



UNIVERSITE DES SCIENCES ET TECHNOLOGIES DE LILLE 1

SCIENCE DE LA MATIERE, DU RAYONNEMENT ET DE L'ENVIRONNEMENT

DOCTORAT

Optiques, Lasers, Physico-Chimie, Atmosphère

Laboratoires d'accueil:

IFP Energies Nouvelles, Division: Systèmes Moteurs et Véhicules

et

PC2A, CNRS: Physico-Chimie des Processus de Combustion et de l'Atmosphère

**Mamady KEITA**

MODELING OF SOOT PARTICLES NUCLEATION FROM  
COMBUSTION PROCESSES

Soutenu le 14 décembre 2017

**Composition du Jury :**

<b>Rapporteurs :</b>	M. Guillaume DAYMA	Professeur, Université d'Orléans
	M. Alexander KONNOV	Professeur, Université de Lund
<b>Examineurs :</b>	M <sup>me</sup> Benedetta FRANZELLI	Chargée de Recherche, Université Paris-Saclay
	M <sup>me</sup> Pascale DESGROUX	Directrice de Recherche, Université de Lille 1 Sciences et Technologies
	M. Olivier COLIN	Ingénieur de Recherche, IFP-Energies Nouvelles
<b>Directeur de thèse :</b>	M. Abderrahman El BAKALI	Professeur, Université de Lille1 Sciences et Technologies



## Acknowledgements

Firstly, I would to express my deepest gratitude to my advisors Dr. André Nicolle (ENSTA Paritech, former IFPEN) and Pr. Abderrahman El Bakali (Professor at the University of Lille 1) for the excellent guidance in preparing this thesis and the continuous support of my Ph.D study and related research, for their availability, motivation and immense knowledge. I had a great opportunity not only to explore many research fields and develop skills that can help me to conduct a research but also, skills related to written and verbal communications and Human skills (teamwork, relational skills and curiosity). I could not have imagined having better advisors and mentors for my Ph.D study. I express my deepest appreciation to Dr. Damien Aubagnac-Karkar (Researcher at IFPEN) for his great support in using his soot model and for his advices and suggestions in writing this thesis.

I would like to thank my thesis committee members: Pr. Guillaume Dayma (Professor at the University of Orléans), Pr. Alexander Konnov (Professor at the University of Lund), Dr. Benedetta Franzelli (Research Coordinator at CNRS, University of Paris-Saclay), Dr. Pascale Desgroux (Research Director at CNRS, University of Lille 1) and Dr. Olivier Colin (Research Coordinator at IFPEN), for their availability and for agreeing to assess my work.

I thank Dr. Antonio Pires Da Cruz (Program Manager at IFPEN) and Dr. Christian Angelberger (Expert at IFPEN) for accepting me as the right candidate to take part of this project in the engines and vehicles modeling department of IFPEN. My thoughts also go to all the staff of this division, especially to Stephane Henriot (Head of engine and vehicle systems division at IFPEN). I thank all the staff of PC2A laboratory, Dr. Pascale Desgroux (Research Director at CNRS), Dr. Laurent Gasnot (Head of PC2A laboratory), Dr. Xavier Mercier (Research Coordinator at CNRS) and Christopher Betrancourt (Ph.D candidate at PC2A) for accepting me in their Lab and for providing experimental data in the framework of the ASMAPE (Advanced Soot Model for Aeronautics and Piston Engines) project.

My sincere thanks also go to Dr. Christophe Dujardin (Director of Studies at ENSCL) who provided me an opportunity to join IFPEN first as intern and for his recommendation and advice to accept this Ph.D position. Without his precious support, it would not be possible to conduct this research.

I thank my office colleagues of IFPEN and all the Ph.D candidates of IFPEN for the stimulating discussions and for all the fun we have had in the last three years. I also thank my colleagues of PC2A Laboratory for their kind invitations for lunch and for having diner together.

Last but not the least, I would like to thank my family: my parents, my wife and my brothers and sisters for their unconditional support throughout writing this thesis and my life in general.



## Abstract

To better control soot particles emission and minimize their health and environmental effects, it is crucial to better understand their formation mechanisms in particularly combustion processes. The first step of these particulates matter formation is their precursors PAH (Polycyclic Aromatic Hydrocarbons) formation, followed by the nucleation process which links the gas-phase (PAH chemistry) and solid-phase (particles).

In the first part of this work, we developed a new detailed chemical kinetic mechanism describing accurately both low and high-temperature ignition and combustion of a wide range of liquid transportation and laboratory fuels as well as the formation of PAH up to coronene, suspected to be major soot precursors. Surrogate mixtures containing n-decane, iso-octane and n-propylbenzene were selected to represent liquid transportation fuels based on their cetane numbers (CN) and threshold sooting index (TSI). Including new reactions paths from recent studies resulted in the improvement of mechanism predictivity (ignition delay times, laminar flame speeds and species mole fractions) over a wide range of experimental conditions (shock tubes, jet stirred reactor, burner stabilized premixed flames, and freely propagating premixed flames). Then, this mechanism was utilized to analyze some key intermediate species as well as PAHs formation pathways for a variety of fuels.

In the second part of this work, a sectional soot model is used with the developed kinetic mechanism in order to investigate soot particles nucleation mechanisms in reproducing experimental data tendencies (soot volume fractions and particles diameters). This model accounts for soot particle inception, condensation, surface growth, coagulation and oxidation processes and directly predicts the Soot Volume Fraction (SVF) and the Soot Number Density Function (SNDF) at each time and location. This couple of kinetic and soot models is run on the detailed kinetic solver Cantera in order to solve both the gas and disperse solid phases in steady laminar flame conditions. The soot model used with the developed detailed kinetic mechanism is validated over premixed laminar methane, ethylene and n-butane flames at various equivalence ratios. Homomolecular and Heteromolecular dimerizations of modest size of PAHs from pyrene to coronene (mass of monomer ranging from 200 to 300 amu) have been considered for particle nucleation modeling.

**Keywords:** Soot, Nucleation, Kinetic Mechanism, PAH, Modeling, Sectional Method, Flames



## Résumé

Pour mieux contrôler l'émission des particules de suies et minimiser leurs impacts sur l'environnement et la santé publique, il est crucial de mieux comprendre leurs mécanismes de formation, en particulier dans les processus de combustion des hydrocarbures. La première étape de formation de ces matières carbonées est la formation de leurs précurseurs appelés HAP (Hydrocarbures Aromatiques Polycycliques), suivie de l'étape de nucléation qui fait le lien entre la phase gaz où les HAP sont formés et la phase solide qui correspond à la formation des particules de suies.

La première partie de ce travail de recherche est focalisée sur le développement d'un nouveau schéma cinétique détaillé, décrivant avec précision non seulement l'auto-inflammation et la combustion basse et haute températures des carburants liquides de transport et ceux du laboratoire, mais aussi la formation des HAP jusqu'au coronène car ces HAP sont suspectés d'être les principaux précurseurs de suies. Des mélanges de carburants modèles contenant le n-décane, l'iso-octane et le n-propylbenzène ont été sélectionnés pour représenter les carburants liquides de transport (Essence, Kérosène et Diesel), en se basant sur leurs nombres de cétane (CN) et leurs indices de suies (TSI). L'ajout de nouvelles voies de réactions issues des études récentes a permis l'amélioration de la prédictivité (délais d'auto-inflammation, vitesses de flamme et fractions molaires des espèces) sur une large gamme de conditions expérimentales (tubes à chocs, réacteurs parfaitement agités, flammes stabilisées sur un brûleur). Ensuite, ce schéma cinétique détaillé a été utilisé pour analyser les voies de formation de quelques espèces intermédiaires clés ainsi que les HAP lors de la combustion d'une grande variété de carburants.

Dans la deuxième partie de ce travail, un modèle sectionnel de suies est utilisé avec le présent schéma cinétique afin d'investiguer les mécanismes de formation des particules de suies en reproduisant les tendances des données expérimentales (fractions volumiques de suies, diamètres des particules). Ce modèle de suies décrit la nucléation, la condensation, la croissance en surface, la coagulation et l'oxydation des particules de suies. Les calculs sur les suies ont été effectués sur un solveur cinétique Cantera afin de résoudre la phase gaz et la phase solide dispersée dans des conditions de flammes laminaires stationnaires. Le couple "schéma cinétique-modèle sectionnel de suies" a été validé sur les flammes prémélangées laminaires de méthane, d'éthylène et de n-butane à différentes richesses. Les dimérisations homomoléculaire et hétéromoléculaire des HAP de taille modérée (du pyrène au coronène) ont été considérées pour la modélisation de la nucléation des particules de suies.

**Mots clés:** Suies, Nucléation, Schéma Cinétique, HAP, Modélisation, Méthode Sectionnelle, Flammes





## Table of Contents

Acknowledgements.....	3
Abstract.....	5
Résumé .....	7
Table of Contents .....	9
Chapter 1: Introduction .....	13
1.1. General context.....	13
1.1.1. Soot formation process.....	16
1.2. Outline of the thesis.....	17
Chapter 2: Literature Review .....	19
2.1. Proposed PAHs molecule for nucleation.....	19
2.2. Main PAH formation pathways.....	26
2.2.1. HACA mechanism .....	26
2.2.2. HAVA (Hydrogen Abstraction and Vinyl Addition) mechanism.....	31
2.2.3. Phenyl Addition and Cyclization (PAC) pathway:.....	33
2.3. Soot formation mechanism.....	35
2.3.1. Gaseous precursors of soot particles.....	37
2.3.2. Soot particles nucleation .....	38
2.3.3. Mass growth of soot particles .....	38
2.3.4. Oxidation of PAHs and soot particles.....	39
2.3.5. Aggregation of soot particles .....	39
2.4. Soot nucleation mechanisms.....	39
2.5. Soot models .....	42
2.5.1. Empirical models .....	42
2.5.2. Kinetic models.....	43
2.5.2.1. Method of moments .....	44
2.5.2.2. Sectional method .....	44
2.6. Conclusions .....	44
Chapter 3: Modeling Tools and Methods .....	47
3.1. One dimensional premixed laminar flames: governing equations .....	47
3.2. The 1D premixed flame code.....	48
3.3. Sensitivity analysis .....	50

3.4.	Rate of production analysis .....	50
3.5.	Sectional Soot Method .....	51
3.5.1.	Governing equations and variables in the model .....	51
3.5.2.	Volume discretization.....	52
3.5.3.	Soot particles volume number in a section $i$ .....	53
3.5.4.	Collisional source terms .....	54
3.5.5.	Inception and condensation .....	55
3.5.6.	Surface chemistry .....	56
3.5.7.	Surface growth.....	57
3.5.8.	Oxidation .....	57
3.5.9.	Parameter $\alpha$ : fraction of soot surface radical sites available for reactions.....	58
Chapter 4: Gas-phase Chemistry.....		61
4.1.	Objective .....	61
4.2.	Surrogate fuels formulation .....	61
4.3.	Development of a detailed chemical kinetic mechanism.....	66
4.4.	Mechanism Validation Results and Discussions.....	70
4.4.1.	Premixed laminar flames configuration .....	72
4.4.1.1.	Saturated aliphatic hydrocarbon flames .....	72
4.4.1.1.1.	Methane flame .....	72
4.4.1.1.2.	N-butane flames.....	76
4.4.1.1.3.	n-butane doped with n-propylbenzene flames.....	94
4.4.1.1.4.	Iso-octane flame.....	103
4.4.1.1.5.	n-decane flame .....	111
4.4.1.2.	Unsaturated aliphatic hydrocarbon flames .....	117
4.4.1.2.1.	Ethylene flames.....	117
4.4.1.3.	Benzene and monoalkyles aromatic flames .....	129
4.4.1.3.1.	Benzene flame .....	129
4.4.1.3.2.	n-propylbenzene flame.....	138
4.4.1.4.	Liquid transportation fuel flames .....	145
4.4.1.4.1.	Jet fuel flame.....	146
4.4.1.4.2.	Gasoline flame .....	153
4.4.2.	Jet Stirred Reactor (JSR) Configuration .....	158
4.4.2.1.	Jet fuel combustion .....	158
4.4.2.2.	Diesel fuel.....	160

4.4.3.	Ignition delay times and laminar flame speeds.....	162
4.4.3.1.	Gasoline.....	162
4.4.3.2.	Jet fuel.....	164
4.4.3.3.	Diesel fuel.....	166
4.5.	Conclusions .....	169
<b>Chapter 5: Solid phase: Soot particles Nucleation Modeling.....</b>		<b>171</b>
5.1.	Objective .....	171
5.2.	Nucleation modeling: soot precursors considered.....	171
5.3.	Collision efficiency.....	173
5.4.	Results and Discussions .....	181
5.4.1.	Methane flame .....	182
5.4.2.	Ethylene flame .....	189
5.4.3.	n-butane flames.....	195
5.5.	Comparison between investigated flames .....	209
5.6.	Conclusions .....	211
<b>Chapter 6: Conclusions and Future Work .....</b>		<b>213</b>
<b>References .....</b>		<b>217</b>
<b>Appendices .....</b>		<b>237</b>



# Chapter 1: Introduction

## 1.1. General context

Combustion is an old technology of mankind that has been used for several years. Most of the worldwide energy support (about 90%) in traffic, heating, or electric power generation is provided by combustion [1]. Following the continuous growth in demand of energy and the need of reduction of pollutants emitted to produce energy, the formation of pollutants from combustion processes has become one of the key topics for researchers. In automotive sector for example, pollutants emission mitigation is really important not only for fuel engine efficiency, but also for the human health and environment. Given the upcoming of new regulations in terms of pollutants emissions into the environment, there is a worthwhile cause to study properly this process.

### - Norms in automotive sector

The current pollutants under European regulations are the following: carbon monoxide (CO), nitrogen oxides (NOx), unburned hydrocarbons and particulate matter (PM). These pollutants are products of an incomplete combustion process and have a huge impact on the air quality. Carbon dioxide (CO<sub>2</sub>) is also of the main combustion products that is not currently under regulation, but is known to cause a global warming as a greenhouse gas. Figure 1 shows the evolution of regulations on pollutant emissions for land cars in Europe, United States of America and Japan [2].

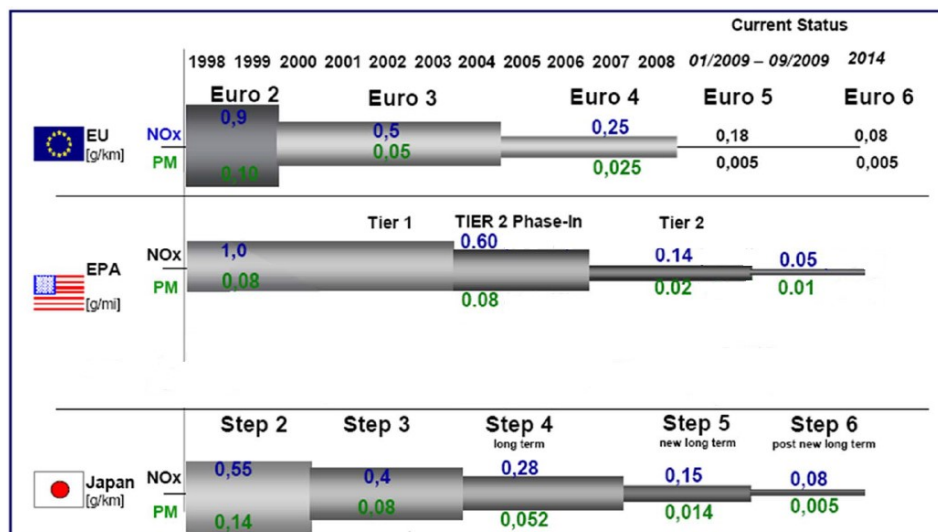


Figure 1 : Exhaust emissions regulations around the world for nitrogen oxides (NOx) and for particulate matter (PM) [2].

It can be seen that the amount of exhaust emissions has drastically decreased from 1998 to 2014 for all the regulations. For example, within the EU regulation, a reduction factor of 20 for PM and a factor of 11 for NO<sub>x</sub> have been achieved. The amount of PM decreased from 0.10 to 0.005 g/km, while that of NO<sub>x</sub> is decreased from 0.9 to 0.08 g/km. The development of advanced technologies including advanced combustion devices and advanced aftertreatment systems has allowed reaching such goals. The amount of the other pollutants according to the EURO 6 regulation is presented as follows in

Table 1:

Norm [mg/km]	Euro 6 Gasoline	Euro 6 Diesel
Nitrogen oxides (NO <sub>x</sub> )	60	80
Carbon monoxide	1000	500
Unburned hydrocarbons	100	-
Unburned non-methane hydrocarbons	68	-
Unburned hydrocarbons + NO <sub>x</sub>	-	170
Particulate matter (PM)	4.5	5
Number of particulate matter [# /km]	$6 \times 10^{12}$	$6 \times 10^{11}$

**Table 1 : Pollutants emissions under EURO 6 regulation.**

Both technologies: gasoline and diesel fuel engines are presented. A particular attention is given to diesel engines regarding NO<sub>x</sub> formation since these systems operate at lean condition ( $\phi < 1$ ), where a great amount of NO<sub>x</sub> can be formed through oxygen combination with nitrogen at high temperature ( $> 2300$  K) [2]. Gasoline engines operate at stoichiometric condition ( $\phi = 1$ ). The specific mass of CO allowed for spark ignition (SI) engines is two times higher than that of diesel engines. There is no regulation on unburned hydrocarbons for diesel engines, while gasoline engines are limited to 100 mg/km for unburned hydrocarbons and 68 mg/km for unburned non-methane hydrocarbons. However, the amount of unburned hydrocarbons + NO<sub>x</sub> for diesel engines is limited to 170 mg/km. Regarding particulate matter, SI engines are allowed to emit ten times more particles than diesel engines. In the latter case, the amount and the number of particulate matter is important due to the non-premixed

combustion that take place, the local equivalence ratio in diesel engines can be very high. As a result, soot particles which are one form of particulate matter can be formed in these conditions, where the concentration of oxygen is very low. Pischinger et al. [3] proposed a diagram that explains the formation of soot and NOx as a function of relative molar air/fuel ratio as depicted in Figure 2.

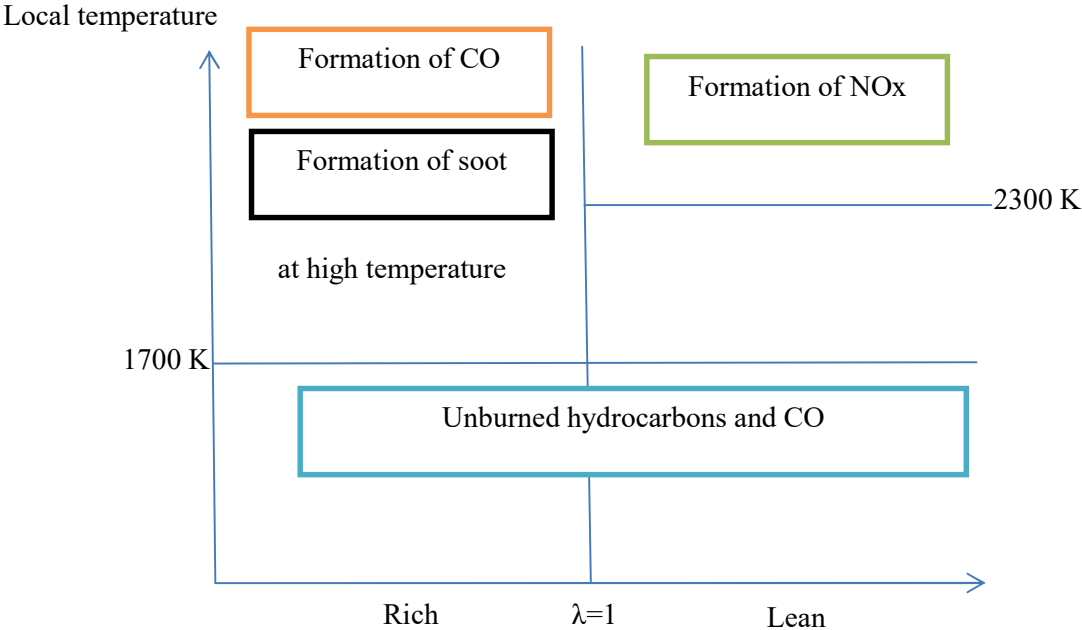


Figure 2 : Formation of pollutants according to Pischinger diagram [3].  $\lambda$  represents the relative air fuel ratio.

It can be seen from this diagram that NOx formation is favored at lean condition and at temperature above 2300 K. Soot and CO are formed at rich condition and at temperature above 1700 K. The formation of unburned hydrocarbons and CO below 1700 K is a phenomenon controlled by the kinetics [2].

Despite the severity of current regulations on pollutant emissions, there is still need to avoid their production from combustion processes not only for human health, but also for the global warming and the technical damages to devices. On one hand, even if gasoline engines emit less PM than diesel ones, both technologies produce PM. On the other hand, the constantly growing number of diesel engines particularly in Europe pleads for the intensification of particulate matter emissions. New regulations for the future will require more limitations on pollutants emissions and new pollutants such as aldehydes can also be regulated. Aldehydes are already under regulation for gasoline engines in California, since they are found to play an important role in photo-oxidation pollution [2]. While

motivations for pollutants mitigation are provided, the understanding of their formation process as well as scientific tools are required to model all the processes involved. With this in mind, the present work focuses on both soot particles and their gaseous precursors formation mechanism since their harmfulness has been clearly demonstrated.

### **1.1.1. Soot formation process**

Soot is one form of particulate matter that is formed from incomplete combustion processes. In the transportation field, soot is mainly produced from diesel engines (up to 87 % mass of cases in transportation field) [4]. Non negligible contribution also comes from spark engines and in aeronautics field. There are several reasons to better understand and control soot particles formation. Among these reasons, one can put forward:

- The fine particle toxicity: fine particle can easily penetrate into human body to cause heart and lung diseases [5].
- The significant contribution to climate change (contribution to radiative forcing).
- The radiative impact and interaction with turbine blades: technical damage in industries.
- The formation of contrail related to cloud albedo: in aircraft's wake.

Soot particles can be classified as fine particles (diameter < 2.5  $\mu\text{m}$ ). In epidemiological studies, fine particles are found to increase mortality due to serious health attack such as heart and lung diseases. In United States for example, the fine particles may cause up to 60,000 deaths per year [6]. Soot particles are associated with Poly Aromatic Hydrocarbons (PAH), which are adsorbed onto their surface. These PAH are found to be mutagenic or tumorigenic. For example, benzo[a]pyrene (5 aromatic rings) causes lung cancer [7]. Soot particles are also found to be suspended in the atmosphere as aerosols (air pollutants), forming brown cloud that causes regional warming. Soot deposition might be responsible for 95% of the polar ice melting [8]. It may cause several technical damages in industries such as the coating of combustion chambers and their interaction with turbine blades (gas turbines damages in power generation). Figure 3 shows a general overview of soot particles formation from homogeneous gaseous mixtures.



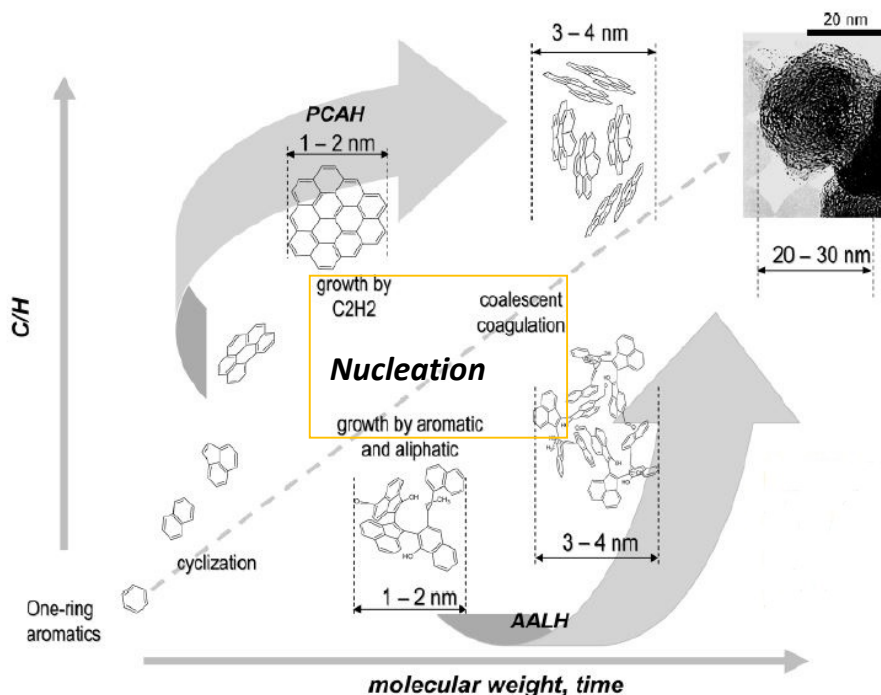


Figure 3 : Soot particles formation process in premixed flames [9]. PCAH stands for PeriCondensed Aromatic Hydrocarbon and AALH denotes Aromatic Aliphatic Linked Hydrocarbon. The term AALH is related to the proposed nucleation mechanism where PAHs are linked by  $\sigma$  bonds.

Soot and PAH formation have been investigated for decades by numerous research groups [8,10–13]. Their formation still remains poorly understood, mainly the nucleation step. It is widely accepted within combustion community that the gaseous species known as Polycyclic Aromatic Hydrocarbons (PAH) are precursors of soot particles as shown on the caption above. Therefore, reliable detailed kinetic mechanisms that describe accurately PAH formation is required to account for soot particles formation modeling. The gas-phase chemistry is a crucial part of the modeling study and need to be carefully elaborate in order to develop robust soot models. Soot formation and their emission must be controlled to cleanup environment and reduce human health attack and also to promote efficient utilization of petroleum based fuels and biofuels. Combustion processes must be well understood for developing cleaner and more economic combustion equipment. For that, physical and chemical processes involved in combustion process have to be better understood.

## 1.2. Outline of the thesis

As stated in the previous section, soot particles nucleation modeling from gaseous species (PAHs) must be carefully investigated. The present work focuses on the chemical understanding of precursor formation including PAHs and nascent soot formation mechanism. The elucidation of chemical

reactions network is required for predicting the soot particles formation and for improving our knowledge on chemical processes involved in combustion. For that, two principal components are investigated:

- (1) Gas-phase chemistry: development of a detailed chemical kinetic mechanism that describes accurately liquid transportation as well as laboratory fuels combustion. Determining of a large set of gas-phase species and reactions.
- (2) Computational modeling of soot nucleation from gaseous species: investigating the role of PAHs widely involved in the nucleation process.

One dimensional premixed laminar flames are considered for soot particles nucleation modeling. In practical systems such as SI engines, combustion is turbulent. In premixed turbulent flames, combustion is a more-dimensional phenomenon and may as such not be treated as a one-dimensional problem. However, both premixed and turbulent premixed flames have the same physical processes and many turbulent flame theories are based on underlying laminar flame structure.

A brief description of each chapter is presented as follows:

In chapter 2, general information concerning soot gaseous precursors (PAHs) used in the previous works, different proposed soot nucleation mechanisms and PAHs formation pathways as a function of fuels are presented.

In chapter 3, modeling tools and methods used to develop a detailed chemical kinetic mechanism and to investigate soot nucleation mechanism are presented.

In chapter 4, the precursor gas-phase chemistry is mainly discussed. A methodology describing commercial surrogate fuels formulation as well as the development of a detailed chemical kinetic mechanism for both commercial and laboratory (single component) fuels combustion modeling. The modeling results for the mechanism validation are presented.

In chapter 5, the particle nucleation modeling (solid phase) is presented. A description of nucleation modeling methodology as well as the investigation of the chosen PAH molecules for soot particles inception are discussed. Finally, results obtained for particles nucleation modeling are presented and discussed.

In chapter 6, the summary of the present study and future work are presented.

## Chapter 2: Literature Review

### 2.1. Proposed PAHs molecule for nucleation

While PAHs are considered by many research groups as soot precursors, the nature of those involved in the nucleation process remains ambiguous and very difficult to determine. This question has been a topic of research for decades. Due to experimental findings limitations, numerical simulations [14–17] are widely used for such investigations.

Frenklach et al. [18,19] concluded that the dimerization of pyrene was necessary to reproduce soot particle size distributions. Miller et al. [20] claimed that the soot nucleation process is most likely if the PAH size is at least four times larger than pyrene. These results are based on the computed lifetimes of dimers under flame conditions. Subsequently, Frenklach et al. [21] performed molecular dynamics calculations and concluded that aromatic dimers of species as small as pyrene can survive long enough to evolve into soot nuclei. From these results, pyrene dimerization was widely used as the key of soot nucleation step but no definitive experimental findings support this assumption. Sabbah et al. [22] presented an experimental and theoretical study of pyrene dimerization at temperatures ranging from 60 to 470 K. Figure 4 shows the results obtained from this study. In Figure 4 (b) (at 120 K), the signal first increases linearly with the increase of pyrene concentration. Above a certain pyrene concentration value, a sudden decrease of pyrene monomer signal is observed. The authors explained this loss of monomer signal by the onset of nucleation and proposed that at these higher degrees of supersaturation, pyrene dimers may be considered as critical nuclei within the framework of classical nucleation theory [23]. In Figure 4 (a) (at 235 K), an excellent linearity is observed between pyrene monomer signal and pyrene monomer concentration, indicating the absence of nuclei formation.

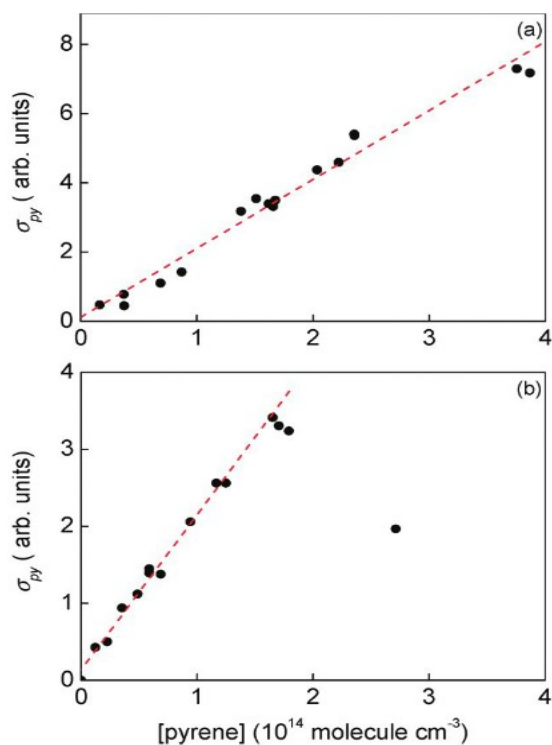


Figure 4 : Plots of the pyrene monomer signal ( $\sigma_{py}$ ) as a function of the nominal density (pyrene concentration at each flow temperature employed). The upper panel (a) demonstrates the absence of significant nucleation at 235 K at pyrene densities up to  $4.10^{14}$  molecules  $\text{cm}^{-3}$  for reaction times of 143  $\mu\text{s}$  at a total density of  $2.06 \cdot 10^{16}$  molecules  $\text{cm}^{-3}$ . In the lower panel (b), nucleation at a temperature of 120 K is evidenced by the collapse of the pyrene monomer signal above a nominal pyrene density of  $1.7 \cdot 10^{14}$  molecules  $\text{cm}^{-3}$  for a reaction time of 118  $\mu\text{s}$  and a total density of  $1.96 \cdot 10^{16}$  molecules  $\text{cm}^{-3}$ .

According to their predictions, dimerization occurs at 235 K if the pyrene partial pressure is in the range of  $0.8\text{-}3.9 \times 10^{-5}$  bar which is in good agreement with their experimental findings. Further, the partial pressure at which 10% conversion to the pyrene dimer may occur at high temperature (up to 1500 K) is in excess of 40 bar. Such high value of partial pressure of pyrene can clearly not be reached in flames conditions or any other combustion environment.

Violi and Elvati [15] conducted a thermodynamic analysis of the physical growth of poly-aromatic hydrocarbons using atomistic molecular dynamics simulations that take into account the entropic contributions that can effect dimerization or trimerization of PAHs. These results clearly showed that even at 1000 K, only the formation of dimers of species such as ovalene or heavier are favored over their corresponding free monomers, ruling out the dimerization of pyrene as the only step for soot formation. These results are consistent with Wang's [8] thermodynamic calculations demonstrating that dimerization of a PAH molecule as big as coronene ( $\text{C}_{24}\text{H}_{12}$ ) is not feasible beyond 1000 K.

From these calculations, only the dimerization of PAH molecules at least as heavy as circumcoronene ( $C_{54}H_{18}$ ) is probable at 2300 K. Teini et al. [24] determined the PAH molecules that would most likely contribute in soot production by measuring their fringe length which is a function of the number of carbon atoms in the molecule, the fuel composition and the temperature history. They investigated acetylene pyrolysis in a rapid compression machine at 10 atm over the temperature range of 1600-2000 K. The mean fringe length of the soot forming PAH clusters was 0.65 nm corresponding to a PAH molecule with 20 carbon atoms and the size of PAH did not change considerably within the soot particles, showing that neither temperature history nor residence time had a significant impact on the distribution of these molecules. Additionally, PAH molecules deposited on both nascent and aged soot particles were shown to have a constant size distribution. Moreover, Dobbins et al. [25] investigated experimentally the chemical evolution and the PAH components of soot particles extracted from the centerline of a laminar ethylene diffusion flame. They found that the thermodynamically stable PAH species also called stabilomers with a mass ranging between 202 amu ( $C_{16}H_{10}$ ) and 374 amu ( $C_{30}H_{14}$ ) are the constituents of the soot precursors particles. However, PAH species  $C_{20}H_{12}$ ,  $C_{22}H_{12}$  and  $C_{24}H_{12}$  with atomic mass units of 252, 276 and 300 respectively had the highest concentrations. In a recent investigation, Saffaripour et al. [26] have improved their soot models for jet fuel (jet A-1) diffusion flames by implementing some changes in their models such as the nature of soot particle precursors (PAH molecules). They replaced pyrene ( $C_{16}H_{10}$ ) by benzopyrene ( $C_{20}H_{12}$ ) in their models according to results from the above-mentioned study by Teini et al. [24]. This modification of their model resulted in an improvement related to physical soot formation prediction, notably the chemical composition of soot particles. This improvement is observed by comparing the soot concentration on the flame wings, at lower flame heights, for the pyrene based model (for which the overprediction was more important) and benzopyrene based model. They attributed this improvement to the slower formation of benzopyrene compared to pyrene. The same observations have been performed in the flame centerline region (at intermediate flame heights) where the concentration of Benzo(a)pyrene is higher than that of pyrene, allowing a better prediction of soot volume fraction in that flame region. However, despite the improvement brought to the model (good prediction of soot particle size and structure), an underprediction by up to a factor of 5 in soot concentration in the flame centerline region

is still observed. Chung [27] investigated the dimerization of PAH molecules and their collision efficiency by numerical simulations. He calculated accurate rates for pyrene dimerization and also the dimerization of larger PAH molecules with different sizes and morphologies. He defined nucleation rate through dimerization in terms of the collision efficiency and collision frequency of two molecules.

The nucleation rate  $r_{nuc}$  is expressed as follows:

$$r_{nuc} = \frac{1}{2N_A} \sum_{i=1}^{\infty} \sum_{j=1}^{\infty} \beta_{ij} N_i N_j \quad \text{Equation 1}$$

Where  $N_A$  is the Avogadro number and  $N_i, N_j$  are respectively the number density of  $i$  and  $j$  species,  $\beta_{ij}$  is the collision frequency. Assuming a free-molecular regime,  $\beta_{ij}$  is expressed as follows:

$$\beta_{ij} = \beta \cdot \sigma_{ij} \sqrt{\frac{8k_B T}{\pi \mu_{ij}}} \quad \text{Equation 2}$$

Where  $\beta$  is the collision efficiency,  $\sigma_{ij}$  is the reaction cross section between species  $i$  and  $j$  and  $\mu_{ij}$  is the reduced mass of species  $i$  and  $j$ . It is worth noting that  $\beta$  is not a constant and depends considerably on temperature. The expression of the collision efficiency  $\beta$  given by the authors depends on the PAH mass (number of aromatic rings) and the temperature:

$$\beta = \exp(p_0 + p_1 \times AR + p_2 \times T^2 + p_3 \times T \times AR + p_4 \times AR^2 + p_5 \times T^3 + p_6 \times T^2 \times AR + p_7 \times T \times AR^2 + p_8 \times AR^3)$$

Where AR denotes the number of aromatic rings, T is the temperature and  $p_0$  to  $p_7$  are the fitting parameters.

If the colliding species are the same, the nucleation rate can be written as:

$$r_{nuc} = \beta \cdot N_A d_{PAH}^2 \cdot \sqrt{\frac{4\pi k_B T}{m_{PAH}}} [PAH]^2 \quad \text{Equation 3}$$

Where  $d_{PAH}$  is the diameter of the PAH molecule,  $m_{PAH}$  is the mass of the PAH molecule and  $[PAH]$  is the PAH concentration.

Figure 5 below shows the collision efficiency for three PCAH molecules. The effect on molecular mass and temperature are clearly observed. One can note that there is a difference in the magnitude of variation depending on molecular mass of PCAH. In the case of molecule III<sub>0</sub>, the collision efficiency drops from 0.400 at 500 K to 0.050 at 1500 K. In the case of molecule I<sub>0</sub>, the collision efficiency drops considerably from 0.10 at 500 K to  $2.5 \times 10^{-4}$  at 1500 K. Since soot zone

is within this range of temperature, the pyrene (molecule  $I_0$ ) dimerization route depends highly on flame conditions, while molecule  $III_0$  dimerization route is likely to occur at various temperature conditions.

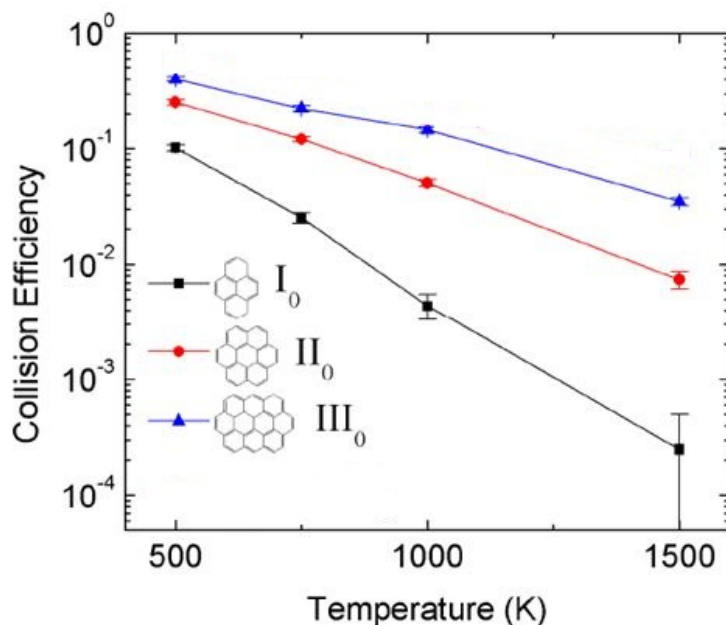


Figure 5: Collision efficiency for 3 peri-condensed aromatic hydrocarbon  $I_0$ : Pyrene;  $II_0$ : Coronene;  $III_0$ : circumcoronene [27].

Other authors such as D'anna et al. [28], Vander Wal et al. [29] and Franklin et al. [30] have focused their research on morphology, chemical evolution and internal structure of particles formed in flames. D'Anna et al. [28] focused on the morphology and number of molecules in the clusters at particle inception and they have computed by sectional method, the mass of particles, H content and internal structure. Their model was able to distinguish clearly between single high molecular mass molecules, clusters of molecules and aggregates of clusters. On the one hand, the above authors indicated that ordered and disordered aromatics coexist in incipient soot particles. The ordered ones are formed from planar (stacked) PAH, corresponding to PAH with only six-membered rings, while the disordered ones are formed from non-planar PAH and/or randomly oriented [30]. They argued that particles with ordered structures are formed preferably at higher temperature and for long residence time in flame, while particles with disordered structures are favored at lower temperature and for short residence time. Moreover, they provided detailed information on the nature of PAH as shown in Figure 6 below: PCAH that contain only  $\pi$  bonds

between C atoms (low H/C ratio) and incompletely condensed aromatics that contain  $\pi$  and  $\sigma$  bonds (high H/C ratio).

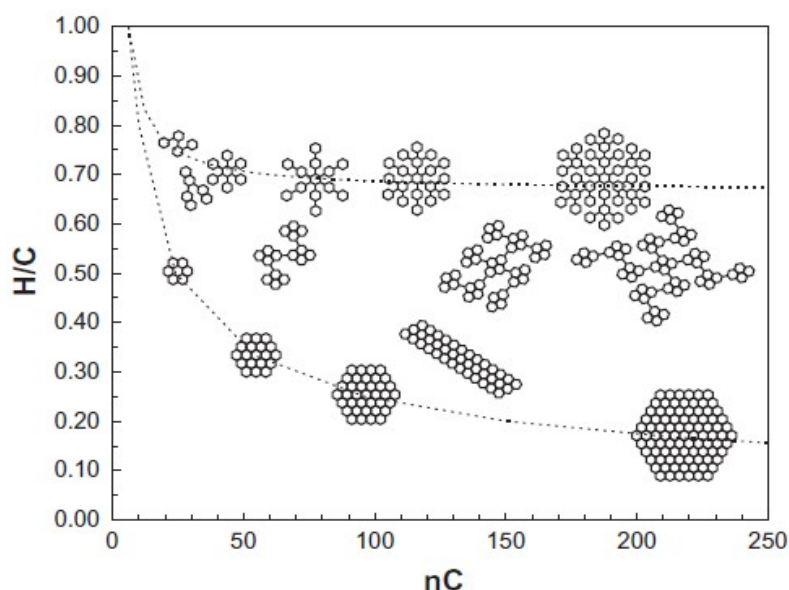


Figure 6 : Representation of aromatic compounds for  $C_{24}$ - $C_{250}$ . Lines represent the limits of oligomers of benzene [28].

On the other hand, D'Anna et al. have examined the number of molecules in the clusters at different heights above the burner. They found that at particle inception, clusters comprise 2 to 8 molecules, in agreement with experimental data from HR-TEM (High Resolution Transmission Electronic Microscope). They also mentioned that at particle inception, three mass peaks are observed: molecules of aromatic compounds having masses up to 1000 amu, their clusters (nanoparticles) with masses up to 5000 amu and isolated particles (first single particles). However, they did not precise the nature of PAHs at particle inception step.

#### - Heteromolecular dimerization

Most of soot models only account for homomolecular dimerization, meaning that the two colliding species are assumed to have the same chemical structure. The heteromolecular dimerization, which assumes that two or more reactants that have different chemical structure is rarely considered. This assumption is found to be an interesting route for soot nucleation comprehension. Indeed, experiments showed that several PAHs have been detected and quantified and collisions between these PAHs can potentially lead to soot particles inception, instead of considering only one PAH physical agglomeration.



Chung and Violi [31] investigated soot mass concentration prediction in a plug flow reactor. Figure 7 shows results obtained by considering collision between two molecules of pyrene and collision between pyrene and coronene molecules.

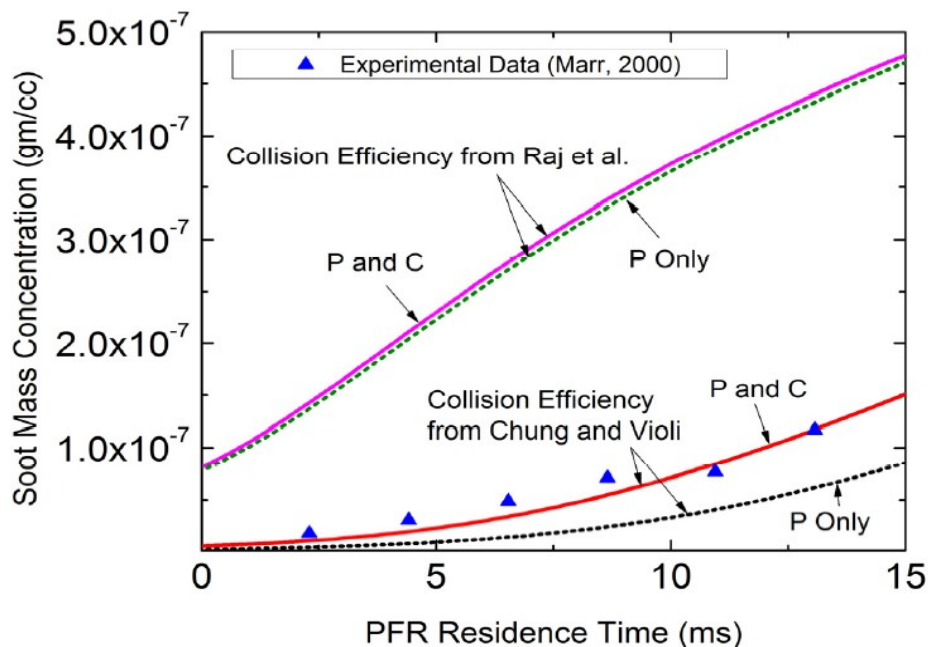


Figure 7: Heteromolecular dimerization compared to homomolecular dimerization for soot mass concentration prediction in a plug flow reactor configuration [32]. P denotes pyrene and C denotes coronene.

The results clearly show that including the heteromolecular dimerization (reaction between pyrene and coronene molecules) results in a much better prediction of soot mass concentration than the homomolecular dimerization alone (reaction between two molecules of pyrene). This is probably due to the collision efficiency effect ( $5 \times 10^{-4}$  for the homomolecular dimerization against  $3 \times 10^{-3}$  for the heteromolecular pyrene/coronene dimerization at  $T=1500$  K), which increases with the molar mass [27]. Since the mean molar mass of coronene and pyrene is higher than that of pyrene only, one should expect to get higher collision efficiency in the coronene and pyrene case. However, one should not omit the effect of the mass action law that can significantly impact results even the collision efficiency is higher. Results obtained from Chung and Violi are also compared to those of Raj et al. [33] in term of collision efficiency between PAHs. One can notice that the collision efficiency obtained by Raj et al. [33] leads to an overprediction of the soot mass concentration. Moreover, no significant difference is observed by comparing homomolecular to heteromolecular dimerization. These results clearly show the significant influence of precursors on soot formation. Consequently, investigation on the

dimerization of a large pool of reactive PAH molecules (multi-precursors nucleation) is necessary to better understand the soot formation mechanism.

## **2.2. Main PAH formation pathways**

### **2.2.1. HACA mechanism**

The nature of PAHs molecules widely involved in nucleation process raises many questions within combustion community as the mechanism involved is poorly understood because of experiment findings, which are very limited. From the previous reviews, PAHs molecules with moderate size (not larger than 300 amu) are found to be soot precursors [34]. However, understanding PAHs chemistry (gas-phase chemistry) is a key step in soot formation modeling as their respective contributions vary from one fuel structure to another, which influence nucleation in a complex way.

Starting from the first aromatic ring (benzene), PAH chemistry has been investigated by many researchers [11,35,36] during the last decades. Pathways leading to their formation remain controversial. It was reported that  $C_3$  species combination plays a dominant role in benzene formation for the combustion of acetylene,  $C_3$  fuels (propene, propane), n-heptane and n-decane flames [35], ethylene [36] and methane flames [37]. In  $C_4$  fuels such as but-1,3-diene [35] or n-butane [38], ethylene [11,39,40] and iso-octane [35,40]:  $C_3$  species combination and  $C_4$  species reaction with acetylene seem to be dominant pathways leading to benzene production. In cyclohexane flame [35] benzene is mainly produced via the sequential dehydrogenation of the initial fuel. In the hexadiene doped methane diffusion flame [37] authors reported that benzene is mainly produced via cyclopentadienyl radical combination with methyl radical, while in the corresponding non doped methane diffusion flame, propargyl radicals combination is the dominant benzene production pathway. A large amount of cyclopentadiene in this doped flame has been observed, leading to cyclopentadienyl radical creation. In toluene flame [40] benzene is directly produced via fuel decomposition, which is faster than  $C_3$  species combination or  $C_4$  species and acetylene reaction.

Beyond benzene formation, several pathways leading to two-ring aromatic hydrocarbon (naphthalene) production have been proposed. Among them, the well-known HACA mechanism (H-abstraction- $C_2H_2$ -addition) [10] has received much attention. Castaldi et al. [36] reported that cyclopentadienyl

radicals combination might play a key role for naphthalene formation in ethylene flames. Colket et al. [41] and McEnally et al. [12] focused their investigation on benzyl radical route, indicating that benzyl radical reacts with propargyl radical to create directly naphthalene [41] or benzyl radical reacts with acetylene to form indene, which is subsequently converted into naphthalene by methyl radical addition [12]. Anderson et al. [42] have evaluated both routes (HACA and benzyl radical) in their investigation and suggested that the importance of HACA route in naphthalene formation is proportional or related to the maximum phenylacetylene concentration in flame, while that of benzyl route is proportional to the maximum toluene concentration. Moreover, authors suggested that both routes constitute the main naphthalene production pathways in the flames studied. Recent investigations carried out by Slavinskaya et al. [39] and Appel et al. [11] involved  $C_4$  species reaction with phenyl radical (or benzene) besides HACA route (with phenylacetylene) and cyclopentadienyl radicals combination route. Wang et al. [40] studied different fuel structures: ethylene, n-heptane, iso-octane, benzene and toluene, and postulated that major pathways leading to naphthalene are  $C_4$  species ( $i-C_4H_5$ ;  $C_4H_3$ ) reaction with phenyl radical or benzene and cyclopentadienyl radicals combination.

Regarding larger PAH formation (up to pyrene), the HACA mechanism is widely used. Castaldi et al. [36], Appel et al. [11] and Marinov et al. [43] have considered solely phenanthryl reaction with acetylene as the main pathway leading to pyrene in their kinetic mechanism. However, they observed that pyrene concentration was underpredicted and concluded that additional pathways beyond HACA mechanism might contribute to pyrene production as well. Slavinskaya et al. [39] proposed that species such as acetylene, diacetylene ( $C_4H_2$ ), cyclopentadienyl radical, phenyl radical and phenylacetylene might play a crucial role in PAH growth process, starting from the first aromatic ring. For example, for pyrene production, authors reported that acenaphthylene with diacetylene combination, phenanthryl radical with acetylene combination and phenylacetylene radical with phenylacetylene combination appear as the major pyrene production pathways. In recent investigations on different fuel structures: ethylene, n-heptane, iso-octane, benzene and toluene, Wang et al. [40] suggested that naphthyl radical with naphthalene combination might also play a role in pyrene production. An overview of aromatics formation pathways can be depicted as in Figure 8.

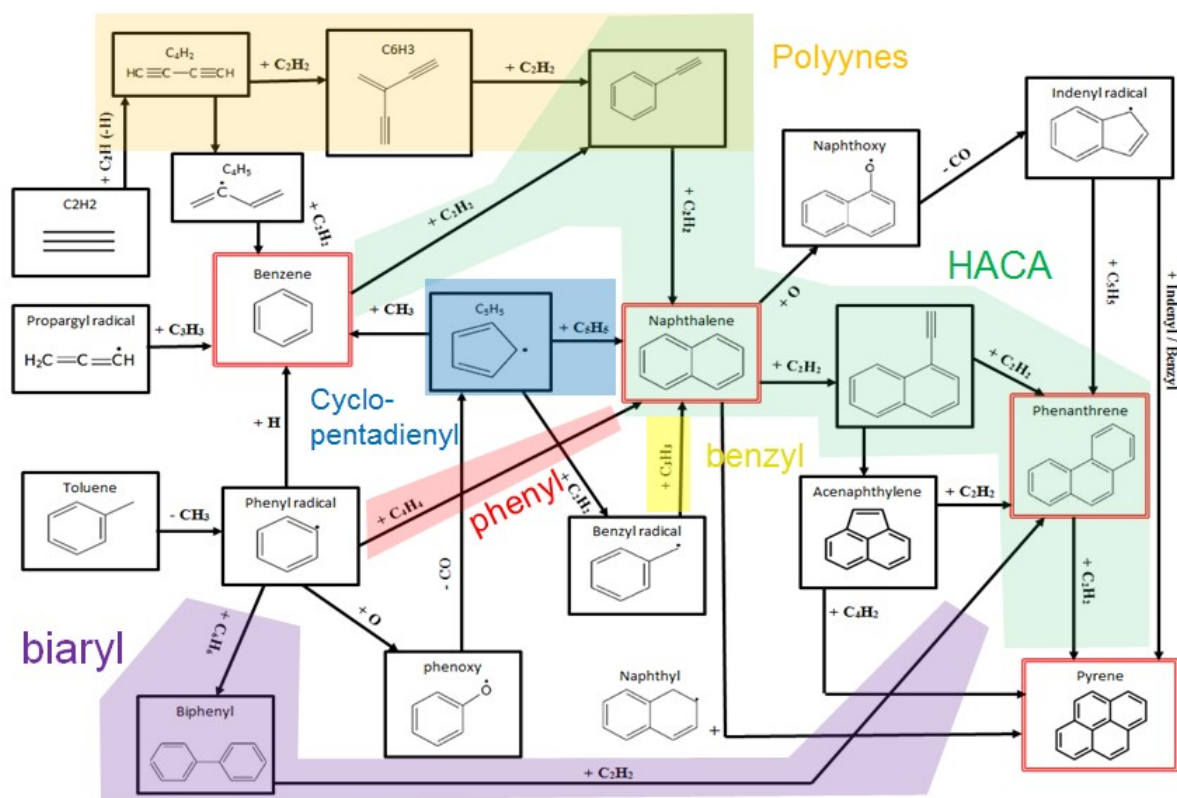


Figure 8 : Overview of different aromatics (up to Pyrene) formation pathways.

Computational studies (DFT) shows that the gaseous acetylene molecule plays a key role in PAHs growth process. The reaction mechanism of PAHs from acenaphthylene ( $C_{12}H_8$ ) to Pyrene ( $C_{16}H_{10}$ ) have been examined by Unterreiner et al. [44]. Authors brought to light the role of acetylene as a key species and considered the Hydrogen-Abstraction-Acetylene-Addition mechanism as one of the major paths in PAHs production. Results obtained from their work are presented as follows:



Figure 9 shows the reaction enthalpies at 298 K for the acetylene addition to naphthyl radical [1] to yield acenaphthylene [6] and hydrogen. The reaction is exothermic by  $163 \text{ kJ.mol}^{-1}$ . The highest barrier of the total reaction path (relative to the educts) is  $19 \text{ kJ.mol}^{-1}$ . The reaction begins with the formation of [2] which proceeds to either [3] via hydrogen migration or to [4] under hydrogen atom loss. At B3LYP level the way to [3] shows a barrier of  $26 \text{ kJ.mol}^{-1}$ , significantly lower than the one to [4] of  $150 \text{ kJ.mol}^{-1}$ . The barrier of the ring cyclization of [3] to [5] is  $42 \text{ kJ.mol}^{-1}$ . Forming [6] under hydrogen loss has an activation barrier of  $192 \text{ kJ.mol}^{-1}$ , the transition state is  $2 \text{ kJ.mol}^{-1}$  above the energy of the final product.

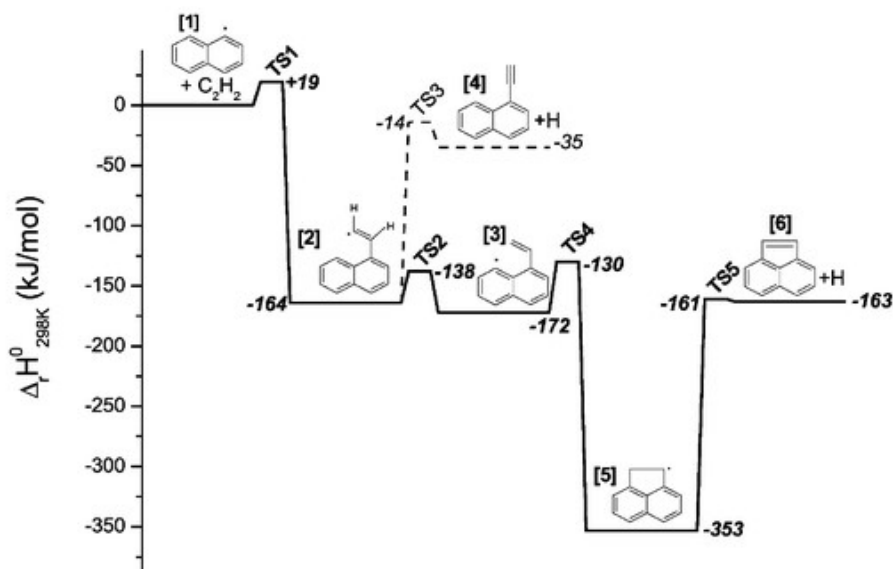


Figure 9 : Potential energy diagram of the reaction naphthyl [1] + acetylene → acenaphthylene [6] + H. The dashed line is a second reaction path. The reaction enthalpies are calculated from harmonic frequencies at 298 K and 0.1 MPa on B3LYP/SV(P) level [44]. The number indicated in the bracket stands for molecule identification as shown in the caption.

- Phenanthryl formation pathway :  $C_{12}H_7$  [6a] +  $C_2H_2 \rightarrow C_{14}H_9$  [17]

Figure 10 shows the reaction enthalpies at 298 K for the acetylene addition to acenaphthylenyl to yield phenanthryl radical.

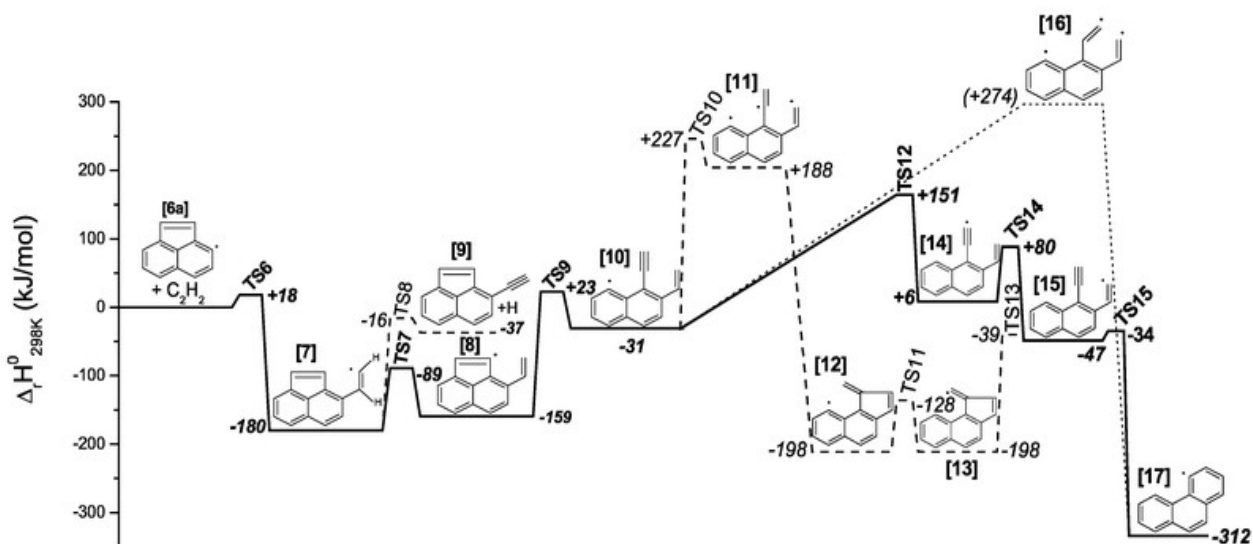


Figure 10 : B3LYP/SV(P) potential energy diagram of the reaction acenaphthylenyl [6a] + acetylene → phenanthryl [17]. The solid line is the most probable reaction pathway, the dashed and dotted lines are other pathways [44]. The number indicated in the bracket stands for molecule identification as shown in the caption.

This reaction is a transformation reaction from a five to six-membered ring. The reaction is exothermic by  $312 \text{ kJ}\cdot\text{mol}^{-1}$ . The HACA mechanism proceeds through formation of [11] and [16], respectively and the highest barrier of the reaction path is found to be  $227 \text{ kJ}\cdot\text{mol}^{-1}$  for the formation of [11].

- **Pyrene formation pathway:**  $C_{14}H_9$  [17] +  $C_2H_2 \rightarrow C_{16}H_{10}$  [23] + H

Figure 11 shows the reaction enthalpies at 298 K for the acetylene addition to phenanthryl to form pyrene.

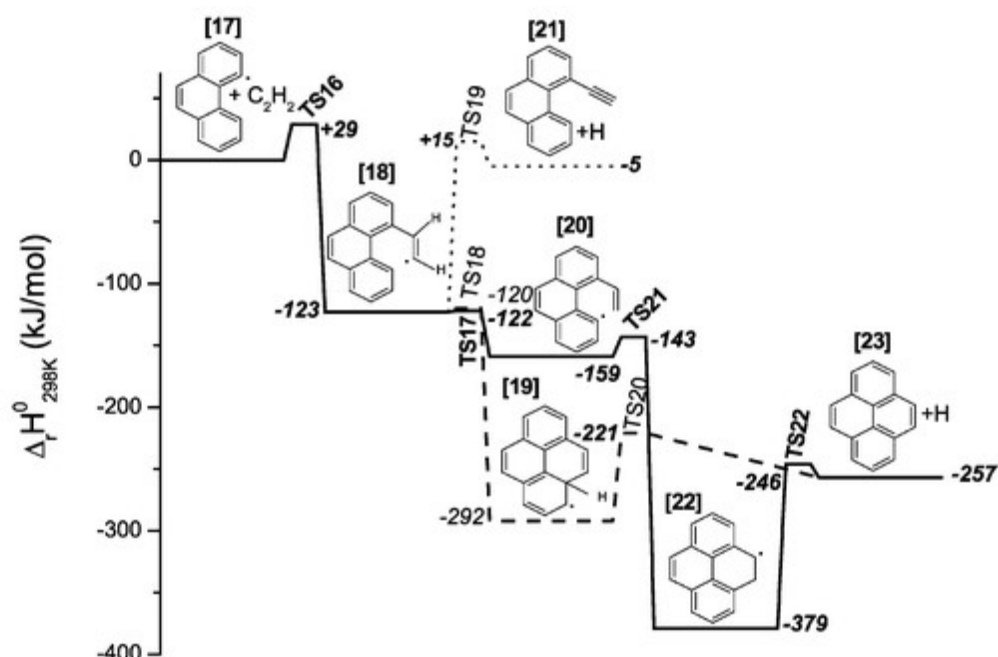


Figure 11 : Potential energy diagram of the reaction phenanthryl [17] + acetylene  $\rightarrow$  pyrene [23] + H. Values calculated at B3LYP/SV(P) level. The solid, dashed and dotted lines are three different pathways [44]. The number indicated in the bracket stands for molecule identification as shown in the caption.

This reaction is six-membered ring cyclization with an exothermic reaction of  $257 \text{ kJ}\cdot\text{mol}^{-1}$ . The highest barrier of the total path is calculated to be  $29 \text{ kJ}\cdot\text{mol}^{-1}$ . Starting after the formation of [18] the radical has three possibilities to react. For the first way, molecule [21] is obtained under hydrogen loss. The second way leads to [19] via ring cyclization and the last way is a H-migration from the  $C_2H_2$  group to the six-membered ring [20] followed by ring cyclization [22]. Both radicals, [19] and [22], decompose to pyrene [23].

- **Fluoranthene formation pathway:**  $C_6H_6$  [1] +  $C_{10}H_7$  [2a]  $\rightarrow C_{16}H_{10}$  [8] +  $H_2$  + H.

Figure 12 shows the reaction enthalpies at 298 K for the benzene addition to naphthyl radical to form fluoranthene.

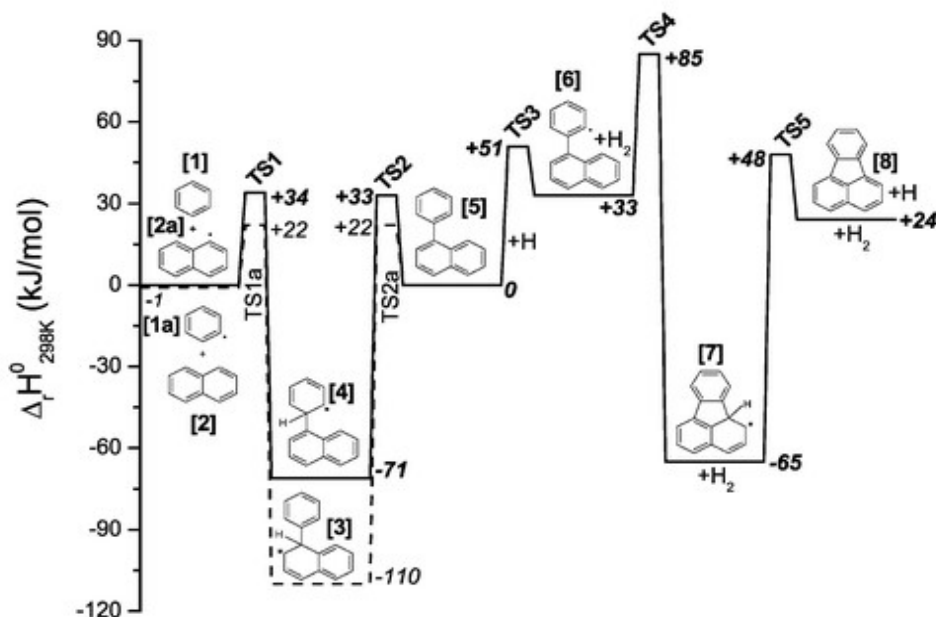


Figure 12 : Potential energy diagram of the aromatic condensation reaction benzene [1] + naphthyl [2a] → fluoranthene [8] + H + H<sub>2</sub>. Calculated at B3LYP/SV(P) level. The dashed line is the reaction pathway for phenyl [1a] + naphthalene [2] [44].

This reaction shows the aromatic condensation of benzene [1] with a naphthyl radical [2a]. The reaction is endothermic by 24 kJ.mol<sup>-1</sup> and the highest barrier of the reaction path, relative to the educts, is obtained to be 85 kJ.mol<sup>-1</sup>. The analogous reaction of phenyl [1a] and naphthalene [2] is also calculated (dashed line). [3] is lower in energy than [4] by 39 kJ.mol<sup>-1</sup>. This is due to the stabilization of the radical through the  $\pi$ -system. The next step is the separation of a hydrogen atom leading to [5]. The energy of the barrier from [3] to [5] is found to be 132 kJ.mol<sup>-1</sup> and from [4] to [5] it is 104 kJ.mol<sup>-1</sup>. The following step is a hydrogen abstraction under formation of H<sub>2</sub> and [6] with a barrier of 51 kJ.mol<sup>-1</sup>. The barrier of the ring cyclization forming a fluoranthenyl radical [7] has been computed to be 52 kJ.mol<sup>-1</sup>. The final step is the decomposition to fluoranthene [8], through a barrier of 113 kJ.mol<sup>-1</sup>.

Some alternative mechanisms that may compete with the HACA based mechanism and all the possible reactions quoted above are proposed. A brief description of these alternative mechanisms is given as follows:

### 2.2.2. HAVA (Hydrogen Abstraction and Vinyl Addition) mechanism

A novel route for PAH growth in HACA based mechanisms was proposed by Shukla et al. [45] in investigating acetylene and ethylene pyrolysis, where small aliphatic hydrocarbon products to large

PAHs (up to 324 uma) were observed. They showed that PAH growth take place by addition of any  $C_2H_x$  species (radical or neutral) such as  $C_2H_2/C_2H$  (ethyne/ethynyl) and  $C_2H_4/C_2H_3$  (ethene/ethenyl), since they are produced in significant concentrations and they further accelerate the formation of a wide range of products including PAHs. Moreover, they suggest that production of naphthalene from benzene via HACA mechanism is less probable, assuming that HAVA mechanism seems to be more promising for producing PAHs during aliphatic hydrocarbon pyrolysis. Experimental evidence supports the HAVA mechanism as shown on the following reaction sequence (Figure 13) during ethylene pyrolysis:

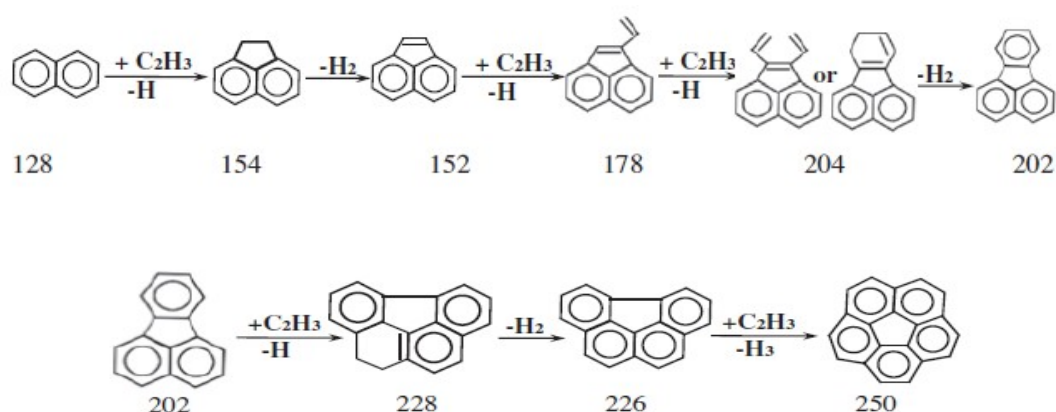


Figure 13 : PAH growth process via vinyl radical addition from ethylene pyrolysis [45].

The time of flight mass spectrometer (TOFMS) experiments shows that from naphthalene to fluoranthene, a repetitive addition of  $C_2H_3$  radical is observed with regular mass number intervals of 26. Similarly, from fluoranthene to corannulene, a repetitive addition of  $C_2H_3$  radical is also observed.

In the case of acetylene pyrolysis, HACA mechanism is proposed for the PAHs growth as shown in Figure 14:

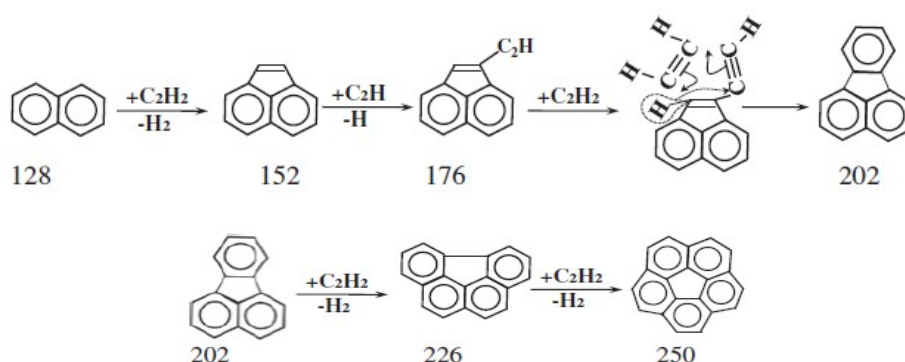


Figure 14 : PAH growth process ethynyl radical addition from acetylene pyrolysis [45].



As for ethylene pyrolysis,  $C_2H_2/C_2H$  ratio has a major impact on PAH growth from naphthalene to corannulene, where a regular mass number interval of 24 is observed.

Therefore, the nature of species involved in the growth process depends considerably on fuel structure and operating conditions. The formation of cyclopentaring fused-PAHs (fluoranthene to corannulene) is possible and might be preferred over currently accepted reaction that forms benzenoid-PAHs (PCAHs) (pyrene to coronene) especially in aliphatic hydrocarbon pyrolysis/oxidation. Moreover, these authors reinforce the validity of HACA/HAVA mechanism for PAHs growth from naphthalene to large PAHs (up to corannulene) even if kinetic data for HAVA mechanism are not yet available.

### 2.2.3. Phenyl Addition and Cyclization (PAC) pathway:

Shukla and Koshi [45] have investigated the role of phenyl radical during benzene pyrolysis with or without addition of acetylene in a flow tube reactor conditions. They detected PAHs such as polyphenyl-PAHs, cyclopentafused-PAHs and larger PAHs up to  $C_{36}H_{22}$  (454 amu). They observed an appearance of mass peaks at regular mass number intervals of 76, corresponding to phenyl radical addition followed by hydrogen elimination. Since HACA mechanism is only found efficient for producing symmetrical PAHs by filling a triple fusing site, the PAC pathway is found to be efficient to continue the endless growth of PAHs.

The authors proposed the following sequence of reactions at low temperature region ( $< 1300$  K) that clearly shows PAH growth by phenyl radical addition (Figure 15), where the number in the bracket represent atomic mass of the corresponding species.

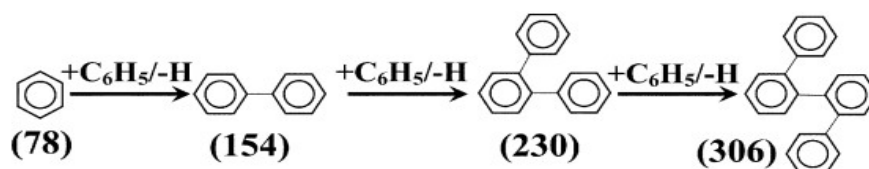


Figure 15 : PAH growth process via phenyl radical addition from benzene pyrolysis [45].

The mass peaks at regular intervals of mass number 76 from benzene to quaterphenyl are produced by successive phenyl radical addition at each step. However, the mass spectra analysis cannot provide the preference sites of addition leading to isomers of terphenyl (o-; m- p- terphenyl), and isomers of quaterphenyl (1, 1':2',1''-terphenyl, 4'-phenyl; 1,1': 3'1''-terphenyl, 5'-phenyl; o-quaterphenyl;

m-quaterphenyl; p-quaterphenyl). Mass peaks are found diminishing with appearance of -2 mass number peaks with increasing temperatures as shown in Figure 16:

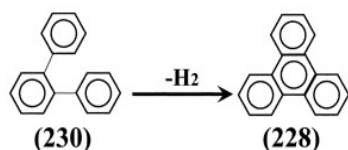


Figure 16 : Ring closure by hydrogen loss under the effect of temperature [45].

o-Terphenyl ( $m/z=230$ ) is dehydrogenated/dehydrocyclized to yield terphenylene ( $m/z=228$ ). That is probably due to the thermal conversion (effect of temperature) and is not expected in the case of m- or p-terphenyl. Similarly, two new species can be produced from o-quaterphenyl ( $m/z= 306$ ) by increasing temperature as shown in Figure 17:

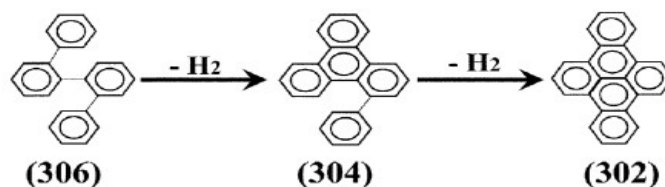


Figure 17 : Effect of temperature in more condensed PAH formation [45].

Only o-quaterphenyl can efficiently produce these two new species: o-phenylterphenylene ( $m/z=304$ ) and dibenzo (fg, op) naphthacene ( $m/z= 302$ ).

In the high temperature region ( $> 1300$  K), phenyl addition sequence starting from naphthalene ( $m/z= 178$ ) to produce larger PAHs such as phenylnaphthalene ( $m/z= 204$ ) and phenylfluoranthene ( $m/z= 278$ ) can be observed as shown in Figure 18:

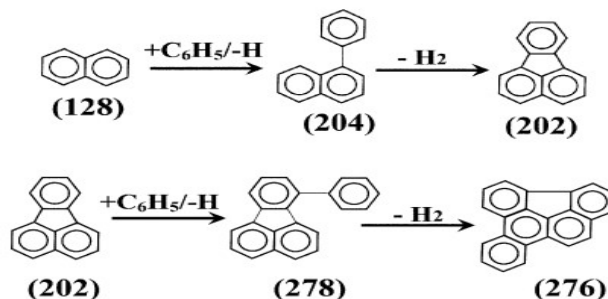


Figure 18 : Cyclopentafused PAHs growth process via phenyl addition/H abstraction [45].

Phenyl addition products are accompanied by stable dehydrocyclized ones, which are most probably fluoranthene and indeno [3,2,1,7, defg] chrysene.

Norinaga et al. [46] have investigated benzene pyrolysis in a flow reactor at atmospheric pressure and at temperature ranging from 1123 to 1223 K, residence time up to 4s. They found that benzene oligomers such as biphenyl ( $C_{12}H_{10}$ ), terphenyl ( $C_{18}H_{14}$ ), quaterphenyl ( $C_{24}H_{18}$ ) and quinquephenyl ( $C_{30}H_{22}$ ) were primarily products and important intermediates of carbonaceous particles in benzene pyrolysis. Therefore, they found necessary to include reactions leading to these benzene oligomer formations in their chemical kinetic mechanism.

All the above results indicate that the PAC route might be an efficient route for PAH growth since it increases the mass by 74 with respect to 24 and 26 in respectively the HACA and HAVA cases. PAC pathway is found efficient for ring growth from any fusing site of a PAH since it generates two new sites at each step and can continue the endless growth. However, it is inefficient to produce symmetrical PAHs, while HACA is only efficient for the ring growth from a triple fusing site of a PAH to generate symmetrical PAHs such as coronene or corannulene. Despite the separate advantages of both routes (PAC and HAVA), PAC or HAVA alone cannot explain the fast growth of PAHs and consequently soot particles formation process. By combining the contribution of all possible routes to PAHs production, one should expect to account for PAHs growth rate and to better predict their formation.

### **2.3. Soot formation mechanism**

The soot particles formation process is a complex process that is not fully known. Soot particles are formed from hydrocarbon fuels conversion at higher temperature and their concentration is increased by increasing the fuel equivalence ratio (relative fuel-air ratio with respect to stoichiometry). The least understood step is probably the particles nucleation step that makes the link between the gas-phase and the solid-phase. Figure 19 illustrates the entire soot formation mechanism.

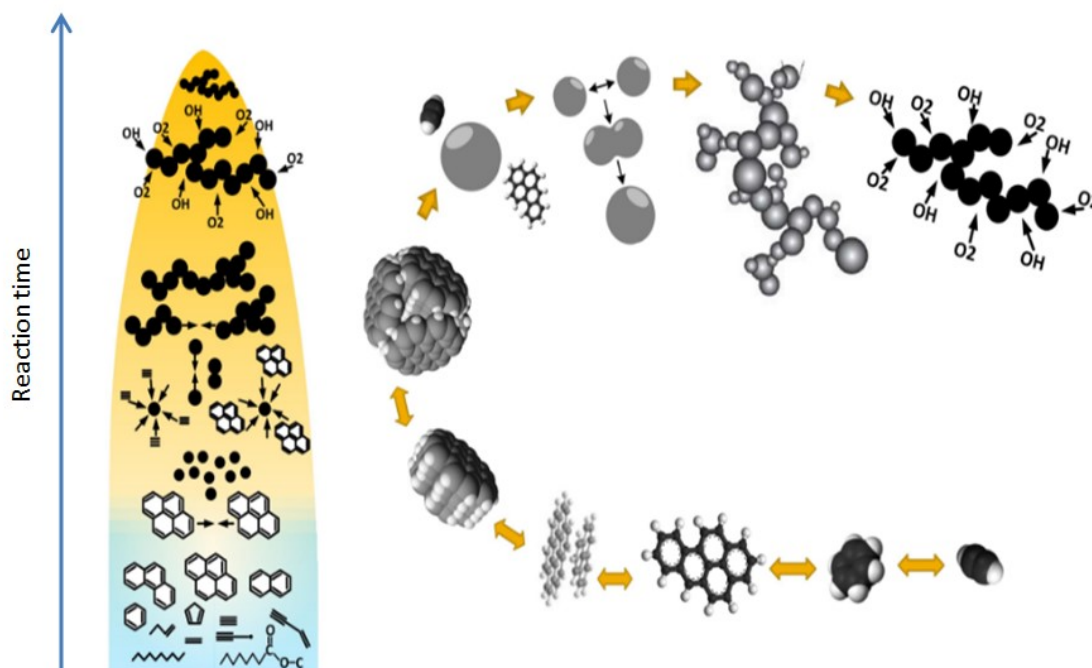


Figure 19 : Soot particles formation mechanism from hydrocarbon combustion.

The blue part of this caption shows the flame zone where PAHs are formed. The production of particulate matter induces a change in flame color changes from blue to yellow. Despite the misunderstanding of all process of soot formation, experimental investigations namely in laminar premixed or non-premixed flames of several hydrocarbon allowed to identify the main steps of this complex process. The PAHs formation mechanisms have been presented in the previous section as well as the potential chemical species involved. The identified processes involved in soot formation mechanism can be summarized as follows:

- (1) Soot gaseous precursors formation: such as  $C_2H_2$ , PAHs
- (2) Nucleation: the smallest particles formation from gaseous species
- (3) Condensation
- (4) Coagulation
- (5) Particles surface growth
- (6) Particles oxidation
- (7) Particles aggregation

The above-mentioned processes can be discussed as follows:

### 2.3.1. Gaseous precursors of soot particles

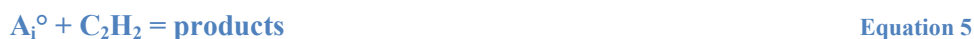
It is suspected that PAHs with size of 500-1000 amu are molecular precursors of soot particles [47]. The chemical growth of light aromatics (1 or 2 aromatics ring) to heavy PAHs (4 to 7 and more) is described by the addition of C<sub>2</sub>, C<sub>3</sub> and other small units to the light PAHs. Among these growth processes, the Hydrogen-Abstraction-Acetylene-Addition mechanism (HACA) has received much attention. The term HACA was introduced by Frenklach and Wang [18]. HACA implied a repetitive reaction sequence of two successive steps:

- (1) abstraction of hydrogen atom from the reacting hydrocarbon by a gaseous hydrogen atom:



Where A<sub>i</sub>-H represents the hydrocarbon and A<sub>i</sub><sup>°</sup> the hydrocarbon radical

- (2) Addition of a gaseous acetylene (C<sub>2</sub>H<sub>2</sub>) molecule to the radical site formed:



However, the inability of the HACA mechanism to be an effective way to ring formation for PAHs formation beyond naphthalene has come under scrutiny by Parker et al. [48]. This compelling study performed under 300 Torr and 1200 K shows that HACA mechanism is unable to form tricyclic PAHs (phenanthrene or anthracene) from naphthyl radical reacting with acetylene. In fact, naphthyl radical reaction with acetylene would form predominantly acenaphthylene (C<sub>12</sub>H<sub>8</sub>) which is a precursor to nonplanar PAHs (or PAHs containing a five-membered ring) such as corannulene and probably fullerene. Naphthyl radical reaction with one acetylene molecule forms an intermediate (C<sub>12</sub>H<sub>9</sub>) that turns by cyclization to acenaphthylene (C<sub>12</sub>H<sub>8</sub>). Mebel et al. [49] showed that this cyclization is much faster than the second addition of acetylene molecule to the intermediate C<sub>12</sub>H<sub>9</sub> leading to C<sub>14</sub>H<sub>11</sub> followed by H atom abstraction to yield a third aromatic ring (anthracene or phenanthrene). These findings suggest that the HACA mechanism is not the most significant mechanism in mass growth to heavy PAHs. Acetylene is not the only species that can be envisioned to propagate the growth of aromatic rings. Several alternate pathways have been put forward such as methyl, propargyl (C<sub>3</sub>), vinylacetylene (C<sub>4</sub>) addition, cyclopentadienyl (C<sub>5</sub>) radicals and phenyl (C<sub>6</sub>) radicals addition and

cyclization [36,41,50–53]. These proposals are based on the resonantly stabilized structure of the reacting radicals, assuming that hydrocarbons with conjugated structures and their derivatives are critical intermediates to soot nucleation [54]. It is found that the pool of species involved in PAH formation growth process depends considerably on fuel structure [55]. For example, in aromatic flames such as benzene, phenyl radicals which exist in high concentration, accelerate PAHs growth and formation. In acetylene flame, acetylene and other small species such as vinyl radicals ( $C_2H_3$ ) exist in high concentration and can contribute significantly to PAHs formation process.

### **2.3.2. Soot particles nucleation**

The soot particles inception step is probably the least understood of all as the transition from gas-phase to solid phase still remains unclear. It could be defined as the transition from gaseous hydrocarbons to macromolecular building blocks [56] (nanoparticles with a mass around 1000-2000 uma and an effective diameter of about 1.5 nm) that turn probably into soot. The combustion conditions (high temperatures and large pools of radicals) make this process very complex. Stein and Fahr [57] have found that heavy PAHs are stable enough at flame temperatures, and the majority consensus on soot particle inception is that the soot particle form via PAHs dimerization. Base on thermodynamic consideration, Wang [8] suggested that PAHs as big as coronene ( $C_{24}H_{12}$ ) dimer cannot be stable in flame at temperature higher than 700 K, since the entropic contribution to free energy tears the dimer apart. From his assumptions, only PAHs as big as circumcoronene ( $C_{54}H_{18}$ ) dimer might remain stable but not at temperature higher than 1600 K. However, since flame temperature can reach 2000 K or more, the nature or the exact stable structures involved in the soot nucleation mechanism remain unclear. The present work aims to discuss the PAHs molecules that could potentially be involved in this process.

### **2.3.3. Mass growth of soot particles**

The mass of nascent soot is increased via the addition of gas phase species such as acetylene ( $C_2H_2$ +soot contributes to surface growth) and PAHs (PAH+soot contributes to condensation) and the collisions between solid particles (soot+soot contributes to coagulation) which significantly increase the particles size and decrease particles number as they merge. For the surface growth, H-atom abstraction from soot surface leads to an active site creation (radical site), which further reacts with a

gaseous species such as acetylene. Soot surface activity decreases when H-atom concentration decreases (limiting active sites production) or due to surface defects causing active sites deactivation [58,59]. By considering soot particles as spherical before and after coagulation, equations governing soot mass growth such as Smoluchowski equation [60] are implemented in most of soot models.

#### **2.3.4. Oxidation of PAHs and soot particles**

The oxidation of PAHs and soot leads to mass loss by elimination of CO and CO<sub>2</sub> molecules. This process may compete with the formation of PAH and soot. The main oxidation reactants are found to be OH, O and O<sub>2</sub>. In fuel-rich conditions, OH is the main oxidation reactant while O<sub>2</sub> is the main reactant in the case of fuel-lean conditions. However, due to the low temperature effect, the rate of oxidation process is not sufficient to lead to the consumption of all soot particles.

#### **2.3.5. Aggregation of soot particles**

Soot particles agglomeration starts when their growth is finished. The resulting particles called mature soot, agglomerate to form a long chain structure.

Soot formation process has received much attention from several research groups and many studies have been performed to better understand the inception step. A lot of operating parameters (fuel type, global and local equivalence ratio, temperature and pressure) have to be taken into account to get a full insight about soot inception. Thus, the good understanding of chemical reactions network in fuel combustion could be a crucial way to increase our knowledge on soot and PAHs formation and to predict soot properties (reactivity) from parent fuel. This support can be offered by computational simulation which allows a critical testing of chemical reaction networks.

### **2.4. Soot nucleation mechanisms**

Soot nucleation mechanism remains poorly understood due to its very fast reaction rate constant and the lack of detailed experimental data. However, three nucleation pathways have been postulated in the literature but they are still much debated. Figure 20 shows a representation of the proposed nucleation mechanisms, indicating the ratio carbon to hydrogen (C/H), the nucleation mechanism type (A, B or C) and the proponent of the mechanism. In addition, all these three different conceptual pathways consider PAHs molecules as soot particle precursors, which is a common point of view within combustion chemistry community.

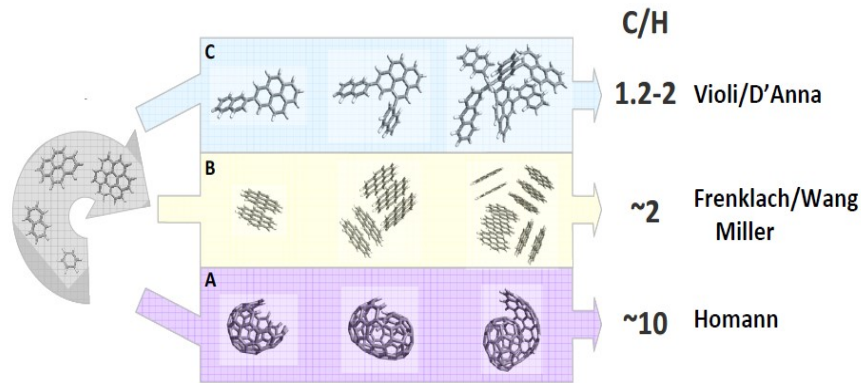


Figure 20 : Postulated soot nucleation mechanisms.

As depicted in Figure 20, paths A, B and C are described as follows:

**Path A:** proposed by Homann [61], it is represented by the growth of two-dimensional PAHs into fullerene-like structures (curved). This soot particle nucleation mechanism type is ruled out since it leads to a mono-modal particle distribution function while experimental findings showed a bimodal particle distribution function, as depicted in Figure 21. Moreover, it seems too slow to account for rates observed for soot nucleation. Consequently, this mechanism may not be a plausible pathway since experimental data are not reproduced by this mechanism alone.

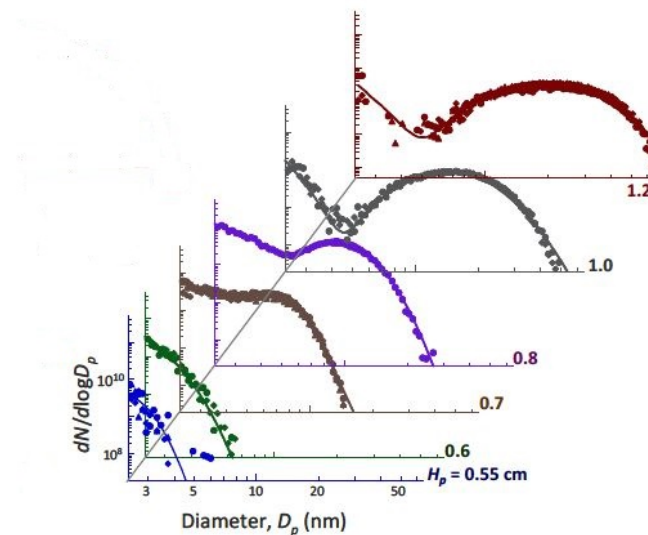


Figure 21 : Detailed particle Distribution Function in ethylene flame ( $C_2H_4/O_2/Ar$   $\phi = 2.1$ ) [8], where  $H_p$  is the height above the burner.

**Path B:** proposed by Frenklach and coworkers [62], this mechanism involves the physical coalescence of PAH molecules into stacked clusters. However, the nature of PAHs molecules that are widely involved in the soot nucleation process remains unclear. Moreover, the binding energies and number of stacked PAH molecules that could lead to soot particle are poorly understood. Path B seems to be

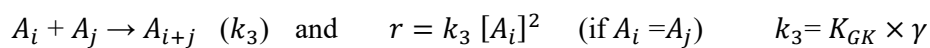


plausible at low temperature conditions because physical coalescence is favored, so, PAHs molecules can collide to form particles. However, under high temperature conditions, the mechanism is not found plausible since high temperature conditions do not favor stacking because of sticking efficiency of PAH molecules decreases with temperature rising. Consequently, this mechanism might be plausible at low temperature conditions but not important at high temperature conditions. Since soot particles are also formed under high temperature conditions, Path B cannot exclusively accounts for nucleation and complementary mechanisms should exist. An alternative mechanism (path C) combined with path B has been proposed by Violi and D'Anna [63].

**Path C:** proposed by Violi and D'Anna [63] path C involves the chemical coalescence or reaction of PAHs molecules into crosslinked three-dimensional structure. The authors found this mechanism to be important at high temperature conditions since a large amount of radical species favoring chemical coalescence are formed. Authors have evaluated in detail the importance of paths B and C (physical growth and chemical growth respectively). They concluded that path B or physical growth is favored at lower temperature and lower radical concentrations while path C or chemical growth is favored at higher temperature and higher radical concentrations.

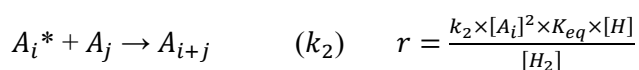
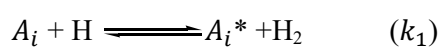
They described paths B and C as follows:

-Path B: physical coalescence:



Where  $A_i$  and  $A_j$  represent the colliding PAHs molecules,  $r$  is the physical rate of nucleation process,  $k_3$  is the reaction rate constant,  $[A_i]$  is the concentration of PAH molecule,  $K_{GK}$  is the gas collision constant and  $\gamma$  is the sticking efficiency. One can note that  $k_3$  is a function of  $K_{GK}$  and  $\gamma$  that depend on temperature and also the rate constant of a non-reversible reaction that leads to soot particles. As the temperature increases,  $\gamma$  decreases and consequently, the physical growth might be neglected (since  $k_3$  decreases) with respect to the chemical coalescence.

-Path C: chemical coalescence:



Where  $A_i$  and  $A_j$  represent PAHs molecules,  $A_i^*$  is the radical formed from  $A_i$  by hydrogen abstraction,  $k_1$  and  $k_2$  are rate constants of reactions,  $K_{eq}$  is the equilibrium constant of reaction that forms  $A_i^*$ ,  $[H]$  and  $[H_2]$  are concentrations of hydrogen and molecular hydrogen respectively and  $r$  is the chemical rate of nucleation process. One can note that  $k_2$  is the rate constant of a non-reversible reaction that leads to soot particle and follows Arrhenius formulation. The higher temperature, the higher  $k_2$  and the chemical coalescence may become the major pathway to explain soot particle nucleation at high temperature.

## **2.5. Soot models**

Soot formation modeling is a challenging task that is not yet fully successful, especially soot inception process that remains unclear. In the current EURO 6 regulation, limit on particles number and size must be defined from combustion devices mainly for land vehicles. Soot models must be capable of accurately predicting soot particles number and their size. An accurate prediction of soot formation should enable optimization of combustion processes and combustion devices design for lowering soot emissions.

The models proposed fall into two categories. The first ones are based on the predicted soot yield by using one or several empirical parameters such as equivalence ratio and the temperature of the flame. The second ones are based on the detailed kinetic modeling of flame structures. Both models are described as following:

### **2.5.1. Empirical models**

Empirical models are widely used in automotive field. They correlate soot production with operating conditions. There are several empirical or semi-empirical models used to predict soot formation and references [64–66] give some examples of those frequently encountered in the literature. Typically, a critical equivalence ratio ( $\phi_c$ ) is measured to determine a general fuel sooting tendency. Fuels that exhibit high  $\phi_c$  have low tendency to form soot. Takahashi et al. [67] show that sooting tendency seems depending on C/H ratio and the number of carbons instead of fuel structure. In the case of premixed flame and constant temperature, authors showed that the logarithm of the critical sooting equivalence ratio linearly decreases with the number of C-C bond in hydrocarbon fuels. A double and a triple CC bond counts for two and three C-C bonds, respectively. Based on these observations and

comparing for example, benzene and toluene, benzene has lower sooting tendency than toluene. In the case of diffusion flames, the sooting tendency of a hydrocarbon is traditionally characterized by the smoke height  $H$ , which is the height of that hydrocarbon jet flame at the smoke point. These smoke heights measured in a particular setup may be converted into setup-independent threshold sooting index (TSI), by the following equation:

$$\text{TSI} = A \cdot \frac{\text{MW}_i}{H} + B \quad \text{Equation 6}$$

Where  $\text{MW}_i$  is the molecular weight of the hydrocarbon and  $A$  and  $B$  are apparatus specific constants. For example, TSI of ethane is found to be 0, contrary to that of naphthalene, which equals to 100. These TSI have been measured by McEnally and Pfefferle [68] for around 100 hydrocarbons, and a quantitative relationship between TSI and molecular structure has been derived, allowing to predict the TSI for some other hydrocarbons. Since the  $H$  parameter depends inversely on sooting tendency, it is small and difficult to measure it precisely for heavily sooting hydrocarbons, such as aromatics. As a result, McEnally and Pfefferle have established a new expression for measuring sooting tendency: the maximum soot volume fraction ( $f_{v,\text{max}}$ ) measured on the centerline of a co-flow and non-premixed flame of methane/air, whose fuel is doped with 400 ppm of the test hydrocarbon. Similarly to smoke points, these soot volume fractions can be converted into apparatus-independent yield sooting indexes (YSI) by the equation:

$$\text{YSI} = C \cdot f_{v,\text{max}} + D \quad \text{Equation 7}$$

Where  $C$  and  $D$  are apparatus specific parameters. According to measurements performed by McEnally and Pfefferle, benzene has a YSI of 30, toluene has a YSI = 43.5, n-propylbenzene has a YSI = 55.9 and naphthalene has a YSI = 100. These results are consistent with the findings of Takahashi et al. [67]. In addition, authors showed that compounds having similar C/H ratios and identical total C atom number may have highly different YSI, demonstrating that the fuel structure may play a role in soot formation.

### 2.5.2. Kinetic models

Authors of these models have developed detailed kinetic models that are able to predict soot concentration in hydrocarbons flames based on their predicted flames structures. The methods widely used for solving the soot population balance are: method of moments and sectional method. The input

of these models is a detailed gas-phase chemical kinetic model that includes chemical species to consider for soot modeling. Therefore, gas-phase is differentiated from the solid phase in these models.

#### **2.5.2.1. Method of moments**

Developed by Frenklach and coworkers [11,69], the most efficient computationally numerical approach is the method of moments. This method only gives mean properties (number, diameter and mass) of all soot particle populations. It describes particles system evolution via mass or particle dimensions distribution function moments. In general, the knowledge of the three first distribution function moments is needed to calculate the main characteristics of particles population, namely the total number of soot particle, their mean mass, their mean diameter or their total equivalent spherical area. A mathematical details associated with the determination of moments can be found in the work of Frenklach et al. [70,71].

#### **2.5.2.2. Sectional method**

Developed by Howard and coworkers [72,73] and D'Anna and Kent [74], the sectional approach gathers gas-phase and aerosol chemistry into a unique kinetic model. In this method, particle populations are divided into particle size classes called sections, which allows a detailed representation of particle size distribution. A sectional soot method requires a minimum number of sections due to the long calculation time since more precisions are obtained. Therefore, the method of moments is a very simple method that does not require long calculation time since general information is given on soot particles population. Sectional soot method is adopted in the present work and details on governing equations as well as the methodology used to describe particles evolution are presented in Chapter 3.

### **2.6. Conclusions**

In this chapter, we investigated potential soot precursors considered in previous soot models. Most of the soot models focused on pyrene dimerization and considered as relevant for particle nucleation modeling. However, several studies rule out this possibility based on thermodynamics calculations [8,14,15]. While PAH molecules are accepted as soot precursors within combustion community, the nature of those involved in the particles inception step raises many questions and remains still

ambiguous. Due to experimental findings limitations, numerical simulations are employed for such investigations.

A promising particle nucleation modeling might be the heteromolecular dimerization of PAH molecules [31], which implies at least two reactants that have different chemical structure. Only few studies addressed this option. Among different proposals of particles nucleation mechanism, most of previous investigations focused on collisional phenomena, i.e collisions between PAH molecules that lead to soot nuclei.

For a better prediction of soot particle formation, a good knowledge of PAHs chemistry network is required. It was observed that PAHs formation paths vary as a function of fuels. Several pathways leading to aromatics species formation have been highlighted from different configurations and experimental conditions. This intertwining of chemical pathways makes the understanding of PAHs chemistry very difficult and must be carefully examined.

In the present work, we aim to develop a detailed chemical kinetic mechanism that describes accurately laboratory as well as liquid transportation fuels combustion, including both low and high temperature reactions and to integrate a large pool of PAH molecules (up to coronene). Soot particles nucleation is modeled by physical agglomeration pathway (collisional phenomena) between PAH molecules. Both homomolecular and heteromolecular dimerizations are considered and investigated for particles inception modeling. Details on the soot sectional model used [75] in this work are presented in Chapter 3.



## Chapter 3: Modeling Tools and Methods

### 3.1. One dimensional premixed laminar flames: governing equations

In the case of a laminar and premixed one dimensional flat flame stabilized on a burner, the properties depend on coordinate  $z$ , which is the height above the burner surface and perpendicular to the burner surface. The evolution along  $z$  axis of the temperature and mole fractions of chemical species is referred to as the flame structure. The typical structure of a one dimensional, premixed laminar flame consists of three main zones, as depicted in Figure 22.

- The zone 1: represents the preheating zone, where the fresh mixture is present.
- The zone 2: represents the flame front where the radical or intermediate species are present. The combustion took place in this zone, where heat transfer and consumption rates of reactants reach their peaks. From chemical point of view, the flame front zone is the most important zone to analyze.
- The zone 3: represents the zone of burnt gases, where the combustion products are found.

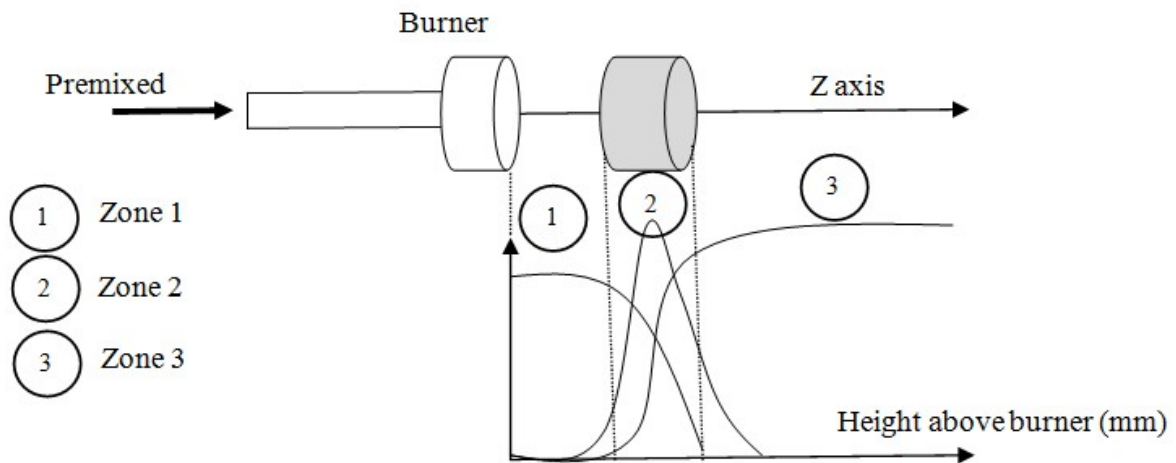


Figure 22 : Structure of a one dimensional premixed laminar flame stabilized on a burner.

For laminar one-dimensional premixed flames, the species conservation equation can be simplified as follows: for  $k^{\text{th}}$  species ( $k \in \{1, \dots, N - 1\}$ )

$$\frac{\partial \rho Y_k}{\partial t} + \frac{\partial}{\partial z} (\rho(\mathbf{u} + \mathbf{V}_k)Y_k) = \dot{\omega}_k \quad \text{Equation 8}$$

Where  $Y_k$  denotes the mass fraction,  $u$  the reacting flow velocity,  $V_k$  the diffusion velocity and  $\dot{\omega}_k$  the volume specific mass source term due to reactions.

Considering a chemical system of  $N$  species reacting through  $M$  reactions, the mass reaction rate  $\dot{\omega}_k$  for species  $k$  is the sum of rates  $\dot{\omega}_{kj}$  produced by all  $M$  reactions.

$$\dot{\omega}_k = \sum_{j=1}^M \dot{\omega}_{kj} = W_k \sum_{j=1}^M v_{kj} Q_j \quad \text{Equation 9}$$

Where  $W_k$  is the atomic weight of species  $k$ ,  $v_{kj}$  is defined as  $v_{kj} = v''_{kj} - v'_{kj}$  and  $v''_{kj}, v'_{kj}$  are the stoichiometric coefficients of species  $k$  in reaction  $j$ .  $Q_j$  is the rate of progress of reaction  $j$  and can be rewritten as follows:

$$Q_j = k_{dir,j} \prod_{k=1}^N [X_k]^{v'_{kj}} - k_{rev,j} \prod_{k=1}^N [X_k]^{v''_{kj}} \quad \text{Equation 10}$$

Where  $[X_k]$  is the molar concentration of species  $k$ .  $k_{dir}$  and  $k_{rev}$  are respectively the forward and reverse rates of reaction  $j$  and they are modeled using the Arrhenius formalism as describes in Appendix A.

The diffusion coefficient  $D_i^M$  of species  $i$  into the mixture of the other species is defined as

$$D_i^M = \frac{1-Y_i}{\sum_{j \neq i} \frac{x_j}{D_{ij}}}, \quad Y_i \text{ is the mass fraction of species } i, D_{ij} \text{ the multicomponent diffusion coefficients, } x_j$$

the mole fractions of species  $j$ .

### 3.2. The 1D premixed flame code

The kinetic code allows the use of a detailed description of gas-phase chemistry that includes several species and reactions. As presented above, a chemically reacting flow can be described in time and space by its pressure  $P$ , its temperature  $T$ , its velocity  $u$  and the density  $\rho_i$  of each species that it contains. For all of our flame structure calculations, the pressure  $P$  is constant. Considering that the density  $\rho_i$  of each of the  $N$  chemical species constituting the flame is giving by the product of its mass fraction  $Y_k$  with the total density  $\rho$ ,  $N + 2$  variables remain unknown:  $Y_k, Y_{k+1} \dots Y_{N-1}, T, u$  and  $\rho$ .

At each distance of the burner surface, the  $N + 2$  unknown variables are determined by the kinetic solver using the conservation equations, based on a chemical kinetic model, thermodynamic and transport data of involved compounds and the boundary conditions of the flame. If a flame



temperature profile is provided from experiment, calculations can be performed without solving the energy conservation equation. In this case, only the species transport equations are solved. The general principle of the kinetic code for a premixed laminar one dimensional flame stabilized on a burner is depicted in Figure 23. The system of equations is determined first on the basis of input data and conservation equations. Secondly, the system of equations is solved using Newton's method. This one determines a sequence of iterations or appropriate solutions that approach the true solution. In case of convergence difficulties, transient equations are solved using backward Euler method. The convergence level can be adjusted and considerably affects the calculation time. The quality of the initial guess, the size of the chemical kinetic model and the number of involved chemical species also affect the calculation time. When the solver succeeds to converge, an output file is written with the calculated flame structure.

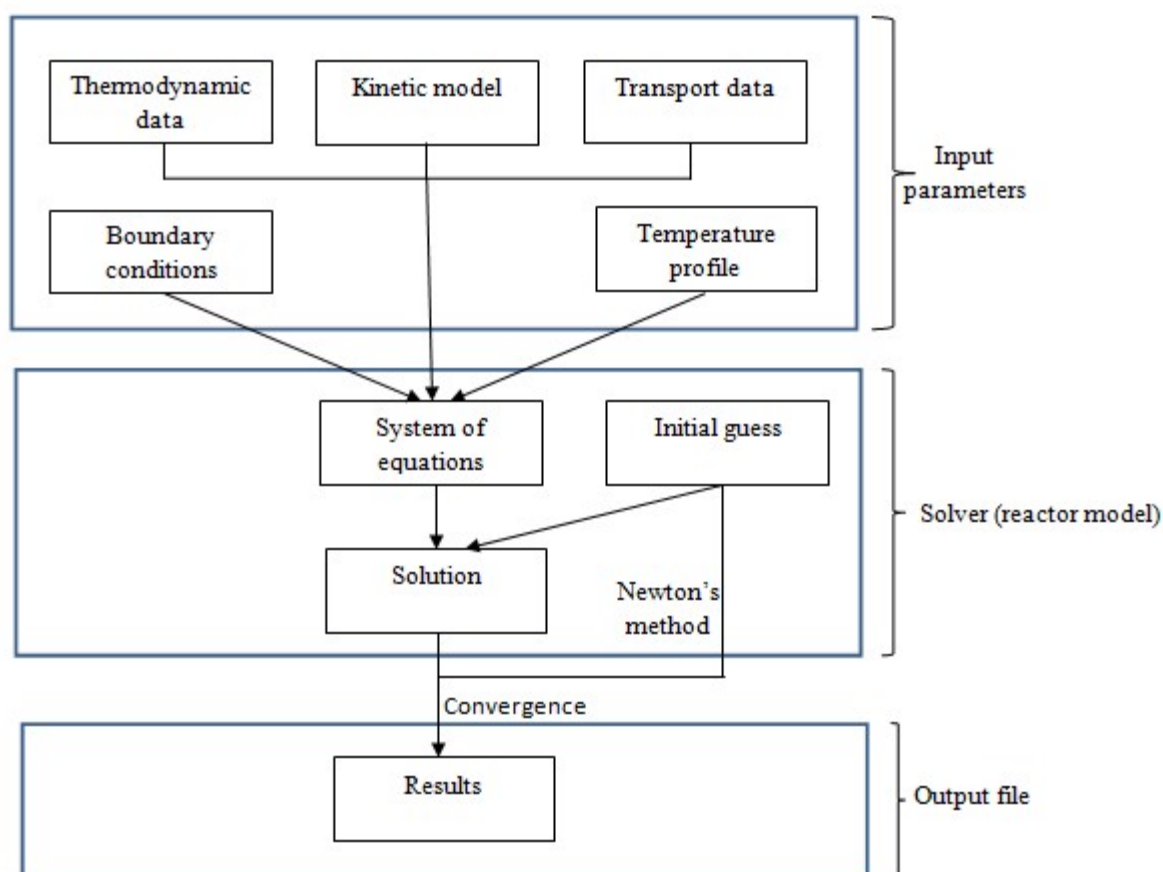


Figure 23 : General functioning structure of the kinetic solver for a premixed laminar one dimensional flame stabilized on a burner. This kinetic solver generates chemical species concentration profiles, rates of production or of consumption, species sensitivity analysis, laminar flame speed, etc. The thermokinetic and transport formalism used in the reactor model are presented in Appendix A.

Kinetic modeling was performed with the PREMIX and AURORA libraries of Chemkin-PRO package, version 1.5.1.3.1 [76]. Cantera software [77] was used for soot calculations. As the latter software has similar operating conditions with Chemkin PRO, only Chemkin general functioning is presented. For all premixed flames calculations, gradient and curvature criteria for mesh refinement were set both to 0.2 and a mixture-averaged transport approach was used as the full multi-component formulation was computationally too intensive for the present mechanism.

### 3.3. Sensitivity analysis

Sensitivity analysis is a tool that helps to understand quantitatively how the solution to a model depends on parameters in the model and also helps to interpret the results from a model. Sensitivity can be calculated from species mass fraction to rate constants. Thus, a sensitivity coefficient for species  $j$  for a reaction  $i$  is expressed as follows:

$$S_{j,i} = \frac{\partial \ln Y_j}{\partial \ln k_i} = \frac{k_i}{Y_j} \frac{\partial Y_j}{\partial k_i} \quad \text{Equation 11}$$

Where  $k_i$  is the rate constant of reaction  $i$ ,  $Y_j$  the mass fraction of species  $j$ . As a result, a positive sensitivity coefficient means that the concentration of species  $j$  increases with the rate constant  $k_i$ . A negative sensitivity coefficient indicates that the concentration of species  $j$  decreases when the rate constant  $k_i$  increases.

### 3.4. Rate of production analysis

This analysis determines the contribution of each reaction  $i$  to the formation or the consumption of species  $j$ . The total rate of production  $r_{f,j}$  and total rate of consumption  $r_{c,j}$  for species  $j$  from all the  $N$  reactions in the mechanism are expressed as follows:

$$r_{f,j} = \sum_{i=1}^N r_{f,j,i} \quad (\text{Total rate of production}) \quad \text{Equation 12}$$

$$r_{c,j} = \sum_{i=1}^N r_{c,j,i} \quad (\text{Total rate of consumption}) \quad \text{Equation 13}$$

The rate of production  $ROP_{f,j}$  and the rate of consumption  $ROC_{f,j}$  for a reaction  $i$  are defined as follows:

$$ROP_{f,j} = \frac{r_{f,j,i}}{r_{f,j}} \quad (\text{rate of production}) \quad \text{Equation 14}$$

$$ROC_{f,j} = \frac{r_{c,j,i}}{r_{f,j}} \quad (\text{rate of consumption}) \quad \text{Equation 15}$$

### 3.5. Sectional Soot Method

The sectional soot modeling approach has been briefly introduced previously. In this section, a description of the soot model used in the present study is given. Modeling of soot particles formation is a challenging task that is not yet fully known. Soot models must be capable of accurately predicting the number and size of particles emitted. Firstly, an accurate prediction of soot particles emissions would facilitate the legislative regulations. Secondly, it will enable optimization of combustion processes and even combustion devices design for lowering emissions of soot particles. Modeling of soot formation implies two main challenges:

- (1) To model accurately the PAHs chemistry that leads to particles nucleation, which processes according to the phenomenological basis through the clustering of PAHs to form soot particles with a size of few nanometers.
- (2) To model particle growth, condensation, coagulation and oxidation-degradation-fragmentation.

The present work is mainly focused on the particles nucleation step, as it is poorly understood and is the very beginning of mature soot formation. We aimed to consider a large pool of PAHs with different structure, in order to point out those widely involved in the particle nucleation step. This service can be performed by sectional approach and the main governing equations of the soot model are described in the next sections.

#### 3.5.1. Governing equations and variables in the model

The soot sectional model used in the present work considers that soot particles are solid and modeled as a distinct disperse phase, interacting with the gaseous phase. This soot model is based on the previous work of Netzell and coworkers [78] and Aubagnac-Karkar et al. [75,79,80], where investigation on development and application of detailed kinetic models for the soot particle size distribution function has been carried out.

Considering a turbulent reactive flow, the soot particles population is evaluated by using a sectional approach, or otherwise, the soot particles are separated with respect to their volume into discrete sections. In each section  $i$ , representing the soot particles of a given volume range, the standard transformation equation for the soot mass fraction  $\tilde{Y}_{soot,i}$  is governed as follows:

$$\frac{\partial \bar{\rho} \tilde{Y}_{soot,i}}{\partial t} + \nabla \cdot (\bar{\rho} \tilde{u} \tilde{Y}_{soot,i}) = \nabla \cdot (\bar{\rho} D_{t,soot} \nabla \tilde{Y}_{soot,i}) + \bar{\rho} \tilde{\omega}_{soot,i} \quad \text{Equation 16}$$

Where  $\bar{\rho}$  is the gas-phase density,  $\tilde{u}$  the gas velocity,  $D_{t,soot}$  the turbulent diffusion coefficient of soot and  $\tilde{\omega}_{soot,i}$  the soot source term in section  $i$ .

A detailed representation of the phenomena involved in the soot formation process can be depicted in Figure 24.

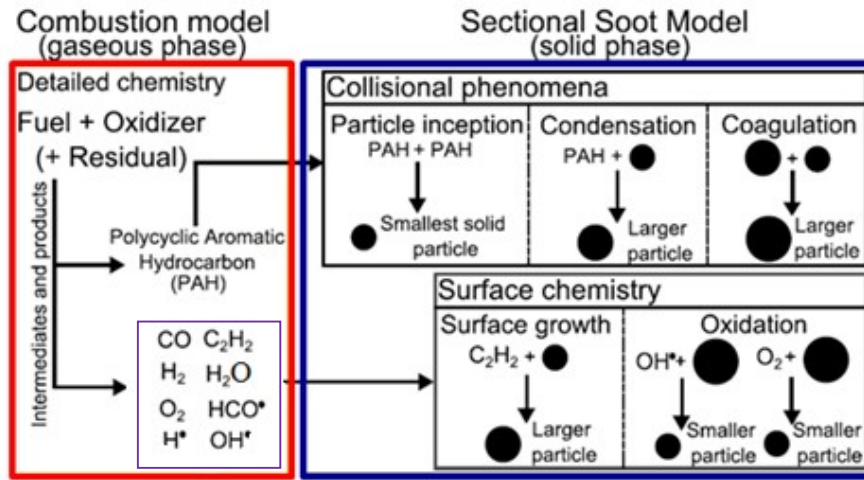


Figure 24 : Soot particles formation and evolution process in the model [75].

Two main stages are described in the model: the collisional phenomena and the surface chemistry.

- The collisional phenomena include particle inception from gaseous species (PAHs) to generate the smallest solid particle or nuclei. Condensation describes the collision of the nuclei with gaseous species to form larger particle. Coagulation describes collision between solid particles to form larger particle and more dense.
- The surface chemistry model includes the particles surface growth that describes the particle growth by chemical reactions such as a gaseous species (acetylene) reaction with soot solid particle. The oxidation reactions aimed to reduce considerably the soot particles size to form smaller particles.

### 3.5.2. Volume discretization

A fixed interval of volume range  $[V_{min}; V_{max}]$  is divided into  $n$  sections.  $V_{min}$  indicates the smallest considered particles and is defined as the carbon equivalent volume of the carbon atoms number of

soot precursors (the colliding PAHs). Carbon equivalent volume for two carbon atoms can be expressed as follows:

$$V_{C_2} = \frac{2M_C}{N_A \rho_{soot}} \quad \text{Equation 17}$$

Where  $M_C$  represents the carbon molar mass,  $N_A$  is Avogadro's number and  $\rho_{soot}$  is the soot density assumed constant and equal to  $1.86 \times 10^{-3} \text{ kg.m}^{-3}$  [78].

Considering two soot precursors containing  $n$  atoms of carbon ( $C_n H_m$ ),  $V_{min}$  is equal to  $n \cdot V_{C_2}$  and all hydrogen atoms taken from the gas phase are sent to  $H_2$  to close the hydrogen balance since all volumes exchanged between phases are given with respect to the exchanged of carbon atoms number. The largest particles diameter  $d_{max}$  is set to  $50\mu\text{m}$  (sphere diameter), to ensure that carbon mass will not be accumulated in the last section.

The soot particles volume in the first section ranges from  $V_{min}$  to  $V_{min} + V_{C_2}$ . Concerning the following sections, particles volume is defined as follows:

$$V_{max,i} = (V_{min} + V_{C_2}) \left( \frac{V_{max}}{V_{min} + V_{C_2}} \right)^{(i-1)/(n_{sections}-1)} \quad \forall i \in \llbracket 2; n_{sections} \rrbracket \quad \text{Equation 18}$$

Based on the computational calculation time, the number of sections is often set to 30 and could be extended to 100 [75], which requires more calculation time. In the present work, all simulations have been performed with 70 sections.

### 3.5.3. Soot particles volume number in a section $i$

The soot volume fraction  $Q_i$  is defined as the soot particles volume in a section  $i$  normalized by the total volume gas and solid phases. Considering that the volume of all soot particles is negligible with respect to the volume of the gas,  $Q_i$  can be written as a function its mass fraction  $\tilde{Y}_{soot,i}$  in Equation 19.

$$Q_i = \frac{\bar{\rho}}{\rho_{soot}} \tilde{Y}_{soot,i} \quad \text{Equation 19}$$

The soot mass fraction source term  $\tilde{\omega}_{soot,i}$  is expressed as follows:

$$\tilde{\omega}_{soot,i} = \frac{\rho_{soot}}{\bar{\rho}} \dot{Q}_i = \frac{\rho_{soot}}{\bar{\rho}} (\dot{Q}_{nucl,i} + \dot{Q}_{cond,i} + \dot{Q}_{sg,i} + \dot{Q}_{ox,i} + \dot{Q}_{coag,i}) \quad \text{Equation 20}$$

Where  $\dot{Q}_{nucl,i}$ ,  $\dot{Q}_{cond,i}$ ,  $\dot{Q}_{sg,i}$ ,  $\dot{Q}_{ox,i}$ ,  $\dot{Q}_{coag,i}$  represent respectively the volume fraction source terms in section  $i$  due to nucleation, condensation, surface growth, oxidation and coagulation.

The soot volume fraction density  $q_i$  in each section  $i$  is given by:

$$q_i = \frac{Q_i}{V_{max,i} - V_{min,i}} \quad \text{Equation 21}$$

Thus, the particle number density  $n_i(v)$  is expressed as follows:

$$n_i(v) = \frac{q_i}{v} \quad \forall v \in [V_{min,i}; V_{max,i}] \quad \text{Equation 22}$$

And then, the soot particles volume number  $N_i$  in a section  $i$  is given by:

$$N_i = \int_{V_{min,i}}^{V_{max,i}} n_i(v) dv = \frac{Q_i}{V_{max,i} - V_{min,i}} \ln \left( \frac{V_{max,i}}{V_{min,i}} \right) \quad \text{Equation 23}$$

$N_i$  allows to calculate finally the Soot Number Density Function (SNDF) in each section  $i$ , at each time and each position.

#### 3.5.4. Collisional source terms

Smoluchowski equation, introduced briefly in chapter 1 is the one that describes collisional phenomena (particle inception, condensation and coagulation). It is expressed in the continuous form as follows:

$$\dot{F}_a(t) = \frac{1}{2} \int_0^a \beta_{a-b,b} F_b(t) F_{a-b}(t) db - \int_0^\infty \beta_{a,b} F_a(t) F_b(t) db \quad \text{Equation 24}$$

Where  $F_x(t)$  is the number of particles of size  $x$ ,  $\dot{F}_x(t)$  is its variation rate and  $\beta_{x,y}$  is the collision frequency between particles of size  $x$  and size  $y$ . This latter is obtained from the theory of aerosol science by Kazakov and Frenklach [81]. Depending on regime applied that in turn depends on Knudsen number value  $k_n$ , collision frequencies can be evaluated.

$$k_n = \frac{\gamma_{gas}}{d} \quad \text{Equation 25}$$

Where  $\gamma_{gas}$  is the gas mean free path,  $d$  is the particle diameter.

The regime considered in this model is that of free molecular collision and collision frequencies are expressed as in [81].

### 3.5.5. Inception and condensation

Particle inception involves collision between two soot precursors (two PAHs) to generate the nuclei or smallest particle, while condensation involves collision between a soot precursor (one PAH) and soot solid particle. Considering the volume number of PAHs,  $N_{PAH}$ , the rate of volume fraction variation  $\dot{Q}_{nucl}$  of the smallest soot given by Smulochwski equation Equation 24 combined with Equation 21 and Equation 22.

$$\dot{Q}_{nucl} = \frac{1}{2} V_{PAH} \beta_{PAH,PAH}^{fm} N_{PAH}^2 \quad \text{Equation 26}$$

Where  $V_{PAH}$  is the volume of one PAH (soot precursor containing  $n$  atoms of carbon) and  $\beta_{PAH,PAH}^{fm}$  is the collision frequency in free molecular regime between two PAHs.

The collision frequency can be linked to the collision efficiency through the following expression [27]:

$$\beta_{PAH,PAH}^{fm} = C_E \times \sigma_{PAH,PAH} \sqrt{\frac{8k_B T}{\pi \mu_{PAH,PAH}}} \quad \text{Equation 27}$$

Where  $C_E$  is the collision efficiency,  $\sigma_{PAH,PAH}$  is the reaction cross section between PAHs and  $\mu_{PAH,PAH}$  is the reduced mass of PAHs.

As a result, the global volume amount of precursors that collide with all soot particles per unit time

$\dot{Q}_{cond}^{PAH}$  is given by:

$$\dot{Q}_{cond}^{PAH} = V_{PAH} N_{PAH} \sum_{i=1}^{i_{max}} \beta_{PAH,i}^{fm} \int_{V_{min,i}}^{V_{max,i}} n_i(v) dv \quad \text{Equation 28}$$

Where  $\beta_{PAH,i}^{fm}$  is the collision frequency between precursors and soot solid particles of section  $i$ .

The volume number of PAH ( $N_{PAH}$ ) is determined based on steady state assumption between PAH formation reaction and PAH consumption by the two collision phenomena (nucleation and condensation) in all sections. Then, the volume fraction reaction rate of PAH is given as follows:

$$r_{PAH} = 2V_{PAH} \beta_{PAH,PAH}^{fm} N_{PAH}^2 + \left( V_{PAH} \sum_{i=1}^{i_{max}} \beta_{PAH,i}^{fm} \int_{V_{min,i}}^{V_{max,i}} n_i(v) dv \right) N_{PAH} \quad \text{Equation 29}$$

By solving this polynomial equation, the positive root gives  $N_{PAH}$  expression and is found to be:

$$N_{PAH} = \frac{-k_{cond} + \sqrt{k_{cond}^2 + 4r_{PAH}k_{nucl}}}{2k_{nucl}} \quad \text{Equation 30}$$

Where  $k_{nucl} = 2V_{PAH} \beta_{PAH,PAH}^{fm}$ ,  $k_{cond} = V_{PAH} \sum_{i=1}^{i_{max}} \beta_{PAH,i}^{fm} \int_{V_{min,i}}^{V_{max,i}} n_i(v) dv$ .

It is worth nothing that the particle inception rate is given by (Equation 26) and equal to  $k_{nucl}$ . The condensation rates cannot directly be deduced from (Equation 28) since the volume fraction computed represents the global volume fraction transferred from gas phase to solid phase. Details on post nucleation processes including condensation and coagulation and their associated rates are described in [75].

### 3.5.6. Surface chemistry

The surface growth and oxidation of soot is described consistently with the gas-phase kinetics. The surface growth is implemented using HACA mechanism [11] and through PAH condensation. The gaseous species involved in the present surface chemistry are: H, H<sub>2</sub>, O<sub>2</sub>, OH, H<sub>2</sub>O, CO, HCO and C<sub>2</sub>H<sub>2</sub>. The surface reactions implemented in the soot model are describes in Table 2:

Reactions	$k = AT^n \exp\left(-\frac{E_a}{RT}\right)$		
	A (cm <sup>3</sup> .mol <sup>-1</sup> .s <sup>-1</sup> )	n	E (kcal.mol <sup>-1</sup> )
$C_{soot} + H \rightarrow C_{soot}^* + H_2$	$4.2 \times 10^{13}$	0.0	13.0
$C_{soot}^* + H_2 \rightarrow C_{soot} + H$	$3.9 \times 10^{12}$	0.0	11
$C_{soot} + OH \rightarrow C_{soot}^* + H_2O$	$1.0 \times 10^{10}$	0.734	1.43
$C_{soot}^* + H_2O \rightarrow C_{soot} + OH$	$3.68 \times 10^{08}$	1.139	17.1
$C_{soot}^* + H \rightarrow C_{soot}$	$2.0 \times 10^{13}$	0.0	0.0
$C_{soot}^* + C_2H_2 \rightarrow C_{soot} + H$	$8.0 \times 10^7$	1.56	3.8
$C_{soot}^* + O_2 \rightarrow C_{soot} + 2 CO$	$2.2 \times 10^{12}$	0.0	7.5
$C_{soot} + OH \leftrightarrow C_{soot}^* + HCO$	$1.62 \times 10^{11}$	0.50	0.0

Table 2 : Surface chemistry mechanism [11].

The kinetics of surface reactions is described in term of surface sites. These sites are carbon atoms saturated with hydrogen (C-H) or dehydrogenated (C\*).



### 3.5.7. Surface growth

The surface growth is described by the gaseous acetylene ( $C_2H_2$ ) addition to soot particles. The volume fraction rate of soot particles in section  $i$  which grow to move to the next section  $i + 1$  is expressed as follows:

$$\dot{Q}_{SG,i}^{out} = N_A K_{SG,i} \int_{V_{max,i}-V_{C_2}}^{V_{max,i}} (v + V_{C_2}) \frac{1}{v} \left( \frac{v}{V_{C_2}} \right)^{\frac{\theta}{3}} dv \quad \text{Equation 31}$$

Where  $K_{SG,i}$  is the reaction rate of acetylene addition to a soot radical site,  $(v + V_{C_2})$  is the volume of soot particle that increases due to  $C_2H_2$  addition, and  $\frac{1}{v} \left( \frac{v}{V_{C_2}} \right)^{\frac{\theta}{3}}$  denotes the available reaction surface variation depending on the volume.

As a result, the surface growth source terms applied to each section is given as follows:

$$\dot{Q}_{SG,1} = -\dot{Q}_{SG,1}^{out} + \dot{Q}_{SG,1}^{gas} \quad \text{Equation 32}$$

$$\dot{Q}_{SG,i} = \dot{Q}_{SG,i-1}^{out} - \dot{Q}_{SG,i}^{out} + \dot{Q}_{SG,i}^{gas} \quad \forall i \in \llbracket 2; n_{sect} - 1 \rrbracket \quad \text{Equation 33}$$

$$\dot{Q}_{SG,n_{sect}} = \dot{Q}_{SG,n_{sect}}^{out} + \dot{Q}_{SG,n_{sect}}^{gas} \quad \text{Equation 34}$$

### 3.5.8. Oxidation

Soot particles oxidation is described by the reaction of soot with oxygen ( $O_2$ ) or hydroxyl (OH) where carbon atoms are removed from soot particles. This process is similar to that of surface growth but the size of particle is reduced due to carbon removal. The volume fraction rate of soot moved from section  $i$  to section  $i - 1$  is give as follows:

$$\dot{Q}_{OX,i}^{out} = N_A K_{OX,i} \int_{V_{min,i}}^{V_{min,i}+V_{C_2}} (v - V_{C_2}) \frac{1}{v} \left( \frac{v}{V_{C_2}} \right)^{\frac{\theta}{3}} dv \quad \text{Equation 35}$$

Where  $K_{OX,i}$  is the reaction rate of oxygen or hydroxyl with soot particles. The oxidation source terms applied to each section are given by:

$$\dot{Q}_{OX,1} = -\dot{Q}_{OX,2}^{out} + \dot{Q}_{OX,1}^{gas} \quad \text{Equation 36}$$

$$\dot{Q}_{OX,i} = \dot{Q}_{OX,i+1}^{out} - \dot{Q}_{OX,i}^{out} + \dot{Q}_{OX,i}^{gas} \quad \forall i \in \llbracket 2; n_{sect} - 1 \rrbracket \quad \text{Equation 37}$$

$$\dot{Q}_{OX,n_{sect}} = -\dot{Q}_{OX,n_{sect}}^{out} - \dot{Q}_{OX,n_{sect}}^{gas} \quad \text{Equation 38}$$

In addition to the surface growth phenomena, Frenklach and Wang [18] introduced a new parameter  $\alpha$  which is the fraction of surface sites available for reactions.  $\alpha$  was introduced into a kinetic model of

soot surface growth after investigation for chemical alternatives to account for the difference between the low and high temperature flames was exhausted.  $\alpha$  was supposed to quantify the changing morphology of soot particle surface and that change was found to be correlated to the particle surface temperature. As a result, the value given to  $\alpha$  considers the growing surface of soot particles as being composed of graphitic edges that contain sites available for reactions and some parts of the surface are comprised of unreactive basal aromatic planes. Authors clearly claimed this temperature dependency upon parameter  $\alpha$  as their conclusions were later experimentally confirmed by Faeth et al. [82,83] for the post flame region of laminar premixed flames. The established correlations and the values of parameter  $\alpha$  used in previous soot models are describes in the next section.

### 3.5.9. Parameter $\alpha$ : The fraction of soot surface radical sites available for reactions

Due to the scarcity of experimental data,  $\alpha$  was expressed as a constant value in most of soot models [84–86]. Frenklach et al. [87] claimed that parameter  $\alpha$  representing a kind of steric factor decreases with the increase of flame temperature. They concluded that at high temperature, soot particle structural units are expected to be more mobile and align themselves in a more concentric manner, and then, the access of gaseous species to the reactive site on soot particle surface is limited. Authors show that parameter  $\alpha$  significantly decreases with the increase of maximum flame temperature. Figure 25 shows results obtained from their study.

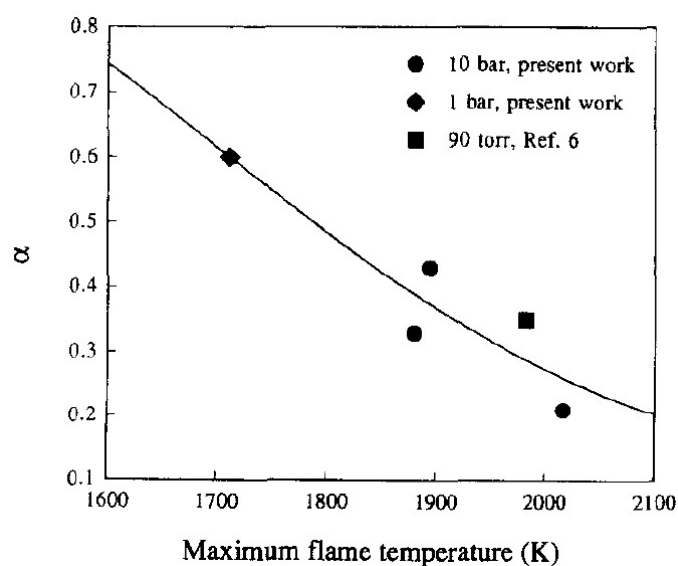


Figure 25 : The fraction of soot surface radical sites available for reaction  $\alpha$  as a function of maximum flame temperature,  $T_{\max}$ . The line is a fit to the data [87].

The correlation established is given as follows:

$$\alpha = \frac{[\tanh(\frac{8168}{T_{max}} - 4.57) + 1]}{2} \quad \text{Equation 39}$$

Numerical calculations show that predictions of soot volume fractions are extremely sensitive to the value of  $\alpha$  considered. A few years later, Appel et al. [11] proposed a correlation that takes into account temperature of soot particles size effects. A critical particle diameter was defined to match the experimentally observed diameters of primary soot particles. The expression proposed by the authors is given as follows:

$$\alpha = \tanh\left(\frac{a}{\log \mu_1} + b\right) \quad \text{Equation 40}$$

Where  $\mu_1$  is the first size moment of the soot particle distribution,  $a$  and  $b$  are the fitted parameters.

Braun-Unkhoff et al. [86] investigated premixed laminar high pressure ethylene flames at different pressure (from 5 to 20 bars) and different equivalence ratios (from 2.04 to 2.76). They showed that the value of parameter  $\alpha$  varies from 0.2 to 0.6. An increase of the  $\alpha$  value was observed by increasing the flame equivalence ratio. However, the pressure dependency was not discussed. Authors performed the  $\alpha$  value variation to match the experimental soot volume fraction measurements. Mouton et al. [85] studied premixed laminar methane flames at low pressure (200 Torr) where a constant value of  $\alpha$  was used. The equivalence ratio of the flames investigated varies from 2.05 to 2.32 and they used constant value for  $\alpha$  0.115 and 0.35 respectively. As a result, the  $\alpha$  value is increased by increasing the equivalence ratio. Chernov et al. [84] used a constant value of 0.15 for parameter  $\alpha$  for both non-premixed ethylene co-flow flame, where good agreement with experiments were obtained. Dworkin et al. [88] investigated laminar co-flow ethylene diffusion flame and used a constant value of 0.078 in their soot model to match experimental data. This value is set to 1.0 if the mechanism of Appel et al. was used. Eaves et al. [89] investigated co-flow ethane-air diffusion flame at different pressures ranging from 2 to 15 atm. Authors concluded that  $\alpha$  value is found to be between 0.055 and 0.067 since the predicted peak soot volume fraction for all flames were within experimental error. Therefore, a constant value of  $\alpha$  found to be 0.061 was adopted since a good agreement with experiments was obtained. In addition, they concluded that no pressure effect on parameter  $\alpha$  was observed over the ranges of pressures simulated (1-15 atm). This conclusion is in line with that of Kim et al. [90] where

experimental investigation on ethylene-air diffusion and premixed flames from 1 to 8 atm did not show any pressure dependency on parameter  $\alpha$ . Consequently, authors claimed that  $\alpha$  value does not need to be altered to predict the trends in peak soot volume fraction as pressure is increased. Aubagnac et al. [75] used a constant value of 0.27 for  $\alpha$  in modeling commercial diesel fuel combustion and in engine conditions. A satisfactory agreement with measurements on soot particles size distribution was obtained.

The parameter  $\alpha$  remains poorly understood since no clear correlation was established. Its ranges have been found to probably change with fuel structure, equivalence ratio, flame temperature or soot particles size. The value of  $\alpha$  is usually determined by fitting experimental data that significantly depends on the chemical kinetic mechanism used.

In the present work, we initially kept constant the value of  $\alpha$  that is set to 0.05 for PAHs homomolecular (mono-precursor) and heteromolecular (multi-precursors) dimerizations. Then, a parametric variation over  $\alpha$  is performed to match experimental data (soot volume fractions and particle diameters) for the investigated laminar premixed methane, ethylene and n-butane flames.

## Chapter 4: Gas-phase Chemistry

### 4.1. Objective

Soot gaseous precursors must accurately be predicted to account for a better understanding of particles inception mechanism. Thus, it is necessary to develop and validate a kinetic model for gas-phase soot precursor formation.

In this chapter, a methodology describing commercial fuel surrogates development as well as a detailed chemical kinetic model development and validation over a wide range of experimental conditions is presented. The availability of experimental and modeling data (thermokinetic, transport) for hydrocarbons combustion can on the one hand, help to formulate surrogate fuels based on two global combustion parameters: cetane number (CN) and threshold sooting index (TSI). On the other hand, detailed kinetic models can be developed. They can also help to analyze with some confidence, the PAHs formation pathways as a function of fuels. The system chosen for the computational investigation of the PAHs formation paths is that of the one dimensional premixed laminar flame configuration.

### 4.2. Surrogate fuels formulation

Due to high complexity of liquid transportation fuels, surrogate fuels composed of few hydrocarbons (from 1 to 12 components) [91] are often used to represent them. To reduce computational time (strongly dependent on the number of species to be transported) and simplify as much as possible the analysis and design of ever more complex engine technologies, combustionists desperately need flexible, simple and reliable chemical surrogate mixtures. As for most of the computational fluid dynamics (CFD) models, evaporation surrogates and chemical surrogates are still distinct, the choice was made to focus on the development of a purely chemical surrogate. A complete physico-chemical surrogate accounts for a number of important targets including H/C ratio, average molecular weight, autoignition quality, heat release rate, extinction, flame adiabatic temperature, sooting behavior, etc. A variety of surrogates formulations were proposed in the literature [92–96] but there is no one that

models liquid transportation fuels with the same three components by varying their respective concentrations as a function of fuel type. The present ternary chemical surrogate does not aim to reproduce volatility nor H/C ratio nor PIONA (n-Paraffin, Iso-paraffin, Olefin, Naphthene, and Aromatic) composition, it was optimized to reproduce CN and TSI parameters accounting for both autoignition and soot production rate. We herein assess the robustness of this approach and PAHs formation during liquid transportation fuels combustion. Yang et al. [97] proposed that two global combustion parameters, namely the derived cetane number (DCN) and the threshold sooting index (TSI), could be considered for formulating a chemical surrogate. Based on these two global parameters, we considered a chemical surrogate for transportation fuels combustion composed of three components: iso-octane, n-decane and n-propylbenzene. The fractions of components in the surrogate mixture are provided in Table 3.

	Diesel surrogate (%vol.)	Jet A-1 surrogate (%vol.)	Gasoline surrogate (%vol.)
n-decane	61.6	53.2	5.0
Iso-octane	0.3	21.6	75.0
n-propyl-benzene	38.1	25.2	20.0

	Diesel	Diesel surrogate	Jet A-1	Jet A-1 surrogate	Gasoline	Gasoline surrogate
CN	49.0	53.7	46.0	48.3	17.0	15.9
TSI	28.0 [98]	26.9	21.4 [99]	20.0	16.0 [98]	17.3

**Table 3 : Surrogate fuels formulation and considered to represent real fuels [100].**

The global optimization of surrogate composition was performed using a genetic optimization algorithm implemented in the blend optimizer from Chemkin PRO software [76].

The Cetane Number of mixtures was calculated by a volume-fraction-weighted sum:

$$CN_{\text{mixture}} = \sum v_i CN_i \quad \text{Equation 41}$$

While the TSI was evaluated from a mole-fraction-weighted sum:

$$TSI_{\text{mixture}} = \sum x_i TSI_i \quad \text{Equation 42}$$

In terms of fuel composition representativity, n- and iso-paraffins are massively present in all liquid transportation fuels [101,102]. Aromatic compounds are also usually present in petroleum-based liquid transportation fuels [101–103] and have to be included in the blend to predict correctly soot volume fraction produced in fossil distillates combustion. N-propylbenzene was chosen as a good trade-off between light and heavier aromatics (from benzene to methylnaphthalene). Moreover, the combustion chemistry of n-decane, iso-octane and n-propylbenzene is presently relatively well modeled and several kinetic mechanisms have been validated over a wide range of conditions [104].

A variety of surrogate formulation for liquid transportation fuels may be suggested as depicted in Table 4 and Table 5. For example, Violi et al. [105] proposed a jet surrogate fuel (JP-8) containing six components. Farell et al. [106] proposed a diesel surrogate containing 4 components and also argued about components that may be of interest in the future.

Components	Kerosene (JP-8) surrogate (%vol)
iso-octane	10
n-dodecane	30
n-tetradecane	20
methylcyclohexane	20
m-xylene	15
Tetralin	5

Table 4 : Jet fuel surrogate [105].

Diesel surrogates	
Current components	Prospective components
n-decane	n-hexadecane
iso-octane	Heptamethylnonane
Methylcyclohexane	n-decylbenzene
Toluene	1-methylnaphthalene

Table 5 : Diesel fuel surrogate [106].

Since a surrogate fuel must be as simple as possible, but not simpler, the more accurately it captures the compositional characteristics of the target fuel (commercial fuels), the more accurately it also embodies the target fuel properties. A higher compositional accuracy requires a larger number of compounds with molecular structures and weights that are more representative of those found in target fuel, while a lower compositional accuracy implies a smaller number of readily available compounds and easy to procure and blend. Mueller et al. [107] recently investigated diesel surrogates formulation in balancing multiple trade-offs including: molecular structure, molecular weight, ignition quality, boiling and melting points, component availability, density, viscosity, purity, cost, safety and availability of chemical kinetic mechanisms. Surrogate candidate components proposed in Mueller's investigation are depicted in Figure 26:

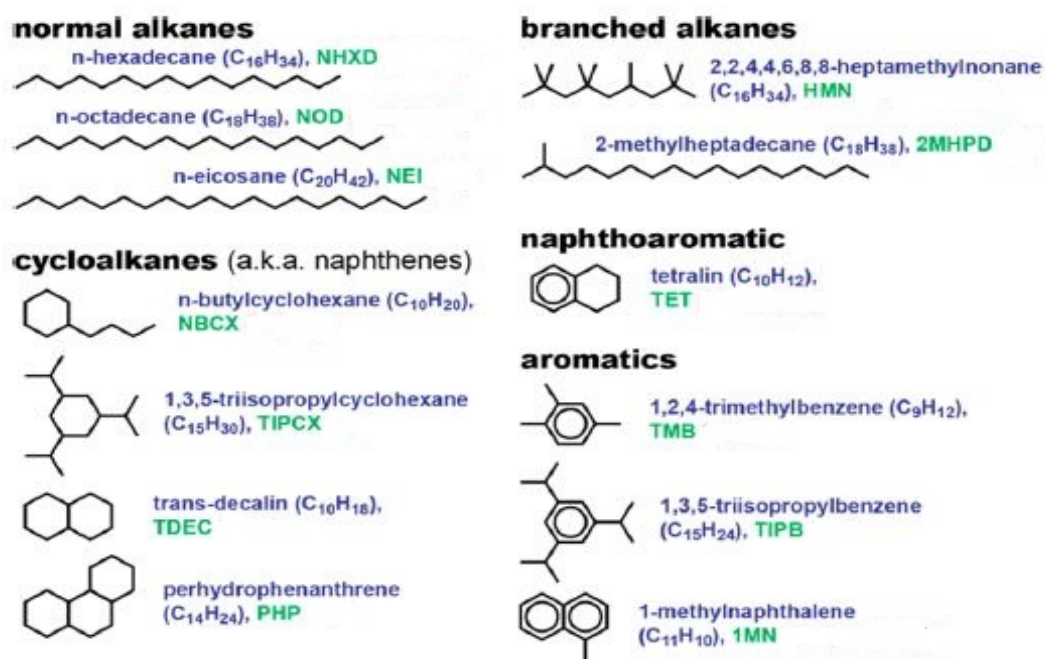


Figure 26 : Diesel surrogate palette compounds [107].

Authors proposed four surrogates from lower to higher compositional accuracy as depicted in Table 6. They showed that surrogate 4 describes better the target fuel properties namely its hydrocarbon class mass fractions, the carbon type mole fractions, peroxide contents, volatility, density, lubricity and cloud point. With soot emissions under diesel combustion conditions, surrogate 2 is expected to best match the soot emissions of the commercial fuels. All the four surrogates represent well the commercial diesel fuels in term of carbon and hydrogen mass fractions (elementary analysis). However, neither combustion experiment nor computational study using these surrogate mixtures was



published. Thus, it remains difficult to assess which proposed surrogate is more representative of commercial fuels.

Component abbreviation (see Figure 26)	Diesel surrogate 1 %wt (4 components)	Diesel surrogate 2 %wt (5 components)	Diesel surrogate 3 %wt (8 components)	Diesel surrogate 4 %wt (9 components)
NHxD	32.2	0.0	3.2	0.0
NOD	0.0	32.1	27.3	15.1
NEI	0.0	0.0	0.0	1.2
HMN	42.0	32.8	35.1	0.0
2MHPD	0.0	0.0	0.0	10.2
NBCX	0.0	0.0	3.8	14.8
TIPCX	0.0	0.0	0.0	12.8
TDEC	10.5	0.0	4.0	0.0
PHP	0.0	0.0	0.0	6.4
TMB	0.0	8.0	4.8	0.0
TIPB	0.0	0.0	0.0	16.6
TET	0.0	14.8	10.8	12.0
1MN	15.3	12.3	10.9	10.9

**Table 6 : Diesel surrogate fuels composition from Mueller et al. work [107].**

In the same way, Gou et al. [108] and Dooley et al. [92] proposed jet-A1 surrogates by matching molecular structure and functional groups: CH<sub>3</sub>, CH<sub>2</sub>, CH, C and phenyl of a commercial jet fuel. The components selected in their investigation are presented in Table 7:

Components	Gou et al. jet surrogate % mol	Dooley et al. jet surrogate % mol	Commercial jet fuel
n-decane	0.0	42.7	normal, branched, cyclic alkanes, aromatics, naphthalenes
iso-octane	0.0	33.0	
Toluene	27.2	24.3	
n-dodecane	50.9	0.0	
2,5-dimethylhexane	21.9	0.0	
H/C	1.98	2.02	1.96
Molecular weight	136.5	126.3	142 ± 20

**Table 7 : Jet surrogate fuels proposed by Gou et al. [108] and Dooley et al. [92].**

They concluded that these surrogate fuel mixtures can reproduce well combustion characteristics in a homogeneous ignition and flow reactor combustion process over a wide temperature range.

For gasoline surrogates, most of previous works use a Primary Reference Fuels (PRF) that is a mixture of n-heptane and iso-octane or a toluene reference fuels (TRF) that is a mixture of toluene and primary reference fuels [109–112]. These surrogates were proposed based on their capability to reproduce gasoline auto-ignition properties in engine conditions, density, global atom content and lower heating value. Table 8 summarizes some surrogates encountered in the literature.

Surrogate components	Mehl et al. [113] gasoline surrogate (% mol)	Cai et al.[111] gasoline surrogate (% vol)	Cai et al. [111] gasoline surrogate PRF (% vol)	Y.-z. An et al.[110] gasoline surrogate (% mol)
n-heptane	0.0	19.4	13.0	17.0
Iso-octane	47.0	42.2	87.0	55.0
Toluene	35.0	38.3	0.0	28.0
1-hexene	18.0	0.0	0.0	0.0
MON	94.6	83.4	87.0	85.0
RON	103.7	90.5	87.0	88.0
H/C ratio	1.84	1.750	2.260	1.971

Table 8 : Some proposed gasoline surrogates in the literature.

### 4.3. Development of a detailed chemical kinetic mechanism

A new detailed chemical kinetic mechanism describing the combustion of our and literature surrogates was derived from different subsets. Iso-octane and n-decane sub-mechanisms were extracted from Dooley et al. [92] and n-propylbenzene sub-mechanism comes from the study of Darcy et al. [114]. These 3 sub-mechanisms were merged to build a base mechanism. Whenever several thermokinetic data were present for the same reaction in both individual sub-mechanisms, those of Dooley et al. [92] were retained. The C<sub>0</sub>, C<sub>1</sub>, C<sub>2</sub> and C<sub>3</sub> sub models were extracted directly from the mechanism of Dooley et al. [92]. Reactions were subsequently added to improve agreement with experimental data obtained over a broad range of conditions such as ignition delay times, laminar flame speeds, PAH and important C<sub>1</sub>-C<sub>6</sub> intermediates concentration profiles. Table 9 summarizes all mechanisms used for the model construction. Reactions added for improving C<sub>2</sub> species (acetylene, ethylene, ethane) formation were taken from Alzueta et al. [115] and from AramcoMech [116]. For C<sub>3</sub> species (allene, propyne, propene), additional reactions were taken from Hansen et al.[117]. For C<sub>4</sub>/C<sub>6</sub> species (butadienes, butenes, cyclopentadiene, benzene), reactions were taken from Wang et al. [118], Zeng et al. [119] and Colket et al. [120]. In addition to low temperature reactions from Dooley et al. [92], some additional n-heptane, iso-octane and n-decane low temperature reactions were extracted from the work of Ranzi et al. [121]. This low temperature subset allowed improving ignition delay times predictions over the 600-900 K range, which is crucial in Diesel engine operation. For monoaromatic species (toluene, styrene, phenylacetylene), reactions were taken from Yuan et al. [122]. The PAH subset (up to coronene and including polyphenyls) was built from the works of Yuan et al. [122], Slavinskaya et al. [123], Miyoshi et al. [124], Norinaga et al. [125], Kousoku et al. [126] and Djokic et al. [127].

Mechanisms	Subsets
Dooley et al. [92]	n-decane and iso-octane subsets including H <sub>2</sub> /CO, C <sub>1</sub> -C <sub>6</sub> subsets
Darcy et al. [114]	n-propylbenzene subset
Alzueta et al. [115]	C <sub>2</sub> subset
Metcalfe et al. [116]	C <sub>2</sub> subset
Hansen et al. [117]	C <sub>3</sub> /C <sub>4</sub> subset
Colket et al. [41,120]	C <sub>4</sub> /C <sub>6</sub> subset
Wang et al. [118]	C <sub>4</sub> /C <sub>6</sub> subset
Zeng et al. [119]	C <sub>4</sub> /C <sub>6</sub> subset
Ranzi et al. [121]	n-decane/iso-octane low temperature reactions
Yuan et al. [122]	Monoaromatics (toluene, styrene, phenylacetylene) subset
Yuan et al.[122], Slavinskaya et al. [123], Miyoshi et al. [124], Norinaga et al. [125], Kousoku et al. [46] and Djokic et al. [127]	PAH up to coronene subset

**Table 9 : Mechanistic sources for model construction.**

In the present reaction model, dibenzofuran (DIBZFUR) subset was taken from Ranzi et al. [128] and from Sebbar et al. [129] as shown in Table 10.

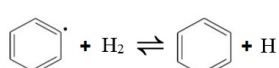
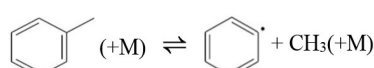
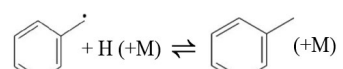
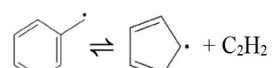
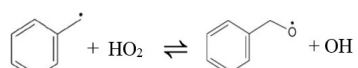
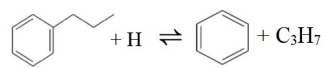
Reactions	A (cm, mol, s)	n	E (kcal.mol <sup>-1</sup> )	Ref.
<chem>C6H5O+C6H5O=&gt;DIBZFUR+H2O</chem>	$4.0 \times 10^{13}$	0.00	11.0	[128]
<chem>DIBZFUR+H=DIBZFURNYL+H2</chem>	$2.5 \times 10^{14}$	0.00	16.0	p.w
<chem>DIBZFURNYL+O2=DIBZFURNOXY+O</chem>	$1.5 \times 10^{19}$	-0.89	18.1	[129]
<chem>DIBZFUR+OH=&gt;CO+NAPHT+HCO</chem>	$2.0 \times 10^{13}$	0.00	0.0	[128]

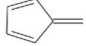
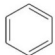
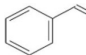
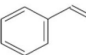
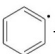

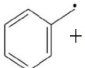
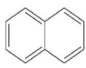
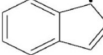
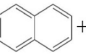
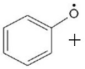
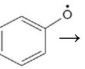
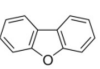
**Table 10: Dibenzofuran submechanism used in the present work.**

Dibenzofuran (DIBZFUR) is produced from phenoxy radicals recombination and may be consumed through H abstraction or oxidation by OH. The rate constant of phenoxy recombination is in line with theoretical and experimental data published so far. The rate constant for H abstraction from dibenzofuran to yield dibenzofuranyl was herein assumed to be identical to that of H abstraction from naphthalene. Benzene oxidation in moderately rich flames can yield significant quantities of resonantly stabilized phenoxy radicals (> 10 ppm) [130] which readily recombine to dibenzofuran [131]. This reaction path has been so far studied mainly in the context of oxygenated fuel oxidation. The rate constant from Ranzi et al. [128] mechanism adopted in the present study is smaller by a factor of two than Grotheer et al. rate constant [132]. Further, it is in good agreement with the Gibbs free energy of activation obtained by Asatrya et al. [131] in their electronic structure calculations of phenoxy dimer dehydration. As there is not sufficient experimental data to directly validate dibenzofuran path kinetics in jet A premixed flames, we assessed this path against dibenzofuran

oxidation experiments in very diluted conditions, showing a correct agreement of naphthalene concentration profile with measurements from [133]. This tends to indicate that the contribution of this path to naphthalene production is indeed accounted for by the present kinetic model at  $T > 1000$  K.

The  $C_0$ - $C_1$  subset contains 34 species and 171 reactions. The  $C_2$ - $C_3$  subset contains 96 species and 582 reactions. The  $C_4$ - $C_5$  subset contains 210 species and 1170 reactions. The  $C_6$ - $C_7$  subset contains 196 species and 770 reactions. The  $C_8$ - $C_9$  subset contains 192 species and 856 reactions. The  $C_{10}$ - $C_{11}$  subset contains 132 species and 487 reactions. The  $C_{12+}$  subset contains 154 species and 514 reactions. To allow compatibility of the present mechanism with older chemkin versions, pressure dependency has been described using Troe's formalism. An example of fit of Troe can be seen in Appendix F, showing the rate constant fitting as a function of temperature for different constant pressures. The vast majority (98%) of reactions implemented in the mechanism are bidirectional. Some lumped reactions were assumed to be unidirectional as  $\Delta rG \ll 0$  over the whole temperature range of interest (300-2500 K) and because making them bidirectional may result in convergence issues for premixed flame calculations. The most important added reaction kinetic parameters based on sensitivity analyses performed for benzene and naphthalene are listed in Table 11.

Reactions	A (cm, mol, s)	n	E (kcal/mol)	Reference
$C_2H_3(+M) = C_2H_2+H(+M)$	$A_\infty = 3.9 \times 10^8$ $A_0 = 2.6 \times 10^{27}$	$n_\infty = 1.62$ $n_0 = -3.40$	$E_\infty = 37.0$ $E_0 = 35.0$	[134]
	$5.7 \times 10^4$	2.43	6.2	[135]
	$A_\infty = 1.9 \times 10^{27}$ $A_0 = 1.0 \times 10^{98}$	$n_\infty = -3.16$ $n_0 = -22.96$	$E_\infty = 100.0$ $E_0 = 120.0$	[136]
	$A_\infty = 7.2 \times 10^{13}$ $A_0 = 3.0 \times 10^{136}$	$n_\infty = 0.06$ $n_0 = -33.35$	$E_\infty = -0.04$ $E_0 = 55.0$	[136]
	$6.0 \times 10^{13}$	0.00	70.0	[137]
	$1.2 \times 10^9$	1.03	-2.2	[138]
	$5.8 \times 10^{13}$	0.00	8.0	[139]

$C_2H_3 + C_2H \rightleftharpoons 2 C_2H_2$	$3.0 \times 10^{13}$	0.00	0.0	[115]
$2 C_2H_3 \rightleftharpoons C_2H_4 + C_2H_2$	$6.3 \times 10^{13}$	0.00	0.0	[115]
$2 C_2H_3 \rightleftharpoons H_2C=C-\dot{C}H+CH_3$	$1.8 \times 10^{13}$	0.00	0.0	[115]
$HC\equiv C-CH_3 + H \rightleftharpoons H_2C=C-\dot{C}H+H_2$	$3.6 \times 10^4$	2.80	4.8	[140]
$2 H_2C=C-\dot{C}H \rightleftharpoons$ 	$7.2 \times 10^{65}$	-16.00	25	[141]
$2 H_2C=C-\dot{C}H \rightleftharpoons$ 	$1.6 \times 10^{66}$	-15.90	28	[142]
 + H $\rightleftharpoons$  + H <sub>2</sub>	$6.7 \times 10^6$	2.53	6.1	[11]
 + HC≡C-CH=CH <sub>2</sub> $\rightleftharpoons$  + H	$3.3 \times 10^{33}$	-5.70	130.0	[11]
 + H <sub>2</sub> C=C-\dot{C}H $\rightleftharpoons$  + 2H	$2.0 \times 10^{13}$	0.35	5.0	[38]
 + CH <sub>3</sub> $\rightleftharpoons$  + 2H	$3.0 \times 10^{18}$	0.00	37.0	[143]
 +  $\rightarrow$  + H <sub>2</sub> O	$4.0 \times 10^{13}$	0.00	11.0	[128]

**Table 11 : Kinetic rate parameters ( $k = A (T / 1 K)^n \exp (- E / RT)$ ) of most important added reactions for naphthalene production.**

To better account for diesel intermediate temperature oxidation, the rate parameters of the reaction between benzyl and hydroperoxy radical forming benzoyl radical (see Table 11), which is important from 800 to 1000 K, were modified. Despite modest deviation with other proposed rate constants [114,138,144,145], that of Da Silva et al. [138] results in a better agreement with experimental ignition delays. In the present work, phenyl+vinylacetylene and benzyl+propargyl pathways are represented as lumped reactions. In fact, production of naphthalene from these two pathways proceed respectively through the formation of phenyl vinylacetylenyl [146] and methyleneindanyl [147]. Figure 27 shows the rate constants proposed for phenyl+vinylacetylene and benzyl+propargyl reactions yielding naphthalene.

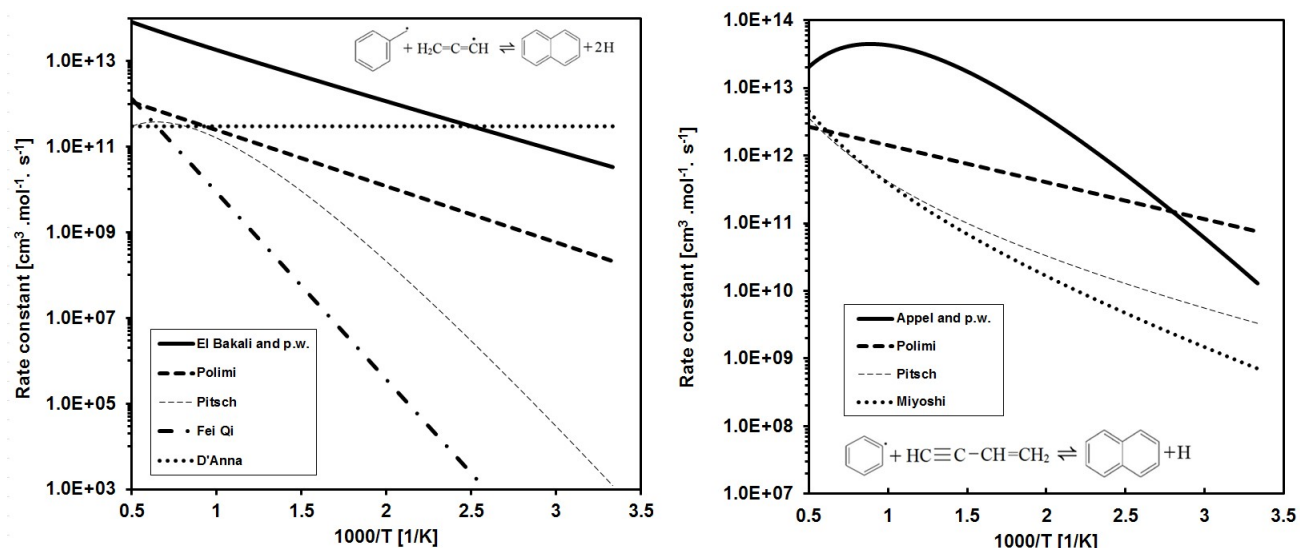


Figure 27 : The proposed rate constants for phenyl+vinylacetylene and benzyl+propargyl reactions. Units are in mol, s, cm<sup>3</sup>, cal, K.

The rate constant herein adopted for phenyl+vinylacetylene pathway follows the recommendation of Appel et al. [11] exhibiting a negative curvature unlike that recommended by Miyoshi et al. [124]. For benzyl+propargyl reaction, large discrepancies still subsist between recommended rate parameters. The rate constant proposed previously by El Bakali et al. [148] was used. The final mechanism contains 1014 species and 4550 most reversible reactions and also accounts for both low and high temperature combustion regimes. The nomenclature of some important species including PAHs used in the present kinetic model as well as the heat of formation of all species is presented in Appendices B and C. The sub-mechanisms used for benzene as well as for naphthalene and pyrene formation and consumption are presented in Appendix G.

#### 4.4. Mechanism Validation Results and Discussions

The performance of the mechanism was assessed against experimental data and several major mechanisms from the literature (see figures for references). A wide range of experimental conditions involving both pure components and commercial fuels combustion have been considered in validating the mechanism. The robustness of the mechanism can be verified by its validation over a wide range of operating conditions such as the nature of fuel (alkanes, alkenes, alkynes, aromatics and commercial fuels), the effects of pressure, temperature, equivalence ratio and the type of the studied system configuration (stabilized flame on a burner, jet stirred reactor, plug flow reactor and shock tube). The determining of this robustness is crucial to assess the acceptable deviation of the kinetic model. Table

12 presents an overview of experimental data used for model validation and Table 13 provides information of those reaction models included in comparison of species profiles taken from literature, with number of species and reactions and their range of validation.

Fuel structure	Configuration	Reference
Methane	Premixed laminar flame, 0.263 atm $\phi=2.05$ ; $\phi=2.32$	[148]
Acetylene	Oxidation in Plug flow reactor, 1 atm, $\phi=7.50$	[115]
Ethylene	Premixed laminar flame, 1 atm, $\phi=3.06$	[36]
N-butane	Premixed laminar flame, 1 atm, $\phi=1.60$ ; $\phi=1.75$ ; $\phi=1.95$	[149]
N-butane/n-propylbenzene	Premixed laminar flame, 1 atm, $\phi=1.75$ ; $\phi=1.95$	[149]
Benzene	Premixed laminar flame, 30 Torr, $\phi=2.00$	[150]
Iso-octane	Premixed laminar flame, 1 atm, $\phi=1.90$	[151]
N-decane	Premixed laminar flame, 1 atm, $\phi=1.70$	[152]
Styrene	Premixed laminar flame, 30 Torr, $\phi=1.70$	[153]
Ethylbenzene	Premixed laminar flame, 30 Torr, $\phi=1.79$	[154]
N-propylbenzene	Premixed laminar flame, 30 Torr, $\phi=1.79$	[118]
Gasoline		
	Premixed laminar flame, 30 Torr, $\phi=1.73$	[155]
	Ignition delay times 20-40 bar: shock tube	[156]
	Laminar flame speeds, $\phi=0.50-1.50$	[157]
Jet Fuel		
	Premixed laminar flame, 1 atm, $\phi=1.70$	[152]
	Oxidation in jet stirred reactor, 1 atm, $\phi=2.00$	[158]
	Ignition delay times 20 atm: shock tube	[159]
	Laminar flame speeds, $\phi=0.70-1.40$	[160]
Diesel Fuel		
	Oxidation in jet stirred reactor, 1 atm, $\phi=2.00$	[96]
	Ignition delay times 6 atm: shock tube and rapid compression machine	[161]
	Laminar flame speeds, $\phi=0.70-1.50$	[162]

Table 12 : The overview of experimental data used for model validation.

Reaction models from literature	Number of species/reactions	Range of validation
Slavinskaya et al. [123]	94 species and 722 reactions	Methane and ethene flames
Polimi [128]	200 species and 6826 reactions	Gasoline, Jet Fuels, Diesel: PRFs, heavy n-alkanes, Isocetane, Decalin, Tetralin
Battin-Leclerc et al. [163]	662 species and 3884 reactions	$\alpha$ -methyl-naphthalene/air and $\alpha$ -methyl-naphthalene/n-decane/air mixtures
Yuan et al. [153]	290 species and 1786 reactions	Styrene flames
Dooley et al. [92]	1599 species and 6633 reactions	Jet fuel surrogate
Raj et al. [164]	231 species and 1350 reactions	Gasoline surrogate fuels
LLNL [165]	2885 species and 11,754 reactions	Diesel fuel surrogate

Table 13 : Models included in the validation process against experiments.

Modeling results were compared to experimental data previously published on a few atmospheric pressure premixed flames of ethylene ( $\phi=3.0$ ) [36], n-butane ( $\phi=1.75$  and  $1.95$ ) [149], iso-octane ( $\phi=1.9$ ) [151], n-decane ( $\phi=1.7$ ) [152] and jet fuel ( $\phi=1.7$ ) [152] and low pressure premixed flame of methane ( $\phi=2.05$  and  $2.32$ ) [148], benzene ( $\phi=2.0$ ) [166], styrene ( $\phi=1.7$ ) [153], ethylbenzene ( $\phi=1.8$ ) [167], n-propylbenzene ( $\phi=1.8$ ) [118] and gasoline ( $\phi=1.7$ ) [155]. In jet stirred reactor configuration, jet fuel ( $\phi=2.0$ ) [158] at atmospheric pressure and diesel fuel oxidation ( $\phi=1.5$ ) [96] at a pressure of 10 bar were modeled. The prediction of ignition delays times and laminar flame speeds of gasoline [156], jet-A1 fuel [159] and diesel fuel [161] was also considered. Results obtained for a variety of other fuels are provided in Appendix D.

#### **4.4.1. Premixed laminar flames configuration**

Species that are of major interest in the sooting flame analysis are acetylene and PAHs. The accepted dominant soot growth mechanisms are the addition of acetylene through HACA mechanism and PAH condensation. Therefore, comparing the measurements and predicted mole fractions of such species is crucial and allows determining of the performance of the kinetic model in order to build a robust soot model.

##### **4.4.1.1. Saturated aliphatic hydrocarbon flames**

The alkane flames investigated in the present work are those of methane, n-butane iso-octane and n-decane. In the next sections, comparison between predicted concentration profiles and the measured ones are presented. The rate of production and consumption of most of measured species are also presented and discussed.

###### **4.4.1.1.1. Methane flame**

Methane combustion modeling is of prime importance as energies carrier and the primary component of natural gas. As a simple fuel, methane combustion is necessary to generate a detailed understanding of that of complex hydrocarbons. Combustion characteristics such as ignition delay time, flame speed and emissions of such small hydrocarbons are of critical importance in describing that of practical fuels. A low pressure (0.263 atm) rich methane premixed flame at  $\phi=2.32$  has been simulated to assess the capability of the present kinetic model in predicting concentrations of species of major interest such as benzene, pyrene and fluoranthene. The comparison between experimental data and the



predicted one is shown in Figure 28. The predicted mole fractions of acetylene as well as PAHs that are not experimentally measured can be seen in Appendix D.

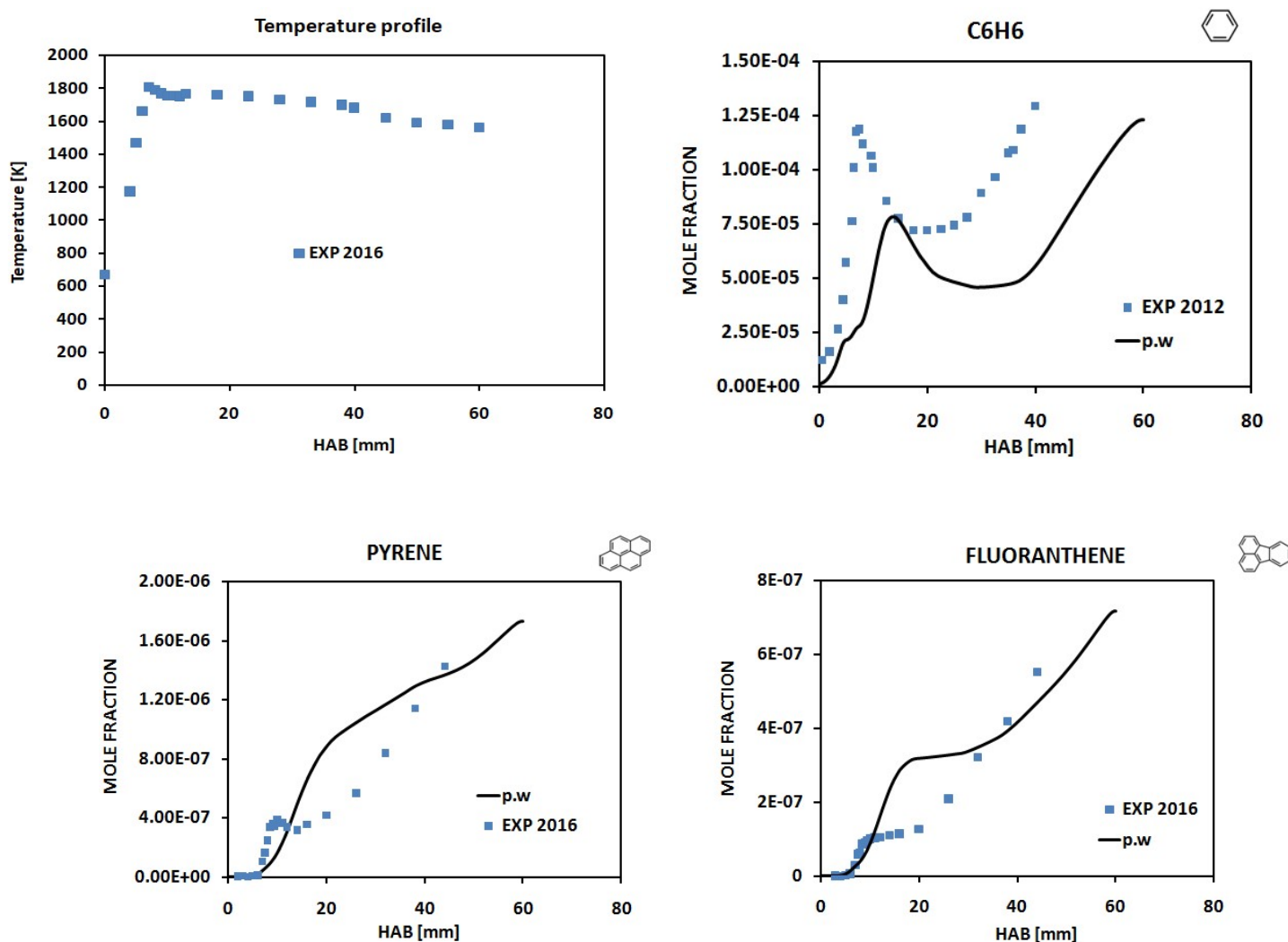


Figure 28 : Low pressure (0.263 atm) methane premixed flame,  $\phi=2.32$ :  $\text{CH}_4$  (46.2% in mol.)/ $\text{O}_2$  (39.8%)/ $\text{N}_2$  (14.0%). Species mole fraction profiles. The symbols represent experimental data from [148,168]; the lines represent modeling results from the present work.

In Figure 28, only the mole fractions for benzene, pyrene and fluoranthene were reported. The predicted mole fractions of the other PAHs are shown in Appendix D to get an insight into gas phase concentrations, since they will be considered as soot precursors for particles nucleation modeling.

In this low pressure flame of methane at  $\phi=2.32$ , it can be seen that the computed concentration profiles of species agree fairly well with the measured ones, despite a slight underprediction for benzene. The shift observed between measurements and prediction is due to the uncertainties about the microprobe position, since species concentration profiles were measured by using this device. The microprobe induces a shift that is tricky to determine in such experimental conditions.

- **Rate of production/consumption Analysis**

**Methane consumption pathways**

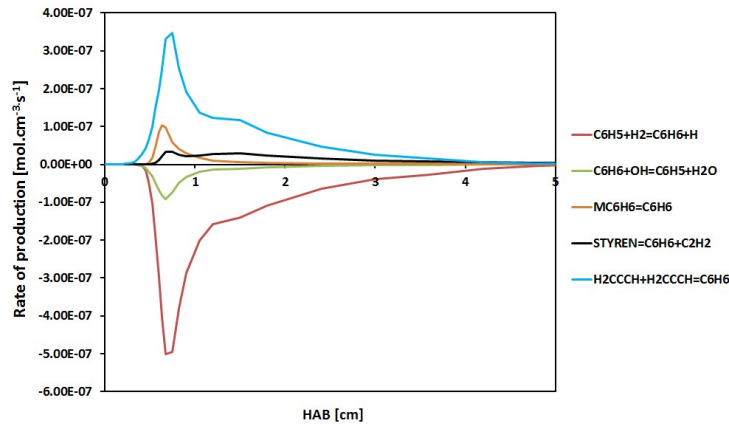
The methane fuel is consumed mainly by H atom abstraction by its reaction with H, OH and O radicals. At a temperature of 1767 K, the main methane consumption reactions are:



At this temperature, methane consumption is dominated by 70% of (R54), followed by 20% contribution of (R56) and 10% of (R55).

**Benzene formation/consumption**

In the above experimental conditions, benzene formation is dominated by recombination reaction of propargyl ( $\text{C}_3$  species) radical. Propargyl comes from propyne, which is mainly formed from acetylene. Figure 29 shows the rate of production and consumption of benzene.



**Figure 29 : Benzene rate of production and consumption in low pressure methane rich flame ( $\phi=2.32$ ).**

The main benzene formation reactions as a function of the height above the burner (HAB) are:



It can be seen that the reaction (R3745) predominates not only in the reaction zone but also in the higher distance from the burner surface. This reaction is followed by the isomerization (R3330) of dimethylene cyclobutene ( $\text{MC}_6\text{H}_6$ ) and then styrene decomposition (R3448) reaction to yield benzene

and acetylene. The major source of benzene consumption is benzyl radical formation,  $C_6H_6 + H = C_6H_5 + H_2$  (R3227) and  $C_6H_6 + OH = C_6H_5 + H_2O$  (R3230).

### Pyrene formation/consumption

As depicted in Figure 30, pyrene formation is dominated by the HACA mechanism, represented by the phenanthryl radical reaction with acetylene,  $A3-4 + C_2H_2 = PYRENE + H$  (R4055).

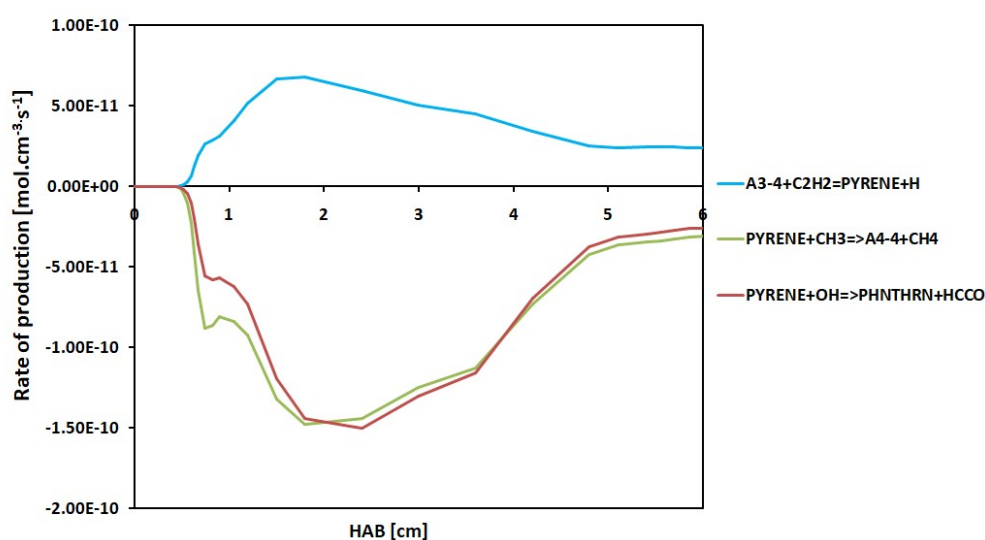


Figure 30 : Pyrene rate of production and consumption in low pressure methane rich flame ( $\phi=2.32$ ).

Pyrene consumption is dominated by the pyrenyl radicals formation through the reaction between pyrene and methyl radical,  $PYRENE + CH_3 = A4-2 + CH_4$  (R4070) and  $PYRENE + CH_3 = A4-4 + CH_3$  (R4072). These reactions are also a source of methane production. The minor discrepancies observed between measured and predicted pyrene concentration can be due to the lack of reactions that are involved in its consumption and probably its production. Reliable kinetic parameters are required for pyrene production in this flame and this issue must be carefully examined in the future work.

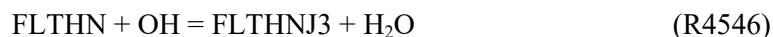
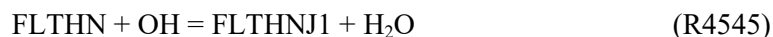
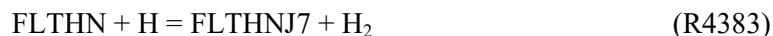
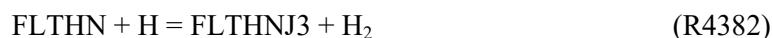
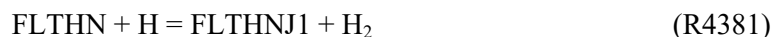
### Fluoranthene (FLTHN) formation/consumption

Fluoranthene formation is dominated by the isomerization reactions from acephenanthrylene (A3R5) and from aceanthrylene (A3LR5):



Reactions (R4389) and (R4391) are found to produce fluoranthene near the burner surface (at low HAB) and at higher HAB (burnt gas zone). Between both zones, they represent a major source of

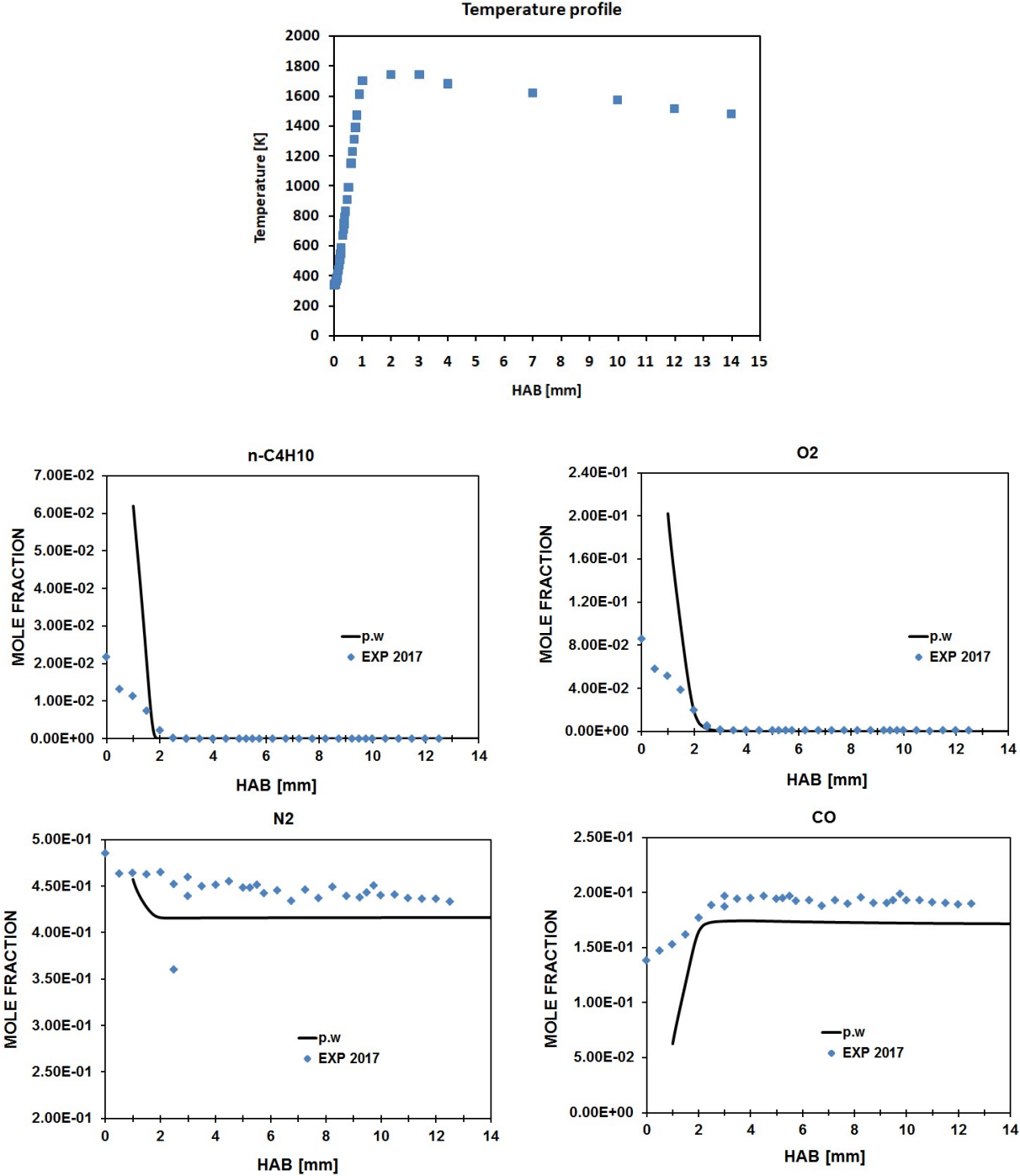
fluoranthene consumption. Fluoranthene is also consumed to yield fluoranthenyl radicals (FLTHNJ1, FLTHNJ3 and FLTHNJ7).



#### 4.4.1.1.2. N-butane flames

The n-butane is one of the simplest hydrocarbons contained in commercial fuel (gasoline) and is a major constituent of liquefied petroleum gas (LPG) that is an important alternative fuel for engines. Therefore, the modeling of n-butane combustion is important for understanding the combustion process in engines. This fuel exhibits two-stage ignition and cool flame that are properties relevant to abnormal combustion problems such as knock. A better understanding of n-butane combustion behavior will help elucidate the study of complex hydrocarbon constituents in practical fuels. Three atmospheric pressure n-butane premixed flames have been simulated to get insight into the capability of the present kinetic model in predicted species of major interests such as acetylene. The modeling of this flame is of prime importance due to the availability of experimental data over soot volume fractions that will be later modeled. Therefore, the importance of modeling of this flame is twofold: get insight into the robustness of the mechanism and better understanding of soot formation process from its gaseous precursors. The comparison between experimental mole fractions of species and the predicted ones for the three equivalence ratios  $\varphi=1.60$ ; 1.75 and 1.95 is shown from Figure 31 to Figure 33. The experimental data come from a parallel work to the present one in the framework of Advanced Soot Models for Aeronautic and Piston Engines (ASMAPE). The studied flames were stabilized for mainly soot volume fraction measurements and the reactivity near the burner surface was completely ignored. As can be seen in the captions below, the reactivity near the burner surface is high of importance and these flames are not suitable to investigate the progress of chemical species in the flame. However, reliable quantitative information in the reaction as well as the soot formation zone can be obtained. In contrast to the temperature profile measurement, the species mole fractions were

measured by using a microprobe. Therefore, the shift indicated (+1 mm) was necessary to match the species maximum concentration, mainly due to uncertainties over the microprobe positions that are difficult to precise.



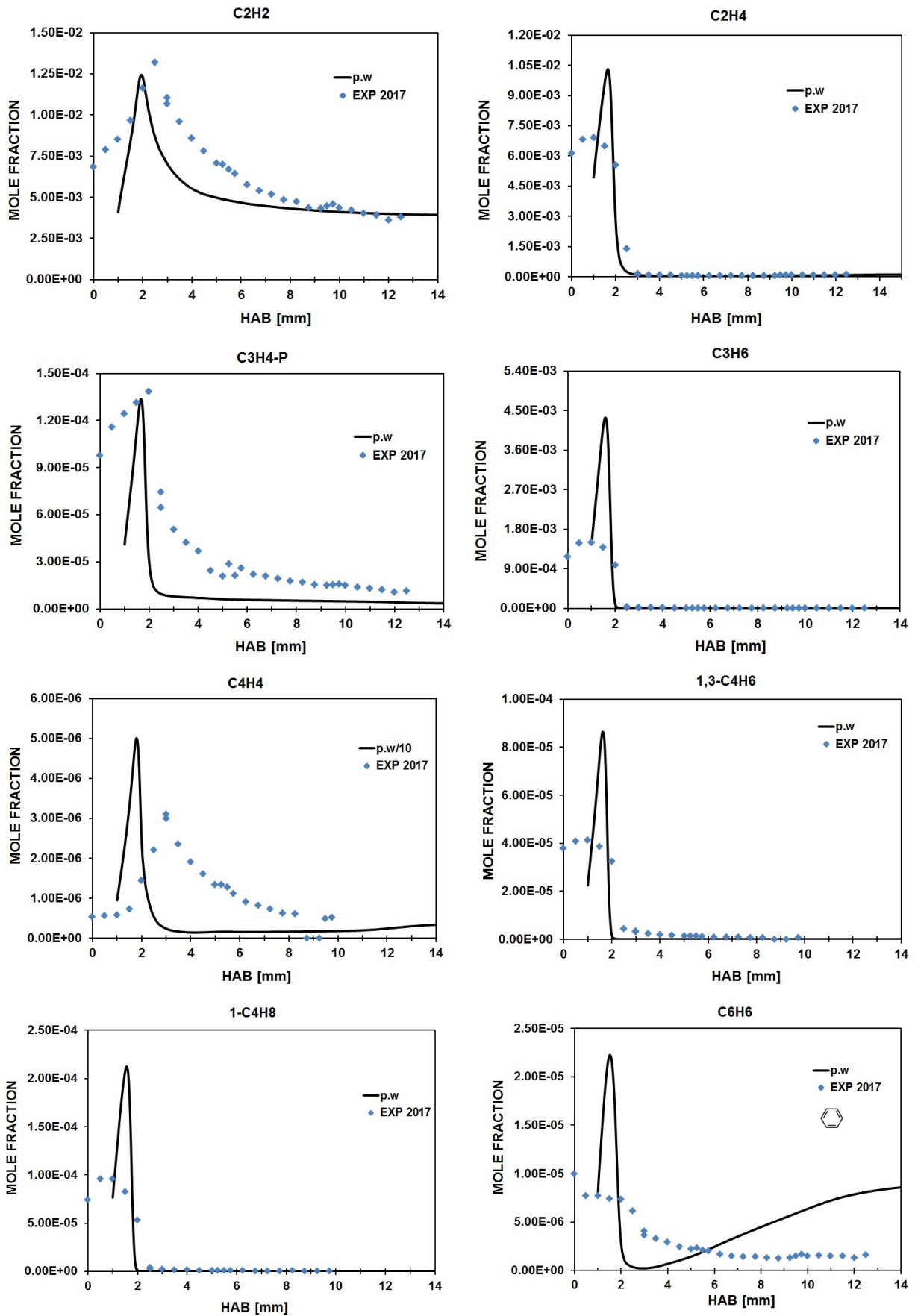
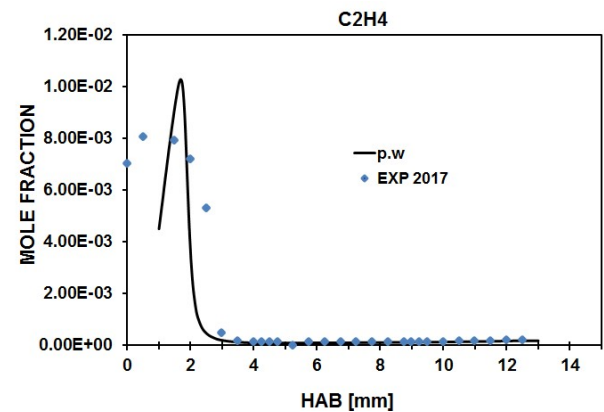
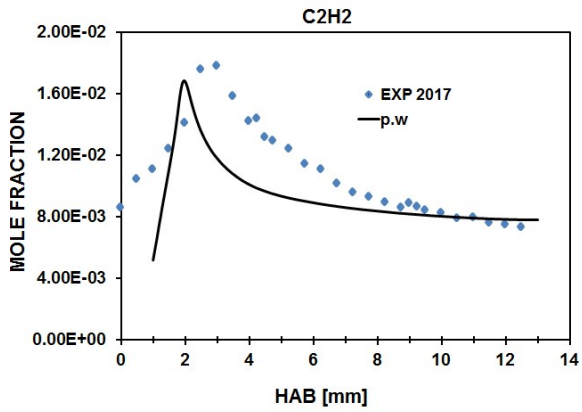
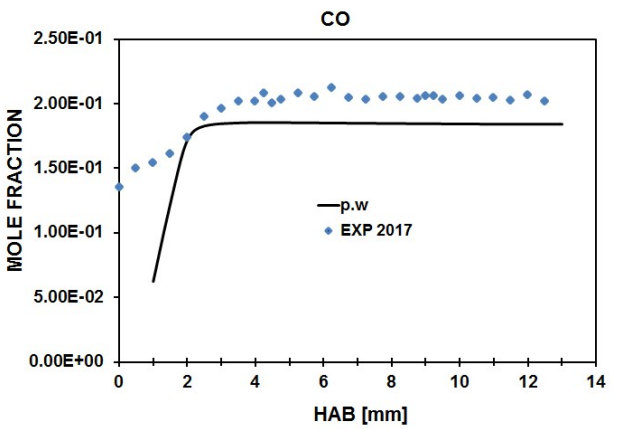
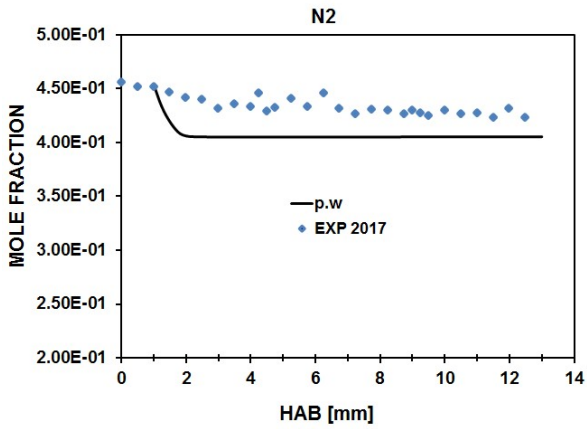
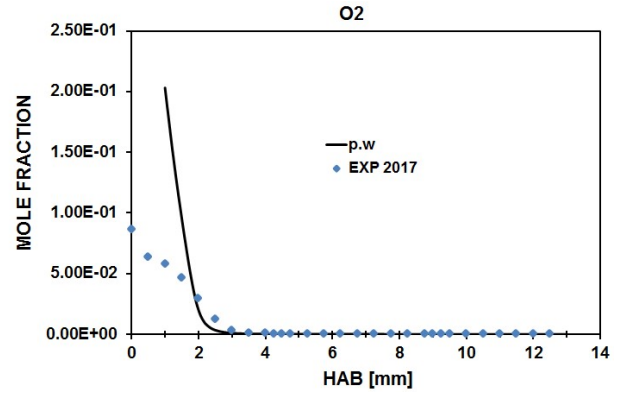
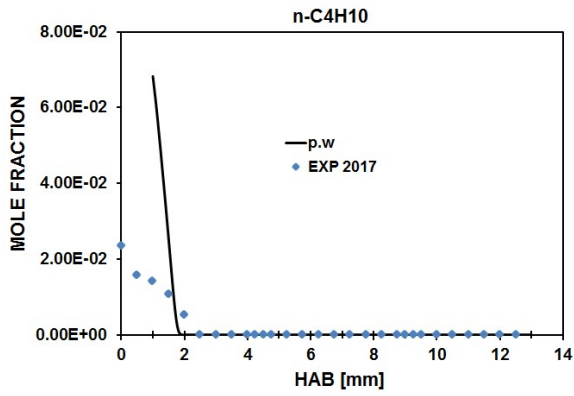
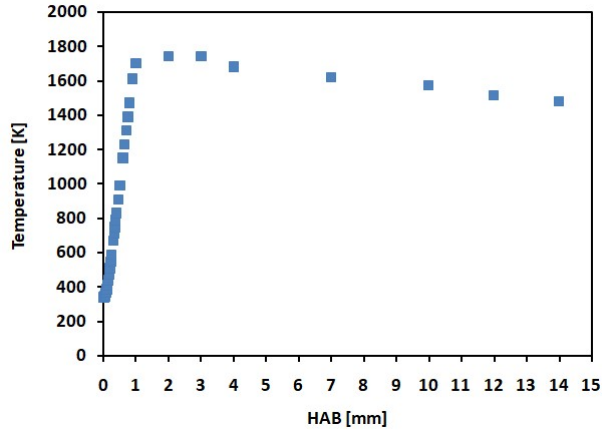


Figure 31 : Atmospheric n-butane premixed flame,  $\phi=1.60$ :  $n\text{-C}_4\text{H}_{10}$  (8.8% in mol.)/ $\text{O}_2$  (35.9%)/ $\text{N}_2$  (55.3%). Species mole fraction profiles. The symbols represent experimental data from [149]; the lines represent modeling results from the present work. p.w/10 denotes that the prediction results are divided by 10.

Temperature profile



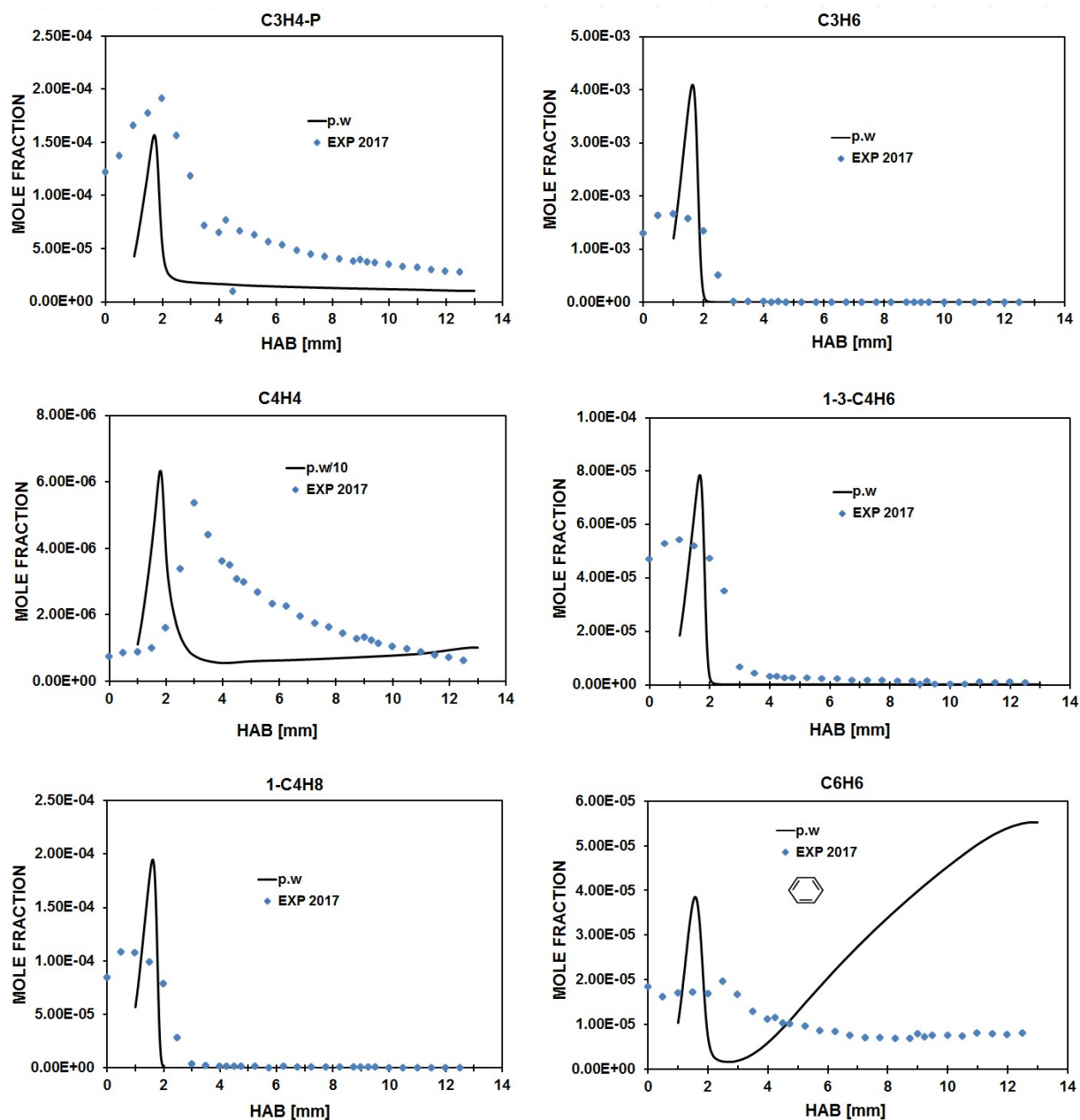
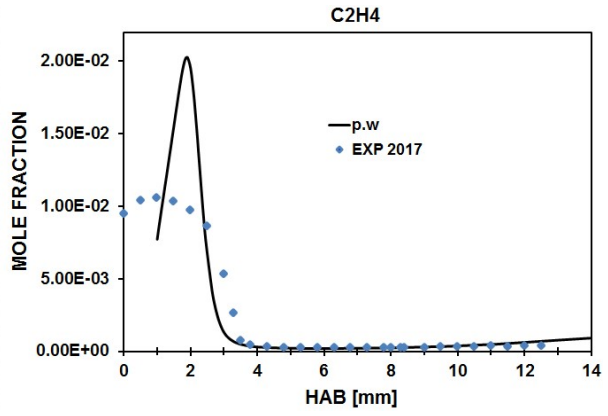
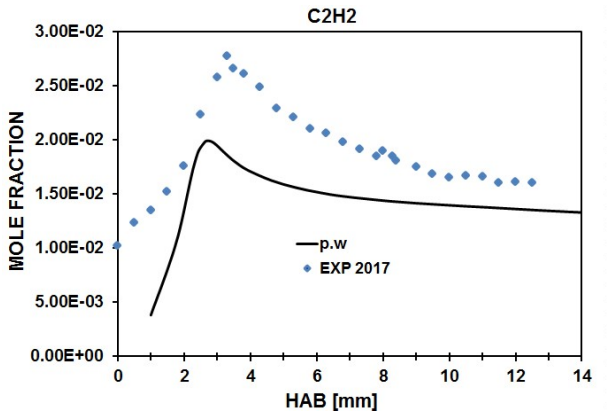
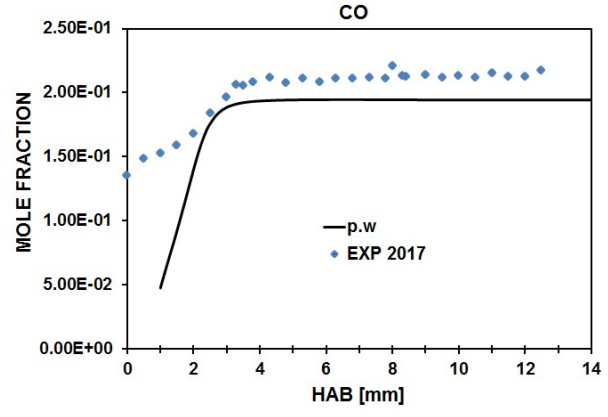
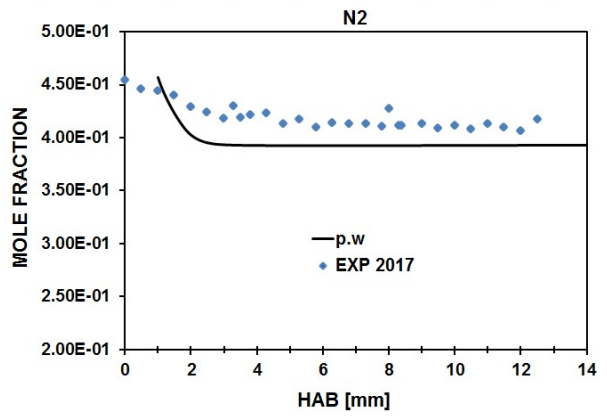
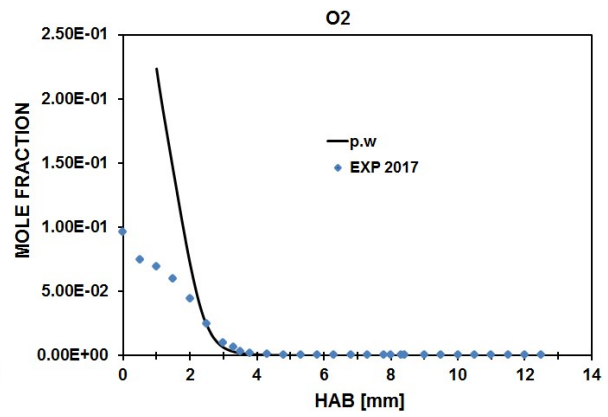
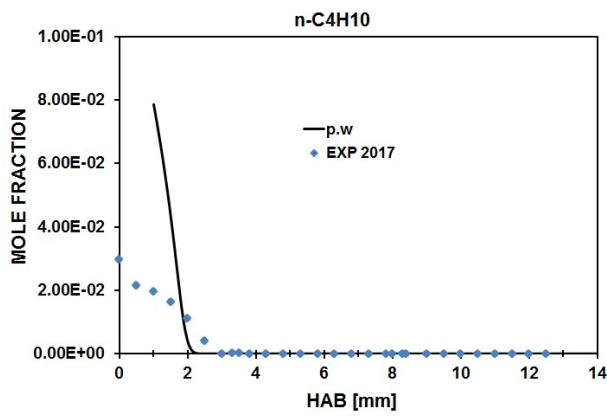
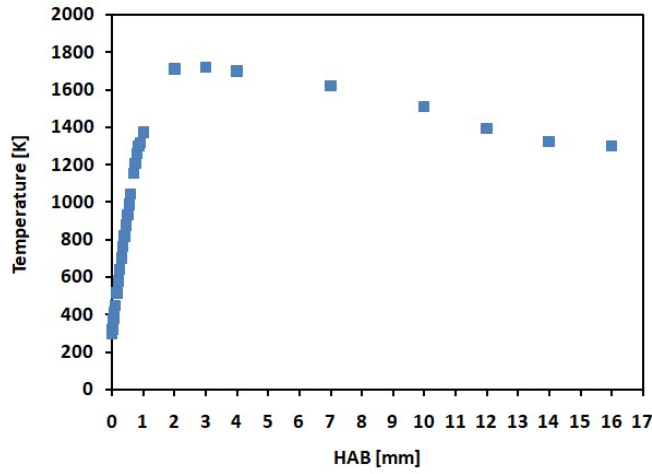


Figure 32 : Atmospheric n-butane premixed flame,  $\phi=1.75$ : n-C<sub>4</sub>H<sub>10</sub> (9.46% in mol.)/O<sub>2</sub> (35.22%)/N<sub>2</sub> (55.32%). Species mole fraction profiles. The symbols represent experimental data from [149]; the lines represent modeling results from the present work. p.w/10 denotes that the prediction results are divided by 10.



Temperature profile



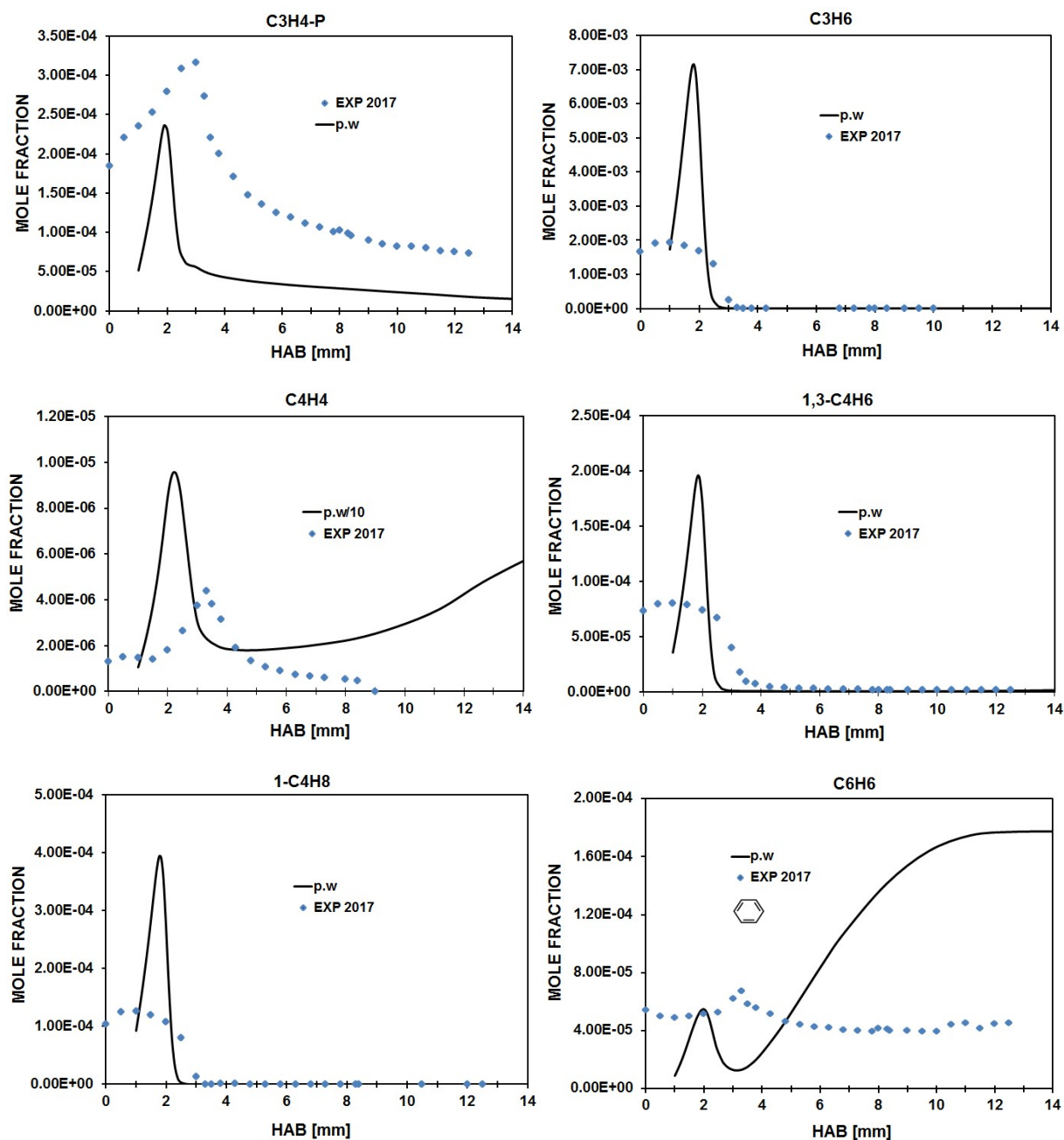


Figure 33 : Atmospheric n-butane premixed flame,  $\phi=1.95$ : n-C<sub>4</sub>H<sub>10</sub> (10.30% mol.)/O<sub>2</sub> (34.31%)/N<sub>2</sub> (55.39%). Species mole fraction profiles. The symbols represent experimental data from [149]; the lines represent modeling results from the present work. p.w/10 denotes that the prediction results are divided by 10.

In both flames at  $\phi=1.60$  and  $\phi=1.75$ , most of measured species profiles show a good agreement with the computed ones (within a factor of 2). Some species of major interest such as acetylene, ethylene, propyne, propene, but-1,3-diene and but-1-ene are satisfactorily represented. Some discrepancies are observed for vinylacetylene C<sub>4</sub>H<sub>4</sub> (within an overprediction of a factor of 10) and benzene, where a continuous increase of concentration is observed at higher HAB, while the measurement shows a constant evolution. From the rate of production analysis, the reactions involved in the benzene production are discussed in the next sections.

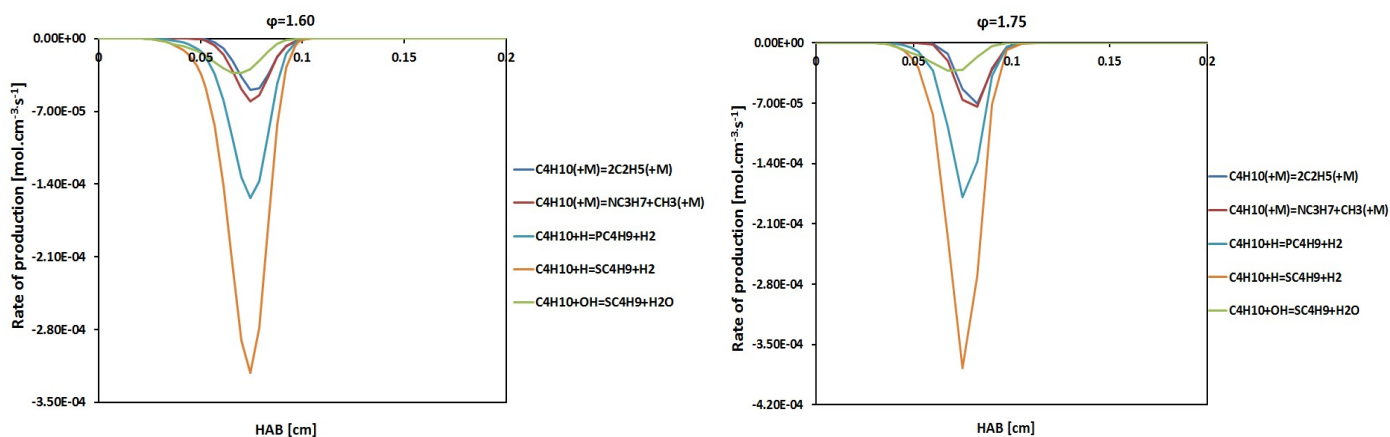
In the flame at  $\phi=1.95$ , similar observations as for  $\phi=1.75$  can be seen. However, the predicted acetylene and propyne maximum concentration peaks are lower than the measured ones, but the concentration profiles are well represented.

#### - Rate of production/consumption Analysis

The formation pathways of measured intermediate species and the comparison between the three flames at different equivalence ratios can be discussed as follows:

#### n-butane

For the three flames, the n-butane is predominantly consumed by H atom abstraction by H and OH, followed by thermal decomposition. The main reactions involved in butane decay are presented in Figure 34.



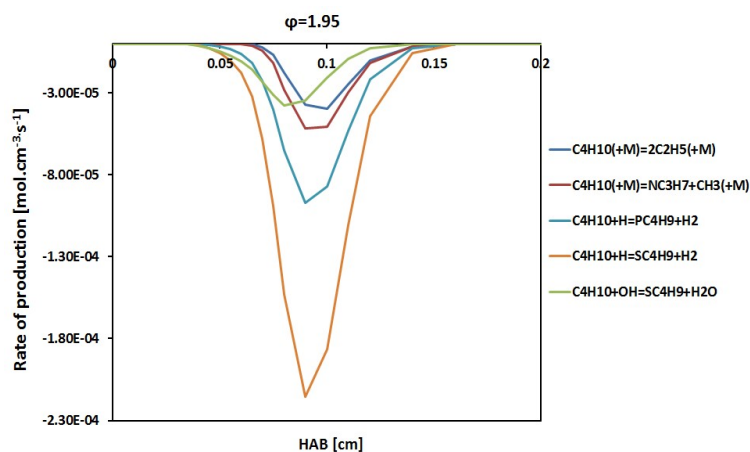


Figure 34 : n-butane decay pathways.

The predominant reaction (R671) starts near the burner surface, followed by the reaction (R670) that yields respectively but-2-yl ( $SC_4H_9$ ) and but-1-yl ( $PC_4H_9$ ). The reaction (R657) produces n-propyl radical and methyl and the reaction (R656) yields two ethyl radicals ( $C_2H_5$ ). In contrast with the two flames at  $\phi=1.60$  and  $\phi=1.75$ , reaction (R673) involving n-butane oxidation by OH is as important as n-butane thermal decomposition (R656) and also takes place near the burner surface. It can be seen that the three flames exhibit similar results in terms of reactions involved in n-butane decay. However, the reaction zone is larger in the flame at  $\phi=1.95$  than in  $\phi=1.60$  and  $\phi=1.75$  due to diffusion processes.

At temperature above 800 K,  $SC_4H_9$  is mainly consumed to produce propene,  $SC_4H_9 = C_3H_6 + CH_3$  (R700), while  $PC_4H_9$  predominantly decays to yield ethylene and ethyl radical  $PC_4H_9 = C_2H_5 + C_2H_4$  (R699). The formation of ethylene and but-1-ene from n-butane decay is clearly understandable, since they are ones of the main n-butane combustion products measured in higher concentrations.

### Acetylene formation/consumption

Acetylene is mainly produced from vinyl radical decay, followed by a modest contribution of propyne in the three flames. Figure 35 shows the comparison between the three flames.

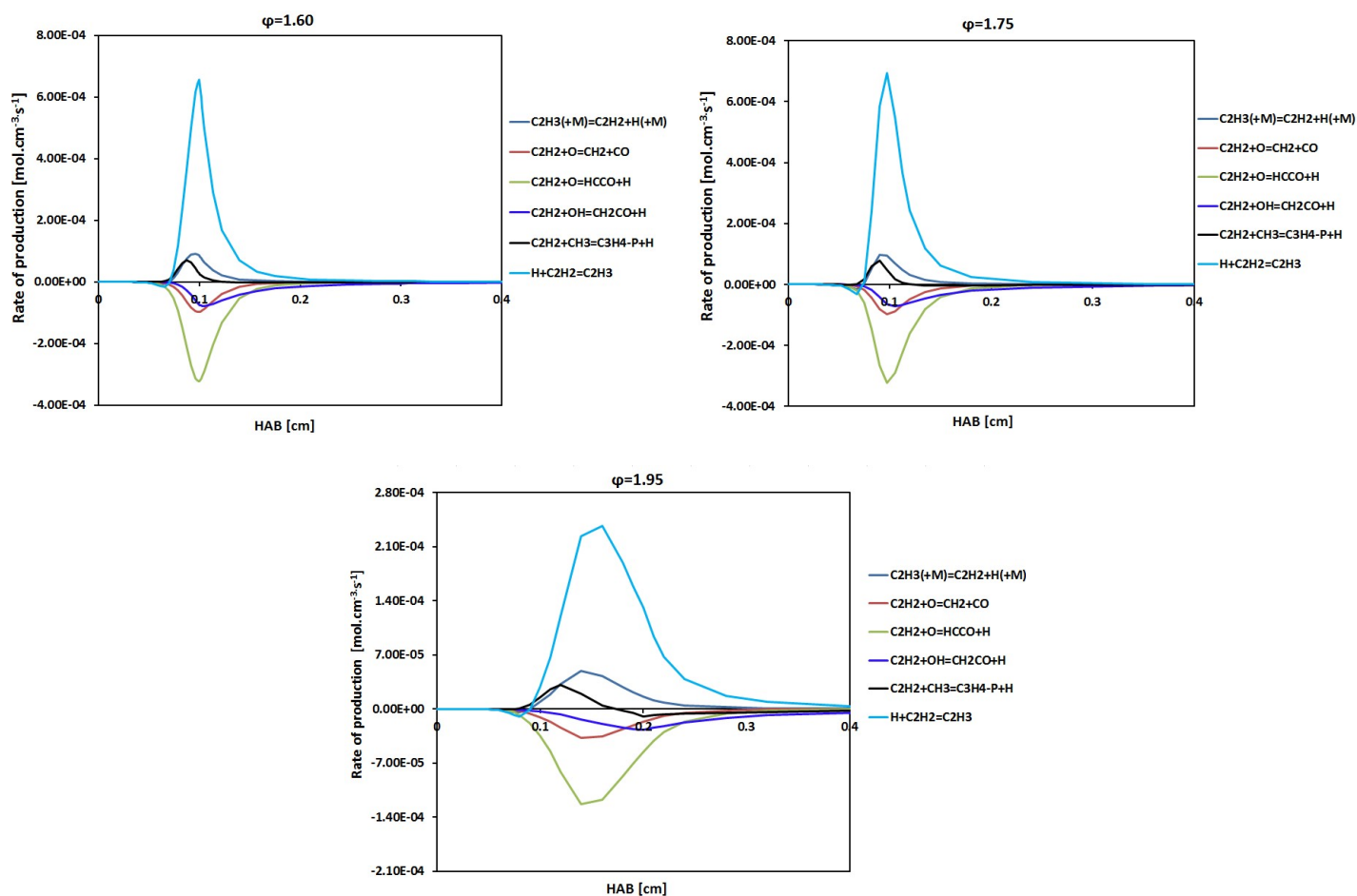


Figure 35 : Acetylene rate of production analysis in the three n-butane premixed flames.

The main reactions involved in acetylene production are:



Vinyl radical ( $\text{C}_2\text{H}_3$ ) is predominantly formed from ethylene H abstraction by H atom,  $\text{C}_2\text{H}_4 + \text{H} = \text{C}_2\text{H}_3 + \text{H}_2$  (R253). Acetylene consumption pathways involved oxygen radical and OH as follows:



The acetylene consumption products such as HCCO is found to contribute in ethylene and carbon monoxide production,  $\text{CH}_3 + \text{HCCO} = \text{C}_2\text{H}_4 + \text{CO}$  (R3724). Methylene ( $\text{CH}_2$ ) is one of the major source of HCO,  $\text{CH}_2 + \text{O}_2 = \text{HCO} + \text{OH}$  (R123) and HCO is found to be the main precursor of carbon

monoxide,  $\text{HCO} + \text{M} = \text{H} + \text{CO} + \text{M}$  (R26).  $\text{CH}_2\text{CO}$  formed from acetylene reaction with OH is also a production source of HCCO,  $\text{CH}_2\text{CO} + \text{H} = \text{HCCO} + \text{H}_2$  (R238). It is mainly consumed to yield methyl and carbon monoxide,  $\text{CH}_2\text{CO} + \text{H} = \text{CH}_3 + \text{CO}$  (R237).

### Ethylene formation/consumption

As can be seen in Figure 36, ethylene formation is dominated from ethyl radical decay, followed by the decomposition of but-1-yl ( $\text{PC}_4\text{H}_9$ ), propene and HCCO.

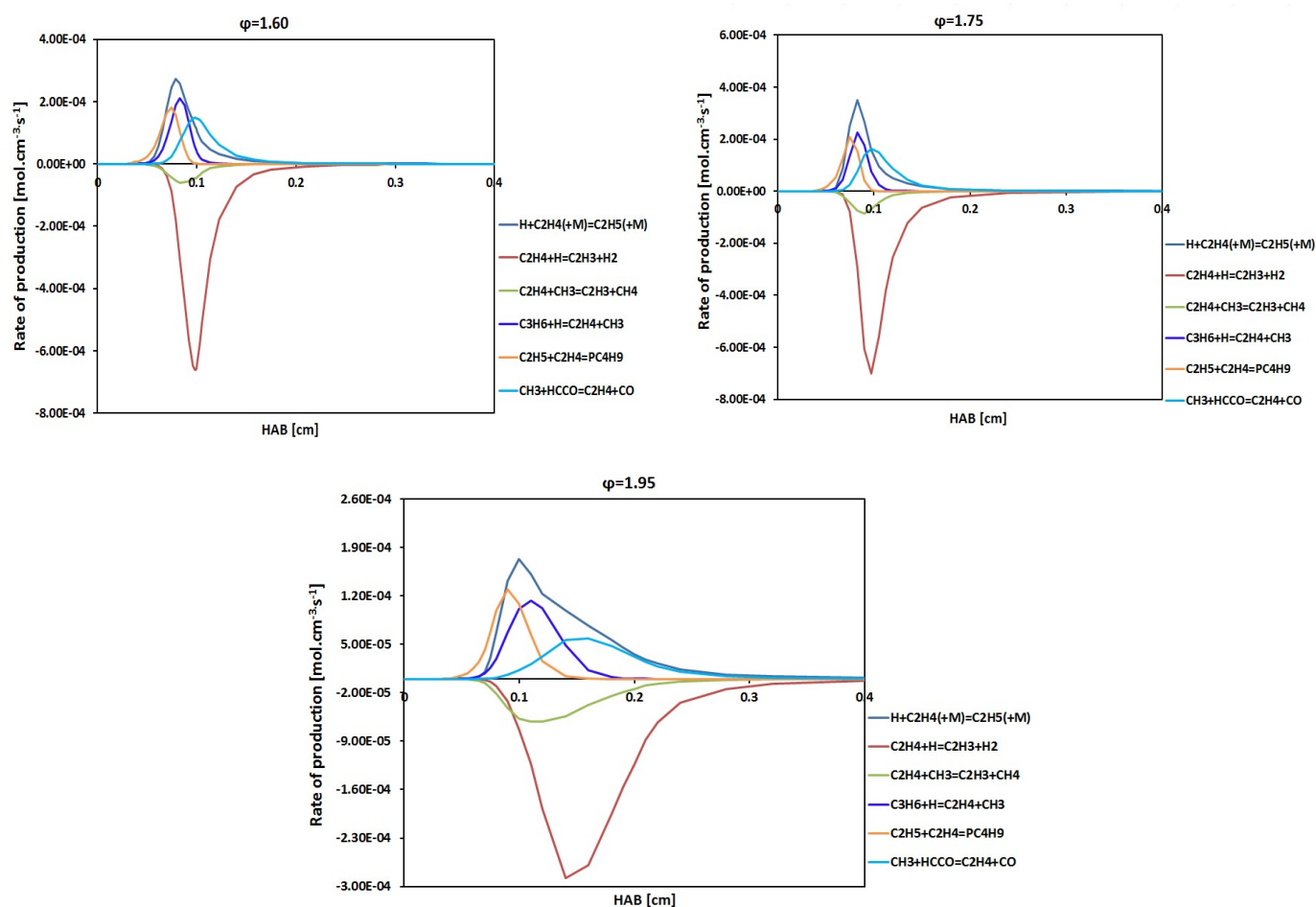


Figure 36 : Ethylene rate of production analysis in the three n-butane premixed flames.

Ethylene is mainly produced by (R699) near the burner surface (lower HAB). As a reminder,  $\text{PC}_4\text{H}_9$  is formed from n-butane (the fuel) decomposition, then, its contribution to ethylene production at that

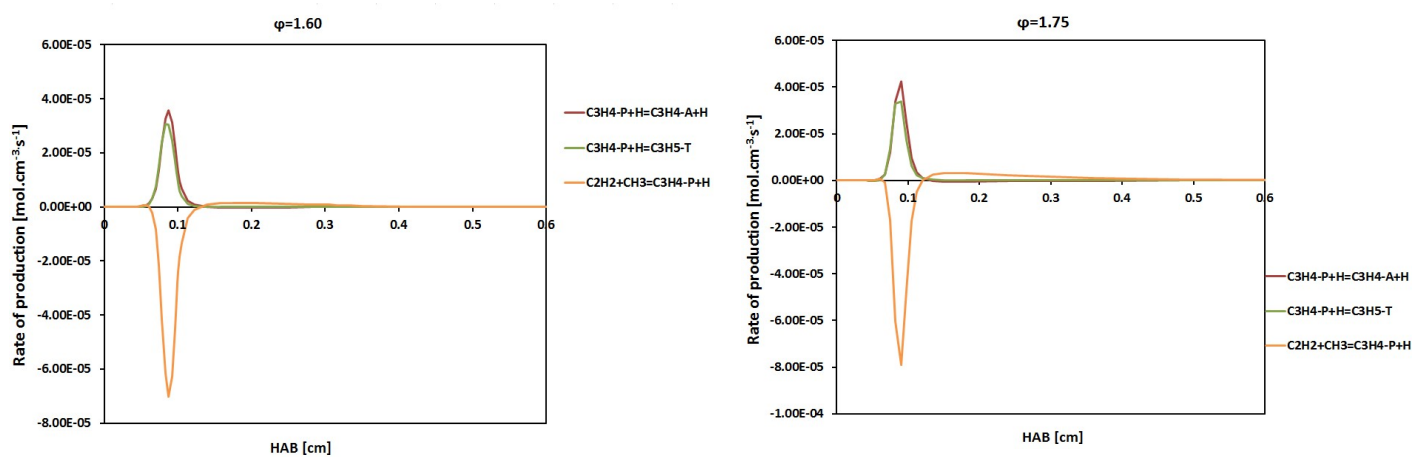
zone is reasonable. At higher distance from the burner surface  $\text{PC}_4\text{H}_9$  is no longer a main source of ethylene and is overtaken by ethyl radical, propene and HCCO contribution. At higher temperature ( $> 1500 \text{ K}$ ), ethyl radical is mainly produced by H abstraction from ethane,  $\text{C}_2\text{H}_6 + \text{H} = \text{C}_2\text{H}_5 + \text{H}_2$  (R160) and ethane is formed from methyl radical recombination,  $2\text{CH}_3 (+\text{M}) = \text{C}_2\text{H}_6 (+\text{M})$  (R52).

The reactions leading to ethylene consumption are mainly its reaction with H atom and methyl radical to yield vinyl radical, which is the main source of acetylene.



### Propyne formation/consumption

Figure 37 shows the main reactions involved in propyne formation and consumption. Propyne is mainly formed from allene ( $\text{C}_3\text{H}_4\text{-A}$ ) and from allyl radical ( $\text{C}_3\text{H}_5\text{-T}$ ).



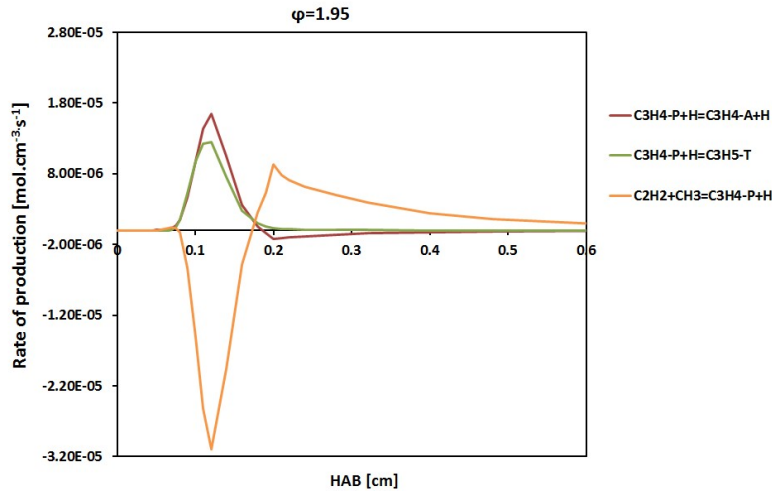


Figure 37 : Propyne rate of production analysis in the three n-butane premixed flames.

Allene is predominantly formed from propargyl radical ( $C_3H_3$ ) and from allyl radical ( $C_3H_5-A$ ):



The major source of allyl radicals ( $C_3H_5-A$ ) is propene,  $C_3H_6 + H = C_3H_5-A + H_2$  (R442). Propargyl radical is formed mainly from acetylene,  $C_2H_2 + CH_2 = C_3H_3 + H$  (R3713). It can be seen that reaction (R514) which produces propyne until  $HAB = 1.8$  mm, becomes a source of consumption to form back allene.

Propyne is mainly consumed to yield acetylene and methyl radical,  $C_2H_2 + CH_3 = C_3H_4-P + H$  (R525). Then the latter reaction starts to produce propyne at higher distance from the burner ( $HAB > 1.8$  mm) and becomes the major source of propyne in the burnt gas zone.

### Propene formation/consumption

Propene is mainly formed from  $SC_4H_9$  thermal decomposition and a contribution of allyl radical reaction with H atom:



It can be seen in Figure 38, that  $SC_4H_9$  starts to produce propene near the burner surface, due to  $SC_4H_9$  formation directly from the fuel decay. Beyond  $HAB=0.8$  mm, reaction (R700) is no longer the major pathway that lead to propene formation and is overtaken by reaction (R425), which involved allyl radical.



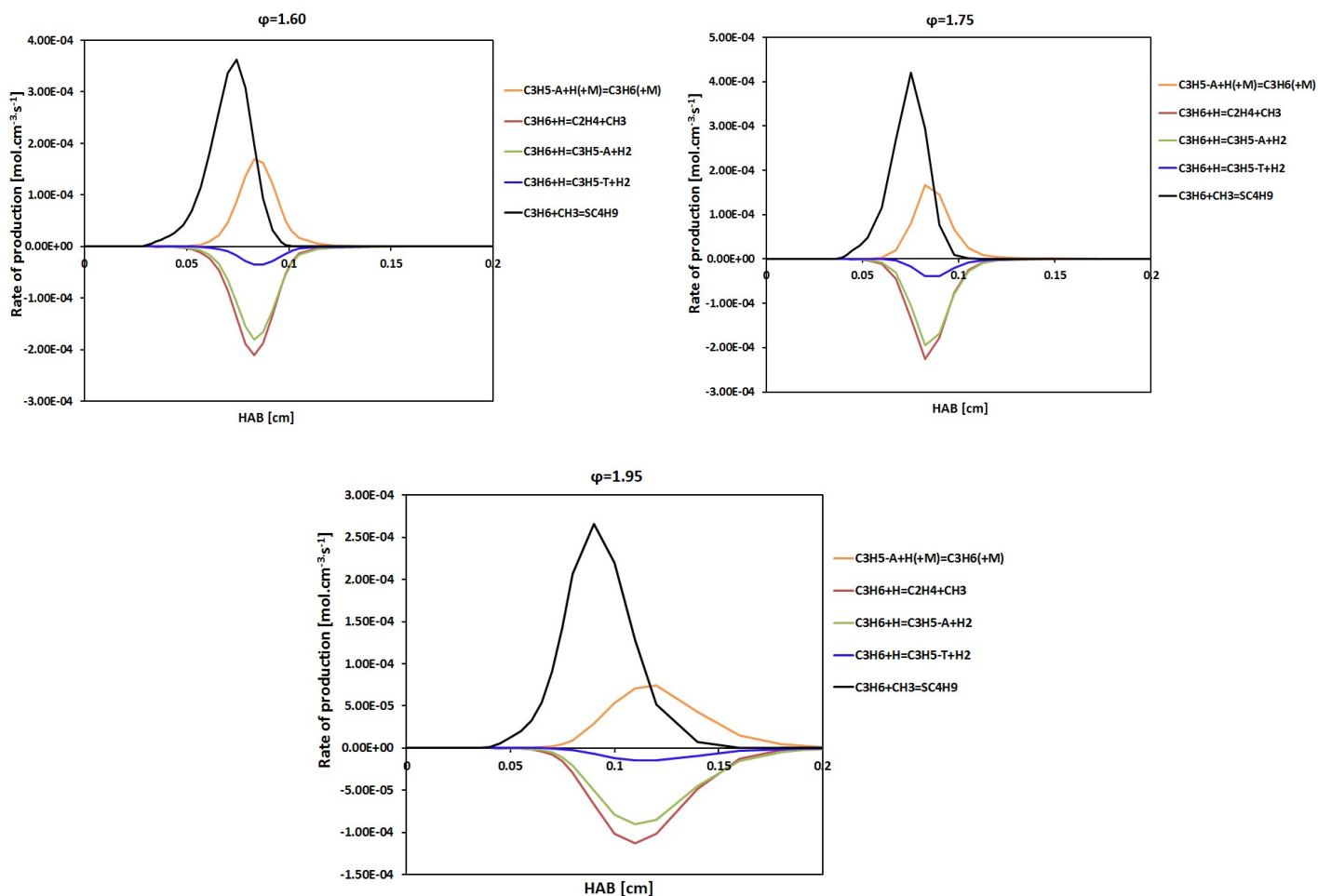
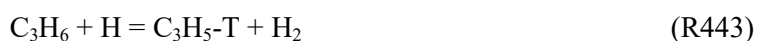


Figure 38 : Propene rate of production analysis in the three n-butane premixed flames.

Reactions involved in the propene consumption are:



It can be observed that allyl radical that is involved in propene production, contributes also to its consumption, indicating that the main source of propene is  $\text{SC}_4\text{H}_9$ .

### **Butadiene (but-1,3-diene) formation/consumption**

but-1,3-diene is mainly formed from  $\text{C}_4\text{H}_7$  radicals hydrogen loss and a light contribution of  $\text{C}_7\text{H}_{13}$  for the richest flame ( $\phi=1.95$ ) and cyclopentadienyl radical ( $\text{C}_5\text{H}_5$ ) for the flames at  $\phi=1.60$  and  $\phi=1.75$ .

The main reactions are presented in Figure 39:



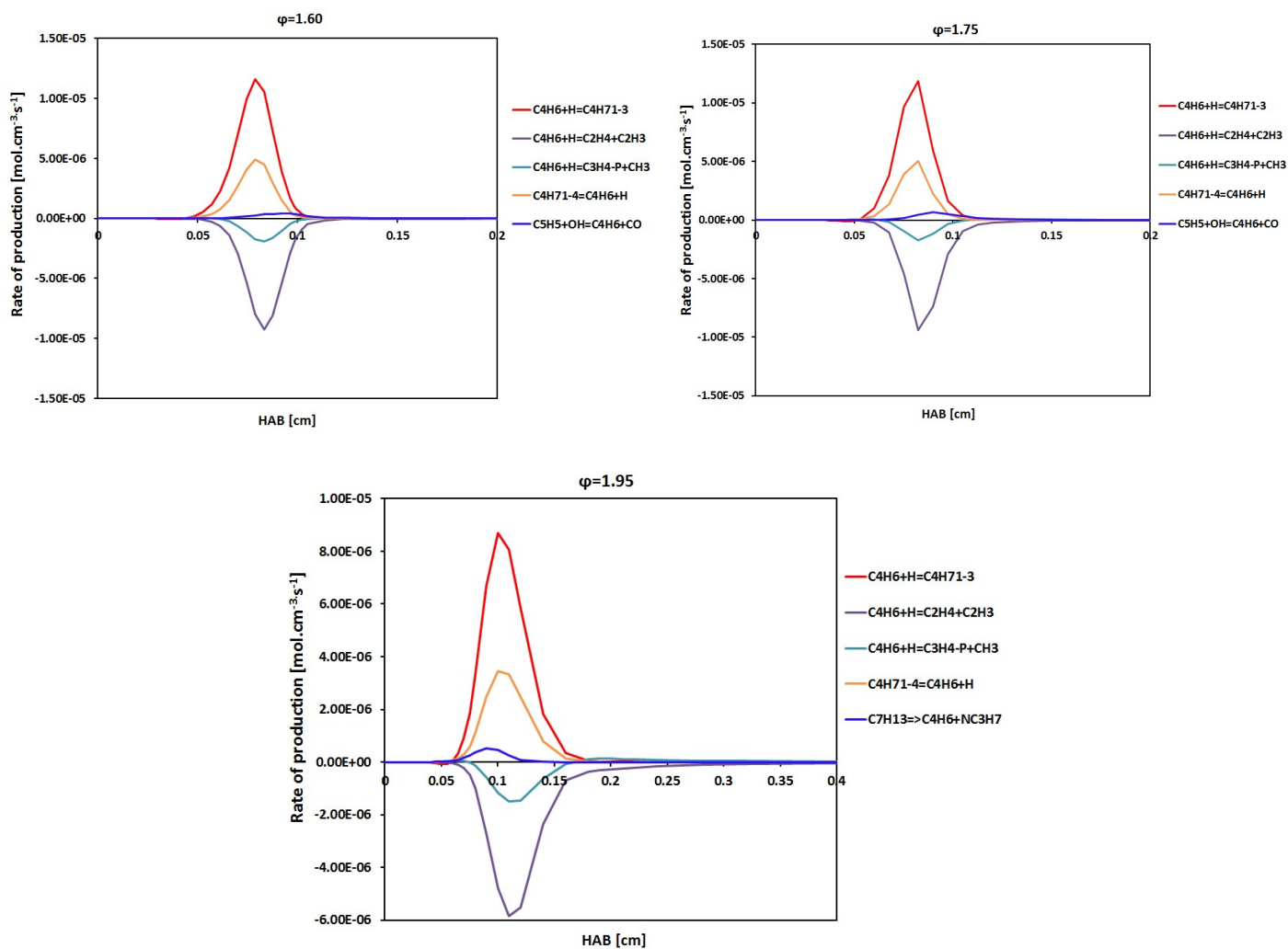


Figure 39 : But-1,3-diene rate of production analysis in the three n-butane premixed flames.

The species  $C_4H_71-3$  and  $C_4H_71-4$  are formed mainly from but-1-ene as follows:



But-1-ene is predominantly formed from allyl radical,  $C_3H_5-A + CH_3 (+M) = C_4H_8-1 (+M)$  (R469) and is consumed to yield  $C_4H_71-3$  (R712);  $C_4H_71-4$  (R713) and  $SC_4H_9$ ,  $C_4H_8-1 + H = SC_4H_9$  (R703).

But-1,3-diene also contributes to ethylene and propyne production, since they are mainly the but-1,3-diene consumption products:



## Vinylacetylene (C<sub>4</sub>H<sub>4</sub>) formation/consumption

As can be seen in Figure 40, the main reaction involved in vinylacetylene production is vinyl radical (C<sub>2</sub>H<sub>3</sub>) reaction with ethynyl (C<sub>2</sub>H) for the three n-butane flames:



Vinylacetylene is consumed mainly by H abstraction reactions and its oxidation by O atoms:

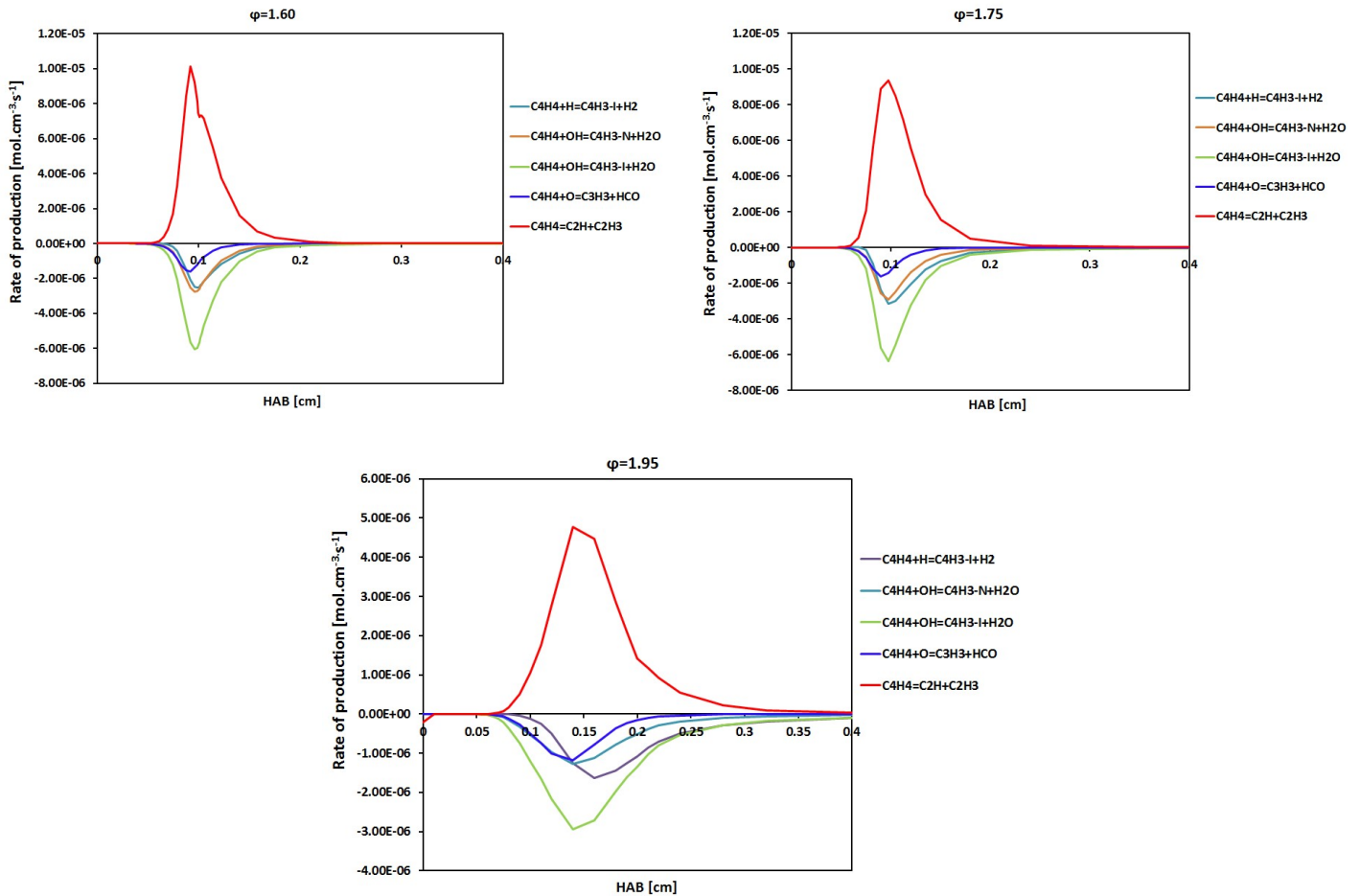
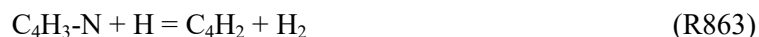


Figure 40 : Vinylacetylene rate of production analysis in the three n-butane premixed flames.

Reaction (R858) produces HCO that is found to be the major carbon monoxide precursor. The species C<sub>4</sub>H<sub>3</sub>-I and C<sub>4</sub>H<sub>3</sub>-N are found to be ones of acetylene and C<sub>4</sub>H<sub>2</sub> precursors:

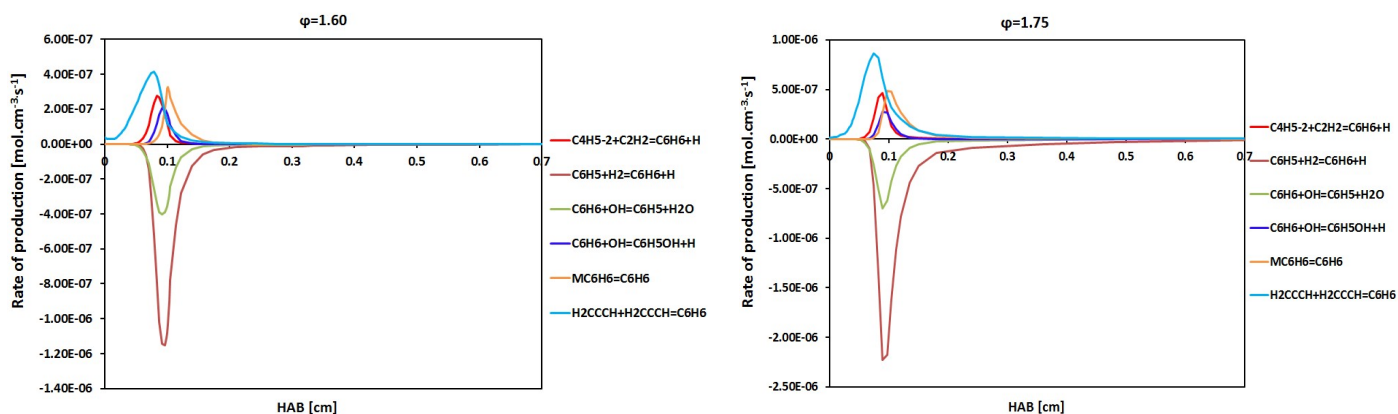




It is observed that the present kinetic model overpredicts by a factor of 10 vinylacetylene concentration in all the flames. The formation and consumption of this species must be examined in the future work, in order to propose more reliable kinetic model that accounts for such species good prediction.

### Benzene formation/consumption

As can be seen in Figure 41, the main reactions involved in benzene production in all the three flames are varied. It is observed that benzene formation starts near the burner surface by propargyl radical recombination. This reaction is followed by  $\text{C}_4/\text{C}_2$  pathway contribution, involving  $\text{C}_4\text{H}_5\text{-2}$  (2-butyn-1-yl radical) and acetylene and then, the significant contribution of phenol ( $\text{C}_6\text{H}_5\text{OH}$ ) and dimethylene cyclobutene ( $\text{MC}_6\text{H}_6$ ) in benzene production.



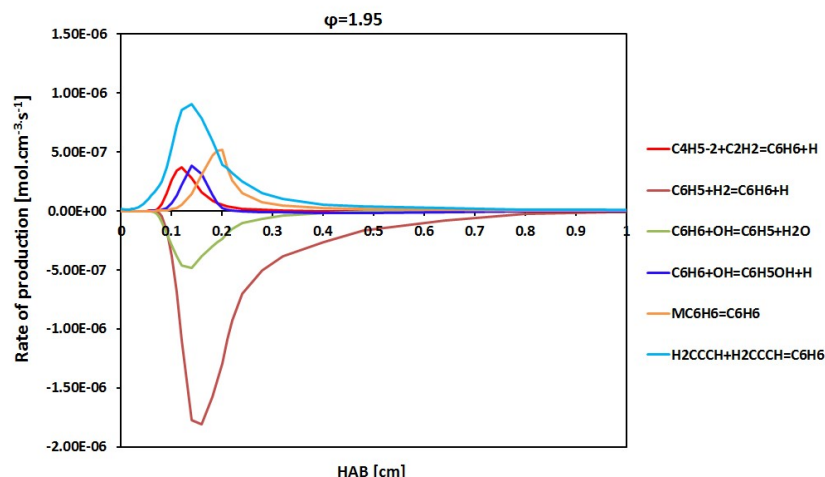


Figure 41 : Benzene rate of production analysis in the three n-butane premixed flames.

In the flame at  $\phi=1.60$ , the recombination reaction of propargyl radicals is predominant in benzene production until  $HAB = 1$  mm, then this reaction is overtaken by  $MC_6H_6$  isomerization at higher  $HAB$ . In contrast with this flame, reaction (R3755) remains mostly predominant in benzene production in the flames at  $\phi=1.75$  and  $\phi=1.95$ .

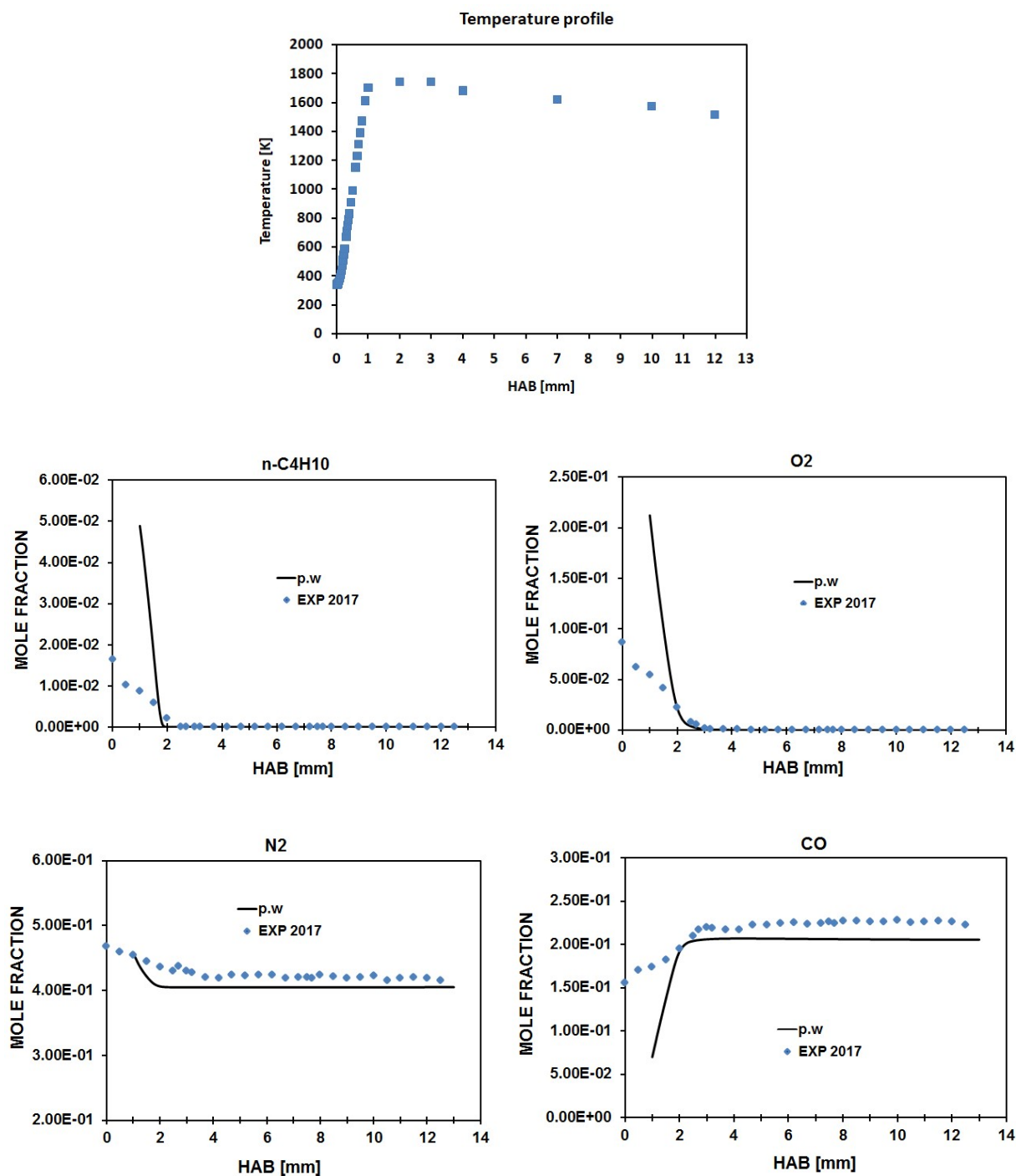
Propargyl radical is formed mainly from propyne, allene and acetylene,  $C_3H_4-P + H + H_2CCCH + H_2$  (R3753);  $C_3H_4-A + H + H_2CCCH + H_2$  (R3749);  $CH_2(S) + C_2H_2 = H_2CCCH + H$  (R3324). The species  $C_4H_5-2$  is mainly formed from cyclopentadiene reaction with methyl radical,  $C_4H_5-2 + C_2H_4 = C_5H_6 + CH_3$  (R817) and from 2-butyne H abstraction,  $C_4H_6-2 + H = C_4H_5-2 + H_2$  (R831).  $MC_6H_6$  is mainly formed from fulvene isomerization reaction,  $MC_6H_6 = FULVENE$  (R3329). Phenol ( $C_6H_5OH$ ) is predominantly produced from phenoxy radical reaction with H atom,  $C_6H_5O + H (+M) = C_6H_5OH (+M)$  (R3248). The main benzene consumption reactions involved H atom abstraction and oxidation by OH to yield phenyl radical.



The measured amount of benzene formed in the richest flame ( $\phi=1.95$ ) is three times higher than in  $\phi=1.75$  and nearly six times higher than in  $\phi=1.60$ . These observations are in line with the benzene rates of production obtained in each of the investigated flames.

#### 4.4.1.1.3. n-butane doped with n-propylbenzene flames

The enrichment of n-butane flames with n-propylbenzene has been proposed to assess the robustness of the present mechanism in order to capture gaseous soot precursors concentration profiles. n-butane flames have been doped with 20% of an aromatic species “n-propylbenzene”. The comparison between the measured mole fractions of species and the predicted ones are presented in Figure 42 and Figure 43.



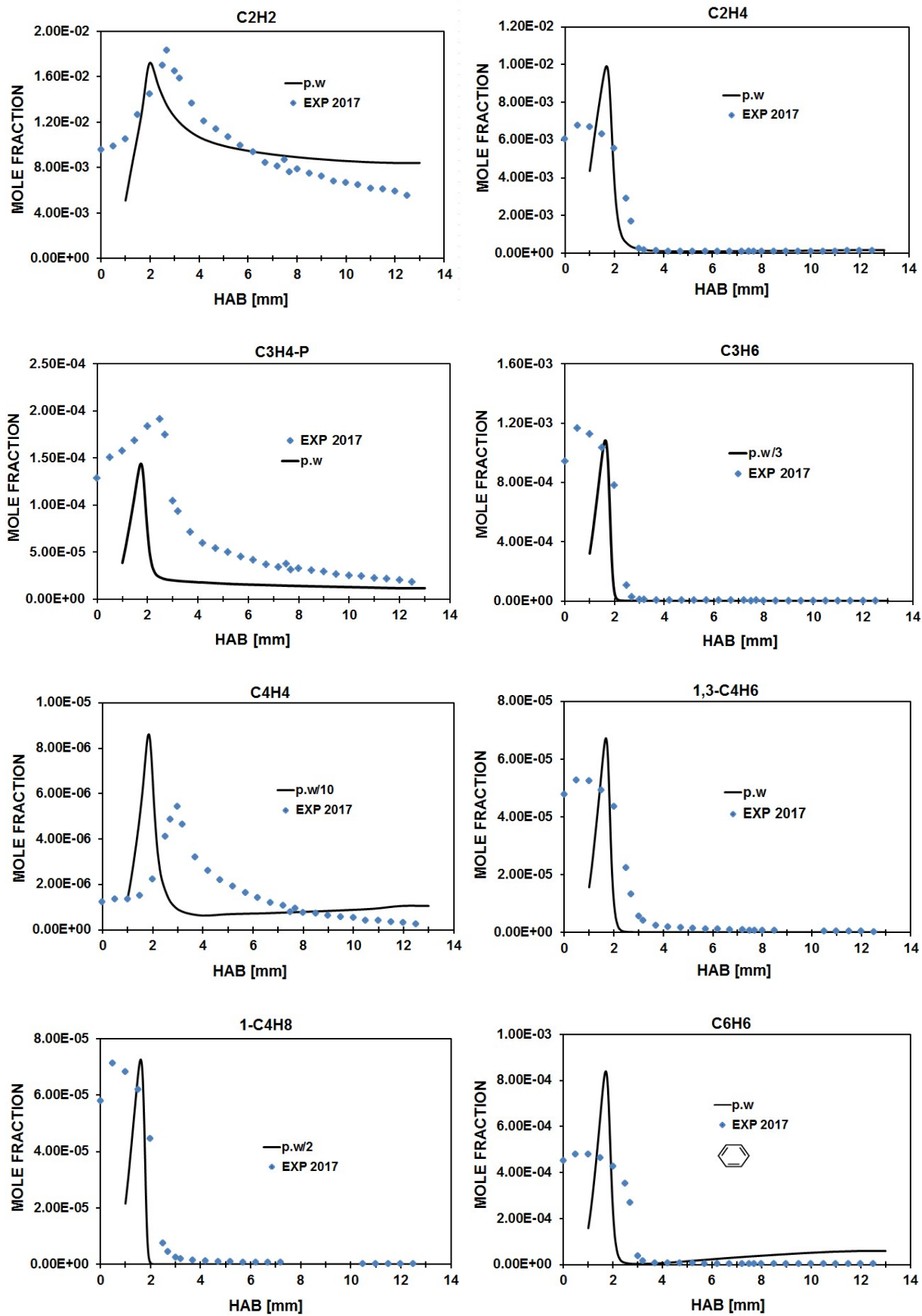
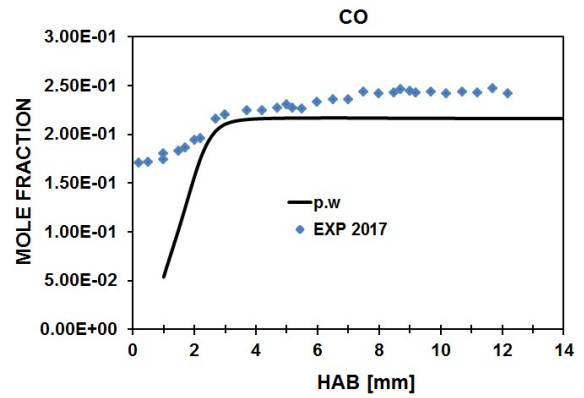
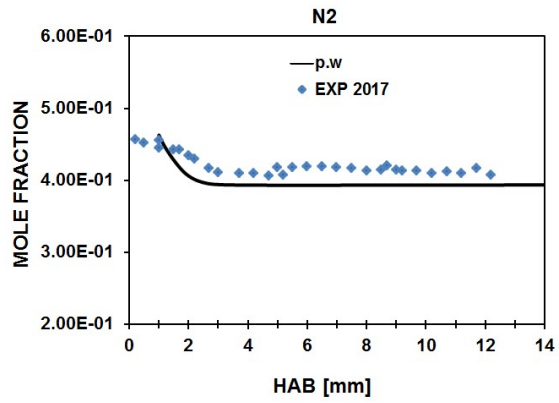
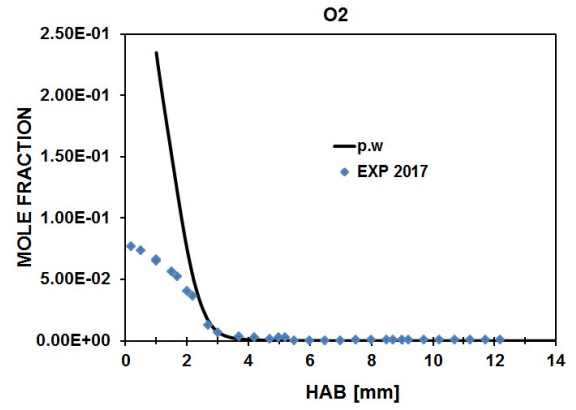
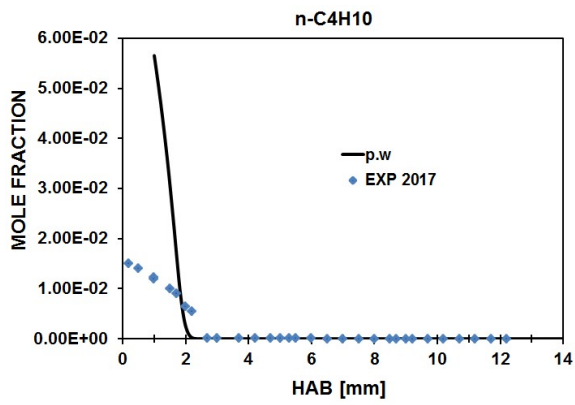
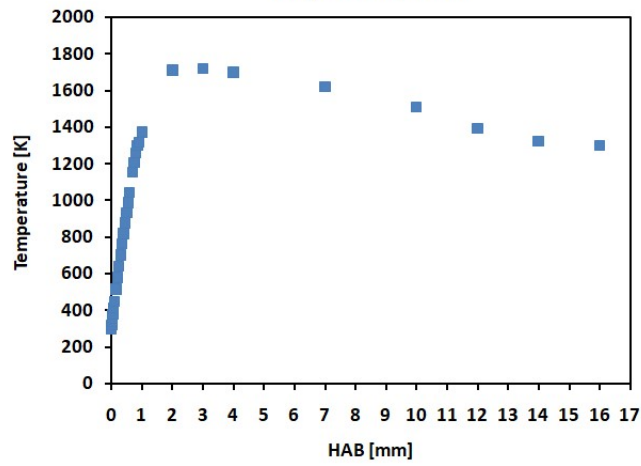


Figure 42 : Atmospheric n-butane/n-propylbenzene premixed flame,  $\phi=1.75$ : n-C<sub>4</sub>H<sub>10</sub> (6.69% in mol.)/n-C<sub>9</sub>H<sub>12</sub> (1.67%)/O<sub>2</sub> (36.32%)/N<sub>2</sub> (55.32%). Species mole fraction profiles. The symbols represent experimental data from [149]; the lines represent modeling results from the present work. p.w/10 denotes that the predictions are divided by 10.

Temperature profile





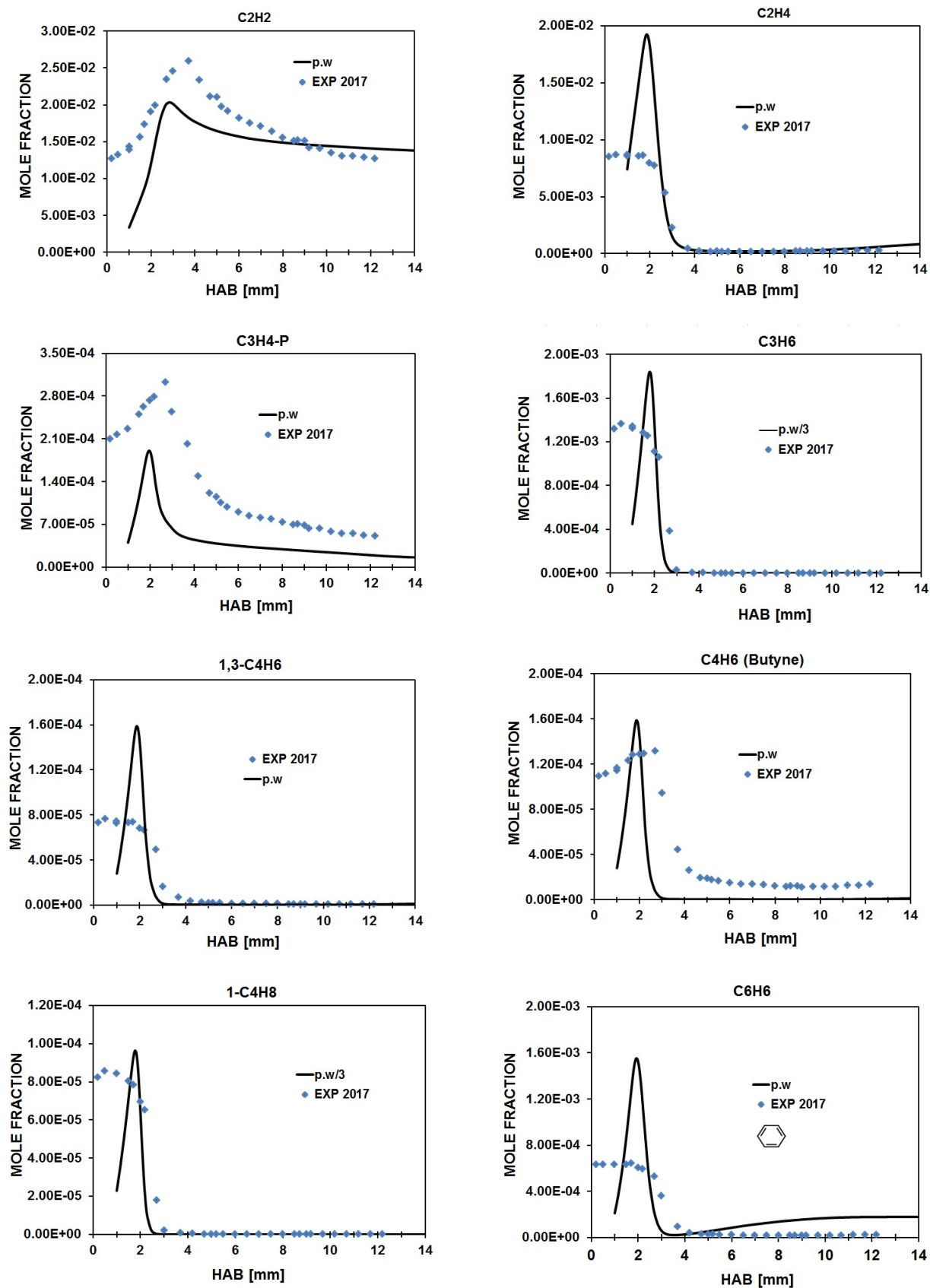


Figure 43 : Atmospheric n-butane/n-propylbenzene premixed flame,  $\phi=1.95$ : n-C<sub>4</sub>H<sub>10</sub> (7.30% in mol.)/n-C<sub>9</sub>H<sub>12</sub> (1.82%)/O<sub>2</sub> (35.56%)/N<sub>2</sub> (55.32%). Species mole fraction profiles. The symbols represent experimental data from [149]; the lines represent modeling results from the present work. p.w/10 denotes that the predictions are divided by 10.

Much better results between measurements and computations are obtained with the addition of an aromatic compound to a paraffinic one. That is understandable since n-propylbenzene is a part of the base mechanism and such improvements are due to its chemistry that is well represented. As a reminder, the present mechanism is composed of 5 sub-sets: C<sub>0</sub>-C<sub>6</sub>, iso-octane, n-decane, n-propylbenzene and PAHs.

In the flame at  $\varphi=1.75$  as well as in  $\varphi=1.95$ , some key species such as acetylene and benzene concentration profiles are satisfactorily represented. The other important species such as ethylene, propyne, propene, but-1,3-diene and but-1-ene are also fairly represented within uncertainties of a factor of 2. Large discrepancies are obtained for vinylacetylene (C<sub>4</sub>H<sub>4</sub>) within a factor of 10.

### - Rate of production/consumption Analysis

#### n-butane

In the n-butane/n-propylbenzene mixture premixed flame, n-butane decays as in the previous discussions on 100% n-butane flames. The addition of n-propylbenzene shows any impact.

#### n-propylbenzene

As can be seen in Figure 44, n-propylbenzene (PBZ) decays to form mainly benzyl radical (PHCH<sub>2</sub>) and ethyl radical.

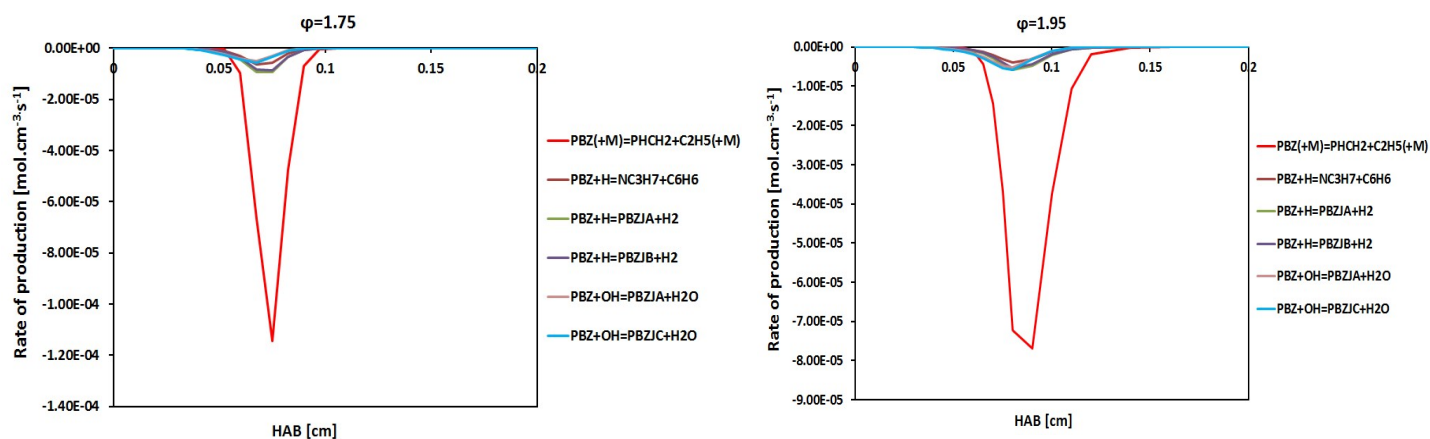


Figure 44 : n-propylbenzene decay pathways in n-butane/n-propylbenzene flames.

The H atom abstraction reactions from n-propylbenzene as well as the oxidation by OH are found to be neglected with respect to reaction (R3509) in the HAB range of 0.5-1 mm. However, these

reactions are found much important near the burner surface ( $HAB < 0.5$  mm), where n-propylbenzene reaction with OH and H atom lead to phenyl propyl radicals formation.



It worth noting that n-propylbenzene reaction with H atom at that zone starts to from benzene and n-propyl radical formation,  $PBZ + H = NC_3H_7 + C_6H_6$  (R3518). The increase of equivalence from 1.75 to 1.95 lead to a broaden reaction zone as for 100% n-butane flames.

### Acetylene formation/consumption

As for n-butane flames, acetylene formation is dominated by vinyl radical hydrogen loss in both flames  $\phi=1.75$  and  $\phi=1.95$  (Figure 45). This reaction is followed by propyne decay contribution. In contrast to 100% n-butane flames, an additional pathway that leads to acetylene production is observed. In fact, cyclopentadienyl radical decays to yield acetylene and propargyl radical. The main reactions involved in acetylene production are:

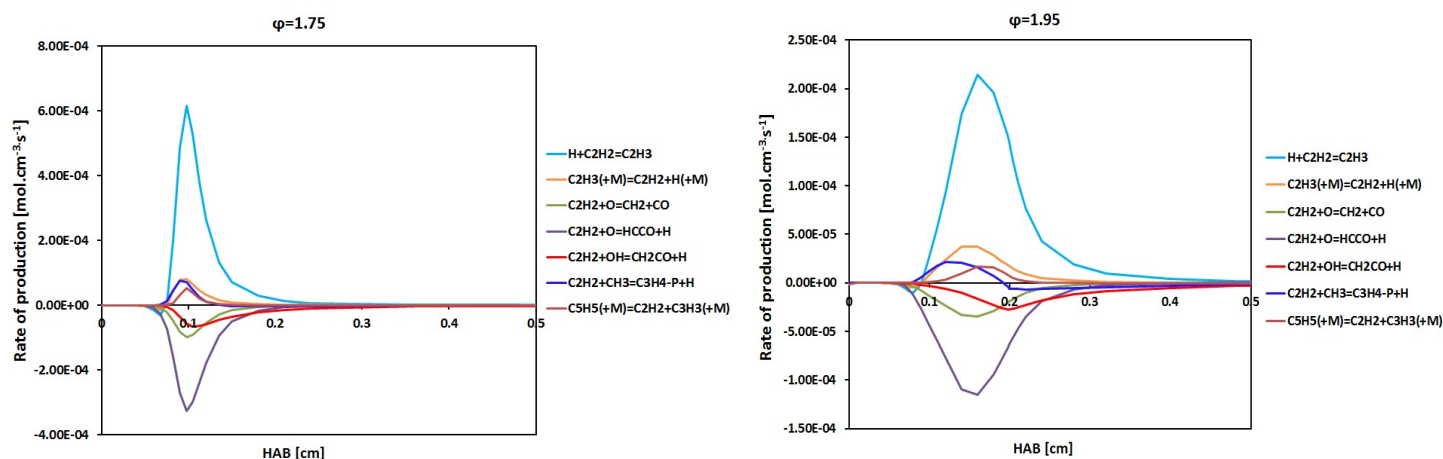
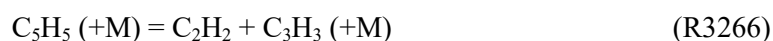


Figure 45 : Acetylene rate of production analysis in n-butane/n-propylbenzene premixed flames.

It can be observed that near the burner surface, vinyl radical consumed first acetylene produced by propyne and cyclopentadienyl. Then, this reaction starts to produce (at HAB=0.65 mm) and remains the most important acetylene source. Reaction (R525) that produces acetylene until HAB=2 mm, becomes a consumption pathway at higher HAB for the richest flame. Cyclopentadienyl radical is mainly formed from phenoxy decay,  $C_6H_5O = CO + C_5H_5$  (R3250) and from cyclopentadiene ( $C_5H_6$ ) H atom abstraction reaction,  $C_5H_6 + H = C_5H_5 + H_2$  (R3258). Cyclopentadiene is mainly formed from phenol decomposition,  $C_6H_5OH = C_5H_6 + CO$  (R3249). Reactions involved in acetylene consumption are similar to those involved in the previous 100% n-butane flames. Acetylene consumption is dominated by HCCO formation,  $C_2H_2 + O = HCCO + H$  (278).

### Ethylene formation/consumption

The main reactions involved in ethylene formation and consumption in these flames are similar to those of 100% n-butane flames previously discussed.

### Propene formation/consumption

As can be seen in Figure 46, reactions involved in propene production and consumption are similar to those previously discussed in 100% n-butane flames. However, it is observed that an additional pathway leading to propene production appears in the n-butane/n-propylbenzene mixture flames:

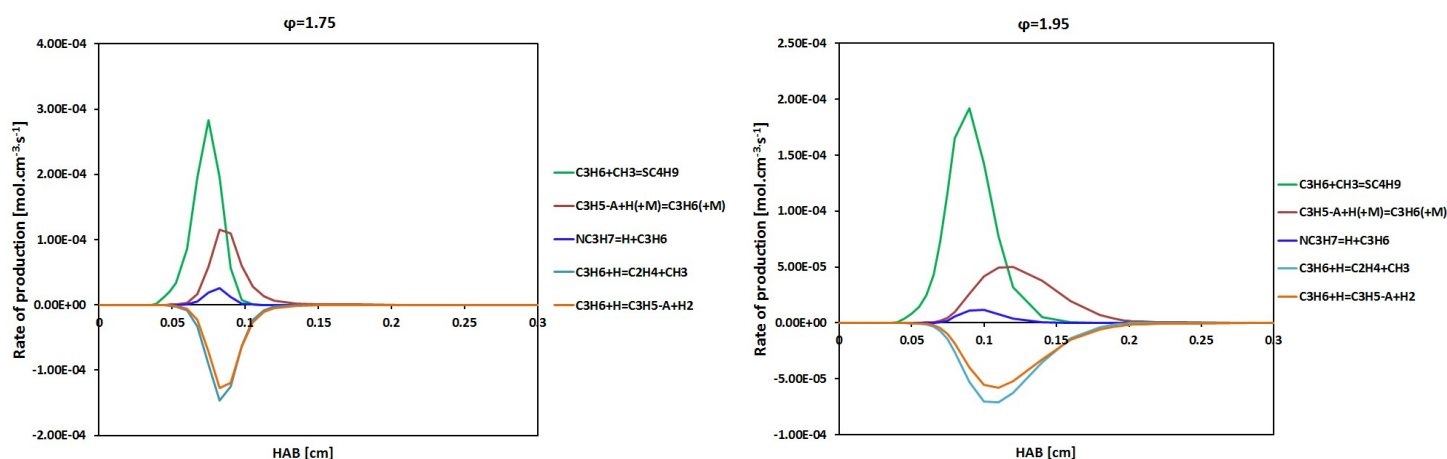


Figure 46 : Propene rate of production analysis in n-butane/n-propylbenzene premixed flames.

The modest contribution of n-propyl ( $NC_3H_7$ ) to propene production in these flames is understandable due to the addition effect of n-propylbenzene in n-butane. It was observed that n-propylbenzene

produce earlier (near the burner surface) n-propyl and benzene (see Figure 44). In 100% n-butane flames, the main source of propene is found to be  $SC_4H_9$ , which is directly formed from n-butane hydrogen loss.

### Propyne formation/consumption

As shown in Figure 47 and as for neat n-butane flames, propyne is mainly produced from allene, allyl radical and an additional pathway which is propargyl radical reaction with H atom.



In the flame at  $\phi=1.75$ , reaction (R529) is only a source of propyne production, while in the richest flame ( $\phi=1.95$ ), the reverse of this reaction takes place at about  $HAB = 2.3$  mm to consume propyne.

Propargyl is mainly formed from cyclopentadiene and cyclopentadienyl radical:

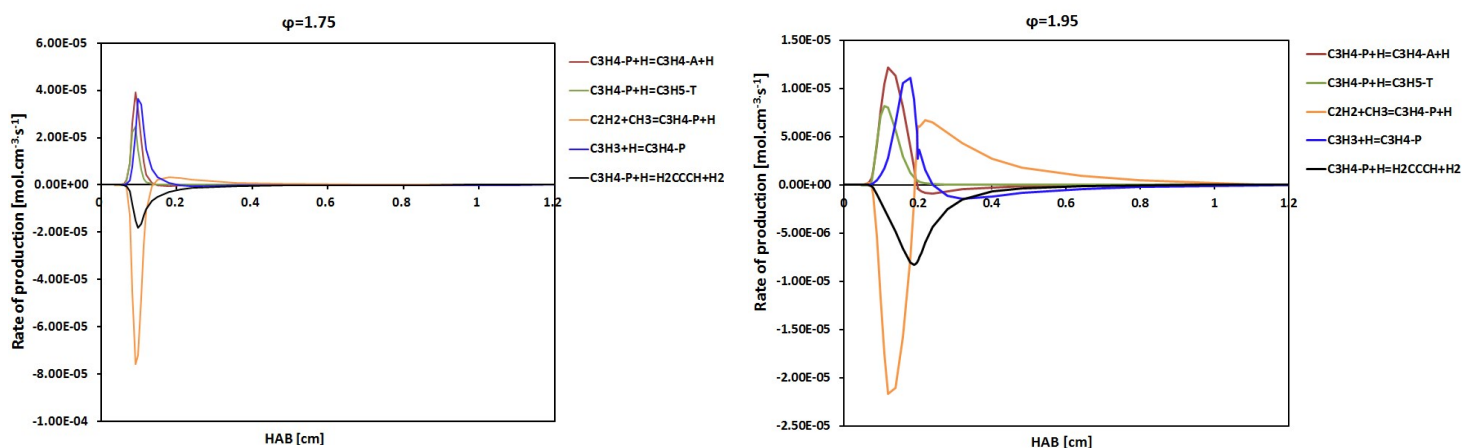
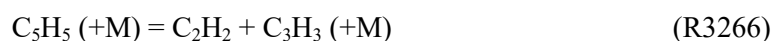


Figure 47 : Propyne rate of production in n-butane/n-propylbenzene premixed flames.

As for neat n-butane flames, similar reactions that consumed propyne are observed. This consumption is dominated by acetylene and methyl radical formation.

### But-1,3-diene formation/consumption

As shown in Figure 48, reactions involved in but-1,3-diene formation are similar to those observed in neat n-butane flames, where cyclopentadienyl radical contribution was found negligible with respect to those of  $C_4H_7$ 1-3 and  $C_4H_7$ 1-4. In the n-butane/n-propylbenzene flames,  $C_4H_7$ 1-3 and  $C_4H_7$ 1-4 are found to be butadiene major precursors in lower HAB zone, while  $C_5H_5$  reaction route is predominant in higher HAB zone, starting from 0.9 mm for  $\phi=1.75$  and about 1.3 mm for  $\phi=1.95$ . The addition of

n-propylbenzene has significantly increased the contribution of cyclopentadienyl in producing but-1,3-diene, since this latter is mainly produced from phenoxy radical and n-propylbenzene is a major source of aromatic production in such conditions. As for neat n-butane flames, but-1,3-diene is mainly consumed to form ethylene and propyne.

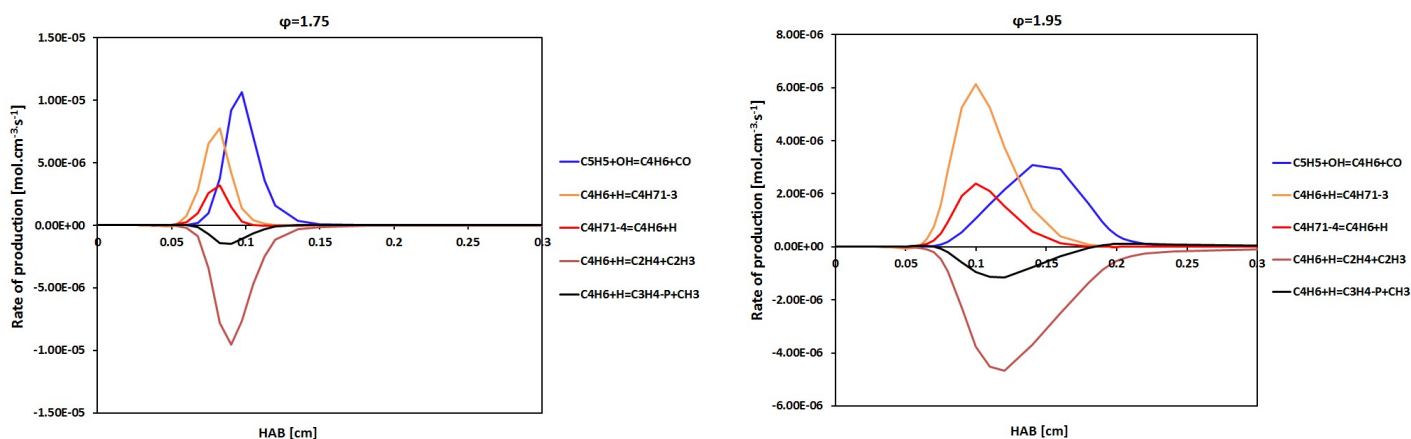


Figure 48 : But-1,3-diene rate of production analysis in n-butane/n-propylbenzene premixed flames.

### Benzene formation/consumption

As can be seen in Figure 49, benzene formation pathways in neat n-butane flames and n-butane/n-propylbenzene mixtures are completely different. It was observed previously that benzene production is dominated by  $C_3$  species recombination reactions in neat n-butane flames. The only aromatic species observed in benzene formation was phenol contribution. In n-butane/n-propylbenzene mixtures, benzene production is dominated by aromatic species H atom abstraction by H. the main reactions involved in benzene production are:



It can be seen that propargyl radicals,  $\text{MC}_6\text{H}_6$  and  $\text{C}_4/\text{C}_2$  reaction routes are no longer important in these flames. The effect of n-propylbenzene addition is clearly observed and induces large modifications to species such as benzene formation pathways with respect to neat n-butane. Toluene is mainly formed from benzyl radical, which is initially produced from n-propylbenzene,  $\text{PHCH}_2 + \text{H}$

(+M) = TOLUEN (+M) (R3383). Biphenyl is mainly formed from benzyl reaction with cyclopentadienyl radical,  $C_5H_5 + PHCH_2 \Rightarrow BIPHENYL + 2H$  (R4514).

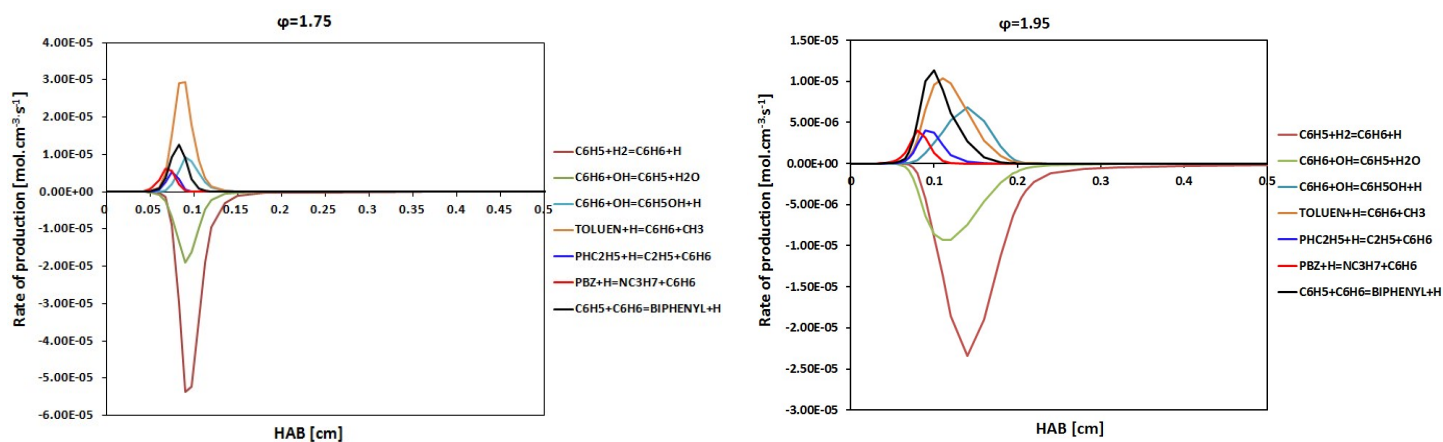
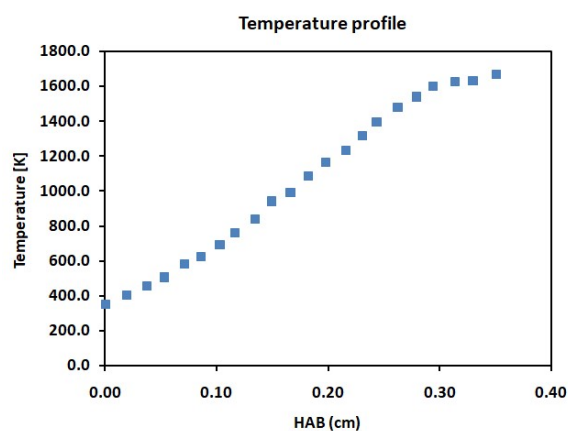


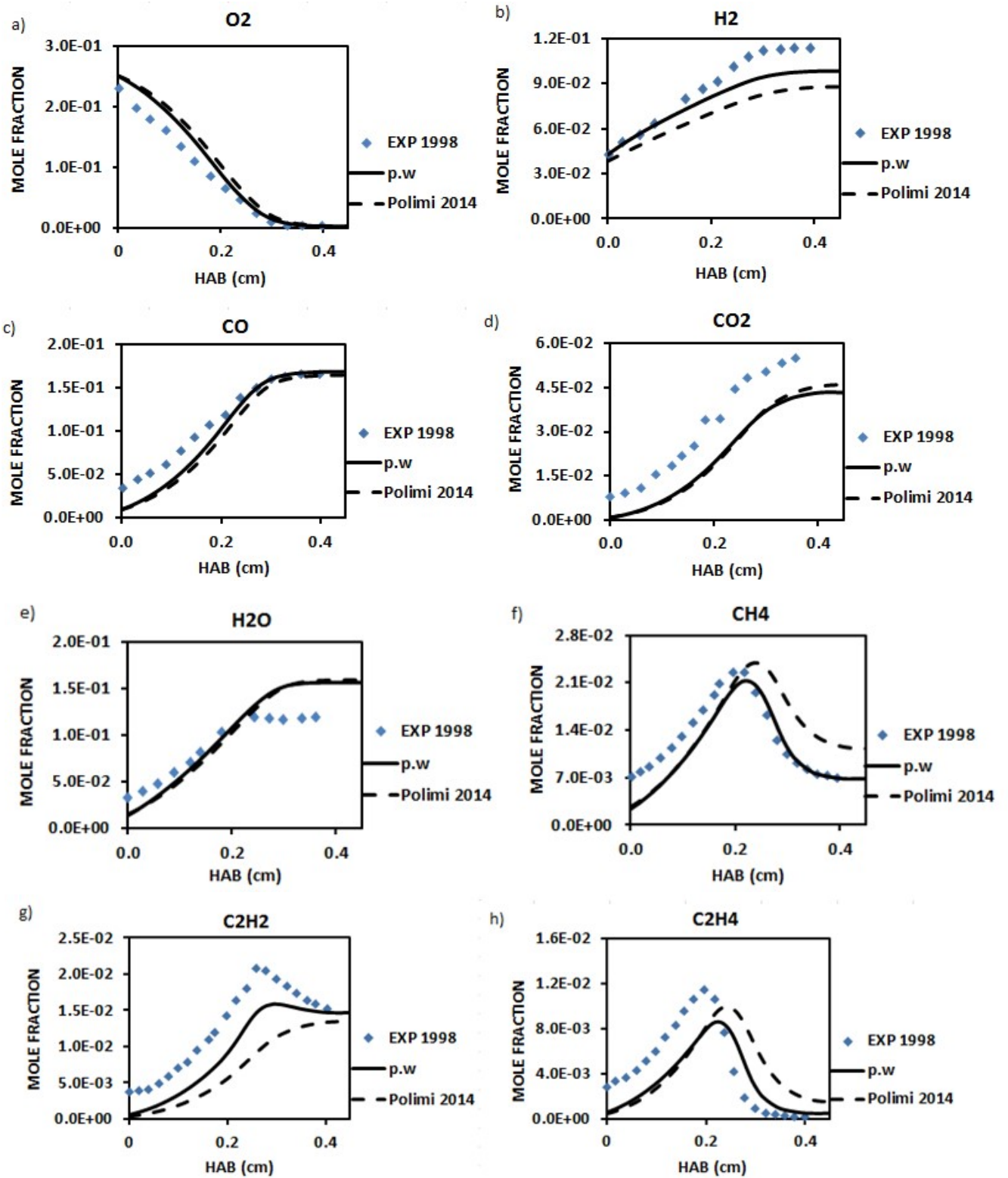
Figure 49 : Benzene rate of production analysis in n-butane/n-propylbenzene premixed flames.

As for neat n-butane flames, benzene is mainly consumed to form phenyl radical by H atom abstraction and its oxidation by OH.

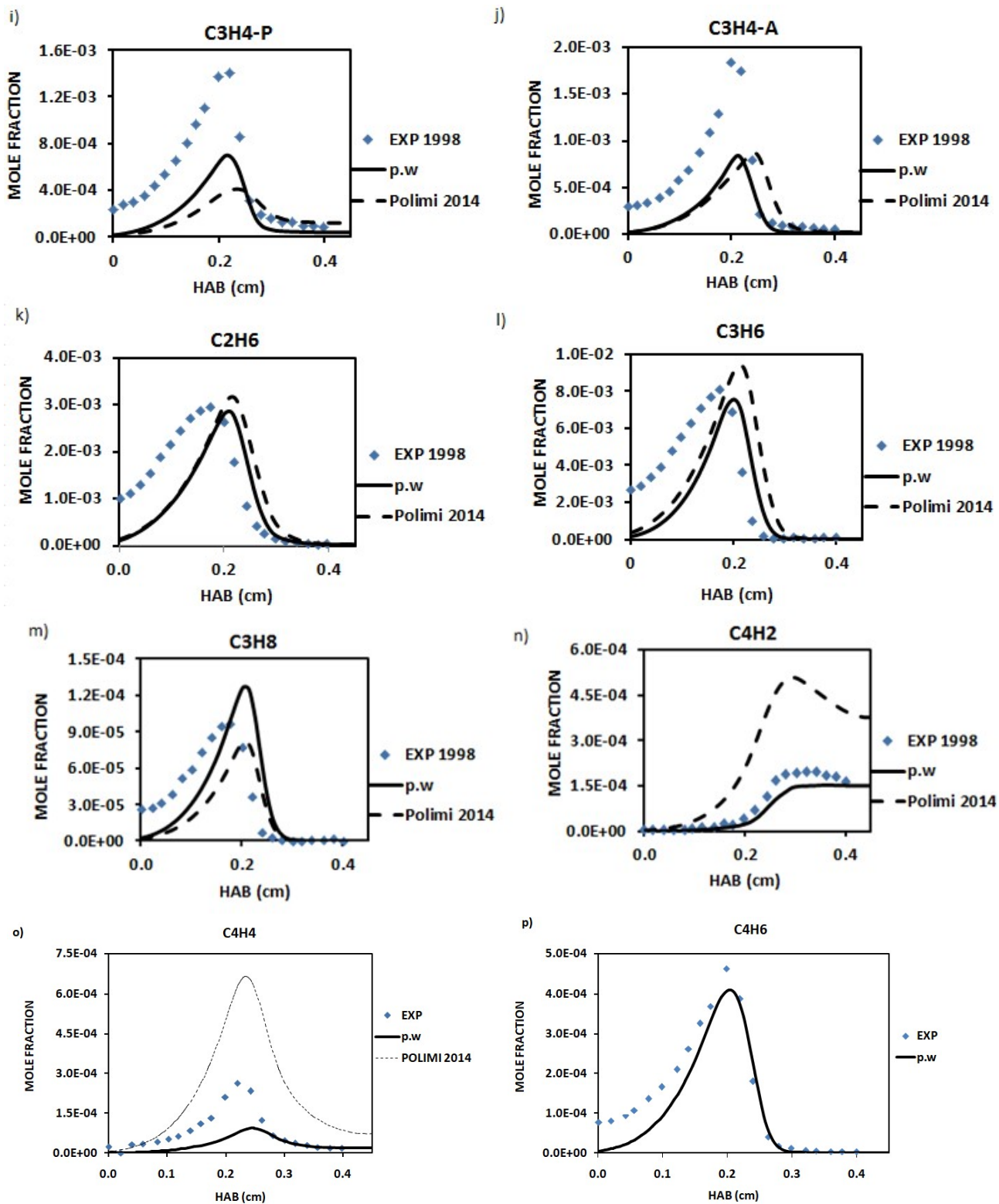
#### 4.4.1.1.4. Iso-octane flame

Iso-octane is an important component of gasoline fuels and is also a key component used in gasoline surrogates to investigate the combustion characteristics of commercial gasoline. The atmospheric pressure iso-octane premixed flame ( $\phi=1.9$ ) has been modeled to assess the performance of the kinetic model that is expected to mimic the combustion behavior of gasoline. As a main subset of the present mechanism, it is crucial to model iso-octane combustion in order to determine the acceptable deviation of the kinetic model. In Figure 50, model predictions are compared with measurements.









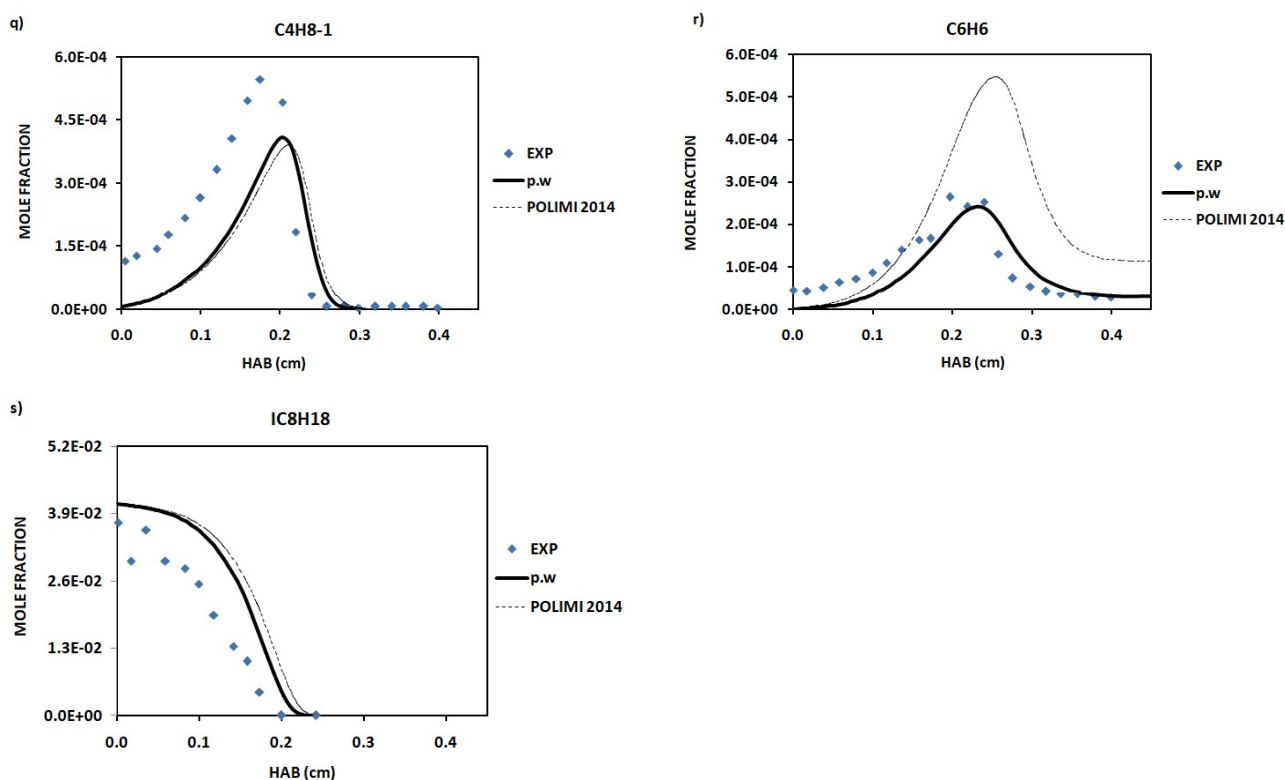


Figure 50 : Atmospheric pressure iso-octane laminar premixed flame :  $iC_8/O_2/N_2$  : 0.0423/0.278/ in mole fraction;  $\phi=1.9$  ;  $V=5.26 \times 10^{-3}$  g/cm<sup>2</sup>/s ; Predicted and experimental mole fraction of a): oxygen, b): hydrogen, c): carbon monoxide, d): carbon dioxide, e): water, f): methane, g): acetylene, h): ethylene, i): propyne, j): allene, k): ethane, l): propene, m): propane, n): diacetylene, o): vinylacetylene, p): 1,3-butadiene, q): but-1-ene, r): benzene, s): iso-octane. The symbols represent experimental data from [151]; the continuous lines represent the modeling results from the present work; dashed lines: Polimi mechanism [128].

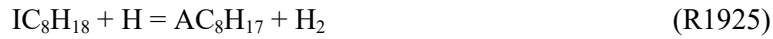
Computations from the present kinetic mechanism clearly show a good agreement with measurements. The small key species measured such as methane, acetylene, ethylene, ethane, allene, propene, propene, diacetylene and vinylacetylene are well represented within a factor of 2. Polimi mechanism [128] shows similar results for all the species. As iso-octane is one of the surrogate component and an important sub-set in the present mechanism, it is crucial to identify the robustness of this sub-set and the above results obtained clearly determine the iso-octane sub-mechanism performance in a rich atmospheric pressure premixed flame.

#### - Rate of production/consumption Analysis

##### Iso-octane decay pathways:

The main reactions involved in the iso-octane decay are those of H atom abstraction by H to yield iso-octyl radicals and its thermal decomposition to form heptyl ( $YC_7H_{15}$ ) and methyl radicals as well as T-butyl and iso-butyl radicals.

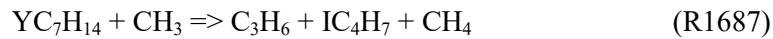
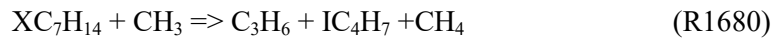




At a HAB=0.2 cm corresponding to a temperature of 1163 K and the position where iso-octane is highly consumed in the reaction zone, reaction (R1921) is predominant, followed by the H abstraction reactions, (R1925), (R1927), (R1926).

### Methane formation/consumption

The main reactions involved in methane formation are presented in Figure 51:



Methane formation is dominated by reaction (R54) from the burner surface to a HAB=0.27 cm. This reaction is also the main pathway of methane consumption to form methyl radical, starting from a HAB=0.27 cm. Then, methane production is dominated by ethylene contribution (R257) from HAB=0.27 cm to the burnt gas zone.

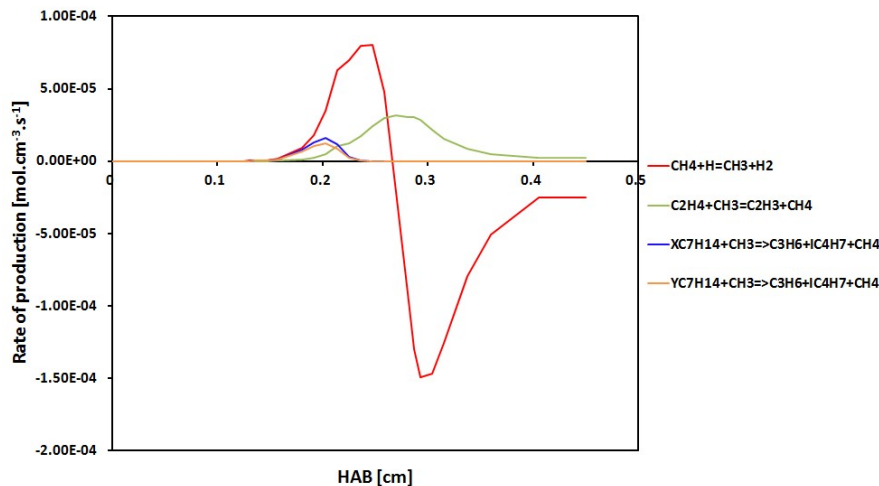


Figure 51 : Methane rate of production in a rich iso-octane premixed flame.

### Acetylene formation/consumption

As can be seen in Figure 52, acetylene formation is initiated by H addition on propyne. Vinyl radical becomes the main source of acetylene at higher HAB.

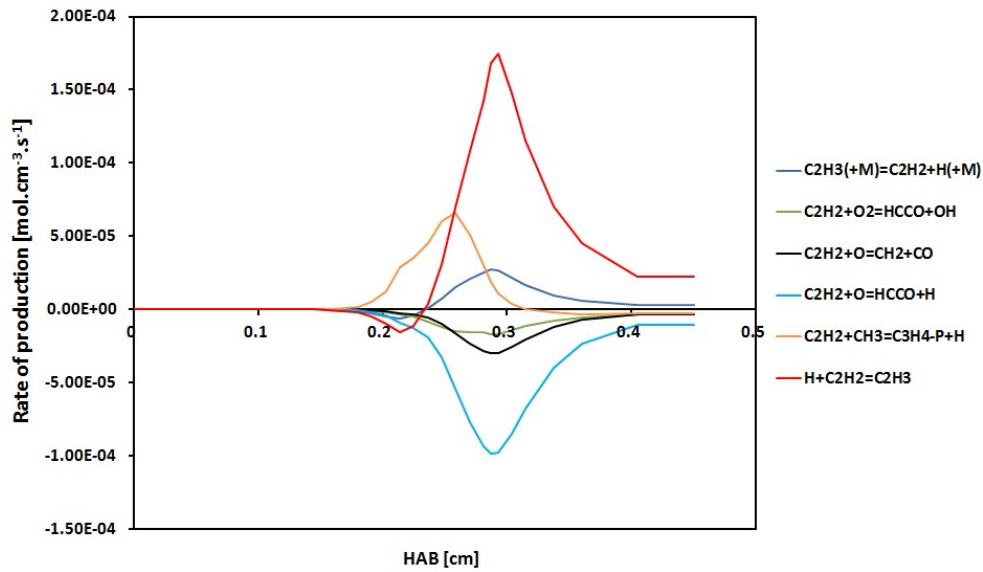


Figure 52 : Acetylene rate of production in a rich iso-octane premixed flame.

It can be seen that reactions (R3768) and (R267) firstly consume acetylene near the burner surface (lower HAB) before starting to its production at HAB=0.23 cm. As discussed previously in the n-butane flames, acetylene is mainly consumed to form HCCO and methylene ( $\text{CH}_2$ ).



### Ethylene formation/consumption

Ethylene formation is dominated near the burner surface by propene reaction with H atom. At higher HAB, ethyl radical decomposition and HCCO reaction with methyl radical are the main sources of ethylene (Figure 53).





Ethylene is mainly consumed to form vinyl radical ( $\text{C}_2\text{H}_3$ ) through H atom abstraction and oxidation by OH. Ethylene is also found to contribute to HCO production, which the main carbon monoxide precursor.

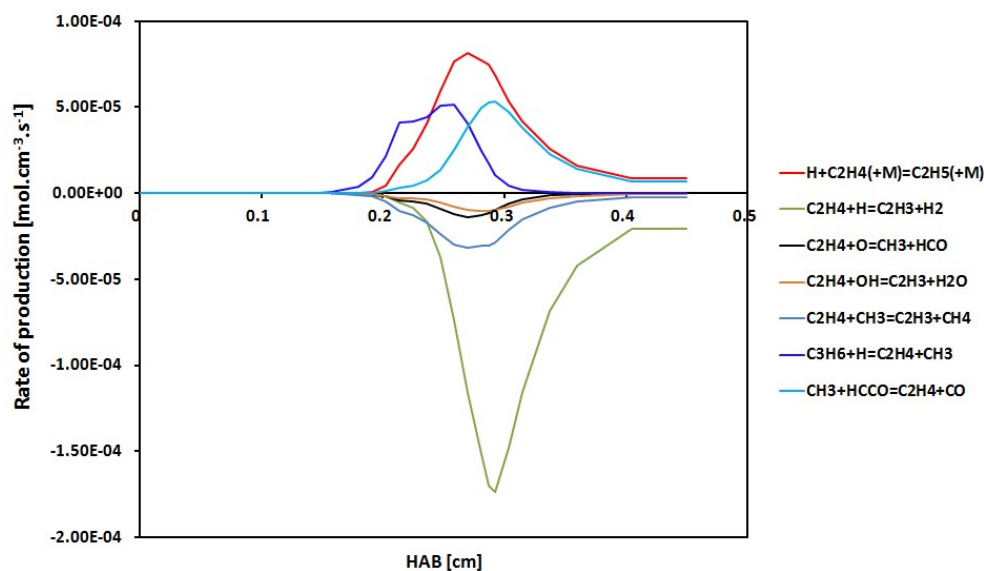


Figure 53 : Ethylene rate of production in a rich iso-octane premixed flame.

### Propene formation/consumption

As shown in Figure 54, propene is mainly produced from iso-propyl radical, followed by the contributions of iso-butyl and iso-butene.



Iso-propyl ( $\text{IC}_3\text{H}_7$ ) is mainly formed from propane decomposition reaction,  $\text{H} + \text{C}_3\text{H}_8 = \text{H}_2 + \text{IC}_3\text{H}_7$  (R382).  $\text{IC}_4\text{H}_9$  formed from the fuel (iso-octane) governs  $\text{IC}_4\text{H}_8$  formation by H elimination.

In this flame, the main products formed from propene consumption are found to be ethylene and allyl radical.

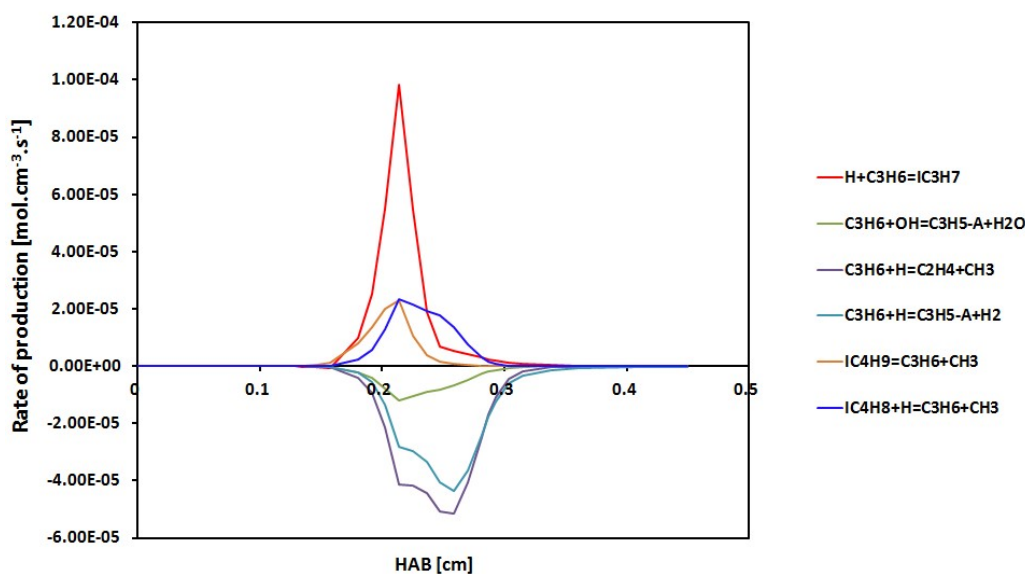


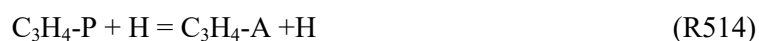
Figure 54 : Propene rate of production in a rich iso-octane premixed flame.

### Propyne formation/consumption

As for n-butane flames, the main reaction involved in propyne are allene (R514) and allyl radical ( $\text{C}_3\text{H}_5\text{-T}$ ) (R515). Propyne is mainly consumed to form acetylene (R525) and propargyl radical (R3753). Reaction (R525) that initially consumes propyne is found to be the major source of propyne at the burnt gas zone.

### Allene ( $\text{C}_3\text{H}_4\text{-A}$ ) formation/consumption

Allene is found to be mainly formed from  $\text{IC}_4\text{H}_7$ ,  $\text{IC}_4\text{H}_7 = \text{C}_3\text{H}_4\text{-A} + \text{CH}_3$  (R1274).  $\text{IC}_4\text{H}_7$  is predominantly formed from iso-butene ( $\text{IC}_4\text{H}_8$ ). The reactions involved in its consumption are mainly propyne production, followed by a minor production of propargyl radical, allyl radical and acetylene.





The reverse of reaction (R504) is observed at higher HAB as allene formation pathway in the burnt gas zone (starting from HAB=0.23 cm).

### **But-1,3-diene (C<sub>4</sub>H<sub>6</sub>) formation/consumption**

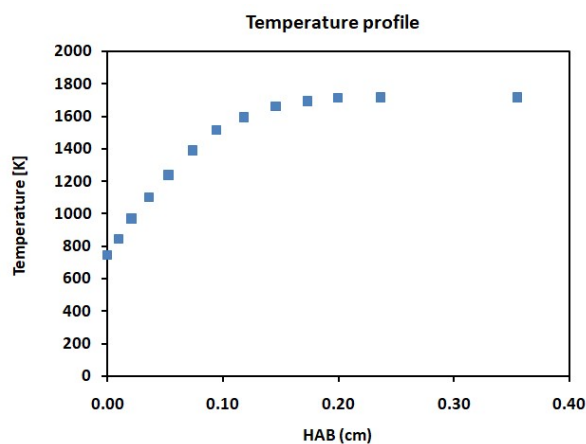
The main reactions involved in 1,3 butadiene formation are:

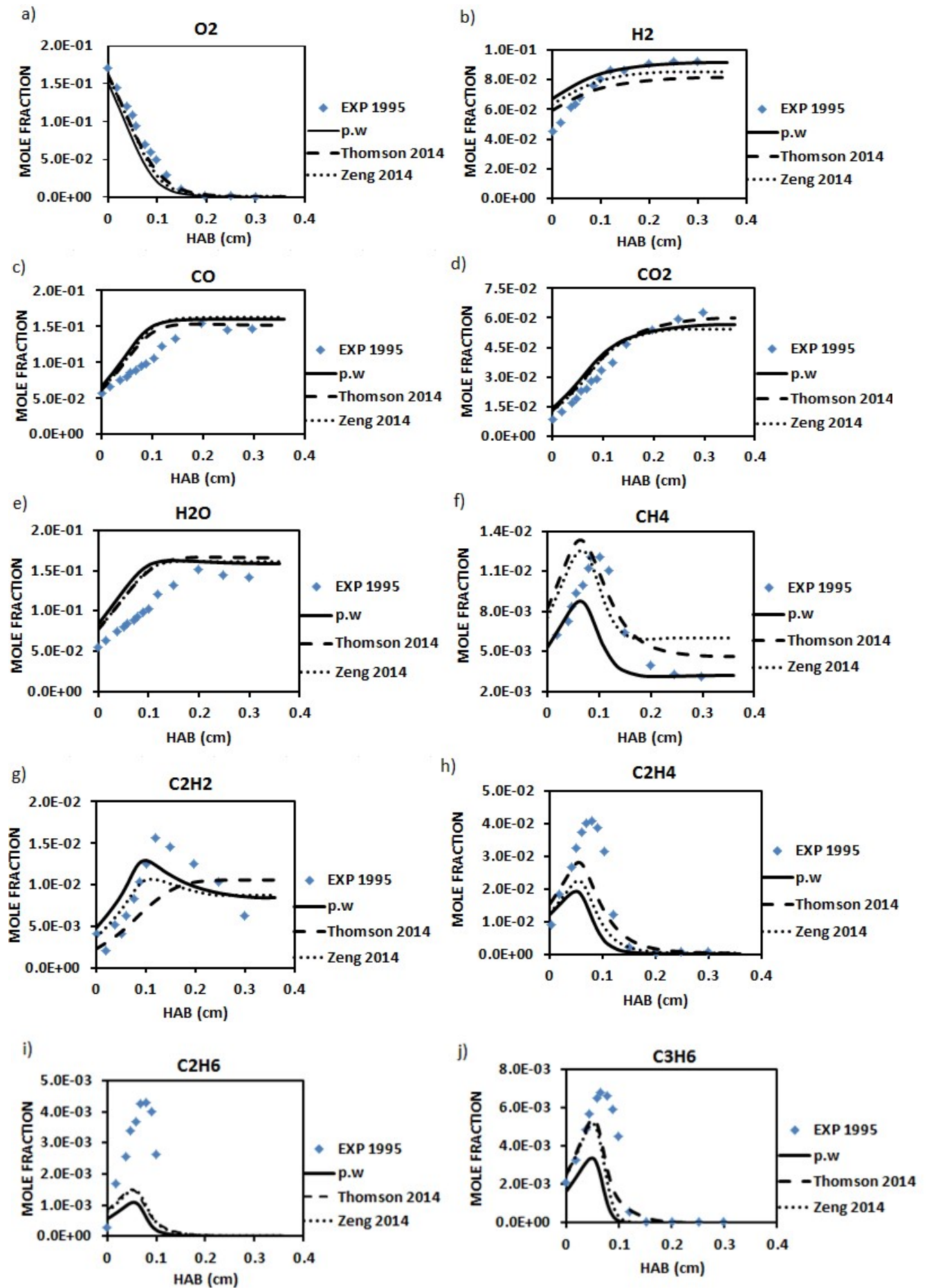


But-1,3-diene formation is dominated at lower HAB by allene reaction with methyl (R774) until HAB=0.22 cm. Then, reaction (R751) becomes the main 1,3 butadiene source, followed by the contribution of reactions (R791) and (R3269). The main reaction involved its consumption is ethylene and vinyl radical production,  $\text{C}_4\text{H}_6 + \text{H} = \text{C}_2\text{H}_4 + \text{C}_2\text{H}_3$  (R772).

#### **4.4.1.1.5. n-decane flame**

High linear alkanes represent an important class of practical fuels such as diesel and kerosene. The oxidation of large hydrocarbon is an important element in modeling combustion in engines including pollutant emissions. Since n-decane is one of the high linear alkane, the accurate prediction of its combustion is major of interest. The atmospheric pressure n-decane premixed flame ( $\phi=1.7$ ) has been modeled and the comparison between predictions and measurements can be seen in Figure 55.







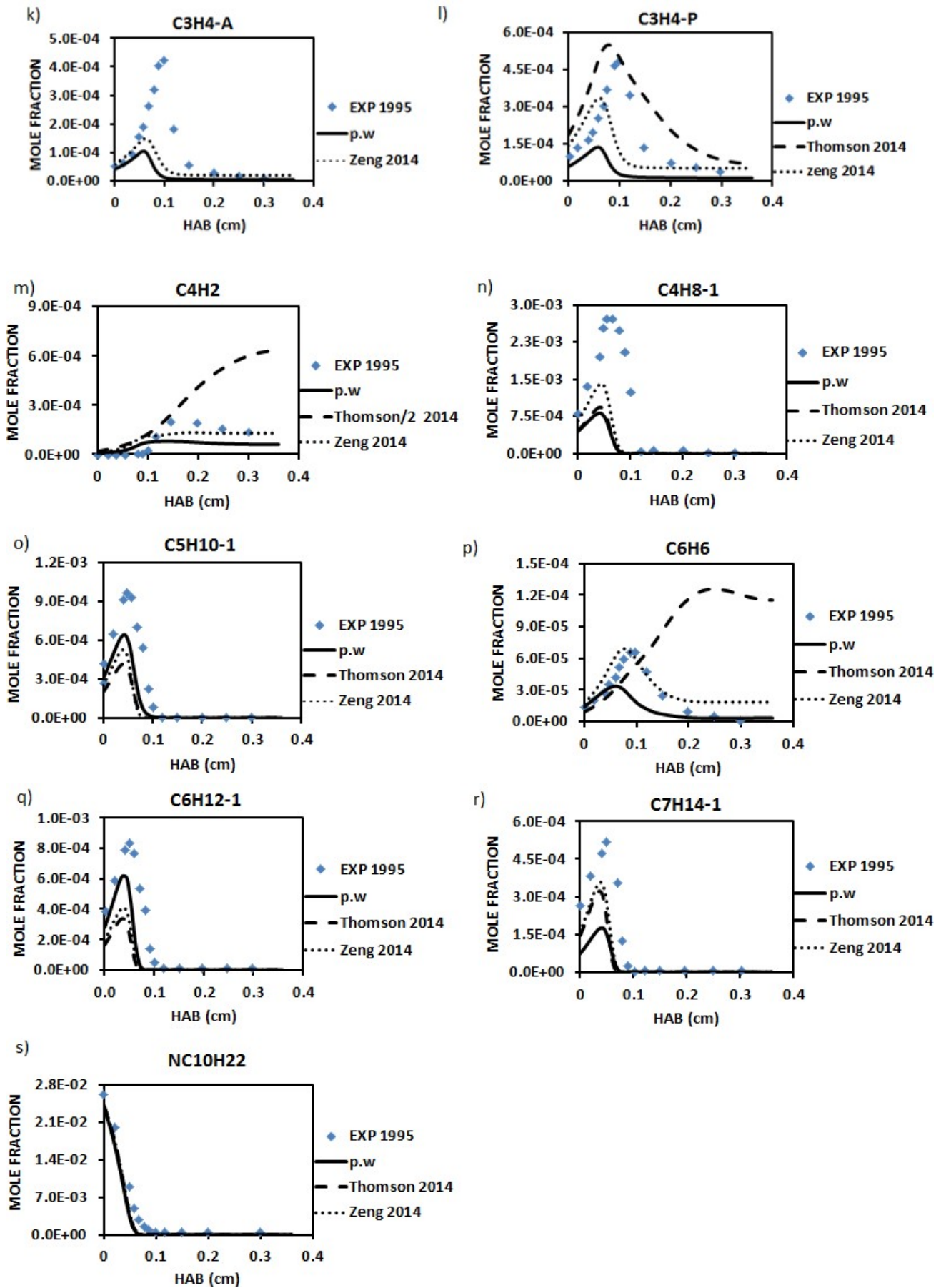


Figure 55 : Atmospheric pressure n-decane premixed laminar flame :  $n_{C_{10}/O_2/N_2} : 0.032/0.286/0.682$  in mole fraction ;  $\phi=1.7$  ;  $V=11.7$  cm/s ; Predicted and experimental mole fraction of a): oxygen, b): hydrogen, c): carbon monoxide, d): carbon dioxide, e): water, f): methane, g): acetylene, h): ethylene, i): ethane, j): propene, k): allene, l): propyne, m):

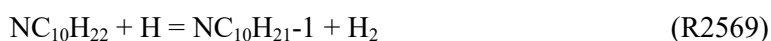
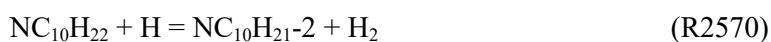
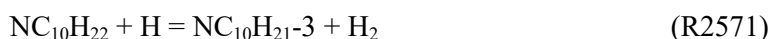
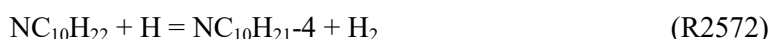
diacetylene, n): but-1-ene, o): pent-1-ene, p): benzene, q): hex-1-ene, r): hept-1-ene, s): n-decane. The symbols represent experimental data from [152]; the continuous lines represent the modeling results from the present work; dashed lines: Thomson et al. mechanism for n-decane combustion [26]; dotted lines: Zeng et al. mechanism for n-decane combustion [119].

As for iso-octane premixed flame, the present mechanism operates satisfactorily in a rich atmospheric pressure n-decane premixed flame. The tested mechanisms from the literature show similar results. However, discrepancies are observed with the Thomson et al. mechanism [26], where this mechanism fails to reproduce acetylene and benzene mole fraction profiles. One of the possible explanations to these discrepancies could be the lack of reactions that lead to benzene production. In the Thomson et al. mechanism [26], for the C<sub>3</sub>H<sub>4</sub> species, only propyne has been considered and the authors did not include allene molecule.

#### - Rate of production/consumption Analysis

##### n-decane decay pathways

n-decane decays mainly to formed n-decyl radicals as following:



The H abstraction reactions are followed by the OH reaction with n-decane that formed the above-mentioned radicals. N-decane is also found to dissociate by forming n-octyl-1 radical and ethyl radical, C<sub>8</sub>H<sub>17-1</sub> + C<sub>2</sub>H<sub>5</sub> = NC<sub>10</sub>H<sub>22</sub> (R2565).

##### Acetylene formation/consumption

As discussed in the previous sections, acetylene is mainly formed from vinyl radical (R3768) followed by propyne contribution (R525). It is mainly consumed by reactions (R278) and (R277) that produce HCCO and CH<sub>2</sub> respectively.

##### Ethylene formation/consumption

As can be seen in Figure 56, reactions involved in ethylene production as a function HAB are given:





Starting from the near burner surface, reactions involved in ethylene production are (R699), followed by (R419), (R170), (R441) and then (R3724). The predominant reactions in the burnt gas zone are (R3724) and (R170). Ethylene is mainly consumed to form vinyl radical, that is the main source of acetylene,  $\text{C}_2\text{H}_4 + \text{H} = \text{C}_2\text{H}_3 + \text{H}_2$  (R253).

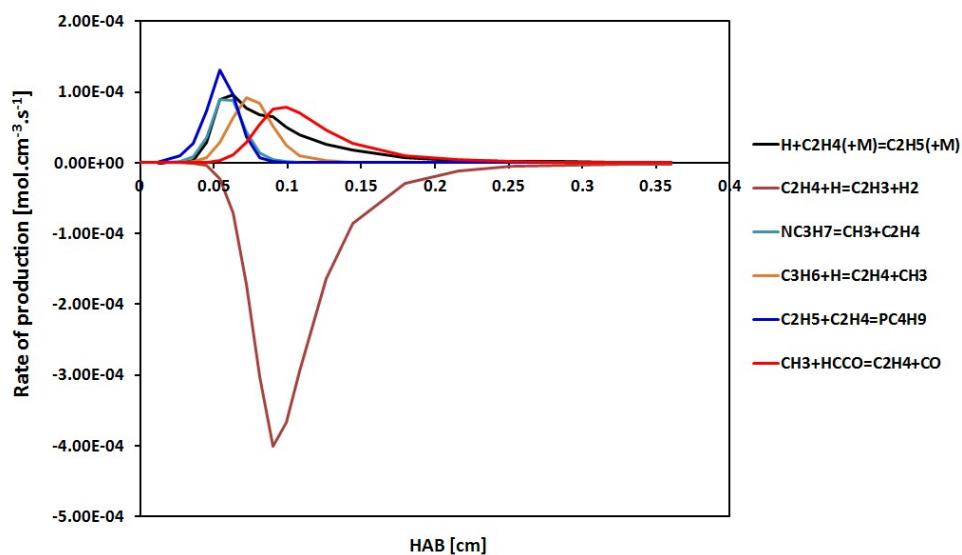
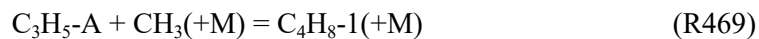


Figure 56 : Ethylene rate of production in a rich n-decane premixed flame.

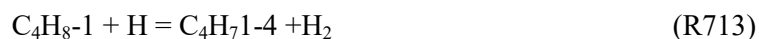
### But-1-ene formation/consumption

But-1-ene is mainly formed from n-decyl radical ( $\text{C}_{10}\text{H}_{21}\text{-3}$ ) thermal decomposition and from allyl radical reaction with methyl.



$\text{C}_{10}\text{H}_{21}\text{-3}$  is directly formed from n-decane decay. The main reactions involved in 1-butene consumption are:





### Benzene formation/consumption

As for n-butane flames, similar reactions involved in benzene production and consumption are observed. Propargyl radical recombination reaction (R3754) that produces benzene near the burner surface is followed by  $\text{C}_4/\text{C}_2$  reaction (R816) contribution. Then, phenol (R3231) and  $\text{MC}_6\text{H}_6$  isomerization reaction (R3330) also contribute significantly to benzene production. As can be seen in Figure 57, the relative importance of the above reactions as a function of HAB clearly evolves. At HAB= 0.1 cm corresponding to a temperature of 1513 K, reaction (R3231) is predominant, followed by propargyl radical recombination (R3754), reaction (R816) and then (R3330).

Benzene is mainly consumed to form phenyl radical through reactions (R3227) and (R3230).

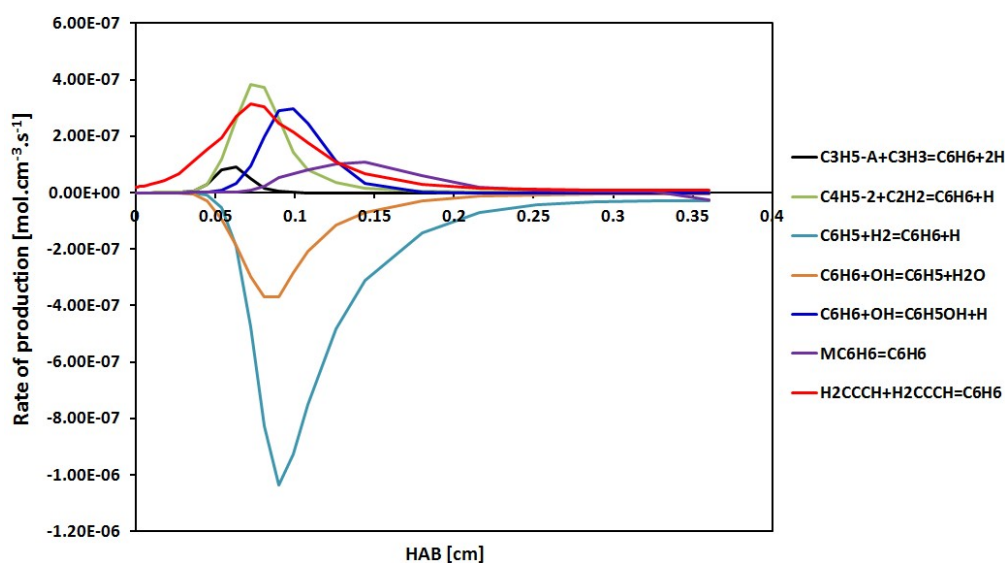


Figure 57 : Benzene rate of production in a rich n-decane premixed flame.

### Pent-1-ene formation/consumption

Pent-1-ene is mainly formed near the burner surface from  $\text{C}_{10}\text{H}_{21}-4$  decomposition, which is directly formed from n-decane decay.



Pent-1-ene is mainly consumed to form  $\text{C}_5\text{H}_91-3$ ,  $\text{C}_5\text{H}_{10}-1 + \text{H} = \text{C}_5\text{H}_91-3 + \text{H}_2$  (R1530).

### Hex-1-ene formation/consumption

Hex-1-ene is mainly formed near the burner surface from C<sub>10</sub>H<sub>21</sub>-5 decomposition, which is directly formed from n-decane decomposition. A minor contribution of n-octyl radical is also observed.



Hex-1-ene is mainly consumed to form n-propyl and allyl radical,  $\text{C}_6\text{H}_{12-1} = \text{NC}_3\text{H}_7 + \text{C}_3\text{H}_5\text{-A}$  (R2392).

### Hept-1-ene formation/consumption

As for Hex-1-ene, hept-1-ene is mainly formed from C<sub>10</sub>H<sub>21</sub>-5 decomposition reaction:



Hept-1-ene is mainly consumed to form 1-butyl and allyl radicals:

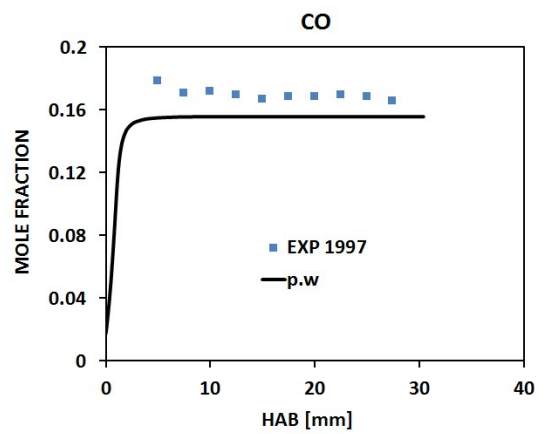
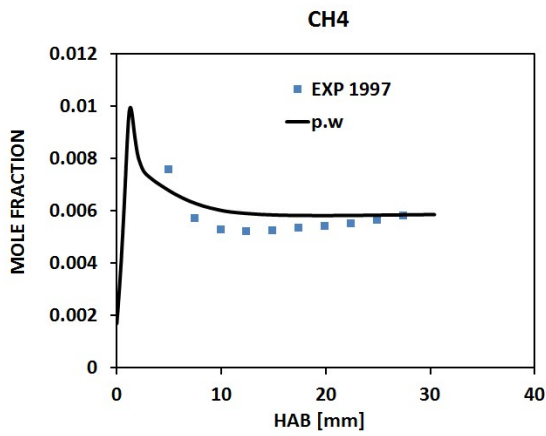
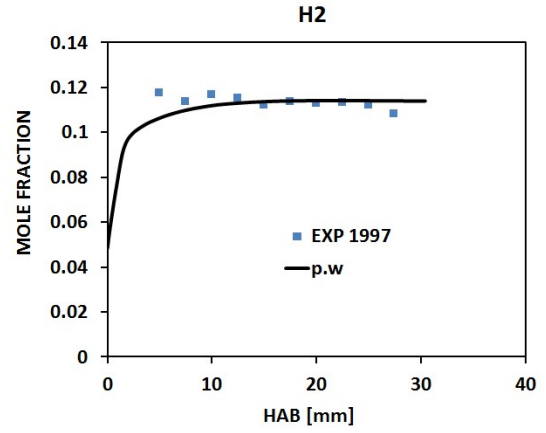
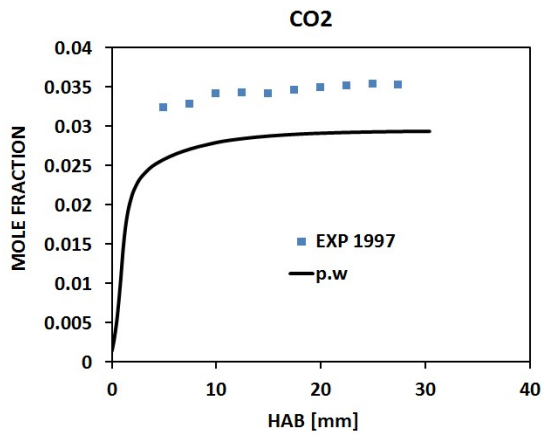
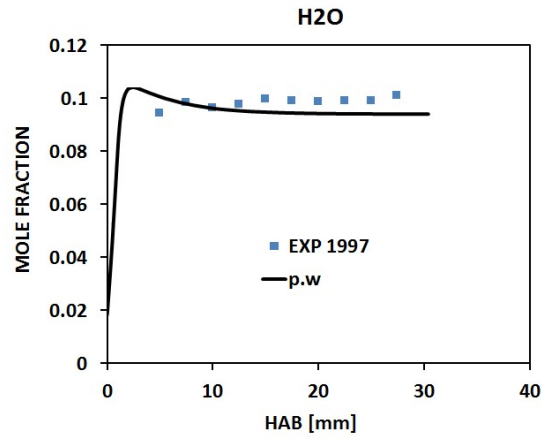
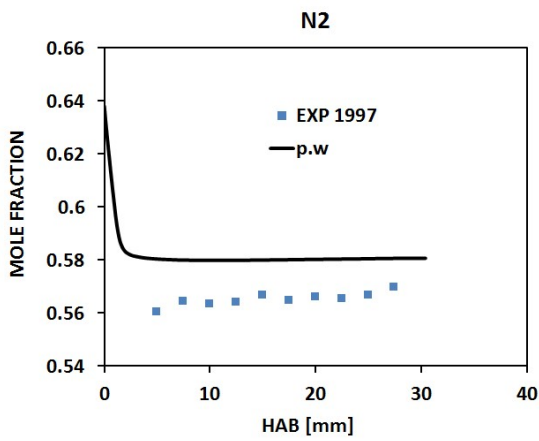
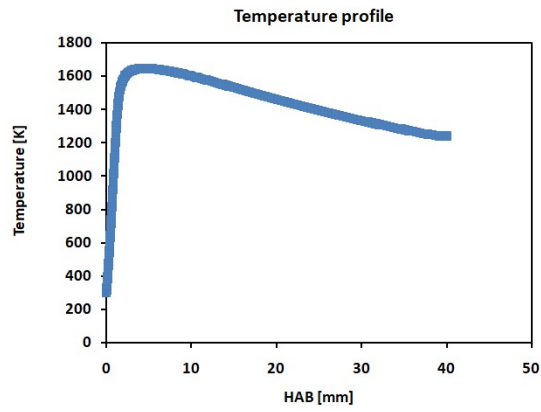


#### **4.4.1.2. Unsaturated aliphatic hydrocarbon flames**

The reactive system of alkene such as ethylene fuel has been examined in validating the present kinetic model. The rate of production and consumption analysis of species of interest has also been processed.

##### **4.4.1.2.1. Ethylene flames**

The reactivity of such small hydrocarbon and intermediates is of critical importance in understanding and accurately describing the combustion characteristics of practical fuels. The kinetics of ethylene combustion as well as for acetylene is of considerable importance since it is formed as intermediates in combustion of larger hydrocarbons and plays a key role in the overall combustion process. Any attempt to kinetically model larger hydrocarbons or complex fuels will require kinetic mechanisms that accurately describe such small species (ethylene, acetylene). Two atmospheric pressure ethylene premixed flames at  $\phi=2.34$  and  $\phi=3.06$  have been simulated (Figure 58Figure 59). A large pool of species of major interest from hydrogen to pyrene has been measured and the prediction of the kinetic model is compared to the measurements.



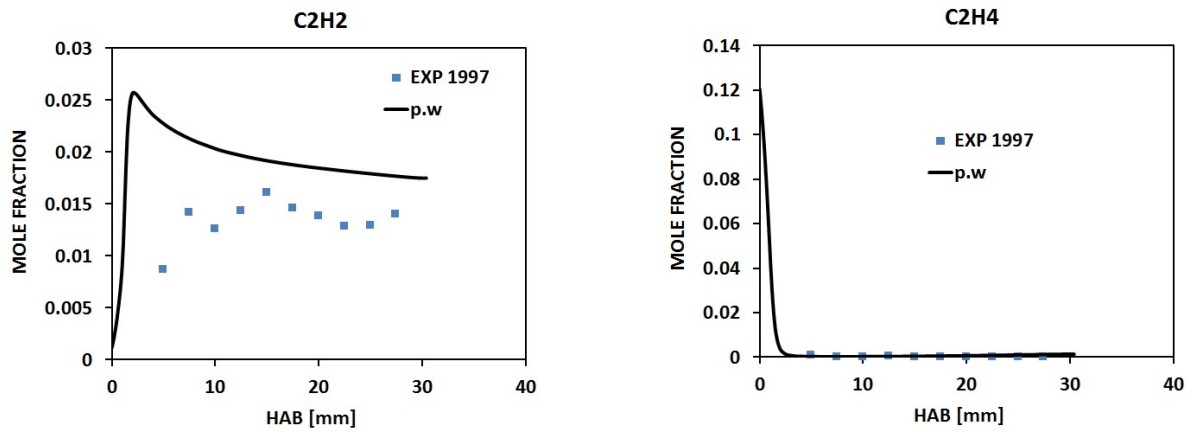
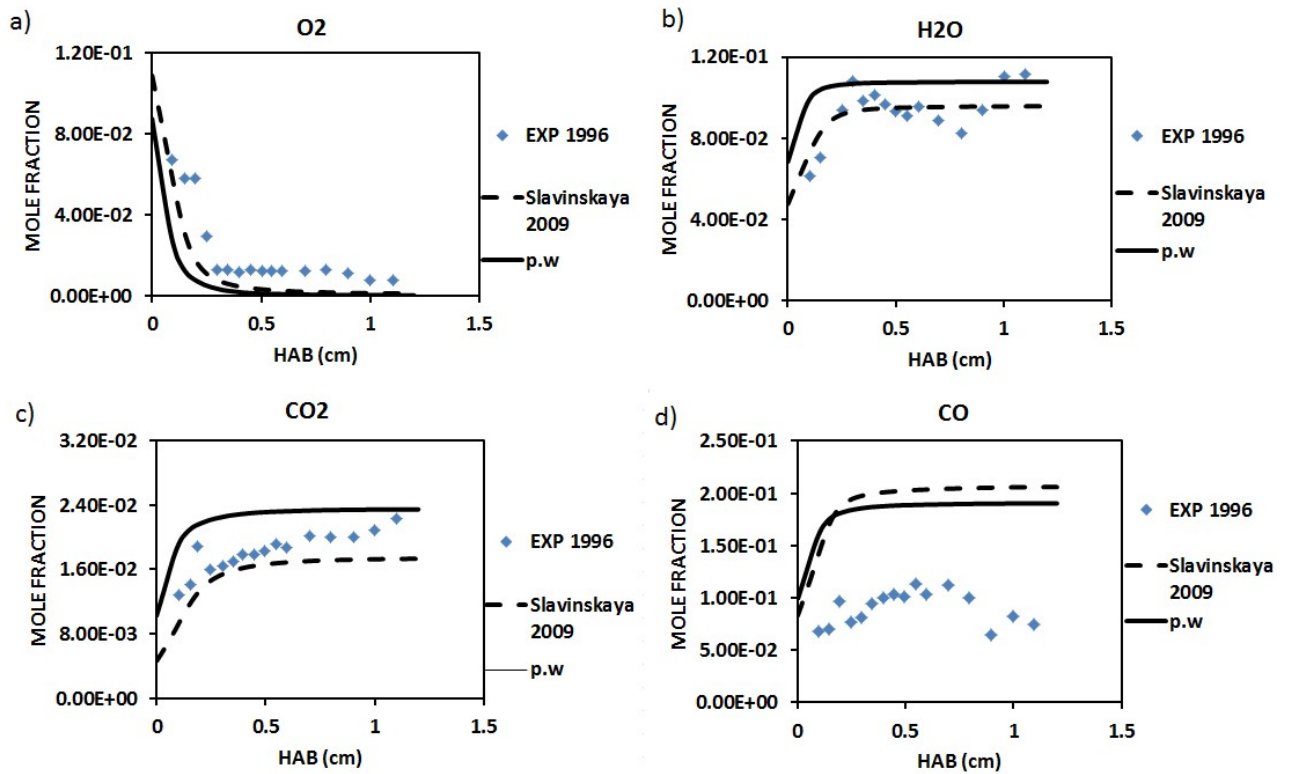
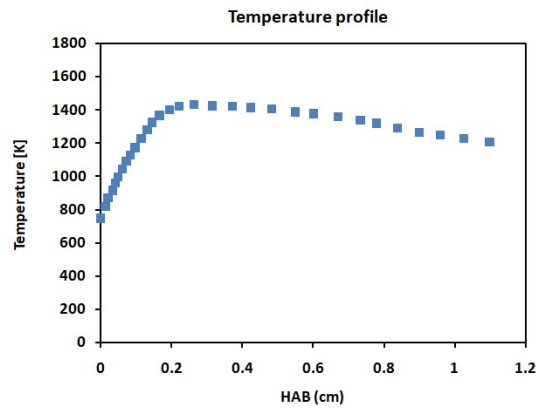
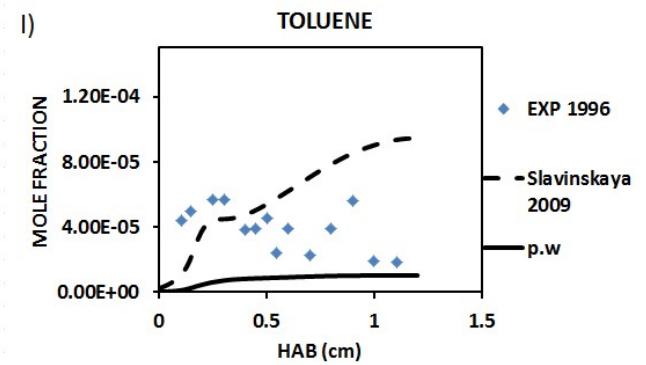
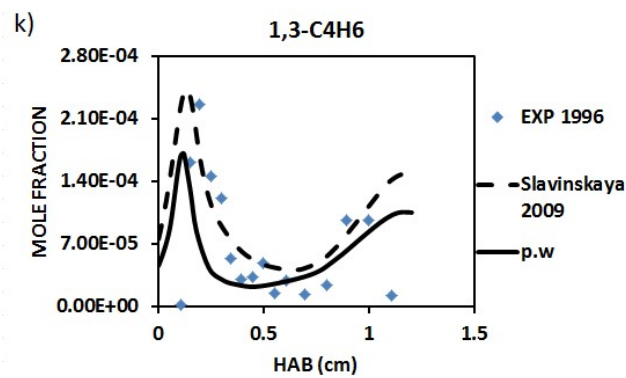
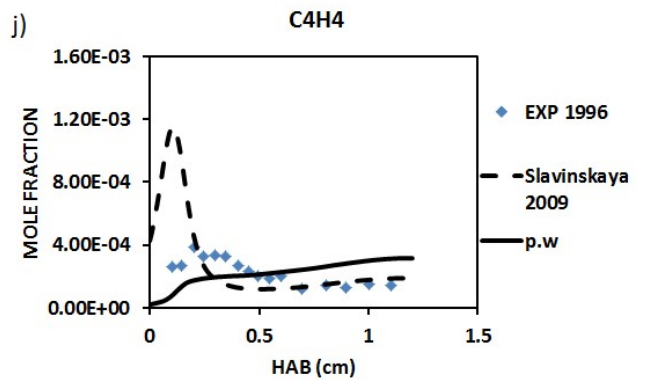
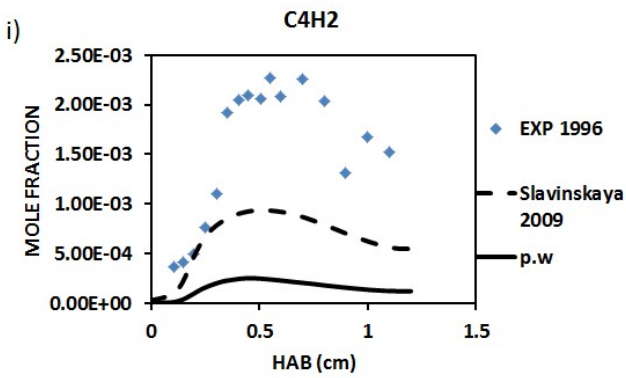
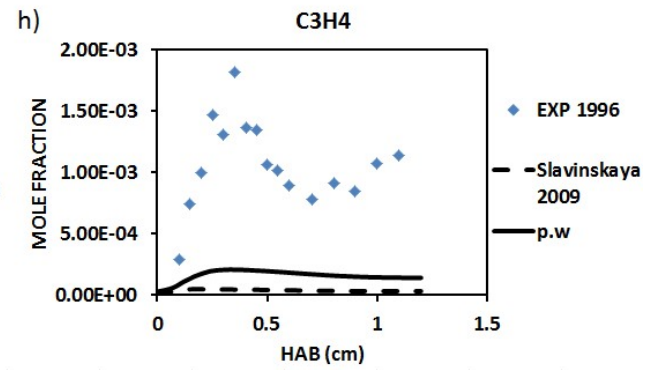
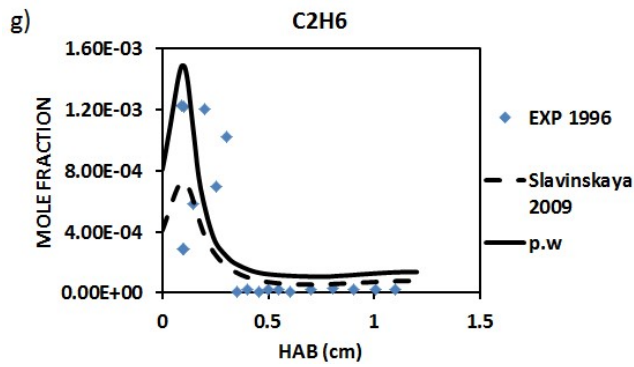
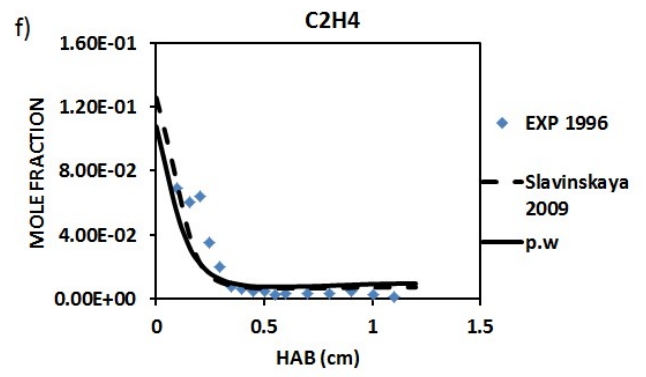
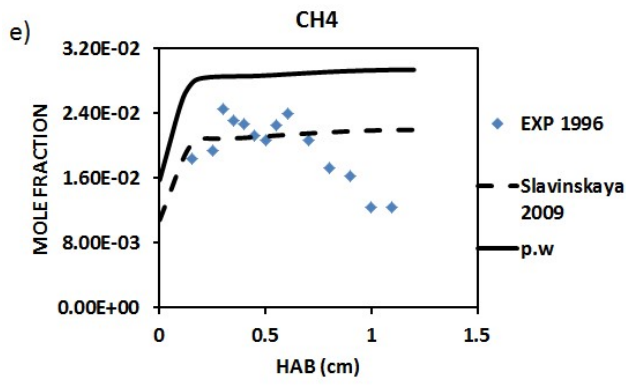
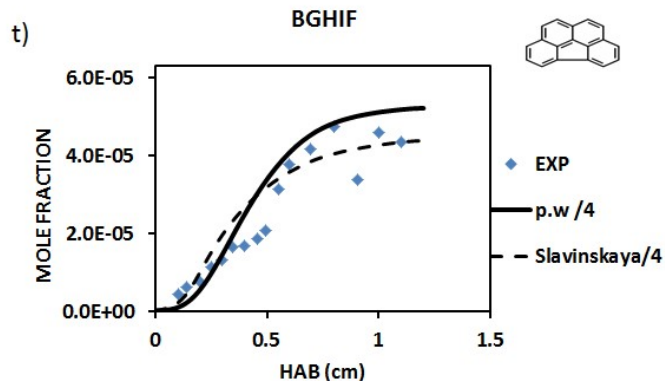
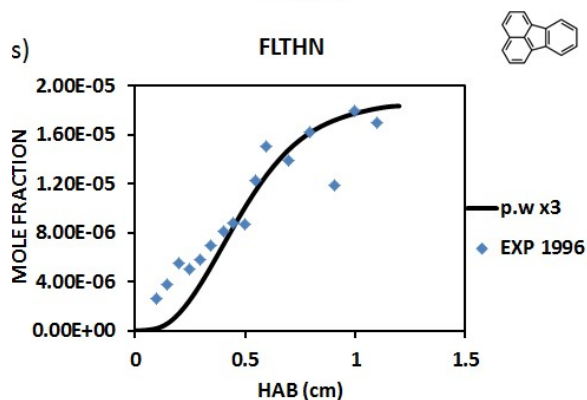
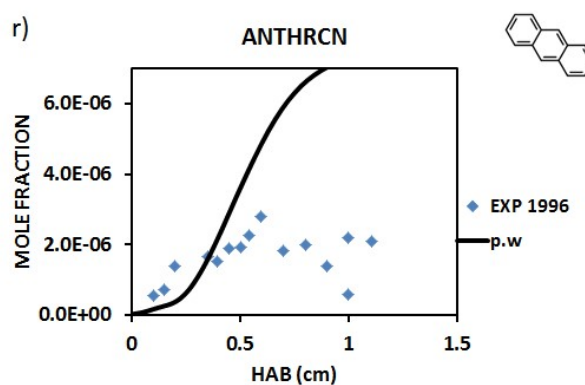
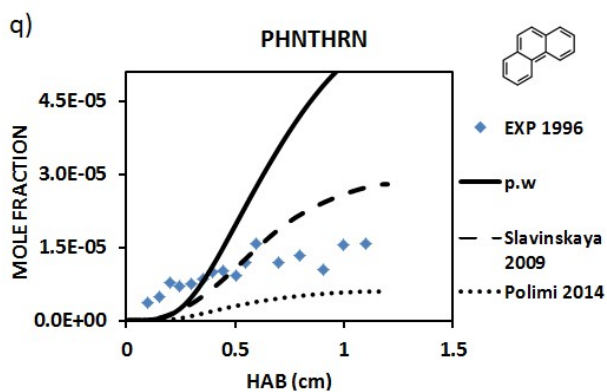
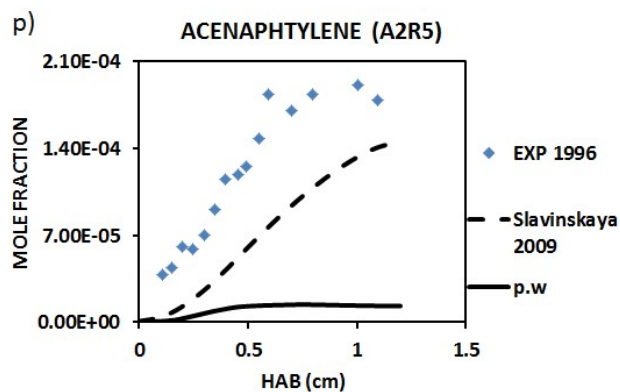
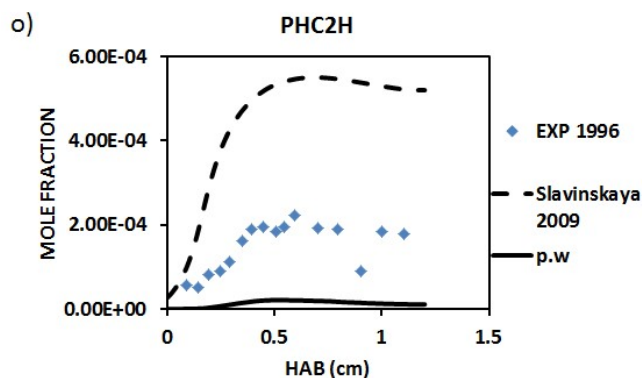
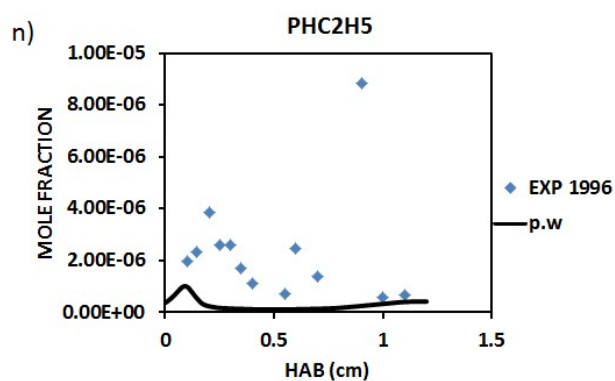
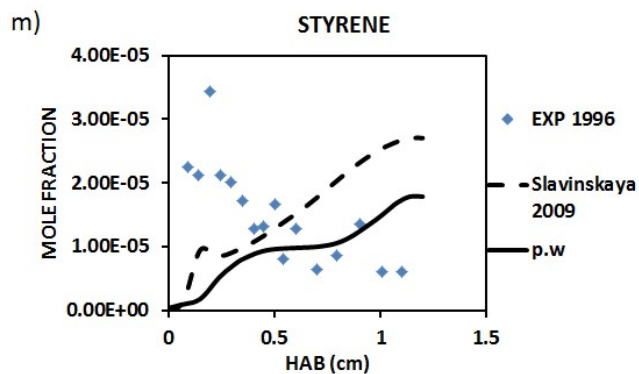


Figure 58 : Atmospheric ethylene premixed flame,  $\phi=2.34$ :  $C_2H_4$  (14.08% mol.)/ $O_2$  (18.05%)/ $N_2$  (67.87%). Species mole fraction profiles. The symbols represent experimental data from [82]; the lines represent modeling results from the present work.









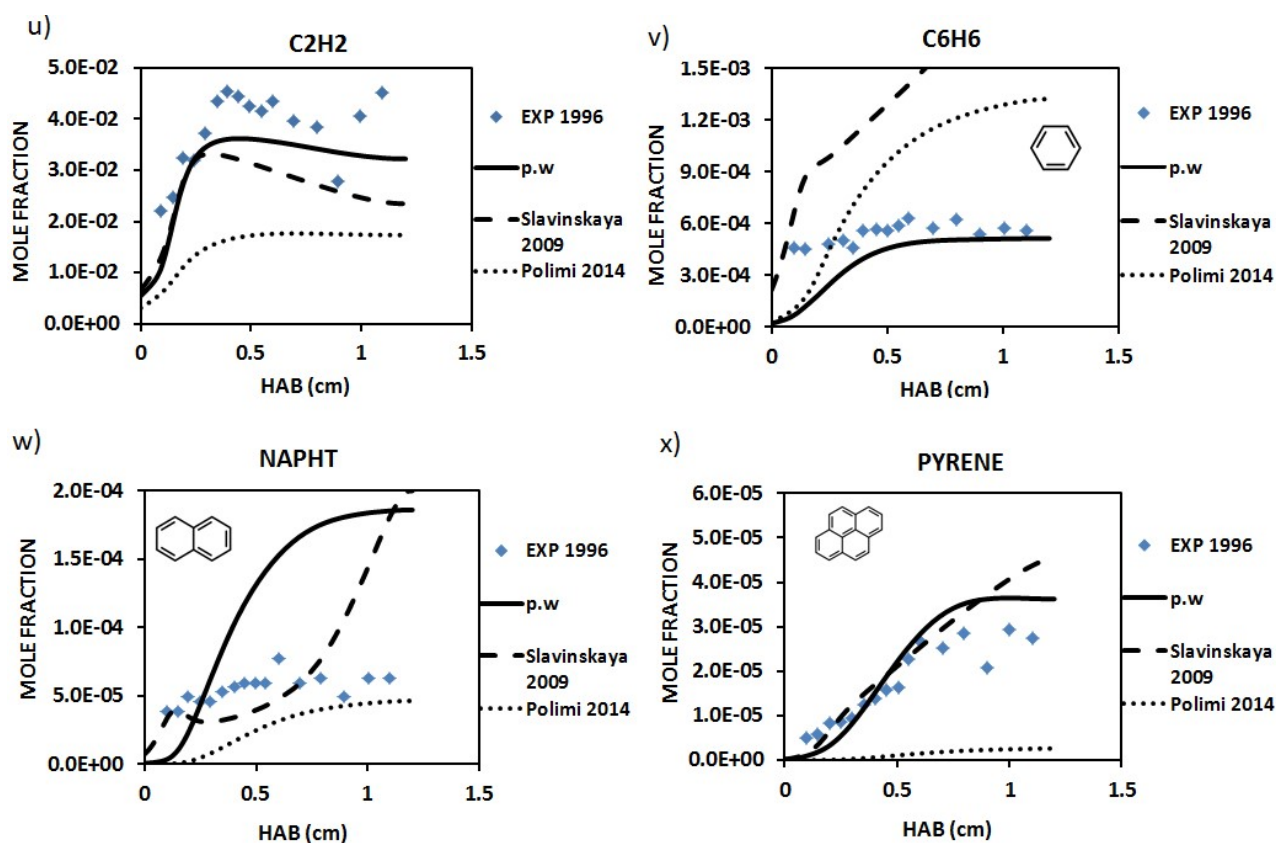


Figure 59 : Ethylene premixed flame ( $\phi=3.06$ ;  $P=1$  atm). Predicted and experimental mole fraction of a): oxygen, b): water, c): carbon dioxide, d): carbon monoxide, e): methane, f): ethylene, g): ethane, h): allene+propyne, i): diacetylene, j): vinylacetylene, k): but-1,3-diene, l): toluene, m): styrene, n): ethylbenzene, o): phenylacetylene, p): acenaphthylene, q): phenanthrene, r): anthracene, s): fluoranthene, t): benzo(ghi) fluoranthene, u): acetylene, v): benzene, w): naphthalene, x): pyrene. The symbols represent the experimental data [36]; the continuous lines represent the modeling results from the present work; dashed lines: Slavinskaya et al. mechanism [123] and dotted lines: Polimi mechanism [128].

In the ethylene premixed flame at  $\phi=2.34$ , a good agreement between measurements and prediction is obtained. However, there is no reported data over PAHs mole fraction. A key species such as acetylene concentration profile is presented and is well captured by the model.

In the ethylene premixed flame at  $\phi=3.06$ , satisfactory results are obtained despite some discrepancies observed for some species. A good agreement between measured and predicted mole fractions of acetylene, benzene, naphthalene (within a factor of 3) and pyrene is obtained. These encouraging are due to the better prediction of small species such as  $\text{CH}_4$ ,  $\text{C}_2\text{H}_4$ ,  $\text{C}_2\text{H}_6$ ,  $\text{C}_4\text{H}_4$  and  $1,3\text{-C}_4\text{H}_6$  that are potential precursors acetylene, benzene and naphthalene. Large discrepancies are observed for some species such as  $\text{C}_3\text{H}_4$  (allene+propyne),  $\text{C}_4\text{H}_2$  and acenaphthylene ( $\text{A}_2\text{R}_5$ ). All the tested mechanisms fail to reproduce satisfactorily  $\text{C}_3\text{H}_4$  concentration profile, while that of Slavinskaya et al. presents acceptable profiles over  $\text{C}_4\text{H}_2$  and acenaphthylene. The other measured PAHs fluoranthene and benzo(ghi)fluoranthene mole fractions are predicted within a factor of 3 (underpredicted) and a factor

of 4 (overpredicted) respectively. Slavinskaya et al. mechanism shows the similar trend for benzo(ghi)fluoranthene (within a factor of 4). The discrepancies are consistent with Slavinskaya et al. mechanism over benzene and naphthalene mole fraction profiles, while polimi mechanism totally underpredicted the pyrene mole fraction within a factor of more than 10.

### Sensitivity on benzene and naphthalene formation/consumption

Figure 60 shows sensitivity analyses for benzene formation in ethylene premixed flame.

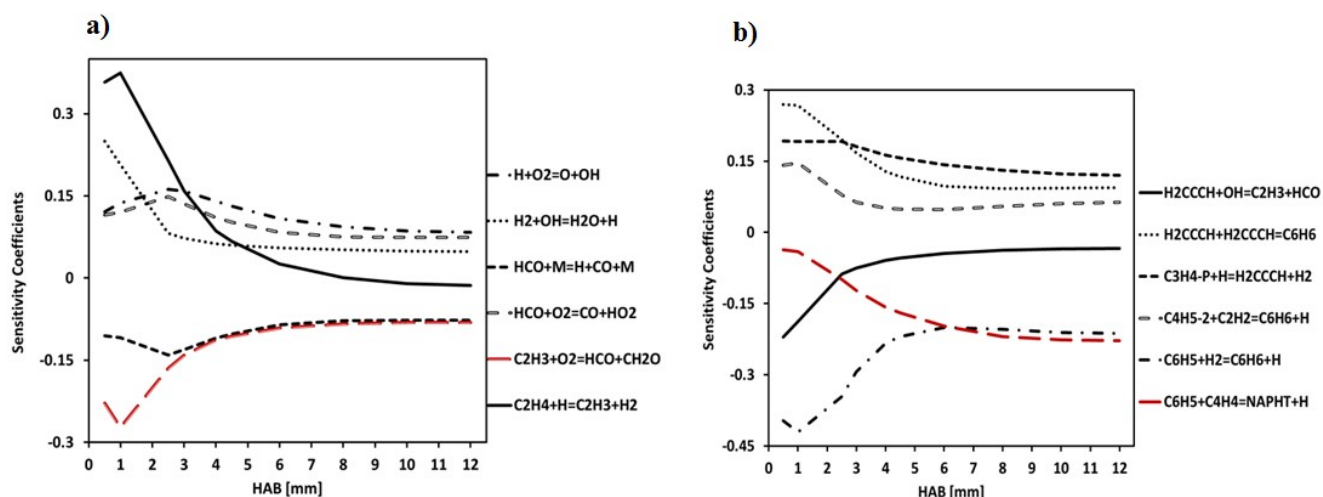


Figure 60 : Normalized sensitivities for benzene formation in ethylene premixed flame ( $\phi=3.06$ ,  $P=1\text{atm}$ ).

As expected, the core  $\text{H}_2\text{-O}_2$  reaction system plays an important role in benzene chemistry. Reactions  $\text{H}+\text{O}_2=\text{O}+\text{OH}$ ;  $\text{H}_2+\text{OH}=\text{H}_2\text{O}+\text{H}$  and  $\text{HCO}+\text{O}_2=\text{CO}+\text{HO}_2$  show positive sensitivities, indicating that reactions involving OH, H and  $\text{HO}_2$  may contribute to benzene formation process through the formation of its precursors. Reaction  $\text{HCO}+\text{M}=\text{H}+\text{CO}+\text{M}$  produces H atom but a negative sensitivity is observed. In this case, formyl (HCO) decomposition may contribute to remove carbon from benzene production paths and H atom production through this step may favor H-abstraction on benzene forming phenyl. It is observed that reactions favoring the formation of vinyl radical, propargyl radical, fulvene, benzene and phenol show positive sensitivities, while those consuming vinyl radical, propargyl radical, phenyl radical, benzene and phenoxy radical show negative sensitivities. This is consistent with the fact that these species could be benzene precursors. One can note that the highest negative sensitivity is observed for reaction  $\text{C}_6\text{H}_5+\text{H}_2=\text{C}_6\text{H}_6+\text{H}$ . In addition, propargyl radicals play a key role in benzene production in all flame zones.

Figure 61 shows sensitivity analyses for naphthalene formation in ethylene rich premixed flame. The core  $H_2-O_2$  reaction system plays an important role as for benzene formation. Reactions favoring naphthalene formation such as phenyl radical reaction with vinylacetylene; propargyl radical recombination or production from propyne and vinyl radical production from ethylene exhibit positive sensitivities. Benzene is found to be a dominant precursor of naphthalene since reactions that favor its formation such as propargyl radical recombination or its derived product such as phenyl radical show positive coefficients for naphthalene formation. Reactions consuming naphthalene such as naphthyl radical, indenyl radical and phenylacetylene formation or its precursors such as phenyl radical oxidation to yield phenyl peroxy radical ( $C_6H_5OO$ ) show negative sensitivities. It is worth noting that the impacts of these reactions (except naphthyl radical formation reaction) on naphthalene formation tend to vanish at higher HAB ( $> 3$  mm). That could be explained by the drop of sensitivity coefficients of reactions that favor naphthalene production, indicating there might be a competition between naphthalene reaction route and other reaction routes that produce indenyl radical such as  $C_5H_5+C_4H_2$  [169] and phenylacetylene such as  $C_6H_5+C_2H_2$  [170]. Phenyl peroxy ( $C_6H_5OO$ ) may contribute to phenoxy radical ( $C_6H_5O$ ) production, which is a precursor of cyclopentadienyl radicals which can then yield naphthalene by recombination [36,52].

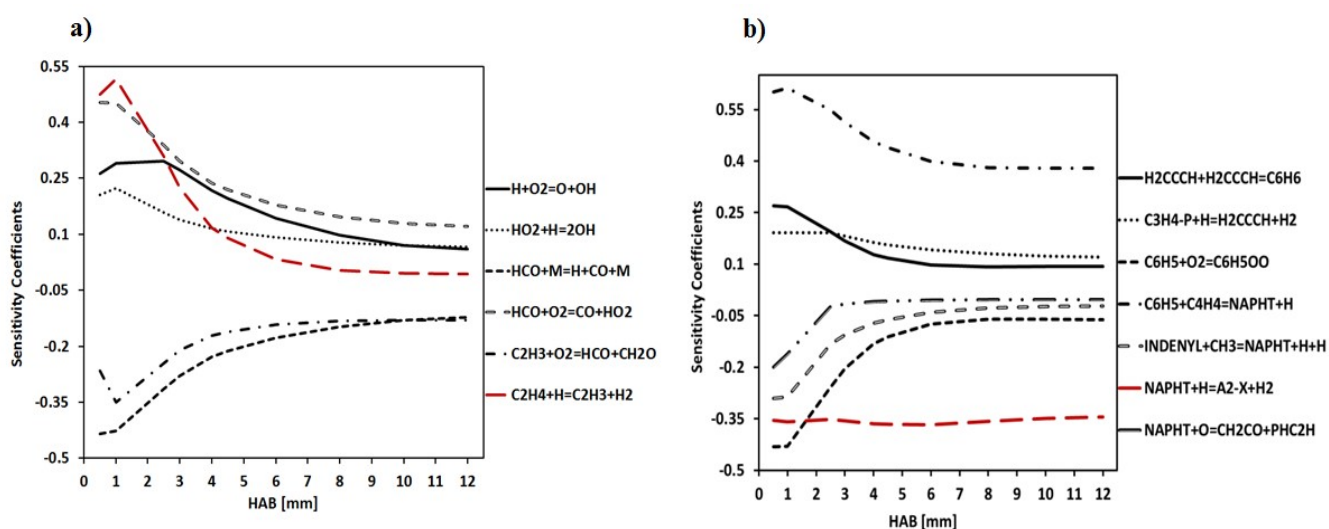


Figure 61 : Normalized sensitivities for naphthalene formation in ethylene premixed flame ( $\phi=3.06$ ,  $P= 1atm$ ).

- Rate of production/consumption Analysis in ethylene flame ( $\phi=3.06$ )

**Acetylene formation/consumption**

As discussed in the previous sections, acetylene is mainly formed from vinyl radical decomposition (R3768) and is mainly consumed to yield HCCO (R278), which is a major precursor of ethylene through reaction (R3724),  $\text{CH}_3 + \text{HCCO} = \text{C}_2\text{H}_4 + \text{CO}$ .

**Benzene and naphthalene formation/consumption**

The present mechanism was subsequently used to analyze benzene and naphthalene production pathways in ethylene flame (Figure 62). Rates of production were obtained at the inflection point of benzene mole fraction profile which corresponds to a HAB of 2.5 mm (55.0% of ethylene conversion). The absolute net reaction fluxes by numerical values are indicated next to the corresponding arrows. The boundary value corresponds to 1 nanomole per cubic centimeter per second and the relative contribution of reactions directly involved in benzene and naphthalene production is indicated in percent.

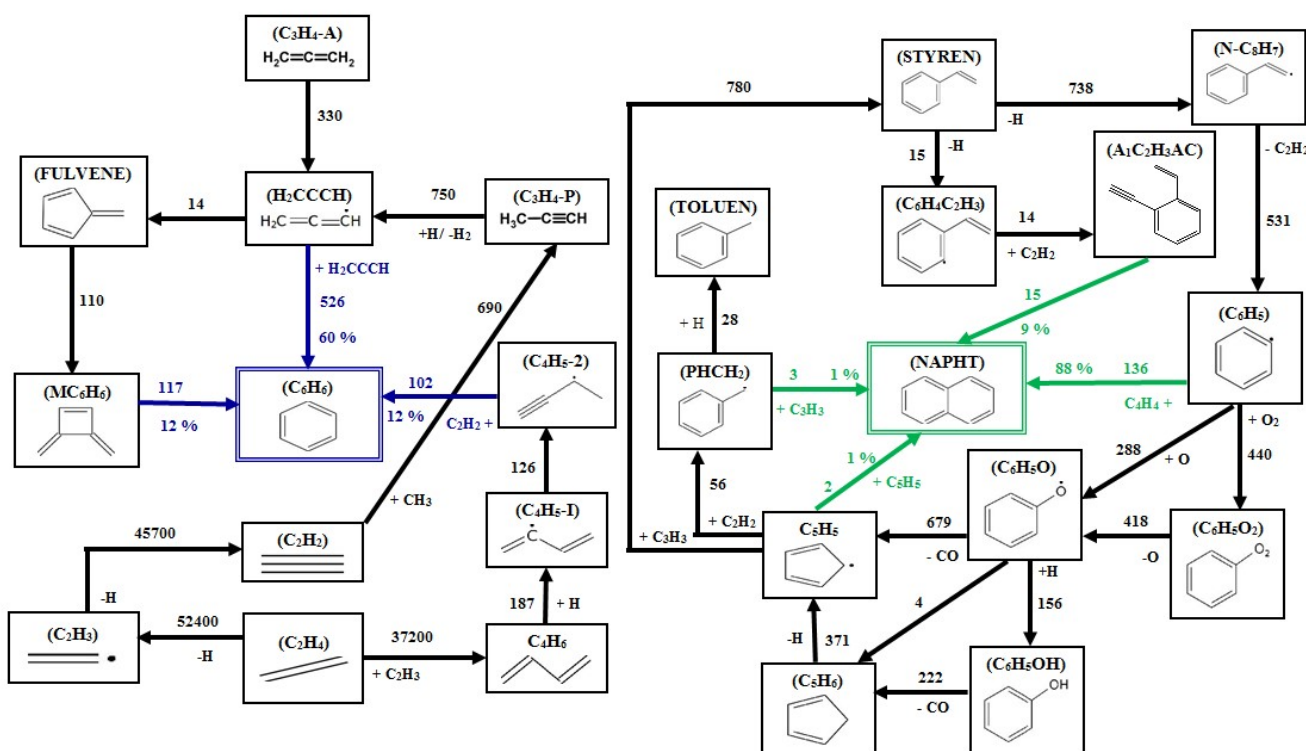


Figure 62 : Major benzene and naphthalene formation pathways in ethylene flame [36]; HAB=2.5 mm (T=1429 K);  $\phi=3.06$ ; P= 1 atm; Reaction fluxes are expressed in nanomole per cubic centimeter per second.

As can be seen in Figure 62, benzene production is dominated by  $\text{C}_3$  species (propargyl radicals) recombination (60%), followed by isomerization reaction of dimethylene cyclobutene ( $\text{MC}_6\text{H}_6$ ) (12%),

and produced from fulvene, C<sub>4</sub> species (but-2-ynyl C<sub>4</sub>H<sub>5</sub>-2) reaction with acetylene (12%), 7% contribution from phenol decomposition reaction, and a minor contribution from styrene decomposition to yield vinyl radical (4%), from toluene de-alkylation (3%), and biphenyl decomposition to yield phenyl radical (2%). Naphthalene is mainly produced from phenyl radical reaction with vinylacetylene (88%), followed by vinyl phenyl acetylene (A<sub>1</sub>C<sub>2</sub>H<sub>3</sub>AC) rearrangement (9%) and minor contributions of cyclopentadienyl radicals recombination (1%) and benzyl reaction with propargyl (1%).

We also investigated the main reactions that produce benzene and naphthalene as a function of HAB (see Figure 63 and Figure 64), from 0.5 to 12.0 mm.

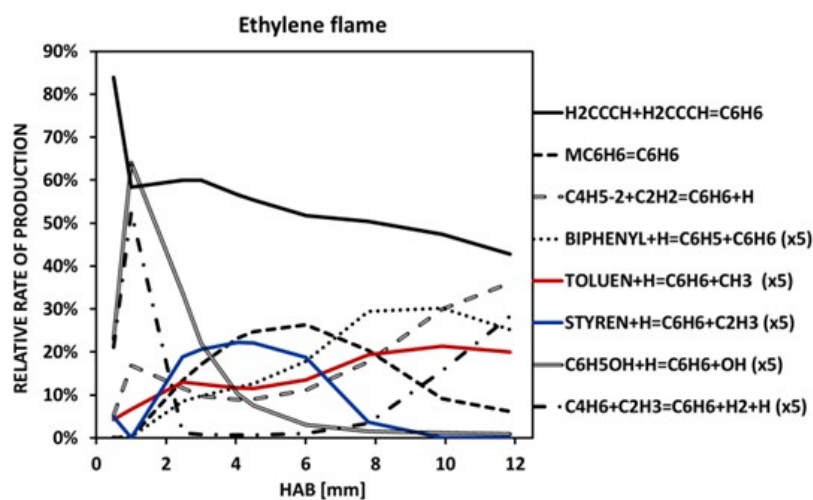


Figure 63 : Relative rates of benzene production normalized by the total rate of production in ethylene flame. The contributions of some reactions are multiplied by 5 as depicted in caption.

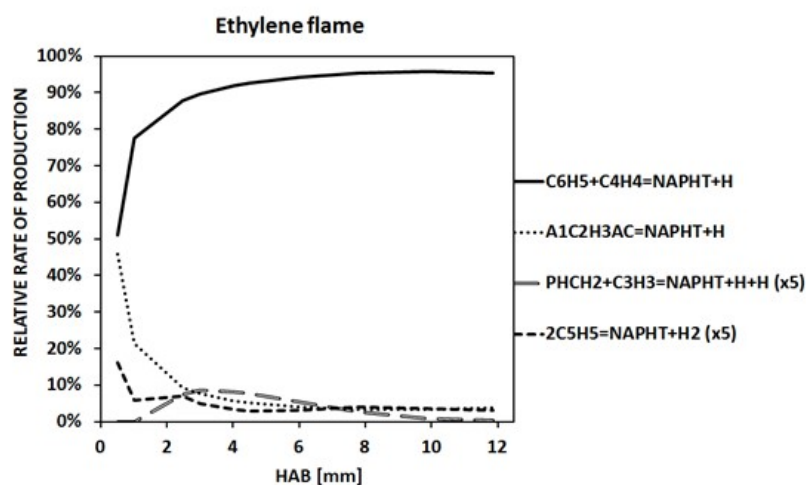


Figure 64 : Relative rates of naphthalene production normalized by the total rate of production in ethylene flame. The contributions of some reactions are multiplied by 5 as depicted in caption.

In Figure 63, we can notice that propargyl radicals recombination reaction, the fulvene derived product dimethylene cyclobutene (MC<sub>6</sub>H<sub>6</sub>) and butyn-2-yl (C<sub>4</sub>H<sub>5</sub>-2) reaction with acetylene appear as the main benzene production paths in atmospheric ethylene rich flame. In Figure 64, naphthalene production is dominated by phenyl reaction with vinylacetylene. Phenyl radical may probably exist in large concentration and vinylacetylene can be easily produced from acetylene reaction with vinyl radical reaction. It can also be observed in Figure 64 that the HACA mechanism contribution (represented here by vinyl phenyl acetylene, A<sub>1</sub>C<sub>2</sub>H<sub>3</sub>AC path) is significant, while that of cyclopentadienyl radical recombination reaction contributes barely to 5% of naphthalene production.

As can be seen in Figure 65, benzene is mainly consumed to form phenyl radical:

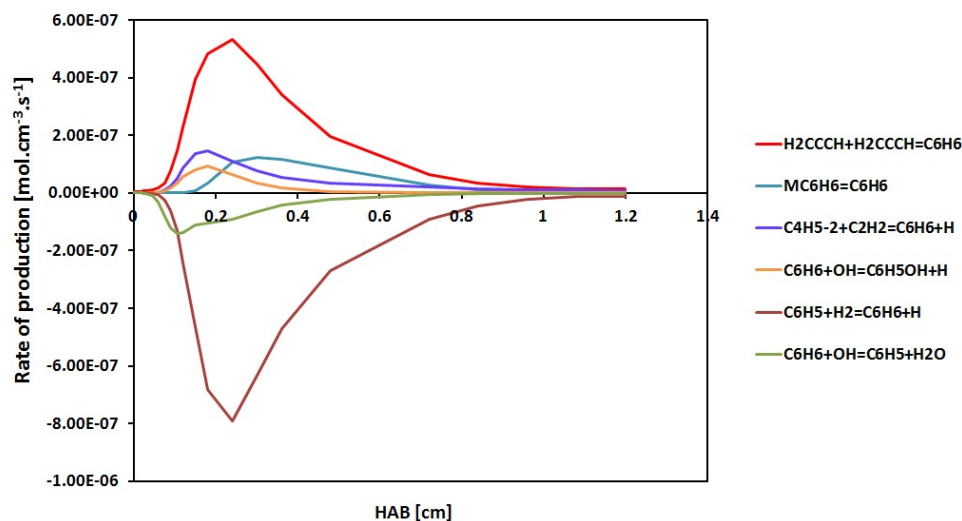


Figure 65 : Benzene rate of production in a rich ethylene premixed flame.

In Figure 66, naphthalene is mainly consumed to form naphthyl radical, indenyl radical and phenanthrene as follows:



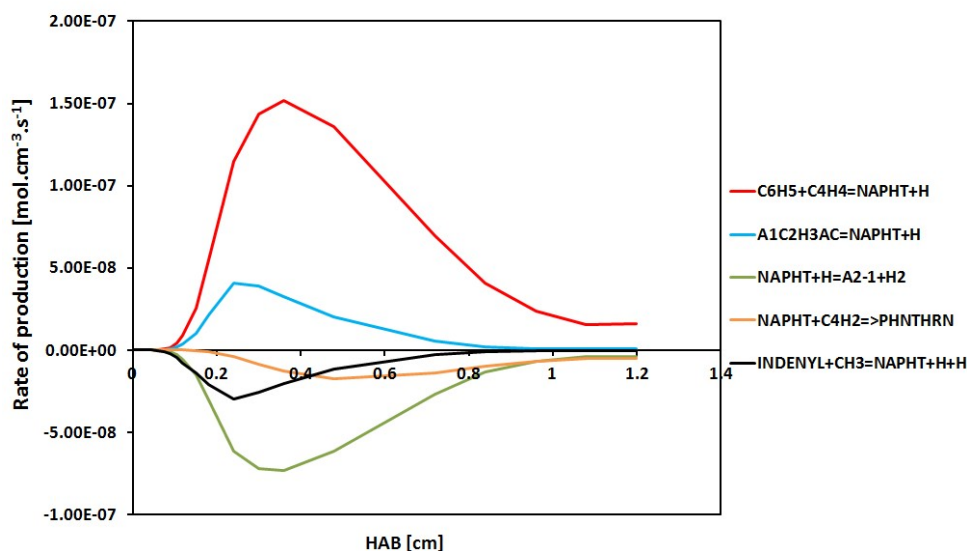
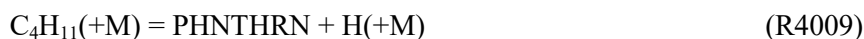


Figure 66 : Naphthalene rate of production in a rich ethylene premixed flame.

### Phenanthrene (PHNTHRN) formation/consumption

Phenanthrene is mainly formed from naphthalene reaction with  $C_4H_2$  (R4192), followed by the contribution of stilbene radical ( $C_{14}H_{11}$ ) and a minor contribution of phenyl reaction with phenylacetylene and anthracene isomerization reaction:



Phenanthrene is mainly consumed by forming phenanthryl radical ( $A_3-1$  and  $A_3-4$ ):



### Pyrene formation/consumption

As can be seen in Figure 67, pyrene is mainly formed through HACA mechanism, represented by the reaction of acetylene with phenanthryl radicals:







Reactions involved in pyrene consumption are mainly pyrenyl radicals formation ( $\text{A}_4\text{-1}$ ,  $\text{A}_4\text{-2}$  and  $\text{A}_4\text{-4}$ ) and benzo(a)pyrene (BAPYR) formation as follows:

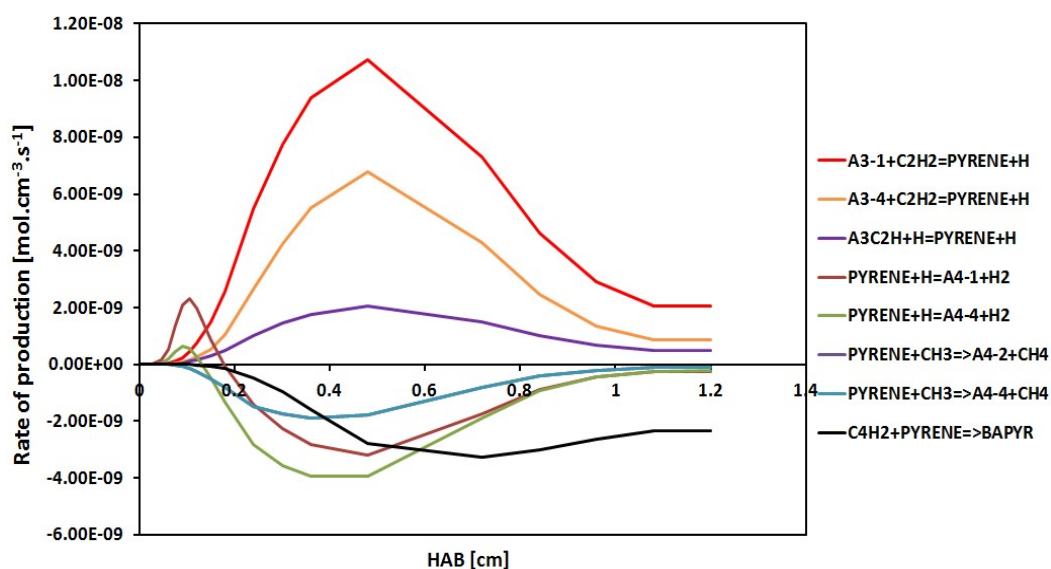


Figure 67 : Pyrene rate of production in a rich ethylene premixed flame.

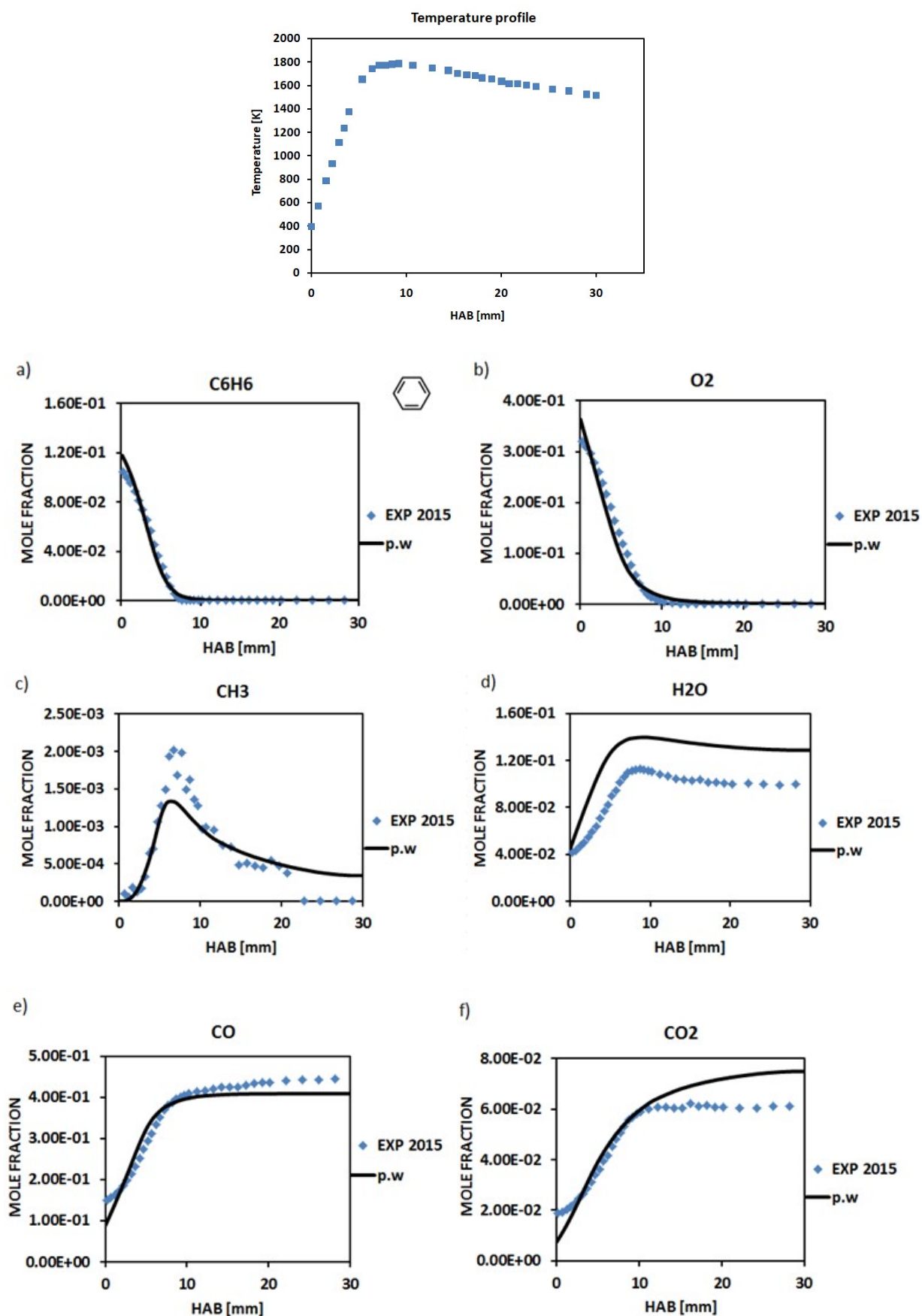
#### 4.4.1.3. Benzene and monoalkyles aromatic flames

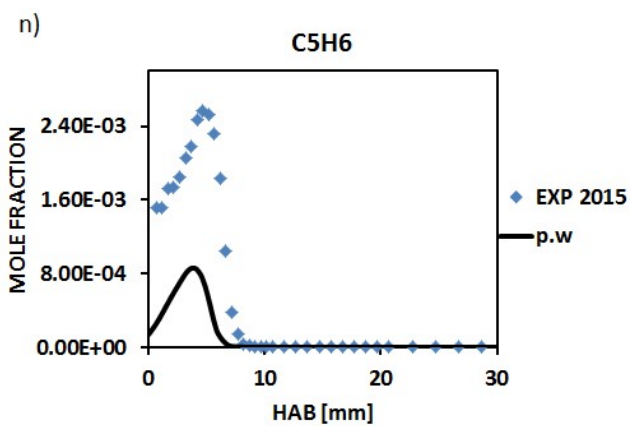
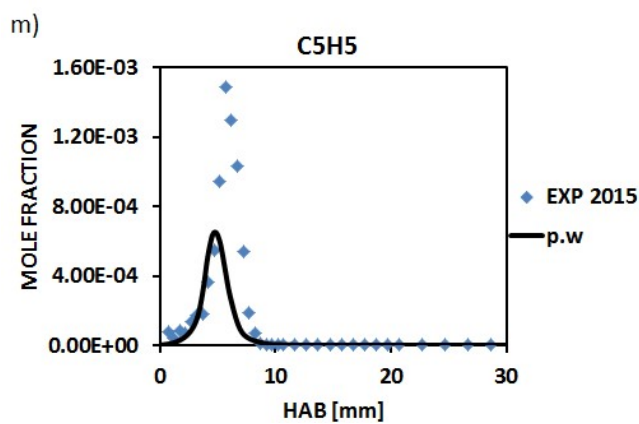
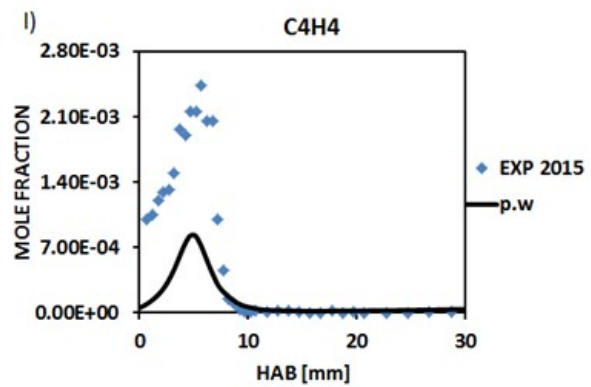
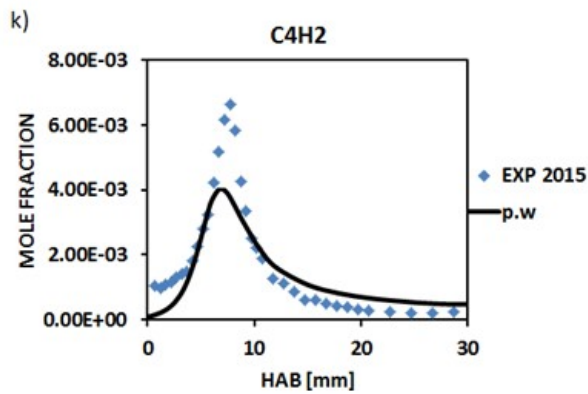
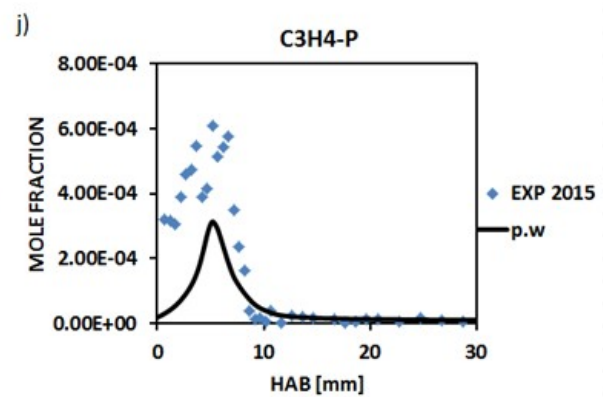
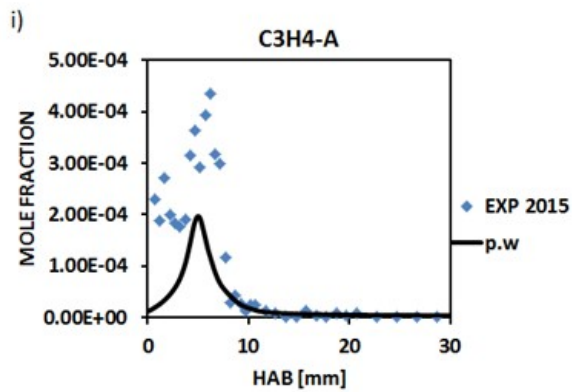
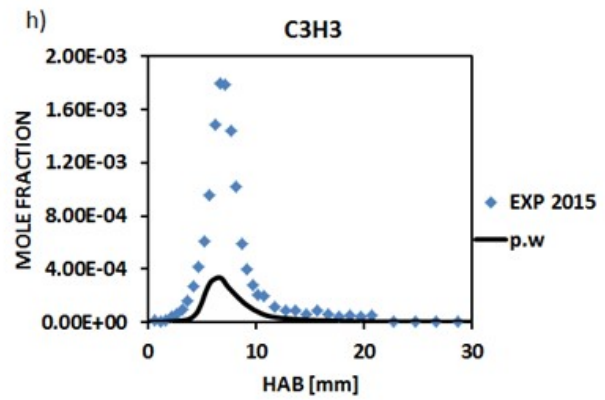
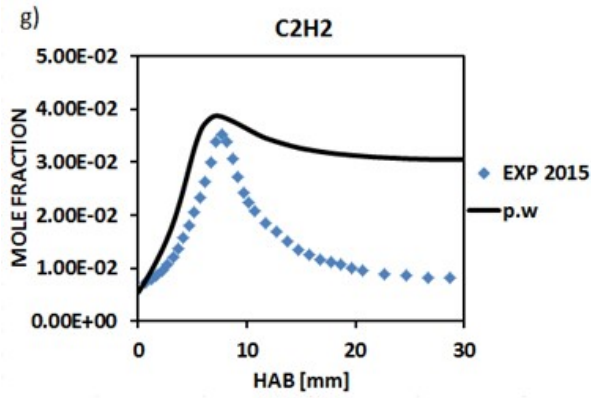
The reactive systems chosen for aromatic hydrocarbons combustion modeling are those of benzene and n-propylbenzene. The effect of the presence of a monoalkyle chain in term of species formation pathways in both systems has been examined.

##### 4.4.1.3.1. Benzene flame

Aromatic hydrocarbons are important fuel component including jet fuel, gasoline and diesel fuel and atmospheric pollutants. The understanding of aromatics combustion provides useful information on their decay as well as their production pathways. Low pressure (30 Torr) aromatic premixed flame

( $\phi=2.0$ ) has been modeled to validate the present kinetic model. In Figure 68, model predictions are compared with experimental mole fraction profiles up to phenanthrene.





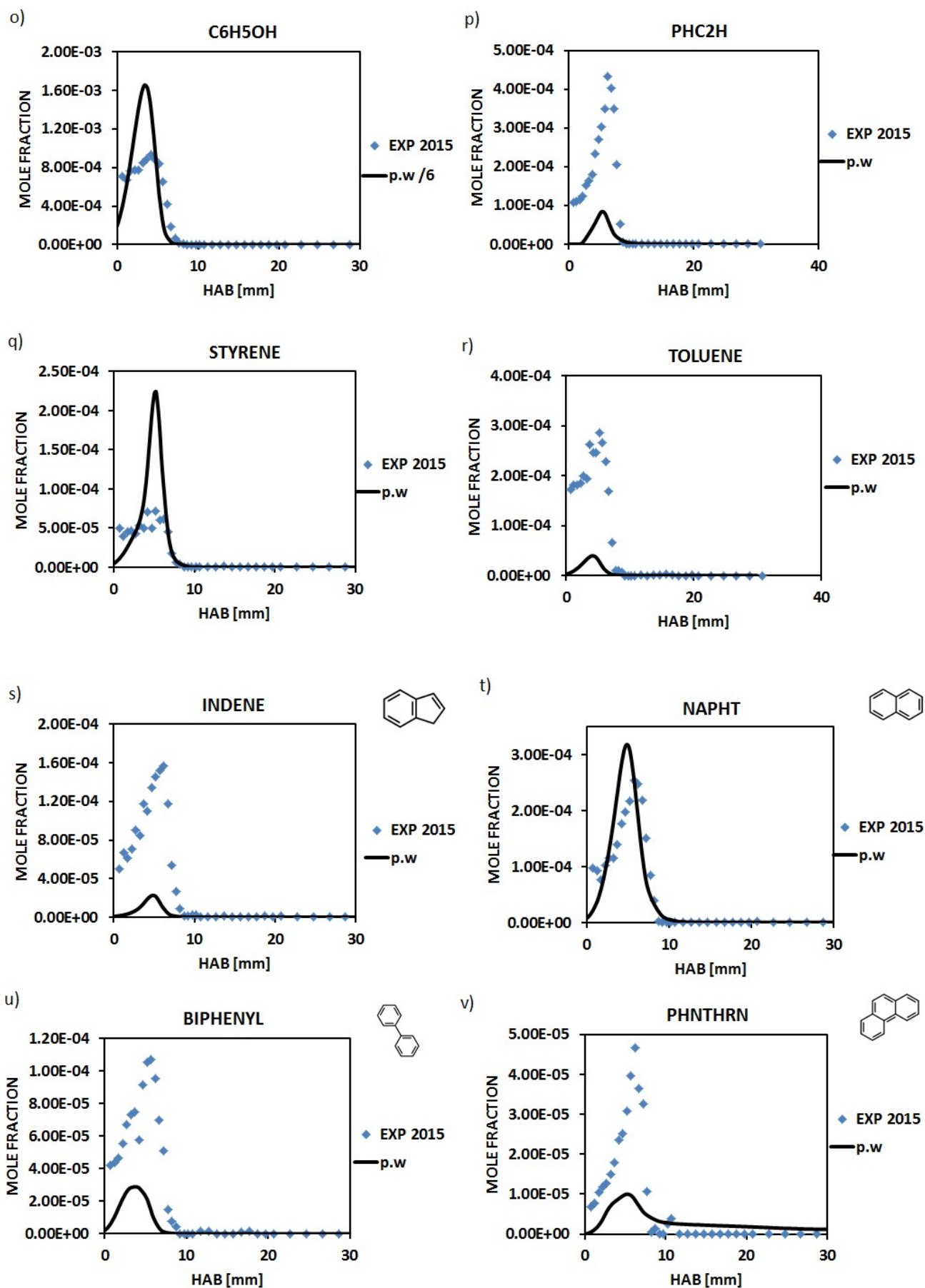


Figure 68 : Low pressure (30 Torr) benzene premixed flame,  $\phi=2.00$ . Predicted and experimental mole fraction of a): benzene, b): oxygen, c): methyl radical, d): water, e): carbon monoxide, f): carbon dioxide, g): acetylene, h): propargyl radical, i): allene, j): propyne, k): but-1,3diene, l): vinylacetylene, m): cyclopentadienyl radical, n): cyclopentadiene,

o): phenol, p): phenylacetylene, q): styrene, r): toluene, s): indene, t): naphthalene, u): biphenyl, v): phenanthrene. The symbols represent the experimental data [150]; the continuous lines represent the modeling results from the present work.

It can be seen that a satisfactory agreement is obtained between measured and predicted mole fractions for most of the key radical as well as molecular species within a factor of 2. Radical species such as methyl, propargyl and cyclopentadienyl mole fraction profiles are well reproduced within experimental uncertainties. Molecular species such as benzene decay, allene, propyne, diacetylene, vinylacetylene and cyclopentadiene are fairly represented. A good agreement with acetylene concentration profile can be seen from the burner surface to 10 mm above the burner. Large discrepancies are observed from 10 mm to the burnt gas zone. In contrast with the modeling result, where a constant evolution of the mole fraction is obtained, the measurements show a decreasing trend within a factor of 3. While positive results are obtained for monoaromatic species such as phenylacetylene (PHC<sub>2</sub>H), styrene, and toluene, a fairly agreement between predicted PAHs mole fraction and the measured ones such as indene, naphthalene, biphenyl and phenanthrene can be seen. These results are online with the better prediction of these PAHs precursors such as acetylene, vinylacetylene, diacetylene, propargyl and cyclopentadienyl.

#### - Rate of production/consumption Analysis

##### Benzene decay pathways

Benzene decays mainly by its reaction with H atom and OH to yield phenyl radical. Phenoxy radical (C<sub>6</sub>H<sub>5</sub>O) is also found to be formed near the burner surface.



In addition to benzene decomposition pathways, it is formed later by styrene decay reaction as follows:



### **Acetylene formation/consumption**

As discussed previously, the main source of acetylene is vinyl radical decay reaction (R3768) and propyne dissociation reaction (R525). In this benzene flame, an additional pathway involving cyclopentadienyl is found to play a significant role in lower HAB zone:

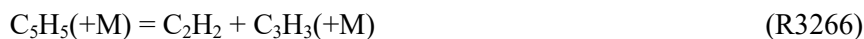


The importance of this reaction in acetylene production is related to the high amount of phenyl radical production from benzene, since cyclopentadienyl is mainly formed from phenoxy radical, which is directly produced from phenyl radical reaction with oxygen atom. For a temperature range of 1380-1770 K corresponding to a HAB range of 4-7 mm, (R3266) is predominant, followed by (R3768) and then (R525). At higher HAB, (R3768) is predominant.

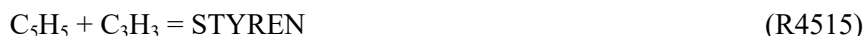
Acetylene is mainly consumed to yield HCCO (R278) and CH<sub>2</sub> (R277) as discussed in the previous sections.

### **Propargyl radical (C<sub>3</sub>H<sub>3</sub>) formation/consumption**

Propargyl formation is dominated by cyclopentadienyl decomposition (R3266) and a minor contribution of phenyl radical as follows:



The reactions involved in its consumption are mainly styrene, propyne and allene production.



### **Propyne formation/consumption**

Propyl formation is dominated by propargyl contribution, followed by allene isomerization reaction:

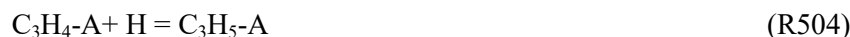


In contrast with benzene flame, propyne formation is dominated by allene and allyl radical contributions in alkane premixed flames. That is understandable due to the high concentration of propargyl precursor ( $C_3H_3$ ) in such aromatic flames.

As for alkane flames, propyne is mainly consumed to form acetylene (R525) in this benzene flame.

### **Allene formation/consumption**

Allene is mainly formed from allyl radical as for alkane flames, and a major contribution of propargyl:



Reaction (R530) is found to be predominant in the burnt gas zone, starting from  $HAB = 8$  mm that corresponds to a temperature 1770 K, while reaction (R504) is the predominant one in alkane flames.

It is mainly consumed to yield propyne and a minor contribution in acetylene production:



### **Cyclopentadiene ( $C_5H_6$ ) formation/consumption**

Cyclopentadiene is found to be mainly formed from phenol ( $C_6H_5OH$ ):



It is produced at lower HAB zone (near the burner surface) by cyclopentadienyl reaction route, then this reaction becomes the main consumption path of cyclopentadiene at temperature  $> 1600$  K.



### **Cyclopentadienyl ( $C_5H_5$ ) formation/consumption**

Cyclopentadienyl formation is dominated by phenoxy radical decomposition reaction, followed by a minor contribution of cyclopentadiene thermal decomposition:



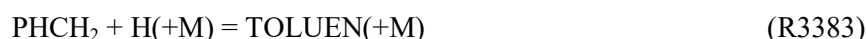


Cyclopentadienyl is mainly consumed to form acetylene, propargyl, styrene and a minor contribution in but-1,3-diene formation as follows:

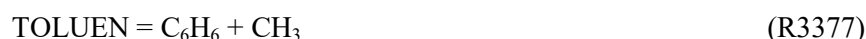


### **Toluene formation/consumption**

Toluene formation is dominated by benzyl radical reaction with H atom:



It is mainly consumed by through the reverse of reaction (R3383) to formed back benzyl. Benzene is also produce through its decomposition reaction:



### **Styrene formation/consumption**

Styrene is mainly formed from cyclopentadienyl reaction with propargyl:



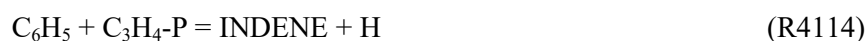
The main reactions involved in styrene consumption lead to phenyl and benzene formation as follows:



### **Indene formation/consumption**

Indene is mainly formed near the burner surface by cyclopentadienyl reaction with cyclopentadiene.

Then, phenyl reaction with propyne and allene are found to play a key role in indene production.







Indene is mainly consumed to form indenyl radical:



### **Biphenyl (BIPHENYL) formation/consumption**

Biphenyl is mainly formed from cyclopentadienyl reaction with benzyl, followed by a minor contribution of phenyl radical recombination reaction:



Biphenyl is mainly consumed to form benzene and phenyl through its decomposition, then biphenyl radical ( $\text{P}_2^-$ ) formation:



In the lower HAB zone (near the burner surface) and due to the high amount of phenyl and benzene in that zone, biphenyl formation is initiated by reaction (R4165) that becomes later its major consumption pathway.

### **Naphthalene formation/consumption**

As for ethylene premixed flame, naphthalene formation is dominated by the phenyl reaction with vinylacetylene ( $\text{C}_4\text{H}_4$ ), followed by the contribution of HACA reaction route represented by  $\text{A}_1\text{C}_2\text{H}_3\text{AC}$  and a minor contribution of cyclopentadienyl radical recombination:



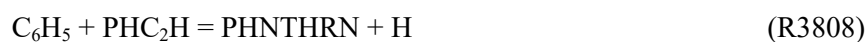
Reaction (R4130) which is the naphthalene predominant production pathway is found to be a source of consumption at higher HAB ( $T > 1770 \text{ K}$ ). Thus, only reaction (R3656) continues to produce naphthalene in that flame zone.

Naphthalene is mainly consumed to form naphthyl radical, phenylacetylene and then indenyl radical:



#### **Phenanthrene (PHNTHRN) formation/consumption**

Phenanthrene formation is dominated by phenyl reaction with phenylacetylene, followed by naphthalene reaction with diacetylene ( $\text{C}_4\text{H}_2$ ):



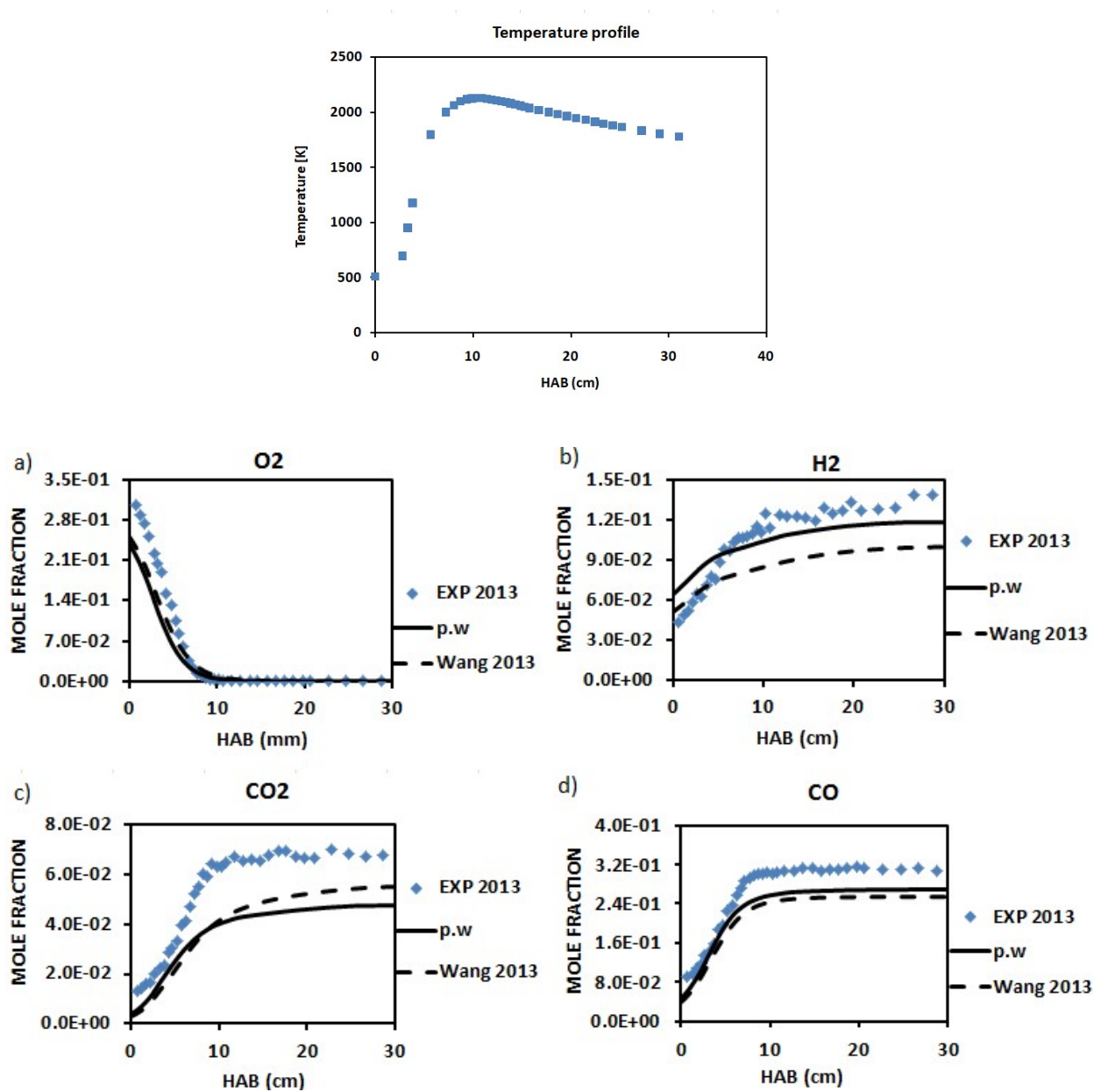
Phenanthrene is mainly consumed to form phenanthryl radical ( $\text{A}_3\text{-1}$ ;  $\text{A}_3\text{-4}$ ), which is found to be widely involved in pyrene formation process through the HACA mechanism.

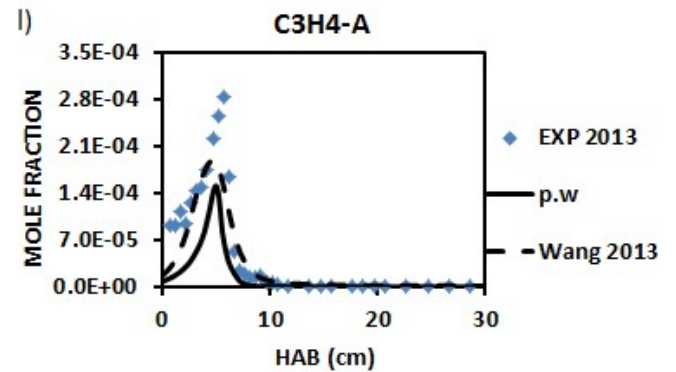
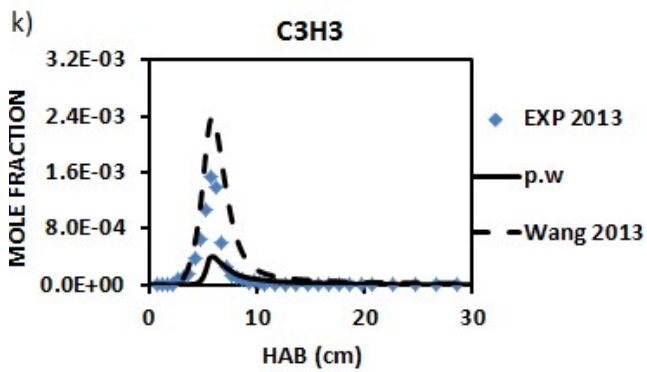
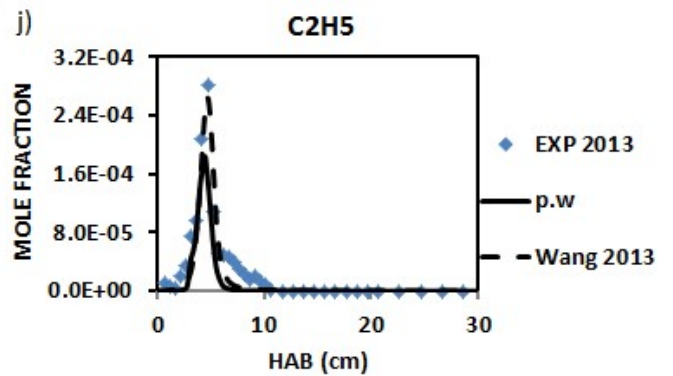
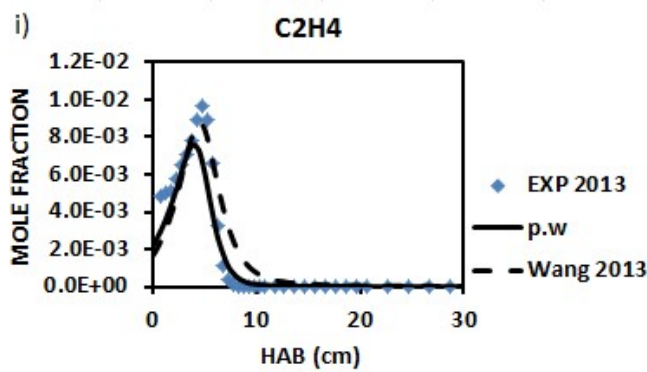
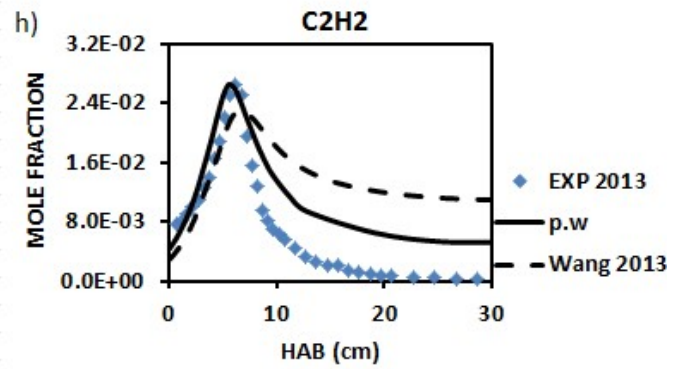
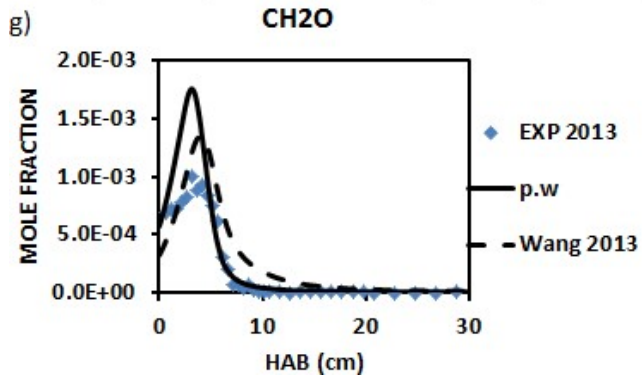
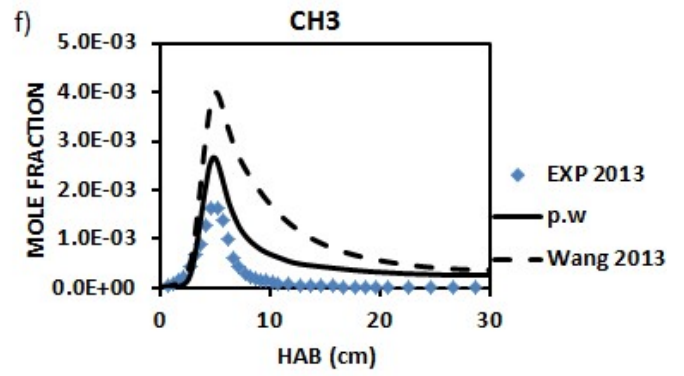
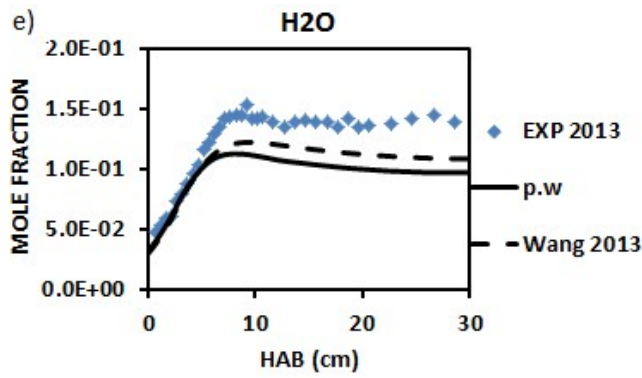


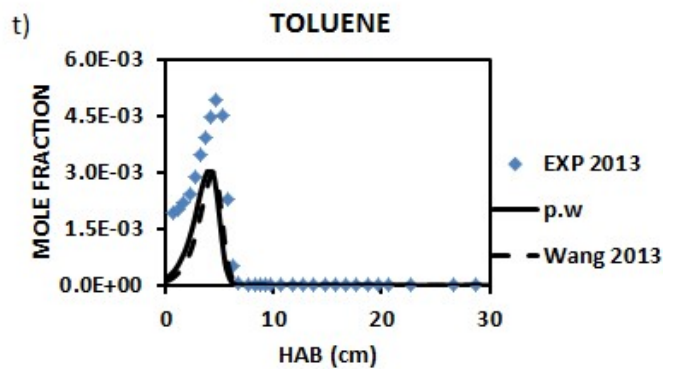
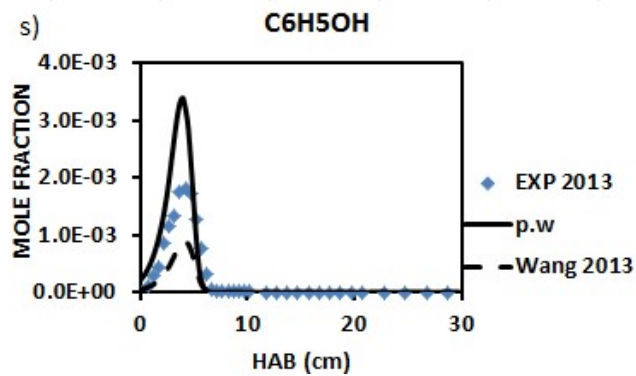
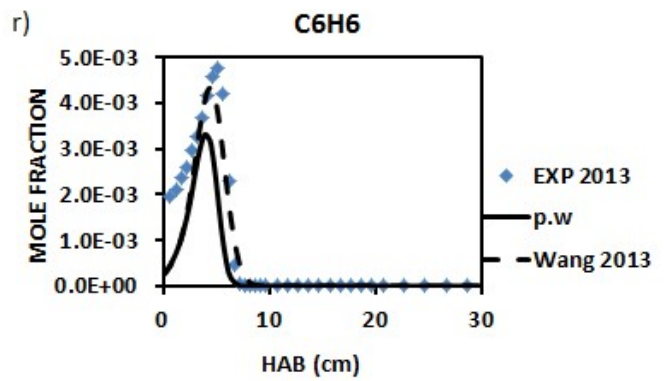
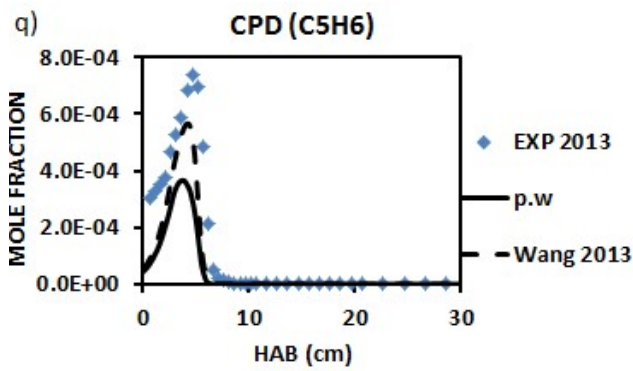
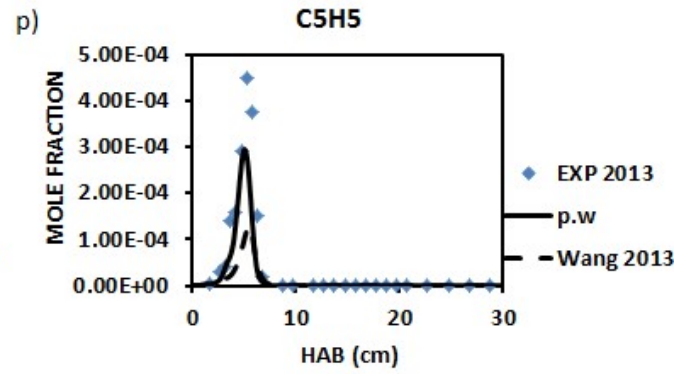
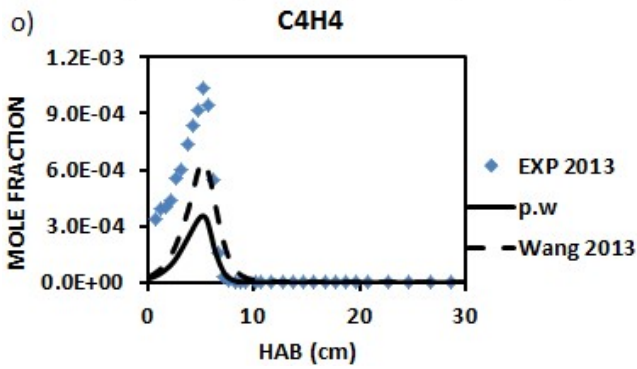
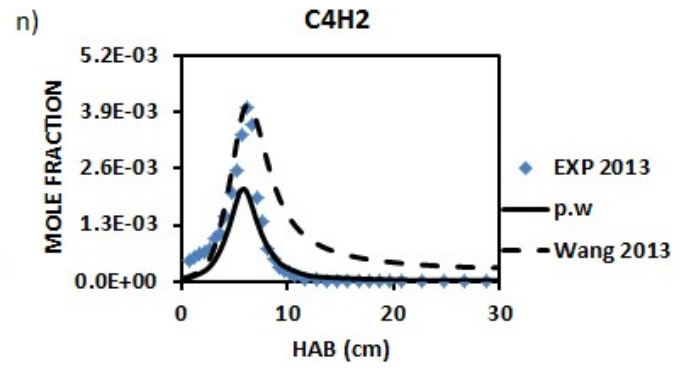
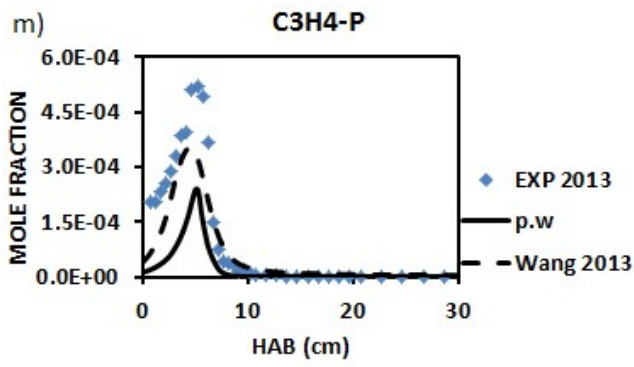
#### **4.4.1.3.2. n-propylbenzene flame**

As for benzene combustion and a main subset of the present mechanism, n-propylbenzene is an aromatic hydrocarbon which combustion properties are useful to understand since this kind of component widely exists in practical fuels. Aromatic hydrocarbons are known to significantly contribute to the soot production by enhancing the soot precursors such as PAHs. The understanding of aromatic hydrocarbon combustion will help for the development of clean combustors. Compared with benzene, n-propylbenzene has longer alkyl chain and higher energy density. It is serves in most of studies as a representative component in diesel or jet surrogate fuels. A low pressure (30 Torr) rich

premixed flame of n-propylbenzene ( $\phi=1.79$ ) has been modeled and compared with the experimental mole fractions of small species as well as PAHs up to naphthalene (Figure 69).







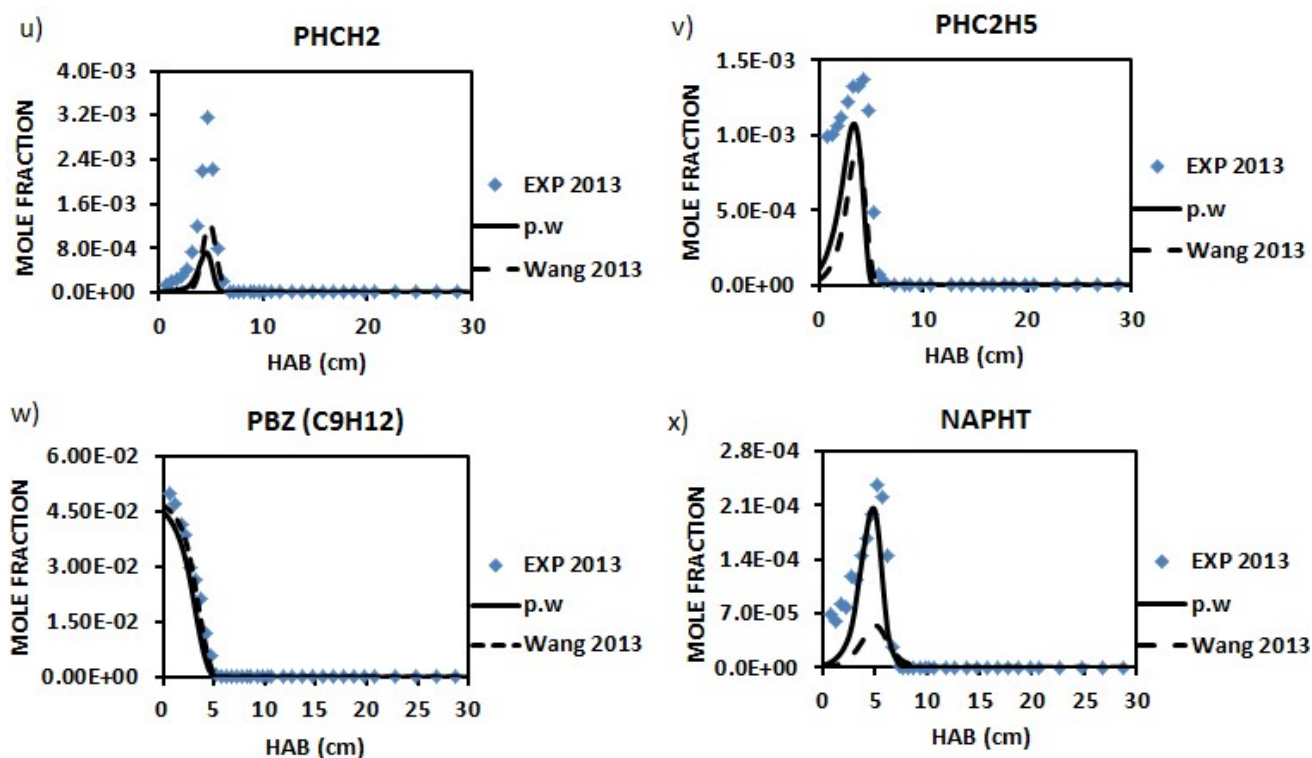


Figure 69 : Low pressure (30 Torr) n-propylbenzene premixed laminar flame : PBZ/O<sub>2</sub>/Ar :0.05/0.32/0.63 in mole fraction ;  $\phi = 1.79$  ;  $V = 50$  cm/s ; Predicted and experimental mole fraction of a): oxygen, b): hydrogen, c): carbon dioxide, d): carbon monoxide, e): water, f): methyl, g): formaldehyde, h): acetylene, i): ethylene, j): ethyl, k): propargyl radical, l): allene, m): propyne, n): diacetylene, o): vinylacetylene, p): cyclopentadienyl, q): cyclopentadiene, r): benzene, s): phenol, t): toluene, u): benzyl, v): ethylbenzene, w): n-propylbenzene, x): naphthalene. The symbols represent experimental data from [118]; the continuous lines represent the modeling results from the present work; dashed lines: Wang et al. mechanism for n-propylbenzene combustion [118].

As for iso-octane flame, a good agreement for all species measured with the predictions can be observed. Radical species as well as molecular species including acetylene, benzene, monoaromatics (n-propylbenzene decay, benzyl radical, phenol, toluene and ethylbenzene) and naphthalene are well reproduced. These results also indicate the performance of the present mechanism for a rich low pressure aromatic premixed flame. The mechanism of Wang et al. [118] shows similar results as for the present mechanism. Discrepancies are observed mainly for acetylene and naphthalene mole fractions prediction. For the acetylene, Wang et al. mechanism [118] overpredicts measurements (within a factor  $> 4$ ) in the burnt gas zone, while for naphthalene, an underprediction within a factor of 3 is obtained.

#### - Rate of production/consumption Analysis

##### n-propylbenzene decay pathways

n-propylbenzene consumption is initiated near the burner surface by H atom abstraction with H and OH, followed by thermal decomposition reactions:



At a temperature higher than 1800 K, reaction (R3509) is the predominant one.

### **Acetylene formation/consumption**

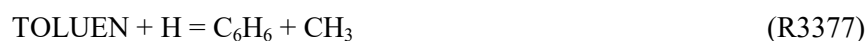
As for benzene flame, similar reactions are involved in acetylene formation. In contrast with benzene flame, acetylene formation is dominated by vinyl radical decomposition (R3768) in all the flame zones, followed by cyclopentadienyl decomposition reaction (R3266) and propyne contribution (R525). However, an additional reaction involving benzyl radical (PHCH<sub>2</sub>) in n-propylbenzene flame is observed:



PHCH<sub>2</sub> is directly formed from n-propylbenzene decay and this reaction is not found important in the case of benzene premixed flame. The presence of an alkyl chain on monoaromatic shows an impact on species such as acetylene formation pathways. The main reactions involved in acetylene consumption are similar to those previously discussed in the case of benzene flame.

### **Benzene formation/consumption**

Benzene is mainly produced near the burner surface by n-propylbenzene decomposition reaction, followed by a major contribution of toluene, biphenyl and styrene decomposition reactions:





As for n-butane/n-propylbenzene mixture flames, benzene formation is controlled mainly by aromatic species decomposition. At a temperature of 1700 K, benzene formation is dominated by toluene decomposition (R3377), followed by biphenyl decomposition (R4165) and then styrene (R3471) and n-propylbenzene decomposition (R3518). The main reactions involved in benzene consumption are phenyl radical formation as discussed in the previous sections.

### **Toluene formation/consumption**

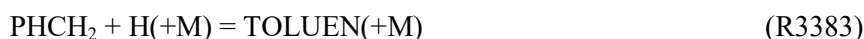
No difference between benzene and n-propylbenzene premixed flames is observed concerning toluene formation and consumption pathways. Reactions observed are similar to those previously discussed in the case of benzene flame.

### **Benzyl (PHCH<sub>2</sub>) formation/consumption**

Benzyl is mainly formed from n-propylbenzene decomposition reaction that takes place near the burner surface through the following reactions:



Benzyl is found to be a major source of toluene, cyclopentadienyl, ethylbenzene, biphenyl and naphthalene as following:



Reaction (R3420) that initially consumes benzyl becomes its source of production at higher HAB ( $T > 1700$  K). Also, reaction (R3383) that is the predominant benzyl consumption path becomes a major source of its production in the burnt gas zone.



## Naphthalene formation/consumption

In contrast with the benzene flame, naphthalene formation is dominated by benzyl reaction propargyl, followed by the HACA mechanism and phenyl reaction with vinylacetylene:



As can be seen in Figure 70, reaction (R4130) exhibits different trend. It is found to play a significant role in naphthalene production, then, it becomes a major source of naphthalene consumption at  $T > 1800$  K. The latter reaction was found predominant in the case of benzene flame and becomes a major source of naphthalene consumption at  $T > 1750$  K. However, reaction (R4265) was not found as important in naphthalene production in benzene flame. The effect of the alkyl chain is clearly observed on aromatics production pathways, since the nature of species involved varies. Reactions involved in naphthalene consumption are similar to those discussed in benzene flame, where naphthyl, indenyl and phenylacetylene are the main products.

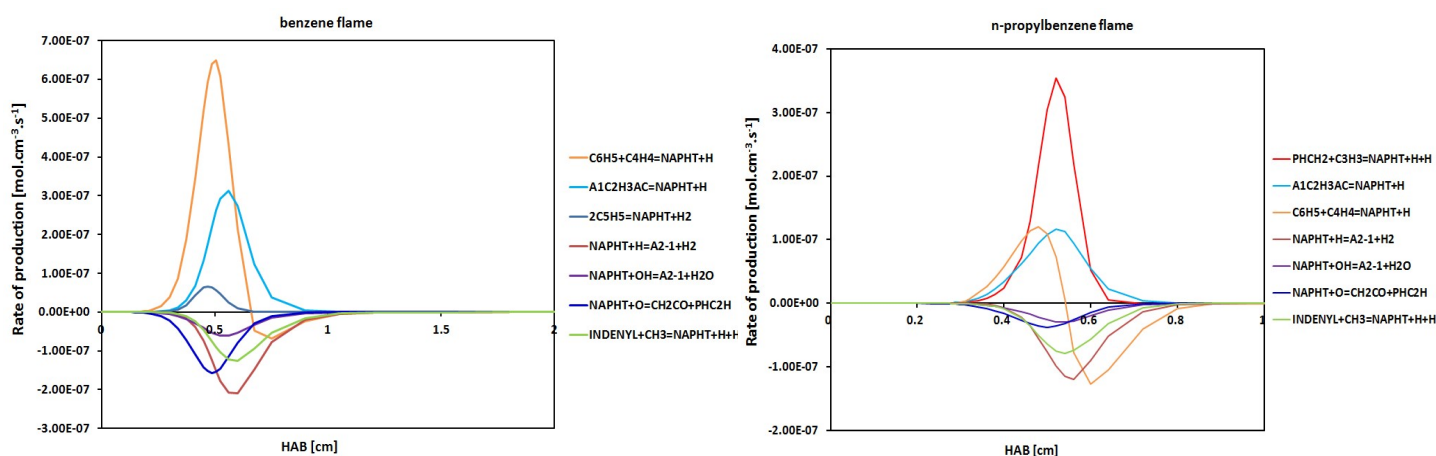


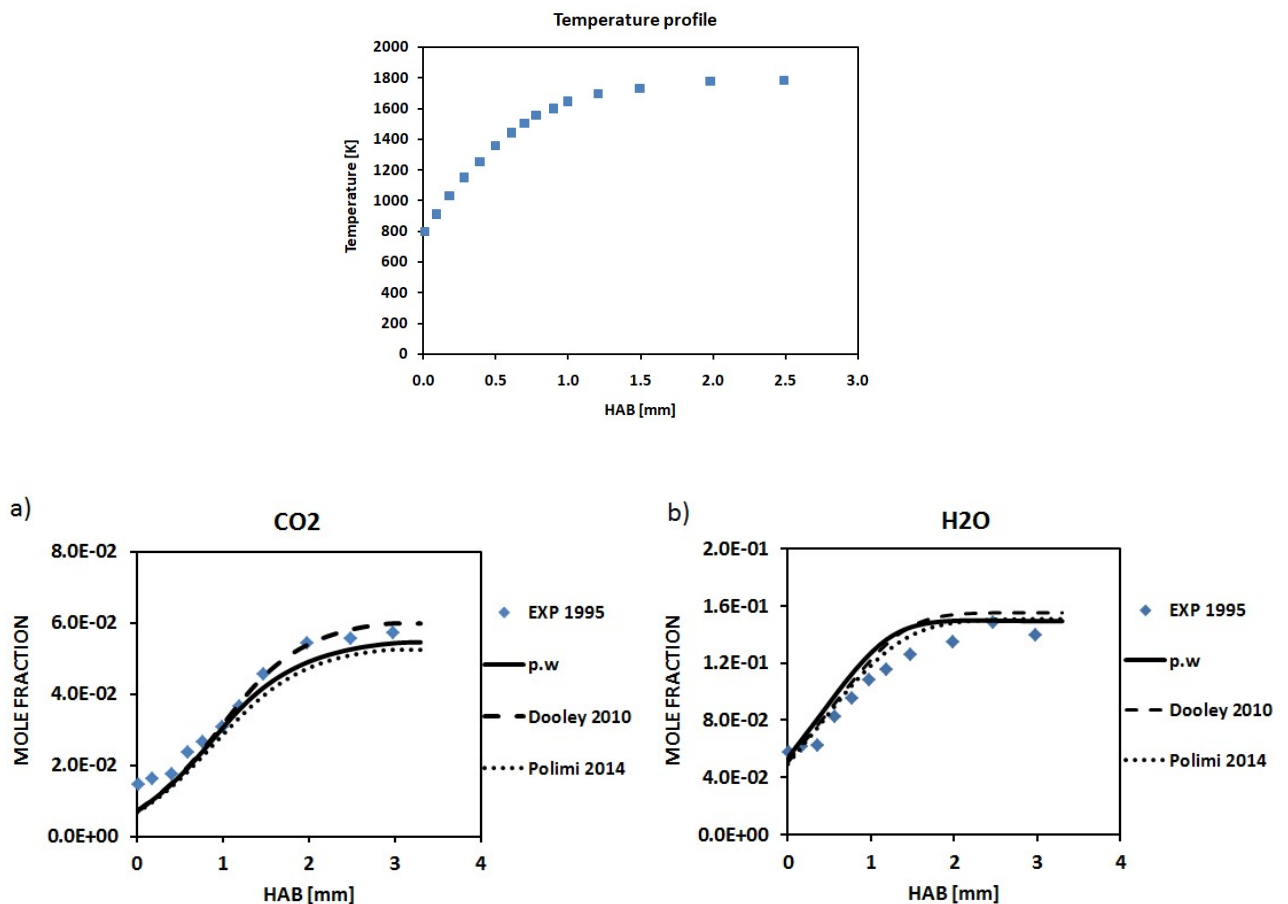
Figure 70 : Naphthalene rate of production analysis in benzene and n-propylbenzene premixed flames.

### 4.4.1.4. Liquid transportation fuel flames

Modeling of the combustion of jet fuel as well as gasoline has been performed in validating the present detailed mechanism. Due to the unavailability of experimental data over diesel fuel flame, the performance assessment of the mechanism is limited to the two above mentioned practical fuels.

#### 4.4.1.4.1. Jet fuel flame

For modeling the combustion of aviation fuels that consist of complex hydrocarbon mixtures, it is often necessary to use surrogate mixtures. The present kinetic model consisting of a few larger hydrocarbons is used to mimic the combustion of commercial jet fuel. The detailed modeling of jet fuels combustion is useful to better control and to reduce emissions and fuel consumption. Due to the complexity of such fuels composed of hundreds of hydrocarbons: alkanes, cycloalkanes, aromatics and polycyclic compounds, such modeling is a real challenge. In Figure 71, the atmospheric pressure jet fuel flame ( $\phi=1.70$ ) has been modeled by using the surrogate considered (n-decane/iso-octane/n-propylbenzene, see Table 3, section 4.2) in the present work. The comparison between measurements and predictions are presented. The largest species measured is benzene and there no available experimental data over higher hydrocarbons.



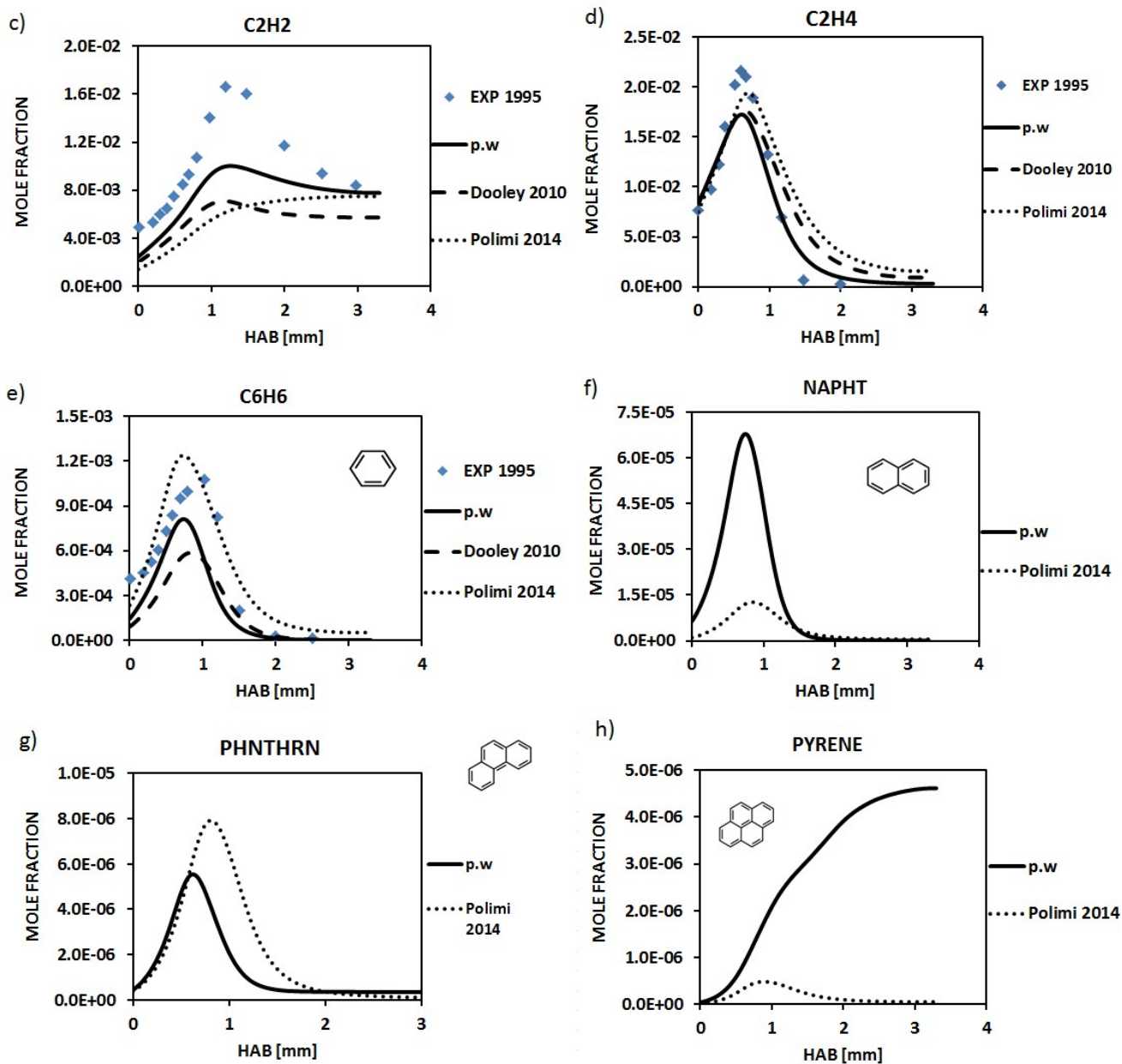


Figure 71 : Atmospheric pressure Jet fuel flame,  $\phi=1.70$ . Predicted and experimental mole fractions of a): carbon dioxide, b): water, c): acetylene, d): ethylene, e): benzene, f): naphthalene, g): phenanthrene and h): pyrene in jet fuel premixed flame. The symbols represent experimental data [152]; the continuous lines represent the modeling results from the present work; dashed lines: jet surrogate mechanism from Dooley et al. [92] and dotted lines: Polimi mechanism [128].

The present mechanism has also been validated over a rich atmospheric pressure commercial jet fuel premixed flame. The combustion products  $CO_2$  and  $H_2O$  and some measured key species such as acetylene and benzene are satisfactorily predicted. Among the mechanisms taken from the literature, some discrepancies with the Polimi mechanism [128] are observed over acetylene mole fraction profile and the amount of PAHs (naphthalene and pyrene) formed is significantly lower than that obtained from the present work mechanism. Due to the lack of experimental data for these PAHs, it is tricky to compare both mechanisms in such conditions. Nevertheless, the surrogate fuel proposed in

this work to mimic commercial jet fuel shows clearly positive results in premixed 1D flame configuration.

### Sensitivity analysis on benzene and naphthalene production

As the present mechanism was shown to perform fairly well over an extended range of operating conditions, it could be used with some confidence to perform local sensitivity analyses by computing the logarithmic derivatives of benzene and naphthalene concentrations with respect to the kinetic preexponential factors. The main aim of this analysis was to gain an overview not only on the nature of reactions which potentially affects benzene and naphthalene chemistry but also the nature of those conditioning benzene and naphthalene production in liquid transportation surrogate fuels.

Figure 72 shows sensitivity analyses for benzene formation in jet A-1 premixed flames.

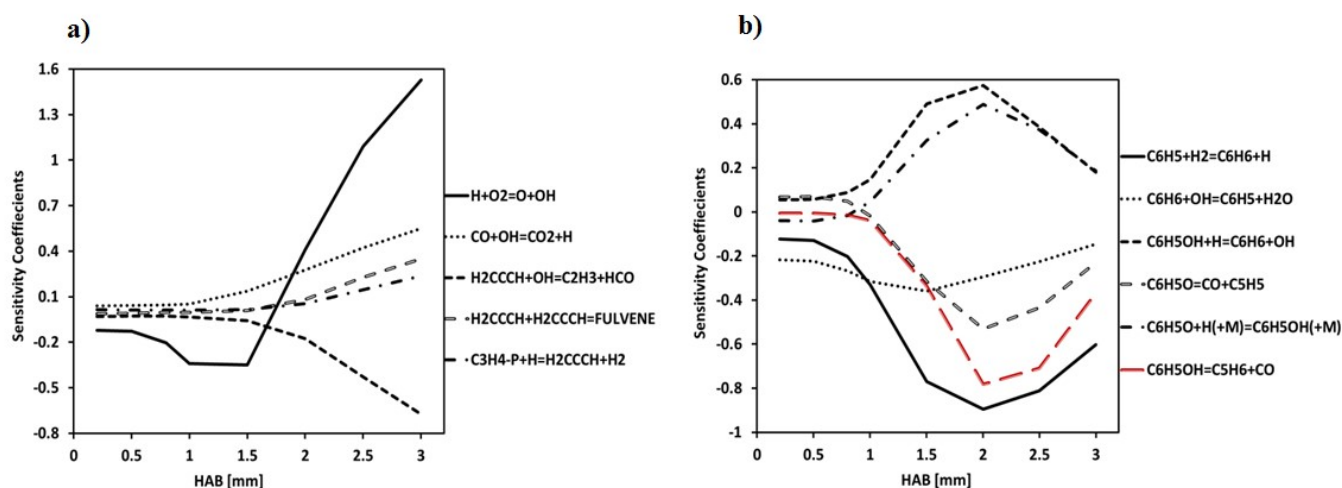


Figure 72 : Normalized sensitivities for benzene formation in jet A-1 premixed flame ( $\phi=1.70$ ,  $P=1\text{atm}$ ).

As expected, the core  $\text{H}_2\text{-O}_2$  reaction system plays an important role in benzene chemistry in jet A-1 flame. It can be seen that reactions involved in propargyl consumption by oxidation shows negative sensitivities, while those involved in its production shows positive sensitivities, indicating that propargyl might be widely involved in benzene formation process. It is observed that reactions favoring the formation of fulvene, benzene and phenol show positive sensitivities, while those consuming benzene and phenoxy which is the main precursor of phenol show negative sensitivities. This is consistent with the fact that these species could be benzene precursors. One can note that the highest negative sensitivity is observed for reaction  $\text{C}_6\text{H}_5+\text{H}_2=\text{C}_6\text{H}_6+\text{H}$ . In addition, reactions involving phenol impact considerably benzene production from 1.0 to 3.0 mm (burnt gas zone).

Figure 73 shows sensitivity analyses for naphthalene formation in jet A-1 flame. The core  $H_2-O_2$  reaction system plays an important role as for benzene formation.

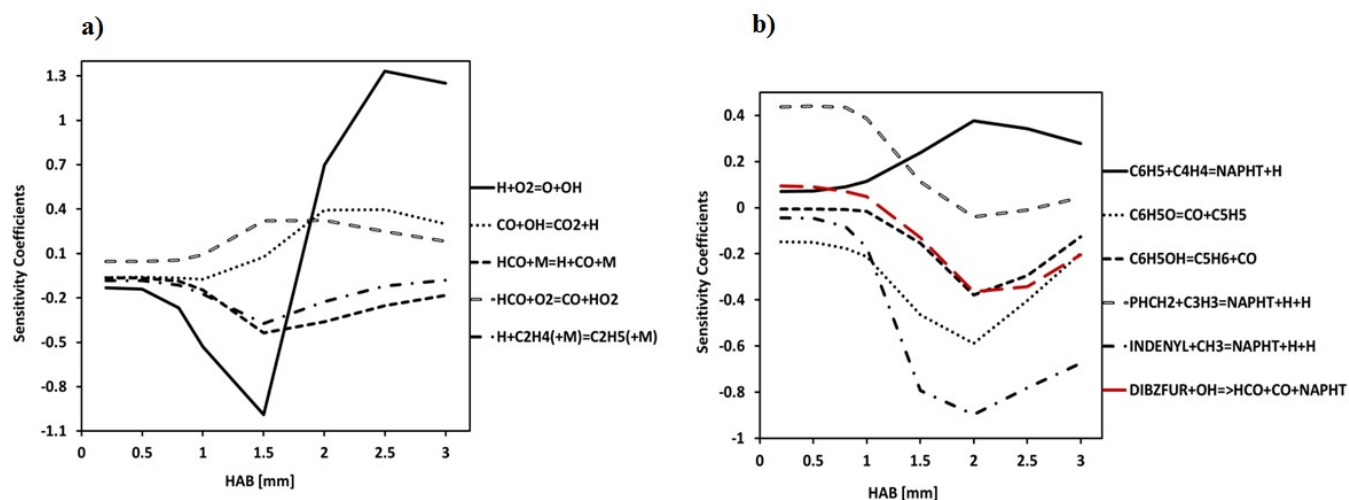


Figure 73 : Normalized sensitivities for naphthalene formation in jet A-1 premixed flame ( $\phi=1.70$ ,  $P=1\text{ atm}$ ).

Benzyl reaction with propargyl shows positive sensitivities from 0.2 to 1.8 mm. Beyond 1.8 mm, this reaction does no longer impact naphthalene formation, implying that benzyl reaction route might be an important pathway from 0.2 to 1.8 mm. Phenyl reaction with vinylacetylene shows positive sensitivities, indicating that this reaction may play an important role [52,171] for naphthalene production from 1.0 mm to 3.0 mm (in burnt gas zone). Dibenzofuran oxidation reaction shows a contrasted behavior. The negative sensitivities observed for this reaction could be explained by the consumption of its precursor (i.e phenoxy), which also exhibits negative sensitivities by yielding cyclopentadienyl radical. In that case, cyclopentadienyl radicals do not seem to play an important role in naphthalene production since phenoxy radical consumption effect is more important than their production. Negative sensitivities observed for phenol decomposition reaction to yield cyclopentadiene ( $C_5H_6$ ) shows that this reaction may also impact naphthalene production.

#### - Rate of production Analysis

##### Acetylene formation/consumption

In jet A-1 flame, acetylene formation is dominated by the contribution of vinyl radical (R3768) and propyne (R525) as previously discussed. It is mainly consumed to produce HCCO (R278) and  $CH_2$  (R277).

### **Benzene and naphthalene formation/consumption**

The present mechanism was subsequently used to analyze benzene and naphthalene production pathways in jet A-1 surrogate fuel. In Figure 74, rates of production were obtained at the inflection point of benzene mole fraction profile which corresponds to a HAB of 0.4 mm (56.2% of jet A-1 fuel conversion). The absolute net reaction fluxes by numerical values are indicated next to the corresponding arrows. The boundary value corresponds to 1 nanomole per cubic centimeter per second and the relative contribution of reactions directly involved in benzene and naphthalene production is indicated in percent.

Figure 74 shows the main reaction paths governing benzene formation in the rich atmospheric jet A-1 flame. Benzene formation is dominated by the consumption of n-propylbenzene (50%) and biphenyl (15%) by hydrogen atoms. C<sub>3</sub> species recombination reactions account for 11%, 8% from toluene dealkylation, 7% from ethylbenzene, 5% from styrene and a minor contribution of 3% from benzaldehyde and phenol. Naphthalene formation is dominated by benzyl reaction with propargyl (51%), followed by 31% contribution from dibenzofuran oxidation by OH, 13% contribution from vinyl phenyl acetylene (A<sub>1</sub>C<sub>2</sub>H<sub>3</sub>AC) rearrangement and a minor contribution of 5% from phenyl reaction with vinylacetylene. The self-recombination of cyclopentadienyl radical reaction was found to be negligible in our conditions.

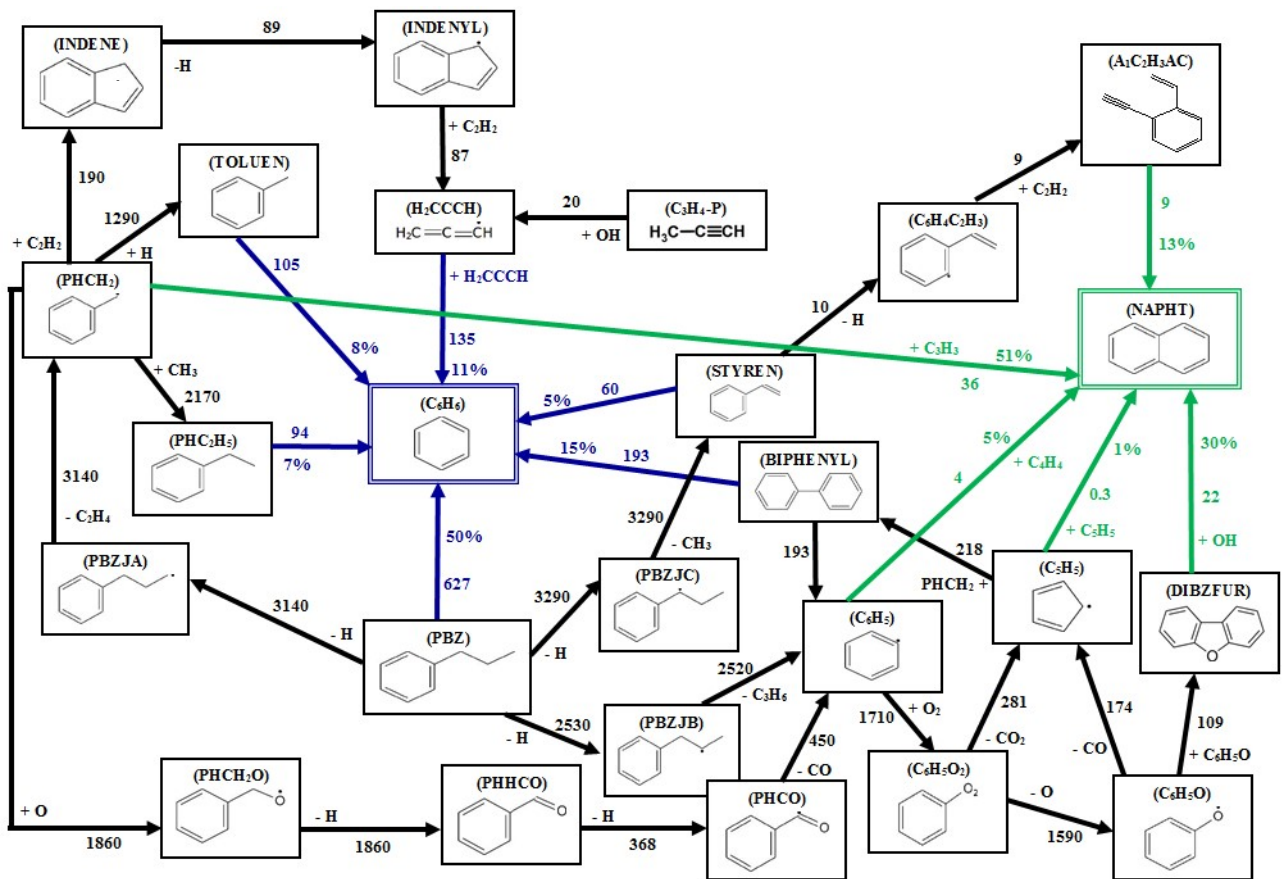


Figure 74 : Major benzene and naphthalene formation pathways in jet A-1 fuel flame [152]: HAB=0.4 mm;  $\phi=1.70$ ; P= 1 atm; Reaction fluxes are expressed in nanomole per cubic centimeter per second.

We also investigated the main reactions that produce benzene and naphthalene as a function of HAB from 0.1 to 3.3 mm (Figure 75 and Figure 76).

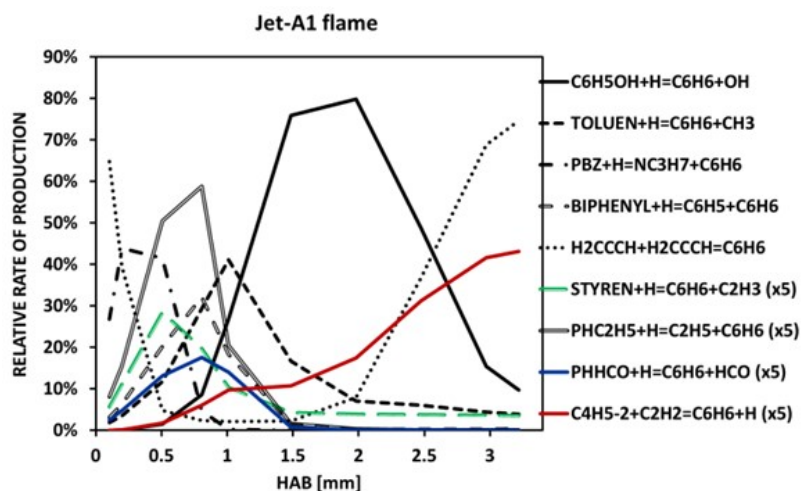


Figure 75 : Relative rates of benzene production normalized by the total rate of production in jet A-1 flames. The contributions of some reactions are multiplied by 5 as depicted in caption.

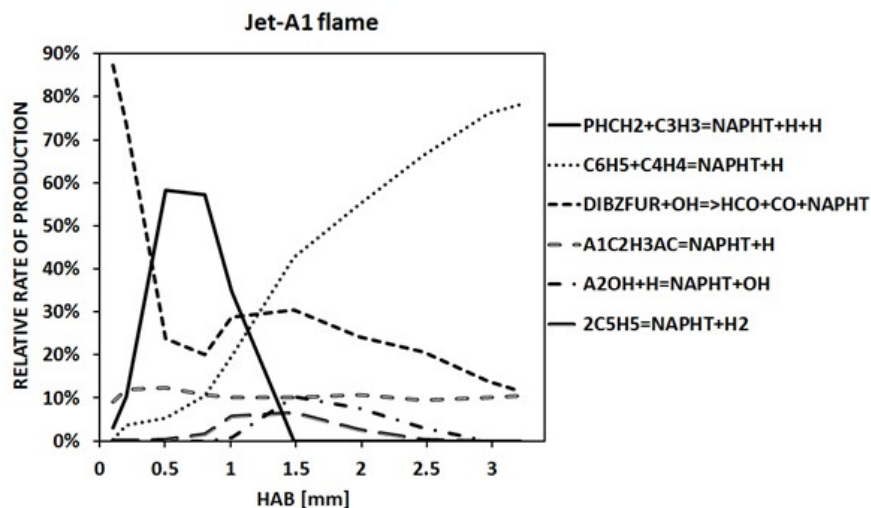


Figure 76 : Relative rates of naphthalene production normalized by the total rate of production in jet A-1 flames. The contributions of some reactions are multiplied by 5 as depicted in caption.

In Figure 75 and Figure 76, we can notice that the nature of the intermediates involved in benzene production differs from those involved in alkanes and alkenes flames previously discussed. From the current kinetic mechanism, benzene appears to be mainly formed from aromatic species such as toluene, biphenyl, ethylbenzene, n-propylbenzene and phenol. This is consistent with the fact that aromatics are well represented in jet A-1 and diesel fuels. Naphthalene production is dominated by benzyl reaction with propargyl. As many of the aromatic hydrocarbons in diesel and jet A-1 fuels contain alkylic side chains [172], they can readily produce benzyl radical by decomposition. The second important reaction identified for naphthalene production is that of dibenzofuran oxidation. Tritz et al. [133] proposed that dibenzofuran oxidation or pyrolysis could lead to naphthalene production proceeding through phenylacetylene intermediate. From the present kinetic study on jet A-1 surrogate oxidation, dibenzofuran decomposition process seems to emerge as one major naphthalene production pathway. The contribution of dibenzofuran oxidation to naphthalene production as a function of HAB in the investigated jet A-1 flame can be seen in Figure 76. It continuously produces naphthalene from HAB=0.1 mm (as a major pathway) to the burnt gas zone (HAB=3.3 mm), while benzyl radical does no longer contribute to naphthalene production at HAB > 1.5 mm since it is almost totally converted. While the present study only confirms the already established involvement of phenyl+vinylacetylene and benzyl+propargyl pathways in naphthalene production [173], the significant contribution of dibenzofuran was not proposed previously for jet A-1 premixed flames.

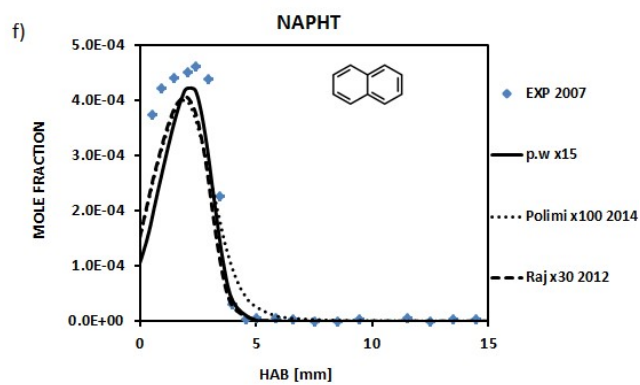
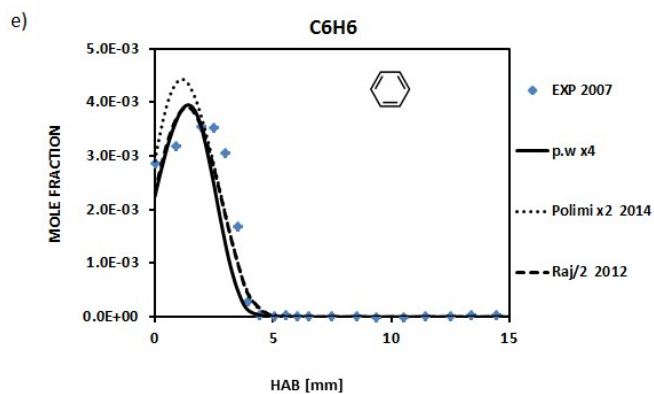
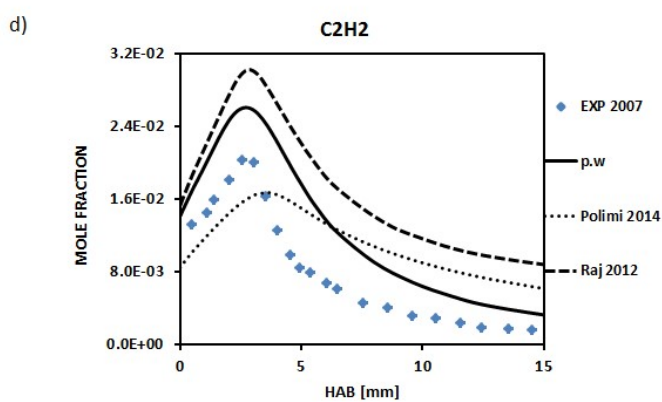
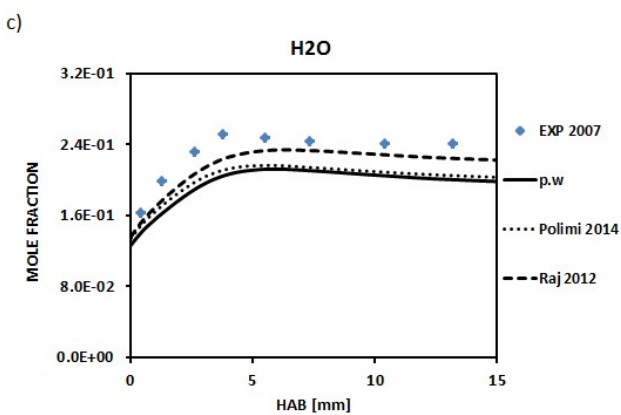
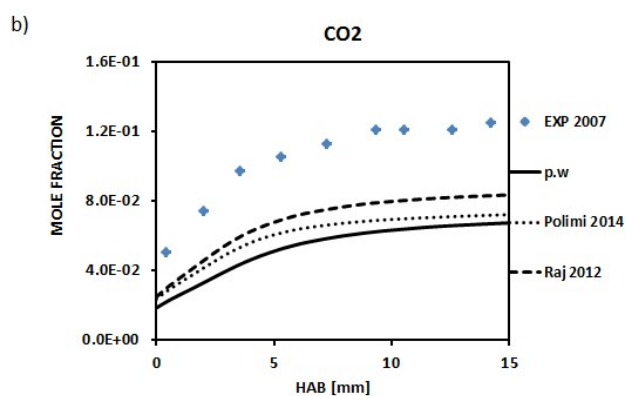
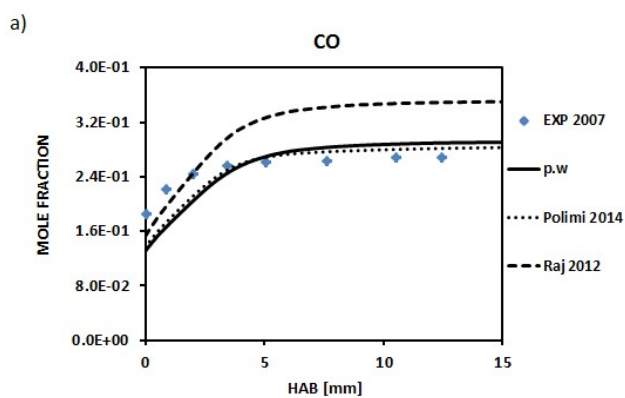
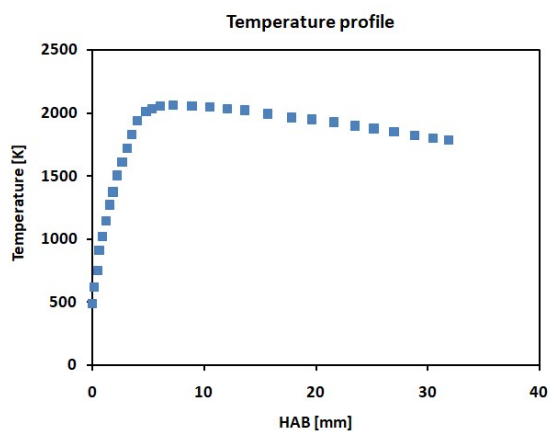


It can also be observed in Figure 76 that the HACA mechanism contribution (represented here by vinyl phenyl acetylene ( $A_1C_2H_3AC$ ) path) is significant, while that of cyclopentadienyl radicals recombination reaction contributes barely to 5% of naphthalene production. Although Marinov and coworkers [36] concluded from their detailed modeling that cyclopentadienyl radicals route reaction could be the dominant naphthalene formation pathway in premixed aliphatic flames, McEnally and Pfefferle [174] deduced that benzyl addition to propargyl and HACA mechanism are viable routes from direct experimental evidence. The present results are consistent with this later assessment. However, dibenzofuran contribution to naphthalene formation had not been highlighted in the context of premixed flame literature prior to the present study.

In summary, the reactions path analyses carried out on the formation of the first aromatic rings reinforce the oxygenate involvement hypothesis in the activation of PAHs formation at high temperature. In this activation process, our calculations show that the phenoxy radical takes a central role. Unlike most of the literature mechanisms which consider that phenoxy is only a source of cyclopentadienyl radicals, the present mechanism introduced a competition of the preceding step with that leading to a direct dibenzofuran formation. The presence of both reactions routes offers not only a better range of PAHs products, but also possible amphiphilic PAHs soot precursors due to the electronegative character of oxygen atoms.

#### **4.4.1.4.2. Gasoline flame**

As for jet fuels, modeling of gasoline combustion is a major of interest for both economical and environmental concerns. The gasoline surrogate proposed in the present work (n-decane/iso-octane/n-propylbenzene, see Table 3, section 4.2) with the present kinetic model is assessed for emulating commercial gasoline combustion behavior. A low pressure (30 Torr) rich gasoline premixed flame ( $\varphi=1.70$ ) has been modeled to get insight into the capability of the present kinetic model. In Figure 77, comparison between predictions and measurements is presented.



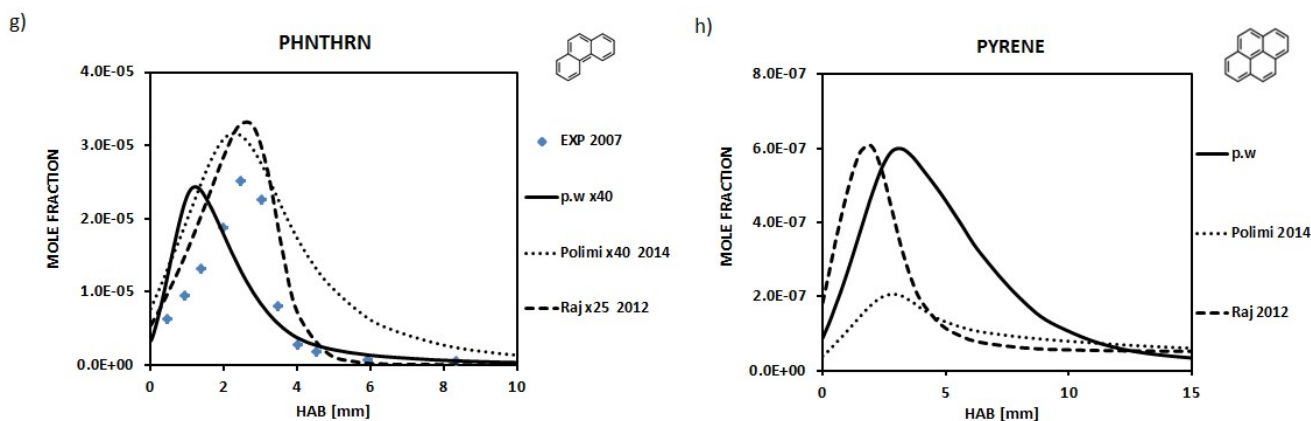


Figure 77 : Low pressure (30 Torr) gasoline flame,  $\phi=1.70$ . Predicted and experimental mole fractions of a): carbon monoxide, b): carbon dioxide, c): water, d): acetylene, e): benzene, f): naphthalene, g): phenanthrene and h): pyrene in gasoline premixed flame. The symbols represent experimental data [155]; the continuous lines represent the modeling results from the present work; dashed lines: Raj et al. mechanism for gasoline surrogate [164] using (n-heptane/iso-octane/toluene: 13.7% (%vol)/42.9%/43.4 from [157]) and dotted lines: Polimi mechanism [128].

As can be seen in Figure 77, the disagreement with experimental data is more important for gasoline premixed flame for which multiple sources of uncertainties may exist, notably the surrogate model, the kinetic model and experimental measurements. As shown in Figure 78, the carbon balance for this flame has been performed and it is found that the ratio of the mass of carbon (outlet) and the mass of carbon (inlet) is decreased by nearly 45%. That may indicate experimental uncertainties over measurements.

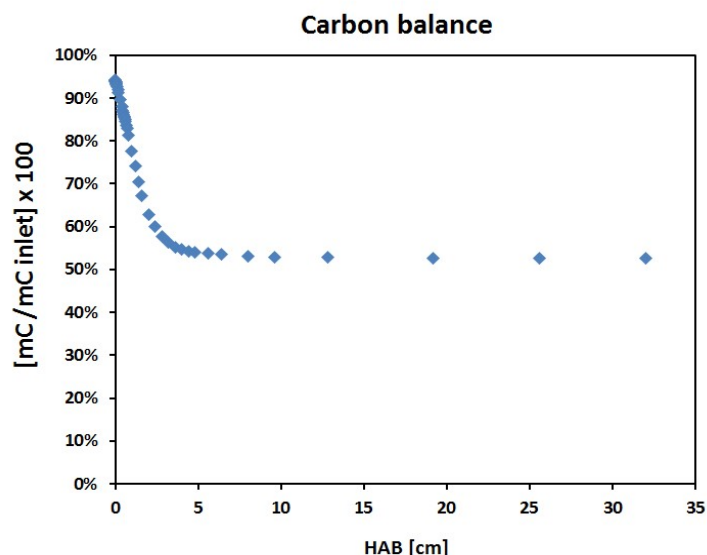


Figure 78 : Carbon balance for the gasoline premixed flame.

Among the tested mechanisms (Raj et al. and Polimi), the present one gives the closest prediction of naphthalene mole fraction (within a factor of 15). A good prediction of acetylene concentration profile is obtained while benzene concentration is underestimated within a factor of 4. Polimi mechanism

[128] underpredicts benzene mole fraction within a factor of 2, while Raj et al. [164] mechanism overpredicts within a factor of 2. For larger molecule measured such as phenanthrene, Raj et al. mechanism shows the closest prediction within a factor of 25. These results clearly show that the proposed gasoline surrogates need to be widely improved by adding more components to match more commercial gasoline properties such as molecular weight, density and the distillation curves. As a reminder, the present gasoline surrogate was proposed to satisfactorily match two global combustion parameters: the cetane number and the threshold sooting index.

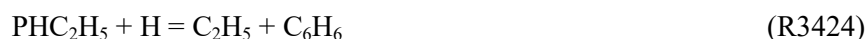
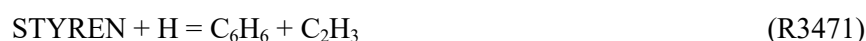
- **Rate of production analysis**

**Acetylene formation/consumption**

As in jet-A1 flame, similar reactions involved in acetylene production and consumption in this rich gasoline flame are observed.

**Benzene formation/consumption**

As can be seen in Figure 79 and as for jet-A1 flame, benzene formation is dominated by the decomposition reactions of aromatic species such as toluene, n-propylbenzene, styrene and ethylbenzene:



Benzene is found to be produce near the burner surface from reaction (R3518), followed by the contribution of toluene, ethylbenzene and styrene.

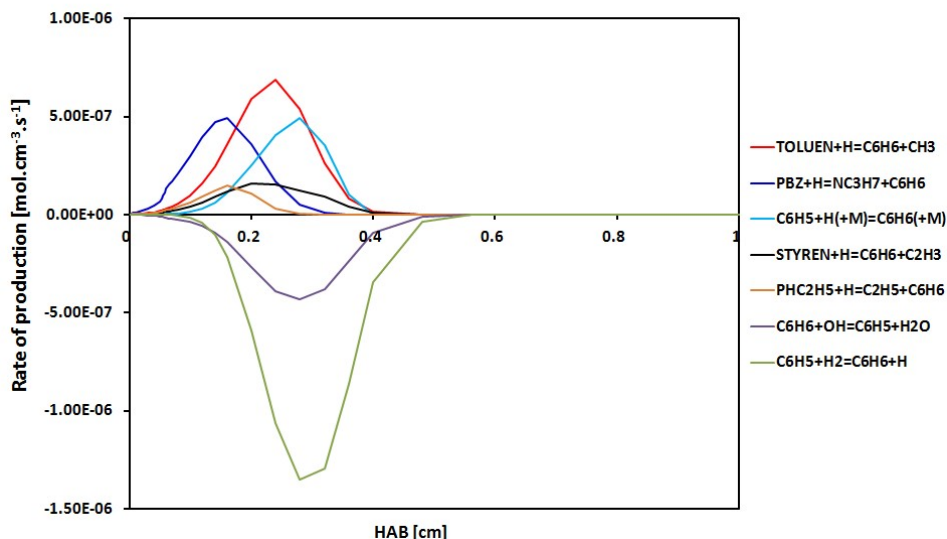


Figure 79 : Benzene rate of production in a rich gasoline premixed flame.

Benzene is mainly consumed to form phenyl radical through reactions (R3227) and (R3230) as previously discussed.

### Naphthalene formation/consumption

As in n-propylbenzene flame, similar reactions involved in naphthalene formation and consumption are observed and no clear difference between pathways involved in both flames is observed (Figure 80), indicating that the impact of aromatic addition to alkanes such as n-decane and iso-octane is predominant as for n-butane/n-propylbenzene mixture flames.

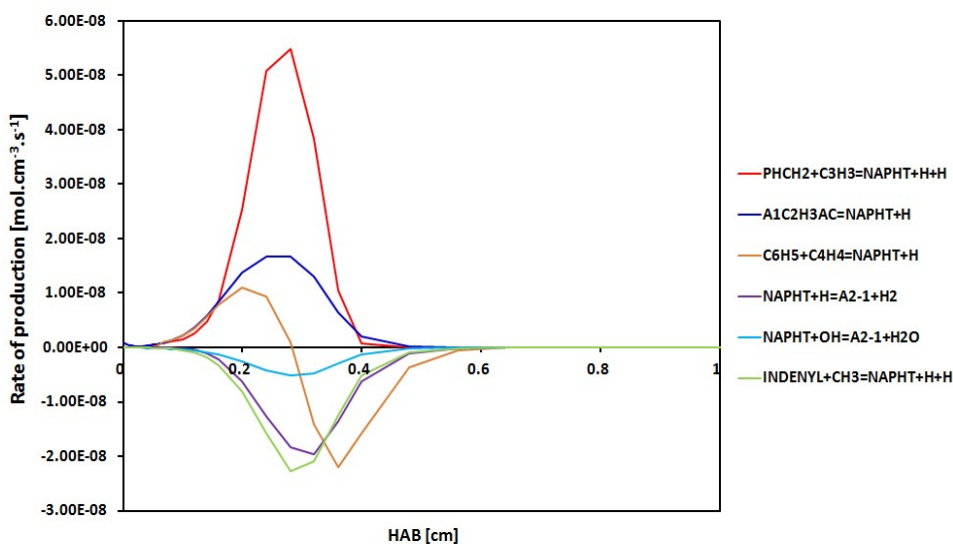
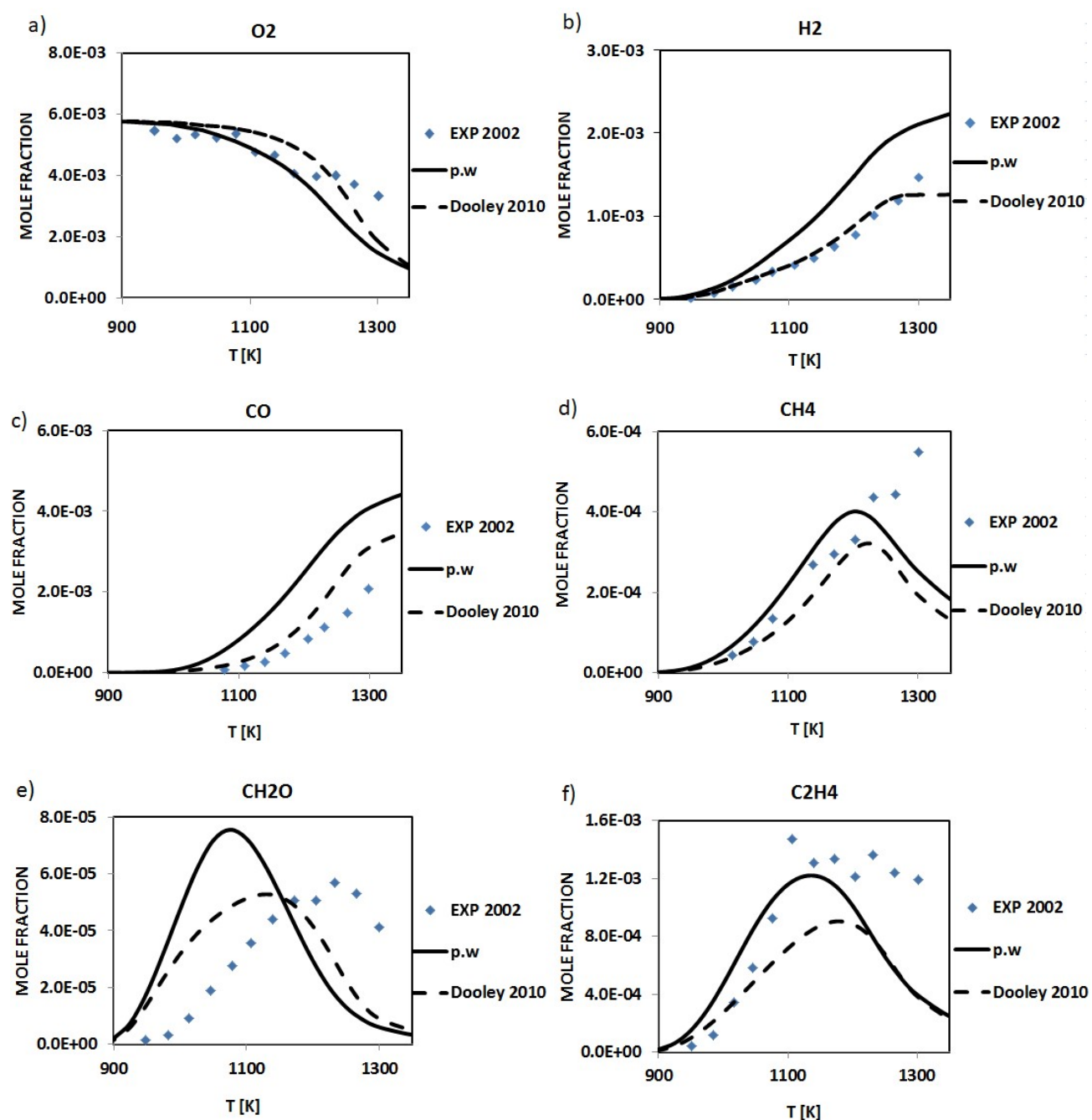


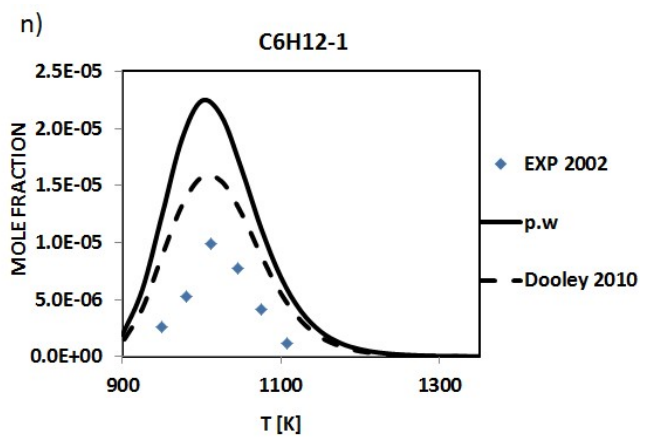
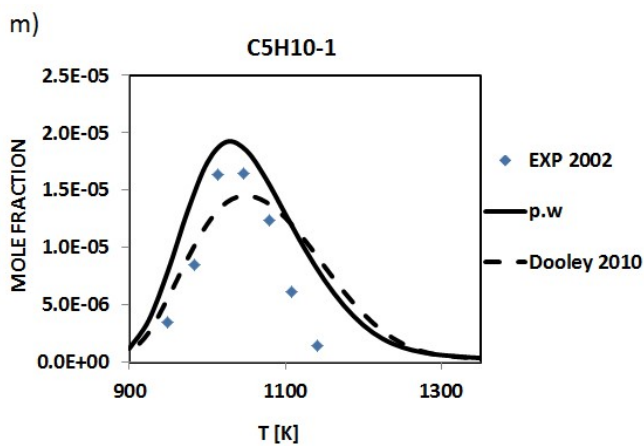
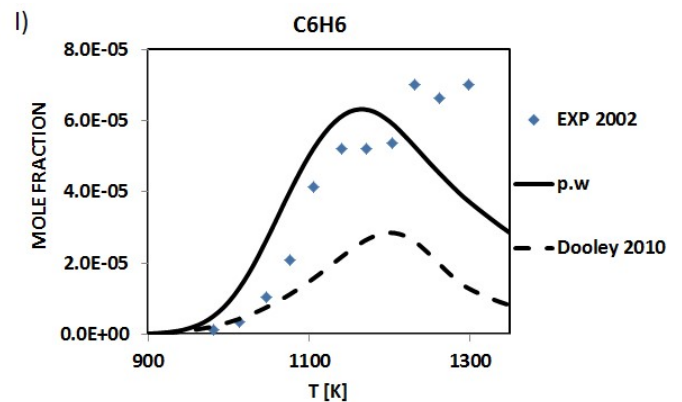
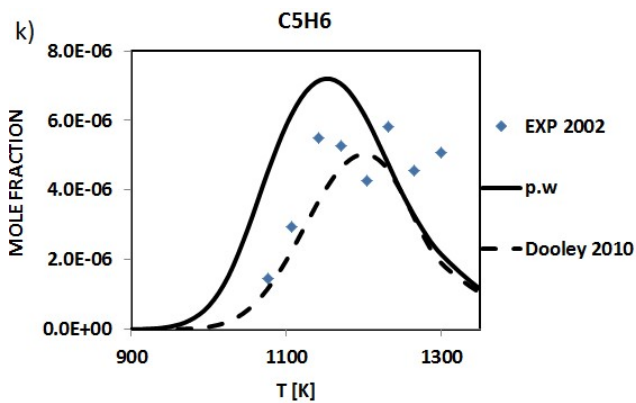
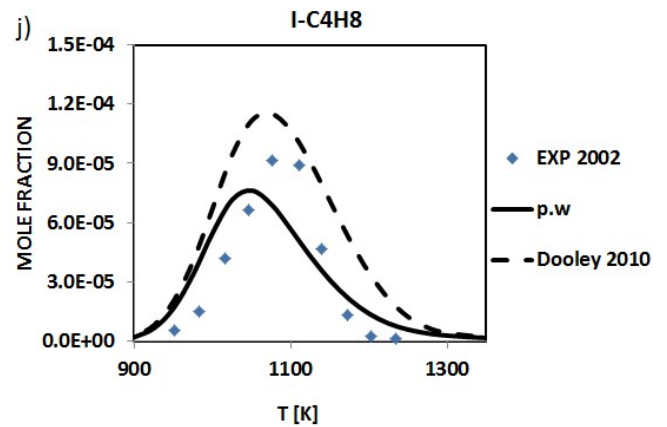
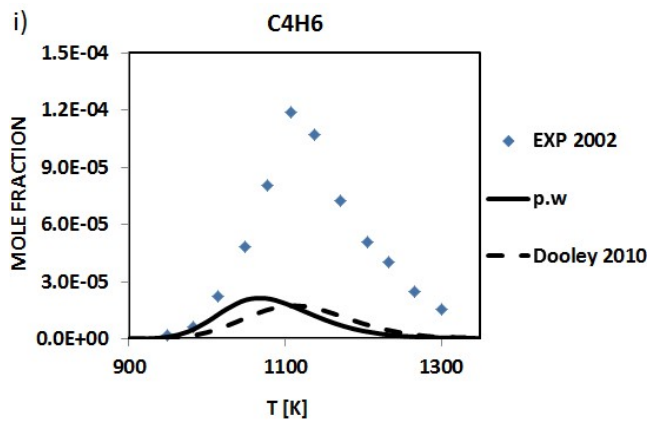
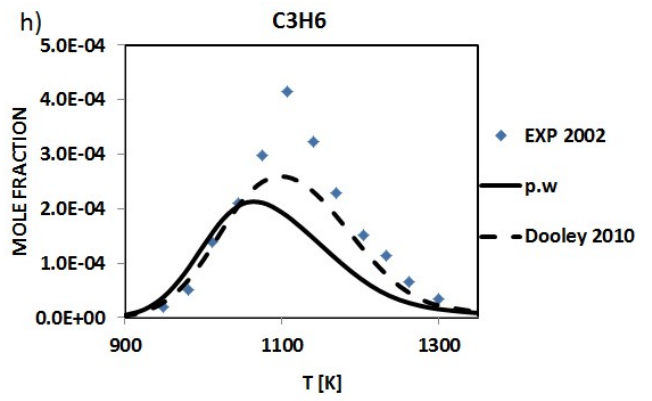
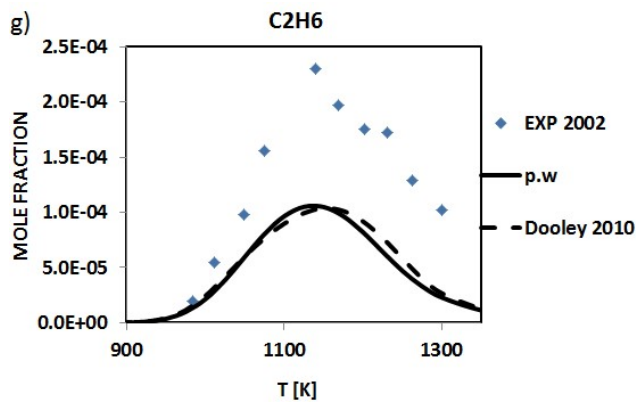
Figure 80 : Naphthalene rate of production in a rich gasoline premixed flame.

## 4.4.2. Jet Stirred Reactor (JSR) Configuration

### 4.4.2.1. Jet fuel combustion

In Figure 81, modeling results of commercial jet fuel ( $C_{11}H_{22}$ ) in jet stirred reactor configuration at a pressure of 1 atm and an equivalence ratio of  $\phi=2.0$  is presented. Several species including alkanes, alkenes, formaldehyde and aromatics up to toluene have been measured and modeled. Comparison between predictions and measurements is presented as follows:





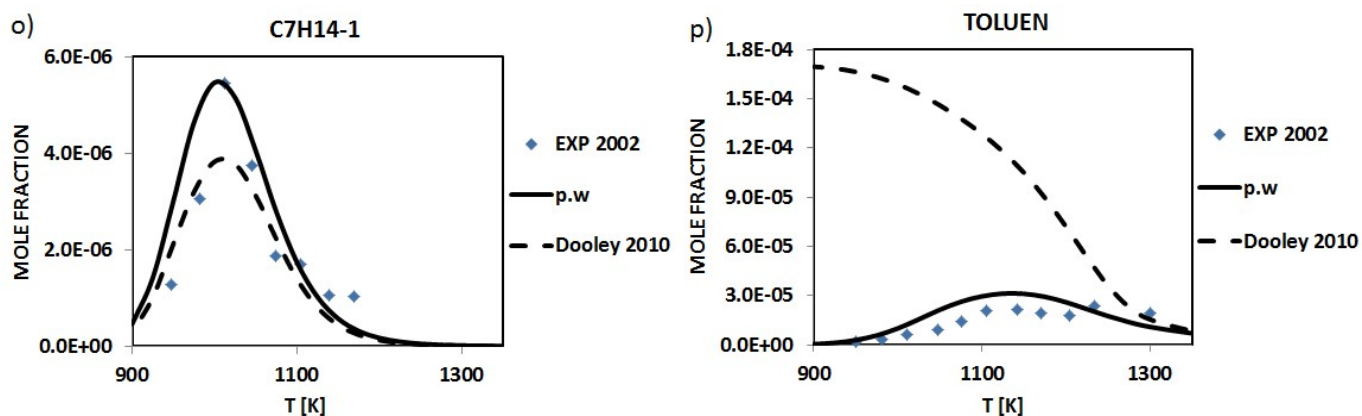
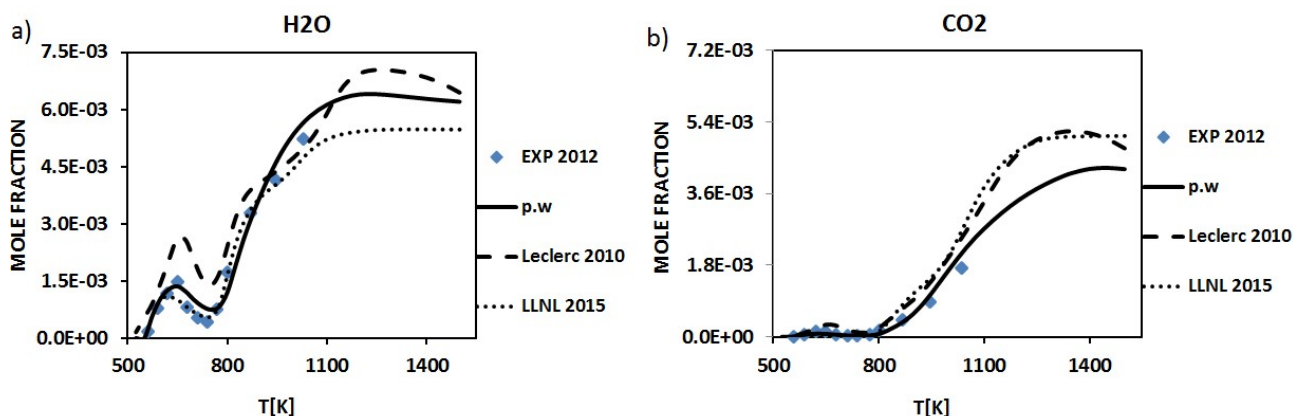


Figure 81: Atmospheric pressure jet fuel ( $C_{11}H_{22}$ ) diluted combustion in jet stirred reactor: jet fuel/ $O_2/N_2$ :0.07/0.58/99.35 in %mol.  $\phi = 2.0$ ;  $\tau = 0.07$ s; Predicted and experimental mole fraction of a): oxygen, b): hydrogen, c): carbon monoxide, d): methane, e): formaldehyde, f): ethylene, g): ethane, h): propene, i): but-1,3-diene, j): iso-butene, k): cyclopentadiene, l): benzene, m): pent-1-ene, n): hex-1-ene, o): hept-1-ene, p): toluene. The symbols represent experimental data from [158]; the continuous lines represent the modeling results from the present work; dashed lines: Dooley et al. mechanism (nC10/iC8/Toluene : 42.67% (%mol)/33.02%/24.31%) [92].

#### 4.4.2.2. Diesel fuel

Diesel fuel ( $C_{15,64}H_{29,34}$ ) oxidation in jet stirred reactor at a pressure of 10 bar and equivalence ratio of  $\phi = 1.5$  has been modeled. Predictive capability of the present kinetic model with the proposed diesel surrogate fuel (n-decane/iso-octane/n-propylbenzene, see Table 3, section 4.2) is also examined. Some key intermediate species from acetylene to but-1-ene have been measured and compared to the modeling results as shown in Figure 82.





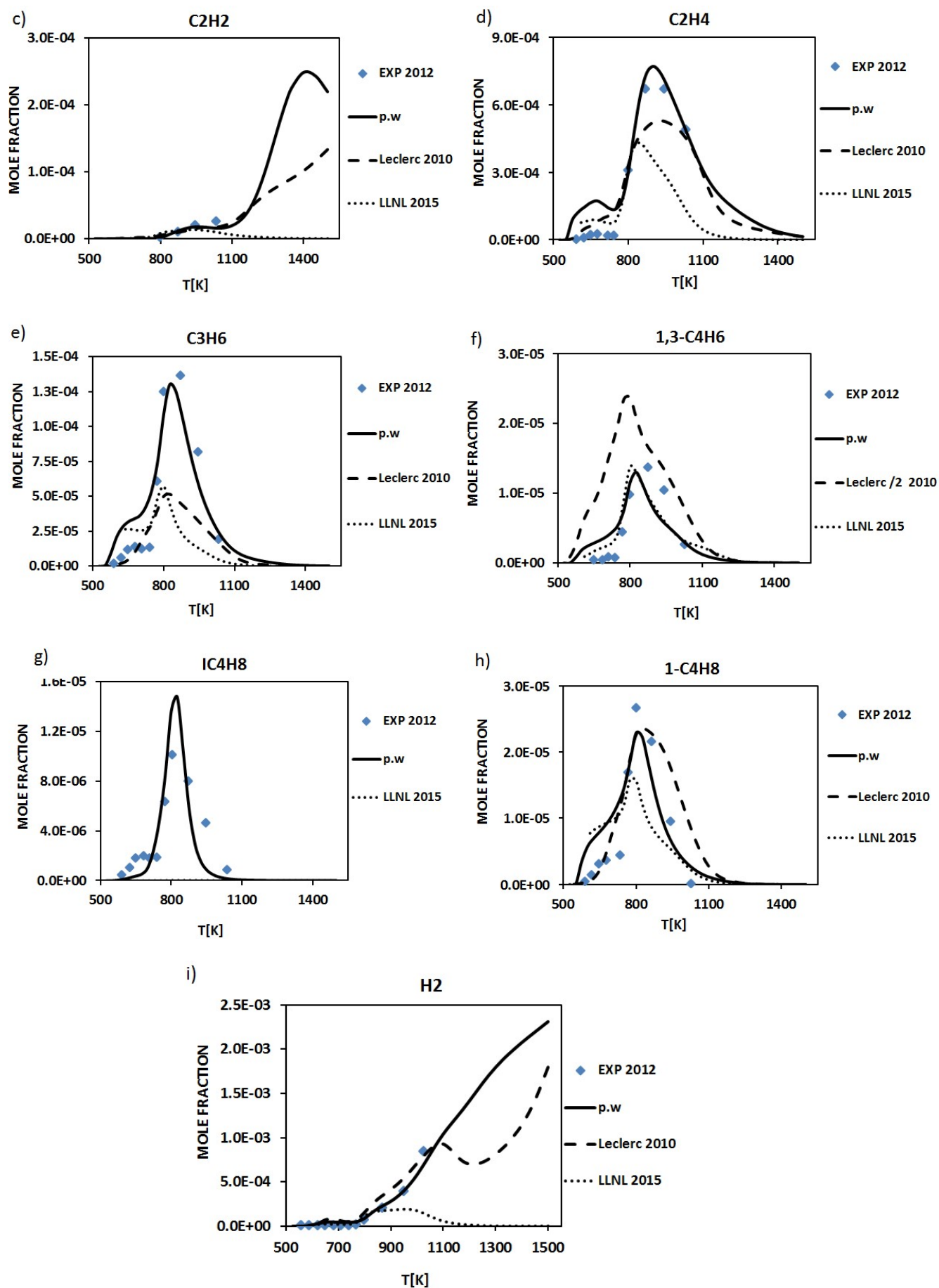


Figure 82 : Diesel fuel ( $C_{15,64}H_{29,34}$ ) combustion in Jet stirred reactor: diesel fuel/ $O_2/N_2$ :650/10,000/989,400 in ppmv.  $\Phi=1.5$ ;  $P=10$  bar;  $\tau=1s$ ; predicted and experimental mole fractions of a) water, b) carbon dioxide, c) acetylene, d) ethylene, e) propene, f) 1,3-butadiene, g) isobutene, h) 1-butene, i) hydrogen.

ethylene, e); propene, f); but-1,3-diene, g); iso-butene, h); but-1-ene and i); hydrogen. The symbols represent experimental data [96]; the continuous lines represent the modeling results from the present work; dashed lines: Battin-Leclerc mechanism for diesel surrogate (n-decane/1-methylnaphthalene: 70(%mol)/30) [163]; dotted lines: Lawrence Livermore National Laboratory mechanism for diesel surrogate (n-dodecane/m-Xylene: 77 (%vol)/23) (LLNL) [165].

The performance of the present reaction model with respect to practical fuels combustion modeling in JSR configuration has been examined. It can be seen that a good agreement between experimental data and the modeling results is obtained in both cases (jet fuel and diesel fuel). It is clearly encouraging results with the surrogate fuels proposed in this study, since some species of major interest such acetylene and benzene mole fractions are correctly reproduced.

### **4.4.3. Ignition delay times and laminar flame speeds**

#### **4.4.3.1. Gasoline**

Ignition delay response of gasoline have been modeled near 20 and 40 bar, temperature ranging from 630 to 900 K and an equivalence ratio  $\phi=1.0$ . The present kinetic model prediction is compared to that of Lawrence Livermore National Laboratory mechanism (LLNL), which uses a gasoline surrogate composed of n-heptane/iso-octane/toluene in respectively 13.7%/42.8%/43.5% in mol. In the present work, a ternary mixture of n-decane/iso-octane/n-propylbenzene in respectively 4.1%/72.9%/23.0% in mol. is proposed. In Figure 83 and Figure 84, the effect of the kinetic model as well as the gasoline surrogate content can be observed. In Figure 85, the prediction of laminar burning velocity of gasoline at atmospheric pressure and an unburned gas mixture temperature ( $T_u$ ) of 358 K is illustrated for large equivalence ratios range (0.6 to 1.5).

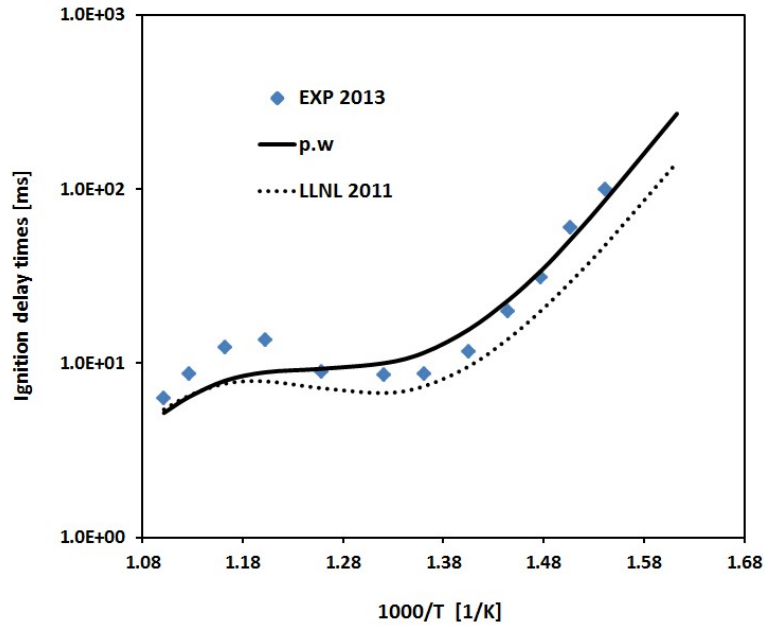


Figure 83 : Ignition delay response of gasoline in a rapid compression machine:  $\phi=1$  ;  $P = 20$  bar ;  $T = 640-900$  K ; The symbols represent experimental data from [156]. The continuous lines represent the modeling results from the present work; the dotted lines: LLNL mechanism [175] (nC7/iC8/Toluene: 13.7% (mol)/42.8%/43.5%, composition from [109]).

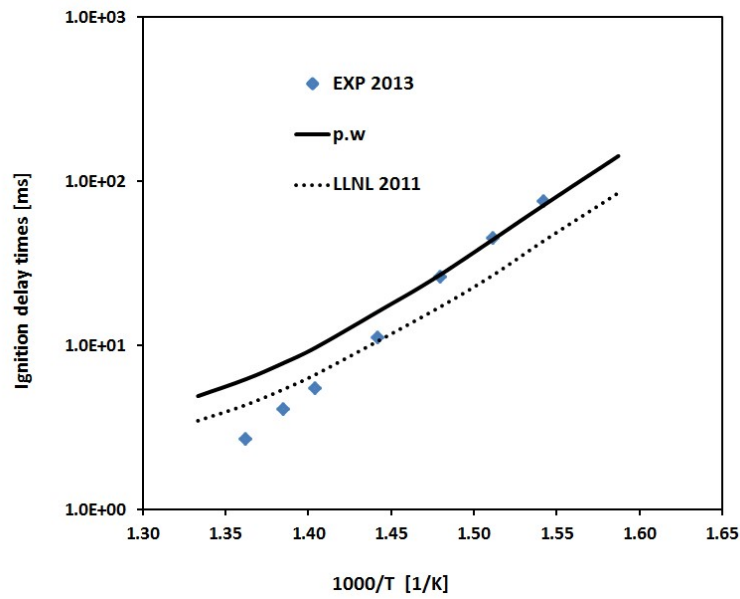


Figure 84 : Ignition delay response of gasoline in a rapid compression machine:  $\phi=1$  ;  $P = 40$  bar ;  $T = 630-740$  K ; The symbols represents experimental data from [156]. The continuous lines represent the modeling results from the present work; the dotted lines: LLNL mechanism [175] (nC7/iC8/Toluene: 13.7% (mol)/42.8%/43.5%, composition from [109]).

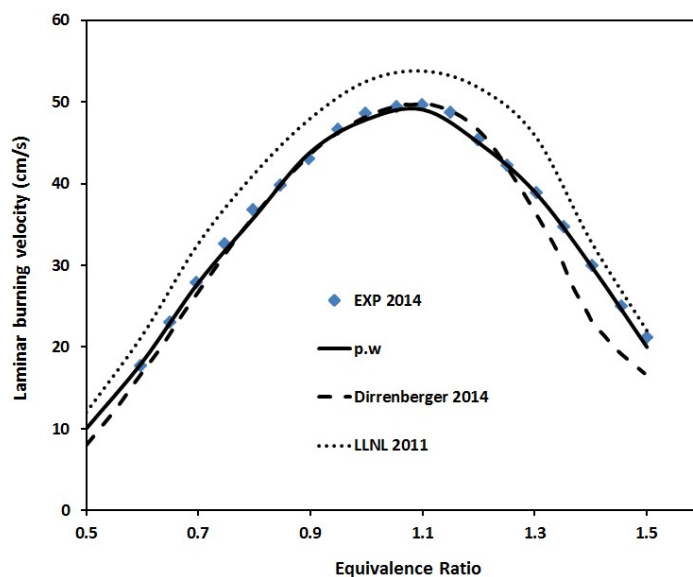


Figure 85 : Laminar burning velocity of gasoline : P = 1 atm ; Tu = 358 K ; The symbols represents experimental data from [157]; the continuous lines represent the modeling results from the present work; the dashed lines: Dirrenberger et al. mechanism [157]; the dotted lines: LLNL mechanism [175] (nC<sub>7</sub>/iC<sub>8</sub>/Toluene: 13.7% (mol)/42.8%/43.5%, composition from [109]).

The proposed gasoline surrogate in this study has been examined over gasoline ignition delay times and laminar flame speeds. Flame speed is a fundamental property of fuel-air mixture which significantly influences combustion engine design parameters such as flame stabilization, auto-ignition, emissions characteristics and combustion dynamics. Laminar flame speed serves as a global parameter which accounts for the diffusivity, exothermicity and reactivity of mixtures. Therefore, accurate prediction of laminar flame speed would help to capture these effects. As such, laminar flame speed proves to be of high importance in validating kinetic models. In contrast with laminar premixed flame configuration, it can be seen that the present reaction model and the proposed surrogate show a good agreement with experimental data. Despite some minor discrepancies for ignition delay times prediction at a temperature range of 800-1000 K, the present kinetic model captures well the negative temperature coefficient (NTC) behavior as well as the low temperature region (600-800 K). The tested mechanisms almost show similar results. For the laminar flame speeds, the present kinetic model satisfactorily reproduces the experimental trend from low to high equivalence ratio values.

#### 4.4.3.2. Jet fuel

In Figure 86, the prediction of jet fuel ignition delay times near 20 atm, an equivalence ratio of  $\phi=1.0$  and temperature ranging from 600 to 1230 K is presented. The present work result is compared to that of Dooley et al. [92] mechanism that considered different jet surrogate fuel from the present one. In

Figure 87, the prediction of laminar flame speed of jet fuel at atmospheric pressure and unburned gas mixture temperature of 400 K is illustrated for a large equivalence ratios range (0.7 to 1.4).

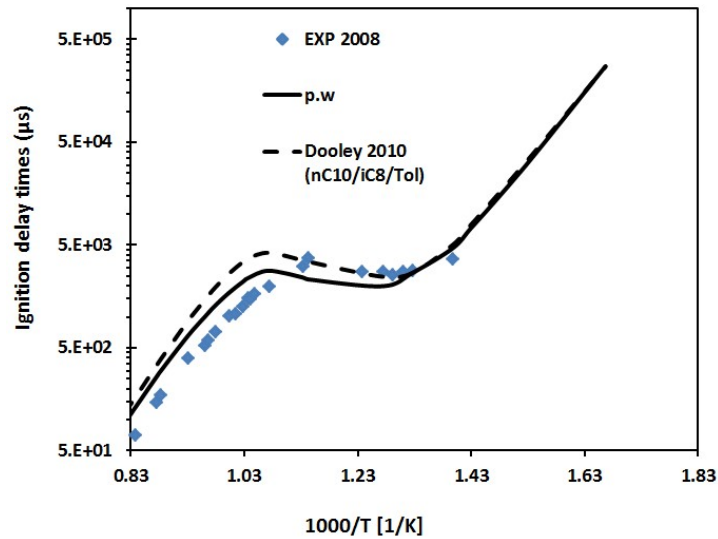


Figure 86 : Jet fuel ignition delay times prediction,  $\phi=1$ ;  $P= 20$  atm;  $T = 600-1230$  K;  $X_{fuel}/O_2/N_2: 1.3\%/20.7\%/78.0\%$  in mole fraction. The symbols represent experimental data from [159]; The continuous lines represent the modeling results from the present work; dashed lines: Dooley et al. mechanism (nC10/iC8/Toluene:42.67% (%mol)/33.02%/24.31%) [92].

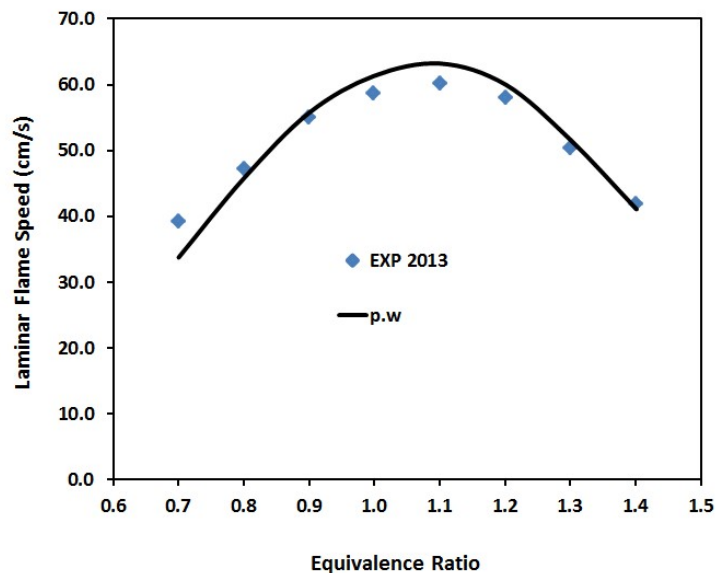


Figure 87 : Laminar burning velocity of jet A flame :  $P= 1$  atm ;  $T_u = 400$  K ; The symbols represent experimental data from [160].

The simulations agree well with the experimental data in ignition delay times prediction from 700 to 1200 K. the NTC zone is well captured and the tested mechanism shows similar results. For the laminar flame speeds, a good agreement is also obtained despite a minor disagreement at lower equivalence ratio ( $\phi=0.7$ ).

### 4.4.3.3. Diesel fuel

In Figure 88, the modeling of ignition behavior of diesel fuel at a pressure of 6 atm, an equivalence ratio of  $\phi=0.5$  and temperature ranging from 600 to 1300 K is presented. The present prediction is compared to literature mechanisms such as Battin-Leclerc et al. mechanism [163] where the authors used n-decane/ $\alpha$ -methyl naphthalene (70%/30% in mol.) mixture as diesel surrogate and the LLNL mechanism [165] where the authors used n-dodecane/ m-xylene (77%/23% by vol.) mixture as diesel surrogate. In Figure 89, the prediction result of the diesel fuel laminar flame speeds at atmospheric pressure and unburned gas mixture temperature of 470 K is illustrated for a large equivalence ratios range (0.75 to 1.5). The modeling result from the present work is compared with that from Pistch et al. mechanism [176], where the authors used only the n-dodecane as diesel surrogate fuel.

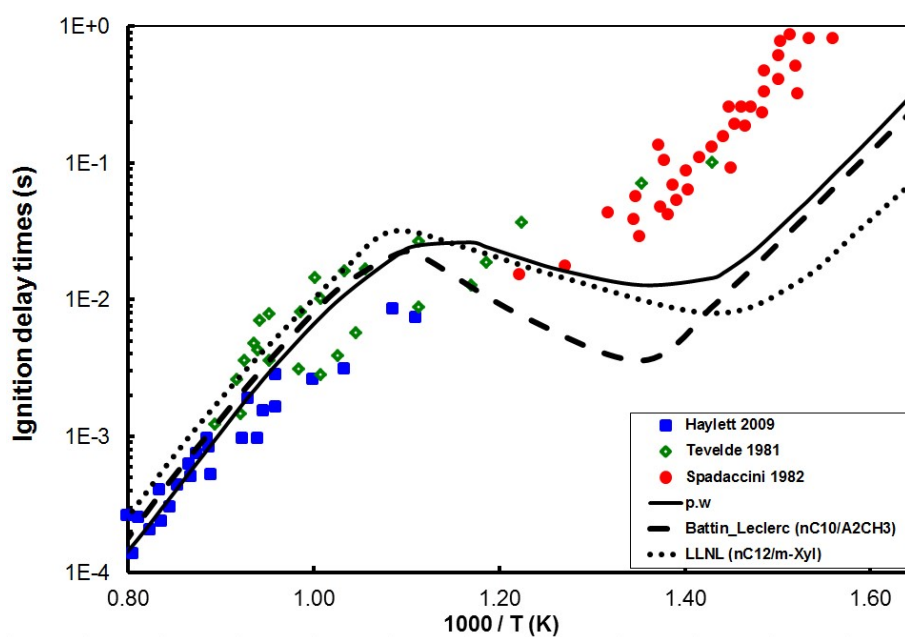


Figure 88 : Diesel ignition delay times measurement in shock tube: diesel fuel (0.7%)/O<sub>2</sub>/Ar;  $\phi= 0.5$  ; P=6 atm ; T=600-1300 K ; The symbols represent experimental data from [161]; the continuous lines represent the modeling results from the present work; dashed lines: Battin-Leclerc et al. mechanism [163]; dotted lines: LLNL mechanism for diesel surrogate [165].

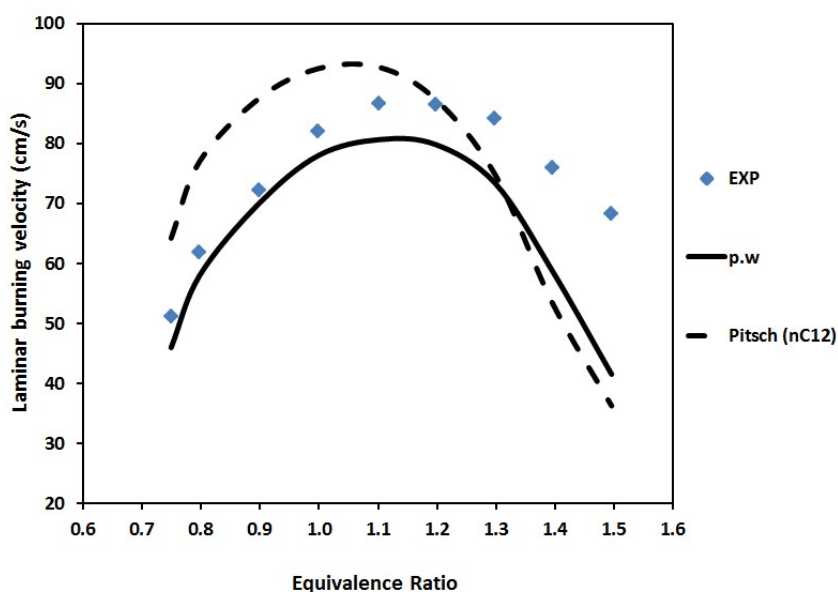


Figure 89 : Laminar burning velocity of diesel fuel :  $P=1$  atm ;  $T_u=470$  K ; The symbols represent experimental data from [162]; the continuous lines represent the modeling results from the present work; dashed lines: Pitsch et al. mechanism for diesel surrogate (n-dodecane) [176].

As can be seen, the present kinetic model is also able to correctly reproduce ignition delay times of diesel fuel. From the higher temperature (1250 K) to the NTC zone, all the tested mechanisms (except that of Battin-Leclerc et al. [163] for the NTC zone) follow the experimental trends. None of the mechanisms is able to predict the measured ignition delay times at the lower temperature zone (600-700K) due to uncertainties surrounded experimental data. It is suspected that the heat losses were not taken into account during experiments. In Figure 90, one can observed that by introducing a heat loss flux of 0.1 calorie per second (0.4 Watts) into simulations, prediction with the present kinetic model in the lower temperature zone is slightly improved. Due to convergence issues, none of the used kinetic models allows the introduction of higher heat flux ( $> 0.1$  calorie/second) during simulations.

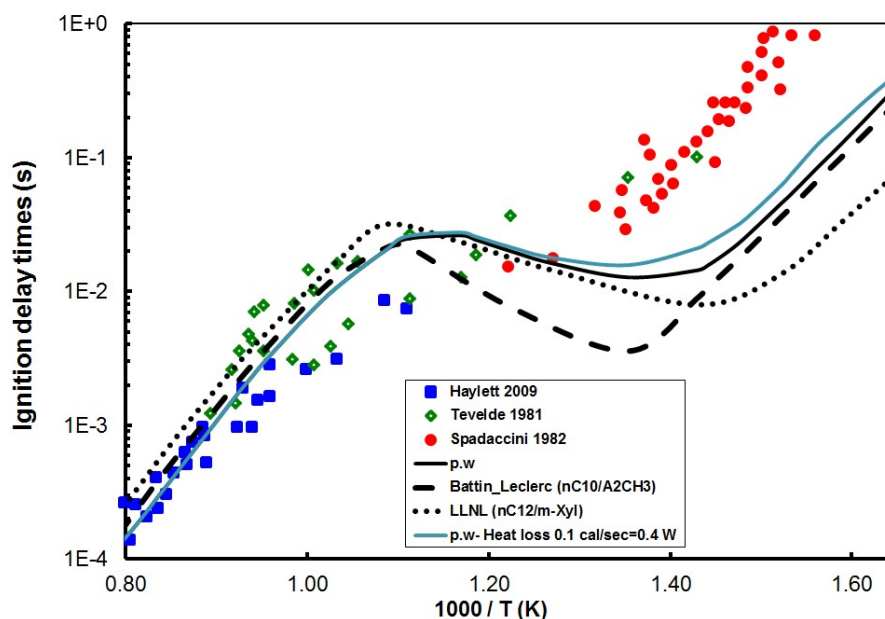


Figure 90 : Diesel ignition delay times measurement in shock tube: diesel fuel (0.7%)/O<sub>2</sub>/Ar;  $\phi=0.5$ ; P=6 atm; T=600-1300 K; Prediction from the present work with a heat loss flux of 0.1 cal/sec (blue line).

For the laminar flame speeds, a good agreement is obtained from the present work from  $\phi=0.75-1$  and a poor agreement can be seen for higher equivalence ratios. In contrast with the present kinetic model and the proposed surrogate (mixture of n-decane/iso-octane/n-propylbenzene, see Table 3, section 4.2) for diesel fuel, Pitsch et al. [176] models (kinetic and surrogate) fail to reproduce satisfactorily experimental data. Indeed, no aromatic species were considered in their surrogate fuel and that can significantly impact the results.

The present mechanism was used to model premixed flames presented above, different fuels structures ranging from C<sub>1</sub> to C<sub>10</sub> species including liquid fuels, alkanes, alkenes, alkynes and aromatics. The overall agreement between predicted and experimental results remains satisfactory. The performance of this reaction model with respect to practical fuels combustion modeling (ignition delay times and laminar flame speeds prediction) shows clearly encouraging results with the surrogate fuel proposed in this study. Satisfactory results are obtained in predicting ignition delay times, laminar flame speeds and species mole fraction profiles in jet stirred reactor configuration. As can be seen from Figure 28 to Figure 89, the disagreement with experimental data is more consistent for gasoline premixed flame for which multiple sources of uncertainties may exist, namely surrogate and kinetic models. Further, for acetylene and benzene, a good agreement with experimental mole fraction profiles is obtained for all flames studied.



The current mechanism was subsequently used in low and atmospheric pressure premixed flame configuration to study some key intermediates and aromatic species formation pathways based on fuel structure. Since no aromatic species concentration profile is available in atmospheric premixed laminar flame configuration for diesel fuel, the latter fuel has not been examined in term of aromatic production pathways.

#### **4.5. Conclusions**

Aromatics formation pathways for commercial liquid transportation fuels are seldom discussed in the literature and the present study aimed at determining the most significant ones in the light of the recent rate constant evaluations. A new detailed chemical kinetic mechanism was herein developed to describe accurately the combustion of liquid transportation fuels (jet A-1 and diesel fuel) as well as laboratory fuels (single components of alkanes, alkenes and aromatics) over an extended range of equivalence ratios, temperatures, pressures and dilution levels. For the gasoline, a good agreement between predictions and measurements is obtained in predicting the ignition delay times and laminar flame speeds, while large discrepancies exist for a rich premixed gasoline flame in predicting aromatic species formation. Given the validations conditions shown in this work, this mechanism is expected to work properly for the combustion of n-decane/iso-octane/n-propylbenzene mixtures for equivalence ratios ranging from 0.5 to 3, temperatures ranging from 600 K to 2500 K and pressures ranging from 0.01 atm to 10 atm. Ternary surrogate mixtures of n-decane, iso-octane and n-propylbenzene were chosen to represent liquid transportation fuels, based on their Derived Cetane Number and Threshold Sooting Index. The impact of fuel formulation on aromatics formation pathways was examined. From the present modeling results, it turns out that jet-A1 and diesel fuels can be satisfactorily represented by the proposed chemical surrogate, while gasoline may not be satisfactorily represented due to its high iso-octane concentration (75% vol. liq.), which is not representative of the actual gasoline composition in terms of PAH precursors, despite its ability to reproduce the sooting level through a relevant TSI value.

In line with previous studies from other groups, this work highlights the discrepancies between aromatics production pathways involved in laboratory flames (widely used in most academic soot formation studies) such as ethylene flame and those involved in actual liquid transportation fuel

flames, calling for more representativity in the choice of reactive systems. Regarding PAH (naphthalene) formation, common pathways were noticed for both laboratory and practical surrogate fuels. According to the present mechanism, phenyl+vinylacetylene and benzyl+propargyl reactions were shown to contribute massively to naphthalene production based on the retained rate constants for these reactions. In ethylene flame for example, phenyl+vinylacetylene reaction is the main path for naphthalene formation, while in jet-A1 flame phenyl+vinylacetylene and benzyl+propargyl are dominant naphthalene production pathways. The importance of reactions involved in aromatics (benzene and naphthalene) production was also seen to depend strongly on HAB. The HACA mechanism represented here by vinyl phenyl acetylene ( $A_1C_2H_3AC$ ) also plays a significant role in naphthalene production for both types of fuels. It is worth noting that an additional pathway involving dibenzofuran oxidation to produce naphthalene was noticed in practical surrogate fuel (jet-A1 flame case). To the best of our knowledge, this reaction had not been evidenced previously as a significant naphthalene production pathway in the context of liquid fuel premixed flames. We herein claim that based on state-of-the art kinetic estimate for dibenzofuran production, this pathway can contribute significantly to naphthalene production over the whole combustion and post-combustion region. This pleads for further development and validation of oxygenated aromatics combustion mechanisms (such as dibenzofuran) as they might play a key role in PAH production for liquid transportation fuels flames. Further, more experimental data on the benzyl+propargyl interaction would be needed to validate the recent theoretical rate constants proposed. Other potential mechanisms such as the alternative HAVA (Hydrogen-Abstraction-Vinyl-Addition) mechanism would also deserve further studies.

## Chapter 5: Solid phase: Soot particles Nucleation Modeling

### 5.1. Objective

While pyrene molecule is widely used in most of previous soot models as a key species in nucleation, there is still no definitive experimental evidence. Several PAHs molecules including pyrene have been experimentally observed from combustion processes [177,178]. The nature of those actually involved in the nucleation process remains elusive. The goal of this chapter is to investigate potential soot precursors, the experimentally observed PAHs molecules that could lead to particles inception through physical agglomeration.

Following the validation of the present kinetic model, it has been used in a soot model based on a sectional approach developed in [75]. Both homomolecular and heteromolecular dimerizations of PAHs in the mass range between 200 and 300 amu have been examined. Results obtained from this investigation can serve for further studies in accurate PAHs concentrations prediction for a variety of fuels. The particles nucleation rates can also be obtained from the used soot model. Several premixed laminar one-dimensional flat flames stabilized on burner have been considered in the present work.

### 5.2. Nucleation modeling: soot precursors considered

Particles inception is usually represented as the collision between of two modest sized PAHs, namely pyrene molecule. This assumption is supported by several works [17,34], while many others [22,31,179] clearly rule out this possibility based on the thermodynamic stability of the corresponding dimers in flame environments. Due to experimental limitations for the particle nucleation, numerical simulations have been mainly carried out to determine the mechanism involved.

While the PAH are commonly accepted as soot particles precursors [56–58,180], the nature of those considerably involved in the nucleation process from hydrocarbons combustion remains ambiguous and has been the subject of many works [17,28,84]. On the one hand, most of soot models discussed about homomolecular dimerization, which indicates that the two colliding species have the same chemical structure and the heteromolecular dimerization, which implies two or more reactants that

have different chemical structure is rarely considered. On the other hand, most of previous soot models are focused and validated on C<sub>1</sub>-C<sub>2</sub> hydrocarbons flames [84,87,88,181] such as methane, acetylene, ethane and ethylene. Only a few works [27,75,182] investigated larger hydrocarbons sooting behavior and the heteromolecular dimerization (pyrene+coronene) [27,31] for the soot mass concentration prediction. These results clearly show that the influence of precursors on nucleation has been only marginally addressed in previous studies.

Molecular dynamics studies indicated that the nucleation process probably depends on larger PAH as big as circumcoronene (C<sub>54</sub>H<sub>18</sub>) involvement. In this work, the particles nucleation is assessed based on the modest-size PAHs dimerization (from pyrene to coronene). The present kinetic model and the sectional soot model developed in [75,79,80] are used to investigate particles inception mechanism in three premixed laminar flames: methane ( $\phi=2.32$ ) [85], ethylene ( $\phi=2.34$ ) [82] and n-butane flames ( $\phi=1.75$ ;  $\phi=1.95$  and  $\phi=2.32$ ) [38,149]. The importance of modeling these flames is discussed in Chapter 4 (section 4.4.1). In addition, both sooting and nucleation flames are investigated in the present study. Regarding the nucleation process modeling, homomolecular and heteromolecular dimerizations of PAHs were taken into account in order to reproduce the experimental data tendencies (soot volume fractions and diameters) in each of the above-mentioned flames. The effect of the choice of the precursors was illustrated using several sets of precursors. It is worth noting that one could define dozens of combinations of precursors.

The PAHs considered for soot particles nucleation modeling (ranging from pyrene (202 amu) to coronene (300 amu)) in the three premixed flames are presented in Figure 91. They include five-membered ring aromatics as well as those containing six-membered rings based on experimental results from fuels pyrolysis [125,183] and oxidation [177,184] and have been put forward as significant PAH in combustion. Although thermodynamic stability calculations indicate that only PAH as big as circumcoronene dimer can survive in flame environments, such molecules were not experimentally quantified in combustion.

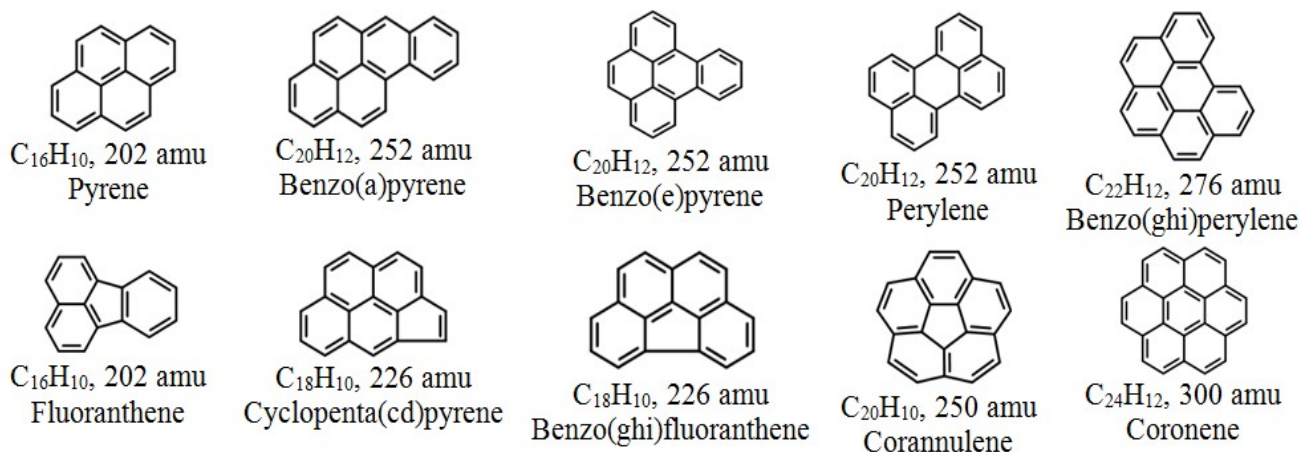


Figure 91 : Pool of investigated molecules for particles nucleation modeling.

### 5.3. Collision efficiency

In most soot models, PAHs molecules collide to form soot particles. One of the accepted key soot parameters which determines the soot inception and growth rates is the probability that PAHs will stick upon collision. This parameter is called the collision or sticking efficiency and is defined as the ratio of successful collisions (i.e collisions which produce clusters) to the total number of collisions [33,185].

Many research groups [27,33,185,186] investigated the PAHs collision efficiencies in order to implement them in soot models. The collision efficiency is found to be dependent not only of the colliding PAH mass and the collision diameter [34,185,187] but also the flame temperature [188]. As a result, several expressions of collision efficiency as a function of the colliding PAH mass, diameter and/or temperature have been proposed by several research groups. Raj et al. [33] established a temperature-independent correlation for collision efficiency as a function of PAHs mass and the collision diameter. Their findings are based on experimentally observed mass spectra for ethylene premixed flames investigated. Authors claimed that the collision efficiency is strongly dependent on the mass and collision diameter of the smaller of the two colliding species. In addition, authors concluded that due to the low value of collision efficiency required to properly predict the position of the maxima of PAH dimers in the spectra, if the mass of one of the colliding species is less than 360 amu and a diameter less than 10 Å, collisions involving species smaller than pyrene may not be successful at high temperature. Totton et al. [186] determined the collision efficiencies by the temperature and the mass of the colliding species via molecular dynamics modeling. The correlation

established is a fit of simulation data, using a least-squares algorithm based on the reduced mass of the colliding species. Authors mentioned that PAH molecules as small as pyrene cannot play a significant role in soot particle nucleation even at a temperature of 500 K and only large PAH as big as circumcoronene dimers can exist in flame temperature conditions (~1500 K). Blanquart et al. [189] proposed a correlation based only on the monomer mass since both experiments and numerical modeling have shown that the collision efficiency increases with the size of the colliding species. In his correlation, a constant is used to match experimental concentrations of PAHs. D'Alessio et al. [185] proposed a correlation that is a function of PAH molecules size and temperature. The potential well depth of species is investigated in order to take into physical chemistry phenomena. However, that expression is established for nanoparticles sticking ( $\geq 2$  nm) and if one interpolates to the PAH mass ranging from 200 to 300 amu (i.e. from Pyrene to coronene), the collision efficiencies values obtained are very low by using the same Hamaker constant, which determines the strength of particle-particle potential energy interactions. This constant is expected to increase towards the value of graphite ( $\sim 5.0 \times 10^{-19} J$ ) [185] during the carbonization process. Authors estimated the lower limit value of Hamaker constant to be  $3.0 \times 10^{-20} J$ . Chung et al. [27] presented an empirical relation of collision efficiency that includes PAH morphology, size and temperature effect. The temperature-dependent dimerization collision efficiency was calculated using molecular dynamics simulations. Authors investigated peri-condensed aromatics dimerization collision efficiency as well as PAH linked by aliphatic chains.

The expressions of collision efficiency established by the above mentioned authors are presented in Table 14:

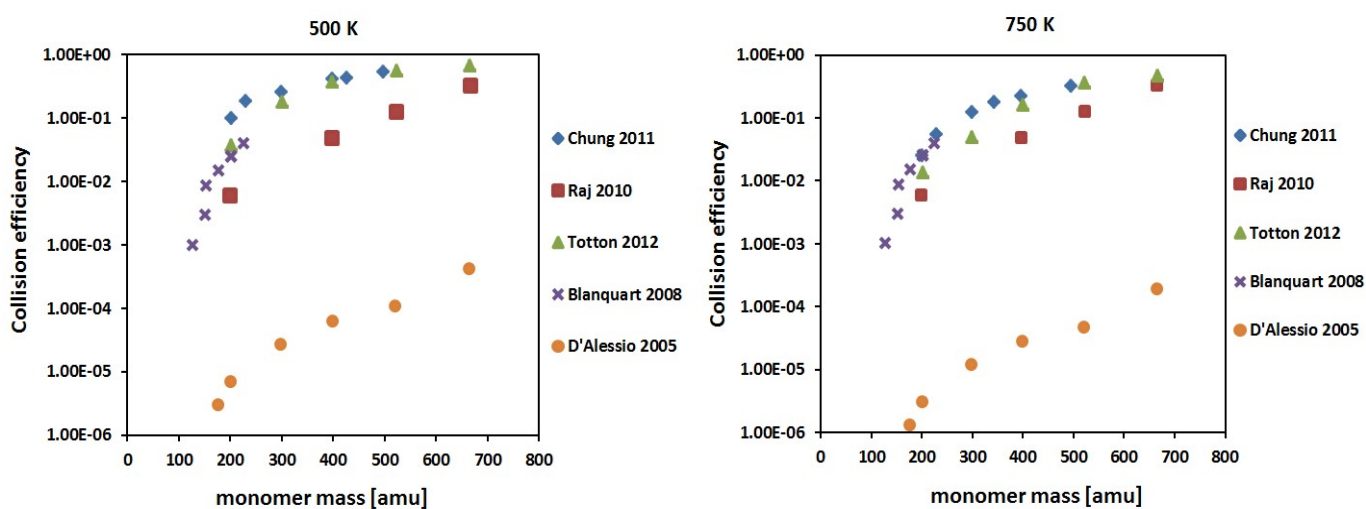
References	Expressions
Raj et al.[33]	$C_E = \frac{1}{1 + \exp\left(-\left(A \times \frac{D_{min}^3}{M_{min}} + \left(\frac{M_{min}}{B}\right)^6 - C\right)\right)}$ <p>Where <math>A</math>, <math>B</math> and <math>C</math> are the fitting parameters. <math>A=2</math> g/(mol Å<sup>3</sup>); <math>B=980</math> g/mol ; <math>C=10</math> (dimensionless). <math>M_{min}</math> and <math>D_{min}</math> are respectively the</p>

	mass and the collision diameter of the smaller of the two colliding PAH.																					
Totton et al. [186]	$C_E = 1 + \frac{\mu}{a\mu + b} - \frac{1}{a}$ <p>Where <math>\mu</math> is the reduced mass of the two colliding PAHs. <math>a</math> and <math>b</math> are the fitting parameters and are determined as a function of the temperature:</p> <table border="1"> <thead> <tr> <th colspan="3">Parameters</th> </tr> <tr> <th>T [K]</th> <th><math>a</math></th> <th><math>b</math></th> </tr> </thead> <tbody> <tr> <td>500</td> <td>0.5074</td> <td>54.13</td> </tr> <tr> <td>750</td> <td>0.6822</td> <td>190.0</td> </tr> <tr> <td>1000</td> <td>0.8032</td> <td>441.3</td> </tr> <tr> <td>1250</td> <td>0.8425</td> <td>714.2</td> </tr> <tr> <td>1500</td> <td>0.8858</td> <td>1322</td> </tr> </tbody> </table>	Parameters			T [K]	$a$	$b$	500	0.5074	54.13	750	0.6822	190.0	1000	0.8032	441.3	1250	0.8425	714.2	1500	0.8858	1322
Parameters																						
T [K]	$a$	$b$																				
500	0.5074	54.13																				
750	0.6822	190.0																				
1000	0.8032	441.3																				
1250	0.8425	714.2																				
1500	0.8858	1322																				
Blanquart et al. [189]	$C_E = C_N \times m_i^4$ <p>Where <math>m_i</math> is the PAH mass. <math>C_N</math> is an adjustment factor to match PAHs experimental concentrations.</p>																					
D'Alessio et al. [185]	$C_E = 1 - \left(1 + \frac{\phi_0(D)}{KT}\right) \exp\left[-\frac{\phi_0(D)}{KT}\right]$ <p>Where <math>\phi_0</math> is the potential well depth which is calculated using the Hamaker constant of the colliding species[190]. The potential well depth is linearly proportional to the reduce mass of the colliding species[191]. <math>K</math> is the Boltzmann constant. <math>T</math> is the temperature.</p>																					
Chung et al. [27]																						

$C_E = \exp(p_0 + p_1 \times AR + p_2 \times T^2 + p_3 \times T \times AR + p_4 \times AR^2 + p_5 \times T^3 + p_6 \times T^2 \times AR + p_7 \times T \times AR^2 + p_8 \times AR^3)$	
<p>Where <math>AR</math> is the number of aromatic rings in the PAH molecule. <math>T</math> is the temperature and <math>p_0, p_1, p_2, p_3, p_4, p_5, p_6, p_7, p_8</math> are the fitting coefficients. The coefficient values are listed as follows:</p>	
$p_0$	-1.864
$p_1$	-0.006943
$p_2$	-3.56E-06
$p_3$	0.001282
$p_4$	-0.1041
$p_5$	1.07E-09
$p_6$	3.71E-08
$p_7$	-5.24E-05
$p_8$	0.004242

Table 14 : Expressions of the collision efficiency.

Figure 92 shows the comparison between the collision efficiency values calculated from the above expressions.





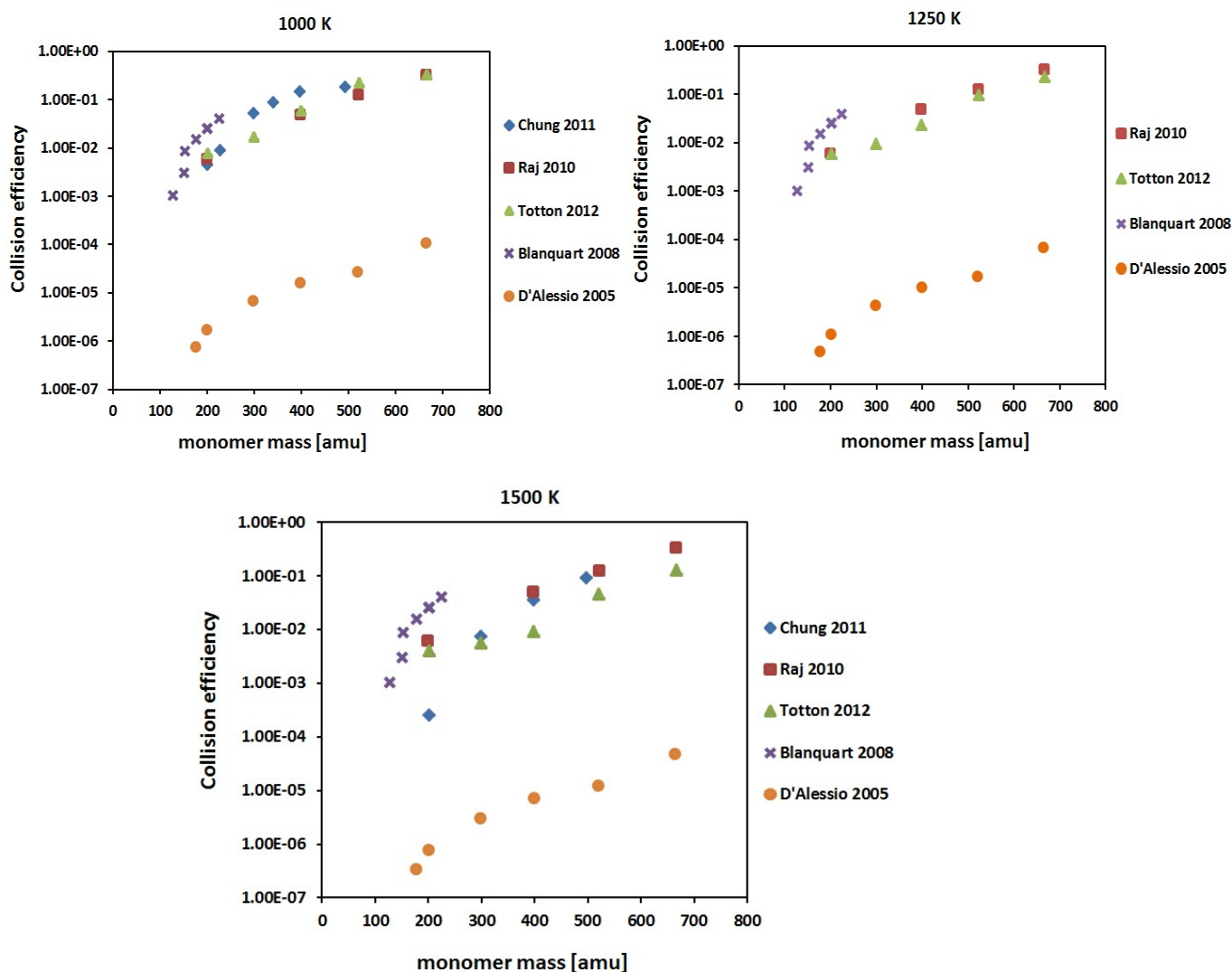


Figure 92 : Collision efficiency values obtained from different correlations as a function of PAH size and temperature.

Firstly, it is clearly observed that the correlations proposed by Chung et al. [27], Raj et al. [33], Totton et al. [186] and Blanquart et al. [189] give roughly the same collision efficiencies from 500 to 1500 K. Then, all of the above correlations show the same qualitative trends. However, the collision efficiency values given by D'Alessio et al. [185] correlation are significantly lower than the other ones. That is due to the Hamaker constant chosen for particles with a minimum diameter value of 2 nm. The Hamaker constant used is more relevant of particles sticking rather than gaseous PAH molecules.

According to the collision efficiency models, it is found to increase with the monomer mass. At 1500 K for example, the collision efficiency values vary from  $2.5 \times 10^{-4}$  (Chung et al.[27]) to  $3.2 \times 10^{-1}$  (Raj et al.[33]) for respectively monomer mass of 200 amu (pyrene) and 667 amu (circumcoronene). The effect of temperature (from 500 to 1500 K) is also observed since the values vary from  $3.7 \times 10^{-2}$  (Totton et al. [186] /  $1.0 \times 10^{-4}$  for Chung et al. [27]) to  $2.5 \times 10^{-4}$  (Chung et al.[27] /

$3.9 \times 10^{-3}$  for Totton et al. [186]). The correlation given by Raj et al. and Blanquart et al. do not consider the impact of temperature. Only the monomer mass impact is observed.

A correlation based on the one proposed by D'Alessio et al. [185] is adopted in the soot model used in the present work [79,80]. It describes the collision efficiency evolution depending on temperature and the colliding particles size as most of the previously introduced functions from the literature. It appears to contain the relevant nucleation phenomenology. In fact, the interaction potential between two reactants that turn into soot nuclei and the effect of temperature were taken into account. Its main difference is a parameter  $E_d$  which can be modified to reproduce either collision efficiencies close to the ones obtained using D'Alessio et al. [185] or close to the ones obtained by Chung et al. [27], Raj et al. [33] and Totton et al. [186]. This choice has been done because it eases the investigation of the collision efficiency influence on the soot phase evolution.

We adjust the parameter  $E_d$  in order to match the values obtained by Chung et al. [27], Raj et al. [33] and Totton et al. [186] since all these correlations give mostly the same collision efficiency trends. The adopted collision efficiency expression is given as follows:

$$C_E = 1 - \left(1 + \frac{D_1 \times D_2 \times E_d}{k_B T}\right) \exp\left[-\frac{D_1 \times D_2 \times E_d}{k_B T}\right] \quad \text{Equation 43}$$

Where  $D_1$  and  $D_2$  are the diameters of the colliding species.  $k_B$  is the Boltzmann constant.  $T$  is the temperature.  $E_d$  is the adjustment factor that we used to match the collision efficiency values obtained by other correlations. The best agreement with the other correlations was found by setting  $E_d$  value at  $5 \times 10^{-3}$ . In fact, a higher value of  $E_d$  typically  $5 \times 10^{-2}$  leads to an overprediction of collision efficiencies of about a factor of 40 with respect to those obtained with  $E_d = 5 \times 10^{-3}$ , while a lower value of  $E_d$  ( $5 \times 10^{-4}$ ) leads to an underprediction of about a factor of 90 with respect to collision efficiencies obtained with  $E_d = 5 \times 10^{-3}$ .

Figure 93 shows results obtained from the proposed correlation and compared to the other ones. It can be seen that the collision efficiencies used in this work are close to the literature point of view.

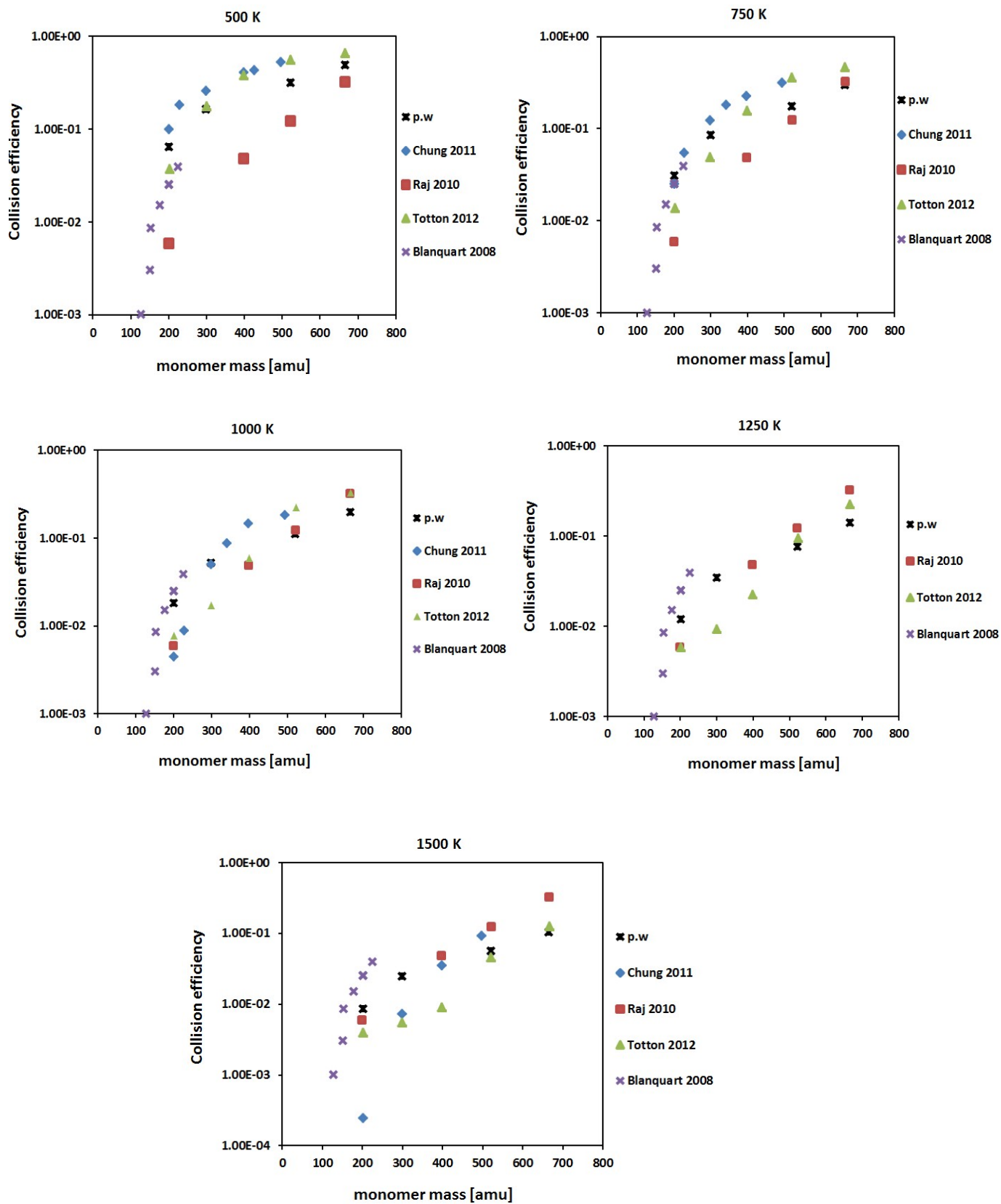
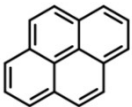
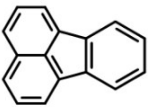
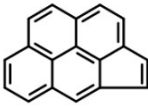
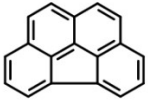

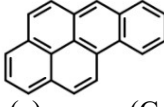
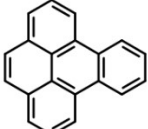
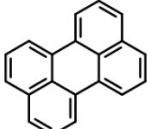



Figure 93 : Comparison of the collision efficiency values calculated from different correlations.

The collision efficiency values considered for the investigated PAH molecules are given in Table 15:

PAH structure	Molecular weight (amu)	Collision efficiency (present work) T=1700 K	Collision efficiency (Yang et al.[181] (temperature-independent)
 Pyrene (C <sub>16</sub> H <sub>10</sub> )	202	6.6 x10 <sup>-3</sup>	6.0 x10 <sup>-3</sup>
 Fluoranthene (C <sub>16</sub> H <sub>10</sub> )	202	6.6 x10 <sup>-3</sup>	
 Cyclopenta[cd]Pyrene (C <sub>18</sub> H <sub>10</sub> )	226	8.5 x10 <sup>-3</sup>	
 benzo(ghi)fluoranthene (C <sub>18</sub> H <sub>10</sub> )	226	8.5 x10 <sup>-3</sup>	
 Corannulene (C <sub>20</sub> H <sub>10</sub> )	250	1.9 x10 <sup>-2</sup>	
 Benzo(a)pyrene (C <sub>20</sub> H <sub>12</sub> )	252	1.3 x10 <sup>-2</sup>	1.1 x10 <sup>-2</sup>
 Benzo(e)Pyrene (C <sub>20</sub> H <sub>12</sub> )	252	1.3 x10 <sup>-2</sup>	1.1 x10 <sup>-2</sup>
 Perylene (C <sub>20</sub> H <sub>12</sub> )	252	1.3 x10 <sup>-2</sup>	
 Benzo(ghi)perylene (C <sub>22</sub> H <sub>12</sub> )	276	1.9 x10 <sup>-2</sup>	1.4 x10 <sup>-2</sup>


 Coronene (C <sub>24</sub> H <sub>12</sub> )	300	$1.9 \times 10^{-2}$	$2.0 \times 10^{-2}$
--	-----	----------------------	----------------------

Table 15 : Collision efficiency used for the investigated PAH molecules.

#### 5.4. Results and Discussions

The soot volume fractions were computed for the low pressure (0.26 atm) premixed laminar flame of methane ( $\varphi=2.32$ ) [85], atmospheric pressure premixed flame of ethylene ( $\varphi=2.34$ ) [82] and atmospheric pressure premixed flames of n-butane ( $\varphi=1.75$ ;  $\varphi=1.95$ ) [149] and  $\varphi=2.32$  [38]. The soot sectional model [75] has been employed to model the centerline of the above-mentioned premixed flames. Predicted soot volume fractions using homomolecular and heteromolecular dimerization of PAHs and the measurements are shown in this section. The Laser-Induced Incandescence (LII) technique was employed to measure soot volume fractions in methane and n-butane flames, with an excitation wavelength of 1064 nm to detect soot particles. This technique is well suited because of its sensitivity and spatial resolution. More details on this technique can be found in Mouton et al. [85] paper. The laser-extinction technique was employed in soot volume fractions measurement for the ethylene flame [82].

It is worth noting that the investigated PAHs have not been experimentally quantified yet except pyrene molecule in low pressure methane premixed flame. Therefore, a particular attention should be given with respect to the present modeling results, due to the lack of experimental data. An initial constant value of  $\alpha=0.05$  is used to compute soot volume fractions in both homomolecular and heteromolecular dimerizations of PAHs considered. Then,  $\alpha$  is varied in both homomolecular and heteromolecular dimerizations in order to better reproduce measurements.

Firstly, the contribution of each PAH (with  $\alpha=0.05$ ) in reproducing the soot volume fraction profiles is investigated to better understand the nucleation process (impact of precursors and measurement tendencies reproduction). Secondly, the nucleation processes (i.e homomolecular and heteromolecular dimerizations) are examined and compared. The results obtained for the following PAH molecules: benzo(e)pyrene, perylene, benzo(ghi)perylene and coronene have not been reported because of their

very low computed gas-phase concentrations as well as nucleation, condensation and surface growth rates. Therefore, their impacts on the soot volume fraction profiles are insignificant even if they are associated with the other investigated PAHs. Results obtained for the investigated flames are presented in the next sections.

#### 5.4.1. Methane flame

In Figure 94, the prediction of soot volume fraction in the case of exclusive homomolecular dimerization of each PAH from pyrene to corannulene is reported with a constant value of  $\alpha$  that is set to 0.05. In Figure 95, the prediction in presence of heteromolecular dimerization consisting of the contribution of three PAHs pyrene, fluoranthene and benzo(a)pyrene is presented, compared to the contribution of pyrene alone. This reactive system (pyrene/fluoranthene/benzo(a)pyrene) is chosen since these three PAHs are mostly observed and exist at higher concentration (compared to the other ones) in combustion products. The comparison between experimental and predicted mole fraction of pyrene and fluoranthene in this flame is shown in Chapter 4 (section 4.4), where a fairly agreement between measurements and predictions was obtained.

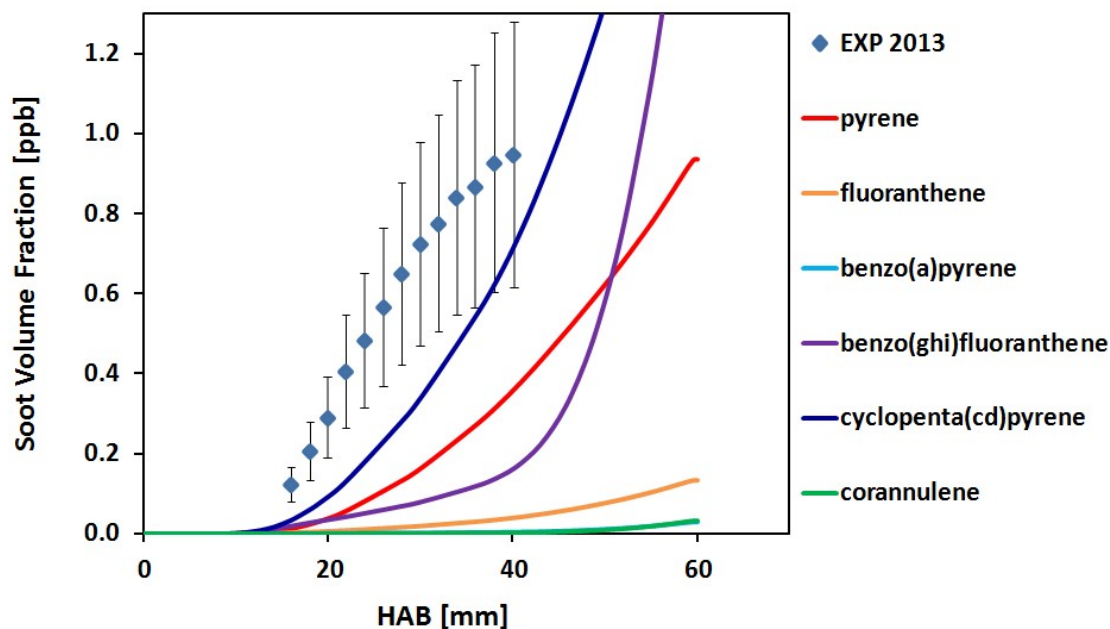


Figure 94 : Low pressure (0.263 atm) methane premixed flame,  $\phi=2.32$ :  $\text{CH}_4$  (46.2% in mol.)/ $\text{O}_2$  (39.8%)/ $\text{N}_2$  (14.0%). Homomolecular dimerization of the investigated PAHs. The symbols represent experimental data from [85]; the lines represent modeling results from the present work. Fraction of reactive surface sites available for reactions ( $\alpha$ ) is set to 0.05.

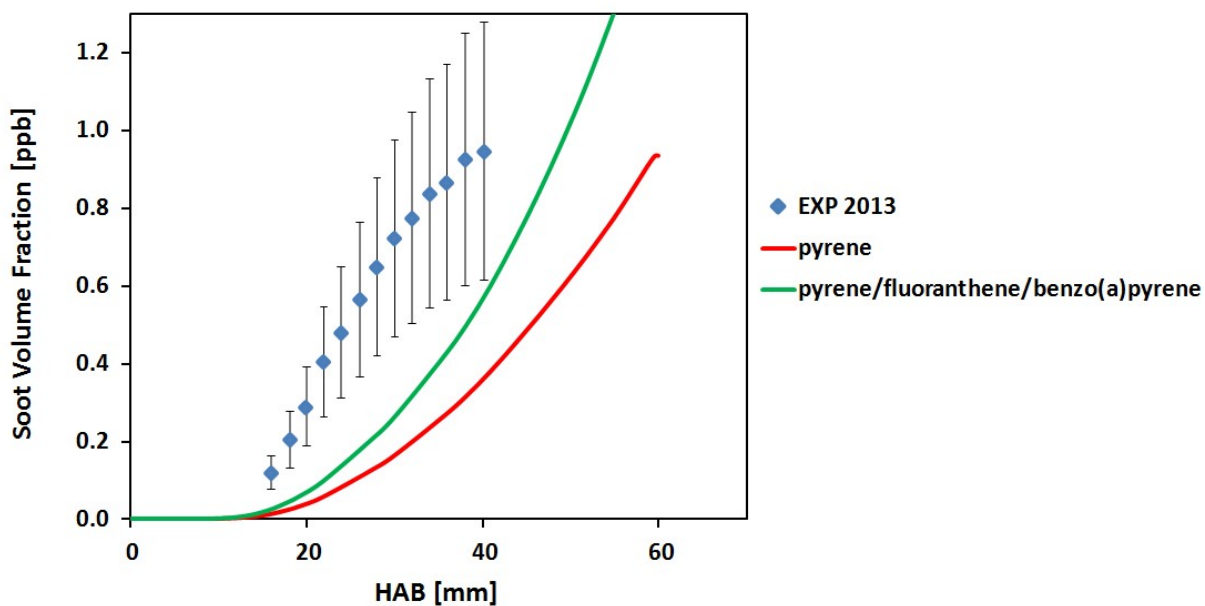


Figure 95 : Low pressure (0.26 atm) methane premixed flame,  $\phi=2.32$ : CH<sub>4</sub> (46.2% in mol.)/O<sub>2</sub> (39.8%)/N<sub>2</sub> (14.0%). Heteromolecular dimerization of pyrene/fluoranthene/benzo(a)pyrene compared to pyrene dimerization. The symbols represent experimental data from [85]; the lines represent modeling results from the present work. Fraction of reactive surface sites available for reactions ( $\alpha$ ) is set to 0.05.

As can be seen in Figure 94, the model only fairly captures the experimental trend in a given HAB range (linear zone) from pyrene and cyclopenta(cd)pyrene homomolecular dimerization, while assuming the dimerization to involve only benzo(ghi)fluoranthene results in a worse quantitative agreement with experiment. At higher HAB (~40 mm), measurements seem to change tendency while computations do not show this feature. That may indicate the oxidation process is very low to account for soot particles oxidation. The better prediction of soot volume fraction obtained by considering cyclopenta(cd)pyrene seems to be related to its predicted gas-phase concentration that is higher than that of pyrene (maximum values respectively of (~2.8 ppm and 1.8 ppm), impacting nucleation rate. Also, the collision efficiency value attributed to cyclopenta(cd)pyrene ( $8.5 \times 10^{-3}$ ) is slightly higher than that of pyrene ( $6.6 \times 10^{-3}$ ). However, the collision efficiency value cannot fully explain the results obtained. It is observed that benzo(a)pyrene dimerization assumption leads to the strong underprediction of measurements, while its collision efficiency is 1.5 times higher that of pyrene.

In Figure 95, the combination of contributions of three different PAHs to nucleation clearly results in an improved result with respect to the case of exclusive pyrene dimerization. According to the present model, pyrene appears to be the major precursor involved in soot nucleation. As can be seen in Figure 96, from the gas-phase to the heteromolecular dimerization process, the concentration of PAHs

involved in the particles inception mechanism are affected at high HAB. That is understandable since they are consumed to create particles. The decrease of species concentration is more important for pyrene than for fluoranthene and benzo(a)pyrene, indicating that pyrene is more consumed and is the main contributor for particles generation. As expected from the heteromolecular dimerization, pyrene is more consumed (about 10%) than in homomolecular dimerization case due to its collision with two more PAHs.

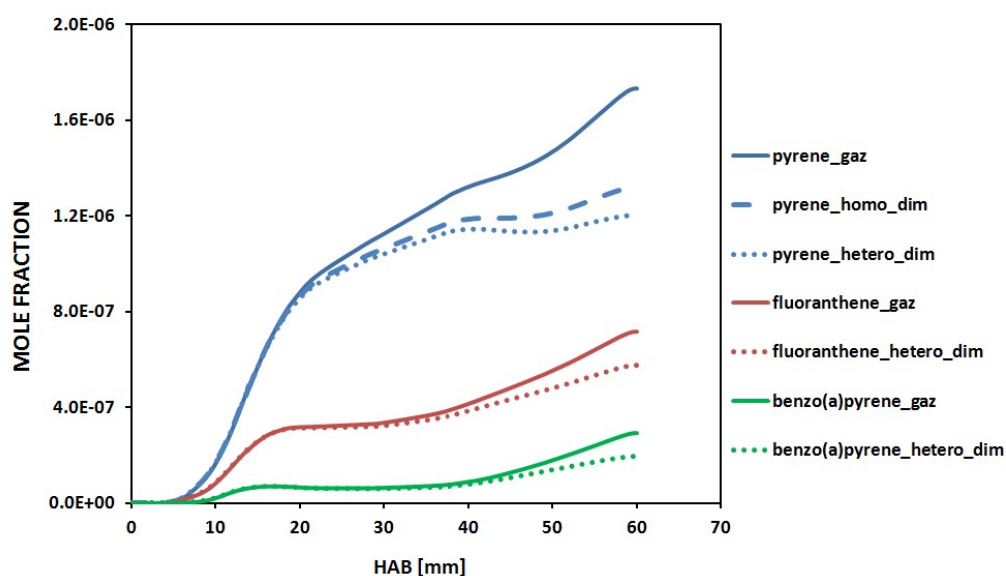


Figure 96 : Methane rich flame ( $\phi=2.32$ ): PAHs concentration in the gas-phase and after their dimerization to generate soot particles. Pyrene\_gaz stands for pyrene concentration in the gas-phase; Homo\_dim stands for homomolecular dimerization (only pyrene); hetero\_dim stands for heteromolecular dimerization (pyrene/fluoranthene/benzo(a)pyrene).

As can be seen in Figure 97, the improved result obtained with the heteromolecular dimerization is due to its higher nucleation, condensation and surface growth rates than in the homomolecular dimerization case.



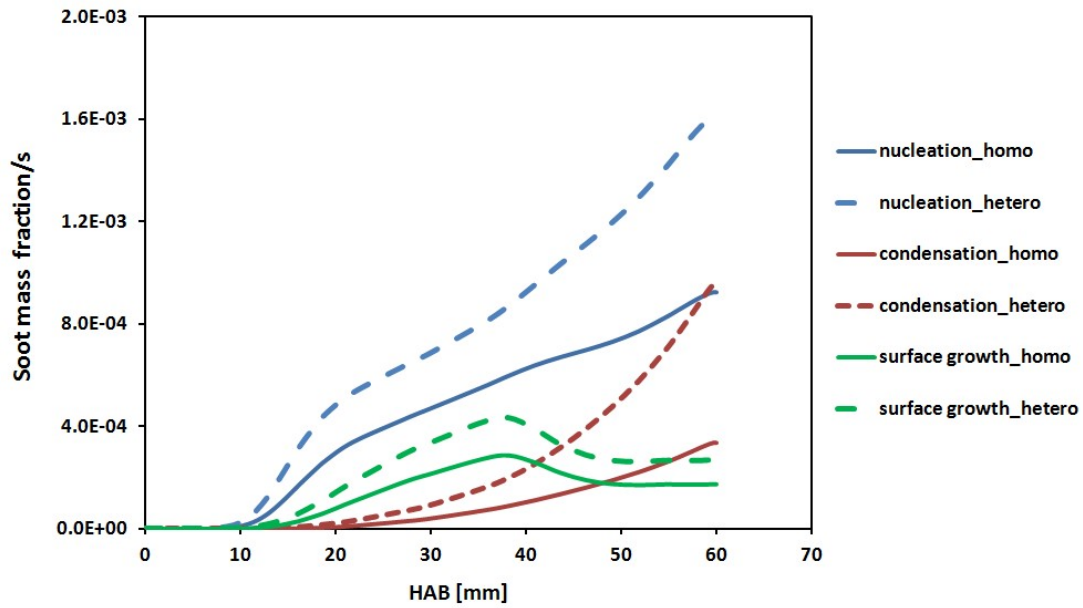


Figure 97 : Methane rich flame ( $\phi=2.32$ ): Comparison between nucleation, condensation and surface growth rates in both homomolecular and heteromolecular dimerization. Homo\_dim stands for homomolecular dimerization (only pyrene); hetero\_dim stands for heteromolecular dimerization (pyrene/fluoranthene/benzo(a)pyrene).

The evolution of the main species which is acetylene involved in the surface growth process has been examined and is found unchanged due to the weak value attributed to  $\alpha$  (0.05). As can be seen in Figure 95, both homo and heteromolecular dimerizations hypotheses lead to the underprediction of measurements. One of the reasons could be the weak value attributed to  $\alpha$ . Thus, it is decided to modify  $\alpha$  value in order to match experimental data. The optimum values of  $\alpha$  obtained for both homo and heteromolecular dimerizations are presented in Figure 98. These values allow to better match the measured soot volume fractions.

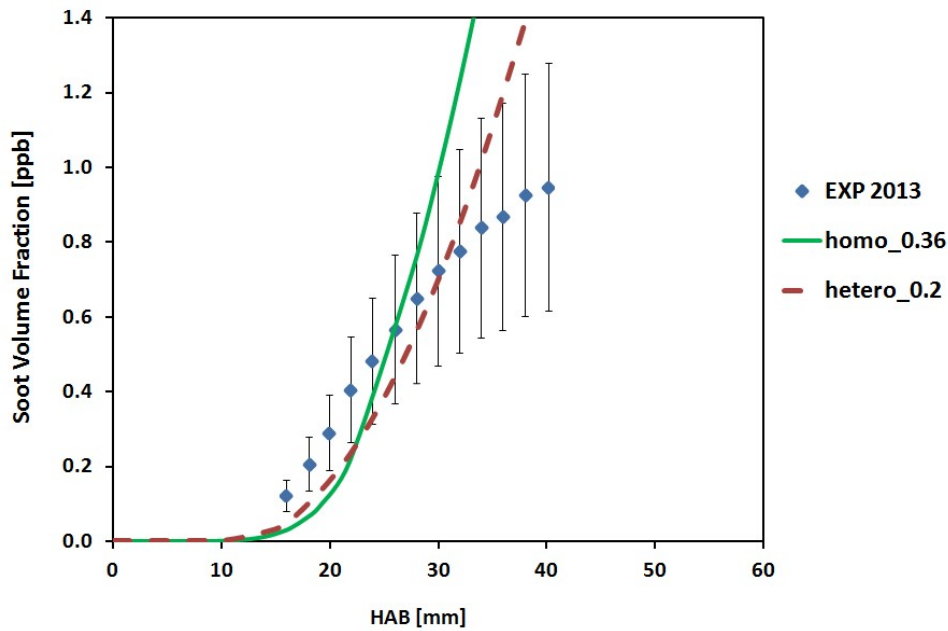


Figure 98 : Methane rich flame ( $\phi=2.32$ ): Determination of the optimum values of  $\alpha$  for both homo and heteromolecular dimerization. Homo\_0.36 stands for:  $\alpha=0.36$  for homomolecular dimerization (if only pyrene is considered); hetero\_0.2 stands for:  $\alpha=0.2$  for heteromolecular dimerization (if pyrene/fluoranthene/benzo(a)pyrene are considered).

If only pyrene is considered as the unique precursor for particles nucleation, the best agreement between prediction and measurements is obtained for  $\alpha=0.36$ , while in the case of heteromolecular dimerization involving three precursors, the best agreement is obtained for  $\alpha=0.2$ . As a result,  $\alpha$  value is increased from 0.05 to 0.36 and 0.2 for respectively homo and heteromolecular dimerizations. Similar value of  $\alpha$  was obtained previously in the work of Mouton et al. [85], where authors used a value of 0.35 in the pyrene homomolecular dimerization. Concerning the shape of predictions, the continuous growth is potentially due to the low oxidation process of soot particles in the burnt gas zone.

The evolution of the concentration profiles of the PAHs involved and the comparison between concentration profiles obtained for  $\alpha=0.05$  and the optimized ones in both homo and the heterodimerization cases are presented in Figure 99 and Figure 100.

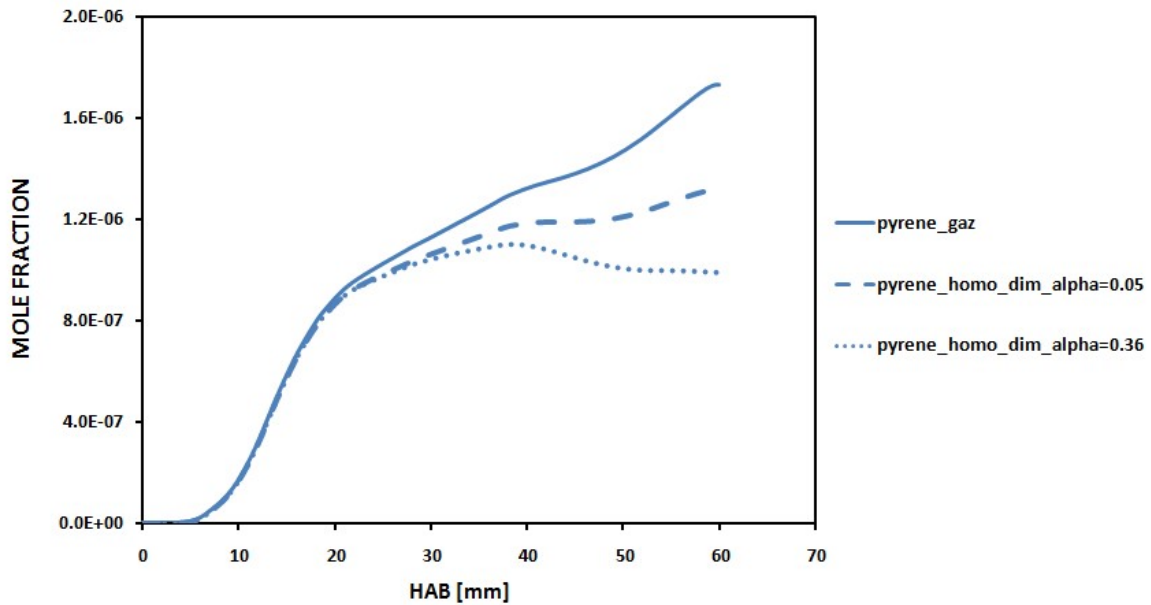


Figure 99 : Methane rich flame ( $\phi=2.32$ ): PAHs mole fraction profiles with the homomolecular (only pyrene) dimerization with the optimized (0.36) and the initial (0.05)  $\alpha$  values.

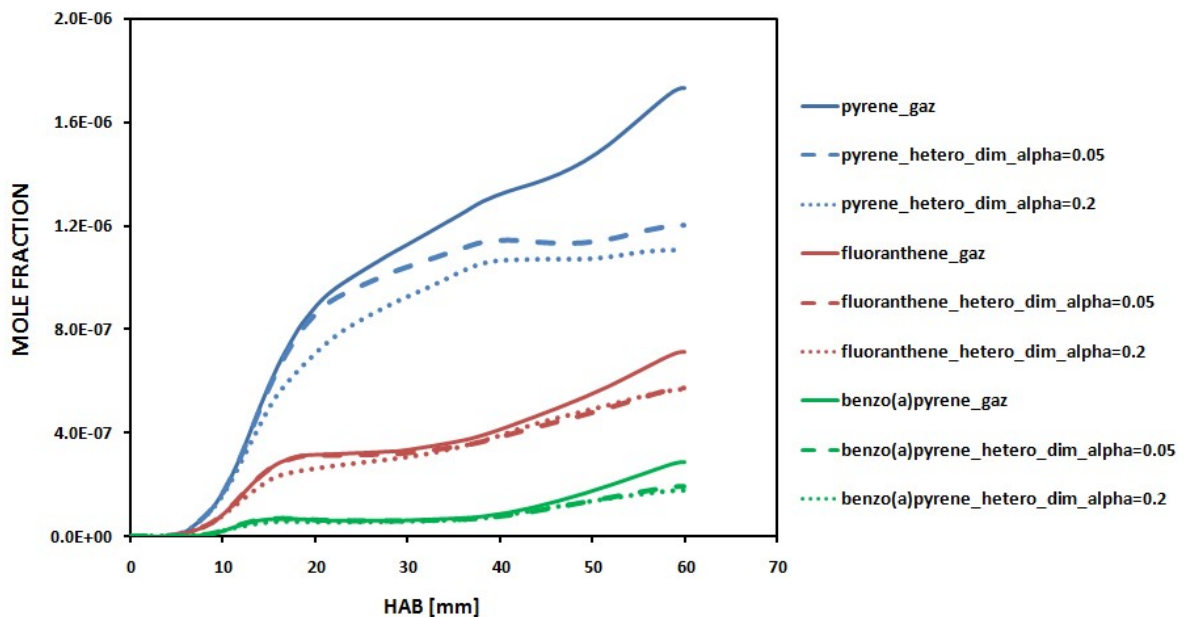


Figure 100 : Methane rich flame ( $\phi=2.32$ ): PAHs mole fraction profiles with the heteromolecular (pyrene/fluoranthene/benzo(a)pyrene) dimerization with the optimized (0.2) and the initial (0.05)  $\alpha$  values.

In the homomolecular dimerization case and as expected, pyrene is more consumed with the increase of  $\alpha$  value from 0.05 to 0.36. With the heteromolecular dimerization, the same observations can be seen for pyrene, while the effect of  $\alpha$  on fluoranthene and benzo(a)pyrene consumption is insignificant. The most consumed PAH is pyrene with respect to the two others and is likely the major contributor in soot particle inception in the reactive system considered.

As can be seen in Figure 101 and Figure 102, these assumptions are confirmed by the higher condensation and surface growth rates obtained with the optimized  $\alpha$  values in both homo and heteromolecular dimerizations cases. A large gap between the optimized  $\alpha$  values and  $\alpha=0.05$  in both dimerizations cases is observed for the surface growth rates, since this latter is highly dependent on the fraction of sites available for reactions on soot particles surface.

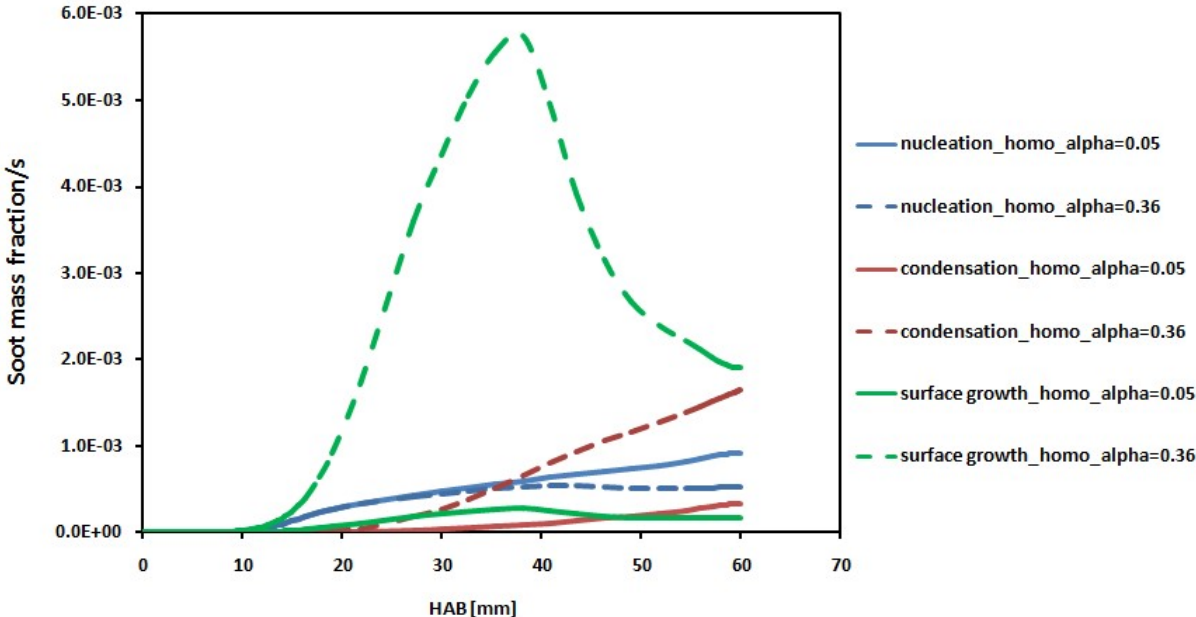


Figure 101 : Methane rich flame ( $\phi=2.32$ ): Comparison of nucleation, condensation and surface growth rates between the results obtained through only pyrene dimerization with the optimized  $\alpha$  values and the initial  $\alpha$  values.

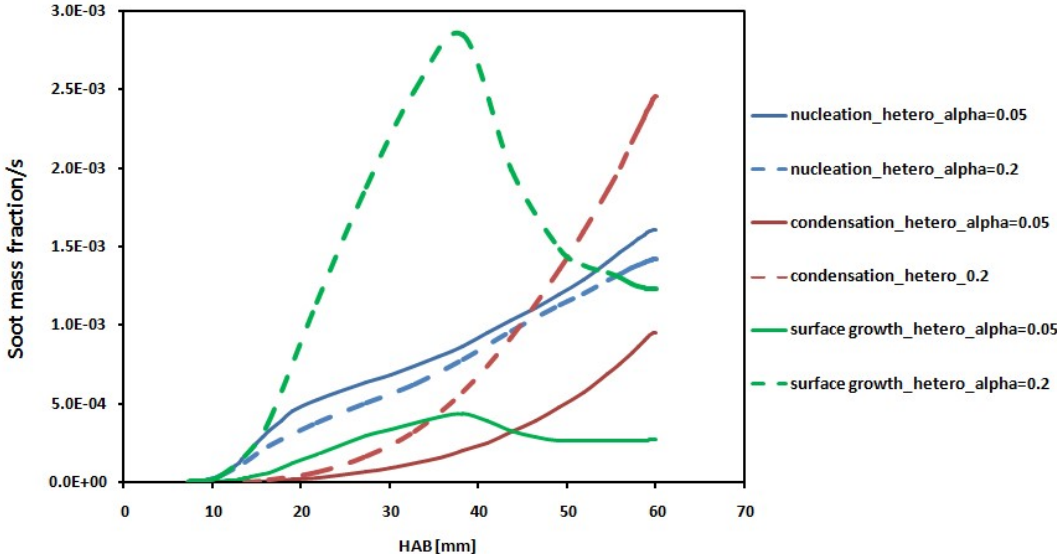


Figure 102 : Methane rich flame ( $\phi=2.32$ ): Comparison of nucleation, condensation and surface growth rates between the results obtained through the heteromolecular dimerization with the optimized  $\alpha$  values and the initial  $\alpha$  values.

### - Soot primary particle diameters prediction

As can be seen in Figure 103, the primary soot particle diameters measured in [85] with the LII technique were modeled using both nucleation processes. The effect of the change of  $\alpha$  values was also examined.

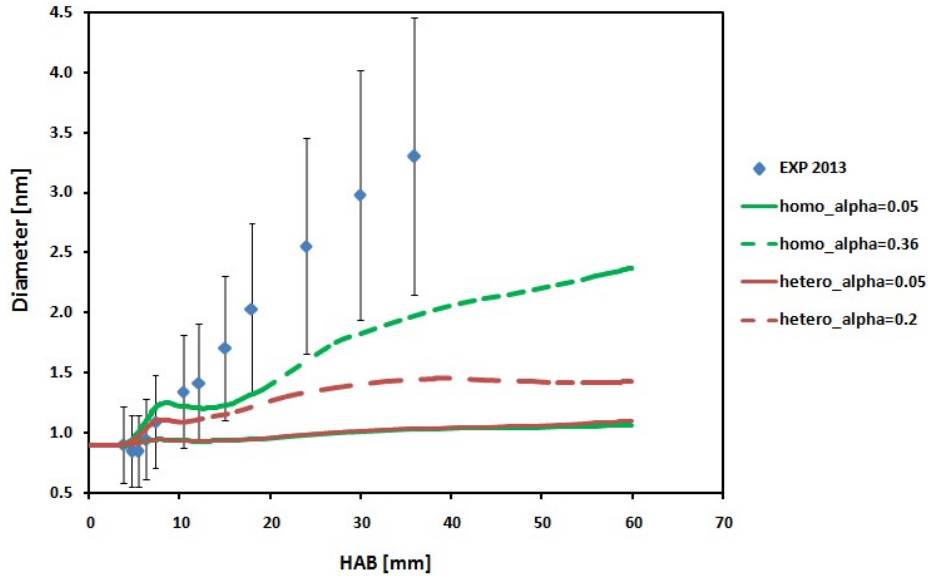


Figure 103 : Methane rich flame ( $\phi=2.32$ ): Soot primary particles prediction in both homo and heteromolecular dimerization with the optimized and the initial  $\alpha$  values. The symbols are experimental data from [85]. The lines and dashed lines represent modeling results from the present work.

In contrast with the measurements trend, the soot model shows nearly a constant evolution of particle diameters in both homo and heteromolecular dimerizations cases if  $\alpha$  value is set to 0.05, indicating lower surface growth rates as discussed previously. With the optimized  $\alpha$  values that allow to better match soot volume fraction profiles in both cases, they failed to reproduce experimental particle diameters. The soot model exhibits a peak at HAB=9 mm, followed by the decrease of particle diameters and then an increase of diameters. The homomolecular dimerization shows a rapid diameter evolution than in the heteromolecular case due to the higher value of  $\alpha$  used (0.36 against 0.20).

#### 5.4.2. Ethylene flame

In Figure 104, prediction with the homomolecular dimerization of each PAH from pyrene to coronene is reported with a constant value of  $\alpha$  (0.05). In Figure 105, prediction with the heteromolecular dimerization consisting of the contribution of three PAHs pyrene, fluoranthene and benzo(a)pyrene is presented, compared to the only contribution of pyrene molecule.

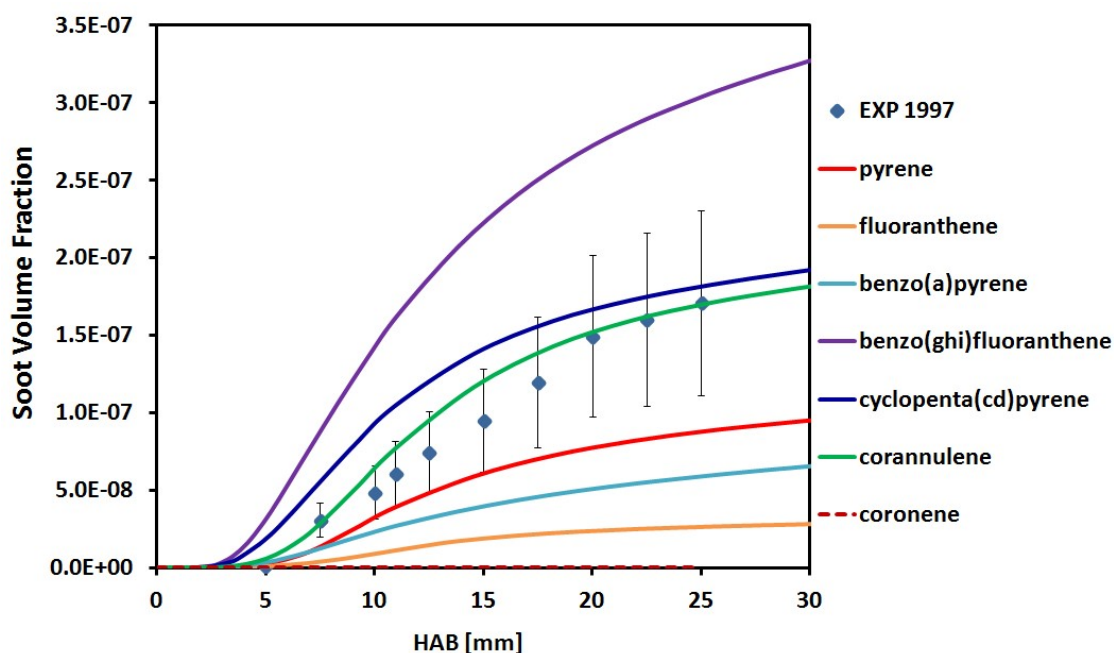


Figure 104 : Atmospheric ethylene premixed flame,  $\phi=2.34$ :  $C_2H_4$  (14.08% in mol.)/ $O_2$  (18.05%)/ $N_2$  (67.87%). Homomolecular dimerization of the investigated PAHs. The symbols represent experimental data from [82]; the lines represent modeling results from the present work. Fraction of reactive surface sites available for reactions ( $\alpha$ ) is set to 0.05.

It can be observed that the homomolecular dimerization of single PAH such as cyclopenta(cd)pyrene, corannulene and pyrene fairly reproduce measurements, while that of benzo(ghi)fluoranthene overpredicts experimental data. The contributions of benzo(a)pyrene and fluoranthene are not enough to account for soot volume fraction prediction. Coronene contribution is clearly insignificant due to its very low gas-phase concentration. As discussed previously, the better agreement obtained for the above-mentioned PAHs is related to their gas-phase concentration and the collision efficiencies. For example, the overprediction showed by benzo(ghi)fluoranthene is understandable since its maximum gas-phase concentration is close to 100 ppm, while that of cyclopenta(cd)pyrene, corannulene and pyrene are respectively 95 ppm, 23 ppm and 20 ppm. However, due to the lack of experimental data on PAH concentration profiles, results obtained from the present kinetic model clearly require more validation in order to fully consider the real contribution of each PAH.

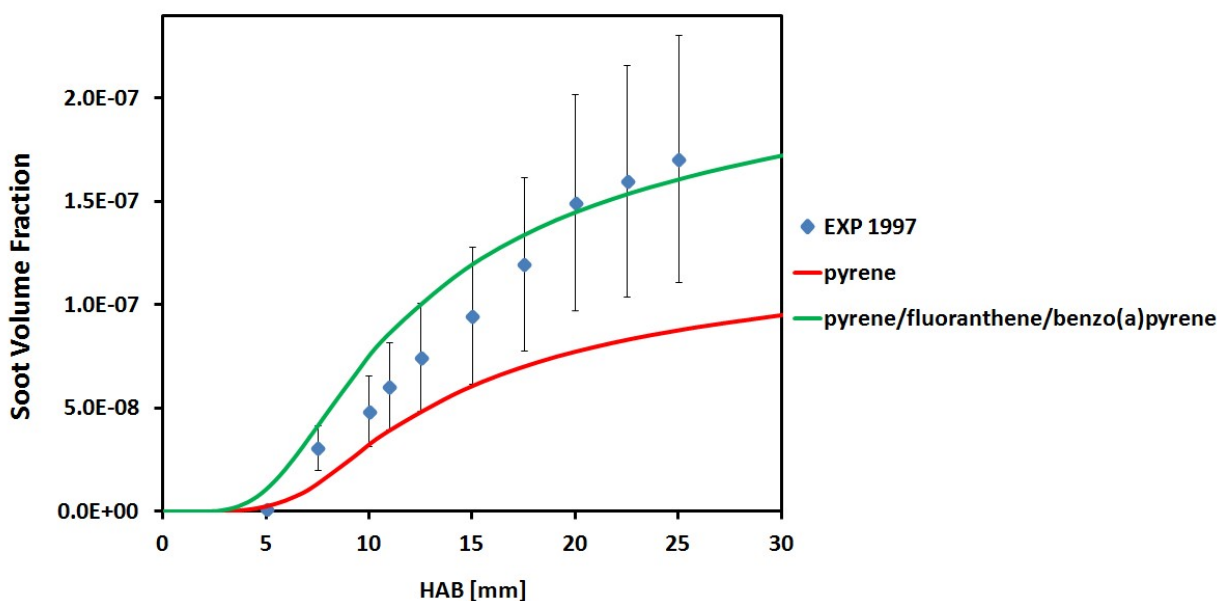


Figure 105 : Atmospheric ethylene premixed flame,  $\phi=2.34$ :  $C_2H_4$  (14.08% in mol.)/ $O_2$  (18.05%)/ $N_2$  (67.87%). Heteromolecular dimerization of pyrene/fluoranthene/benzo(a)pyrene. The symbols represent experimental data from [82]; the lines represent modeling results from the present work. Fraction of reactive surface sites available for reactions ( $\alpha$ ) is set to 0.05.

In Figure 105, soot volume fraction prediction is distinctly improved when adding the heteromolecular dimerization. The evolution of the involved PAHs concentration in both homo and heteromolecular dimerizations is presented in Figure 106. It can be seen that PAHs are drastically consumed to generate soot particles. It can also be observed that the prediction improvement is due to the contributions of the two PAHs (fluoranthene and benzo(a)pyrene) associated with pyrene, since they are clearly consumed to match experimental data. That result is confirmed by the higher nucleation and condensation rates obtained in the heteromolecular dimerization case as previously discussed in the methane rich flame. It is worth noting that this drastic consumption of PAHs with the present soot model is not physical since they are totally consumed to generate soot particles. Experimental measurements do not exhibit such behavior, where PAH mole fractions do not completely tend towards zero at higher HAB.

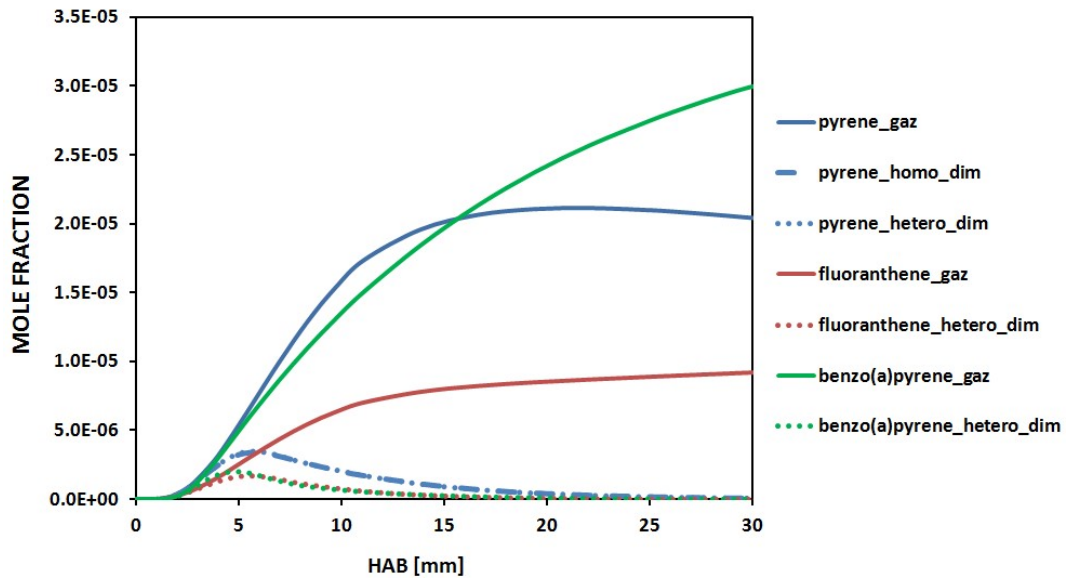


Figure 106 : Ethylene rich flame ( $\phi=2.34$ ): PAHs concentration in the gas-phase and after their dimerization to generate soot particles. Pyrene\_gaz stands for pyrene concentration in the gas-phase; Homo\_dim stands for homomolecular dimerization (only pyrene); hetero\_dim stands for heteromolecular dimerization (pyrene/fluoranthene/benzo(a)pyrene).

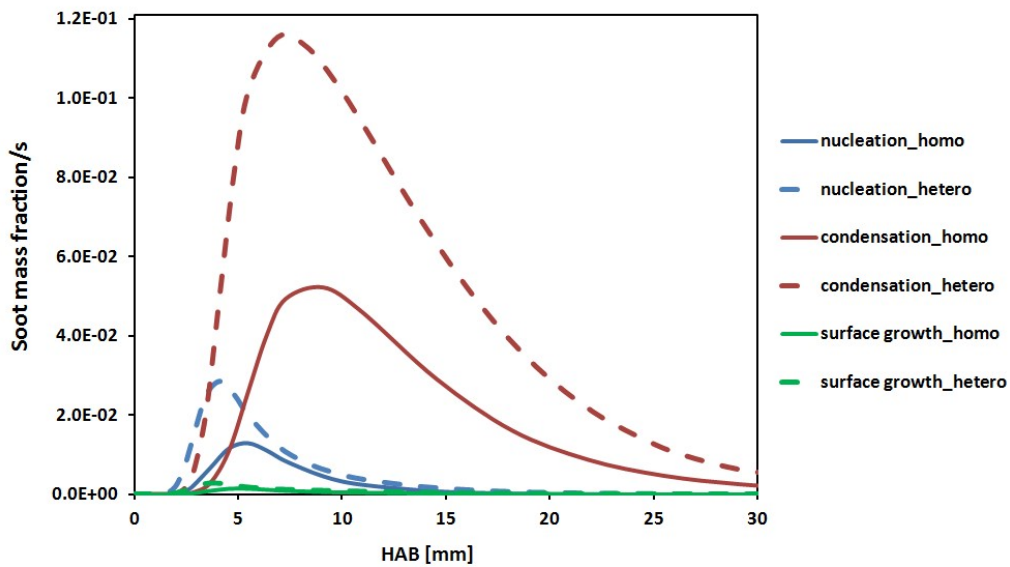


Figure 107 : Ethylene rich flame ( $\phi=2.34$ ): Comparison between nucleation, condensation and surface growth rates in both homomolecular and heteromolecular dimerization. Homo\_dim stands for homomolecular dimerization (only pyrene); hetero\_dim stands for heteromolecular dimerization (pyrene/fluoranthene/benzo(a)pyrene).

As can be seen in Figure 105, the exclusive dimerization of pyrene with a constant  $\alpha$  value of 0.05 underpredicts measurements, while the heteromolecular dimerization fairly reproduces experimental soot volume fraction with this  $\alpha$  value. Thus, it is decided to vary  $\alpha$  value in order to match experimental data if only pyrene should be considered as a unique soot precursor. The optimum value of  $\alpha$  obtained for the latter case is presented in Figure 108 and the best agreement is obtained for a  $\alpha$  value of 1.0 (the maximum value that  $\alpha$  can physically have). In the previous work of Chernov et al.



[84] on ethylene flames in the case of homomolecular dimerization, authors found that  $\alpha$  varies between 0.77 and 1.0 if the chemical mechanism from Appel et al. [11] is used, while Faeth et al. [192,193] found that  $\alpha$  varies between 0.8 and 1.0. Thus, the value of  $\alpha$  determined in the present work is consistent with that obtained in the previous works from other groups such as Chernov et al. [84].

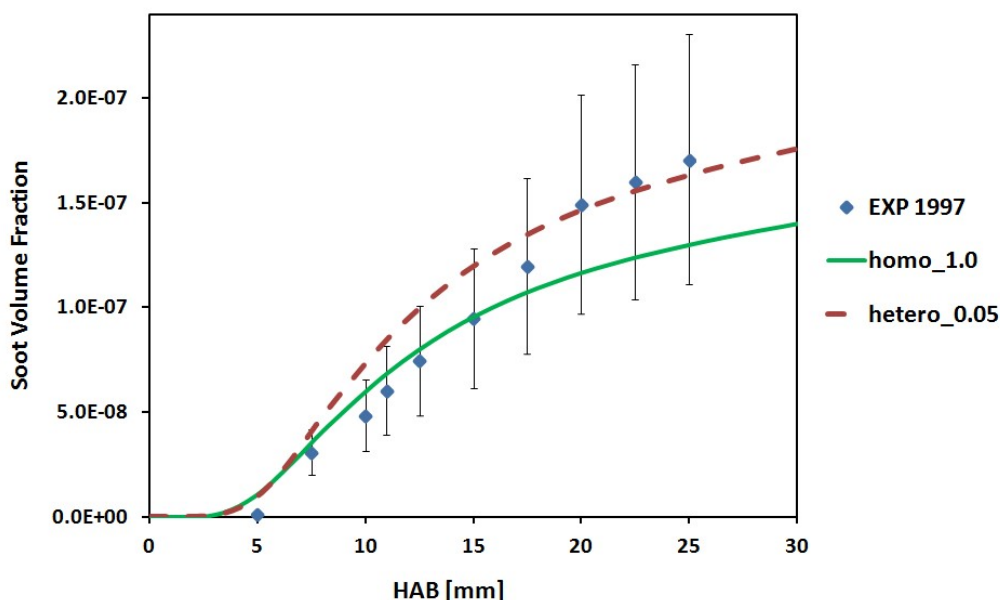


Figure 108 : Ethylene rich flame ( $\phi=2.34$ ): Determination of the optimum value of  $\alpha$  for the homomolecular dimerization. Homo\_1.0 stands for:  $\alpha=1.0$  for homomolecular dimerization (if only pyrene is considered); hetero\_0.05 stands for:  $\alpha=0.05$  for heteromolecular dimerization (if pyrene/fluoranthene/benzo(a)pyrene are considered).

The evolution of the involved PAHs concentrations remains nearly unchanged with the optimized  $\alpha$  compared to that presented in Figure 106. In addition, in the homomolecular dimerization case, the effect of  $\alpha$  (from 0.05 to 1) on pyrene consumption profile remains mostly negligible. However, according to the present model (Figure 109) by considering the homomolecular dimerization case, the surface growth rate is higher with the optimized  $\alpha$  value (1.0) than with  $\alpha=0.05$ . Indeed, this is due to the higher value (1.0) given to  $\alpha$  if only pyrene is considered as the only monomer. One can also notice the higher condensation and nucleation rates are obtained with the lower  $\alpha$  value (0.05).

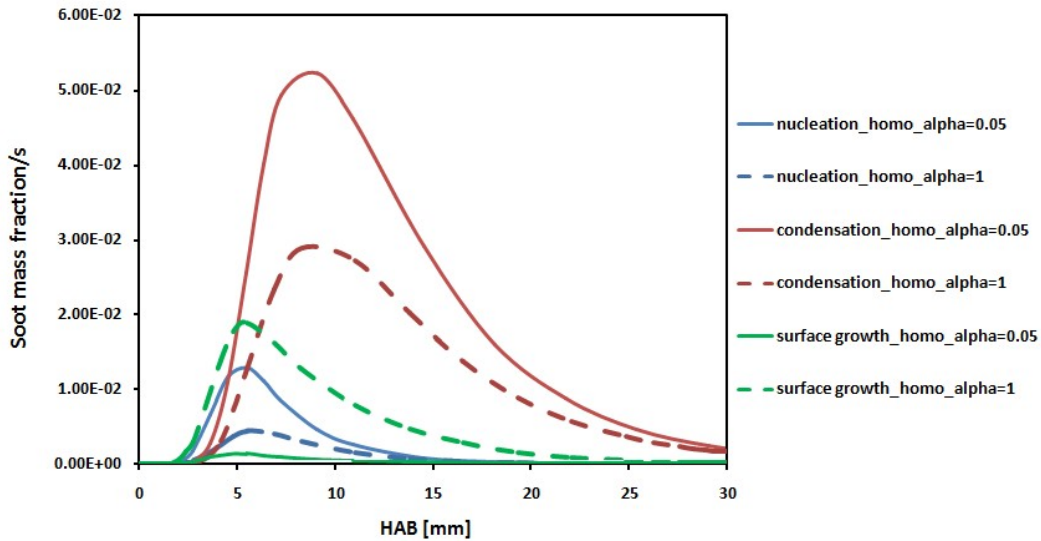


Figure 109 : Ethylene rich flame ( $\phi=2.32$ ): Comparison between nucleation, condensation and surface growth rates in homomolecular dimerization (only pyrene) with the optimized and initial  $\alpha$  values.

- Soot primary particle diameters prediction

In this rich ethylene premixed flame, the available particles mean diameters has been modeled as shown in Figure 110, for both  $\alpha=0.05$  and its optimized value for the homomolecular dimerization of pyrene and the heteromolecular dimerization case. These soot primary particles were obtained from Transmission Electronic Microscope (TEM) by thermophoretic sampling [82].

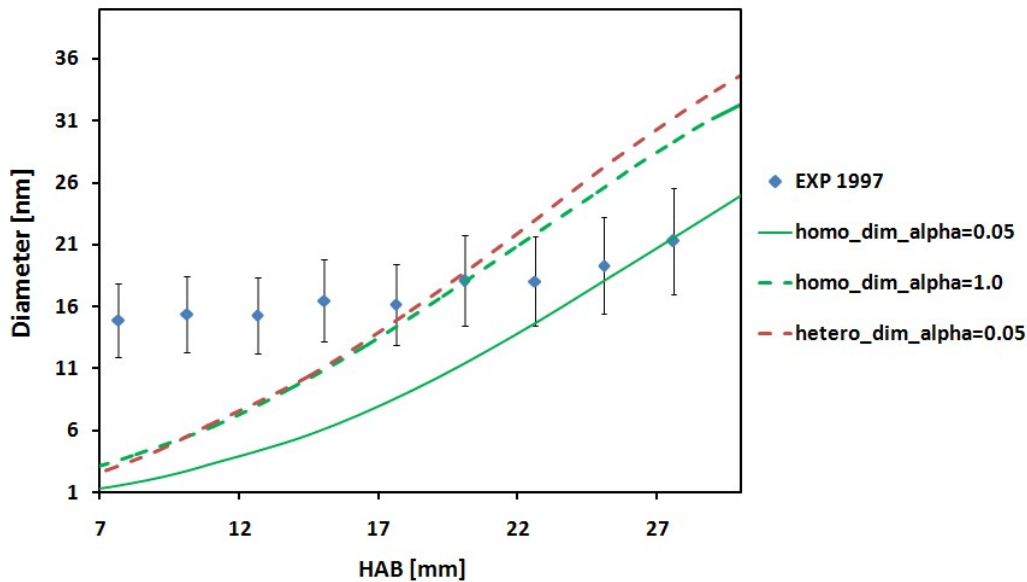


Figure 110 : Soot primary particles prediction in both homo and heteromolecular dimerization ( $\alpha=0.05$ ) and with the optimized  $\alpha$  ( $\alpha=1.0$  for the homomolecular and  $\alpha=0.05$  for the heteromolecular dimerization). The symbols are experimental data from [82]. The lines and dashed lines represent modeling results from the present work.

According to the present soot model for both homo and heteromolecular dimerization cases, the mean particles diameter shows an increase as a function of the height above the burner, while the measurements nearly show a constant evolution of primary particle diameters. The increase of  $\alpha$  value in the homomolecular dimerization case leads to match the prediction given by the heteromolecular dimerization with  $\alpha=0.05$  but the experimental diameters profile is not reproduced. As a reminder, these measurements represent a mean value of diameters obtained from a TEM and uncertainties for such particles diameter determination can be as high as 15% (95% confidence interval) by using thermophoretic sampling [194] and up to 50% for the LII method [195,196]. It is expected from the present soot model to obtain such particle diameter evolution, since condensation and surface growth phenomena occur with nearly no consumption of soot particles.

### **5.4.3. n-butane flames**

Three n-butane premixed flames at various equivalence ratios  $\varphi=1.75$ ; 1.95 and 2.32 were investigated in particles nucleation modeling. There is a major interest in modeling the leanest ( $\varphi=1.75$ ) n-butane flame since it represents a nucleation flame, where the amount of soot formed is very low with a constant particles diameter [197,198]. In contrast with that flame, experimental data for the richest flame ( $\varphi=2.32$ ) are available in order to investigate the behavior of  $\alpha$  for the n-butane premixed flames.

#### **5.4.3.1. n-butane flame ( $\varphi=1.75$ )**

In Figure 111, soot volume fraction prediction with the homomolecular dimerization of each PAH from pyrene to corannulene is reported with a constant value of  $\alpha$  (0.05). In Figure 112, soot volume fraction predictions accounting for heteromolecular dimerization contribution of three PAHs pyrene, fluoranthene and benzo(a)pyrene is presented and compared to pyrene homomolecular dimerization.

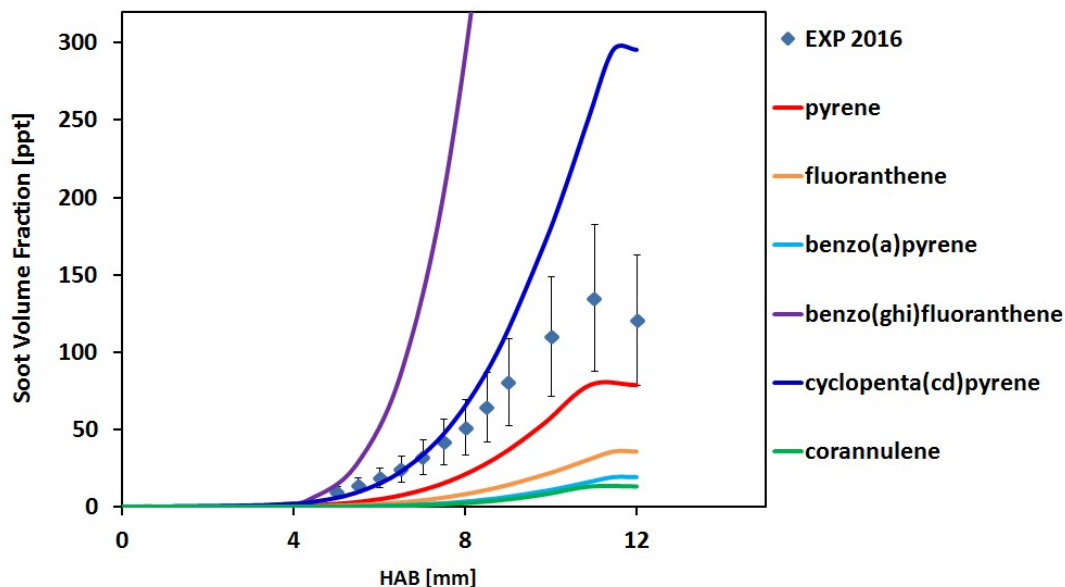


Figure 111 : Atmospheric n-butane premixed flame,  $\phi=1.75$ : n-C<sub>4</sub>H<sub>10</sub> (9.46% in mol.)/O<sub>2</sub> (35.22%)/N<sub>2</sub> (55.32%). Homomolecular dimerization of the investigated PAHs. The symbols represent experimental data from [149]; the lines represent modeling results from the present work. Fraction of reactive surface sites available for reactions ( $\alpha$ ) is set to 0.05.

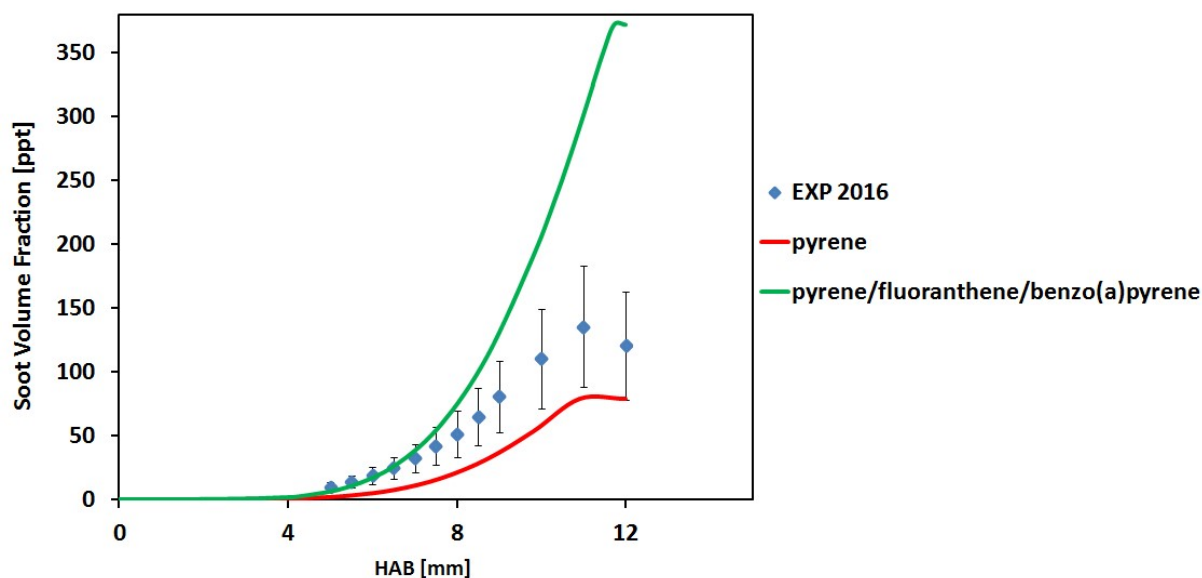


Figure 112 : Atmospheric n-butane premixed flame,  $\phi=1.75$ : n-C<sub>4</sub>H<sub>10</sub> (9.46% in mol.)/O<sub>2</sub> (35.22%)/N<sub>2</sub> (55.32%). Heteromolecular dimerization of pyrene/fluoranthene/benzo(a)pyrene. The symbols represent experimental data from [149]; the lines represent modeling results from the present work. Fraction of reactive surface sites available for reactions ( $\alpha$ ) is set to 0.05.

As can be observed in Figure 111, considering the homomolecular dimerizations of cyclopenta(cd)pyrene ( $\sim 0.8$  ppm predicted maximum gas-phase concentration) and pyrene ( $\sim 0.5$  ppm) leads to an acceptable agreement with measurements ( $\alpha=0.05$ ), while dimerization of benzo(ghi)fluoranthene ( $\sim 1.8$  ppm) highly overpredicts and that of fluoranthene ( $\sim 0.24$  ppm) and benzo(a)pyrene ( $\sim 0.12$  ppm) and corannulene ( $\sim 0.13$  ppm) underpredict experimental measurements.

In Figure 112, soot volume fraction prediction is improved with the heteromolecular dimerization. However, an overprediction within a factor of about 3 can be observed in the higher HAB zone. The evolution of the involved PAHs concentration in both homo and heteromolecular dimerization remains nearly unchanged with respect to their gas-phase concentrations due to the low sooting tendency of this nucleation n-butane flame. As can be seen in Figure 113 and as previously discussed, the addition of fluoranthene and benzo(a)pyrene to pyrene contribution leads to higher nucleation and condensation rates, while the surface growth rate stays comparable.

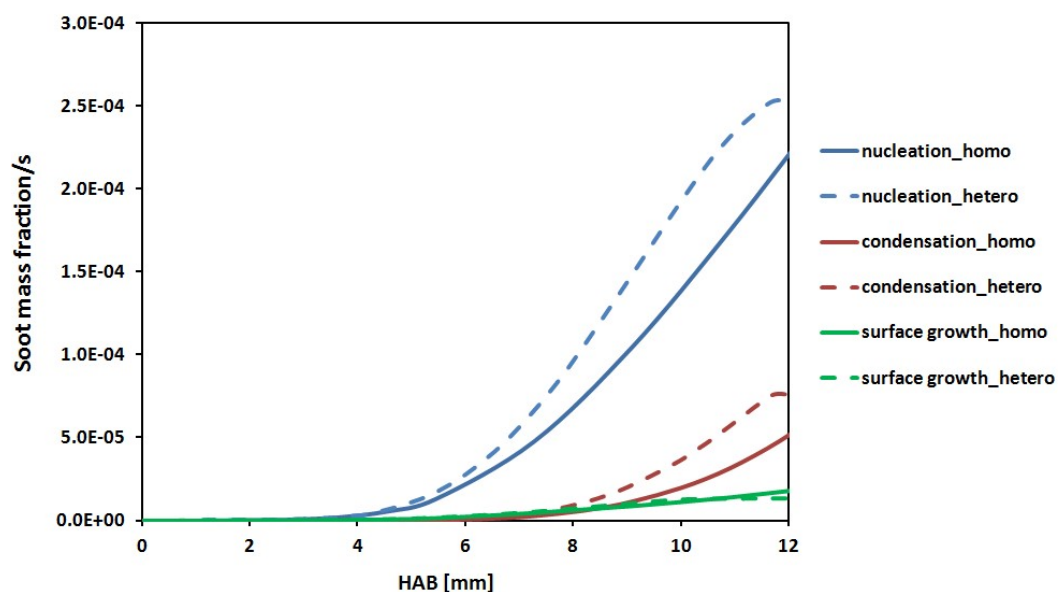


Figure 113 : n-butane flame ( $\phi=1.75$ ): Comparison between nucleation, condensation and surface growth rates in both homomolecular and heteromolecular dimerization. Homo\_dim stands for homomolecular dimerization (only pyrene); hetero\_dim stands for heteromolecular dimerization (pyrene/fluoranthene/benzo(a)pyrene).

It was shown in Figure 112 that considering the exclusive dimerization slightly underpredicts measurements, while the heteromolecular one shows an overprediction within a factor of 3. Therefore, the optimized  $\alpha$  values for this lean flame in both homo and heteromolecular conditions has been determined. Results obtained are presented in Figure 114.

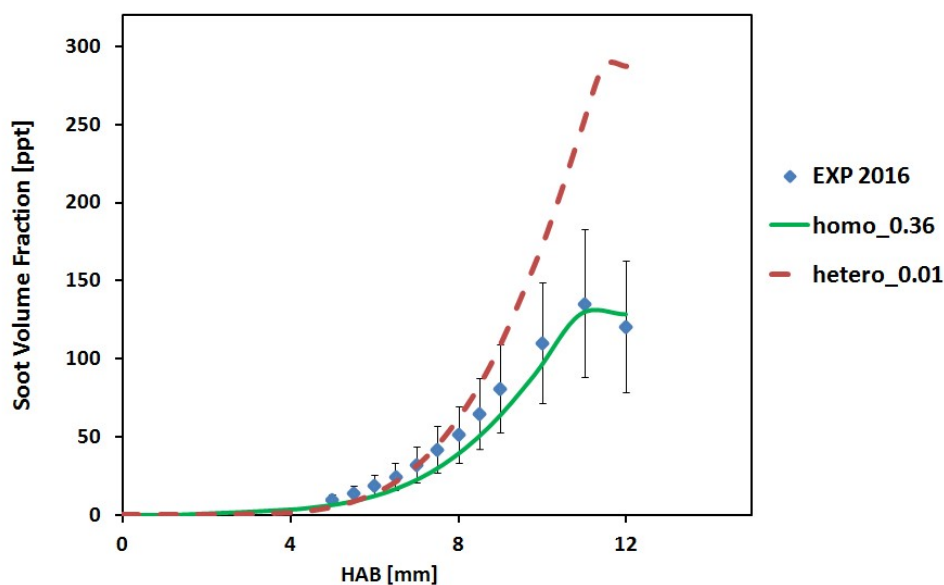


Figure 114 : n-butane flame ( $\phi=1.75$ ): Determination of the optimum value of  $\alpha$  for the homomolecular dimerization. Homo\_0.36 stands for:  $\alpha=0.36$  for homomolecular dimerization (if only pyrene is considered); hetero\_0.01 stands for:  $\alpha=0.01$  for heteromolecular dimerization (if pyrene/fluoranthene/benzo(a)pyrene are considered).

If only pyrene dimerization is considered, the best agreement is obtained for  $\alpha=0.36$  (against 0.05), while in the heteromolecular case, the best agreement is obtained for  $\alpha=0.01$  (against 0.05). In the latter case, the discrepancy between model and experiment was reduced from an overprediction of a factor of 3 to a factor of 2. The evolution of the involved PAHs concentrations remains nearly unchanged with the optimized  $\alpha$  compared to the gas-phase ones. The comparison between nucleation, condensation and surface growth rates using the optimized and the initial  $\alpha$  values in both homo and heteromolecular dimerization is presented in Figure 115 and Figure 116. In the homomolecular dimerization case, the increase of  $\alpha$  from 0.05 to 0.36 leads as expected to higher surface growth rate, while the nucleation and condensation rates is more important with  $\alpha=0.05$  at higher HAB. In the heteromolecular dimerization, both  $\alpha$  values give roughly the same nucleation and condensation rates, while the surface growth rate is slightly more important with  $\alpha=0.05$ . These observations were expected because of the low values attributed to  $\alpha$ .

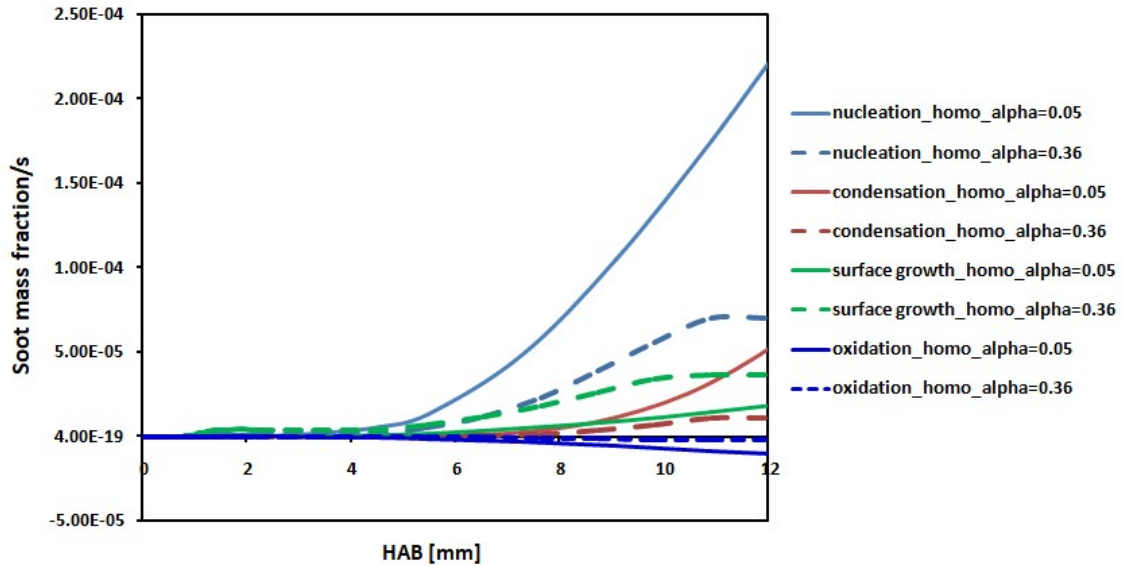


Figure 115 : n-butane flame ( $\phi=1.75$ ): Comparison between nucleation, condensation and surface growth rates in homomolecular dimerization case with the optimized and the initial  $\alpha$  values.

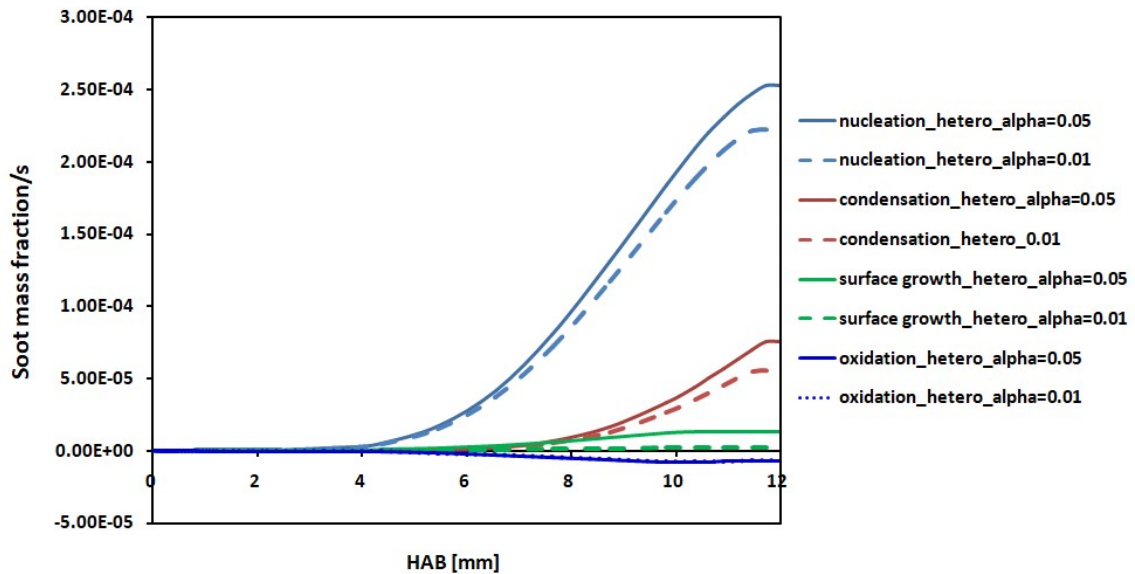


Figure 116 : n-butane flame ( $\phi=1.75$ ): Comparison between nucleation, condensation and surface growth rates in heteromolecular dimerization case with the optimized and the initial  $\alpha$  values.

#### - Soot primary particle diameters prediction

In this flame, it is expected to observe a constant particle size since its sooting tendency is very low [149]. In Figure 117, the predicted soot particle diameters as a function of the height above the burner are presented for both  $\alpha=0.05$  and its optimized values in the pyrene ( $\alpha=0.36$ ) and heteromolecular ( $\alpha=0.01$ ) dimerizations.

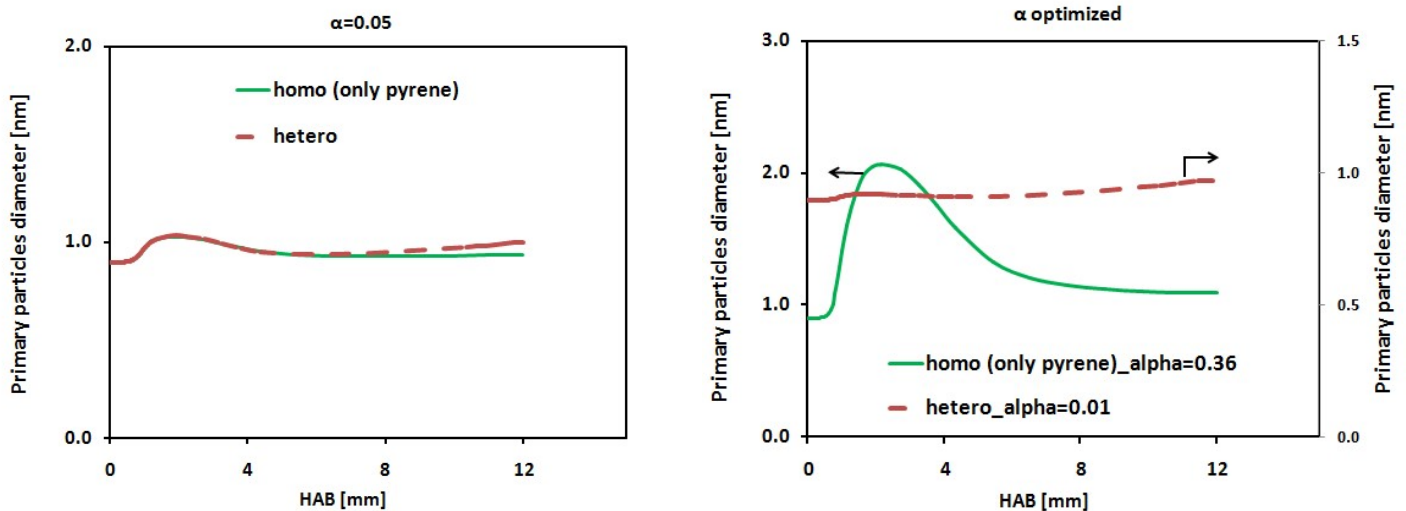


Figure 117 : n-butane flame ( $\phi=1.75$ ): Soot primary particles prediction in both homo and heteromolecular dimerization ( $\alpha=0.05$ ) and with the optimized  $\alpha$  ( $\alpha=0.36$  for the homomolecular and  $\alpha=0.01$  for the heteromolecular dimerization).

As expected, the model exhibits nearly a constant evolution of particles diameter for a weak value of  $\alpha$ . For  $\alpha=0.05$ , both pyrene and heteromolecular cases show the same results and the predicted particle diameters are around 1 nm. For the optimized  $\alpha$  values, which is significantly increased in pyrene dimerization (from 0.05 to 0.36), particles diameter is no longer constant since a peak is observed with a maximum of 2 nm. The decrease of particles diameter is due to their oxidation process. That is understandable since the surface growth rate increases with  $\alpha$ . In the heteromolecular case where the optimized  $\alpha$  value is found to be 0.01, particles diameter is constant and is found to reach 1nm.

#### 5.4.3.2. n-butane flame ( $\phi=1.95$ )

In Figure 118, soot volume fraction predictions with the homomolecular dimerization of each PAH from pyrene to corannulene is reported with a constant value of  $\alpha$  (0.05). In Figure 119, the prediction accounting for the heteromolecular dimerization contribution of three PAHs pyrene, fluoranthene and benzo(a)pyrene is presented and compared to pyrene homomolecular dimerization.



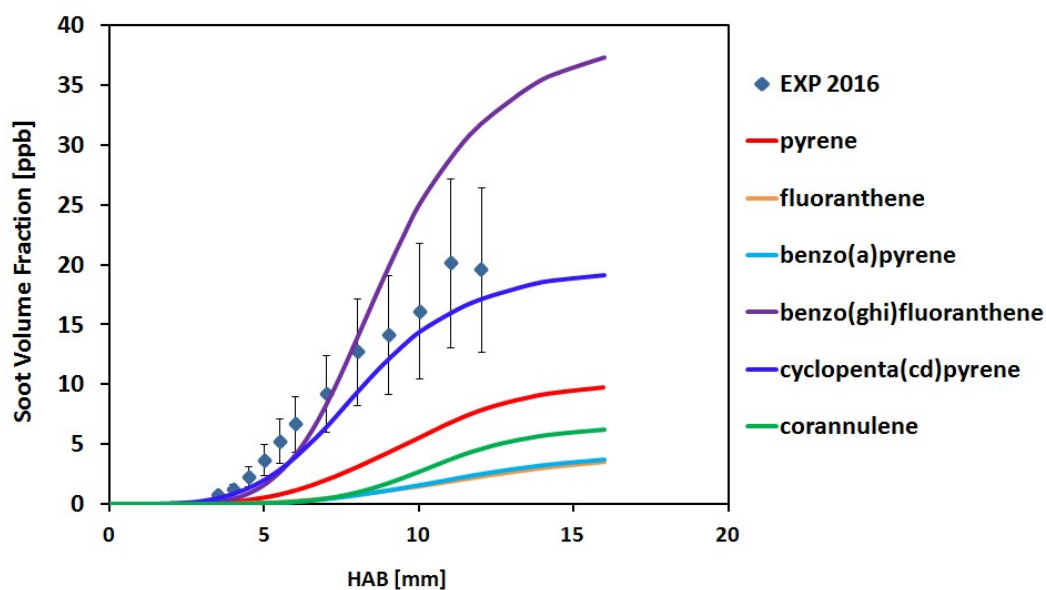


Figure 118 : Atmospheric n-butane premixed flame,  $\phi=1.95$ : n-C<sub>4</sub>H<sub>10</sub> (10.30% in mol.)/O<sub>2</sub> (34.31%)/N<sub>2</sub> (55.39%). Homomolecular dimerization of the investigated PAHs. The symbols represent experimental data from [149]; the lines represent modeling results from the present work. Fraction of reactive surface sites available for reactions ( $\alpha$ ) is set to 0.05.

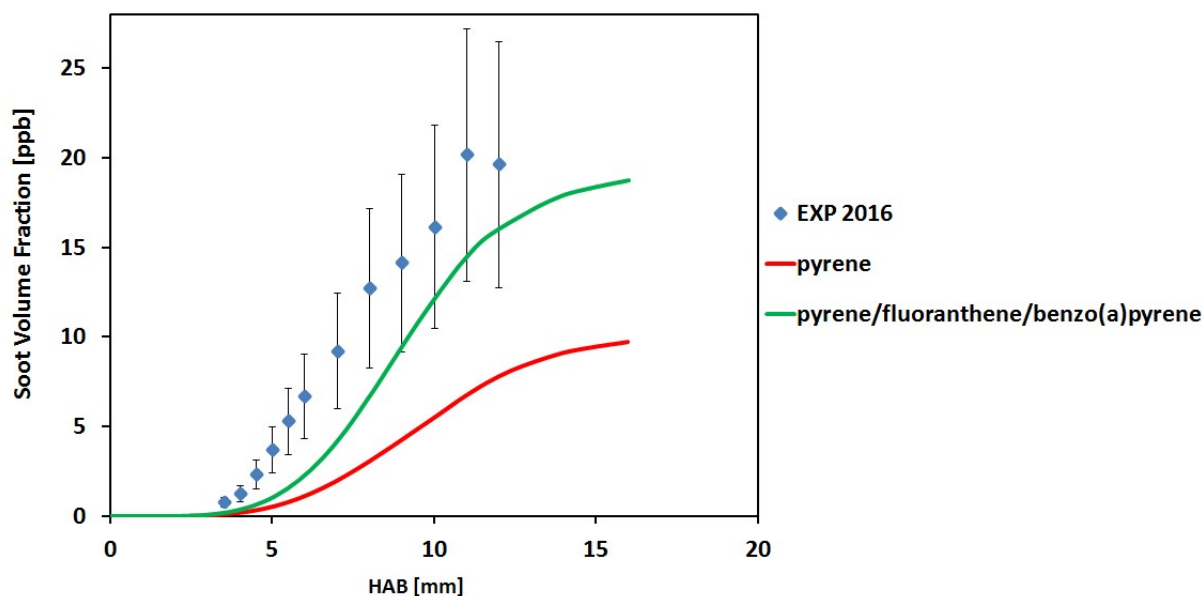


Figure 119 : Atmospheric n-butane premixed flame,  $\phi=1.95$ : n-C<sub>4</sub>H<sub>10</sub> (10.30% in mol.)/O<sub>2</sub> (34.31%)/N<sub>2</sub> (55.39%). Heteromolecular dimerization of pyrene/fluoranthene/benzo(a)pyrene. The symbols represent experimental data from [149]; the lines represent modeling results from the present work. Fraction of reactive surface sites available for reactions ( $\alpha$ ) is set to 0.05.

In Figure 118, the best agreement between measurements and prediction is observed for the homomolecular dimerization of cyclopenta(cd)pyrene. Also, a fair agreement can be observed for benzo(ghi)fluoranthene and for pyrene (within a factor of 2). It would be expected from the computed PAH mole fractions that benzo(ghi)fluoranthene (~20 ppm gas-phase concentration) and

cyclopenta(cd)pyrene (~11 ppm) would lead to a larger amount of soot with respect to pyrene (~5 ppm) and the other PAHs (< 3 ppm).

In Figure 119, soot volume fraction prediction is improved by considering the heteromolecular dimerization for the reasons discussed in the previous sections. The evolution of the involved PAHs concentrations in both homo and heteromolecular dimerizations is shown in Figure 120. It can be seen that PAHs are massively consumed to generate soot particles. Pyrene is more consumed in the case of heteromolecular than in the homomolecular dimerization since it reacts with two more PAHs: fluoranthene and benzo(a)pyrene.

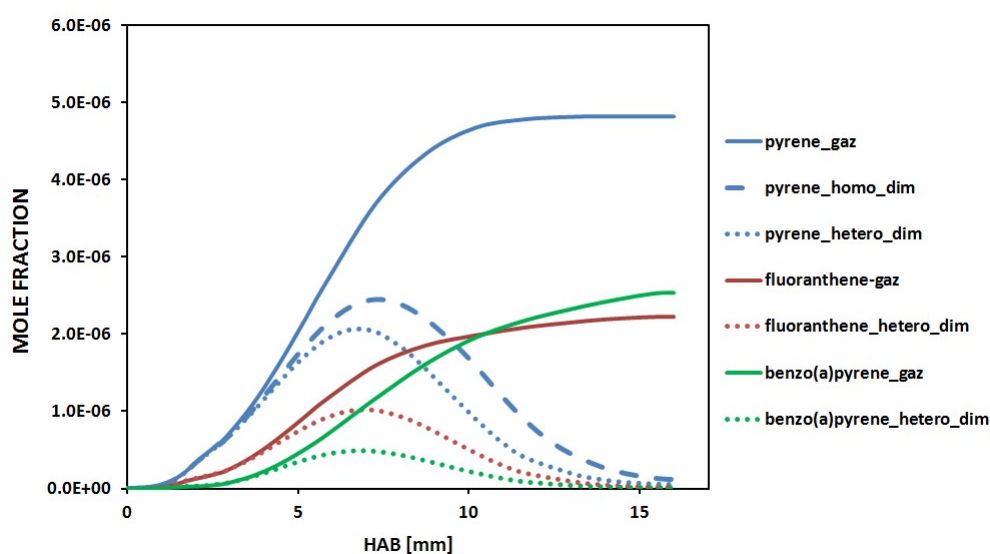


Figure 120 : n-butane flame ( $\phi=1.95$ ): PAHs concentration in the gas-phase and after their dimerization to generate soot particles. Pyrene\_gaz stands for pyrene concentration in the gas-phase; Homo\_dim stands for homomolecular dimerization (only pyrene); hetero\_dim stands for heteromolecular dimerization (pyrene/fluoranthene/benzo(a)pyrene).

As can be seen in Figure 121 and as previously discussed, the addition of the dimerization of fluoranthene and benzo(a)pyrene to pyrene homomolecular dimerization leads to higher nucleation, condensation and surface growth rates.

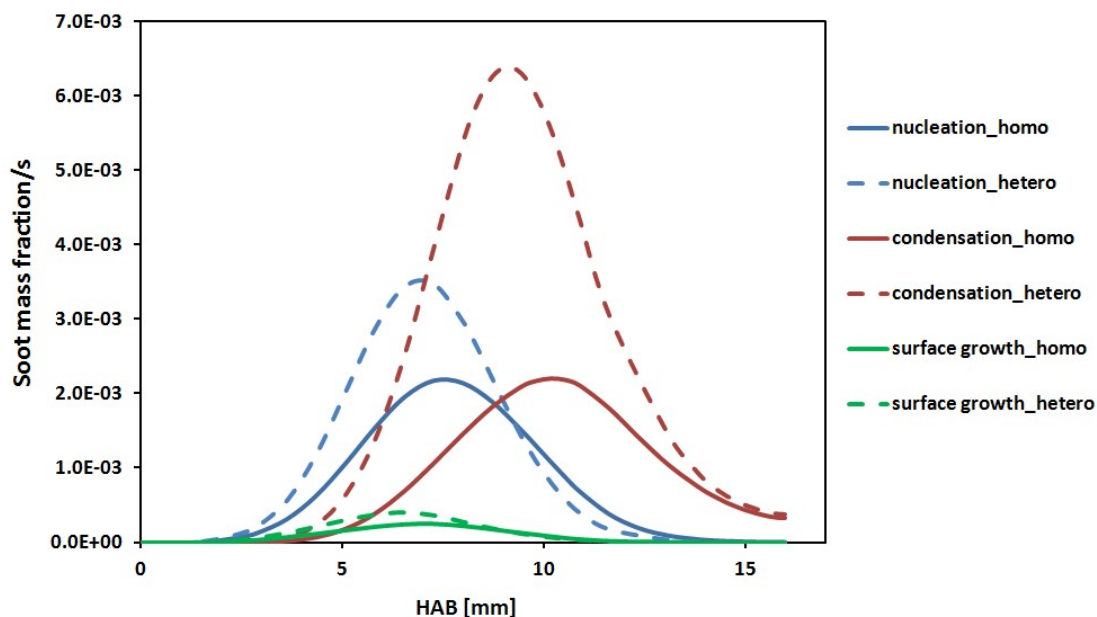


Figure 121 : n-butane flame ( $\phi=1.95$ ;  $\alpha=0.05$ ): Comparison between nucleation, condensation and surface growth rates in both homomolecular and heteromolecular dimerization. Homo\_dim stands for homomolecular dimerization (only pyrene); hetero\_dim stands for heteromolecular dimerization (pyrene/fluoranthene/benzo(a)pyrene).

As observed in Figure 119, the only pyrene dimerization underpredicts measurements within a factor of 2, while a better agreement can be obtained with the heteromolecular dimerization. Therefore, the optimized  $\alpha$  values for this flame in both homo and heteromolecular conditions were determined. Results obtained are presented in Figure 122.

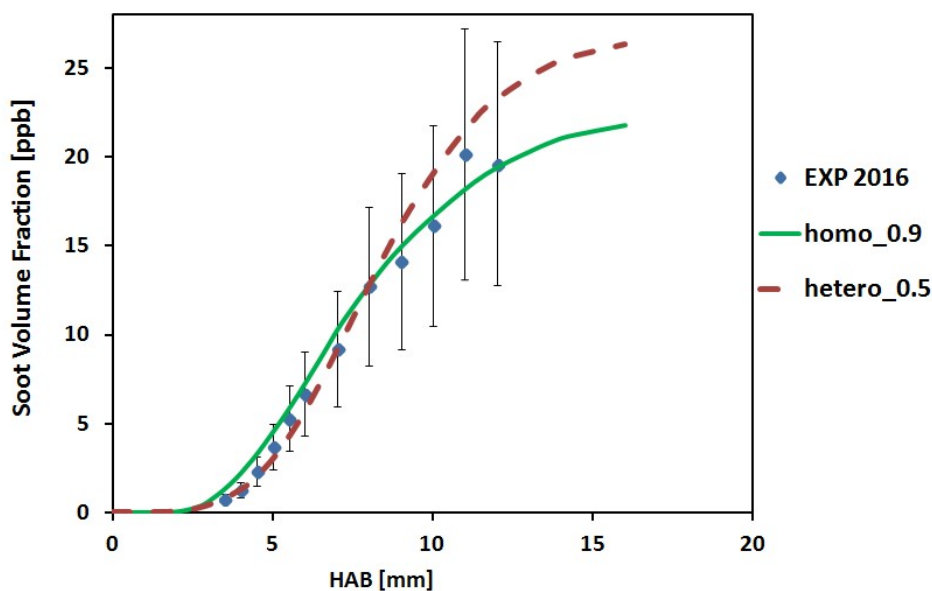


Figure 122 : n-butane flame ( $\phi=1.95$ ): Determination of the optimum value of  $\alpha$  for the homomolecular dimerization. Homo\_0.9 stands for:  $\alpha=0.9$  for homomolecular dimerization (if only pyrene is considered); hetero\_0.5 stands for:  $\alpha=0.5$  for heteromolecular dimerization (if pyrene/fluoranthene/benzo(a)pyrene are considered).

If only pyrene dimerization is considered, the best agreement is obtained for  $\alpha=0.9$  (against 0.05 initially), while in the heteromolecular case, the best agreement is obtained by setting  $\alpha=0.5$  (against 0.05 initially). The effect of the change of  $\alpha$  value on PAH concentration profiles as well as the nucleation, condensation and surface growth rates in both homo and heteromolecular dimerizations is presented from Figure 123 to Figure 126 . With the increase of  $\alpha$  in both cases, PAHs are more consumed than in  $\alpha=0.05$ , since the reactivity is increased. In the heteromolecular dimerization case, pyrene concentration is the most impacted with respect to the two other PAHs: benzo(a)pyrene and fluoranthene. As discussed in the previous sections, the PAH concentrations tend towards zero at higher HAB, indicating the limitations of the present soot model.

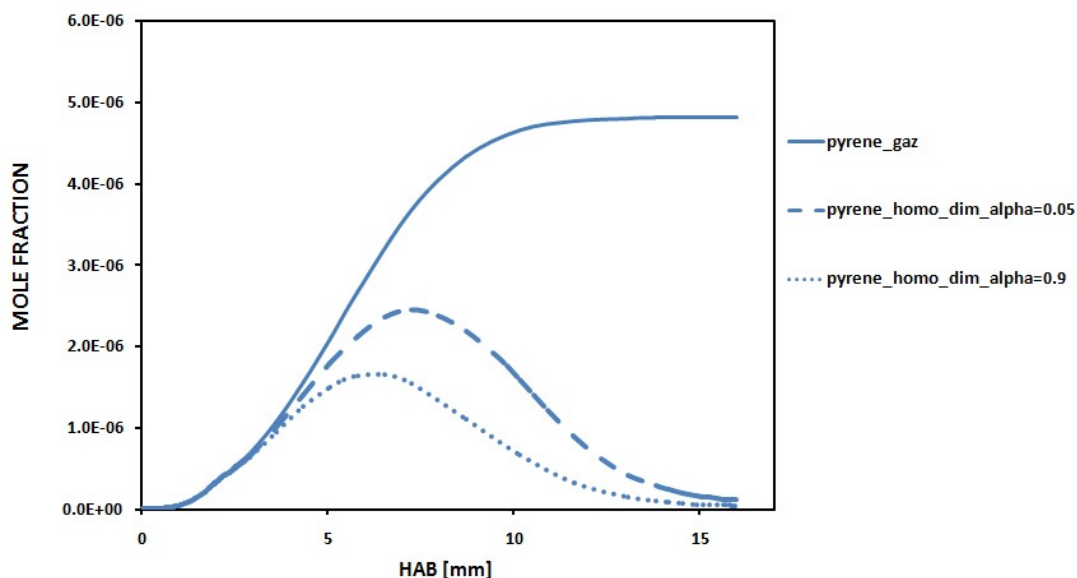


Figure 123 : n-butane flame ( $\phi=1.95$ ): pyrene concentration profiles in the gas-phase and after its homomolecular dimerization with the optimized and the initial  $\alpha$  value.

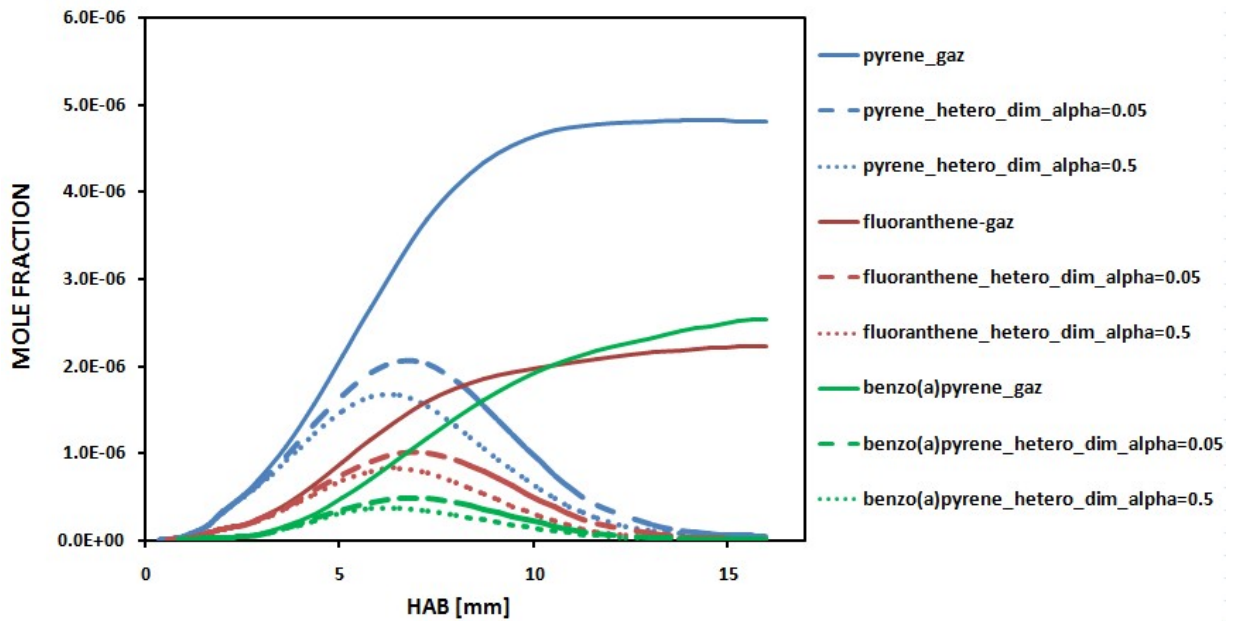


Figure 124 : n-butane flame ( $\phi=1.95$ ): PAH concentration profiles in the gas-phase and after its heteromolecular dimerization with the optimized and the initial  $\alpha$  value.

This fast consumption of PAHs is confirmed as shown in Figure 125 and Figure 126, where the condensation and surface growth rates are significantly increased with respect to the case of  $\alpha=0.05$ . The impact on the surface growth is more significant due to the higher value of  $\alpha$  (0.9 against 0.05 and 0.5 against 0.05 for homo and heteromolecular dimerization respectively).

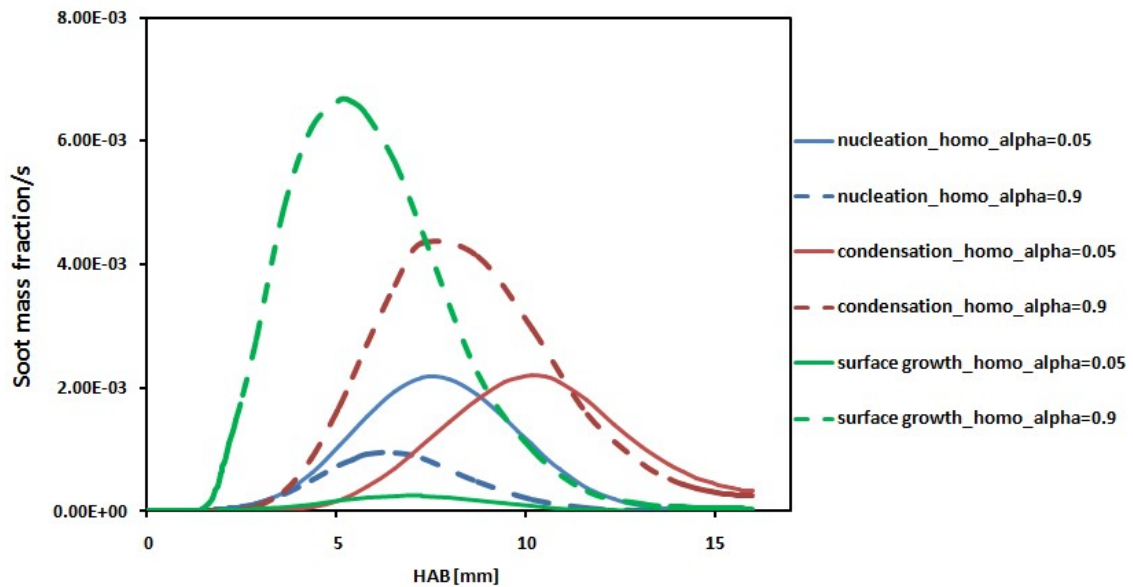


Figure 125 : n-butane flame ( $\phi=1.95$ ): Comparison between nucleation, condensation and surface growth rates in homomolecular dimerization with the optimized and the initial  $\alpha$  values.

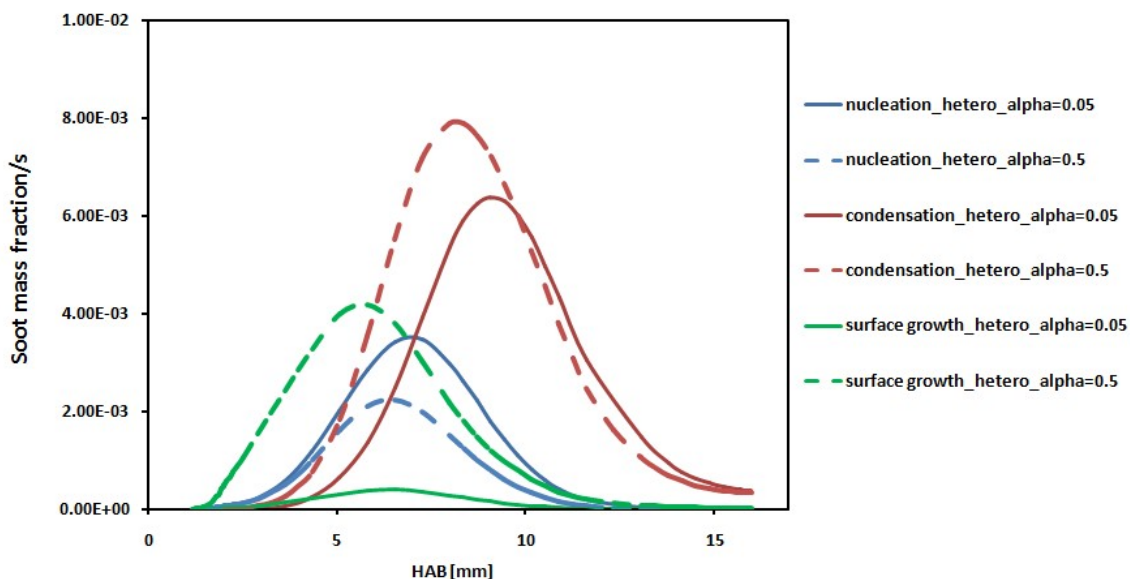


Figure 126 : n-butane flame ( $\phi=1.95$ ): Comparison between nucleation, condensation and surface growth rates in heteromolecular dimerization with the optimized and the initial  $\alpha$  values.

#### 5.4.3.3. n-butane flame ( $\phi=2.32$ )

The richest n-butane ( $\phi=2.32$ ) flame [38] has been investigated in order to examine the behavior of  $\alpha$  within pyrene and heteromolecular dimerizations. It was observed that  $\alpha$  is increased for both homo and heteromolecular cases when the equivalence ratio is increased from 1.75 to 1.95. This flame is of high importance as it allows comparing three hydrocarbon premixed flames: methane, ethylene and n-butane at nearly the same equivalence ratio: 2.32; 2.34 and 2.32 respectively.

Soot volume fraction profile is highly underpredicted with the homomolecular dimerization (only pyrene) and the heteromolecular dimerization (pyrene/fluoranthene/benzo(a)pyrene) with a constant value of  $\alpha$  (0.05). A higher  $\alpha$  value is required to account for soot volume fraction prediction. In Figure 127, the optimized values of  $\alpha$  that allow a better agreement between predictions and measurements is reported for both homo and heteromolecular dimerizations.

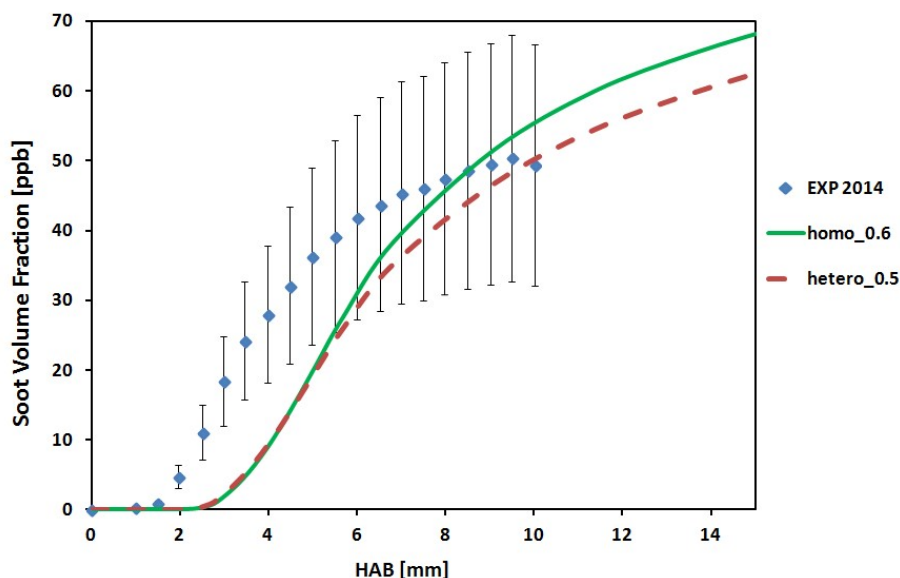


Figure 127 : n-butane flame ( $\phi=2.32$ ): Determination of the optimum value of  $\alpha$  for the homomolecular dimerization. Homo\_0.6 stands for:  $\alpha=0.6$  for homomolecular dimerization (if only pyrene is considered); hetero\_0.5 stands for:  $\alpha=0.5$  for heteromolecular dimerization (if pyrene/fluoranthene/benzo(a)pyrene are considered). The symbols represent experimental data from [38].

The best agreement is obtained for  $\alpha=0.6$  in the homomolecular dimerization, while in the heteromolecular case, the best agreement is obtained by setting  $\alpha=0.5$ . These values are similar to those obtained in the n-butane ( $\phi=1.95$ ) case. The evolutions of PAH concentration profiles in both homo and heteromolecular dimerization cases are presented in Figure 128 and Figure 129. As discussed previously, a significant increase of  $\alpha$  value leads to a high consumption of precursors. In the heteromolecular dimerization case (Figure 129), this consumption is more important for pyrene than fluoranthene and benzo(a)pyrene, confirming pyrene as the major contributor.

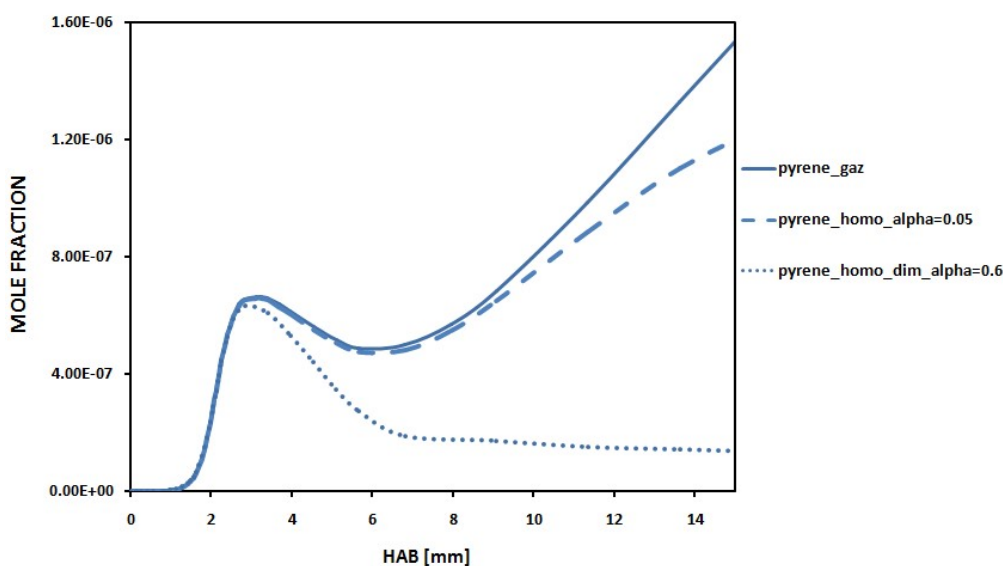


Figure 128 : n-butane flame ( $\phi=2.32$ ): pyrene concentration profile in the gas-phase and after its dimerization with the optimized and initial  $\alpha$  values.

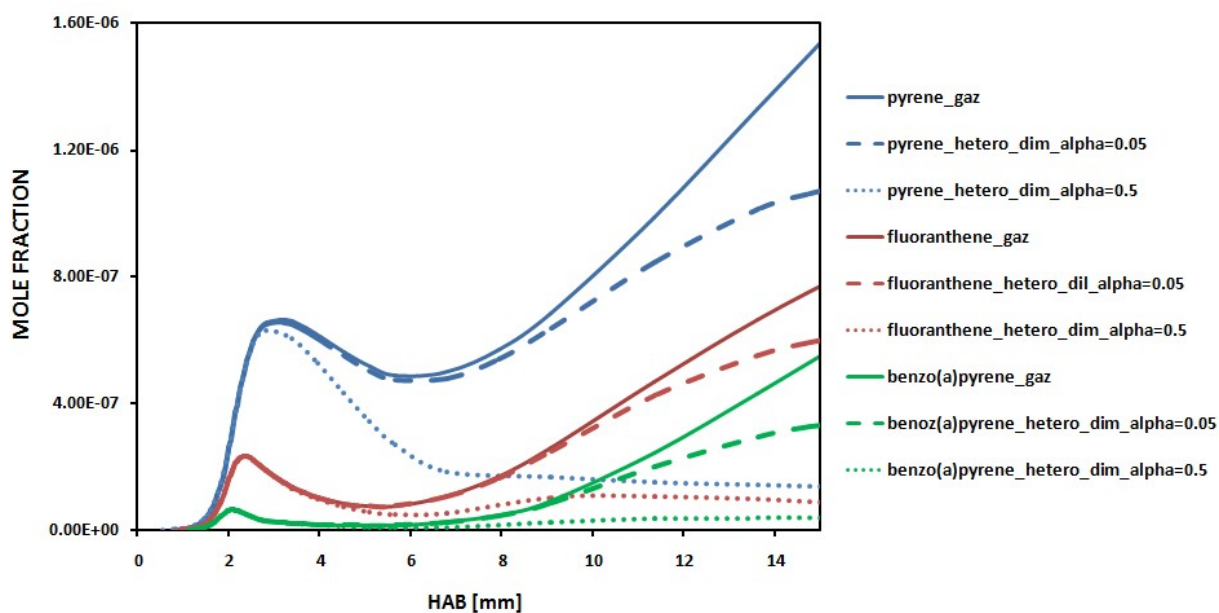


Figure 129 : n-butane flame ( $\phi=2.32$ ): PAHs concentration profiles in the gas-phase and after their dimerization with the optimized and initial  $\alpha$  values.

In Figure 130 and Figure 131, the evolutions of the nucleation, condensation and surface growth rates are presented. As expected, both cases exhibit higher condensation and surface growth rates due to the significant change of  $\alpha$ . For example, in the homomolecular dimerization case, the increase of  $\alpha$  from 0.05 to 0.6 leads to an increase of the maximum surface growth rate within a factor of 500 and a factor of about 300 for the heteromolecular dimerization in this rich n-butane flame.

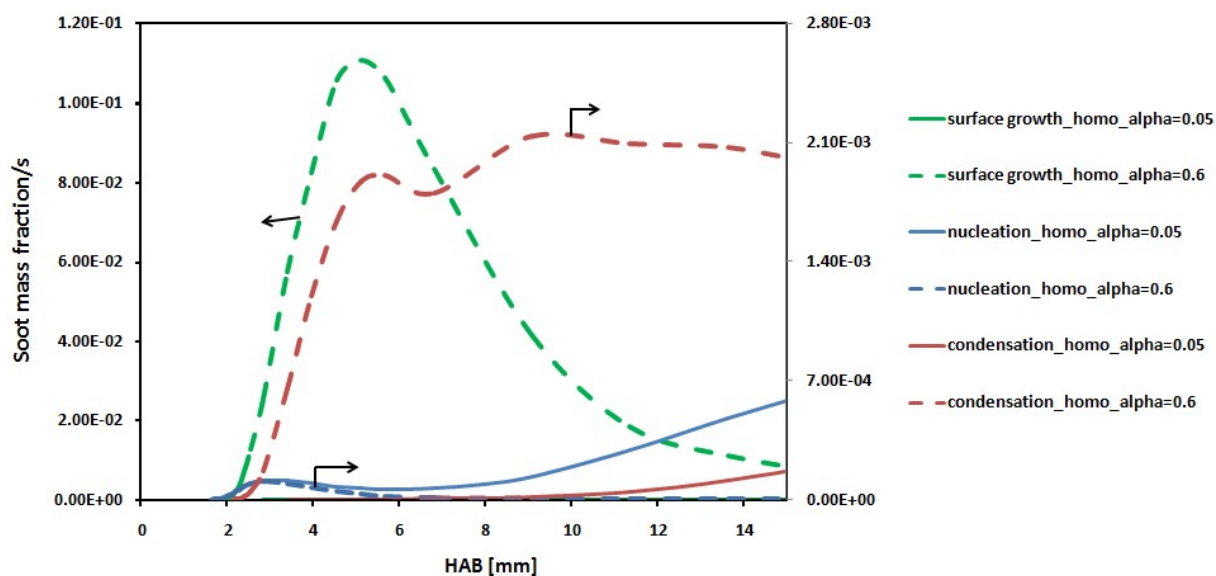


Figure 130 : n-butane flame ( $\phi=2.32$ ): Comparison between nucleation, condensation and surface growth rates in homomolecular dimerization with the optimized and the initial  $\alpha$  values.





Figure 131 : n-butane flame ( $\phi=2.32$ ): Comparison between nucleation, condensation and surface growth rates in heteromolecular dimerization with the optimized and the initial  $\alpha$  values.

### 5.5. Comparison between investigated flames

The contribution of PAHs in term of soot particles inception was examined for three different hydrocarbon flames and at various equivalence ratios. Also, the particles nucleation pathways involving either only pyrene (homomolecular dimerization) or pyrene-fluoranthene-benzo(a)pyrene (heteromolecular dimerization) were investigated. It was found that the predicted soot volume fractions and diameters in light hydrocarbon flames depends highly on soot precursors considered as well as the value given to  $\alpha$ .

Considering  $\alpha=0.05$  and the homomolecular dimerization of each PAH, it is observed that the best agreement between measured and predicted soot volume fractions is obtained with cyclopenta(cd)pyrene in all the investigated hydrocarbon flames. It is also observed that the dimerization of corannulene and pyrene for ethylene flame, pyrene for the n-butane nucleation flame ( $\phi=1.75$ ) and benzo(ghi)fluorathene for the rich n-butane flame ( $\phi=1.95$ ) shows an acceptable sooting tendency. One can note that in the low pressure methane and the atmospheric n-butane nucleation flames, the soot precursors are not drastically consumed as observed in the atmospheric rich ethylene and n-butane flames where the precursors are totally consumed from their dimerization. Table 16 summarizes the optimized values of  $\alpha$  determined as a function of fuels, equivalence ratio ( $\phi$ ),

maximum flame temperature ( $T_{\max}$ ), pressure and the maximum soot volume fraction measured ( $Fv_{\max}$ ).

Fuel	$\varphi$	Pressure (atm)	$T_{\max}$ (K)	$Fv_{\max}$ (ppb)	$\alpha$ (only pyrene)	$\alpha$ (pyrene/fluoranthene/ benzo(a)pyrene+pyrene)	Ratio $\frac{\alpha_{homo}}{\alpha_{hetero} + \alpha_{homo}}$
Methane	2.32	0.263	1805	1.0	0.36	0.2	1.8
Ethylene	2.34	1	1644	171	1.0	0.05	20
n-butane	1.75	1	1740	0.14	0.36	0.01	36
n-butane	1.95	1	1720	20	0.9	0.5	1.8
n-butane	2.32	1	1880	50	0.6	0.5	1.2

**Table 16 : Optimized values of  $\alpha$  obtained from homomolecular and heteromolecular dimerizations in hydrocarbon premixed flames.**

It can be observed that the value of  $\alpha$  is higher in the case of a single soot precursor than for the heteromolecular dimerization which involves in addition to pyrene, two more PAHs: fluoranthene and benzo(a)pyrene. One can notice that the variation of  $\alpha$  from one flame to another is more important with the heteromolecular than in the homomolecular dimerization. For example, between the methane flame ( $\varphi=2.32$ ) and the other flames, a factor of about 3 with ethylene ( $\varphi=2.34$ ) and n-butane ( $\varphi=1.95$ ) flames is observed and a factor of about 2 with n-butane ( $\varphi=2.32$ ). In the heteromolecular dimerization, the variation between methane and ethylene flames is about a factor of 4 and a factor of 20 between methane and the n-butane nucleation flames. A larger  $\alpha$  ratio (defined as the value of  $\alpha$  in the homomolecular dimerization over the value of  $\alpha$  in the heteromolecular dimerization) is observed for the nucleation flame (n-butane flame at  $\varphi=1.75$ ). In the methane rich flame,  $\alpha$  value that allows matching fairly the measurements is found to be 0.36 and 0.2 for respectively homo and heteromolecular dimerization. In the ethylene rich flame, a ratio of 20 over  $\alpha$  value is obtained between both nucleation processes. In the n-butane flames,  $\alpha$  value is increased from  $\varphi=1.75$  to  $\varphi=1.95$  and then decreased in  $\varphi=2.32$  if only pyrene dimerization is considered. That might indicate that the error evolution induced by a homomolecular dimerization is non-linear with the equivalence ratio. Also, one can notice the same observation if the heteromolecular dimerization is considered, where a constant evolution of  $\alpha$  seems to take place from  $\varphi=1.95$  to  $\varphi=2.32$ . However, experimental

investigations are required to elucidate existing correlations between  $\alpha$  and the nature of fuel in question as well as the impact of the temperature. Moreover, additional experimental concentrations of PAHs are also required for determining the deviation of the present soot model.

## 5.6. Conclusions

In this chapter, the contribution of a dozen of PAHs molecules from pyrene to coronene (mass ranging from 202 to 300 amu) and the nucleation processes both homomolecular and heteromolecular dimerizations of PAHs were investigated concerning particulate matter emissions. Particles nucleation was modeled based on the experimental results of soot volume fractions and soot primary particles diameters for premixed laminar flames of methane, ethylene and n-butane at different equivalence ratios and pressures. The effects of fuels, equivalence ratios and the temperature were quantified on particles nucleation process. Predictive capability of a sectional soot model coupled with a detailed chemical mechanism in calculating soot volume fractions and diameters was also been examined.

In the first instance, the homomolecular dimerization of individual PAH from pyrene to coronene by using a constant  $\alpha$  value of 0.05 was examined. Computations show that for this value of  $\alpha$ , the homomolecular dimerization of cyclopenta(cd)pyrene exhibits a good agreement with experimental soot volume fractions in the investigated hydrocarbon flames. It was clearly observed that pyrene likely plays a key role in the particles nucleation process, but its sole contribution and dimerization cannot allow predicting accurately soot formation for all the investigated flames. Also, the dimerization of species such as corannulene and benzo(ghi)fluoranthene shows a major interest in soot particles nucleation modeling, namely in ethylene ( $\phi=2.34$ ) and n-butane flame ( $\phi=1.95$ ). It is worth noting that the five-membered ring PAHs such cyclopenta(cd)pyrene, corannulene and benzo(ghi)fluoranthene seem to be widely involved in the nucleation process if this constant value of  $\alpha=0.05$  is used in the soot model. However, the predicted PAHs concentrations require further validations against experimental measurements. Also, experimental investigations are needed to elucidate existing correlations between  $\alpha$  and the nature of fuels.

In the second phase, the focus was more on only pyrene dimerization, considered as the unique soot precursor. It is found that if only pyrene should be considered as soot precursor,  $\alpha$  value is varied in

each of the above-mentioned flames in order to compensate the error induced by the heteromolecular dimerization simplification. Thus, the optimal value of  $\alpha$  was determined in each investigated premixed flames, which varies as a function of fuels ranging from 0.36 for methane ( $\phi=2.32$ ) and the n-butane nucleation flame ( $\phi=1.75$ ) to 1.0 for ethylene flame ( $\phi=2.34$ ).

Finally, the concept of heteromolecular dimerization which involves two or more PAHs in predicting soot formation has been examined. In this study, the association of three PAHs: pyrene-fluoranthene-benzo(a)pyrene was investigated. This process was found to show a significant contribution for soot inception with the used  $\alpha$  values. Since several PAHs that have different chemical structure were detected and quantified in hydrocarbon premixed flames, they can collide to generate particulate matter. In fact, the homomolecular dimerization which involves only one PAH having the same chemical structure is considered as a part of the heteromolecular dimerization. Computations show that with the heteromolecular dimerization,  $\alpha$  value is varied as a function of fuels, ranging from 0.01 for the n-butane nucleation flame ( $\phi=1.75$ ) to 0.5 for the n-butane flames ( $\phi=1.95$  and  $\phi=2.32$ ). Although several PAHs are detected and quantified during hydrocarbons combustion, there is no experimental evidence identifying those widely involved in the particles nucleation process. From the present study, we found that the heteromolecular dimerization process is an interesting pathway that can lead to soot formation mechanism elucidation. More experimental data are required to clarify the particles nucleation process, namely the transition between the gas-phase and the solid phase.

## Chapter 6: Conclusions and Future Work

This study aimed to investigate the major chemical species (PAHs) widely involved in the particles nucleation process using advanced computational approach such as sectional soot model. This thesis focused on two nucleation models: homomolecular and heteromolecular dimerizations through the physical agglomeration of Polycyclic Aromatic Hydrocarbons.

The first part of this work was focused on the development of a detailed chemical kinetic mechanism that served as input for the sectional soot model. A new detailed kinetic model containing 1014 species and 4550 most reversible reactions has been developed to describe accurately the combustion of liquid transportation fuels as well as single component fuels (ranging from methane to n-propylbenzene) over an extended range of experimental conditions. The surrogate fuel used to build the present kinetic mechanism is composed of three components: n-decane/iso-octane/n-propylbenzene. This ternary mixture has been chosen to represent liquid transportation fuels, based on their Cetane Number (CN) and Threshold Sooting Index (TSI). Several PAHs experimentally observed (detected and quantified) ranging from pyrene to coronene have been included in the current kinetic model in order to examine their contributions in the soot particles inception mechanism, when the kinetic model is coupled with a soot model. The robustness of the present mechanism has been investigated over a wide range of experimental conditions and it is found to simultaneously reproduce chemical species (including PAHs) mole fractions, ignition delay times and flame speeds for a variety of fuels. Based on this mechanism, the impacts of fuels composition and reaction progress (height above the burner) on the relative importance of the aromatics as well as some key intermediates such as acetylene, ethylene, propene, propyne, allene and but-1,3-diene have been characterized. An alternative pathway leading to aromatic production in liquid transportation fuels combustion has been highlighted. Oxygenated compound such as dibenzofuran is found to significantly contribute to naphthalene production during jet-A1 fuel combustion. In addition, three alternative naphthalene production paths, namely benzyl+propargyl, phenyl+vinylacetylene and dibenzofuran oxidation have

been simultaneously considered in the same detailed kinetic mechanism. The relative importance of each of these reactions has been examined in both practical and laboratory fuels combustion. The composition of fuel is found to significantly impact aromatics formation pathways. For example, predominant reactions involved in naphthalene formation in ethylene and jet-A1 surrogate fuel or n-propylbenzene premixed flames are found to differ completely. While phenyl+vinylacetylene is the predominant one in ethylene flame, benzyl+propargyl and dibenzofuran oxidation are found to be the major pathways in jet-A1 surrogate fuel.

The second part of this work was focused on the soot nucleation modeling. The capability in terms of particles inception of a dozen of PAH molecules that have been experimentally observed was investigated. A sectional soot model coupled with the kinetic mechanism developed in this study was employed to investigate particles inception mechanisms. Two nucleation models: homomolecular and heteromolecular dimerizations of PAHs were considered to quantify the impact of each of the examined PAHs as well as the way the nucleation is induced. A monodirectional nucleation model was considered in the present study.

While PAHs are considered as potential soot precursors within the combustion community and due to the lack of experimental evidence on particles nucleation mechanisms, the nature of gaseous species (PAHs) responsible of the first soot particles formation (smallest particles that turn into mature soot) remains elusive. Computational studies are required for such investigations. However, reliable detailed kinetic mechanism and soot model are needed to better understand soot formation mechanism. In the present work, particles nucleation is modeled based on experimental data over soot volume fractions obtained from different fuels combustion: methane ( $\phi=2.32$ ), ethylene ( $\phi=2.34$ ) and n-butane ( $\phi=1.75$ ;  $\phi=1.95$ ;  $\phi=2.32$ ). Computations show pyrene and pyrene based-products such as cyclopenta(cd)pyrene may play a key role in particles nucleation. However, the only contribution of pyrene dimerization cannot allow predicting accurately soot formation. The dimerization of pyrene is considered in most of soot models as the key of nucleation process. In this work, we carefully examined the pyrene dimerization in all the investigated flames and concluded that the role of pyrene is highly dependent on the value of  $\alpha$  used, which varies as a function of the fuel type. The current study also reveals that

for a given value of  $\alpha$  ( $\alpha=0.05$ ), the five-membered ring PAHs such as cyclopenta(cd)pyrene, corannulene and benzo(ghi)fluoranthene seem to be widely involved in nucleation since satisfactory agreement were obtained in some cases. Thus, it is worth noting that the five-membered ring PAHs may potentially play an important role in such process and devote further investigations. Since the nucleation rate is defined in terms of the collision frequency, collision efficiency and gas-phase concentrations of colliding species, according to our simulations results, the dimerization of the following PAHs: benzo(e)pyrene, perylene, benzo(ghi)perylene and coronene are found negligible due to their very low predicted concentrations ( $\sim 1$  ppb).

Finally, the concept of heteromolecular dimerization process has been explored. This process allows associating several PAHs in order to reproduce experimental measurements. It has been proposed based on the fact that the use of only pyrene dimerization as a key of particles inception is not adequate to predict soot formation in the investigated flames. Computations show that the heteromolecular dimerization can be an important process for soot formation modeling. We found this process more realistic since it allows filling the gap when the contribution of only one PAH is not sufficient to reproduce experimental data. Moreover, since several PAHs can exist during hydrocarbon fuels combustion, there is no evidence that excludes the collision between PAHs having different chemical structure to produce soot particles. On the contrary, this is more true than if only a precursor (PAH) is considered for soot formation modeling.

Results obtained from the present work provide a global overview on the soot nucleation process. They can be incorporated into current soot models for more results and details on soot formation process. Therefore, the post-nucleation steps can be improved to build more robust soot models. The nucleation and condensation steps were considered in this work as monodirectional (non-reversible). Recommendations for future work include:

- (1) Develop more reliable detailed chemical mechanisms that can more accurately predict PAHs concentration profiles for a wide range of fuels and over extended experimental conditions.
- (2) Modeling of the concentration profiles of PAHs considered in this work for all the investigated flames.

- (3) Investigate the predictive capability of soot particle diameter profiles in n-butane flames.
- (4) Investigate experimentally the transition between gas-phase and soot particles inception step.
- (5) Investigate experimentally existing correlations between the fraction of surface sites available for reactions on soot particles ( $\alpha$ ) and the nature of fuels, in order to use potential  $\alpha$  values in predicting soot concentrations.
- (6) Investigate the condensation as reversible process that can help to not completely consume PAHs as observed in this work.
- (7) Explore more experimental conditions that can help to better understand soot formation process.



## References

- [1] J. Warnatz, U. Maas, R.W. Dibble, Physical and Chemical Fundamentals, Modeling and Simulation Experiments, Pollutant Formation, Combustion, 2nd Edition 1996.
- [2] Ludovic Russier, IFP Training: Pollution atmosphérique et réglementations, CLM IFPEN 2015.
- [3] F. Pischinger, H. Schulte, and J. Hansen. Grundlagen und entwicklungslinien des dieselmotorischen brennverfahren. In VDI-Berichte, editor, Die Zukunft des Dieselmotors, pages 61–93, Düsseldorf, 1988.
- [4] M. Ba and J. Colosio, Qualité de l'air, une surveillance accrue des particules mais des concentrations à réduire. IFPEN, les données de l'environnement 58, 2000.
- [5] Dockery DW, Pope III CA, Xu X, Spengler JD, Ware JH, Fay ME An association between air pollution and mortality in six US cities N engl J. Med. 329 (1993) 1753-9.
- [6] J. Kaiser, Showdown over clean air science, Science 277 (1997) 466-469.
- [7] D.A. Kaden, R.A. Hites, W.G. Thilly, Mutagenicity of soot and associated polycyclic aromatic hydrocarbon to salmonella typhimurium, Cancer Res. 39 (1979) 4152-9.
- [8] H. Wang, Formation of nascent soot and other condensed-phase materials in flames, 33 rd symp. (Int.) Combust. (2010).
- [9] H. Bockhorn, A. D'Anna, A.F. Sarofim, H. Wang, Combustion Generated Fine Carbonaceous Particles, Karlsruhe University Press, 2009.
- [10] H. Wang, M. Frenklach, Calculations of Rate Coefficients for the Chemically Activated Reactions of Acetylene with Vinylic and Aromatic Radicals, J. Phys. Chem. 98 (1994) 11465–11489.
- [11] J. Appel, H. Bockhorn, M. Frenklach, Kinetic modeling of soot formation with detailed chemistry and physics: laminar premixed flames of C2 hydrocarbons, Combust. Flame 121 (2000) 122-136.
- [12] C.S. McEnally, L.D. Pfefferle, An Experimental Study in Non-Premixed Flames of Hydrocarbon Growth Processes that Involve Five-Membered Carbon Rings, Combust. Sci. Technol. 131 (1998) 323–344.

- [13] M. Commodo, G. Tessitore, G. de Falco, A. Bruno, P. Minutolo, A. D'Anna, Further details on particle inception and growth in premixed flames, *Proc. Combust. Inst.* 35 (2015) 1795–1802.
- [14] J.S. Lowe, J. Y.W. Lai, P. Elvati, A. Violi, Towards a predictive model for polycyclic aromatic hydrocarbon dimerization propensity, *Proc. Combust. Inst.* 35 (2015) 1827–1832.
- [15] P. Elvati, A. Violi: Thermodynamics of poly-aromatic hydrocarbon clustering and the effects of substituted aliphatic chains, *Proc. Comb. Inst.* 34 (2013) 1837-1843.
- [16] A. Violi, Modeling of soot particle inception in aromatic and aliphatic premixed flames, *Combust. Flame* 139 (2004) 279–287.
- [17] C.A. Schuetz, M. Frenklach, Nucleation of soot: Molecular dynamics simulations of pyrene dimerization, *Proc. Combust. Inst.*, 29 (2002) 2307–2314.
- [18] M. Frenklach, H. Wang, Detailed modeling of soot particle nucleation and growth. *Symp.(Int.) Combust.* 23 (1991) 1559-66.
- [19] M. Frenklach, D.W. Clary, J.W.C. Gardiner, S.E. Stein, Detailed kinetic modeling of soot formation in shock-tube pyrolysis of acetylene, *Symp. (Int.) Combust.* 20 (1985) 887-901.
- [20] J.H. Miller, K.C. Smyth, W.G. Mallard, Calculations of the dimerization of aromatic hydrocarbons: Implications for soot formation. *Symp. (Int.) Combust.* 20 (1985) 1139-47.
- [21] C.A. Schuetz, M. Frenklach. Nucleation of soot: Molecular dynamics simulations of pyrene dimerization. *Proc. Combust. Inst.* 29 (2002) 2307-14.
- [22] H. Sabbah, L. Biennier, S.J. Klippenstein, I.R. Sims, Rowe, Bertrand R. Exploring the Role of PAHs in the Formation of Soot: Pyrene Dimerization, *J. Phys. Chem. Lett.* 1 (2010) 2962–2967.
- [23] S.M. Kathmann, G.K. Schenter, B.C. Garrett, Thermodynamics and kinetics of nanoclusters controlling gas-to particle nucleation, *J. Phys. Chem. C* 113 (2009) 10354-10370.
- [24] P.D. Teini, D.M. Karwat, A. Atreya, Observations of nascent soot: Molecular deposition and particle morphology, *Combust. Flame* 158 (2011) 2045-2055.
- [25] R.A. Dobbins, R.A. Fletcher, H.C. Chang, The evolution of soot precursor particles in a diffusion flame, *Combust. Flame* 115 (1998) 285-298.

- [26] M. Saffaripour, A. Veshkini, M. Kholghy, M.J. Thomson, Experimental investigation and detailed modeling of soot aggregate formation and size distribution in laminar coflow diffusion flames of Jet A-1, a synthetic kerosene, and n-decane, *Combust. Flame* 161 (2014) 848–863.
- [27] S.-H. Chung, *Computational Modeling of Soot Nucleation*, PhD Thesis (2011), University of Michigan, USA.
- [28] A. D’Anna, M. Sirignano, J. Kent, A model of particle nucleation in premixed ethylene flames, *Combust. Flame* 157 (2010) 2106-2115.
- [29] R.L. Vander Wal, A. Yezerets, N.W. Currier, D.H. Kim, C.M. Wang, HRTEM Study of diesel soot collected from diesel particulate filters. *Carbon*. 45 (2007) 70-7.
- [30] R.E. Franklin, Crystallite growth in graphitizing and non-graphitizing carbons, *Proc. R. Soc. Lond. A* 209 (1951) 196.
- [31] S.-H. Chung, A. Violi, Peri-condensed aromatics with aliphatic chains as key intermediates for the nucleation of aromatic hydrocarbons. *Proc. Combust. Inst.* 33 (2011) 693-700.
- [32] J.A. Marr, PAH chemistry in a jet-stirred/plug-flow reactor system: Massachusetts Institute of Technology; 1985.
- [33] A. Raj, M. Sander, V. Janardhanan, M. Kraft, A study on the coagulation of polycyclic aromatic hydrocarbon clusters to determine their collision efficiency, *Combust. Flame* 157(3) (2010) 523-34.
- [34] J.D. Herdman, J.H. Miller, Intermolecular potential calculations for polynuclear aromatic hydrocarbon clusters, *J. phys. chem. A* 112 (2008) 6249–6256.
- [35] H.R. Zhang, E.G. Eddings, A.F. Sarofim, C.K. Westbrook, Fuel dependence of benzene pathways, *Proc. Combust. Inst.* 32 (2009) 377–385.
- [36] M.J. Castaldi, N.M. Marinov, C.F. Melius, J. Huang, S.M. Senkan, W.J. Pit, C.K. Westbrook, Experimental and modeling investigation of aromatic and polycyclic aromatic hydrocarbon formation in a premixed ethylene flame, *Symp. (Int.) Combust.* 26 (1996) 693–702.
- [37] S. Sharma, M.R. Harper, W.H. Green, Modeling of 1,3-hexadiene, 2,4-hexadiene and 1,4-hexadiene-doped methane flames: Flame modeling, benzene and styrene formation, *Combust. Flame* 157 (2010) 1331–1345.

- [38] D. Boufflers, Etude expérimentale et Modélisation de la formation des suies et de leurs précurseurs en flamme de prémélange à différentes richesses (cas du n-C<sub>4</sub>H<sub>10</sub>), PhD Thesis (2014), University of Lille 1, France.
- [39] N.A. Slavinskaya, U. Riedel, S.B. Dworkin, M.J. Thomson, Detailed numerical modeling of PAH formation and growth in non-premixed ethylene and ethane flames, *Combust. Flame* 159 (2012) 979–995.
- [40] H. Wang, M. Yao, Z. Yue, M. Jia, R.D. Reitz, A reduced toluene reference fuel chemical kinetic mechanism for combustion and polycyclic-aromatic hydrocarbon predictions, *Combust. Flame* 162 (2015) 2390–2404.
- [41] M.B. Colket, D.J. Seery, Reaction mechanisms for toluene pyrolysis, *Symp. (Int.) Combust.* 25 (1994) 883–891.
- [42] H. Anderson, C.S. McEnally, L.D. Pfefferle, Experimental study of naphthalene formation pathways in non-premixed methane flames doped with alkylbenzenes, *Proc. Combust. Inst.* 28 (2000) 2577–2583.
- [43] N.M. Marinov, W.J. Pitz, C.K. Westbrook, A.M. Vincitore, M.J. Castaldi, S.M. Senkan, C.F. Melius, Aromatic and Polycyclic Aromatic Hydrocarbon Formation in a Laminar Premixed n-Butane Flame, *Combust. Flame* 114 (1998) 192–213.
- [44] B.V. Unterreiner, M. Sierka, R. Ahlrichs, Reaction pathways for growth of polycyclic aromatic hydrocarbons under combustion conditions, a DFT study, *Phys. Chem. Chem. Phys.*, 6 (2004) 4377–4384.
- [45] B. Shukla, M. Koshi, A novel route for PAH growth in HACA based mechanisms, *Combust. Flame* 159 (2012) 3589–3596.
- [46] A. Kousoku, K. Norinaga and K. Miura, Extended Detailed Chemical Kinetic Model for Benzene Pyrolysis with New Reaction Pathways Including Oligomer Formation, *Ind. Eng. Chem. Res.* 53 (2014) 7956–7964.
- [47] H. Richter, J.B. Howard, Formation of polycyclic aromatic hydrocarbons and their growth to soot—a review of chemical reaction pathways, *Prog. in Energ. Combust. Sci.* 26 (2000) 565–608.

- [48] D.S.N. Parker, R.I. Kaiser, B. Bandyopadhyay, O. Kostko, T.P. Troy, M. Ahmed, Unexpected Chemistry from the Reaction of Naphthyl and Acetylene at Combustion-Like Temperatures, *Angew. Chem.* 127 (2015) 5511–5514.
- [49] V. V. Kislov, N. I. Islamova, A. M. Kolker, S. H. Lin, A. M. Mebel, Hydrogen Abstraction Acetylene Addition and Diels–Alder Mechanisms of PAH Formation: A Detailed Study Using First Principles Calculations, *J. Chem. Theory Comput.* 1 (2005) 908–924.
- [50] C. F. Melius, M. E. Colvin, N. M. Marinov, W. J. Pitz and S. M. Senkan, Reaction mechanisms in aromatic hydrocarbon formation involving the C<sub>5</sub>H<sub>5</sub> cyclopentadienyl moiety, *Proc. Combust. Inst.* 26 (1996) 685.
- [51] J.P. Hessler, Calculation of reactive cross sections and microcanonical rates from kinetic and thermochemical data, *J. Phys. Chem. A* 102 (1998) 4517.
- [52] B. Shukla and M. Koshi, Comparative study on the growth mechanisms of PAHs, *Combust. Flame* 158 (2011) 369–375.
- [53] Y. Li, L. Zhang, Z. Tian, T. Yuan, J. Wang, B. Yang, F. Qi, Experimental study of a fuel-rich premixed toluene flame at low pressure, *Energy Fuels* 23 (2009) 1473–1485.
- [54] M. Frenklach, S. Taki, M. B. Durgaprasad and R. A. Matula, Soot formation in shock-tube pyrolysis of acetylene, allene, and 1, 3-butadiene, *Combust. Flame* 54 (1983) 81.
- [55] C.S. McEnally, L.D. Pfefferle, B. Atakan, K. Kohse-Höinghaus, Studies of aromatic hydrocarbon formation mechanisms in flames: Progress towards closing the fuel gap, *Prog. Energ. Combust. Sci.* 32 (2006) 247–294.
- [56] H. Bockhorn, (ed.), *Soot Formation in Combustion: Mechanisms and Models*, Springer-Verlag, Berlin, 1994.
- [57] S.E. Stein, A. Fahr, High-temperature stabilities of hydrocarbons. *J. Phys. Chem.* 89 (17) (1985) 3714-25.
- [58] M. Frenklach, Reaction mechanism of soot formation in flames, *Phys. Chem. Chem. Phys.* 4 (2002) 2028-2037.
- [59] M. Frenkalch, On surface growth mechanism of soot particles. *Proc. Combust. Inst.* (1996) 2285-2293.

- [60] M.V Smoluchowski, Versuch einer mathematischen Theorie der Koagulationskinetic Kolloider Lösungen, 1916.
- [61] K.H. Homann, Fullerenes and Soot Formation-New Pathways to Large Particles in Flames *Angew. Chem, Int Ed.* 37 (1998) 2435-2451.
- [62] M. Frenklach, H. Wang, Detailed Mechanism and Modeling of Soot Particle Formation. In: Bockhorn H. (eds) *Soot Formation in Combustion. Springer Series in Chem. Phys.* 59 (1994) 162-190. Springer, Berlin, Heidelberg.
- [63] A. D'Anna, Combustion-formed nanoparticles, *Proc. Combust. Inst.* 32 (2009) 593-613.
- [64] P.S. Mehlta, S. Das, A correlation for soot concentration in diesel exhaust based on fuel-air mixing parameters, *Fuel* 71 (1996) 689-692.
- [65] J.B Moss, C.D. Stewart, and K.J. Young, Modeling soot formation and nurnout in a high temperature laminar flame burning under oxygen-enriched conditions, *Combust. Flame* 101 (1995) 491-500.
- [66] R. Said, A. Garo and R. Borgui, Soot formation modeling for turbulent flames *Combust. Flame* 108 (1997) 71-86.
- [67] F. Takahashi and I. Glassman, Sooting correlations for premixed flames. *Combust. Sci.Technol.* 37 (1984) 1-19.
- [68] C. Mc Enally, L. Pfefferle, Improved sooting tendency measurements for aromatic hydrocarbons and their implications for naphthalene formation pathways, *Combust. Flame* 148 (2007) 210-222.
- [69] M. Frenklach and H. Wang, Detailed mechanism and modeling of soot particle formation. In H. Bockhorn, editor, *Soot Formation in Combustion: Mechanisms and Models*, pages 165-192. Springer- Verlag, Heidelberg, Germany, 1994.
- [70] M. Frenklach, Method of moments with interpolative closure, *Chem. Eng. Sci* 57 (12) (2002) 2229-2239.
- [71] M. Frenklach, S.J. Harris, Aerosol dynamics modeling using the method of moments, *J. Colloid and Interface Sci.*, 118 (1987) 252-261 1987.

- [72] C.J. Pope and J.B. Howard. Simultaneous particle and molecule modeling (SPAMM): An approach for combining sectional aerosol equations and elementary gas-phase reactions, *Aerosol Sci. Technol.*, 27(1) (1997) 73–94.
- [73] H. Richter, S. Granata, W.H. Green, J.B. Howard, Detailed modeling of PAH and soot formation in a laminar premixed benzene/oxygen/argon low-pressure flame, *Proc. Combust. Inst.* 30 (2005) 1397-1405.
- [74] A. D’Anna and J.H. Kent. Modeling of particulate carbon and species formation in coflowing diffusion flames of ethylene. *Combust. Flame* 144 (2006) 249–260.
- [75] D. Aubagnac-Karkar, J.-B. Michel, O. Colin, P.E. Vervisch-Kljakic, Darabiha, Nasser, Sectional soot model coupled to tabulated chemistry for Diesel RANS simulations, *Combust.Flame* 162 (2015) 3081–3099.
- [76] Reaction Design, Reaction Workbench 15131, Reaction Design: San Diego, USA, 2013.
- [77] D.G. Goodwin, H.K. Moffat, R.L. Speth, Cantera: An object-oriented software toolkit for chemical kinetics, thermodynamics, and transport processes, Version 2.2. 1 (2016).
- [78] K. Netzell, H. Lehtiniemi, F. Mauss, Calculating the soot particle size distribution function in turbulent diffusion flames using a sectional method, *Proc. Combust. Inst.* 31 (2007) 667–674.
- [79] D. Aubagnac-Karkar, A. El Bakali, P. Desgroux, Numerical Investigation on Pyrene Based Nucleation in Laminar Flames, Proceedings of the 8th European Combustion Meeting, 18-21 April 2017, Dubrovnik, Croatia.
- [80] D. Aubagnac-Karkar, A. El Bakali and P. Desgroux, Soot particles inception and PAH condensation modelling applied in a soot model utilizing a sectional method, *Combust. Flame*, article in press.
- [81] A. Kazakov, M. Frenklach, Dynamic Modeling of Soot Particle Coagulation and Aggregation: Implementation With the Method of Moments and Application to High-Pressure Laminar Premixed Flames, *Combust. Flame* 114 (1998) 484–501.
- [82] F. Xu, P.B. Sunderland, G.M. Faeth, Soot formation in laminar premixed ethylene/air flames at atmospheric pressure, *Combust. Flame* 108 (1997) 471–493.

- [83] F. Xu, K.C. Lin, and G.M. Faeth, Soot formation in laminar premixed methane/oxygen flames at atmospheric pressure, *Combust. Flame* 115 (1998) 195-209.
- [84] V. Chernov, M.J. Thomson, S.B. Dworkin, N.A. Slavinskaya, R. Uwe, Soot formation with C1 and C2 fuels using an improved chemical mechanism for PAH growth, *Combust. Flame* 161 (2014) 592–601.
- [85] T. Mouton, X. Mercier, M. Wartel, N. Lamoureux, P. Desgroux, Laser-induced incandescence technique to identify soot nucleation and very small particles in low-pressure methane flames, *Appl. Phys. B* 112 (2013) 369–379.
- [86] M. Braun-Unkhoff, A. Chrysostomou, P. Frank, E. Gutheil, R. Lu'ckerath, W. Stricker, Experimental and numerical study on soot formation in laminar high pressure flames, *Proc. Combust. Inst.* 27(1) (1998) 1565.
- [87] A. Kazakov, H. Wang, M. Frenklach, Detailed Modeling of Soot Formation in Laminar Premixed Ethylene Flames at a Pressure of 10 Bar, *Combust. Flame* 100 (1995) 111-120.
- [88] S.B. Dworkin, Q. Zhang, M.J. Thomson, N.A. Slavinskaya, U. Riedel, Application of an enhanced PAH growth model to soot formation in a laminar coflow ethylene/air diffusion flame, *Combust. Flame* 158 (2011) 1682–1695.
- [89] N.A. Eaves, A. Veshkini, C. Riese, Q. Zhang, S.B. Dworkin, Murray John Thomson, A numerical study of high pressure, laminar, sooting, ethane–air coflow diffusion flames, *Combust. Flame* 159 (2012) 3179–3190.
- [90] C.H. Kim, F. Xu, G.M. Faeth, Soot surface growth and oxidation at pressures up to 8.0 atm in laminar nonpremixed and partially premixed flames, *Combust. Flame* 152 (3) (2008) 301–316.
- [91] W. Schulz, 12 components jet surrogate formulation, Jet surrogate fuels formulation, *ACS Petrol. Chem. Div. Preprints* 37 (1991) 383–392.
- [92] S. Dooley, S.H. Won, M. Chaos, J. Heyne, Y. Ju, F.L. Dryer, K. Kumar, C.-J. Sung, H. Wang, M.A. Oehlschlaeger, R.J. Santoro, T.A. Litzinger, A jet fuel surrogate formulated by real fuel properties, *Combust. Flame* 157 (2010) 2333–2339.
- [93] P. Dagaut, A. El Bakali, A. Ristori, The combustion of kerosene: Experimental results and kinetic modelling using 1- to 3-component surrogate model fuels, *Fuel* 85 (2006) 944–956.



- [94] M. Mehl, W.J. Pitz, C.K. Westbrook, H.J. Curran, Kinetic modeling of gasoline surrogate components and mixtures under engine conditions, *Proc. Combust. Inst.* 33 (2011) 193–200.
- [95] G. Kukkadapu, K. Kumar, C.-J. Sung, M. Mehl, W.J. Pitz, Autoignition of gasoline surrogates at low temperature combustion conditions, *Combust. Flame* 162 (2015) 2272–2285.
- [96] H. Ramirez Lancheros, Etude expérimentale et modélisation cinétique de l'oxydation, l'auto-inflammation et la combustion de carburants Diesel et bio-Diesel, PhD Thesis (2012), University of Orleans, France.
- [97] Y. Yang, A.L. Boehman, R.J. Santoro, A study of jet fuel sooting tendency using the threshold sooting index (TSI) model, *Combust. Flame* 149 (2007) 191-205.
- [98] R. Lemaire, E. Therssen, P. Desgroux, Effect of ethanol addition in gasoline and gasoline–surrogate on soot formation in turbulent spray flames, *Fuel* 89 (2010) 3952–3959.
- [99] S. Dooley, S.H. Won, J. Heyne, T.I. Farouk, Y. Ju, F.L. Dryer, K. Kumar, X. Hui, C.-J. Sung, H. Wang, M.A. Oehlschlaeger, V. Iyer, S. Iyer, T.A. Litzinger, R.J. Santoro, T. Malewicki, K. Brezinsky, The experimental evaluation of a methodology for surrogate fuel formulation to emulate gas phase combustion kinetic phenomena, *Combust. Flame* 159 (2012) 1444–1466.
- [100] C. Betrancort, P. Desgroux, E. Therssen, Determination of the threshold sooting index in flames of liquid hydrocarbons by laser induced incandescence, Laboratoire PC2A, Lille, 2014, France.
- [101] J.C. Guibet, fuels and engines, Pub. IFP éditions Technip, Rueil-Malmaison, France, 1999.
- [102] P. Dagaut, A. El Bakali, A. Ristori, The combustion of kerosene: Experimental results and kinetic modelling using 1- to 3-component surrogate model fuels, *Fuel* 85 (2006) 944–956.
- [103] N. Grumman, Diesel Fuel Oils 2003, Report NGMS-232 PPS, 2004., N. Grumman, Diesel Fuel Oils 2003,
- [104] W.J. Pitz, N.P. Cernansky, F.L. Dryer, F.N. Egolfopoulos, J.T. Farrell, D.G. Friend, H. Pitsch, Development of an Experimental Database and Chemical Kinetic Models for Surrogate Gasoline Fuels, SAE Paper 2007-01-0175, 2007, USA.
- [105] A. Violi, S. Yan, E.G. Eddings, A.F. Sarofim, S. Granata, T. Faravelli, E. Ranzi, Experimental formulation and kinetic model for JP-8 surrogate mixtures, *Combust. Sci. Technol.* 174 (2002) 399-417.

- [106] J.T. Farrell, N.P. Cernansky, F.L. Dryer, C.K. Law, D.G. Friend, C.A. Hergart, R.M. McDavid, A.K. Patel, C.J. Mueller, H. Pitsch, Development of an experimental database and kinetic models for surrogate diesel fuels, SAE Technical Paper 2007-01-0201, 2007, USA.
- [107] C.J. Mueller, W.J. Cannella, J.T. Bays, T.J. Bruno, K. DeFabio, D.H. Dettman, R.M. Gieleciak, L.M. Huber, C.B. Kweon, S.S. McConnell, W.J. Pitz, M.A. Ratcliff, Diesel Surrogate Fuels for Engine Testing and Chemical-Kinetic Modeling: Compositions and Properties, *Energy Fuels* 30 (2016) 1445-1461.
- [108] J. Yu, Z. Wang, X. Zhuo, W. Wang, X. Gou, Surrogate Definition and Chemical Kinetic Modeling for Two Different Jet Aviation Fuels, *Energy Fuels* 30 (2016) 1375-1382.
- [109] C. Pera, V. Knop, Methodology to define gasoline surrogates dedicated to auto-ignition in engines, *Fuel* 96 (2012) 59–69.
- [110] Y.-z. An, Y.-q. Pei, J. Qin, H. Zhao, S.-p. Teng, B. Li, X. Li, Development of a PAH (polycyclic aromatic hydrocarbon) formation model for gasoline surrogates and its application for GDI (gasoline direct injection) engine CFD (computational fluid dynamics) simulation, *Energy* 94 (2016) 367–379.
- [111] L. Cai, H. Pitsch, Optimized chemical mechanism for combustion of gasoline surrogate fuels, *Combust. Flame* 162 (2015) 1623–1637.
- [112] E. Gianotti, M. Taillades-Jacquín, Á. Reyes-Carmona, G. Taillades, J. Rozière, D.J. Jones, Hydrogen generation via catalytic partial dehydrogenation of gasoline and diesel fuels, *Appl. Catalysis B: Env.* 185 (2016) 233–241.
- [113] M. Mehl, W.J. Pitz, C.K. Westbrook, H.J. Curran, Kinetic modeling of gasoline surrogate components and mixtures under engine conditions, *Proc. Combust. Inst.* 33 (2011) 193–200.
- [114] D. Darcy, M. Mehl, J.M. Simmie, J. Würmel, W.K. Metcalfe, C.K. Westbrook, W.J. Pitz, H.J. Curran, An experimental and modeling study of the shock tube ignition of a mixture of n-heptane and n-propylbenzene as a surrogate for a large alkyl benzene, *Proc. Combust. Inst.* 34 (2013) 411–418.

- [115] N.E. Sánchez, A. Callejas, Á. Millera, R. Bilbao, M.U. Alzueta, Influence of the Oxygen Presence on Polycyclic Aromatic Hydrocarbon (PAH) Formation from Acetylene Pyrolysis under Sooting Conditions, *Energy Fuels* 27 (2013) 7081–7088.
- [116] W.K. Metcalfe, S.M. Burke, S.S. Ahmed, H.J. Curran, A Hierarchical and Comparative Kinetic Modeling Study of C<sub>1</sub> – C<sub>2</sub> Hydrocarbon and Oxygenated Fuels, *Int. J. Chem. Kinet.* 45 (2013) 638–675.
- [117] N. Hansen, J.A. Miller, P.R. Westmoreland, T. Kasper, K. Kohse-Höinghaus, J. Wang, T.A. Cool, Isomer-specific combustion chemistry in allene and propyne flames, *Combust. Flame* 156 (2009) 2153–2164.
- [118] Z. Wang, Y. Li, F. Zhang, L. Zhang, W. Yuan, Y. Wang, F. Qi, An experimental and kinetic modeling investigation on a rich premixed n-propylbenzene flame at low pressure, *Proc. Combust. Inst.* 34 (2013) 1785–1793.
- [119] M. Zeng, W. Yuan, Y. Wang, W. Zhou, L. Zhang, F. Qi, Y. Li, Experimental and kinetic modeling study of pyrolysis and oxidation of n-decane, *Combust. Flame* 161 (2014) 1701–1715.
- [120] M.B. Colket, The pyrolysis of acetylene and vinylacetylene in a single-pulse shock tube, *Symp. (Int.) Combust.* 21 (1988) 851–864.
- [121] E. Ranzi, C. Cavallotti, A. Cuoci, A. Frassoldati, M. Pelucchi, T. Faravelli, New reaction classes in the kinetic modeling of low temperature oxidation of n-alkanes, *Combust. Flame* 162 (2015) 1679–1691.
- [122] W. Yuan, Investigation on the pyrolysis and oxidation of toluene over a wide range conditions. I. Flow reactor pyrolysis and jet stirred reactor oxidation, *Combust. Flame* 162 (2015) 3–21.
- [123] N.A. Slavinskaya, P. Frank, A modelling study of aromatic soot precursors formation in laminar methane and ethene flames, *Combust. Flame* 156 (2009) 1705–1722.
- [124] A. Matsugi, A. Miyoshi, Modeling of two- and three-ring aromatics formation in the pyrolysis of toluene, *Proc. Combust. Inst.* 34 (2013) 269–277.
- [125] K. Norinaga, O. Deutschmann, Detailed kinetic modeling of gas-phase reactions in the chemical vapor deposition of carbon from light hydrocarbons, *Ind. Eng. Chem. Res.* 46 (2007) 3547–3557.

- [126] A. Kousoku, K. Norinaga and K. Miura, Extended Detailed Chemical Kinetic Model for Benzene Pyrolysis with New Reaction Pathways Including Oligomer Formation, *Ind. Eng. Chem. Res.* 53 (2014) 7956-7964.
- [127] M.R. Djokic, An experimental and kinetic modeling study of cyclopentadiene pyrolysis: First growth of polycyclic aromatic hydrocarbons, *Combust. Flame* 161 (2014) 2739–2751.
- [128] E. Ranzi, A. Frassoldati, A. Stagni, M. Pelucchi, A. Cuoci, T. Faravelli, Reduced Kinetic Schemes of Complex Reaction Systems: Fossil and Biomass-Derived Transportation Fuels, *Int. J. Chem. Kinet.*, 46 (2014) 512-542.
- [129] N. Sebbar, H. Bockhorn, J.W. Bozzelli, Thermochemical Similarities Among Three Reaction Systems: Vinyl + O<sub>2</sub> – Phenyl + O<sub>2</sub> – Dibenzofuranyl + O<sub>2</sub>, *Combust. Sci. Technol.* 180 (2008) 959-974.
- [130] B. Yang, Y. Li, L. Wei, C. Huang, J. Wang, Z. Tian, R. Yang, L. Sheng, Y. Zhang, F. Qi, An experimental study of the premixed benzene/oxygen/argon flame with tunable synchrotron photoionization, *Proc. Combust. Inst.*, 31 (2007) 555–563.
- [131] R. Asatryan, A. Davtyan, L. Khachatryan, B. Dellinger, Molecular modeling studies of the reactions of phenoxy radical dimers: pathways to dibenzofurans, *J. Phys. Chem. A* 109 (2005) 11198–11205.
- [132] H.H. Grotheer, R. Louw, The reaction of phenoxy radicals with mono-chlorobenzene and its meaning for gas-phase dioxin formation in incineration, *Proc. Combust. Inst.*, 26 (1996) 2405-2411.
- [133] A. Tritz, I. Ziegler-Devin, C. Perrin, P.-M. Marquaire, Experimental study of the oxidation and pyrolysis of dibenzofuran at very low concentration, *J. Env. Chem. Eng.* 2 (2014) 143–153.
- [134] V.D. Knyazev, I.R. Slagle, Experimental and Theoretical Study of the  $C_2H_3 \rightleftharpoons H + C_2H_2$  Reaction. Tunneling and the Shape of Falloff Curves, *J. Phys. Chem.* 100 (1996) 16899-16911.
- [135] A.M. Mebel, M.C. Lin, T. Yu, K. Morokuma, Theoretical study of potential energy surface and thermal rate constants for the  $C_6H_5 + H_2$  and  $C_6H_6 + H$  reactions, *J. Phys. Chem. A* 101 (1997) 3189-3196.

- [136] S.J. Klippenstein, L.B. Harding, Y. Georgievskii, On the formation and decomposition of C<sub>7</sub>H<sub>8</sub>, *Proc. Combust. Inst.* 31 (2007) 221-229.
- [137] R. Bounaceur, I. Da Costa, R. Fournet, F. Billaud, F. Battin-Leclerc, Experimental and modeling study of the oxidation of toluene, *Int. J. Chem. Kinet.* 37 (2005) 25-49.
- [138] G. da Silva, J.W. Bozzelli, Kinetic modeling of the benzyl+HO<sub>2</sub> reaction, Kinetic modeling of the benzyl+HO<sub>2</sub> reaction, *Proc. Combust. Inst.* 32 (2009) 287-294.
- [139] D.L. Baulch, C.T. Bowman, C.J. Cobos, R.A. Cox, T. Just, J.A. Kerr, M.J. Pilling, D. Stocker, Evaluated Kinetic Data for Combustion Modeling: Supplement II, *J. Phys. Chem. Ref. Data* 34 (2005) 757.
- [140] J.A. Miller, J.P. Senosiain, S.J. Klippenstein, Y. Georgievskii, Reactions over Multiple, Interconnected Potential Wells: Unimolecular and Bimolecular Reactions on a C<sub>3</sub>H<sub>5</sub> Potential, *J. Phys. Chem. A* 112 (2008) 9429-9438.
- [141] Y. Georgievskii, S.J. Klippenstein, J.A. Miller, Association rate constants for reactions between resonance-stabilized radicals: C<sub>3</sub>H<sub>3</sub> + C<sub>3</sub>H<sub>3</sub>, C<sub>3</sub>H<sub>3</sub> + C<sub>3</sub>H<sub>5</sub>, and C<sub>3</sub>H<sub>5</sub> + C<sub>3</sub>H<sub>5</sub>, *Phys. Chem. Chem. Phys.* 9 (2007) 4259-4268.
- [142] J.A. Miller, S.J. Klippenstein, The recombination of propargyl radicals and other reactions on a C<sub>6</sub>H<sub>6</sub> potential, *J. Phys. Chem. A* 107 (2003) 7783-7799.
- [143] A. Laskin, Thermal decomposition of indene. Experimental results and kinetic modeling, *Proc. Combust. Inst.* 27 (1998) 313-320.
- [144] K. Brezinski, T. A. Litzinger, I. Glassman, The high temperature oxidation of the methyl side chain of toluene, *Int. J. Chem. Kinet.* 16 (1984) 1053-1074.
- [145] G. Blanquart, P. Pepiot-Desjardins, H. Pitsch, Chemical mechanism for high temperature combustion of engine relevant fuels with emphasis on soot precursors, *Combust. Flame* 156 (2009) 588-607.
- [146] N.W. Moriarty, M. Frenklach, AB initio study of naphthalene formation by addition of vinylacetylene to phenyl, *Proc. Combust. Inst.* 28 (2000) 2563-2568.
- [147] A. Matsugi, A. Miyoshi, Computational study on the recombination reaction between benzyl and propargyl radicals, *Int. J. Chem. Kinet.* 44 (2012) 206-218.

- [148] A. El Bakali, X. Mercier, M. Wartel, F. Acevedo, I. Burns, L. Gasnot, J.-F. Pauwels, P. Desgroux, Modeling of PAHs in low pressure sooting premixed methane flame, *Energy* 43 (2012) 73–84.
- [149] C. Betrancourt, Experimental study of soot formation in laminar premixed flames of fuels of interest for automobile and aeronautics: a focus on the soot nucleation process. PhD Thesis (2017), University of Lille 1, France.
- [150] J. Yang, L. Zhao, W. Yuan, F. Qi, Y. Li, Experimental and kinetic modeling investigation on laminar premixed benzene flames with various equivalence ratios, *Proc. Combust. Inst.* 35 (2015) 855-862.
- [151] A. El Bakali., J.L Delfau, C. Vovelle, Experimental Study of 1 Atmosphere, Rich, Premixed n - heptane and iso-octane Flames, *Combust. Sci. Technol.* 140 (1998) 69–91.
- [152] C. Douté, J.L Delfau, R. Akrich, C. Vovelle, Chemical Structure of Atmospheric Pressure Premixed n -Decane and Kerosene Flames, *Combust. Sci. Technol.* 106 (1995) 327–344.
- [153] W. Yuan, Y. Li, P. Dagaut, J. Yang, F. Qi, Experimental and kinetic modeling study of styrene combustion, *Combust. Flame* 162 (2015) 1868–1883.
- [154] Y. Li, J. Cai, L. Zhang, J. Yang, Z. Wang, F. Qi, Experimental and modeling investigation on premixed ethylbenzene flames at low pressure, *Proc. Combust. Inst.* 33 (2011) 617-624.
- [155] Y. Li, C. Huang, L. Wei, B. Yang, J. Wang, Z. Tian, T. Zhang, L. Sheng, F. Qi, An Experimental Study of Rich Premixed Gasoline/O<sub>2</sub>/Ar Flame with Tunable Synchrotron Vacuum Ultraviolet Photoionization, *Energy Fuels* 21 (2007) 1931–1941.
- [156] G. Kukkadapu, K. Kumar, C.-J. Sung, M. Mehl, W.J. Pitz, Autoignition of gasoline and its surrogates in a rapid compression machine, *Proc. Combust. Inst.* 34 (2013) 345–352.
- [157] P. Dirrenberger, P.A. Glaude, R. Bounaceur, H. Le Gall, da Cruz, A. Pires, A.A. Konnov, F. Battin-Leclerc, Laminar burning velocity of gasolines with addition of ethanol, *Fuel* 115 (2014) 162–169.
- [158] P. Dagaut, On the kinetics of hydrocarbons oxidation from natural gas to kerosene and diesel fuel, *Phys. Chem. Chem. Phys.* 4 (2002) 2079–2094.

- [159] S.S. Vasu, D.F. Davidson, R.K. Hanson, Jet fuel ignition delay times: Shock tube experiments over wide conditions and surrogate model predictions, *Combust. Flame* 152 (2008) 125–143.
- [160] X. Hui, C.-J. Sung, Laminar flame speeds of transportation-relevant hydrocarbons and jet fuels at elevated temperatures and pressures, *Fuel* 109 (2013) 191–200.
- [161] D.R. Haylett, P.P. Lappas, D.F. Davidson, R.K. Hanson, Application of an aerosol shock tube to the measurement of diesel ignition delay times, *Proc. Combust. Inst.* 32 (2009) 477–484.
- [162] C.T. Chong, S. Hochgreb, Measurements of laminar flame speeds of liquid fuels: Jet-A1, diesel, palm methyl esters and blends using particle imaging velocimetry (PIV), *Proc. Combust. Inst.* 33 (2011) 979–986.
- [163] H. Wang, S.J. Warner, M.A. Oehlschlaeger, R. Bounaceur, J. Biet, P.-A. Glaude, F. Battin-Leclerc, An experimental and kinetic modeling study of the autoignition of  $\alpha$ -methyl-naphthalene/air and  $\alpha$ -methyl-naphthalene/n-decane/air mixtures at elevated pressures, *Combust. Flame* 157 (2010) 1976–1988.
- [164] A. Raj, I.D.C. Prada, A.A. Amer, S.H. Chung, A reaction mechanism for gasoline surrogate fuels for large polycyclic aromatic hydrocarbons, *Combust. Flame* 159 (2012) 500–515.
- [165] Y. Pei, M. Mehl, W. Liu, T. Lu, W.J. Pitz, S. Som, A Multicomponent Blend as a Diesel Fuel Surrogate for Compression Ignition Engine Applications, *J. Eng. Gas Turbines Power* 137 (2015) 111502.
- [166] J. Yang, L. Zhao, W. Yuan, F. Qi, Y. Li, Experimental and kinetic modeling investigation on laminar premixed benzene flames with various equivalence ratios, *Proc. Combust. Inst.* 35 (2015) 855–862.
- [167] Y. Li, J. Cai, L. Zhang, J. Yang, Z. Wang, F. Qi, Experimental and modeling investigation on premixed ethylbenzene flames at low pressure, *Proc. Combust. Inst.* 33 (2011) 617–624.
- [168] T. Mouton, X. Mercier, P. Desgroux, Isomer discrimination of PAHs formed in sooting flames by jet-cooled laser-induced fluorescence: application to the measurement of pyrene and fluoranthene, *Appl. Phys.B* (2016) 122: 123.
- [169] V.D. Knjazev, and I.R. Slagle, Kinetics of the reaction between propargyl radical and acetylene, *J. Phys. Chem. A* 106 (2002) 5613–5617.

- [170] S. Granata, T. Faravelli, E. Ranzi, N. Olten, S. Senkan, Kinetic modeling of counterflow diffusion flames of butadiene, *Combust. Flame* 131 (2002) 273–284.
- [171] J. Appel, H. Bockhorn, M. Frenklach, Kinetic modeling of soot formation with detailed chemistry and physics: laminar premixed flames of C2 hydrocarbons, *Combust. Flame* 121 (2000) 122–136.
- [172] R.P. Lindstedt, Modeling of the chemical complexities of flames, *Proc. Combust. Inst.* 27 (1998) 269–285.
- [173] P. Lindstedt, L. Maurice, M. Meyer, Thermodynamic and kinetic issues in the formation and oxidation of aromatic species, *Faraday Disc.* 119 (2001) 409–432.
- [174] C.S. McEnally, L.D. Pfefferle, The use of carbon-13-labeled fuel dopants for identifying naphthalene formation pathways in non-premixed flames, *Proc. Combust. Inst.* 28 (2000) 2569–2576.
- [175] M. Mehl, W.J. Pitz, C.K. Westbrook, H.J. Curran, Kinetic modeling of gasoline surrogate components and mixtures under engine conditions, *Proc. Combust. Inst.* 33 (2011) 193–200.
- [176] K. Narayanaswamy, P. Pepiot, H. Pitsch, A chemical mechanism for low to high temperature oxidation of n-dodecane as a component of transportation fuel surrogates, *Combust. Flame* 161 (2014) 866–884.
- [177] W. J. Grieco, A. L. Lafleur, K. C. Swallow, H. Richter, K. Taghizadeh, J. B. Howard, Fullerenes and PAH in low-pressure premixed benzene/oxygen flames, *Twenty-Seventh Symposium (Int.) on Combustion*, *Combust.* (1998) 1669–1675.
- [178] K. Norinaga, O. Deutschmann, N. Saegusa, J. Hayashi, Analysis of pyrolysis products from light hydrocarbons and kinetic modeling for growth of polycyclic aromatic hydrocarbons with detailed chemistry, *J. Anal. Appl. Pyrolysis*, 86 (2009) 148–160.
- [179] W. Hai, Formation of nascent soot and other condensed-phase materials in flames, *Formation of nascent soot and other condensed-phase materials in flames*, *Proc. Combust. Inst.* 33 (2011) 41–67.
- [180] I. Glassman, *Combustion*, Academic press, San Diego, 1996.



- [181] Y. Wang, A. Raj, S.H Chung, Soot modeling of counterflow diffusion flames of ethylene-based binary mixture fuels, *Combust. Flame* 162 (2015) 586–596.
- [182] G. Blanquart, H. Pitsch, Analyzing the effects of temperature on soot formation with a joint volume-surface-hydrogen model, *Combust. Flame* 156 (2009) 1614–1626.
- [183] N.E. Sánchez, A. Callejas, Á. Millera, R. Bilbao, M.U. Alzueta, Influence of the Oxygen Presence on Polycyclic Aromatic Hydrocarbon (PAH) Formation from Acetylene Pyrolysis under Sooting Conditions, *Energy Fuels* 27 (2013) 7081–7088.
- [184] H. Bockhorn, F. Fetting, and H. W. Wenz: Investigation of the Formation of High Molecular Hydrocarbons and Soot in Premixed Hydrocarbon-Oxygen Flames, *Ber. Bunsenges. Phys. Chem.* 87 (1983), 1067- 1073.
- [185] A. D'Alessio, A.C. barone, R. Cau, A. D'Anna, P. Minutolo, Surface deposition and coagulation efficiency of combustion generated nanoparticles in the size range from 1 to 10nm, *Proc. Combust Inst* 30 (2005) 2595-2603.
- [186] T.S. Totton, A.J. Misquitta, M. Kraft, A quantitative study of the clustering of polycyclic aromatic hydrocarbons at high temperatures, *Phys. Chem. Chem. Phys.* 14 (2012) 4081–4094.
- [187] J.H. Miller, Aromatic excimers: evidence for polynuclear aromatic hydrocarbon condensation in flames, *Proc. Combust. Inst.* 30 (2005) 1381-1388.
- [188] Happold, Karlsruhe University Press (2007) pp. 275–285.
- [189] G. Blanquart, Chemical and Statistical soot modeling, Ph.D Thesis (2008), Stanford University, USA.
- [190] J.N. Israelachvili Intermolecular and surface forces, Academic Press, London ; San Diego, 1991.
- [191] A. Veshkini, N.A. Eaves, S.B. Dworkin, M.J. Thomson, Application of PAH-condensation reversibility in modeling soot growth in laminar premixed and nonpremixed flames, *Combust. Flame* 167 (2016) 335-352.
- [192] F. Xu, A. El-Leathy, C. Kim, G. Faeth, Soot surface oxidation in hydrocarbon/air diffusion flames at atmospheric pressure, *Combust. Flame* 132 (2003) 43–57.

- [193] A. El-Leathy, C. Kim, G. Faeth, Soot Surface Growth in Laminar Hydrocarbon/Air Diffusion Flames, *AIAA J.* 41 (2003) 856–865.
- [194] A.M. Vargas, Ö.L. Gülder, Pressure dependence of primary soot particle size determined using thermophoretic sampling in laminar methane-air diffusion flames, *Proc. Combust. Inst.* 36 (2017) 975-984.
- [195] G.B. Sarnacki, H.K. Chelliah, Uncertainties of Soot Measurement in Counterflow Flames using Laser Induced Incandescence: Soot Volume Fraction, Particle Size, and Number Density, Department of Mechanical and Aerospace Engineering, University of Virginia.
- [196] Emre Cenker. Imaging measurements of soot particle size and soot volume fraction with laserinduced incandescence at Diesel engine conditions. *Engineering Sciences [physics]*. Ecole Centrale Paris, 2014, France.
- [197] P. Desgroux, A. Faccinetto, X. Mercier, T. Mouton, D.A. Karkar, A. El Bakali, Comparative study of the soot formation process in a “nucleation” and a “sooting” low pressure premixed methane flame. *Combust. Flame* 184 (2017) 153-166.
- [198] T. Mouton, X. Mercier, M. Wartel, N. Lamoureux, P. Desgroux, Laser-induced incandescence technique to identify soot nucleation and very small particles in low-pressure methane flames, *Appl. Physics B* 112 (2013) 369.
- [199] S. Gordon and B. J. McBride: Computer program for calculation of complex chemical equilibrium compositions, rocket performance, incident and reflected shocks and Chapman-Jouguet detonations NASA SP-273, 1971.
- [200] I. Ziegler; R. Fournet; P.M. Marquaire, Pyrolysis of propane for CVI of pyrocarbon: Part I. Experimental and modeling study of the formation of toluene and aliphatic species, *J. Anal. Appl. Pyrolysis* 73 (2005) 212-230.
- [201] A. Laskin; H. Wang; C.K. Law, Detailed kinetic modeling of 1, 3-butadiene oxidation at high temperatures, *Int. J. Chem. Kinet.*, 32 (2000) 589-614.
- [202] J.L. Emdee, K. Brezinsky, I. Glassman, A kinetic model for the oxidation of toluene near 1200 K, *J. Phys. Chem.* 96 (1992) 2151-2161.

- [203] M.U. Alzueta; P. Glarborg, Experimental and kinetic modeling study of the oxidation of benzene, *Int. J. Chem. Kinet.* 32 (2000) 498-522.
- [204] C.-C. Chen, J.W. Bozzelli, J.T. Farrell, Thermochemical Properties, Pathway, and Kinetic Analysis on the Reactions of Benzene with OH, *J. phys. chem. A* 108 (2004) 4632–4652.
- [205] T. Seta, M. Nakajima, A. Miyoshi, High-temperature reactions of OH radicals with benzene and toluene, *J. phys. chem. A* 110 (2006) 5081–5090.
- [206] M. Chaos, Z. Zhao, A. Kazakov, P. Gokulakrisnan, M. Angioletti, F.L. Dryer, A PRF+toluene surrogate fuel model for simulating gasoline kinetics. In: *Proc. of the fifth US Combust. Inst. meeting, San Diego, 2007.*
- [207] I. Da Costa, R. Fournet, F. Billaud, F. Battin-Leclerc, Experimental and modeling study of the oxidation of benzene, *Int. J. Chem. Kinet.* 35 (2003) 503–524.
- [208] X. Zhong, J.W. Bozzelli, Thermochemical and kinetic analysis of the H, OH, HO<sub>2</sub>, O, and O<sub>2</sub> association reactions with cyclopentadienyl radical, *J. Phys. Chem. A* 102 (1998) 3537–3555.
- [209] J. Park, G.J. Nam, I.V. Tokmakov, M.C. Lin, Experimental and theoretical studies of the phenyl radical reaction with propene, *J. phys. chem. A* 110 (2006) 8729–8735.
- [210] W.D. Clark, S.J. Price, Free-radical and molecular processes in the pyrolysis of ethylbenzene, *Can. J. Chem.* 48 (1970) 1059-1064.
- [211] Y. Wenhao, Y. Li, P. Dagaut, J. Yang, F. Qi, Investigation on the pyrolysis and oxidation of toluene over a wide range conditions. I. Flow reactor pyrolysis and jet stirred reactor oxidation, *Combust. Flame* 162 (2015) 3–21.
- [212] A. Comandini, T. Malewicki, K. Brezinsky, Chemistry of polycyclic aromatic hydrocarbons formation from phenyl radical pyrolysis and reaction of phenyl and acetylene, *J. phys. chem. A* 116 (2012) 2409–2434.
- [213] H. Wang, M. Frenklach, A detailed kinetic modeling study of aromatics formation in laminar premixed acetylene and ethylene flames, *Combust. Flame* 110 (1997) 173-221.
- [214] C. Saggese, A. Frassoldati, A. Cuoci, T. Faravelli, E. Ranzi, A wide range kinetic modeling study of pyrolysis and oxidation of benzene, *Combust. Flame* 160 (2013) 1168-1190.

- [215] A. Goldanigaa, T. Faravellia, E. Ranzi, The kinetic modeling of soot precursors in a butadiene flame, *Combust. Flame* 122 (2000) 350-358.
- [216] H.Y. Zhang, J.T. McKinnon, Elementary reaction modeling of high-temperature benzene combustion, *Combust. Sci. Technol.*, 107 (1995) 261-300.
- [217] H. Kraus, C. Oehlers, F. Temps, H. G. Wagner, Kinetics of the reactions of carbene (CH<sub>2</sub>)(X3B1) with selected polycyclic aromatic hydrocarbons at temperatures between 296 and 690 K, *J. Phys. Chem.* 97 (1993) 10989-10995.

## Appendices

### A. Thermokinetic and transport formalism

#### 1. The kinetic mechanism

The kinetic mechanism is an important input needed as it describes chemical species involved in flame chemistry and chemical reactions that occur. The size of the kinetic mechanism depends on fuel structure and the desired detailed level of the calculated flame structure. Complex fuels containing a lot of components will require more chemical reactions than a single component fuel. The kinetic mechanism consists of two parts: the first part lists all chemical species involved in the mechanism and the second part lists elementary chemical reactions that may occur. These reactions can be bidirectional or not and the kinetic parameter of each reaction follows the Arrhenius-Kooij law as follows:

$$k = A \cdot T^n \cdot \exp\left(-\frac{E}{RT}\right) \quad \text{Equation 44}$$

Where  $k$  is the rate constant,  $A$  the pre-exponential factor,  $T$  the temperature,  $n$  the temperature exponent,  $E$  the activation energy and  $R$  the ideal gas constant.

Bidirectional and elementary reactions are written in the general form as follows:



Only the forward rate constant ( $k_{dir}$ ) is introduced into the kinetic mechanism file, as the reverse rate constant ( $k_{rev}$ ) can be calculated at each temperature as follows:

$$\frac{k_{dir}}{k_{rev}} = K_{eq} \left(\frac{P}{RT}\right)^{\sum \nu_{products} - \sum \nu_{reactants}} = e^{\frac{-\Delta H - T\Delta S}{RT}} \quad \text{Equation 46}$$

Where  $K_{eq}$  is the gas equilibrium constant and  $\nu$  represents the stoichiometric coefficients.  $\Delta H$  and  $\Delta S$  are respectively the variation in enthalpy and entropy caused by the considered reaction at the temperature  $T$ .  $K_{eq}$  can be expressed as follows:

$$K_{eq} = \frac{P_C P_D}{P_A P_B} \quad \text{and the partial pressures can be calculated as: } P_i = \frac{\rho_i}{M_i} RT$$

The net formation rate of a compound  $i$  can be expressed by subtracting its consumption rate to its production rate.

### 3. Pressure dependent reactions

Unimolecular and recombination reactions are more or less complex since pressure dependency is implied. In fact, collisions are not sufficient in low pressure case, while in high pressure case, they are excessive. This phenomena leads to a competition between the product formation (favored at low pressure) and the reactant re-formation (favored at high pressure). These reactions involve collisions with a non-reactive third-body  $M$ . The rate of these reactions depends on the  $M$  concentration, which depends on the working pressure. A pressure dependent reaction is depicted as follows:



The collision efficiency of each compound  $M$  of the gas-phase is different and can be specified in the kinetic mechanism. For a pressure dependent reaction, 2 regimes can specified as depicted in Figure 132: low pressure limit and fall-off domain.

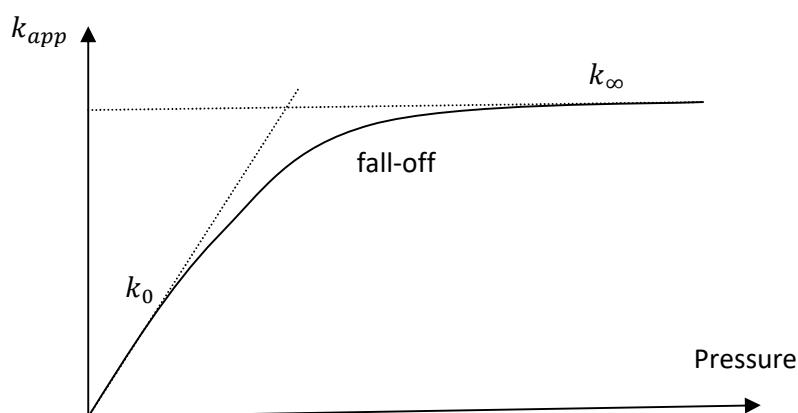
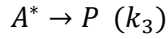
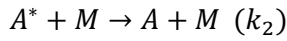
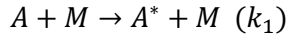


Figure 132: The fall-off phenomenon.

The pressure effect is described by two different fall-off forms: that of Lindemann and that of Troe.

#### - Lindemann formalism

In the case of unimolecular reactions, the main reactions are those of decomposition or isomerization. According to Lindeman theory, unimolecular reaction is decomposed into two steps by forming an activated intermediate product  $A^*$  due to the collision of  $M$  and the reactant and the  $A^*$  forms finally the product. These steps are shown as follows:



By applying the QSSA (Quasi-Steady-State Approximation) to  $A^*$ , the following expression is obtained:

$$\frac{d[A^*]}{dt} = k_1[A][M] - k_2[A^*][M] - k_3[A^*] \approx 0$$

$$[A^*] = \frac{k_1[A][M]}{k_2[M] + k_3}$$

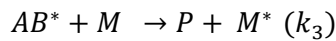
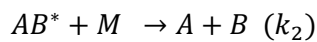
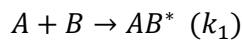
$$\frac{d[P]}{dt} = k_3[A^*] = \frac{k_3 k_1 [M]}{k_2 [M] + k_3} [A] = k_{app} [A]$$

- At low pressure:  $k_2[M] \ll k_3$      $k_{app} \approx k_1[M] = k_0[M]$
- At higher pressure:  $k_2[M] \gg k_3$      $k_{app} \approx \frac{k_1 k_3}{k_2} [A] = k_\infty [A]$
- At intermediary pressure: reaction order is between 1 and 2, and the rate constant is that of the fall-off zone. the rate constant in the fall-off zone can be expressed as follows:

$$k = k_\infty \left( \frac{P_r}{1 + P_r} \right) \cdot F$$

Where:  $P_r$  is the reduced pressure and is expressed as  $P_r = \frac{k_0[M]}{k_\infty}$ ,  $[M] = \sum_i f_i [M]_i$  and  $f_i$  = efficiency coefficient of specie  $i$ .  $F$  is a corrector factor. One can note that  $F = 1$  in the Lindemann's formalism.

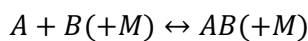
In the case of recombination reaction, the mechanism is described as follows:



By applying the QSSA to  $AB^*$ , one obtains:

$$\frac{d[P]}{dt} = k_3[AB^*][M] = \frac{k_1 k_3 [M]}{k_2 + k_3 [M]} [A][B] = k_{app} [A][B]$$

- **Troe formalism**



The formalism of Troe indicates (with an uncertainty of about 20 %) the influence of pressure over rate constant and is more precised than the Lindemann's formalism. It takes into account the difference observed between experiments findings and Lindemann theory. Four more coefficients a, b, c and d called Troe's parameters, are used to calculate the correction factor  $F$  as expressed below:

$k_{Troe} = F \cdot k_{Lindemann}$  and the factor  $F$  is described as follows:

$$\log F = \left[ 1 + \left( \frac{\log P_r + C}{N - 0.14(\log P_r + C)} \right)^2 \log F_{cent} \right]$$

$$F_{cent} = (1 - a) \exp\left(-\frac{T}{b}\right) + a \exp\left(-\frac{T}{c}\right) + \exp\left(-\frac{d}{T}\right)$$

$$N = 0.75 - 1.27 \log F_{cent}$$

$$C = -0.40 - 0.67 \log F_{cent}$$

$$P_r = \frac{k_0[M]}{k_\infty}$$

$F_{cent}$  is centering parameter;  $N$  and  $C$  are other parameters and  $P_r$  is reduced pressure,  $T$  is temperature. In the kinetic code, the rate constants  $k_0$ ,  $k_\infty$  and the four Troe's parameters a, b, c and d must be specified in order to account for pressure dependence of  $k_{dir}$  and  $k_{rev}$ .

## 2. Thermodynamic database

The thermodynamic data entered for species are those from NASA chemical equilibrium formalism [199]. The enthalpy and entropy are calculated from Kirchhoff relations. Thermodynamic properties are calculated using a polynomial curve fit that consists in two sets of 7 coefficients ( $a_{1,k} - a_{7,k}$ ), corresponding to 2 ranges of temperature: 300 to 1000 K and 1000 to 5000 K. These two sets of coefficients (14 coefficients) allow to calculate specific heat  $C_{p,k}$ , enthalpy  $H_k^0$  and entropy  $S_k^0$  of a compound  $i$  at various temperatures using the following equations:

$$\frac{C_{p,k}}{R} = a_{1,k} + a_{2,k}T + a_{3,k}T^2 + a_{4,k}T^3 + a_{5,k}T^4 \quad \text{Equation 48}$$

$$\frac{H_k^0}{RT} = a_{1,k} + a_{2,k}\frac{T}{2} + a_{3,k}\frac{T^2}{3} + a_{4,k}\frac{T^3}{4} + a_{5,k}\frac{T^4}{5} + \frac{a_{6,k}}{T} \quad \text{Equation 49}$$

$$\frac{S_k^0}{R} = a_{1,k} \ln T + a_{2,k}T + a_{3,k}\frac{T^2}{2} + a_{4,k}\frac{T^3}{3} + a_{5,k}\frac{T^4}{4} + a_{7,k} \quad \text{Equation 50}$$



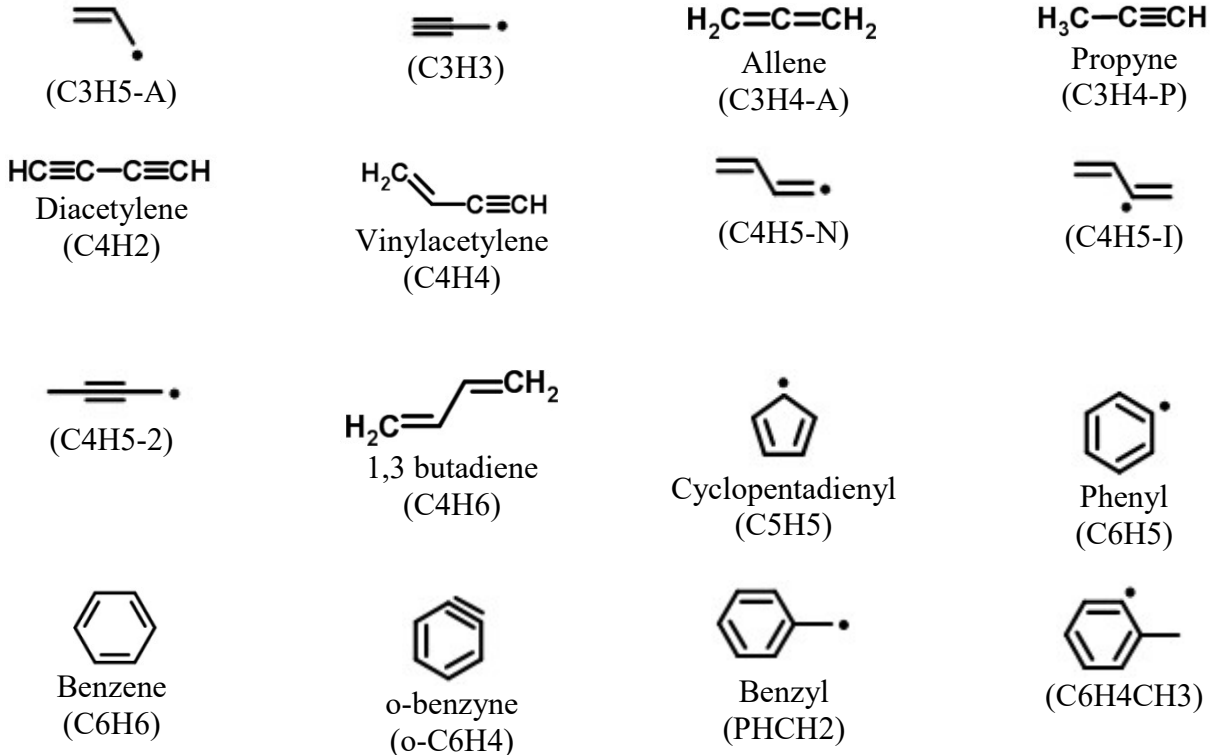
### 3. Transport database

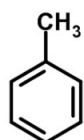
The transport database gives information for calculation of the multicomponent diffusion coefficient  $D_{ij}$ , the thermal diffusion coefficient  $D_i^T$  and the heat conductivity of the mixture  $\lambda$  that are needed to determine the molecular diffusion  $j_i$ .  $D_{ij}$ ,  $D_i^T$  and  $\lambda$  can be calculated by kinetic solver by providing into transport database, six parameters for each chemical species that are: molecule geometry, Lennard-Jones potential ( $\frac{\xi_k}{k_B}$ ), Lennard-Jones collision mean diameter ( $\sigma_k$ ), dipole moment ( $\mu_k$ ), polarisability ( $\alpha_k$ ) and rotational relaxation collision number ( $Z_{rotk}$ ). As an example, a binary diffusion coefficient  $D_{ij}$  in practical application is given by:

$$D_{ij} = \frac{3}{8} \sqrt{\frac{\pi \cdot k_B \cdot T \cdot 2 \frac{m_i \cdot m_j}{m_i + m_j}}{\pi \sigma_{ij}^2 \Omega^{(i,j)}(T_{ij}^*)}} \frac{1}{\rho} \quad \left( \frac{m}{s^2} \right) \quad \text{Equation 51}$$

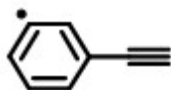
Where  $k_B$  is the Boltzmann constant,  $T$  the temperature,  $\sigma$  the molecular diameter,  $m$  the particle mass (atom, molecule),  $\Omega$  the collision integral,  $T^*$  the reduced temperature.

### B. The nomenclature of species used in the kinetic model

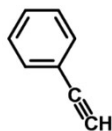




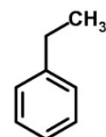
Toluene  
(TOLUEN)



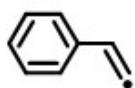
(A1C2H-)



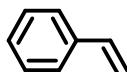
Phenylacetylene  
(PHC2H)



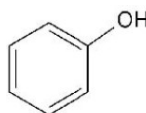
Ethylbenzene  
(PHC2H5)



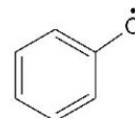
(N-C8H7)



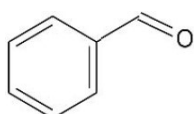
Styrene  
(STYREN)



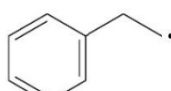
Phenol  
(C6H5OH)



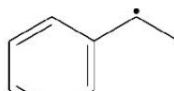
Phenoxy  
(C6H5O)



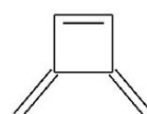
Benzaldehyde  
(PHHCO)



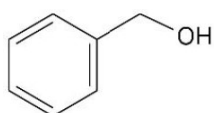
(APHC2H4)



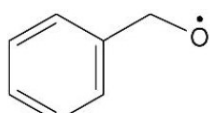
(BPHC2H4)



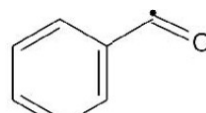
dimethylene  
cyclobutene  
(MC6H6)



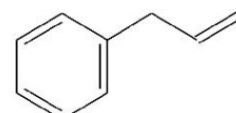
(PHCH2OH)



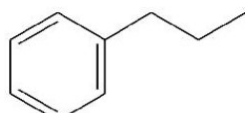
(PHCH2O)



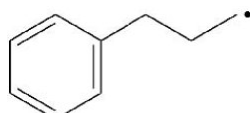
(PHCO)



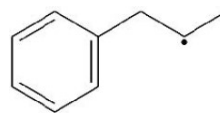
(PHC3H5-1)



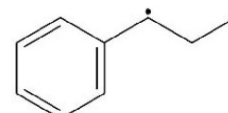
n-propylbenzene  
(PBZ)



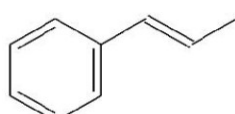
(PBZJA)



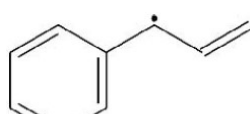
(PBZJB)



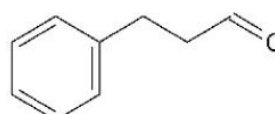
(PBZJC)



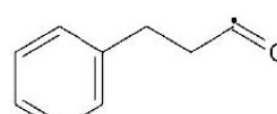
(PHC3H5-2)



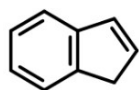
(PHC3H4)



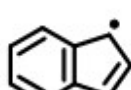
(PHC2H4HCO)



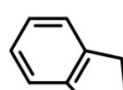
(PHC2H4CO)



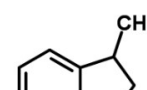
Indene  
(INDENE)



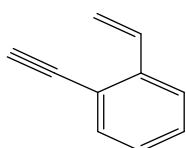
Indenyl  
(INDENYL)



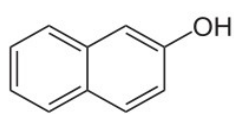
Indane  
(C9H10)



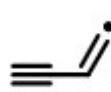
1-methylindane  
(C10H10)



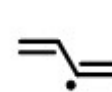
vinyl phenyl acetylene  
(A1C2H3AC)



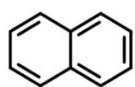
Naphthol  
(A2OH)



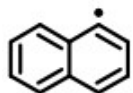
(C4H3-N)



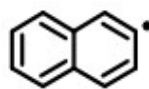
(C4H5-I)



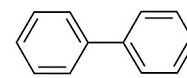
Naphthalene  
(NAPHT)



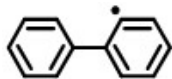
1-naphthyl  
(A2-1)



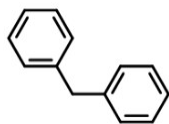
2-naphthyl  
(A2-2)



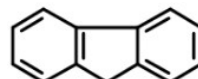
Biphenyl  
(BIPHENYL)



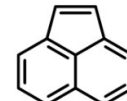
Biphenyl radical  
(P2-)



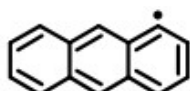
Benzylbenzene  
(BENZYLB)



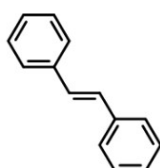
Fluorene  
(FLUORENE)



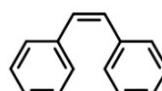
Acenaphthylene  
(A2R5)



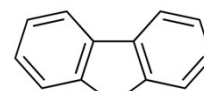
Anthracenyl  
(A3LJX)



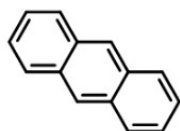
Trans-stilbene  
(C14H12)



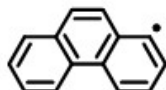
Cis-stilbene  
(C14H12)



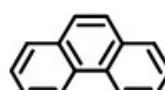
Dibenzofuran  
(DIBZFUR)



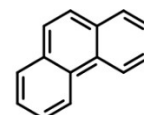
Anthracene  
(ANTHRCN)



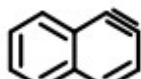
1-Phenanthryl  
(A3-1)



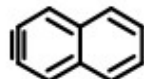
4-Phenanthryl  
(A3-4)



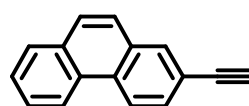
Phenanthrene  
(PHNTHRN)



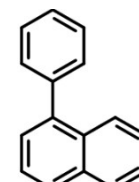
A2T1  
(A2T1)



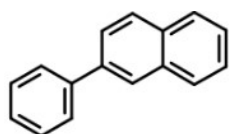
A2T2  
(A2T2)



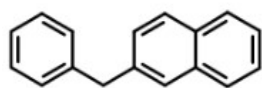
Phenanthrylacetylene  
(A3C2H2)



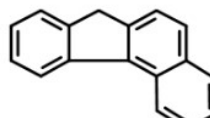
1-Phenyl-naphthalene  
(A2A1-1)



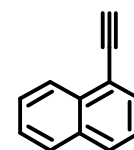
2-phenyl-naphthalene  
(A2A1-2)



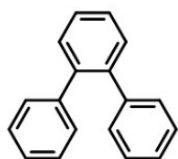
2-benzyl-naphthalene  
(BENZNAP)



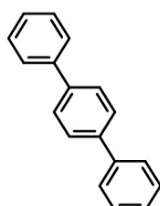
Benzofluoranthene  
(BENZFLRN)



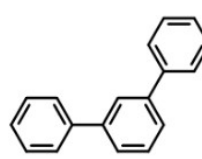
Naphthylacetylene  
(A2C2H2)



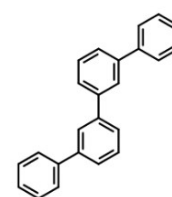
o-Terphenyl  
(TERPHENYL)



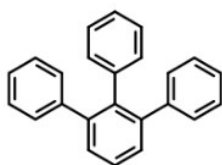
p-Terphenyl  
(TERPHENYL)



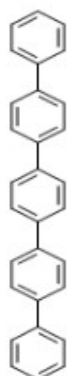
m-Terphenyl  
(TERPHENYL)



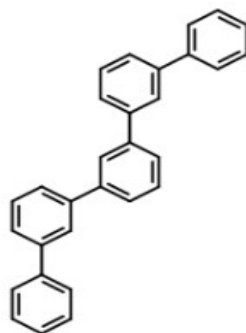
m-Quaterphenyl  
(QUATERPHENYL)



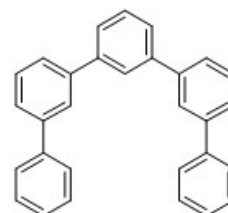
Triphenylbenzene  
(QUATERPHENYL)



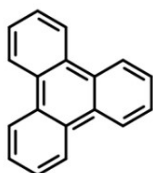
p-Quinquephenyl  
(QUINQUEPHENYL)



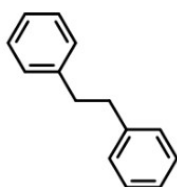
m-Quinquephenyl  
(QUINQUEPHENYL)



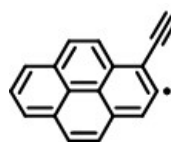
Quinquephenyl  
(QUINQUEPHENYL)



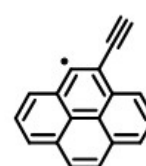
Triphenylene  
(TRIPHENYLENE)



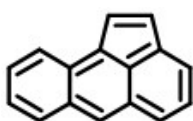
Bibenzyl  
(C<sub>14</sub>H<sub>14</sub>)



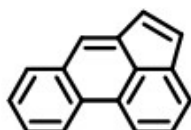
1-Pyrenylacetylene  
(A<sub>4</sub>C<sub>2</sub>H\*)



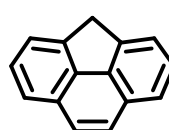
4-Pyrenylacetylene  
(A<sub>4</sub>C<sub>2</sub>H\*S)



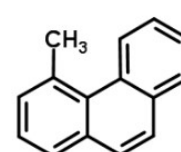
Aceanthrylene  
(A<sub>3</sub>LR<sub>5</sub>)



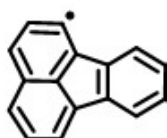
Acephenanthrylene  
(A<sub>3</sub>R<sub>5</sub>)



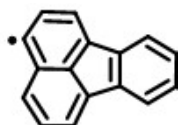
A<sub>3</sub>CH<sub>2</sub>R  
(A<sub>3</sub>CH<sub>2</sub>R)



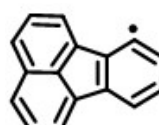
4-methylphenanthrene  
(A<sub>3</sub>CH<sub>3</sub>)



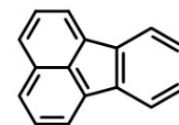
1-Fluoranthenyl  
(FLTHNJ1)



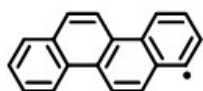
3-Fluoranthenyl  
(FLTHNJ3)



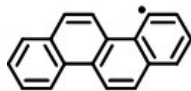
7-Fluoranthenyl  
(FLTHNJ7)



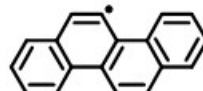
Fluoranthene  
(FLTHN)



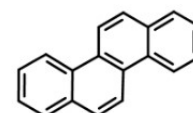
1-chrysenyl  
(CHRYSEN-1)



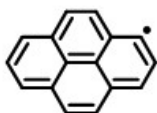
4-chrysenyl  
(CHRYSEN-4)



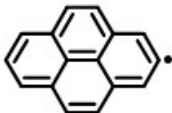
5-chrysenyl  
(CHRYSEN-5)



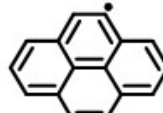
Chrysene  
(CHRYSEN)



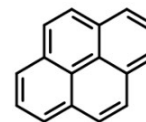
1-Pyrenyl



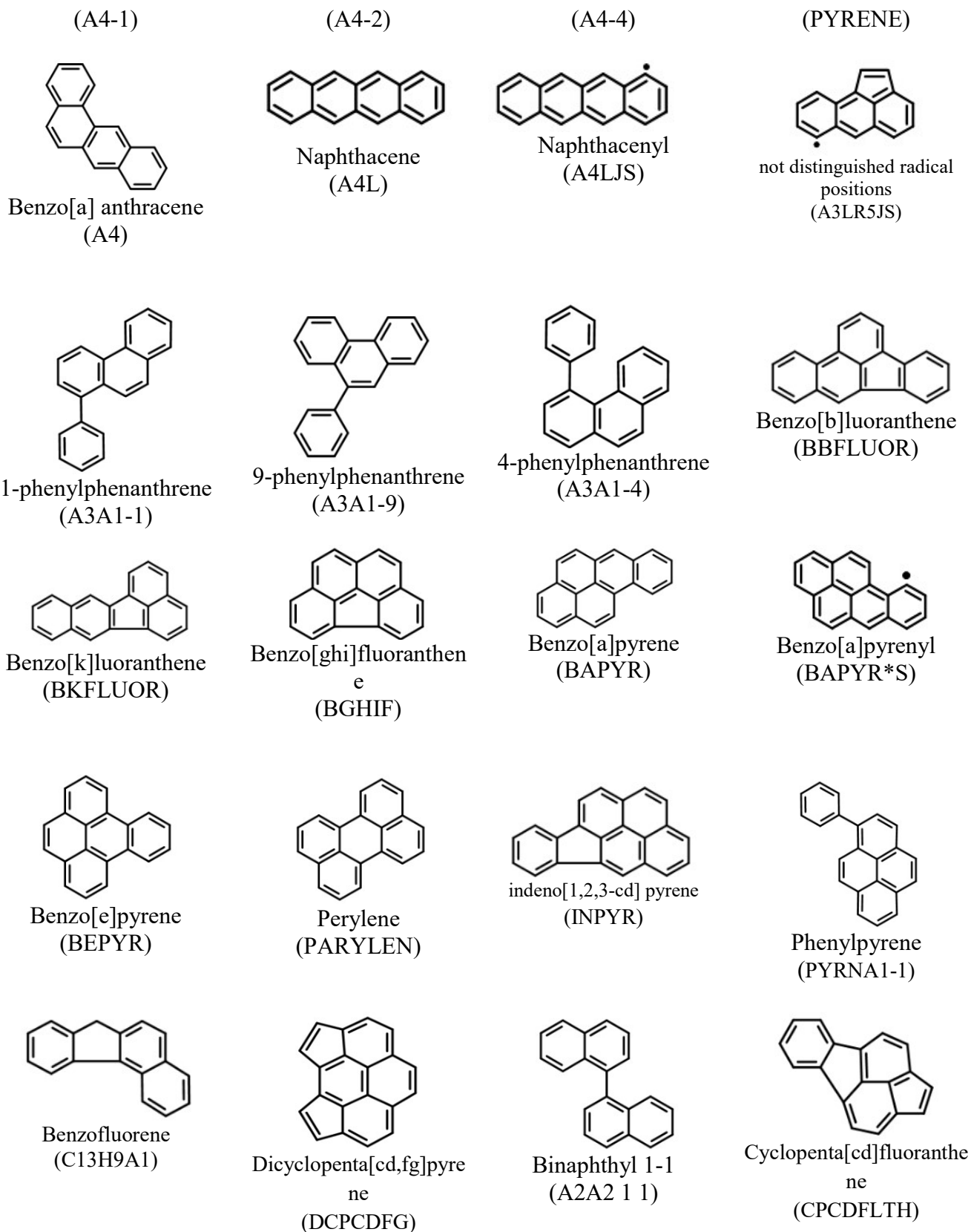
2-Pyrenyl



4-pyrenyl



Pyrene



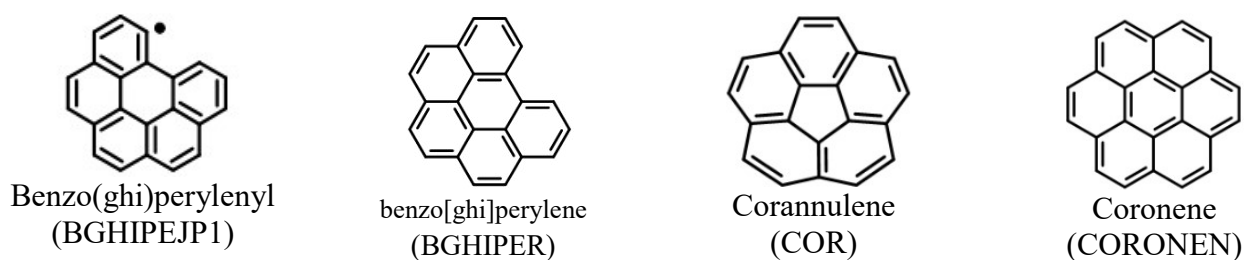


Figure 133 : Molecular structures of some key species and major polycyclic aromatic hydrocarbons involved in the model.

### C. Heat of formation used of all species

Number	Name	H (298 K)	H (T <sub>bath</sub> )	Cp (T <sub>bath</sub> )	S (T <sub>bath</sub> )	G (T <sub>bath</sub> )
		kcal/mol		cal/(mol-K)		kcal/mol
1	NC10H22	-59.85	-59.85	56	130.45	-98.74
2	IC8H18	-53.44	-53.44	45.15	101.21	-83.61
3	PBZ	1.91	1.91	36.06	94.23	-26.18
4	O2	0	0	7.01	49.01	-14.61
5	CO	-26.42	-26.42	6.95	47.22	-40.5
6	N2	0	0	6.95	45.77	-13.65
7	AR	0	0	4.97	37.01	-11.03
8	HE	0	0	4.97	30.15	-8.99
9	CO2	-94.06	-94.06	8.89	51.08	-109.29
10	H2O	-57.8	-57.8	7.99	45.1	-71.25
11	CH3CHOCHO	-31.24	-31.24	20.99	79.65	-54.99
12	HO2CHO	-90.21	-90.21	10.82	59.41	-107.92
13	O2CHO	-38.3	-38.3	9.52	58.82	-55.84
14	OCHO	-38.3	-38.3	9.52	58.82	-55.84
15	CH3O2H	-31.8	-31.8	15.86	65.34	-51.28
16	CH	142.01	142.01	6.95	43.72	128.98
17	HCCOH	20.43	20.43	13.19	58.71	2.93
18	CH3CO3H	-80.49	-80.49	20.48	77.24	-103.52
19	CH3CO3	-42.35	-42.35	19.91	77.37	-65.42
20	CH3CO2	-51.39	-51.39	14.73	63.57	-70.34
21	O2C2H4OH	-41.29	-41.29	21.73	86.96	-67.22
22	C2H5O2H	-40.8	-40.8	20.66	76.4	-63.58
23	C2H4O2H	8.2	8.2	19.98	79.93	-15.63
24	C2H4O1-2	-12.58	-12.58	11.7	57.51	-29.73
25	CH3COCH2O2	-35.38	-35.38	25.6	92.65	-63.01
26	CH3COCH2O2H	-71.49	-71.49	27.63	92.43	-99.05
27	CH3COCH2O	-33.71	-33.71	21.16	80.46	-57.7
28	CH3OCH3	-43.4	-43.4	15.68	63.77	-62.42
29	CH3OCHO	-84.3	-84.3	16.97	71.34	-105.57

30	CH3OCO	-38.39	-38.39	16.18	72.46	-60
31	NC3H7O2H	-45.73	-45.73	26.13	85.82	-71.32
32	IC3H7O2H	-50.01	-50.01	26.21	81.71	-74.37
33	NC3H7O	-9.17	-9.17	19.89	75.07	-31.55
34	IC3H7O	-13.54	-13.54	20.46	73.07	-35.33
35	C3H6O1-2	-21.88	-21.88	17.97	66.31	-41.65
36	C3H6OH	-14.78	-14.78	19.27	80.97	-38.92
37	HOC3H6O2	-49.61	-49.61	27.36	94.95	-77.91
38	PC4H9O2H	-50.67	-50.67	31.62	95.24	-79.06
39	PC4H9O2	-16.86	-16.86	29.55	94.11	-44.92
40	SC4H9O2	-21.13	-21.13	29.67	91.37	-48.37
41	PC4H9O	-14.1	-14.1	25.37	84.49	-39.29
42	SC4H9O	-18.47	-18.47	25.96	83.86	-43.47
43	C4H8O1-3	-27.66	-27.66	21.64	73.66	-49.62
44	C4H8O1-4	-43.63	-43.63	19.13	73.89	-65.66
45	C4H8OH-1O2	-54.62	-54.62	32.84	104.37	-85.73
46	C4H8OOH1-2	-4.31	-4.31	30.83	99.43	-33.96
47	C4H8OOH1-3	-4.31	-4.31	29.9	99.68	-34.03
48	C4H8OOH1-4	-1.66	-1.66	30.81	98.65	-31.07
49	C4H8OOH1-2O2	-41.53	-41.53	38.09	111.31	-74.72
50	C4H8OOH1-3O2	-41.53	-41.53	38.09	111.31	-74.72
51	NC4KET12	-72.57	-72.57	32.16	100.17	-102.43
52	NC4KET13	-74.11	-74.11	33.22	99.36	-103.73
53	C2H5COCH3	-56.89	-56.89	24.06	81.07	-81.06
54	CH2CH2COCH3	-8	-8	23.31	84.49	-33.19
55	CH2CH2CHO	4.5	4.5	18.53	77.53	-18.61
56	IC4H9O2H	-52.91	-52.91	31.35	92.55	-80.5
57	TC4H9O2H	-58.41	-58.41	32.2	86.31	-84.14
58	IO2C4H8OH	-60.2	-60.2	33.45	100.05	-90.03
59	TC4H8OOH-IO2	-45	-45	38.59	107.29	-76.99
60	IC4H8OOH-IO2	-39.5	-39.5	37.67	111.36	-72.71
61	IC4H8OOH-TO2	-45	-45	38.59	107.29	-76.99
62	IC4KETII	-71.61	-71.61	31.77	100.97	-101.71
63	IC4KETIT	-75.84	-75.84	32.36	93.28	-103.65
64	TC3H6OCHO	-39.04	-39.04	26.56	84.25	-64.16
65	TC3H6O2CHO	-39.73	-39.73	30.34	93.5	-67.61
66	TC3H6O2HCO	-38.93	-38.93	31.61	94.4	-67.08
67	IC3H5O2HCHO	-26.83	-26.83	31.69	96.7	-55.66
68	TC4H8CHO	-9.3	-9.3	28.7	89.66	-36.03
69	O2C4H8CHO	-43.39	-43.39	35.75	104.72	-74.62
70	O2HC4H8CO	-42.59	-42.59	36.86	105.62	-74.09
71	AC5H11	12.3	12.3	27.72	85.46	-13.18
72	DC5H11	12.3	12.3	27.72	85.46	-13.18
73	AC6H13	6.64	6.64	33.21	94.88	-21.65
74	BC6H13	1.84	1.84	33.1	95.32	-26.58
75	DC6H13	3.99	3.99	32.38	95.9	-24.6

76	EC6H13	6.64	6.64	33.21	94.88	-21.65
77	IC4H9COCH3	-68.99	-68.99	34.67	97.23	-97.98
78	IC4H9COCH2	-26.68	-26.68	34.46	94.51	-54.86
79	IC3H6CH2COCH3	-19.98	-19.98	33.9	100.65	-49.99
80	TC3H6CH2COCH3	-24.78	-24.78	33.85	101.09	-54.92
81	NC3H7COCH3	-61.82	-61.82	29.51	90.49	-88.8
82	NC3H7COCH2	-19.51	-19.51	29.28	87.77	-45.68
83	C3H6COCH3-2	-15.46	-15.46	27.88	94.93	-43.76
84	AC3H5CHO	-18.05	-18.05	20.91	80.69	-42.11
85	C4H8CHO-1	-5.36	-5.36	29.44	94.99	-33.68
86	C2H5COC2H5	-62.21	-62.21	30.13	89.3	-88.83
87	C2H5COC2H4P	-13.2	-13.2	29.38	94.09	-41.25
88	C2H5COC2H3	-35.72	-35.72	27.32	86.43	-61.49
89	PC2H4COC2H3	13.28	13.28	26.54	89.84	-13.5
90	C7H16-24	-49.54	-49.54	39.25	98.2	-78.81
91	ZC7H15O2	-40.4	-40.4	45.62	112.9	-74.07
92	YC7H15O	-40.17	-40.17	42.27	104.32	-71.28
93	ZC7H15O	-37.74	-37.74	41.67	105.39	-69.17
94	YC7H14OOH-X1	-26.43	-26.43	47.69	117.48	-61.46
95	YC7H14OOH-Z	-29.08	-29.08	46.73	118.51	-64.42
96	YC7H14OOH-X2	-26.43	-26.43	47.69	117.48	-61.46
97	ZC7H14OOH-Y	-29.8	-29.8	46.86	119.27	-65.36
98	YC7H14OOH-X1O2	-62.04	-62.04	54.52	134.24	-102.06
99	YC7H14OOH-X2O2	-62.04	-62.04	54.52	134.24	-102.06
100	YC7H14OOH-Y2O2	-67.54	-67.54	55.5	128.81	-105.94
101	YC7H14OOH-ZO2	-66.31	-66.31	54.69	130.14	-105.11
102	X-Y2C7H14O	-70.28	-70.28	35.25	93.48	-98.15
103	XC7H14OH	-40.79	-40.79	41.4	115.45	-75.22
104	YC7H14OH	-45.09	-45.09	42.03	110.71	-78.1
105	XO2C7H14OH	-77.3	-77.3	49.51	124.95	-114.55
106	YO2C7H14OH	-81.6	-81.6	49.98	122.96	-118.26
107	NEOC5H11O2H	-60.61	-60.61	37.38	95.57	-89.1
108	NEOC5H11O	-24.14	-24.14	31.05	84.82	-49.43
109	NEO-C5H10O	-35.01	-35.01	25.9	79.56	-58.73
110	NEOC5H10OOH-O2	-45.3	-45.3	41.88	116.55	-80.05
111	NEOC5H9Q2	-31.9	-31.9	42.9	121.1	-68.01
112	NEOC5H9Q2-N	-37	-37	45.9	121.5	-73.23
113	NEOC5KET	-78.61	-78.61	37.81	104.8	-109.85
114	NEOC5KETOX	-42.14	-42.14	31.53	94.05	-70.19
115	HC6H13	3.77	3.77	33.68	88.47	-22.61
116	TC4H9CHO	-58.31	-58.31	29.46	82.69	-82.96
117	TC4H9CO	-21.4	-21.4	28.64	83.81	-46.39
118	IC3H6CHCHO	-36.64	-36.64	28.28	83.54	-61.55
119	IC3H6CHCO	-5.74	-5.74	28.12	82.15	-30.23
120	PC7H13O-O	-7.19	-7.19	39.59	100.87	-37.27
121	NC7H15O2	-36.76	-36.76	46.29	115.46	-71.19



122	PC7H15O2	-41.03	-41.03	46.42	110.55	-74
123	QC7H15O2	-36.76	-36.76	46.29	113.28	-70.54
124	NC7H14OOH-N2	-21.56	-21.56	47.54	120.01	-57.34
125	NC7H14OOH-O	-24.21	-24.21	46.61	121.03	-60.3
126	QC7H14OOH-O	-24.21	-24.21	46.61	121.03	-60.3
127	PC7H14OOH-N	-25.83	-25.83	47.7	117.27	-60.8
128	PC7H14OOH-O	-28.48	-28.48	46.75	116.12	-63.1
129	NC7H14OOH-OO2	-62.44	-62.44	55.17	155.58	-108.82
130	QC7H14OOH-OO2	-61.44	-61.44	54.45	130.48	-100.34
131	PC7H14OOH-NO2	-62.44	-62.44	55.17	155.58	-108.82
132	PC7H14OOH-OO2	-65.71	-65.71	54.63	127.75	-103.8
133	N-PC7H14O	-68.48	-68.48	35.64	94.38	-96.62
134	NEOC7KETPN	-97.31	-97.31	49.04	122.36	-133.79
135	NEOC7KETPO	-100.04	-100.04	48.05	118.26	-135.3
136	NEOC7KETQO	-94.01	-94.01	49.89	118.53	-129.35
137	CC8H17O2	-45.53	-45.53	52.44	115.95	-80.11
138	AC8H17O2H	-73.84	-73.84	53.58	123.33	-110.61
139	BC8H17O2H	-78.91	-78.91	53.72	118.41	-114.21
140	CC8H17O2H	-79.34	-79.34	54.51	117.08	-114.25
141	DC8H17O2H	-73.84	-73.84	53.58	121.15	-109.96
142	AC8H17O	-37.27	-37.27	47.2	112.58	-70.84
143	BC8H17O	-41.64	-41.64	47.89	109.77	-74.37
144	CC8H17O	-44.07	-44.07	48.25	107.33	-76.08
145	DC8H17O	-37.27	-37.27	47.2	111.77	-70.6
146	AC8H16OOH-D	-25.63	-25.63	52.82	126.74	-63.42
147	CC8H16OOH-D	-31.13	-31.13	53.71	120.5	-67.06
148	CC8H16OOH-B	-32.98	-32.98	52.73	121.52	-69.22
149	CC8H16OOH-A	-31.13	-31.13	53.71	122.68	-67.71
150	DC8H16OOH-D	-25.63	-25.63	52.82	124.56	-62.77
151	DC8H16OOH-A	-25.63	-25.63	52.82	126.74	-63.42
152	IC8ETERAD	-74.74	-74.74	40.1	93.77	-102.7
153	IC8ETERDD	-47.34	-47.34	42.06	101.59	-77.63
154	AC8H16OOH-AO2	-59.04	-59.04	58.96	138.47	-100.32
155	AC8H16OOH-BO2	-63.71	-63.71	59.39	137.81	-104.8
156	AC8H16OOH-CO2	-65.04	-65.04	59.95	134.5	-105.14
157	BC8H16OOH-CO2	-69.71	-69.71	60.35	131.65	-108.96
158	BC8H16OOH-AO2	-63.71	-63.71	59.39	137.81	-104.8
159	BC8H16OOH-DO2	-63.71	-63.71	59.39	135.63	-104.15
160	CC8H16OOH-BO2	-69.71	-69.71	60.35	131.65	-108.96
161	CC8H16OOH-AO2	-65.04	-65.04	59.95	134.5	-105.14
162	DC8H16OOH-CO2	-65.04	-65.04	59.95	133.69	-104.9
163	DC8H16OOH-DO2	-59.04	-59.04	58.96	137.66	-100.08
164	DC8H16OOH-BO2	-63.71	-63.71	59.39	135.63	-104.15
165	IC8KETAA	-94.14	-94.14	54.03	131.75	-133.42
166	IC8KETAB	-98.41	-98.41	54.17	127.65	-136.47
167	IC8KETAC	-99.64	-99.64	54.94	126.32	-137.3

168	IC8KETBA	-99.21	-99.21	52.77	129.67	-137.87
169	IC8KETBC	-103.44	-103.44	53.44	121.17	-139.57
170	IC8KETBD	-99.21	-99.21	52.77	128.86	-137.63
171	IC8KETDB	-99.11	-99.11	54.11	126.83	-136.93
172	IC8KETDC	-99.07	-99.07	54.61	123.25	-135.82
173	IC8KETDD	-94.84	-94.84	53.97	129.56	-133.47
174	CC8H16OH-B	-53.59	-53.59	47.55	113.23	-87.35
175	BC8H16OH-C	-53.11	-53.11	48.04	115.1	-87.42
176	CC8H16OH-BO2	-88.41	-88.41	55.74	127.21	-126.34
177	CC8H16O-BO2H	-72.55	-72.55	56.79	125.53	-109.98
178	BC8H16OH-CO2	-87.21	-87.21	55.96	126.62	-124.96
179	BC8H16O-CO2H	-71.35	-71.35	57.03	124.94	-108.6
180	DC6H12CHO-D	-30.53	-30.53	40.24	104.9	-61.81
181	IC3H7COC3H6-T	-37.9	-37.9	39.19	101.44	-68.15
182	TC4H9COC2H5	-76.01	-76.01	40.32	102.81	-106.66
183	TC4H9COC2H4S	-36.2	-36.2	39.07	100.44	-66.15
184	HC6H12CHO	-29.53	-29.53	40.14	101.14	-59.69
185	OC7H13OOH-N	-43.13	-43.13	45.29	113.77	-77.06
186	OC7H13O-N	-5.78	-5.78	38.96	103.32	-36.59
187	PC7H13OOH-O	-40.24	-40.24	45.49	110.4	-73.16
188	OC7H13OOH-Q	-42.52	-42.52	45.63	114.24	-76.59
189	OC7H13O-Q	-4.44	-4.44	38.99	101.14	-34.6
190	DC6H11-D	44.69	44.69	30.83	91.58	17.39
191	IC3H6CHCOCH2	-4.42	-4.42	32.17	90.25	-31.33
192	C4H8OH-1	-19.71	-19.71	24.71	90.39	-46.66
193	C5H11O2-1	-21.79	-21.79	35.03	103.53	-52.66
194	C5H11O2H-1	-55.6	-55.6	37.06	104.66	-86.8
195	C5H11O-1	-19.03	-19.03	30.85	93.91	-47.03
196	C5H11O-2	-23.4	-23.4	31.44	93.28	-51.21
197	C5H10OOH1-2	-9.24	-9.24	35.43	109.1	-41.77
198	C5H10OOH1-3	-9.24	-9.24	35.43	109.1	-41.77
199	C5H10OOH1-4	-9.24	-9.24	35.43	109.1	-41.77
200	C5H10OOH2-3	-13.51	-13.51	35.56	106.36	-45.22
201	C5H10OOH1-2O2	-46.46	-46.46	43.56	120.73	-82.46
202	C5H10OOH1-3O2	-46.46	-46.46	43.56	120.73	-82.46
203	C5H10OOH1-4O2	-46.46	-46.46	43.56	120.73	-82.46
204	C5H10OOH2-4O2	-50.74	-50.74	43.7	117.99	-85.91
205	C5H10O1-3	-32.59	-32.59	26.77	81.71	-56.95
206	C5H10O1-4	-52.94	-52.94	25.13	82.69	-77.59
207	NC5KET12	-77.5	-77.5	37.63	109.59	-110.17
208	NC5KET13	-79.04	-79.04	38.7	108.78	-111.47
209	NC5KET14	-79.04	-79.04	38.7	108.78	-111.47
210	NC5KET24	-86.49	-86.49	37.98	107.69	-118.6
211	NC3H7COC2H4P	-18.13	-18.13	34.83	103.51	-48.99
212	C6H12O1-2	-36.67	-36.67	34.04	94.57	-64.87
213	C6H12O1-3	-37.52	-37.52	32.24	92.5	-65.1

214	C6H13O2H-1	-60.53	-60.53	42.48	114.08	-94.54
215	C6H13O2-1	-26.72	-26.72	40.52	112.95	-60.4
216	C6H12OOH1-2	-14.17	-14.17	40.9	118.52	-49.51
217	C6H12OOH1-3	-14.17	-14.17	40.9	118.52	-49.51
218	C6H12OOH1-4	-14.17	-14.17	40.9	118.52	-49.51
219	C6H12OOH1-2O2	-51.4	-51.4	46.82	130.15	-90.2
220	C6H12OOH1-3O2	-51.4	-51.4	46.82	130.15	-90.2
221	C6H12OOH1-4O2	-51.4	-51.4	46.82	130.15	-90.2
222	NC6KET12	-76.43	-76.43	38.57	127.37	-114.4
223	NC6KET13	-83.97	-83.97	44.18	118.2	-119.21
224	NC6KET14	-83.97	-83.97	44.18	118.2	-119.21
225	C6H13O-1	-23.96	-23.96	36.33	103.33	-54.77
226	C7H14-2	-17.84	-17.84	36.56	101.04	-47.97
227	C7H14-3	-17.67	-17.67	36.23	101.42	-47.91
228	C7H15O2-4	-35.92	-35.92	46.08	118.26	-71.18
229	C7H15O2H-1	-65.46	-65.46	47.99	123.5	-102.28
230	C7H15O-1	-28.89	-28.89	41.82	112.75	-62.51
231	C7H14OOH4-2	-23.37	-23.37	46.5	123.83	-60.29
232	C7H14OOH1-2O2	-56.33	-56.33	54.1	139.57	-97.94
233	C7H14OOH1-3O2	-56.33	-56.33	54.1	139.57	-97.94
234	C7H14OOH1-4O2	-56.33	-56.33	54.1	139.57	-97.94
235	C7H14OOH4-2O2	-60.6	-60.6	54.31	136.83	-101.39
236	NC7KET12	-84.96	-84.96	49.1	126.54	-122.69
237	NC7KET13	-88.9	-88.9	49.66	127.62	-126.95
238	NC7KET14	-88.9	-88.9	49.66	127.62	-126.95
239	NC7KET42	-96.74	-96.74	49.55	126.71	-134.52
240	C5H10CHO-1	-10.29	-10.29	34.9	104.41	-41.42
241	C5H10CHO-2	-14.71	-14.71	32.76	105.13	-46.06
242	C5H10CHO-3	-14.71	-14.71	32.76	105.13	-46.06
243	C5H10CHO-4	-14.71	-14.71	32.76	105.13	-46.06
244	C5H10CHO-5	-21.26	-21.26	33.1	98.32	-50.58
245	NC4H9COCH3	-66.75	-66.75	34.98	99.91	-96.54
246	C9H19-3	-8.56	-8.56	48.99	126.84	-46.38
247	C9H19-5	-8.56	-8.56	48.99	126.84	-46.38
248	C9H18-2	-27.7	-27.7	47.49	120.69	-63.69
249	C9H18-3	-27.53	-27.53	47.14	120.26	-63.39
250	C10H21O-1	-43.68	-43.68	58.28	141.01	-85.73
251	C10H21O-2	-48.05	-48.05	58.79	139.01	-89.5
252	C10H21O-3	-48.05	-48.05	58.79	139.01	-89.5
253	C10H21O-4	-48.05	-48.05	58.79	139.01	-89.5
254	C10H21O-5	-48.05	-48.05	58.79	139.01	-89.5
255	C9H19O-1	-38.75	-38.75	52.8	131.59	-77.99
256	C8H17O-1	-33.82	-33.82	47.31	122.17	-70.25
257	C9H19O2-4	-46.16	-46.16	57.01	138.08	-87.33
258	C9H19O2-5	-46.16	-46.16	57.01	138.08	-87.33
259	C10H21O2H-1	-81.04	-81.04	64.46	151.47	-126.2

260	C10H21O2H-2	-84.5	-84.5	64.61	148.66	-128.82
261	C10H21O2H-3	-84.5	-84.5	64.61	148.66	-128.82
262	C10H21O2H-4	-84.5	-84.5	64.61	148.66	-128.82
263	C10H21O2H-5	-84.5	-84.5	64.61	148.66	-128.82
264	C9H19O2H-1	-76.11	-76.11	58.98	142.04	-118.46
265	C8H17O2H-1	-71.18	-71.18	53.48	132.62	-110.72
266	C10OOH2-1	-35.49	-35.49	63.84	152.08	-80.84
267	C10OOH2-6	-38.14	-38.14	62.92	153.1	-83.79
268	C10OOH3-1	-35.49	-35.49	63.84	152.08	-80.84
269	C10OOH3-7	-38.14	-38.14	62.92	153.1	-83.79
270	C10OOH4-7	-38.14	-38.14	62.92	153.1	-83.79
271	C10OOH4-8	-38.14	-38.14	62.92	153.1	-83.79
272	C10OOH5-9	-38.14	-38.14	62.92	153.1	-83.79
273	C9OOH1-2	-29.75	-29.75	57.31	146.49	-73.43
274	C9OOH1-3	-29.75	-29.75	57.31	146.49	-73.43
275	C9OOH1-4	-29.75	-29.75	57.31	146.49	-73.43
276	C9OOH5-3	-33.21	-33.21	57.44	143.67	-76.05
277	C8OOH1-2	-24.82	-24.82	51.83	137.06	-65.69
278	C8OOH1-3	-24.82	-24.82	51.83	137.06	-65.69
279	C8OOH1-4	-24.82	-24.82	51.83	137.06	-65.69
280	C10OOH1-2O2	-72.29	-72.29	70.54	167.15	-122.12
281	C10OOH1-3O2	-72.29	-72.29	70.54	167.15	-122.12
282	C10OOH1-4O2	-72.29	-72.29	70.54	167.15	-122.12
283	C10OOH2-1O2	-72.29	-72.29	70.54	167.15	-122.12
284	C10OOH2-3O2	-75.75	-75.75	70.75	164.34	-124.74
285	C10OOH2-4O2	-75.75	-75.75	70.75	164.34	-124.74
286	C10OOH2-5O2	-75.75	-75.75	70.75	164.34	-124.74
287	C10OOH3-1O2	-72.29	-72.29	70.54	167.15	-122.12
288	C10OOH3-2O2	-75.75	-75.75	70.75	164.34	-124.74
289	C10OOH3-4O2	-75.75	-75.75	70.75	164.34	-124.74
290	C10OOH3-5O2	-75.75	-75.75	70.75	164.34	-124.74
291	C10OOH3-6O2	-75.75	-75.75	70.75	164.34	-124.74
292	C10OOH4-1O2	-72.29	-72.29	70.54	167.15	-122.12
293	C10OOH4-2O2	-75.75	-75.75	70.75	164.34	-124.74
294	C10OOH4-3O2	-75.75	-75.75	70.75	164.34	-124.74
295	C10OOH4-5O2	-75.75	-75.75	70.75	164.34	-124.74
296	C10OOH4-6O2	-75.75	-75.75	70.75	164.34	-124.74
297	C10OOH4-7O2	-75.75	-75.75	70.75	164.34	-124.74
298	C10OOH5-2O2	-75.75	-75.75	70.75	164.34	-124.74
299	C10OOH5-3O2	-75.75	-75.75	70.75	164.34	-124.74
300	C10OOH5-4O2	-75.75	-75.75	70.75	164.34	-124.74
301	C10OOH5-6O2	-75.75	-75.75	70.75	164.34	-124.74
302	C10OOH5-7O2	-75.75	-75.75	70.75	164.34	-124.74
303	C10OOH5-8O2	-75.75	-75.75	70.75	164.34	-124.74
304	C9OOH1-2O2	-67.36	-67.36	65.08	157.73	-114.38
305	C9OOH1-3O2	-67.36	-67.36	65.08	157.73	-114.38

306	C8OOH1-2O2	-62.43	-62.43	59.62	148.31	-106.64
307	C8OOH1-3O2	-62.43	-62.43	59.62	148.31	-106.64
308	C8OOH1-4O2	-62.43	-62.43	59.62	148.31	-106.64
309	C10O2-6	-86.79	-86.79	52.19	119.58	-122.44
310	C10O3-4	-60.76	-60.76	55.89	133.48	-100.55
311	C10O3-7	-86.79	-86.79	52.19	119.58	-122.44
312	C10O4-7	-82.53	-82.53	51.95	128.92	-120.97
313	C9O1-3	-53.2	-53.2	47.97	122.16	-89.62
314	C9O1-4	-73.23	-73.23	46.11	120.13	-109.05
315	C8O1-2	-46.52	-46.52	44.46	115.27	-80.89
316	C10KET1-2	-101.45	-101.45	65.55	154.44	-147.5
317	C10KET1-3	-103.67	-103.67	66.1	155.52	-150.04
318	C10KET1-4	-103.67	-103.67	66.1	155.52	-150.04
319	C10KET2-1	-104.66	-104.66	65.27	156.9	-151.44
320	C10KET2-3	-109.29	-109.29	65.44	153.53	-155.07
321	C10KET2-4	-111.51	-111.51	66.02	154.61	-157.61
322	C10KET2-5	-111.51	-111.51	66.02	154.61	-157.61
323	C10KET3-1	-108.05	-108.05	65.88	157.42	-154.98
324	C10KET3-2	-109.29	-109.29	65.44	153.53	-155.07
325	C10KET3-4	-109.29	-109.29	65.44	153.53	-155.07
326	C10KET3-5	-111.51	-111.51	66.02	154.61	-157.61
327	C10KET3-6	-111.51	-111.51	66.02	154.61	-157.61
328	C10KET4-1	-108.05	-108.05	65.88	157.42	-154.98
329	C10KET4-2	-111.51	-111.51	66.02	154.61	-157.61
330	C10KET4-3	-109.29	-109.29	65.44	153.53	-155.07
331	C10KET4-5	-109.29	-109.29	65.44	153.53	-155.07
332	C10KET4-6	-111.51	-111.51	66.02	154.61	-157.61
333	C10KET4-7	-111.51	-111.51	66.02	154.61	-157.61
334	C10KET5-2	-111.51	-111.51	66.02	154.61	-157.61
335	C10KET5-3	-111.51	-111.51	66.02	154.61	-157.61
336	C10KET5-4	-109.29	-109.29	65.44	153.53	-155.07
337	C10KET5-6	-109.29	-109.29	65.44	153.53	-155.07
338	C10KET5-7	-111.51	-111.51	66.02	154.61	-157.61
339	C10KET5-8	-111.51	-111.51	66.02	154.61	-157.61
340	C9KET1-2	-96.52	-96.52	60.07	145.02	-139.76
341	C9KET1-3	-98.74	-98.74	60.62	146.1	-142.3
342	C8KET1-2	-91.59	-91.59	54.58	135.59	-132.02
343	C8KET1-3	-93.81	-93.81	55.14	136.67	-134.56
344	C8KET1-4	-93.81	-93.81	55.14	136.67	-134.56
345	NC8H17CHO	-74.09	-74.09	52.1	129.26	-112.63
346	NC8H17CO	-37.18	-37.18	51.27	130.38	-76.06
347	C7H15COCH2	-37.85	-37.85	56.42	141.19	-79.95
348	C6COC2H4P	-32.92	-32.92	51.22	131.77	-72.21
349	C5COC2H4P	-27.99	-27.99	45.76	122.35	-64.47
350	C4COC2H4P	-23.06	-23.06	40.27	112.93	-56.73
351	C2H2OH	29.39	29.39	15.8	61.34	11.11

352	C2H3CHOCH2	2	2	19.77	71.82	-19.41
353	C4H6O23	-17.3	-17.3	18.07	67.94	-37.55
354	CH3CHCHCHO	-25.7	-25.7	18.18	79.62	-49.44
355	CC3H4	66.2	66.2	12.67	58.23	48.84
356	CH3CHCO	-19.61	-19.61	17.87	67.8	-39.83
357	CH3CHCHO	-4.7	-4.7	18	70.37	-25.68
358	C2H5CHCO	-24.37	-24.37	22.94	77.6	-47.51
359	NC3H7CO	-12.53	-12.53	23.93	83.28	-37.36
360	H	52.1	52.1	4.97	27.39	43.93
361	H2	0	0	6.9	31.21	-9.31
362	O	59.56	59.56	5.23	38.47	48.09
363	OH	9.32	9.32	7.15	43.88	-3.77
364	HO2	2.5	2.5	8.32	54.73	-13.82
365	H2O2	-32.53	-32.53	10.4	55.66	-49.13
366	CH2O	-27.7	-27.7	8.38	52.25	-43.28
367	HCO	10.4	10.4	8.23	53.66	-5.6
368	HOCH2O	-43.43	-43.43	13.04	64.81	-62.76
369	CH3OH	-48.06	-48.06	10.48	57.28	-65.14
370	CH2OH	-4.1	-4.1	11.29	58.88	-21.66
371	CH3O	3.9	3.9	9.05	54.61	-12.39
372	CH3O2	2	2	13.89	64.21	-17.14
373	CH4	-17.9	-17.9	8.4	44.47	-31.16
374	CH3	34.82	34.82	9.21	46.38	21
375	CH2	92.49	92.49	8.24	46.72	78.56
376	CH2(S)	101.51	101.51	8.07	45.1	88.07
377	C2H6	-20.04	-20.04	12.52	54.73	-36.36
378	C2H5	28.02	28.02	11.28	60.14	10.09
379	C2H4	12.54	12.54	10.18	52.38	-3.08
380	C2H3	68.42	68.42	9.54	55.34	51.92
381	C2H2	54.2	54.2	10.59	48.02	39.88
382	C2H	135.02	135.02	8.89	49.56	120.24
383	CH3CHO	-39.18	-39.18	13.12	63.14	-58.01
384	CH3CO	-5.4	-5.4	12.38	63.75	-24.41
385	CH2CHO	3.12	3.12	12.88	60.41	-14.89
386	CH2CO	-12.4	-12.4	12.4	57.79	-29.63
387	HCCO	42.45	42.45	12.64	60.75	24.34
388	C2H5OH	-56.21	-56.21	15.39	67.11	-76.21
389	C2H5O	-4.24	-4.24	14.42	65.65	-23.81
390	PC2H4OH	-7.2	-7.2	14.63	70.52	-28.23
391	SC2H4OH	-14.09	-14.09	15.79	67.89	-34.33
392	C2H5O2	-7	-7	18.54	75.27	-29.44
393	C2H3O1-2	31.53	31.53	10.35	61.1	13.32
394	CH3COCH3	-51.57	-51.57	17.84	70.1	-72.46
395	CH3COCH2	-7.26	-7.26	18.35	72.06	-28.74
396	C2H3CHO	-20.32	-20.32	17	67.4	-40.42
397	C2H3CO	11.58	11.58	16.82	66.01	-8.1

398	C2H5CHO	-44.5	-44.5	19.29	72.74	-66.19
399	C2H5CO	-7.6	-7.6	18.47	73.86	-29.62
400	C3H8	-24.82	-24.82	17.58	64.57	-44.07
401	IC3H7	18.2	18.2	17.93	60.11	0.28
402	NC3H7	22.6	22.6	18.02	64.14	3.48
403	C3H6	4.65	4.65	15.38	63.82	-14.38
404	C3H5-A	40.75	40.75	14.81	62.06	22.25
405	C3H5-S	63.76	63.76	15.2	65.21	44.32
406	C3H5-T	61.56	61.56	15.04	65.63	41.99
407	C3H4-P	45.77	45.77	14.47	58.9	28.21
408	C3H4-A	47.64	47.64	14.2	57.95	30.36
409	C3H3	83.05	83.05	15.8	61.49	64.71
410	C3H2	129.61	129.61	14.91	64.82	110.29
411	C3H5O	22.15	22.15	17.54	73	0.39
412	C3H6OOH1-2	0.62	0.62	25.54	88.89	-25.88
413	C3H6OOH1-3	3.27	3.27	25.36	89.23	-23.33
414	C3H6OOH2-1	-1	-1	25.59	85.28	-26.43
415	C3H6OOH1-2O2	-36.6	-36.6	32.58	101.89	-66.98
416	C3H6OOH1-3O2	-32.33	-32.33	32.45	104.62	-63.53
417	C3H6OOH2-1O2	-36.6	-36.6	32.58	101.89	-66.98
418	NC3H7O2	-11.93	-11.93	24.05	84.69	-37.18
419	IC3H7O2	-16.2	-16.2	24.17	80.58	-40.23
420	C3H6O1-3	-18.36	-18.36	15.59	64.86	-37.7
421	C3KET12	-67.64	-67.64	26.72	90.75	-94.69
422	C3KET13	-64.91	-64.91	27.61	92.67	-92.54
423	C3KET21	-71.32	-71.32	27.01	90.94	-98.43
424	C3H51-2,3OOH	-20	-20	33.33	104.98	-51.3
425	C3H52-1,3OOH	-17.98	-17.98	32.93	103.8	-48.93
426	AC3H5OOH	-14.23	-14.23	24.03	82.92	-38.95
427	C4H10	-30.26	-30.26	23.25	73.93	-52.3
428	C4H8-1	-0.11	-0.11	20.48	73.62	-22.06
429	C4H8-2	-3.22	-3.22	20.57	71.03	-24.4
430	PC4H9	18.74	18.74	22.51	77.84	-4.47
431	SC4H9	16.09	16.09	21.69	79.74	-7.68
432	C4H71-1	59	59	20.31	75.01	36.63
433	C4H71-2	56.8	56.8	20.14	75.43	34.31
434	C4H71-3	33.39	33.39	18.95	69.81	12.58
435	C4H71-4	48.9	48.9	19.72	77.03	25.93
436	C4H6	26.08	26.08	19.13	66.61	6.22
437	C4H7O	12.92	12.92	23.06	80.33	-11.03
438	C2H5COCH2	-14.58	-14.58	24.38	80.72	-38.65
439	CH3CHCOCH3	-17.08	-17.08	22.73	78.7	-40.55
440	C2H3COCH3	9.38	9.38	20.53	47.62	-4.82
441	NC3H7CHO	-49.44	-49.44	24.73	82.16	-73.93
442	C3H6CHO-1	-0.43	-0.43	23.99	85.57	-25.94
443	C3H6CHO-2	-3.08	-3.08	23.19	86.6	-28.9

444	C3H6CHO-3	-9.63	-9.63	23.48	79.79	-33.42
445	SC3H5CHO	-28.19	-28.19	22.17	75.99	-50.85
446	SC3H5CO	2.71	2.71	22.03	74.6	-19.53
447	IC4H10	-32.5	-32.5	23.04	70.44	-53.5
448	IC4H9	16.5	16.5	22.28	75.16	-5.91
449	TC4H9	11.7	11.7	17.78	76.37	-11.07
450	IC4H8	-3.8	-3.8	21.48	70	-24.67
451	IC4H7	32.3	32.3	20.89	69.62	11.55
452	TC4H9O2	-24.6	-24.6	30.15	85.18	-50
453	IC4H9O2	-19.1	-19.1	29.23	91.42	-46.36
454	TC4H8O2H-I	-9.4	-9.4	31.77	92.45	-36.96
455	IC4H8O2H-I	-3.9	-3.9	30.56	95.97	-32.51
456	IC4H8O2H-T	-8.7	-8.7	30.27	95.77	-37.25
457	IC4H8O	-31.48	-31.48	23.25	71.25	-52.73
458	CC4H8O	-25.53	-25.53	20.33	69.91	-46.38
459	IC4H9O	-16.13	-16.13	25.07	81.8	-40.52
460	TC4H9O	-23.14	-23.14	25.65	75.42	-45.63
461	IC4H7O	13.7	13.7	23.67	80.56	-10.32
462	IC4H8OH	-24.1	-24.1	25.25	88.5	-50.49
463	IC3H7CHO	-51.21	-51.21	23.45	79.66	-74.96
464	TC3H6CHO	-13.5	-13.5	24.04	76.58	-36.33
465	IC3H7CO	-14.3	-14.3	22.63	81.59	-38.63
466	IC3H6CHO	-2.2	-2.2	22.7	83.08	-26.97
467	IC4H7OH	-38.26	-38.26	24.62	82.02	-62.72
468	IC4H6OH	-2.16	-2.16	24.08	80.26	-26.09
469	IC3H5CHO	-27.34	-27.34	23.08	74.65	-49.6
470	IC3H5CO	4.56	4.56	22.92	73.26	-17.28
471	IC3H6CO	-28.06	-28.06	24.18	75.35	-50.53
472	IC4H7OOH	-24.38	-24.38	30.15	91.48	-51.66
473	TC3H6OH	-23.8	-23.8	20.64	77.63	-46.95
474	IC3H5OH	-38.81	-38.81	19.03	72.63	-60.47
475	CH2CCH2OH	27.09	27.09	18.17	76.27	4.35
476	BC5H11	7.7	7.7	27.58	85.9	-17.91
477	AC5H10	-8.56	-8.56	26.59	81.17	-32.76
478	BC5H10	-11.67	-11.67	26.68	79.96	-35.51
479	CC5H10	-7.03	-7.03	25.69	80.35	-30.99
480	AC5H9-A2	27.54	27.54	26	79.42	3.86
481	AC5H9-C	24.94	24.94	25.05	77.36	1.88
482	CC5H9-B	24.23	24.23	23.89	75.29	1.79
483	AC5H9O-C	4.26	4.26	28.97	89.25	-22.35
484	CC5H9O-B	2.08	2.08	29.4	87.09	-23.89
485	AC6H12	-13.49	-13.49	32.05	90.59	-40.5
486	BC6H12	-16.43	-16.43	31.79	89.76	-43.19
487	CC6H12	-14.9	-14.9	31	88.94	-41.42
488	DC6H12	-12.21	-12.21	31.16	89.77	-38.98
489	AC6H11-A2	22.61	22.61	31.45	88.84	-3.88



490	AC6H11-C	20.01	20.01	30.51	86.78	-5.86
491	AC6H11-E	35.51	35.51	31.28	94.01	7.48
492	BC6H11-E	32.57	32.57	31.02	93.18	4.79
493	CC6H11-A	34.1	34.1	30.15	92.36	6.57
494	CC6H11-B	16.4	16.4	29.19	85.25	-9.02
495	AC6H11O-C	-0.67	-0.67	34.43	98.67	-30.09
496	CC6H11O-B	-5.96	-5.96	34.58	95.68	-34.49
497	C4H7CO1-4	12.69	12.69	26.58	91.01	-14.44
498	C5H10-1	-5.04	-5.04	25.94	83.04	-29.8
499	C5H10-2	-7.98	-7.98	25.68	82.2	-32.49
500	C5H91-3	28.46	28.46	24.4	79.23	4.84
501	C5H91-4	41.31	41.31	24.36	87.48	15.23
502	C5H91-5	43.96	43.96	25.17	86.45	18.19
503	CC5H11	9.65	9.65	26.92	86.48	-16.13
504	C5H92-4	25.52	25.52	24.14	78.39	2.15
505	C5H92-5	41.02	41.02	24.91	85.62	15.5
506	C5H9O1-3	7.78	7.78	28.38	91.12	-19.39
507	C5H9O2-4	4.84	4.84	28.01	92.47	-22.73
508	C5H11-2	11.16	11.16	27.14	89.16	-15.42
509	NC4H9CHO	-54.37	-54.37	30.18	91.58	-81.67
510	NC4H9CO	-17.46	-17.46	29.4	92.7	-45.1
511	C4H8CHO-2	-8.01	-8.01	28.64	96.02	-36.64
512	C4H8CHO-3	-8.01	-8.01	28.64	96.02	-36.64
513	C4H8CHO-4	-14.56	-14.56	28.96	89.21	-41.16
514	IC4H7-11	55.31	55.31	21.31	72.76	33.61
515	C5H81-3	16.4	16.4	24.66	74.99	-5.96
516	XC7H15	-0.53	-0.53	38.49	101.61	-30.83
517	YC7H15	-5.33	-5.33	38.3	102.06	-35.76
518	ZC7H15	-3.18	-3.18	37.63	102.64	-33.78
519	XC7H14	-20.66	-20.66	37.28	97.33	-49.68
520	YC7H14	-23.35	-23.35	37.06	96.5	-52.12
521	XC7H13-X1	15.4	15.4	36.69	95.58	-13.1
522	XC7H13-Z	12.8	12.8	35.74	93.52	-15.08
523	XC7H13-X2	28.3	28.3	36.5	100.75	-1.74
524	XC7H13-Y2	23.7	23.7	36.47	101.19	-6.47
525	YC7H13-Y2	7.91	7.91	35.28	91.43	-19.35
526	YC7H13-X2	25.61	25.61	36.29	99.91	-4.18
527	XC7H13O-Z	-7.84	-7.84	39.79	105.41	-39.27
528	YC7H13O-Y2	-14.41	-14.41	40.65	103.24	-45.19
529	YC7H15O2	-41.63	-41.63	46.41	112.94	-75.31
530	YC7H14OOH-Y2	-31.03	-31.03	47.62	119.31	-66.61
531	Y-YC7H14O	-57.05	-57.05	38.1	92.45	-84.61
532	NEOC5H12	-40.3	-40.3	28.99	72.88	-62.03
533	NEOC5H11	8.7	8.7	28.4	79.47	-14.99
534	NEOC5H11O2	-26.8	-26.8	35.29	94.44	-54.96
535	NEOC5H10OOH	-11.6	-11.6	36.57	101.17	-41.77

536	NEOC6H12	-14.07	-14.07	31.62	83.37	-38.93
537	NEOC6H11	42.83	42.83	31.28	85.18	17.44
538	NC7H15	-1.16	-1.16	39.14	100.07	-31
539	OC7H15	-3.81	-3.81	38.31	98.92	-33.3
540	PC7H15	-3.81	-3.81	38.31	98.92	-33.3
541	QC7H15	-1.16	-1.16	39.14	97.89	-30.35
542	OC7H14	-21.94	-21.94	36.81	91.96	-49.36
543	PC7H14	-20.01	-20.01	37.07	92.79	-47.68
544	OC7H13-N	26.98	26.98	36.05	97.55	-2.1
545	PC7H13-N	28.91	28.91	36.29	98.39	-0.42
546	PC7H13-O	13.41	13.41	35.52	88.98	-13.12
547	AC8H17	-4.43	-4.43	44.4	106.81	-36.28
548	BC8H17	-7.08	-7.08	43.55	105.65	-38.58
549	CC8H17	-10.73	-10.73	44.34	105.08	-42.06
550	DC8H17	-5.23	-5.23	44.4	104.63	-36.43
551	IC8H16	-26.49	-26.49	42.92	99.51	-56.16
552	JC8H16	-26.86	-26.86	43.17	100.35	-56.78
553	IC8H15	9.61	9.61	42.32	99.14	-19.95
554	AC8H17O2	-40.03	-40.03	51.55	122.2	-76.47
555	BC8H17O2	-45.1	-45.1	51.69	117.28	-80.07
556	DC8H17O2	-40.03	-40.03	51.55	120.02	-75.82
557	AC8H16OOH-A	-25.63	-25.63	52.82	126.74	-63.42
558	AC8H16OOH-B	-27.48	-27.48	51.8	127.77	-65.58
559	AC8H16OOH-C	-30.93	-30.93	52.73	127.19	-68.86
560	BC8H16OOH-C	-36	-36	52.87	122.28	-72.46
561	BC8H16OOH-A	-29.9	-29.9	52.96	124.01	-66.88
562	BC8H16OOH-D	-29.9	-29.9	52.96	121.83	-66.23
563	DC8H16OOH-C	-30.93	-30.93	52.73	126.39	-68.62
564	DC8H16OOH-B	-27.48	-27.48	51.8	125.59	-64.93
565	IC8ETERAA	-46.4	-46.4	44.08	106.3	-78.1
566	IC8ETERAB	-52.52	-52.52	42.71	103.15	-83.27
567	IC8ETERAC	-76.58	-76.58	41.22	97.3	-105.59
568	IC8ETERBC	-57.58	-57.58	45.55	100.43	-87.52
569	IC8ETERBD	-52.52	-52.52	42.71	100.97	-82.62
570	CC8H16OH-D	-50.94	-50.94	48.46	112.21	-84.39
571	YC7H13OOH-X1	-43.93	-43.93	45.67	116.6	-78.7
572	YC7H13O-X1	-5.85	-5.85	39.2	105.68	-37.36
573	XC7H13OOH-Z	-44.23	-44.23	45.69	115.14	-78.56
574	YC7H13OOH-X2	-44.54	-44.54	45.32	119.68	-80.23
575	YC7H13O-X2	-7.19	-7.19	39.14	109.23	-39.76
576	CC6H11-D	42	42	30.57	90.75	14.95
577	C4H7	32.88	32.88	19.96	72.03	11.41
578	C5H9	28.46	28.46	24.4	79.23	4.84
579	IC5H9	24.94	24.94	25.09	77.36	1.88
580	C5H11-1	13.81	13.81	27.88	87.26	-12.2
581	C5H11O2-2	-26.06	-26.06	35.16	100.79	-56.11

582	C5H10OOH2-4	-13.51	-13.51	35.56	106.36	-45.22
583	C5H10O2-4	-36.96	-36.96	27.38	82.45	-61.55
584	C6H13-1	8.88	8.88	33.43	97.56	-20.21
585	C6H13-2	6.23	6.23	32.59	98.58	-23.16
586	C6H13-3	6.23	6.23	32.59	98.58	-23.16
587	C6H12-1	-9.97	-9.97	31.38	92.46	-37.54
588	C6H12-2	-12.91	-12.91	31.12	91.62	-40.23
589	C6H12-3	-12.74	-12.74	30.79	90.63	-39.76
590	C6H11	20.76	20.76	29.3	88.19	-5.53
591	C6H12O1-4	-57.87	-57.87	30.45	92.11	-85.33
592	C7H15-1	3.95	3.95	38.88	106.98	-27.95
593	C7H15-2	1.3	1.3	38.05	108	-30.9
594	C7H15-3	1.3	1.3	38.05	108	-30.9
595	C7H15-4	1.3	1.3	38.05	106.63	-30.49
596	C7H14-1	-14.9	-14.9	36.82	101.88	-45.28
597	C7H13	18.6	18.6	35.27	98.07	-10.64
598	C7H15O2-1	-31.65	-31.65	45.92	122.37	-68.14
599	C7H14OOH1-2	-19.1	-19.1	46.36	127.94	-57.25
600	C7H14OOH1-3	-19.1	-19.1	46.36	127.94	-57.25
601	C7H14OOH1-4	-19.1	-19.1	46.36	127.94	-57.25
602	C7H14O1-3	-43.33	-43.33	36.92	103.32	-74.14
603	C7H14O1-4	-63.37	-63.37	35.38	101.29	-93.57
604	NC5H11CHO	-59.3	-59.3	35.66	101	-89.41
605	NC5H11CO	-22.39	-22.39	34.84	102.12	-52.84
606	NC4H9COCH2	-24.44	-24.44	34.71	97.19	-53.42
607	C4H7OOH1-4	-21.3	-21.3	28.8	93.25	-49.1
608	C4H7O1-4	16.05	16.05	22.56	82.8	-8.63
609	C10H21-1	-10.84	-10.84	55.24	135.24	-51.16
610	C10H21-2	-13.49	-13.49	54.39	136.26	-54.12
611	C10H21-3	-13.49	-13.49	54.39	136.26	-54.12
612	C10H21-4	-13.49	-13.49	54.39	136.26	-54.12
613	C10H21-5	-13.49	-13.49	54.39	136.26	-54.12
614	C9H19-1	-5.91	-5.91	49.78	125.82	-43.42
615	C9H19-2	-8.56	-8.56	48.99	126.84	-46.38
616	C9H19-4	-8.56	-8.56	48.99	126.84	-46.38
617	C8H17-1	-0.98	-0.98	44.33	116.4	-35.69
618	C8H17-2	-3.63	-3.63	43.5	117.42	-38.64
619	C8H17-3	-3.63	-3.63	43.5	117.42	-38.64
620	C8H17-4	-3.63	-3.63	43.5	117.42	-38.64
621	C10H20-1	-29.69	-29.69	53.2	130.14	-68.5
622	C10H20-2	-32.63	-32.63	52.94	130.11	-71.43
623	C10H20-3	-32.46	-32.46	52.6	129.68	-71.13
624	C10H20-4	-32.46	-32.46	52.6	129.68	-71.13
625	C10H20-5	-32.46	-32.46	52.6	129.68	-71.13
626	C9H18-1	-24.76	-24.76	47.75	120.72	-60.76
627	C8H16-1	-19.83	-19.83	42.3	111.3	-53.02

628	C8H16-2	-22.77	-22.77	42.04	111.27	-55.95
629	C8H16-3	-22.6	-22.6	41.67	110.84	-55.65
630	C8H16-4	-22.6	-22.6	41.67	110.84	-55.65
631	C10H21O2-1	-47.63	-47.63	62.35	150.32	-92.45
632	C10H21O2-2	-51.1	-51.1	62.51	147.51	-95.07
633	C10H21O2-3	-51.1	-51.1	62.51	147.51	-95.07
634	C10H21O2-4	-51.1	-51.1	62.51	147.51	-95.07
635	C10H21O2-5	-51.1	-51.1	62.51	147.51	-95.07
636	C9H19O2-1	-42.7	-42.7	56.96	140.89	-84.71
637	C8H17O2-1	-37.77	-37.77	51.47	131.47	-76.97
638	C8H17O2-4	-41.23	-41.23	51.51	128.66	-79.6
639	C10OOH1-2	-34.68	-34.68	62.78	155.91	-81.17
640	C10OOH1-3	-34.68	-34.68	62.78	155.91	-81.17
641	C10OOH1-4	-34.68	-34.68	62.78	155.91	-81.17
642	C10OOH2-3	-38.14	-38.14	62.92	153.1	-83.79
643	C10OOH2-4	-38.14	-38.14	62.92	153.1	-83.79
644	C10OOH2-5	-38.14	-38.14	62.92	153.1	-83.79
645	C10OOH3-2	-38.14	-38.14	62.92	153.1	-83.79
646	C10OOH3-4	-38.14	-38.14	62.92	153.1	-83.79
647	C10OOH3-5	-38.14	-38.14	62.92	153.1	-83.79
648	C10OOH3-6	-38.14	-38.14	62.92	153.1	-83.79
649	C10OOH4-1	-35.49	-35.49	63.84	152.08	-80.84
650	C10OOH4-2	-38.14	-38.14	62.92	153.1	-83.79
651	C10OOH4-3	-38.14	-38.14	62.92	153.1	-83.79
652	C10OOH4-5	-38.14	-38.14	62.92	153.1	-83.79
653	C10OOH4-6	-38.14	-38.14	62.92	153.1	-83.79
654	C10OOH5-2	-38.14	-38.14	62.92	153.1	-83.79
655	C10OOH5-3	-38.14	-38.14	62.92	153.1	-83.79
656	C10OOH5-4	-38.14	-38.14	62.92	153.1	-83.79
657	C10OOH5-6	-38.14	-38.14	62.92	153.1	-83.79
658	C10OOH5-7	-38.14	-38.14	62.92	153.1	-83.79
659	C10OOH5-8	-38.14	-38.14	62.92	153.1	-83.79
660	C8OOH4-2	-28.28	-28.28	51.97	134.25	-68.31
661	C8OOH4-6	-28.28	-28.28	51.97	134.25	-68.31
662	C10O1-2	-56.39	-56.39	55.46	134.11	-96.37
663	C10O1-3	-58.13	-58.13	53.46	131.58	-97.36
664	C10O1-4	-78.16	-78.16	51.58	129.55	-116.78
665	C10O2-3	-60.76	-60.76	55.89	133.48	-100.55
666	C10O2-4	-62.5	-62.5	53.7	130.95	-101.54
667	C10O2-5	-82.53	-82.53	51.95	128.92	-120.97
668	C10O3-5	-62.5	-62.5	53.7	130.95	-101.54
669	C10O3-6	-82.53	-82.53	51.95	128.92	-120.97
670	C10O4-6	-62.5	-62.5	53.7	130.95	-101.54
671	C8O1-3	-48.27	-48.27	42.47	112.74	-81.88
672	C8O1-4	-68.3	-68.3	40.63	110.71	-101.31
673	NC7H15CHO	-69.16	-69.16	46.61	119.84	-104.89

674	NC6H13CHO	-64.23	-64.23	41.13	110.42	-97.15
675	NC7H15CO	-32.25	-32.25	45.79	120.96	-68.32
676	NC6H13CO	-27.32	-27.32	40.31	111.54	-60.58
677	C6H13COCH2	-32.92	-32.92	51.56	131.77	-72.21
678	C5H11COCH2	-27.99	-27.99	46.42	122.35	-64.47
679	C10H19	13.89	13.89	51	134.12	-26.1
680	C9H17	18.82	18.82	45.55	124.7	-18.36
681	C8H15	23.75	23.75	40.1	115.28	-10.62
682	C6H6	19.81	19.81	19.78	64.37	0.62
683	C6H5	79.44	79.44	20.9	69.83	58.62
684	C6H5OO	31.52	31.52	26	86.21	5.82
685	C6H5O	10.36	10.36	24.66	74.89	-11.97
686	C6H5OH	-25.01	-25.01	25.31	76.95	-47.95
687	C5H6	32	32	16.54	64.46	12.78
688	C5H5	63.85	63.85	19.55	68.15	43.53
689	C5H4O	13.2	13.2	19.35	69.31	-7.46
690	C5H5O	43.35	43.35	21.01	71.38	22.07
691	C4H5-I	77.4	77.4	18.03	68.47	56.99
692	C4H5-N	85.4	85.4	18.68	69.47	64.69
693	C4H4	68.19	68.19	17.41	66.79	48.27
694	C4H3-I	119.2	119.2	19.81	70.19	98.28
695	C4H3-N	127.11	127.11	17.68	67.99	106.83
696	C4H2	111.72	111.72	17.7	59.79	93.89
697	H2C4O	54.6	54.6	17.22	66.44	34.79
698	C5H7	40.71	40.71	16.05	67.98	20.45
699	C*CCJC*C	49.32	49.32	21.05	75.94	26.67
700	C*CC*CCJ	49.12	49.12	22.45	77.21	26.1
701	C*CC*CC	18.21	18.21	24.32	76.58	-4.62
702	CJ*CC*CC*O	52.35	52.35	25.74	81.55	28.03
703	C*CC*CCJ*O	28.14	28.14	25.71	78.77	4.66
704	CJ*CC*O	38.78	38.78	17.39	69.25	18.14
705	C4H612	39.34	39.34	19.21	69.72	18.55
706	C4H6-2	34.67	34.67	18.34	65.98	15
707	CH2CHCHCHO	9.4	9.4	16.78	73.04	-12.37
708	CH3CHCHCO	9.4	9.4	16.78	73.04	-12.37
709	H2CC	99.14	99.14	10.18	52.83	83.39
710	C4H5-2	74.31	74.31	18.77	71.22	53.08
711	HCOOH	-92.62	-92.62	10.67	59.28	-110.29
712	H2CCCH	83.05	83.05	15.8	61.49	64.71
713	C2O	68.51	68.51	10.3	55.68	51.91
714	TOLUEN	11.95	11.95	24.69	76.53	-10.87
715	PHC2H5	7.01	7.01	30.64	85.93	-18.61
716	STYREN	35.24	35.24	29.1	82.31	10.7
717	PHHCO	-8.75	-8.75	25.81	83.34	-33.6
718	C5H4OH	12.31	12.31	22.04	74.13	-9.79
719	NAPHT	36	36	31.62	79.66	12.24

720	INDENE	39.08	39.08	30.56	80.5	15.08
721	PHC3H5-1	32.57	32.57	32.71	95.75	4.03
722	C14H14	34.21	34.21	49.01	115.5	-0.22
723	HEX1245	94.45	94.45	26.78	78.43	71.07
724	C6H615	98.95	98.95	26.66	81.13	74.76
725	MC6H6	80.35	80.35	25.33	71.53	59.02
726	FULVENE	53.45	53.45	25.36	71.53	32.12
727	C6H4O2	-31.1	-31.1	25.93	78.32	-54.45
728	C6H5O2	33.85	33.85	25.98	81.07	9.67
729	C6H5O2H	-0.64	-0.64	27.35	83.78	-25.62
730	C6H3O2	27.53	27.53	25.75	78.62	4.09
731	C6H3O3	-41.61	-41.61	27.39	88.07	-67.87
732	C5H4	111.08	111.08	20.9	70.9	89.94
733	C5H3	135.43	135.43	21	70.55	114.4
734	PHCH2	50.31	50.31	26.08	76.75	27.43
735	PHCH2OH	-24.05	-24.05	28.02	87.32	-50.09
736	PHCH2O	27.2	27.2	24.67	82.11	2.72
737	PHCO	26.05	26.05	25.65	84.74	0.79
738	PHCH2O2	28.98	28.98	31.25	95	0.66
739	APHC2H4	55.13	55.13	30.62	86.87	29.23
740	BPHC2H4	40.33	40.33	29.92	85.71	14.77
741	ASTYRYL	92.55	92.55	28.58	82.19	68.04
742	BSTYRYL	82.34	82.34	27.23	81.23	58.12
743	PHC2H	78.27	78.27	27.49	79.44	54.58
744	C6H4C2H3	93.74	93.74	28.12	82.65	69.1
745	PHCH2HCO	-10.89	-10.89	30.47	95.07	-39.24
746	PHCH2CO	26.01	26.01	29.65	96.19	-2.67
747	PHCOCH2	88.82	88.82	31.01	94.61	60.61
748	C6H5CCO	55.42	55.42	32.4	96.08	26.77
749	PHCHCO	10.97	10.97	31.77	87.83	-15.22
750	PBZJA	50.02	50.02	36	96.33	21.3
751	PBZJB	48.92	48.92	35.86	96.49	20.15
752	PBZJC	35.21	35.21	35.45	94.92	6.91
753	BPHPROPY	46.14	46.14	36.16	94.97	17.82
754	PHC3H5-2	27.36	27.36	34.42	94.62	-0.85
755	PHC3H4	63.47	63.47	33.89	92.06	36.02
756	PHC2H4HCO	-17.15	-17.15	37.64	102.43	-47.69
757	PHC2H4CO	19.75	19.75	36.81	103.55	-11.12
758	PHCH2COCH2	24.4	24.4	36.2	106.14	-7.24
759	PHCOC2H4	83.5	83.5	37.14	104.21	52.43
760	PHCOC2H3	6.06	6.06	33.68	102.34	-24.45
761	BPHC3H5OHA	12.68	12.68	39	109.05	-19.84
762	APHC3H5OHB	9.83	9.83	39.81	107.77	-22.3
763	CPHC3H5OHB	-5.67	-5.67	39.31	106.77	-37.51
764	BPHC3H5OHC	9.33	9.33	37.52	112.21	-24.12
765	PBZOHAQJB	-22.28	-22.28	45.64	123.77	-59.19

766	PBZOHBQJA	-22.28	-22.28	45.64	123.77	-59.19
767	PBZOHBQJC	-25.52	-25.52	45.44	123.94	-62.48
768	PBZOHCQJB	-25.52	-25.52	45.44	123.94	-62.48
769	COPHC3H4-1	44.92	44.92	35.45	102.06	14.5
770	AOPHC3H4-2	44.27	44.27	35.17	97.71	15.14
771	PHCH2CHCO	8.31	8.31	35.22	99.73	-21.42
772	PHCOCH2CH2O2	-15.68	-15.68	44.88	114.97	-49.95
773	PHCOCH2CH2O2H	-50.78	-50.78	46.65	119.41	-86.38
774	PHCOCH2CH2O	-15.32	-15.32	40.35	106.76	-47.15
775	PHCH2COCH2O2	-6.41	-6.41	42.27	121.37	-42.6
776	PHCH2COCH2O2H	-42.51	-42.51	44.3	121.15	-78.64
777	PHCH2COCH2O	-6.12	-6.12	38.47	112.39	-39.63
778	CH3C6H4C2H3	27.55	27.55	34.56	92.86	-0.13
779	C10H9	54.86	54.86	34.25	86.92	28.95
780	C10H10	28	28	34.41	85.89	2.39
781	C6H4C2H	133.61	133.61	26.83	78.83	110.1
782	C7H5	112.29	112.29	26.55	78.54	88.87
783	C7H6	85.2	85.2	24.89	75.8	62.6
784	c-C4H5	72	72	15.35	63.68	53.02
785	c-C5H4	131.13	131.13	17.22	66.69	111.24
786	A1C2HAC	146.53	146.53	36.44	94.86	118.24
787	A2O	34.8	34.8	20.18	102.8	4.15
788	A2OH	-8.06	-8.06	37.84	90.3	-34.99
789	A1C2H3AC	105.17	105.17	36.97	104.07	74.14
790	INDENYL	68.38	68.38	29.51	79.68	44.63
791	INDENOXY	39.64	39.64	22.02	99.59	9.95
792	PHNTHRN	49.51	49.51	44.27	93.93	21.5
793	PHCCH2	86.51	86.51	27.8	81.31	62.26
794	PHCHCH	96.46	96.46	30.34	83	71.71
795	C6H4CH3	73.27	73.27	24.79	81.33	49.02
796	A2CH3-1	27.93	27.93	38.54	90.42	0.97
797	C6H4OH	38.1	38.1	25.2	75.06	15.73
798	PHCC	133.21	133.21	26.29	78.05	109.94
799	C9H10	27	27	35.1	91.7	-0.34
800	C9H9-1	12.47	12.47	10.55	52.45	-3.17
801	A2T2	120.58	120.58	31.88	81.88	96.17
802	A2T1	118	118	31.72	83.15	93.21
803	A2-1	94.7	94.7	30.18	83.15	69.91
804	A2-2	94.31	94.31	30.54	83.35	69.46
805	BIPHENYL	43.54	43.54	39.82	92.94	15.83
806	FLUORENE	41.83	41.83	41.73	92.52	14.25
807	A2C2H2	112.3	112.3	39.83	100.8	82.25
808	A2C2H	90.6	90.6	39.41	91.23	63.4
809	A2R5-	119.42	119.42	37.1	89.6	92.7
810	A2R5	62.1	62.1	36.36	86.36	36.35
811	P2-	102	102	36.79	96.72	73.16

812	C13H12	38.79	38.79	43.3	103.87	7.82
813	C13H9	90.59	90.59	39.78	93.19	62.8
814	A3-1	108.51	108.51	42.59	97.32	79.49
815	A3-4	107.24	107.24	44.12	96.44	78.49
816	A2(C2H)2	176.23	176.23	48.89	102.69	145.61
817	ANTHRCN	55.18	55.18	44.76	93.87	27.19
818	C13H9CH2	90.22	90.22	47.87	104.28	59.13
819	C13H8CH2	65.45	65.45	45.39	96.8	36.59
820	C14H13	67.26	67.26	48.41	115.12	32.94
821	C14H11	90.05	90.05	48.54	108.51	57.7
822	PHC2H-	132.71	132.71	26.3	78.07	109.43
823	C14H13OO	45.56	45.56	54.97	134.76	5.38
824	C14H13OOH	11.36	11.36	57.07	134.54	-28.75
825	C14H13O	47.32	47.32	50.32	126.24	9.69
826	C14H12OOH	45.76	45.76	57.94	130.87	6.74
827	C14H12O2H-1O2	22.62	22.62	62.69	150.7	-22.31
828	C14H11O-1O2H	-16.5	-16.5	57.59	139.69	-58.15
829	o-C6H4	106.61	106.61	19.49	68.04	86.33
830	BICYCLO	85.46	85.46	37.74	87.32	59.42
831	DIBZFUL	13.19	13.19	39.09	89.69	-13.55
832	DIBZFURNYL	76.65	76.65	41.48	69.65	55.89
833	DIBZFURNOXY	13.19	13.19	39.09	89.69	-13.55
834	A3CH3	42.01	42.01	52.63	106.5	10.26
835	A3CH2	79.72	79.72	52.2	104.9	48.44
836	FLTHN	69.79	69.79	48.95	99.34	40.17
837	A3C2H2	130.34	130.34	51.69	112.86	96.69
838	A3C2H	109.1	109.1	51.85	105.31	77.7
839	PYRENE	53.9	53.9	48.39	95.81	25.33
840	A4-1	115.25	115.25	48.5	99.06	85.72
841	A4-2	115.16	115.16	48.77	97.8	86
842	A4-4	115.06	115.06	48.66	99.21	85.48
843	A2R5R5	100.28	100.28	40.43	86.17	74.59
844	C14H12	57.93	57.93	47.97	108.39	25.62
845	CHRYSEN	66.63	66.63	57.3	111.2	33.47
846	CHRYSEN-1	126.68	126.68	56.5	112.32	93.19
847	CHRYSEN-4	126.68	126.68	56.5	112.32	93.19
848	CHRYSEN-5	126.68	126.68	56.5	112.32	93.19
849	A3C2H-2	160.91	160.91	52.55	110.47	127.97
850	A3C2H-1	162.96	162.96	52.39	109.81	130.22
851	C6H2	167.5	167.5	24.88	71.51	146.18
852	C6H	248	248	22.95	74.68	225.73
853	C8H2	223.3	223.3	31.7	83.1	198.52
854	C8H	277.74	277.74	31.65	85.74	252.17
855	C4H	192	192	15.96	63.47	173.07
856	BGHIF	85.69	85.69	53.45	98.35	56.37
857	BAPYR	69.21	69.21	64.95	111.97	35.82



858	BAPYR*S	129.26	129.26	64.21	113.09	95.55
859	A4C2H*	169.26	169.26	58.11	111.83	135.91
860	A3C2H*	170.58	170.58	52.25	107.3	138.59
861	A2C2H*	150.32	150.32	39.34	91.9	122.92
862	A1C2H-	132.71	132.71	26.3	78.07	109.43
863	N-C8H7	93	93	30.46	82.31	68.46
864	C2H5OO	-4.53	-4.53	18.22	74.79	-26.83
865	CH3OOH	-31.65	-31.65	17.45	67.53	-51.78
866	CH3OO	4.3	4.3	13.89	66.56	-15.54
867	C2H5OOH	-39.17	-39.17	19.95	73.74	-61.15
868	HCO3	-31.31	-31.31	13.24	74.08	-53.4
869	HCO3H	-67.41	-67.41	15.18	73.87	-89.43
870	C2-QOOH	8.37	8.37	19.48	79.19	-15.24
871	CH2CHCH2	39.39	39.39	15.77	64.69	20.1
872	CH3CHOOCHO	-33.4	-33.4	26.26	86.17	-59.09
873	CH2CHOOHCHO	-17.48	-17.48	26.1	90	-44.31
874	ETC3H4O2	-62.46	-62.46	20.94	73.71	-84.43
875	CH2OOCHOOHCHO	-53.27	-53.27	32.97	100.9	-83.36
876	C5EN-OO	8.47	8.47	32.42	98.62	-20.93
877	C5EN-QOOH	18.73	18.73	33.82	101.48	-11.52
878	C5EN-OOQOOH-35	-15.46	-15.46	40.62	114.48	-49.59
879	C5EN-OQOOH-35	-54.09	-54.09	34.57	104	-85.1
880	C5H8O	-2.32	-2.32	23.52	80.91	-26.45
881	C5H8	18.05	18.05	25.17	70.87	-3.08
882	CYC5H8	7.82	7.82	19.43	69.61	-12.94
883	NEOC5-QOOH	-12.48	-12.48	36.81	101.3	-42.69
884	NEOC5-OOQOOH	-46.58	-46.58	41.91	117.31	-81.56
885	NEOC5-OQOOH	-79.49	-79.49	37.84	104.51	-110.65
886	NC5H12OO	-28.36	-28.36	35.39	97.3	-57.37
887	NC5-QOOH	-15.46	-15.46	36.65	101.71	-45.78
888	NC5-OOQOOH	-48.59	-48.59	43.31	117.49	-83.62
889	N1C4H9OH	-65.88	-65.88	26.35	85.83	-91.47
890	MEK	-57.37	-57.37	23.77	81.21	-81.58
891	C3H6O2	-80.31	-80.31	22.37	83.38	-105.17
892	C3H7CHO	-50.34	-50.34	25.13	82.24	-74.86
893	NC7-QOOH	-21.41	-21.41	46.67	125.15	-58.72
894	NC7H14O	-62.78	-62.78	36.06	99.62	-92.48
895	NC7-OOQOOH	-69.4	-69.4	49.35	131.28	-108.54
896	NC7-OQOOH	-96.27	-96.27	48.93	129.41	-134.85
897	C3H4O2	-62.46	-62.46	20.94	73.71	-84.43
898	NC7H13OOH	-69.7	-69.7	48.2	121.77	-106.01
899	C7KETONE	-65.45	-65.45	40.21	110.25	-98.32
900	IC8-QOOH	-32.97	-32.97	53.01	132.4	-72.44
901	IC8T-QOOH	-32.97	-32.97	53.01	132.4	-72.44
902	IC8H17	-11.43	-11.43	44.62	102.5	-42
903	IC8H17-OO	-45.87	-45.87	51.72	130.01	-84.63

904	IC8H16O	-67.81	-67.81	41.7	105.49	-99.26
905	IC8-OOQOOH	-67.07	-67.07	59.85	146.08	-110.63
906	IC8-OQOOH	-105	-105	53.69	135.99	-145.55
907	NC10MOOH	-69.7	-69.7	48.2	121.77	-106.01
908	NC10-QOOH	-38.15	-38.15	62.9	156.09	-84.69
909	NC10-OQOOH	-111.5	-111.5	66.05	157.63	-158.49
910	NC10-OOQOOH	-73.06	-73.06	70.69	167.33	-122.95
911	NC3H7OO	-9.45	-9.45	23.73	84.22	-34.56
912	CH3COOH	-103.9	-103.9	15.9	67.43	-124.01
913	TERPHENYL	66.63	66.63	57.3	111.2	33.47
914	P3-	126.68	126.68	56.5	112.32	93.19
915	QUATERPHENYL	89.16	89.16	74.49	148.81	44.79
916	P4-	150.06	150.06	74.07	153.05	104.43
917	TRIPHENYLEN	66.63	66.63	57.3	111.2	33.47
918	A4T-	126.68	126.68	56.5	112.32	93.19
919	QINQUEPHENYL	112.71	112.71	94.65	184.55	57.69
920	P5-	173.72	173.72	94.59	190.9	116.81
921	BENZYL B	38.79	38.79	43.3	103.87	7.82
922	BENZYLBJ	74.14	74.14	44.17	102.95	43.44
923	A1A1CH2-1	71.84	71.84	45.37	103.11	41.1
924	PHCH2CH2	55.96	55.96	29.95	89.58	29.25
925	A1CCA1	99.96	99.96	46.32	106.6	68.18
926	A2C2H-2J3	150.87	150.87	40.79	95.08	122.53
927	A3LJX	116.17	116.17	44.43	96.58	87.37
928	A3LJ2	116.43	116.43	44.49	96.54	87.64
929	A3LJ9	116.31	116.31	44.27	95.36	87.88
930	A2R5YNE1	111.73	111.73	45.44	98.35	82.4
931	A2R5YNE3	113.77	113.77	45.9	99.87	83.99
932	A2R5YNE4	114.65	114.65	45.86	99.42	85.01
933	A2R5YNE5	113.76	113.76	45.65	98.42	84.42
934	A3CH2R	50.55	50.55	44.13	105.13	19.2
935	A3R5	76.94	76.94	49.31	101.12	46.79
936	A2R5YN4J5	177.2	177.2	45.36	99.74	147.46
937	A3R5J7	137.96	137.96	48.95	101.05	107.84
938	A2R5YN5J4	175.78	175.78	45.28	99.18	146.21
939	A3R5J10	137	137	48.9	101.01	106.88
940	A2R5YN3J4	175.86	175.86	45.68	99.47	146.21
941	A2R5YN4J3	176.56	176.56	45.18	98.83	147.09
942	A3LR5JS	142.84	142.84	49.23	106.3	111.15
943	A3LR5	75.23	75.23	49.35	101.23	45.05
944	HB	277.33	277.33	85.89	130.91	238.3
945	A2A1-1	59.12	59.12	52.11	109.71	26.41
946	A2A1-2	59.12	59.12	52.11	109.71	26.41
947	A21C6H4	106.96	106.96	50.38	104.9	75.69
948	A22C6H4	109.25	109.25	49.93	102.4	78.72
949	A2R5YN1J2	177.59	177.59	44.83	98.45	148.23

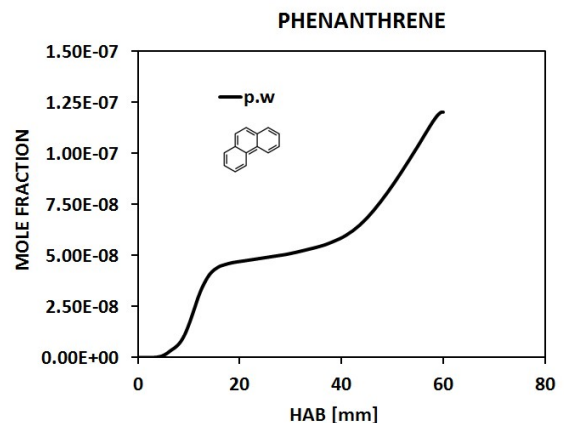
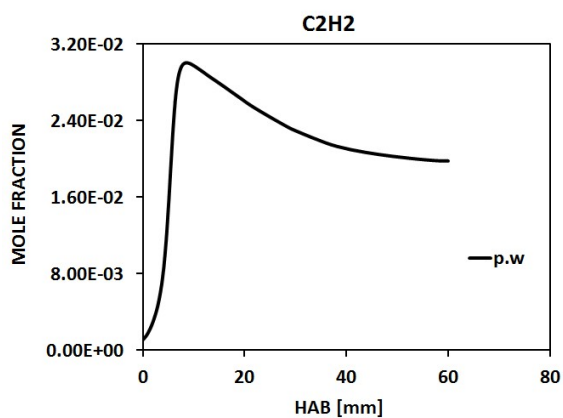
950	FLTHNJ7	130.74	130.74	48.59	100.96	100.64
951	FLTHNJ1	130.82	130.82	48.66	100.76	100.77
952	FLTHNJ3	131.33	131.33	48.58	100.78	101.28
953	BENZNAP	54.69	54.69	57.51	122.25	18.24
954	BENZNAPJP	116.24	116.24	56.74	123.37	79.46
955	BENZFLRN	58.01	58.01	57.6	81.91	33.59
956	A3LC2H-1	107.85	107.85	53.49	108.3	75.56
957	A3LC2H-1P	169.41	169.41	52.58	109.42	136.78
958	A3LC2H-2	107.68	107.68	53.53	108.69	75.27
959	A3LC2H-2P	169.24	169.24	52.73	109.81	136.5
960	A3LC2H-2S	167.74	167.74	52.73	109.81	135
961	A4LJS	135.8	135.8	56.5	112.57	102.24
962	A4L	75.75	75.75	57.3	108.7	43.34
963	A3A1-1	71.46	71.46	66.12	122.77	34.85
964	A3-9	109.23	109.23	43.96	96.52	80.45
965	A3A1-9	71.46	71.46	66.12	122.77	34.85
966	BBFLUOR	84.11	84.11	61.9	115.82	49.58
967	A2A2-12	75.33	75.33	66.12	122.77	38.72
968	BKFLUOR	86.05	86.05	61.89	114.3	51.97
969	FLRNA1-4	65.36	65.36	61.09	121.16	29.23
970	CPTRPHEN	62.35	62.35	57.83	118.19	27.11
971	A4C2H*S	169.26	169.26	58.11	111.83	135.91
972	BEPYREN	73.13	73.13	61.47	114.33	39.04
973	BEPYRENJS	133.18	133.18	60.65	115.45	98.76
974	A3A1-4	71.46	71.46	66.12	122.77	34.85
975	A2A2-11	75.33	75.33	66.12	122.77	38.72
976	PERYLEN	78.31	78.31	61.55	113.9	44.35
977	PERYLENJS	138.36	138.36	60.74	115.02	104.07
978	PYRNA1-1	77.03	77.03	70.39	126.37	39.35
979	PYRNA1-4	77.03	77.03	70.39	126.37	39.35
980	INPYR	91.51	91.51	64.4	114.07	57.5
981	BBFLUORJS	144.16	144.16	61.1	116.94	109.3
982	BGHIFJ	154.42	154.42	53.01	107.11	122.48
983	CPCDFLTH	110.13	110.13	54.79	105.86	78.57
984	CPCDFLTJS	170.19	170.19	54	106.98	138.29
985	BGHIFR	125.06	125.06	55.7	106.8	93.22
986	BGHIFRJS	185.12	185.12	54.92	109.3	152.53
987	COR1	155.82	155.82	64.39	113.91	121.85
988	CPCDPYR	87.27	87.27	54.19	104.98	55.97
989	DCPCDFG	118.47	118.47	59.2	108.49	86.13
990	COR	119.91	119.91	58.98	105.81	88.36
991	CPCDPYRJS	147.33	147.33	53.39	106.1	115.69
992	CORJ	179.92	179.92	58.13	110.11	147.09
993	COR1J	213.82	213.82	63.52	115.11	179.5
994	COR2	188.02	188.02	69.68	119.01	152.54
995	COR2J	246.13	246.13	68.81	120.11	210.31

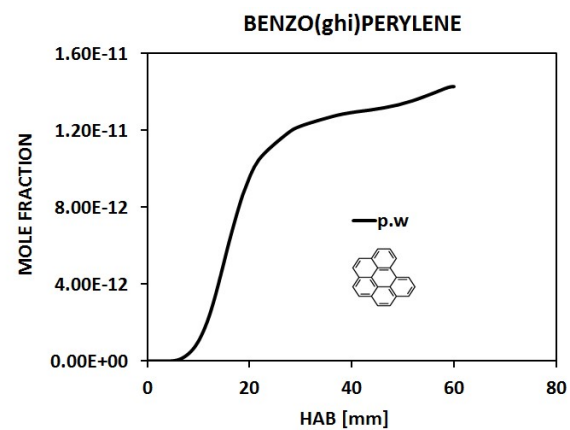
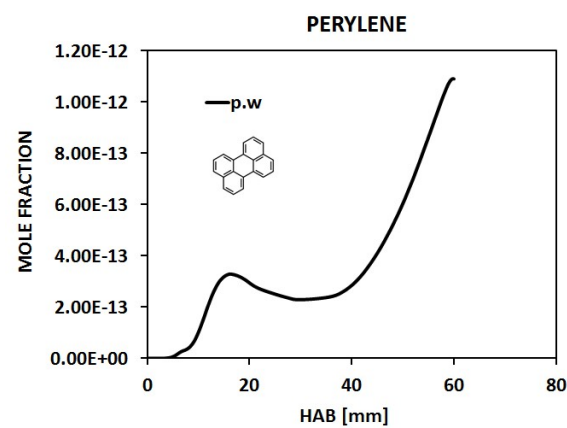
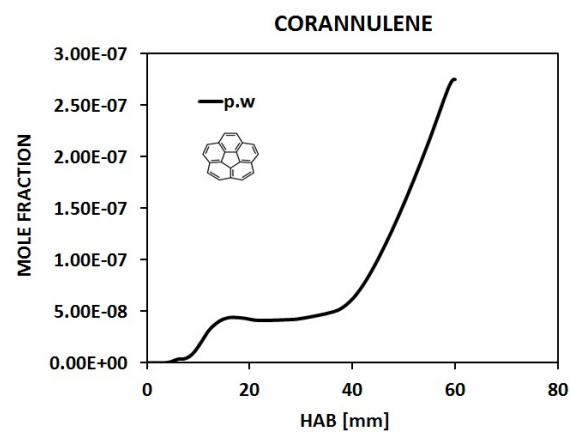
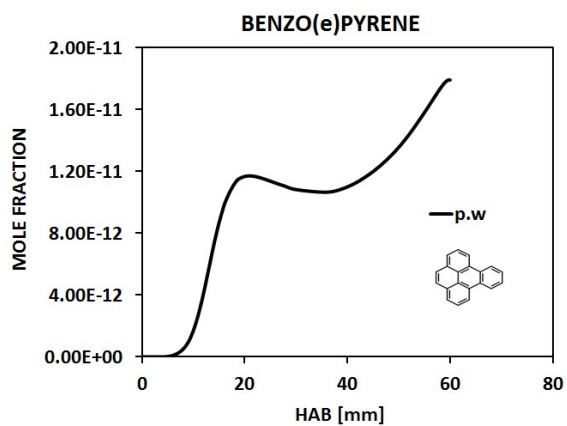
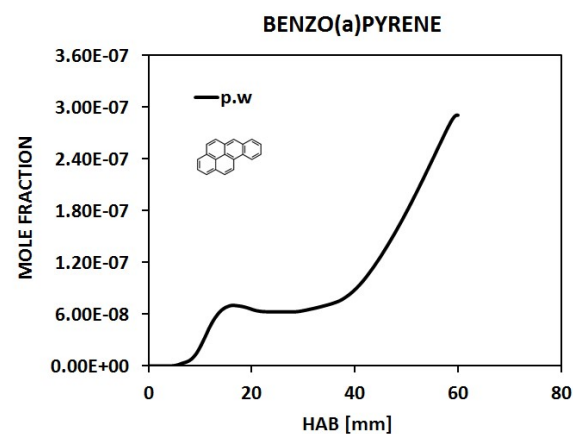
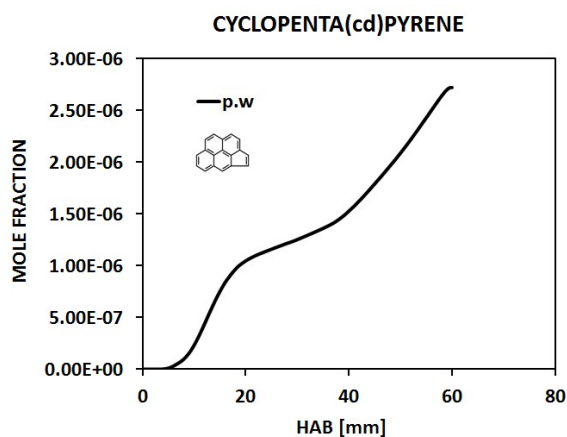
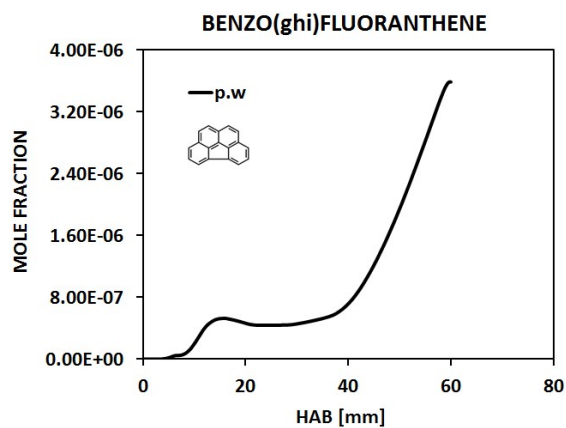
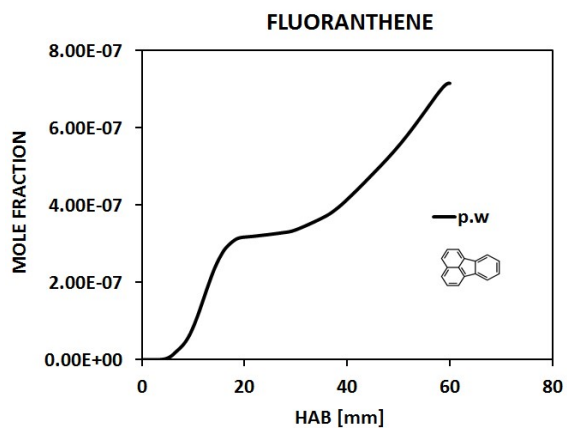
996	COR3	219.72	219.72	75.27	124.01	182.75
997	COR3J	277.73	277.73	74.35	125.11	240.43
998	COR4	250.53	250.53	80.55	129.11	212.03
999	COR4J	308.63	308.63	79.64	130.21	269.81
1000	ANTHAN	74.41	74.41	70.18	112.82	40.77
1001	ANTHANJP	134.46	134.46	70.24	116.69	99.67
1002	ANTHANJS	134.46	134.46	70.24	116.69	99.67
1003	BGHIPER	72.21	72.21	70.18	115.57	37.75
1004	BGHIPEJP1	132.26	132.26	70.24	116.69	97.47
1005	CPBPER	112.59	112.59	70.13	125.39	75.21
1006	BGHIPEJS1	132.26	132.26	70.24	116.69	97.47
1007	CORONEN	77.41	77.41	71.73	114.23	43.35
1008	A3L-O	43.41	43.41	50.24	78.92	19.89
1009	A3O-4	43.02	43.02	50.58	74.95	20.68
1010	A4	68.21	68.21	57.21	111.85	34.86
1011	A3LA1-X	128.26	128.26	56.41	112.97	94.58
1012	A4-O	59.62	59.62	62.66	91.98	32.19
1013	C13H9A1-	93.06	93.06	56.35	75.7	70.49
1014	C13H9A1	59.26	59.26	56.72	80.74	35.19
1015	CORONEN-O	71.21	71.21	71.37	125.46	33.8
1016	CORONENYL	138.31	138.31	67.28	120.67	102.33

Table 17 : Heat of formation used of all species at 298.15 K.

## D. Mechanism Validation and Modeling Results

### 1. Methane premixed flame ( $\phi=2.32$ ): predicted mole fractions of acetylene and PAHs





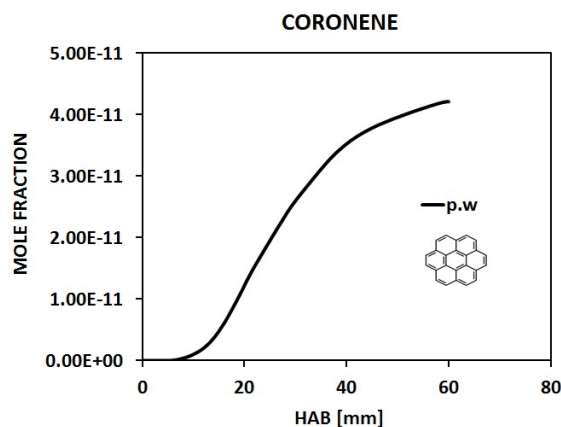
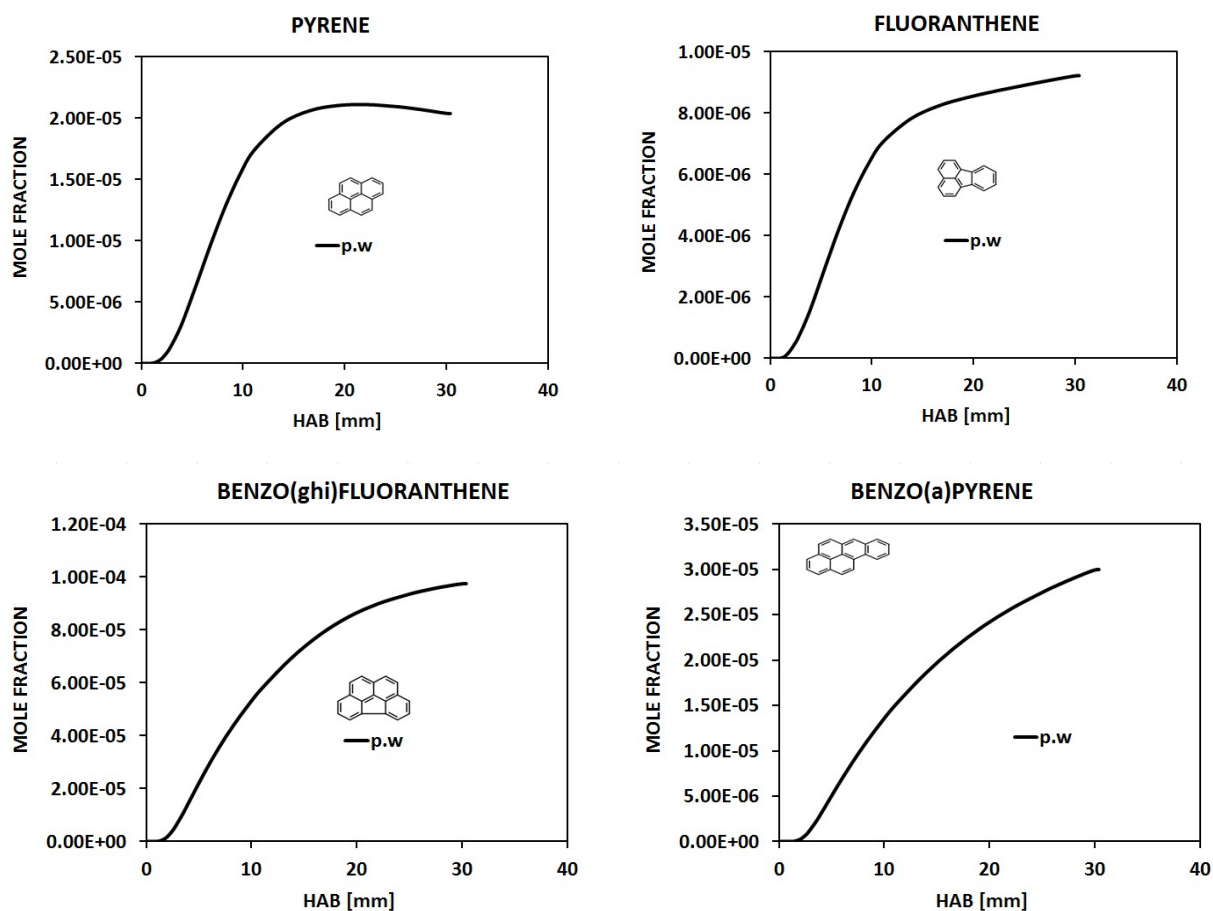


Figure 134 : Low pressure (0.263 atm) methane premixed flame,  $\phi=2.32$ : CH<sub>4</sub> (46.2% in mol.)/O<sub>2</sub> (39.8%)/N<sub>2</sub> (14.0%). Predicted Acetylene and PAHs mole fraction profiles not experimentally measured.

The maximum predicted concentration of fluoranthene, benzo(a)pyrene and coronulene are below 1 ppm, while that of benzo(ghi)fluoranthene and cyclopenta(cd)pyrene are found to be respectively 3.5 and 2.7 ppm, that are at least two times higher than that pyrene. The maximum computed concentrations of benzo(e)pyrene to coronene are below 1 pbb.

## 2. Ethylene premixed flame ( $\phi=2.34$ ): predicted mole fractions of PAHs



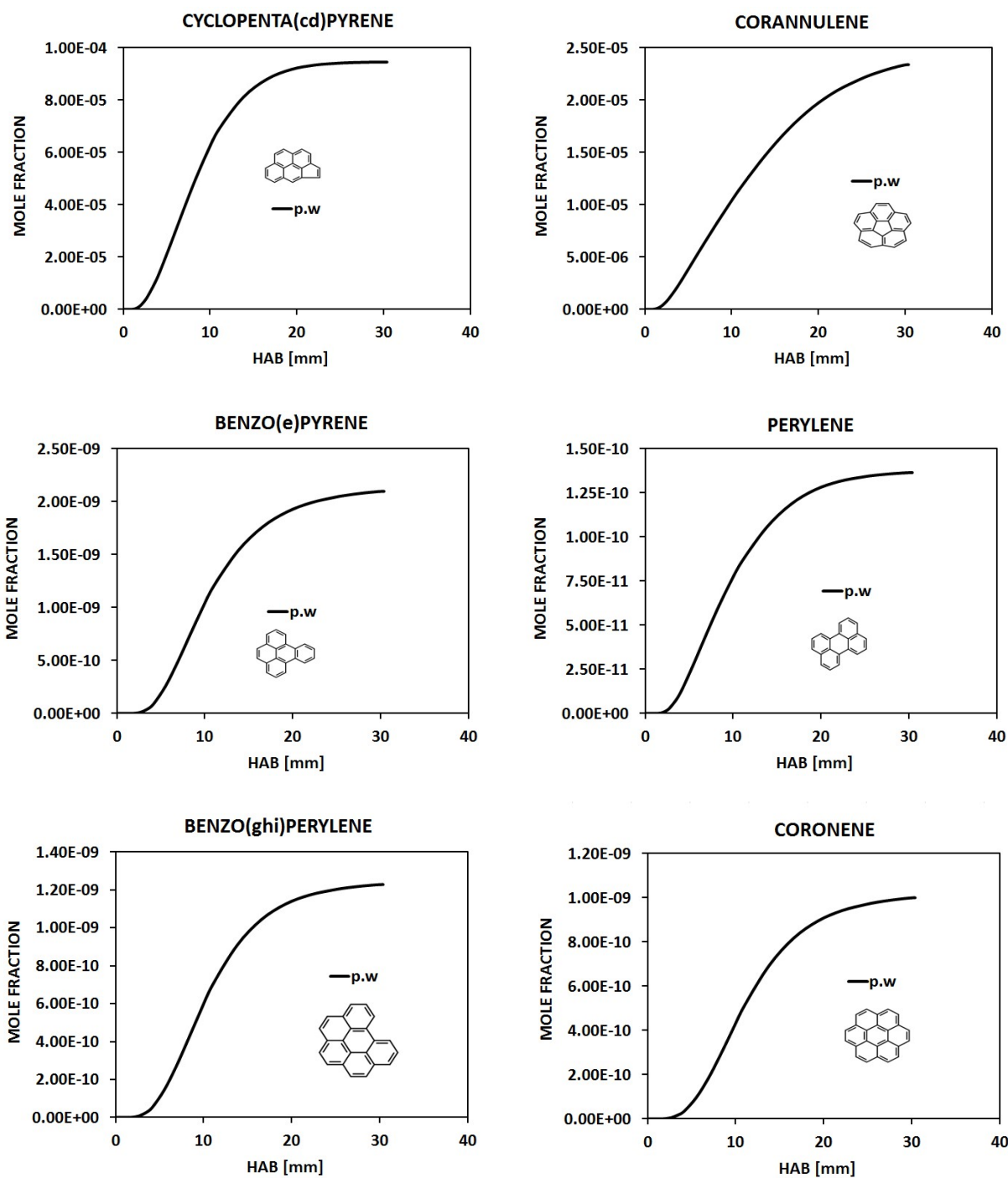
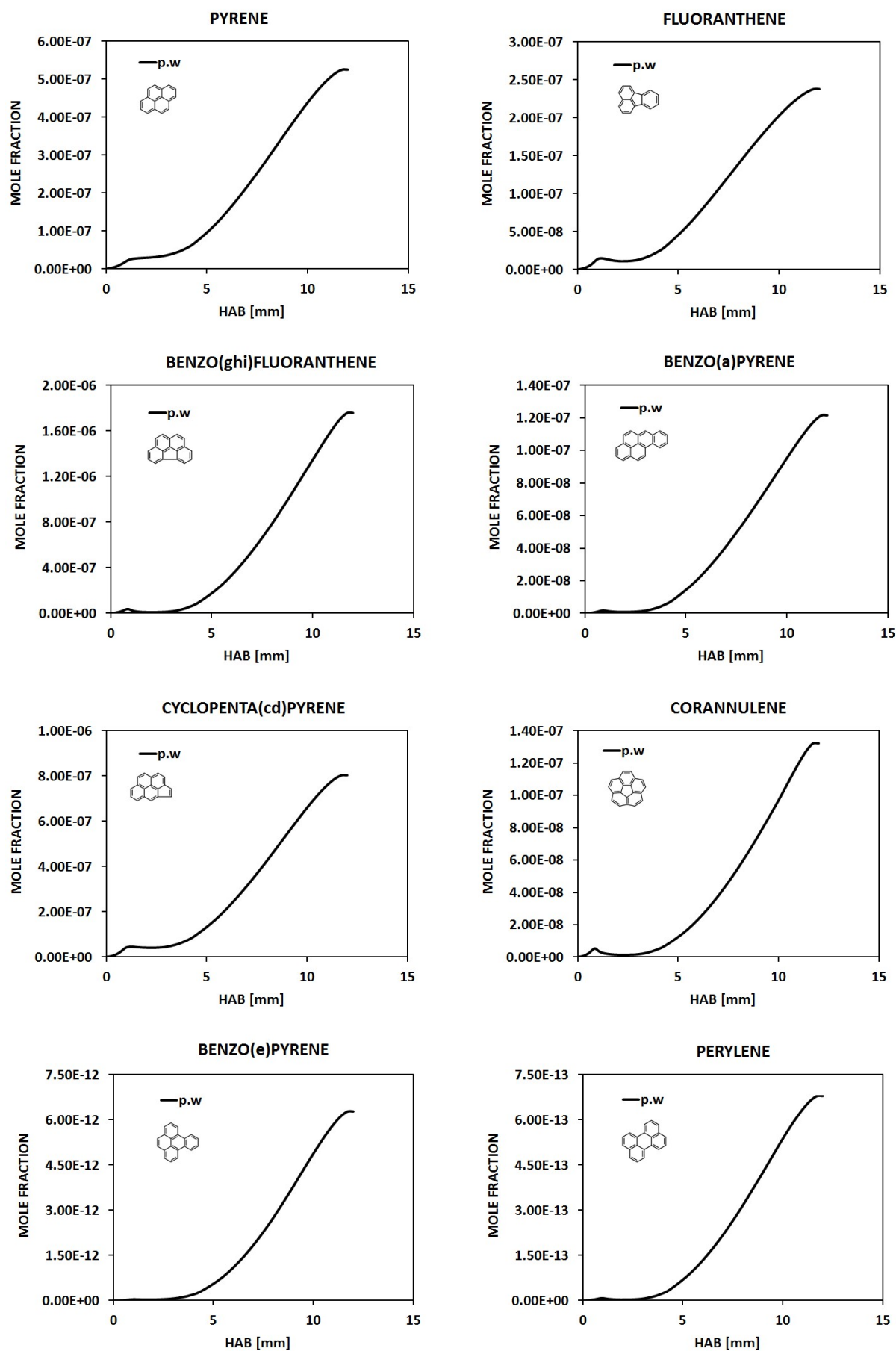


Figure 135 : Atmospheric ethylene premixed flame,  $\phi=2.34$ :  $C_2H_4$  (14.08% mol.)/ $O_2$  (18.05%)/ $N_2$  (67.87%). Predicted PAHs mole fraction profiles not experimentally measured.

The highest concentration is obtained for benzo(ghi)fluoranthene and cyclopenta(cd)pyrene (nearly 100 ppm), followed by benzo(a)pyrene, corannulene and pyrene (20-30 ppm) and then fluoranthene (9 ppm). From benzo(e)pyrene to coronene, the maximum predicted concentrations are closed the pbb ( $10^{-9}$ ) order.

### 3. N-butane premixed flame ( $\phi=1.75$ ): predicted mole fractions of PAHs





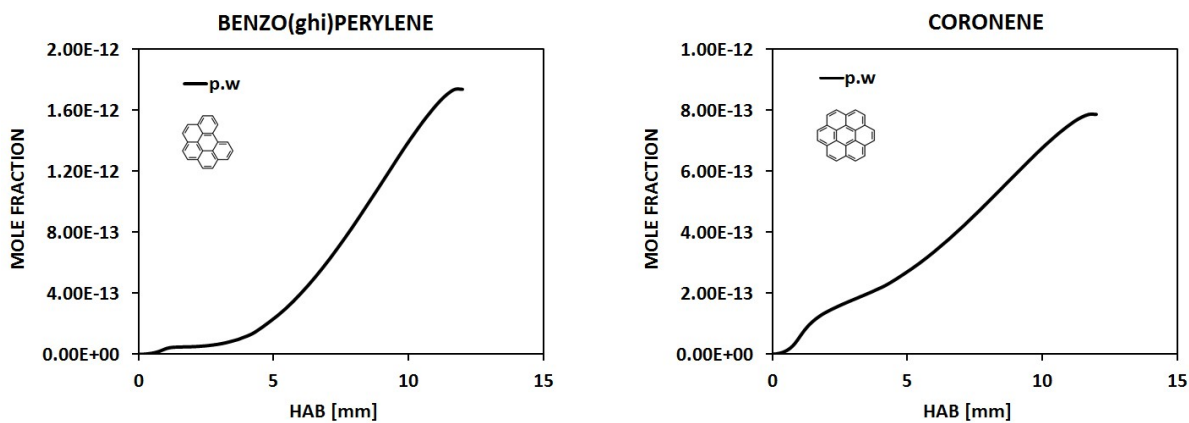
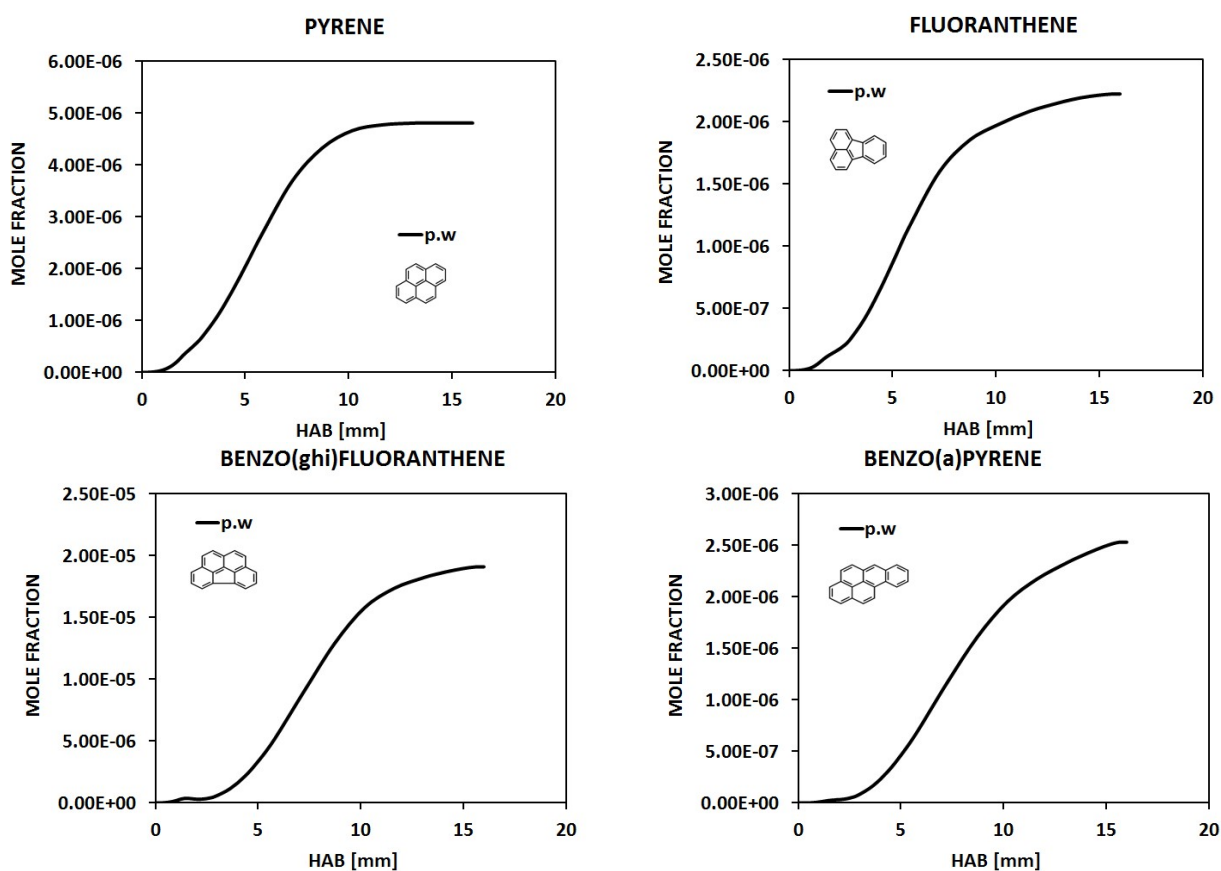


Figure 136 : Atmospheric n-butane premixed flame,  $\phi=1.75$ : n-C<sub>4</sub>H<sub>10</sub> (9.46% in mol.)/O<sub>2</sub> (35.22%)/N<sub>2</sub> (55.32%). Predicted PAHs mole fractions not experimentally measured.

The maximum predicted mole fraction of PAHs from pyrene to coronene are below 1 ppm, except that of benzo(ghi)fluoranthene (~1.7 ppm). It is worth noting that the maximum concentration of PAHs from benzo(e)pyrene to coronene are very low and are closed to the ppt ( $10^{-12}$ ) order.

#### 4. N-butane premixed flame ( $\phi=1.95$ ): predicted mole fractions of PAHs



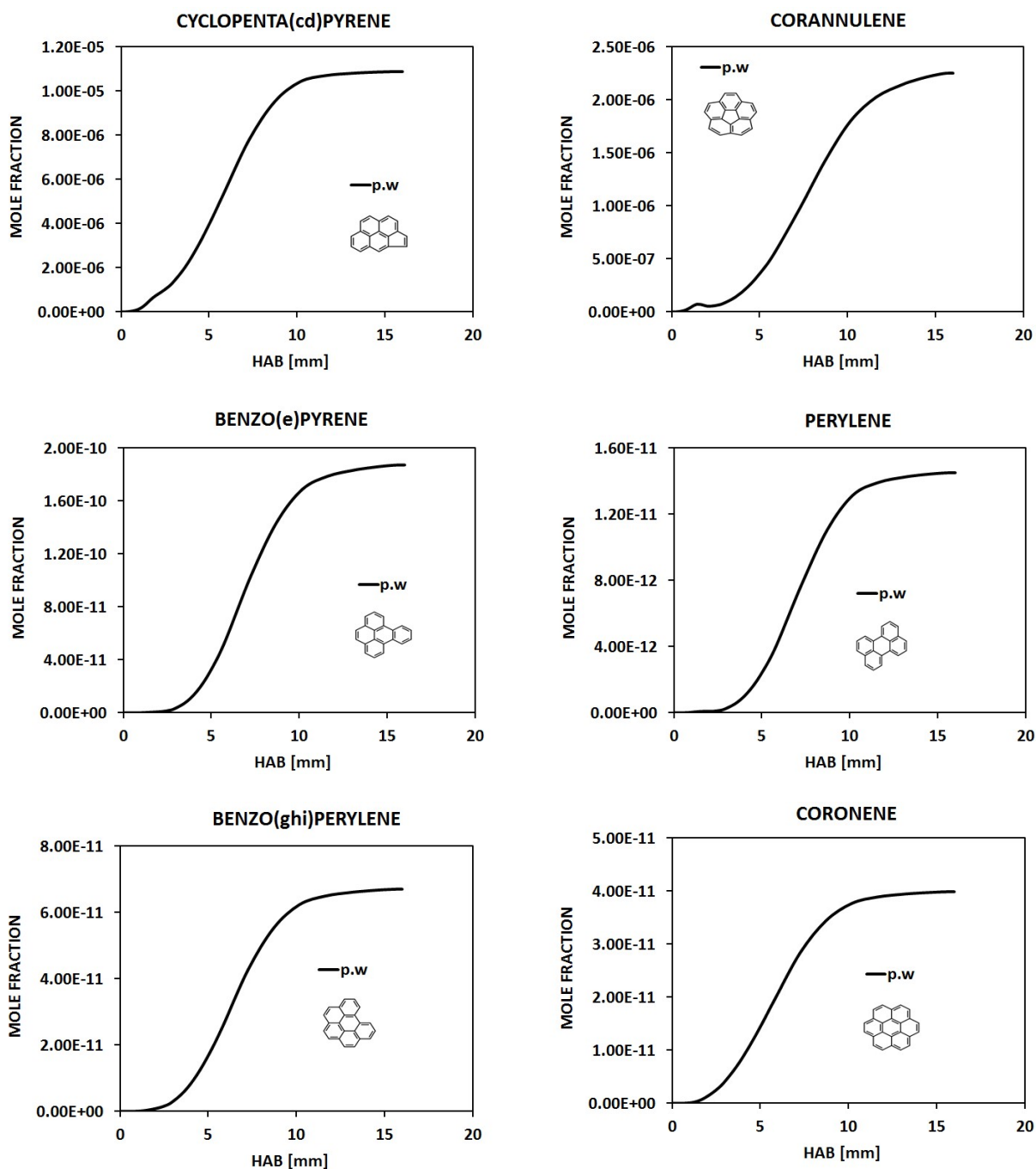
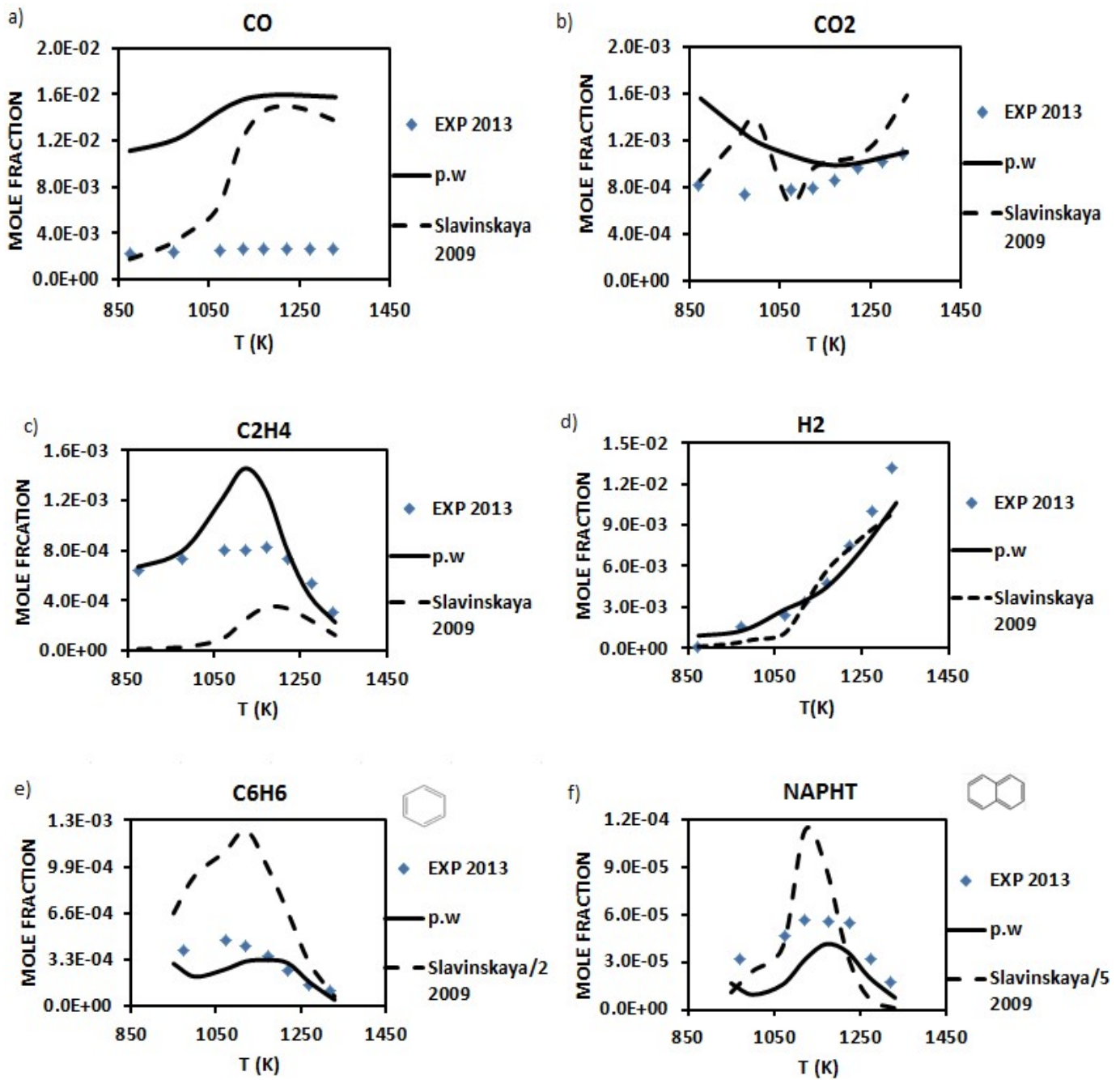
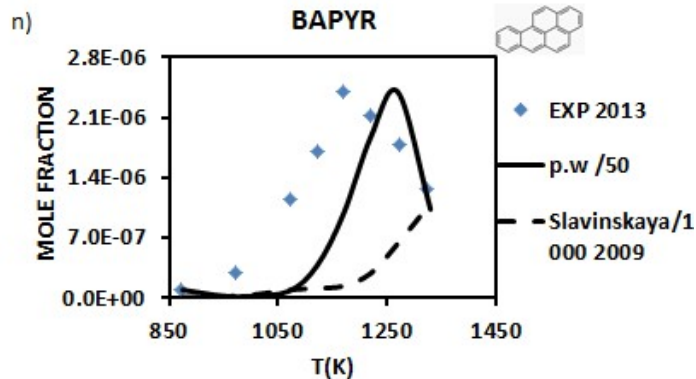
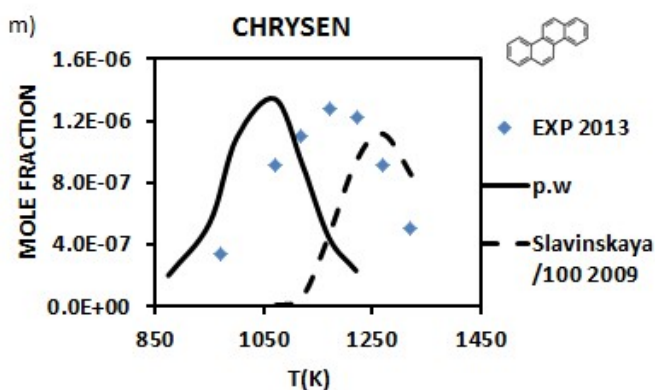
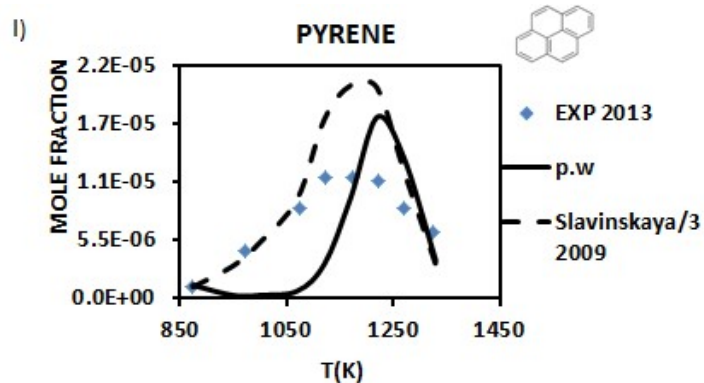
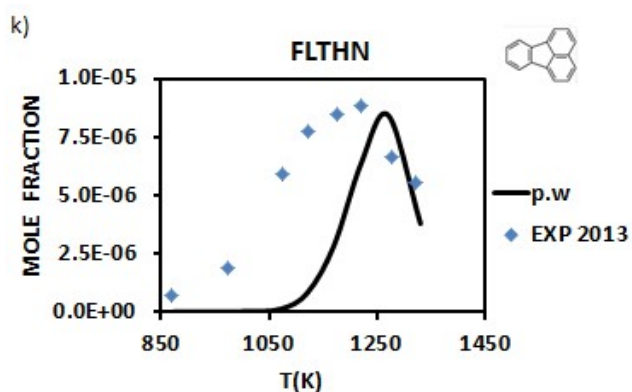
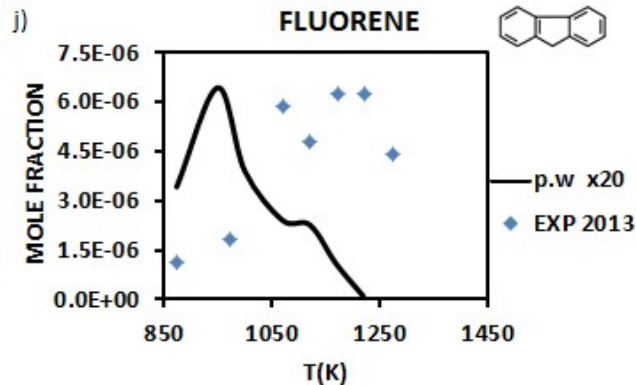
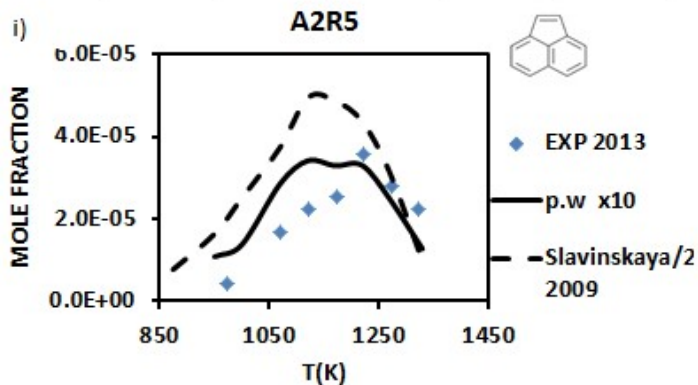
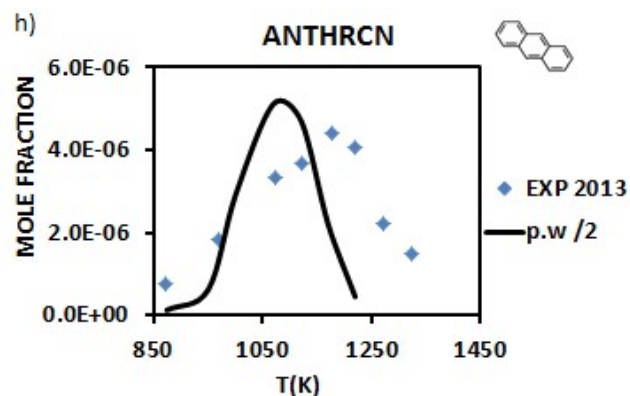
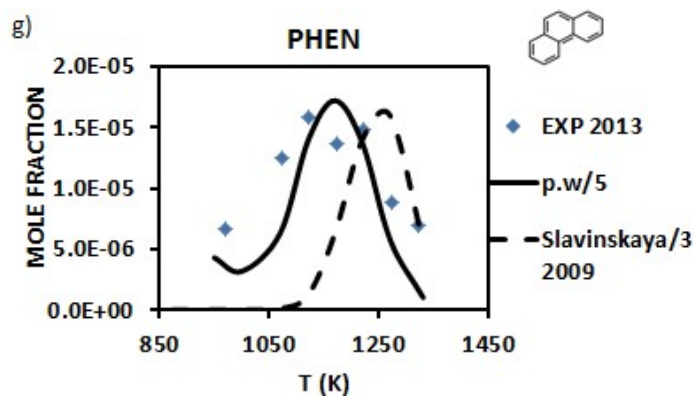


Figure 137 : Atmospheric n-butane premixed flame,  $\phi=1.95$ : n-C<sub>4</sub>H<sub>10</sub> (10.30% mol.)/O<sub>2</sub> (34.31%)/N<sub>2</sub> (55.39%). Predicted PAHs mole fractions not experimentally measured.

The concentrations of PAHs are increased since the equivalence ratio is increased from 1.75 to 1.95. The maximum concentrations of benzo(ghi)fluoranthene and cyclopenta(cd)pyrene reached respectively 20 and 10 ppm, while that of pyrene, fluoranthene, benzo(a)pyrene, corannulene are only a few ppm (2-5 ppm). From benzo(e)pyrene to coronene, computations show low concentration profiles that are below the ppb ( $10^{-9}$ ) order.

5. Acetylene oxidation in a plug flow reactor configuration ( $\phi=7.5$ )





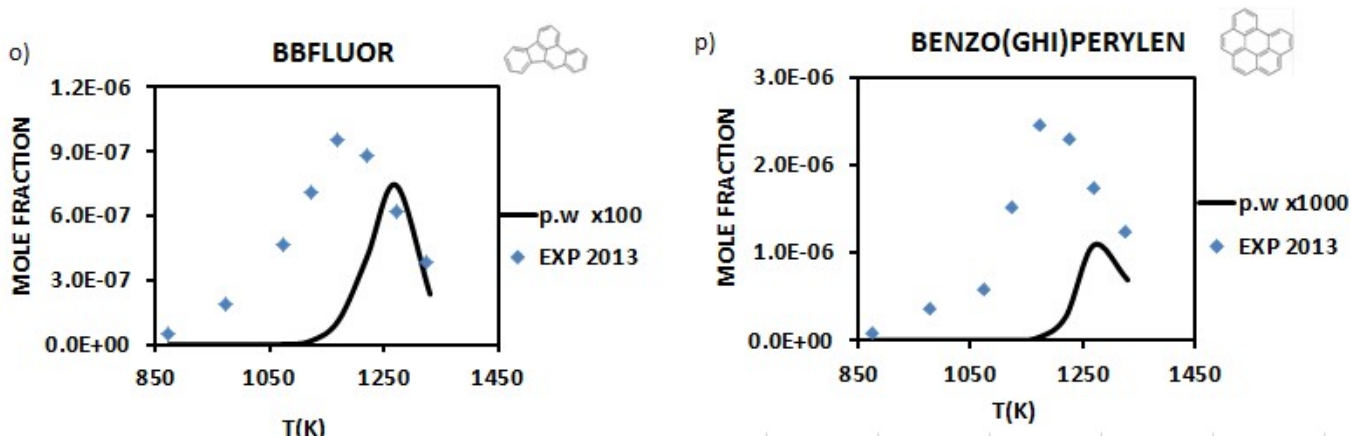
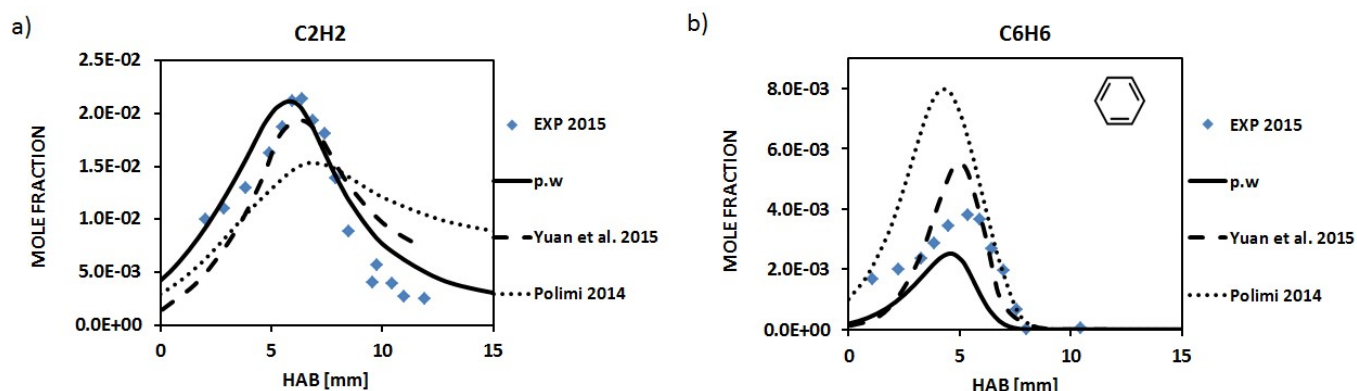


Figure 138 : Acetylene oxidation in plug flow reactor configuration :  $C_2H_2/O_2/N_2$ : 0.03/0.01/0.96 in volume fraction ;  $\phi=7.5$  ;  $P=1$  atm ;  $\tau= 1.5s$  ; Predicted and experimental mole fraction of a): carbon monoxide, b): carbon dioxide, c): ethylene, d): hydrogen, e): benzene, f): naphthalene, g): phenanthrene, h): anthracene, i): acenaphylene, j): fluorene, k): fluoranthene, l): pyrene, m): chrysene, n): benzo(a)pyrene, o): benzo(b) fluoranthene, p): benzo(ghi) perylene. The symbols represent experimental data from [115]; the continuous lines represent the modeling results from the present work; dashed lines: Slavinskaya et al. mechanism [123].

Predictive capability of the kinetic model is tested in the plug flow reactor condition for acetylene oxidation. Some key intermediate species mole fractions such as ethylene and aromatics such as benzene, naphthalene, anthracene, fluoranthene, pyrene and chrysene are satisfactorily reproduced. Large discrepancies are observed for larger PAHs such as benzo(a)pyrene and benzo(ghi)fluoranthene within an important factor ( $> 50$ ). The improvement of the present kinetic model is needed to account for a better understanding of larger PAH molecules chemistry.

## 6. Styrene premixed laminar flame



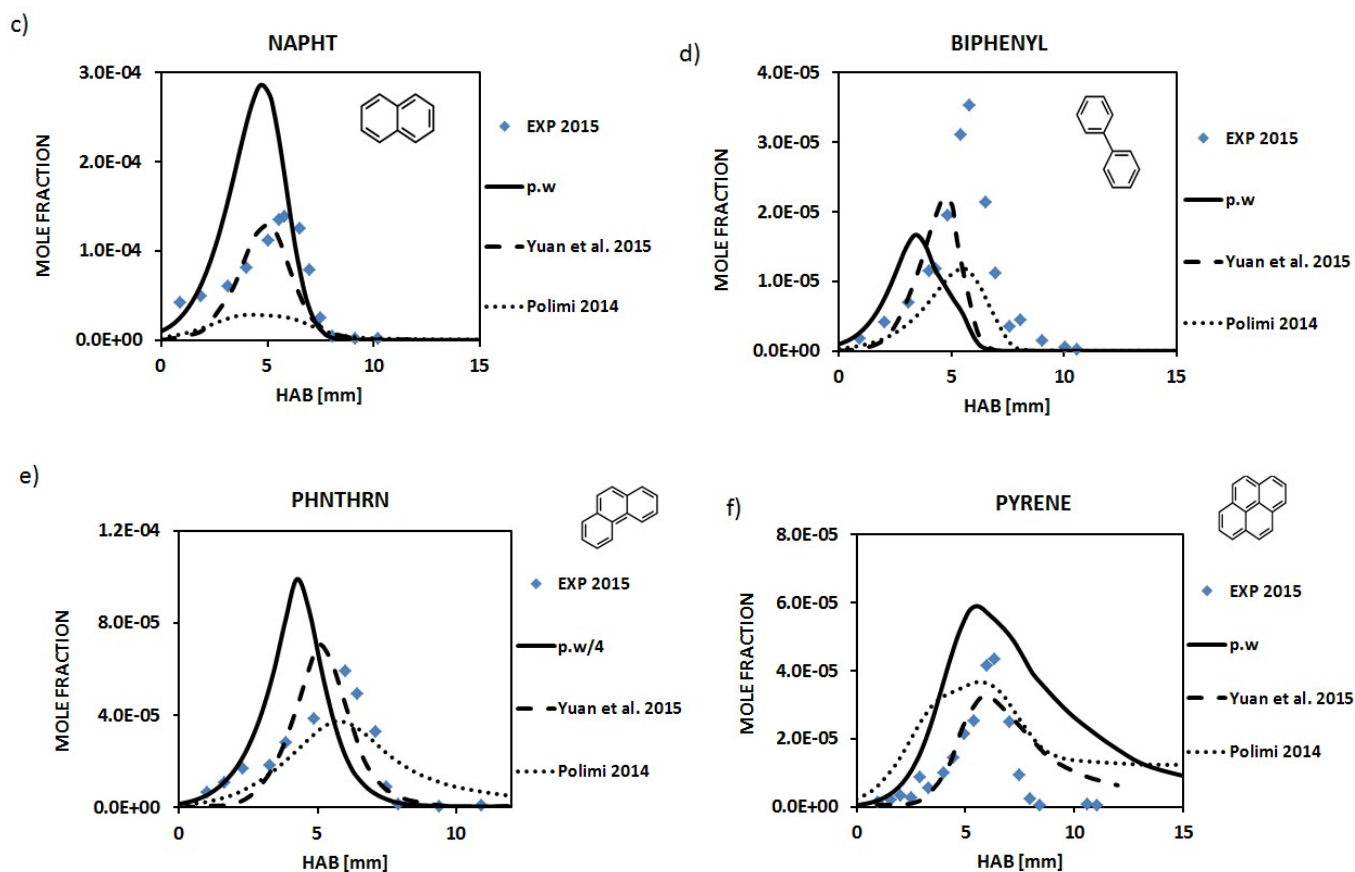


Figure 139 : Styrene premixed laminar flame: Styrene/O<sub>2</sub>/Ar: 0.073/0.427/0.500 in mole fraction;  $\phi = 1.70$ ;  $P = 0.0395$  atm ;  $V = 35$  cm/s ; Predicted and experimental mole fraction of a) acetylene, b) benzene, c) naphthalene, d) biphenyl, e) phenanthrene, f) pyrene. The symbols represent experimental data from [153]; the continuous lines represent the modeling results from the present work; dashed lines: Yuan et al. mechanism for styrene combustion [153]; dotted lines: polimi mechanism [128].

The present mechanism has been tested in monoaromatic with unsaturated aliphatic chain fuel. As can be observed, a good agreement is obtained from acetylene to pyrene molecule. This kinetic is able to describe accurately the combustion of aromatic, monoaromatic with saturated aliphatic chain and monoaromatic with unsaturated aliphatic chain. Based on these results, the present detailed mechanism can be used with some confidence to analyze some key intermediate species as well as aromatics (PAHs) formation pathways.

## E. Main benzene and naphthalene formation pathways

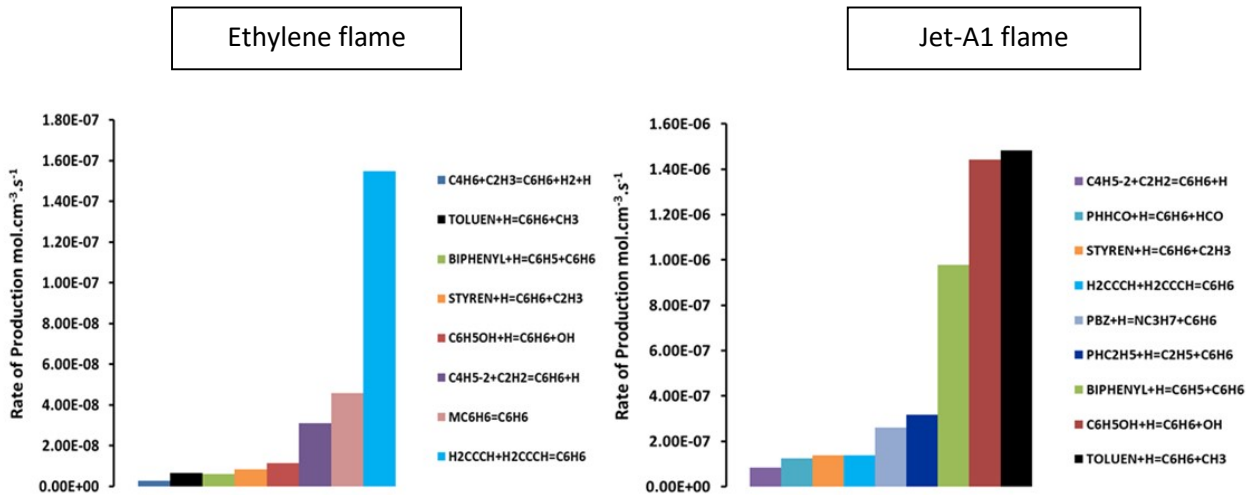


Figure 140 : Benzene production pathways as a function of HAB in ethylene flame [36] ( $\phi=3.06$ ;  $P= 1\text{atm}$ ;  $\text{HAB}= 0.5\text{-}12\text{ mm}$ ) and in jet-A1 fuel premixed flame [152]( $\phi=1.70$ ;  $P= 1\text{atm}$ ;  $\text{HAB}= 0.1\text{-}3.3\text{ mm}$ ). Rates of production indicated correspond to the global contribution to benzene production in the given HAB range.

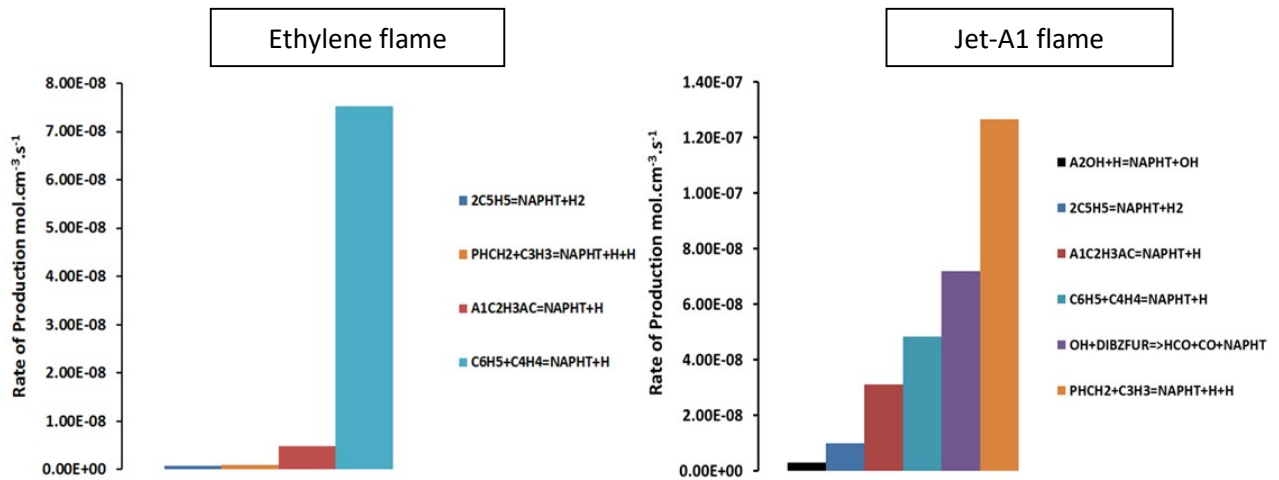
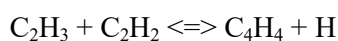


Figure 141 : Naphthalene production pathways as a function of HAB in ethylene flame [36] ( $\phi=3.0$ ;  $P= 1\text{atm}$ ;  $\text{HAB}= 0.5\text{-}12\text{ mm}$ ) and in jet fuel premixed flame [152] ( $\phi=1.70$ ;  $P= 1\text{atm}$ ;  $\text{HAB}= 0.1\text{-}3.3\text{ mm}$ ). Rates of production indicated correspond to the global contribution to naphthalene production in the given HAB range.

## F. Fit of Troe

The rate constant of the following bimolecular reaction has been obtained through the fit of Troe:



	P [atm]		
P [atm]	0.1	1.0	10.0
A	4.60E+016	2.00E+018	4.90E+016
n	-1.25	-1.68	-1.13
E [cal /mol]	8400	10600	11800

Table 18 : Data for different constant pressures.

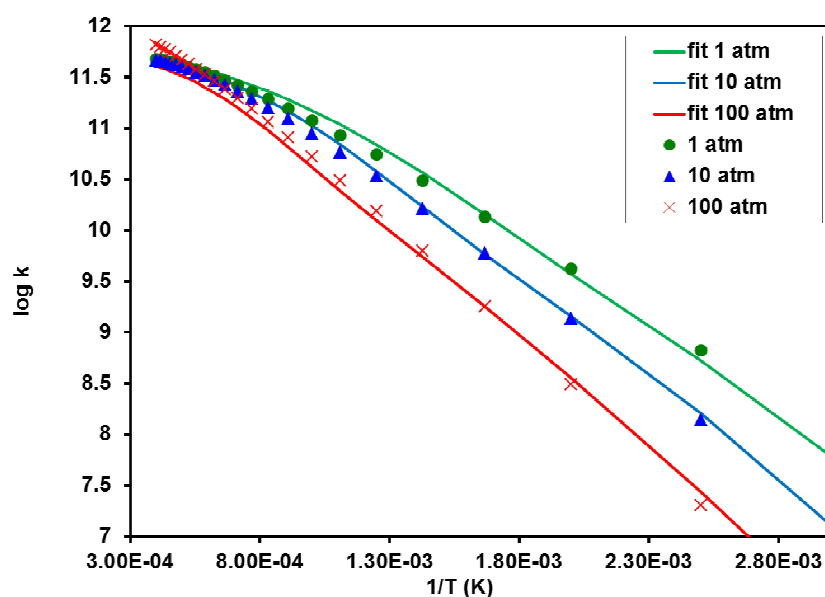


Figure 142 : Fit of the rate constant as a function of temperature.

The optimized fall-off parameters obtained are given as follows:

T*	T**	T***	alpha	A <sub>0</sub>	n <sub>0</sub>	E <sub>0</sub>	A <sub>inf</sub>	n <sub>inf</sub>	E <sub>inf</sub>
1.71x10 <sup>2</sup>	1.07x10 <sup>3</sup>	1.00x10 <sup>-30</sup>	1.00	5.0x10 <sup>4</sup>	-0.75	5.0 x10 <sup>3</sup>	5 x10 <sup>3</sup>	-1.21	1.2 x10 <sup>4</sup>

Table 19 : Fall-off parameters optimization (yellow) with the rate constant parameters in low pressure regime (orange) and high pressure regime (green).



## G. Sub-mechanisms used for benzene, naphthalene and pyrene formation and consumption

Reactions	A (cm, mol, s)	n	E (kcal/mol)	Ref
C3H5-A+C3H3=C6H6+2H	$5.6 \times 10^{20}$	-2.54	1.7	[200]
C3H4-A+C3H3=C6H6+H	$1.4 \times 10^{12}$	0.00	9.9	[200]
2C3H3=C6H6	$2.0 \times 10^{12}$	0.00	0.0	[201]
C4H6+C2H3=C6H6+H2+H	$5.6 \times 10^{11}$	0.00	3.2	[201]
C4H5-N+C2H2=C6H6+H	$1.6 \times 10^{16}$	-1.33	5.4	[201]
C4H5-N+C2H3=C6H6+H2	$1.8 \times 10^{-13}$	7.07	-3.6	[201]
C4H5-2+C2H2=C6H6+H	$5.0 \times 10^{14}$	0.00	25.0	[201]
C6H5+H(+M)=C6H6(+M)	$A_{\infty} = 1.0 \times 10^{14}$ $A_0 = 6.6 \times 10^{75}$	$n_{\infty} = 0.00$ $n_0 = -16.30$	$E_{\infty} = 0.0$ $E_0 = 7.0$	[202]
C6H6+O2=C6H5+HO2	$6.3 \times 10^{13}$	0.00	60.0	[202]
C6H6+O=C6H5O+H	$2.2 \times 10^{13}$	0.00	4.5	[203]
C6H6+O=C6H5+OH	$2.0 \times 10^{13}$	0.00	14.7	[203]
C6H5+H2=C6H6+H	$5.7 \times 10^4$	2.43	6.3	[135]
C6H6+CH3=C6H5+CH4	$7.3 \times 10^{12}$	0.00	18.9	[202]
C6H6+HO2=C6H5+H2O2	$5.5 \times 10^{12}$	0.00	28.9	[202]
C6H6+OH=C6H5+H2O	$1.2 \times 10^0$	4.10	-0.3	[204]
C6H6+OH=C6H5OH+H	$1.3 \times 10^2$	3.25	5.6	[205]
C6H5+CH2O=C6H6+HCO	$8.6 \times 10^4$	2.19	0.04	[206]
C6H5+HCO=C6H6+CO	$8.6 \times 10^4$	2.19	0.04	[206]
C6H5OH+C6H5=C6H5O+C6H6	$4.9 \times 10^{12}$	0.00	4.4	[207]
C5H6+C6H5=C5H5+C6H6	$1.0 \times 10^{-1}$	4.00	0.0	[208]
C5H6+C5H5=C6H6+C4H5-N	$5.0 \times 10^9$	0.00	0.0	[208]
C5H6+C2H3=C6H6+CH3	$2.1 \times 10^{67}$	-16.08	42.4	[208]
MC6H6=C6H6	$3.8 \times 10^{13}$	0.00	22.0	[114]
C6H6+C2H3=C6H5+C2H4	$A_{\text{forward}} = 4.0 \times 10^{-1}$ $E_{\text{reverse}} = 9.4 \times 10^{-3}$	$n_{\text{forward}} = 4.02$ $n_{\text{reverse}} = 4.47$	$E_{\text{forward}} = 88.0$ $E_{\text{reverse}} = 4.5$	[114]
C6H6+C4H5-N=C6H5+C4H6	$4.1 \times 10^{-1}$	4.02	8.8	[114]
C6H6+C4H5-I=C6H5+C4H6	$4.1 \times 10^{-1}$	4.02	8.8	[114]
C6H5+C3H6=C3H5-A+C6H6	$1.3 \times 10^0$	3.82	1.4	[209]
TOLUEN+H=C6H6+CH3	$2.4 \times 10^{13}$	0.00	5.1	[114]
TOLUEN+C6H5=PHCH2+C6H6	$2.1 \times 10^{12}$	0.00	4.4	[114]
PHCH2OH+H=C6H6+CH2OH	$1.2 \times 10^{13}$	0.00	5.1	[114]
PHCH2OH+C6H5=>PHHCO+C6H6+H	$1.4 \times 10^{12}$	0.00	4.4	[114]
PHHCO+H=C6H6+HCO	$1.2 \times 10^{13}$	0.00	5.1	[114]
PHHCO+C6H5=PHCO+C6H6	$7.0 \times 10^{11}$	0.00	4.4	[114]
PHC2H5=C6H6+C2H4	$1.1 \times 10^9$	0.00	51.7	[210]
PHC2H5+H=C2H5+C6H6	$2.4 \times 10^{13}$	0.00	5.1	[114]
STYREN=C6H6+C2H2	$1.6 \times 10^{11}$	0.00	58.4	[114]
STYREN+H=C6H6+C2H3	$2.4 \times 10^{13}$	0.00	5.1	[114]
PHCH2HCO+H=C6H6+CH2CHO	$5.8 \times 10^{13}$	0.00	8.0	[114]
PHC2H+OH=>C6H6+HCCO	$1.0 \times 10^{13}$	0.00	0.0	[114]
PBZ+H=NC3H7+C6H6	$5.8 \times 10^{13}$	0.0 0	8.1	[139]
PBZ+C6H5=PBZJA+C6H6	$7.8 \times 10^{11}$	0.00	20.5	[114]
PBZ+C6H5=PBZJB+C6H6	$7.8 \times 10^{11}$	0.00	16.2	[114]
PBZ+C6H5=PBZJC+C6H6	$7.8 \times 10^{11}$	0.00	16.2	[114]
PHC3H5-1+H=C6H6+C3H5-A	$5.8 \times 10^{13}$	0.00	5.1	[114]

PHC3H5-2+C6H5=PHC3H4+C6H6	$2.8 \times 10^{12}$	0.00	11.2	[114]
C4H4+C2H2=C6H6	$4.4 \times 10^{11}$	0.00	30.0	[118]
H2CCCH+H2CCCH=C6H6	$1.6 \times 10^{66}$	-15.9	27.5	[142]
H2CCCH+H2CCCH=C6H6	$1.2 \times 10^{35}$	-7.40	5.0	[142]
FULVENE+H(+M)=C6H6+H(+M)	$4.5 \times 10^8$	1.16	12.5	[119]
C4H4+C6H5=C6H6+C4H3-N	$1.0 \times 10^{12}$	0.00	0.0	[120]
C4H4+C6H5=C6H6+C4H3-I	$1.0 \times 10^{12}$	0.00	0.0	[120]
C6H5+C2H2=C6H6+C2H	$1.1 \times 10^{12}$	0.0 0	14.1	[120]
H+C14H14=>C6H6+H+STYREN	$2.5 \times 10^{12}$	0.00	5.0	[211]
PHCC+C6H6=PHNTHRN+H	$5.6 \times 10^{12}$	-0.07	7.6	[211]
C14H14+C6H5=C14H13+C6H6	$1.0 \times 10^{14}$	0.00	9.9	[137]
o-C6H4+C6H6=>BICYCLO	$1.1 \times 10^4$	2.52	5.9	[212]
BICYCLO=>o-C6H4+C6H6	$4.9 \times 10^{16}$	0.00	6.7	[212]
A2-1+C6H6=FLTHN+H+H2	$8.5 \times 10^{11}$	0.00	3.9	[211]
C6H6+C2H = PHC2H+H	$1.0 \times 10^{12}$	0.00	0.0	[123]
C4H5-I + C6H6 = INDENE+CH3	$1.4 \times 10^{13}$	0.00	14.0	[123]
INDENE+H = C6H6+C3H3	$2.0 \times 10^{14}$	0.00	24.5	[123]
INDENE+C6H5 = INDENYL+C6H6	$5.0 \times 10^{11}$	0.00	3.0	[143]
C4H5-I+C6H6 => NAPHT+H2+H	$1.0 \times 10^{12}$	0.00	1.5	[123]
C6H5+C6H6 = BIPHENYL+H	$1.1 \times 10^{23}$	-2.92	7.5	[213]
A2-1+C6H6 = PYRENE+H+H2	$1.0 \times 10^{12}$	0.00	2.5	[41]
A2C2H*+C6H6 = CHRYSEN+H	$1.1 \times 10^{24}$	-2.92	8.0	[123]
A2R5-+C6H6 => BGHIF+H2+H	$1.1 \times 10^{25}$	-2.92	8.0	[123]
C6H6+C2H = N-C8H7	$7.0 \times 10^{38}$	-8.02	8.2	[123]
C4H5-I+C2H2=C6H6+H	$1.6 \times 10^{15}$	-1.33	5.3	[123]
P2-+C6H6=TERPHENYL+H	$9.5 \times 10^{75}$	-18.90	39.4	[125]
P2-+C6H6=>TRIPHENYLEN+H2+H	$8.5 \times 10^{11}$	0.00	3.9	[125]
P3-+C6H6=QUATERPHENYL+H	$1.0 \times 10^{83}$	-18.90	39.5	[125]
P4-+C6H6=QINQUEPHENYL+H	$1.0 \times 10^{83}$	-18.90	39.5	[125]
C6H5+C3H4-P=C6H6+C3H3	$1.8 \times 10^4$	2.54	2.8	[124]
BENZYL B+H=C6H6+PHCH2	$1.7 \times 10^8$	1.56	4.4	[124]
BENZYL B+C6H5=BENZYL B J+C6H6	$5.3 \times 10^{13}$	0.00	11.9	[124]
C14H14+H=C6H6+PHCH2CH2	$1.7 \times 10^8$	1.56	4.	[124]
STILBN+C6H5=STILBNJ+C6H6	$2.6 \times 10^2$	3.19	2.8	[124]
A2-1+C6H6=A2A1-1+H	$9.5 \times 10^{11}$	0.00	4.3	[124]
A2-2+C6H6=A2A1-2+H	$9.5 \times 10^{11}$	0.00	4.3	[124]
BENZ NAP+C6H5=BENZ NAP JP+C6H6	$5.3 \times 10^{13}$	0.00	11.9	[124]
A3-1+C6H6=A3A1-1+H	$9.5 \times 10^{11}$	0.00	4.3	[124]
C13H9+C6H6=FLRNA1-4+H	$9.5 \times 10^{11}$	0.00	4.3	[124]
A4-1+C6H6=PYRNA1-4+H	$9.5 \times 10^{11}$	0.00	4.3	[124]

Table 20 : Kinetic rate parameters ( $k = A (T / 1 \text{ K})^n \exp (- E / RT)$ ) of important reactions for benzene production/consumption.

Reactions	A (cm, mol, s)	n	E (kcal/mol)	Ref
2C5H5=NAPHT+H2	1.0×10 <sup>13</sup>	0.00	7.0	[114]
2C5H5=NAPHT+2H	5.0×10 <sup>12</sup>	0.00	8.0	[114]
A1C2H3AC=NAPHT+H	1.0×10 <sup>10</sup>	0.00	4.8	[114]
NAPHT+H=C10H9	5.0×10 <sup>14</sup>	0.00	5.0	[114]
NAPHT=A2-1+H	4.5×10 <sup>15</sup>	0.00	107.4	[114]
NAPHT+H=A2-1+H2	2.5×10 <sup>14</sup>	0.00	16.0	[114]
NAPHT+OH=A2-1+H2O	1.6×10 <sup>8</sup>	1.42	1.4	[114]
NAPHT+CH3=A2-1+CH4	2.0×10 <sup>12</sup>	0.00	15.0	[114]
NAPHT+O=A2O+H	2.2×10 <sup>13</sup>	0.00	4.5	[114]
NAPHT+O=A2-1+OH	2.0×10 <sup>13</sup>	0.00	14.7	[114]
NAPHT+O2=A2-1+HO2	6.3×10 <sup>13</sup>	0.00	60.0	[114]
A2OH+H=NAPHT+OH	2.2×10 <sup>13</sup>	0.00	7.9	[114]
C3H3+C6H4CH3=>NAPHT+H+H	5.0×10 <sup>12</sup>	0.00	3.0	[214]
NAPHT+C4H3-N=>PHNTHRN+H	4.0×10 <sup>13</sup>	0.00	15.9	[211]
NAPHT+C4H3-N=ANTHRCN+H	1.0×10 <sup>13</sup>	0.00	0.0	[211]
BICYCLO=NAPHT+C2H2	7.4×10 <sup>14</sup>	0.09	54.8	[212]
DIBZFUROH=>CO+NAPHT+HCO	2.0×10 <sup>13</sup>	0.00	0.0	[128]
NAPHT+PHC2H=CHRYSEN+H	8.5×10 <sup>11</sup>	0.00	3.9	[211]
C4H5-I+C6H6=>NAPHT+H2+H	1.0×10 <sup>12</sup>	0.00	1.5	[215]
C4H6+C6H5=>NAPHT+H2+H	5.0×10 <sup>11</sup>	0.00	1.5	[215]
C6H5+C4H3-N=NAPHT	3.2×10 <sup>23</sup>	-3.20	2.1	[216]
C6H5+C4H4=NAPHT+H	3.3×10 <sup>33</sup>	-5.70	12.8	[11]
C6H4CH3+H2CCCH=>NAPHT+2H	4.0×10 <sup>11</sup>	0.00	7.0	[123]
INDENE+CH2=>NAPHT+2H	2.0×10 <sup>13</sup>	0.00	4.4	[217]
NAPHT+O=CH2CO+PHC2H	2.2×10 <sup>13</sup>	0.00	2.2	[213]
NAPHT+O=>INDENYL+CO+H	3.6×10 <sup>14</sup>	0.00	22.0	[123]
NAPHT+OH=>PHC2H+CH2CO+H	1.3×10 <sup>13</sup>	0.00	5.3	[213]
NAPHT+C2H=A2-1+C2H2	5.0×10 <sup>13</sup>	0.00	8.0	[216]
NAPHT+C2H=A2C2H+H	5.0×10 <sup>13</sup>	0.00	0.0	[11]
P2+O2=NAPHT+HCO+CO	2.0×10 <sup>12</sup>	0.00	3.7	[123]
NAPHT+C4H2=>PHNTHRN	2.8×10 <sup>4</sup>	2.45	14.6	[11]
NAPHT+C6H=A4-1	7.0×10 <sup>37</sup>	-8.02	8.2	[213]
NAPHT+C6H5=PYRENE+H+H2	1.0×10 <sup>11</sup>	0.00	2.5	[41]
PHC2H+NAPHT=>BGHIF+H2+H	2.1×10 <sup>25</sup>	-2.92	8.0	[123]
N-C8H7+C2H2=NAPHT+H	1.6×10 <sup>16</sup>	-1.33	2.7	[11]
NAPHT+O=N-C8H7+HCCO	2.0×10 <sup>13</sup>	0.00	21.0	[123]
INDENYL+CH3=NAPHT+H+H	3.0×10 <sup>18</sup>	0.00	36.5	[143]
PHCH2+C3H3=NAPHT+H+H	2.0×10 <sup>13</sup>	0.35	5.0	[148]
NAPHT+C6H5=A2A1-1+H	6.4×10 <sup>11</sup>	0.00	4.3	[124]
NAPHT+C6H5=A2A1-2+H	6.4×10 <sup>11</sup>	0.00	4.3	[124]
BENZNAP+H=NAPHT+PHCH2	1.7×10 <sup>8</sup>	1.56	4.4	[124]
NAPHT+PHC2H=A4+H	8.5×10 <sup>11</sup>	0.00	3.9	[124]
NAPHT+A2-1=A2A2-12+H	6.4×10 <sup>11</sup>	0.00	4.3	[124]
NAPHT+A2-1=A2A2-11+H	6.4×10 <sup>11</sup>	0.00	4.3	[124]

Table 21 : Kinetic rate parameters ( $k = A (T / 1 K)^n \exp (- E / RT)$ ) of important reactions for naphthalene (NAPHT) production/consumption.

Reactions	A (cm, mol, s)	n	E (kcal/mol)	Ref
A3-1+C2H2 = PYRENE+H	6.6×10 <sup>24</sup>	-3.36	8.9	[11]
A3-4+C2H2=PYRENE+H	1.9×10 <sup>7</sup>	1.79	3.3	[211]
C13H9+C3H3=PYRENE+H2	1.5×10 <sup>75</sup>	-17.80	39.6	[47]
C13H9+C3H2=PYRENE+H	1.5×10 <sup>75</sup>	-17.80	39.6	[47]
FLUORENE+C3H2=PYRENE+H2	1.5×10 <sup>12</sup>	1.80	56.5	[211]
PHC2H-+PHC2H=PYRENE+H	1.1×10 <sup>23</sup>	-2.90	15.9	[62]
PHCC+PHCC=PYRENE	5.0×10 <sup>12</sup>	0.00	6.0	[211]
PHC2H-+PHC2H-=PYRENE	5.0×10 <sup>12</sup>	0.00	6.0	[211]
PHCC+PHC2H-=PYRENE	5.0×10 <sup>12</sup>	0.00	6.0	[211]
A3C2H+H=PYRENE+H	3.2×10 <sup>09</sup>	1.18	4.6	[33]
A3C2H2(+M)=PYRENE+H(+M)	4.0×10 <sup>28</sup>	-5.00	26.0	[211]
LOW / 1.00E+29 -4.4 8.00E+03/ TROE/ 1.0E-02 1.00E-30 2.0E+04 5.00E+01/				
PYRENE+H=A4-1+H2	2.5×10 <sup>14</sup>	0.00	16.0	[211]
PYRENE+H=A4-2+H2	2.5×10 <sup>14</sup>	0.00	16.0	[211]
PYRENE+H=A4-4+H2	2.5×10 <sup>14</sup>	0.00	16.0	[211]
A4-1+CH4=>PYRENE+CH3	4.5×10 <sup>-02</sup>	4.25	4.3	[211]
PYRENE+CH3=>A4-2+CH4	8.0×10 <sup>-01</sup>	3.93	11.8	[211]
A4-2+CH4=>PYRENE+CH3	4.5×10 <sup>-02</sup>	4.25	4.3	[211]
PYRENE+CH3=>A4-4+CH4	8.0×10 <sup>-01</sup>	3.93	11.8	[211]
A4-4+CH4=>PYRENE+CH3	4.5×10 <sup>-02</sup>	4.25	4.3	[211]
A4-1+H(+M)=PYRENE(+M)	1.0×10 <sup>14</sup>	0.00	0.0	[211]
LOW / 6.6E+75 -16.3 7000./ TROE/ 1.0 0.1 585 6113 /				
A4-2+H(+M)=PYRENE(+M)	1.0×10 <sup>14</sup>	0.00	0.0	[211]
LOW / 6.6e75 -16.3 7000 / TROE/ 1.0 0.1 585 6113 /				
A4-4+H(+M)=PYRENE(+M)	1.0×10 <sup>14</sup>	0.00	0.0	[211]
LOW / 6.6e75 -16.3 7000/ TROE/ 1.0 0.1 585 611 /				
PHNTHRN+C2H=PYRENE+H	1.0×10 <sup>13</sup>	0.00	0.0	[213]
PYRENE+OH=A4-1+H2O	2.3×10 <sup>04</sup>	2.68	0.7	[211]
PYRENE+OH=A4-2+H2O	2.3×10 <sup>04</sup>	2.68	0.7	[211]
PYRENE+OH=A4-4+H2O	2.3×10 <sup>04</sup>	2.68	0.7	[211]
PYRENE+OH=>A3-4+CH2CO	1.3×10 <sup>13</sup>	0.00	10.6	[211]
PYRENE+OH=>PHNTHRN+HCCO	5.5×10 <sup>02</sup>	3.25	5.6	[211]
PYRENE+O=>A3-4+HCCO	2.2×10 <sup>13</sup>	0.00	4.5	[211]
A4-1+O2=>A3-4+CO+CO	2.1×10 <sup>12</sup>	0.00	7.5	[211]
A4-2+O2=>A3-4+CO+CO	2.1×10 <sup>12</sup>	0.00	7.5	[211]
A4-4+O2=>A3-4+CO+CO	2.1×10 <sup>12</sup>	0.00	7.5	[211]
A3CH2+CH2 = PYRENE+H2+H	2.4×10 <sup>14</sup>	0.00	0.0	[123]
N-C8H7+PHC2H => PYRENE+H2+H	1.1×10 <sup>24</sup>	-2.92	8.0	[123]
N-C8H7+A1C2H- = PYRENE+H2	4.3×10 <sup>37</sup>	-6.30	22.5	[123]
INDENYL+C6H4CH3 => PYRENE+2H2	4.3×10 <sup>37</sup>	-6.30	22.5	[123]
2INDENYL => PYRENE+C2H2+H2	4.3×10 <sup>37</sup>	-6.30	22.5	[123]
NAPHT+C6H = A4-1	7.0×10 <sup>37</sup>	-8.02	8.2	[213]
NAPHT+C6H5 = PYRENE+H+H2	1.0×10 <sup>11</sup>	0.00	2.5	[41]
A2-1+C6H6 = PYRENE+H+H2	1.0×10 <sup>12</sup>	0.00	2.5	[41]

A2-1+C6H5 => PYRENE+H2	$4.3 \times 10^{37}$	-6.3	22.5	[123]
A2-1+C6H2 = A4-1	$7.0 \times 10^{37}$	-8.02	8.2	[123]
A2R5-+C4H2 => A4-1	$7.0 \times 10^{37}$	-8.02	8.2	[123]
A2R5-+C4H3-N = PYRENE	$6.4 \times 10^{23}$	-3.20	2.1	[123]
A3C2H+H = PYRENE+H	$9.0 \times 10^{38}$	-7.39	10.4	[11]
CHRYSEN-1+O2 => HCO+CO+PYRENE	$2.0 \times 10^{13}$	0.00	3.7	[123]
C4H2+PYRENE => BAPYR	$6.0 \times 10^{02}$	2.23	-0.6	[123]
N-C8H7+PHC2H- => PYRENE+2H	$4.3 \times 10^{14}$	0.00	4.9	[123]
PYRENE+C6H5=PYRNA1-1+H	$1.3 \times 10^{12}$	0.00	4.3	[124]
PYRENE+C6H5=PYRNA1-4+H	$1.3 \times 10^{12}$	0.00	4.3	[124]

Table 22 : Kinetic rate parameters ( $k = A (T / 1 \text{ K})^n \exp (- E / RT)$ ) of important reactions for pyrene production/consumption.

## H. List of species included in the kinetic model

	Species Considered	Phase	Charge	Molecular Weight	Temperature		Element count					
					Low	High	C	H	O	N	Ar	He
1	NC10H22	G	0	1.42E+02	300	5000	10	22	0	0	0	0
2	IC8H18	G	0	1.14E+02	300	5000	8	18	0	0	0	0
3	PBZ	G	0	1.20E+02	300	3000	9	12	0	0	0	0
4	O2	G	0	3.20E+01	300	5000	0	0	2	0	0	0
5	CO	G	0	2.80E+01	300	5000	1	0	1	0	0	0
6	N2	G	0	2.80E+01	300	5000	0	0	0	2	0	0
7	AR	G	0	3.99E+01	200	6000	0	0	0	0	1	0
8	HE	G	0	4.00E+00	200	6000	0	0	0	0	0	1
9	CO2	G	0	4.40E+01	300	5000	1	0	2	0	0	0
10	H2O	G	0	1.80E+01	300	5000	0	2	1	0	0	0
11	CH3CHOCHO	G	0	7.31E+01	300	5000	3	5	2	0	0	0
12	HO2CHO	G	0	6.20E+01	300	5000	1	2	3	0	0	0
13	O2CHO	G	0	6.10E+01	300	5000	1	1	3	0	0	0
14	OCHO	G	0	4.50E+01	300	5000	1	1	2	0	0	0
15	CH3O2H	G	0	4.80E+01	300	5000	1	4	2	0	0	0
16	CH	G	0	1.30E+01	300	5000	1	1	0	0	0	0
17	HCCOH	G	0	4.20E+01	300	4000	2	2	1	0	0	0
18	CH3CO3H	G	0	7.61E+01	300	5000	2	4	3	0	0	0
19	CH3CO3	G	0	7.50E+01	300	5000	2	3	3	0	0	0
20	CH3CO2	G	0	5.90E+01	300	5000	2	3	2	0	0	0
21	O2C2H4OH	G	0	7.71E+01	300	5000	2	5	3	0	0	0
22	C2H5O2H	G	0	6.21E+01	300	5000	2	6	2	0	0	0
23	C2H4O2H	G	0	6.11E+01	300	5000	2	5	2	0	0	0

24	C2H4O1-2	G	0	4.41E+01	300	5000	2	4	1	0	0	0
25	CH3COCH2O2	G	0	8.91E+01	300	5000	3	5	3	0	0	0
26	CH3COCH2O2H	G	0	9.01E+01	300	5000	3	6	3	0	0	0
27	CH3COCH2O	G	0	7.31E+01	300	5000	3	5	2	0	0	0
28	CH3OCH3	G	0	4.61E+01	300	5000	2	6	1	0	0	0
29	CH3OCHO	G	0	6.01E+01	300	5000	2	4	2	0	0	0
30	CH3OCO	G	0	5.90E+01	300	5000	2	3	2	0	0	0
31	NC3H7O2H	G	0	7.61E+01	300	5000	3	8	2	0	0	0
32	IC3H7O2H	G	0	7.61E+01	300	5000	3	8	2	0	0	0
33	NC3H7O	G	0	5.91E+01	300	5000	3	7	1	0	0	0
34	IC3H7O	G	0	5.91E+01	300	5000	3	7	1	0	0	0
35	C3H6O1-2	G	0	5.81E+01	300	5000	3	6	1	0	0	0
36	C3H6OH	G	0	5.91E+01	300	5000	3	7	1	0	0	0
37	HOC3H6O2	G	0	9.11E+01	300	5000	3	7	3	0	0	0
38	PC4H9O2H	G	0	9.01E+01	300	5000	4	10	2	0	0	0
39	PC4H9O2	G	0	8.91E+01	300	5000	4	9	2	0	0	0
40	SC4H9O2	G	0	8.91E+01	300	5000	4	9	2	0	0	0
41	PC4H9O	G	0	7.31E+01	300	5000	4	9	1	0	0	0
42	SC4H9O	G	0	7.31E+01	300	5000	4	9	1	0	0	0
43	C4H8O1-3	G	0	7.21E+01	300	5000	4	8	1	0	0	0
44	C4H8O1-4	G	0	7.21E+01	300	5000	4	8	1	0	0	0
45	C4H8OH-1O2	G	0	1.05E+02	300	5000	4	9	3	0	0	0
46	C4H8OOH1-2	G	0	8.91E+01	300	5000	4	9	2	0	0	0
47	C4H8OOH1-3	G	0	8.91E+01	300	5000	4	9	2	0	0	0
48	C4H8OOH1-4	G	0	8.91E+01	300	5000	4	9	2	0	0	0
49	C4H8OOH1-2O2	G	0	1.21E+02	300	5000	4	9	4	0	0	0
50	C4H8OOH1-3O2	G	0	1.21E+02	300	5000	4	9	4	0	0	0
51	NC4KET12	G	0	1.04E+02	300	5000	4	8	3	0	0	0
52	NC4KET13	G	0	1.04E+02	300	5000	4	8	3	0	0	0
53	C2H5COCH3	G	0	7.21E+01	300	5000	4	8	1	0	0	0
54	CH2CH2COCH3	G	0	7.11E+01	300	5000	4	7	1	0	0	0
55	CH2CH2CHO	G	0	5.71E+01	300	5000	3	5	1	0	0	0
56	IC4H9O2H	G	0	9.01E+01	300	5000	4	10	2	0	0	0
57	TC4H9O2H	G	0	9.01E+01	300	5000	4	10	2	0	0	0
58	IO2C4H8OH	G	0	1.05E+02	300	5000	4	9	3	0	0	0
59	TC4H8OOH-IO2	G	0	1.21E+02	300	5000	4	9	4	0	0	0
60	IC4H8OOH-IO2	G	0	1.21E+02	300	5000	4	9	4	0	0	0
61	IC4H8OOH-TO2	G	0	1.21E+02	300	5000	4	9	4	0	0	0
62	IC4KETII	G	0	1.04E+02	300	5000	4	8	3	0	0	0
63	IC4KETIT	G	0	1.04E+02	300	5000	4	8	3	0	0	0
64	TC3H6OCHO	G	0	8.71E+01	300	5000	4	7	2	0	0	0
65	TC3H6O2CHO	G	0	1.03E+02	300	5000	4	7	3	0	0	0
66	TC3H6O2HCO	G	0	1.03E+02	300	5000	4	7	3	0	0	0
67	IC3H5O2HCHO	G	0	1.03E+02	300	5000	4	7	3	0	0	0
68	TC4H8CHO	G	0	8.51E+01	300	5000	5	9	1	0	0	0
69	O2C4H8CHO	G	0	1.17E+02	300	5000	5	9	3	0	0	0

70	O2HC4H8CO	G	0	1.17E+02	300	5000	5	9	3	0	0	0
71	AC5H11	G	0	7.11E+01	300	5000	5	11	0	0	0	0
72	DC5H11	G	0	7.11E+01	300	5000	5	11	0	0	0	0
73	AC6H13	G	0	8.52E+01	300	5000	6	13	0	0	0	0
74	BC6H13	G	0	8.52E+01	300	5000	6	13	0	0	0	0
75	DC6H13	G	0	8.52E+01	300	5000	6	13	0	0	0	0
76	EC6H13	G	0	8.52E+01	300	5000	6	13	0	0	0	0
77	IC4H9COCH3	G	0	1.00E+02	300	5000	6	12	1	0	0	0
78	IC4H9COCH2	G	0	9.92E+01	300	5000	6	11	1	0	0	0
79	IC3H6CH2COCH3	G	0	9.92E+01	300	5000	6	11	1	0	0	0
80	TC3H6CH2COCH3	G	0	9.92E+01	300	5000	6	11	1	0	0	0
81	NC3H7COCH3	G	0	8.61E+01	300	5000	5	10	1	0	0	0
82	NC3H7COCH2	G	0	8.51E+01	300	5000	5	9	1	0	0	0
83	C3H6COCH3-2	G	0	8.51E+01	300	5000	5	9	1	0	0	0
84	AC3H5CHO	G	0	7.01E+01	300	5000	4	6	1	0	0	0
85	C4H8CHO-1	G	0	8.51E+01	300	5000	5	9	1	0	0	0
86	C2H5COC2H5	G	0	8.61E+01	300	5000	5	10	1	0	0	0
87	C2H5COC2H4P	G	0	8.51E+01	300	5000	5	9	1	0	0	0
88	C2H5COC2H3	G	0	8.41E+01	300	5000	5	8	1	0	0	0
89	PC2H4COC2H3	G	0	8.31E+01	300	5000	5	7	1	0	0	0
90	C7H16-24	G	0	1.00E+02	300	5000	7	16	0	0	0	0
91	ZC7H15O2	G	0	1.31E+02	300	5000	7	15	2	0	0	0
92	YC7H15O	G	0	1.15E+02	300	5000	7	15	1	0	0	0
93	ZC7H15O	G	0	1.15E+02	300	5000	7	15	1	0	0	0
94	YC7H14OOH-X1	G	0	1.31E+02	300	5000	7	15	2	0	0	0
95	YC7H14OOH-Z	G	0	1.31E+02	300	5000	7	15	2	0	0	0
96	YC7H14OOH-X2	G	0	1.31E+02	300	5000	7	15	2	0	0	0
97	ZC7H14OOH-Y	G	0	1.31E+02	300	5000	7	15	2	0	0	0
98	YC7H14OOH-X1O2	G	0	1.63E+02	300	5000	7	15	4	0	0	0
99	YC7H14OOH-X2O2	G	0	1.63E+02	300	5000	7	15	4	0	0	0
100	YC7H14OOH-Y2O2	G	0	1.63E+02	300	5000	7	15	4	0	0	0
101	YC7H14OOH-ZO2	G	0	1.63E+02	300	5000	7	15	4	0	0	0
102	X-Y2C7H14O	G	0	1.14E+02	300	5000	7	14	1	0	0	0
103	XC7H14OH	G	0	1.15E+02	300	5000	7	15	1	0	0	0
104	YC7H14OH	G	0	1.15E+02	300	5000	7	15	1	0	0	0
105	XO2C7H14OH	G	0	1.47E+02	300	5000	7	15	3	0	0	0
106	YO2C7H14OH	G	0	1.47E+02	300	5000	7	15	3	0	0	0
107	NEOC5H11O2H	G	0	1.04E+02	300	5000	5	12	2	0	0	0
108	NEOC5H11O	G	0	8.71E+01	300	5000	5	11	1	0	0	0
109	NEO-C5H10O	G	0	8.61E+01	300	5000	5	10	1	0	0	0
110	NEOC5H10OOH-O2	G	0	1.35E+02	300	5000	5	11	4	0	0	0
111	NEOC5H9Q2	G	0	1.35E+02	300	5000	5	11	4	0	0	0
112	NEOC5H9Q2-N	G	0	1.35E+02	300	5000	5	11	4	0	0	0
113	NEOC5KET	G	0	1.18E+02	300	5000	5	10	3	0	0	0

114	NEOC5KETOX	G	0	1.01E+02	300	5000	5	9	2	0	0	0
115	HC6H13	G	0	8.52E+01	300	5000	6	13	0	0	0	0
116	TC4H9CHO	G	0	8.61E+01	300	5000	5	10	1	0	0	0
117	TC4H9CO	G	0	8.51E+01	300	5000	5	9	1	0	0	0
118	IC3H6CHCHO	G	0	8.41E+01	300	5000	5	8	1	0	0	0
119	IC3H6CHCO	G	0	8.31E+01	300	5000	5	7	1	0	0	0
120	PC7H13O-O	G	0	1.13E+02	300	5000	7	13	1	0	0	0
121	NC7H15O2	G	0	1.31E+02	300	5000	7	15	2	0	0	0
122	PC7H15O2	G	0	1.31E+02	300	5000	7	15	2	0	0	0
123	QC7H15O2	G	0	1.31E+02	300	5000	7	15	2	0	0	0
124	NC7H14OOH-N2	G	0	1.31E+02	300	5000	7	15	2	0	0	0
125	NC7H14OOH-O	G	0	1.31E+02	300	5000	7	15	2	0	0	0
126	QC7H14OOH-O	G	0	1.31E+02	300	5000	7	15	2	0	0	0
127	PC7H14OOH-N	G	0	1.31E+02	300	5000	7	15	2	0	0	0
128	PC7H14OOH-O	G	0	1.31E+02	300	5000	7	15	2	0	0	0
129	NC7H14OOH-OO2	G	0	1.63E+02	300	5000	7	15	4	0	0	0
130	QC7H14OOH-OO2	G	0	1.63E+02	300	5000	7	15	4	0	0	0
131	PC7H14OOH-NO2	G	0	1.63E+02	300	5000	7	15	4	0	0	0
132	PC7H14OOH-OO2	G	0	1.63E+02	300	5000	7	15	4	0	0	0
133	N-PC7H14O	G	0	1.14E+02	300	5000	7	14	1	0	0	0
134	NEOC7KETPN	G	0	1.46E+02	300	5000	7	14	3	0	0	0
135	NEOC7KETPO	G	0	1.46E+02	300	5000	7	14	3	0	0	0
136	NEOC7KETQO	G	0	1.46E+02	300	5000	7	14	3	0	0	0
137	CC8H17O2	G	0	1.45E+02	300	5000	8	17	2	0	0	0
138	AC8H17O2H	G	0	1.46E+02	300	5000	8	18	2	0	0	0
139	BC8H17O2H	G	0	1.46E+02	300	5000	8	18	2	0	0	0
140	CC8H17O2H	G	0	1.46E+02	300	5000	8	18	2	0	0	0
141	DC8H17O2H	G	0	1.46E+02	300	5000	8	18	2	0	0	0
142	AC8H17O	G	0	1.29E+02	300	5000	8	17	1	0	0	0
143	BC8H17O	G	0	1.29E+02	300	5000	8	17	1	0	0	0
144	CC8H17O	G	0	1.29E+02	300	5000	8	17	1	0	0	0
145	DC8H17O	G	0	1.29E+02	300	5000	8	17	1	0	0	0
146	AC8H16OOH-D	G	0	1.45E+02	300	5000	8	17	2	0	0	0
147	CC8H16OOH-D	G	0	1.45E+02	300	5000	8	17	2	0	0	0
148	CC8H16OOH-B	G	0	1.45E+02	300	5000	8	17	2	0	0	0
149	CC8H16OOH-A	G	0	1.45E+02	300	5000	8	17	2	0	0	0
150	DC8H16OOH-D	G	0	1.45E+02	300	5000	8	17	2	0	0	0
151	DC8H16OOH-A	G	0	1.45E+02	300	5000	8	17	2	0	0	0
152	IC8ETERAD	G	0	1.28E+02	300	5000	8	16	1	0	0	0
153	IC8ETERDD	G	0	1.28E+02	300	5000	8	16	1	0	0	0
154	AC8H16OOH-AO2	G	0	1.77E+02	300	5000	8	17	4	0	0	0
155	AC8H16OOH-BO2	G	0	1.77E+02	300	5000	8	17	4	0	0	0
156	AC8H16OOH-CO2	G	0	1.77E+02	300	5000	8	17	4	0	0	0
157	BC8H16OOH-CO2	G	0	1.77E+02	300	5000	8	17	4	0	0	0
158	BC8H16OOH-AO2	G	0	1.77E+02	300	5000	8	17	4	0	0	0
159	BC8H16OOH-DO2	G	0	1.77E+02	300	5000	8	17	4	0	0	0



160	CC8H16OOH-BO2	G	0	1.77E+02	300	5000	8	17	4	0	0	0
161	CC8H16OOH-AO2	G	0	1.77E+02	300	5000	8	17	4	0	0	0
162	DC8H16OOH-CO2	G	0	1.77E+02	300	5000	8	17	4	0	0	0
163	DC8H16OOH-DO2	G	0	1.77E+02	300	5000	8	17	4	0	0	0
164	DC8H16OOH-BO2	G	0	1.77E+02	300	5000	8	17	4	0	0	0
165	IC8KETAA	G	0	1.60E+02	300	5000	8	16	3	0	0	0
166	IC8KETAB	G	0	1.60E+02	300	5000	8	16	3	0	0	0
167	IC8KETAC	G	0	1.60E+02	300	5000	8	16	3	0	0	0
168	IC8KETBA	G	0	1.60E+02	300	5000	8	16	3	0	0	0
169	IC8KETBC	G	0	1.60E+02	300	5000	8	16	3	0	0	0
170	IC8KETBD	G	0	1.60E+02	300	5000	8	16	3	0	0	0
171	IC8KETDB	G	0	1.60E+02	300	5000	8	16	3	0	0	0
172	IC8KETDC	G	0	1.60E+02	300	5000	8	16	3	0	0	0
173	IC8KETDD	G	0	1.60E+02	300	5000	8	16	3	0	0	0
174	CC8H16OH-B	G	0	1.29E+02	300	5000	8	17	1	0	0	0
175	BC8H16OH-C	G	0	1.29E+02	300	5000	8	17	1	0	0	0
176	CC8H16OH-BO2	G	0	1.61E+02	300	5000	8	17	3	0	0	0
177	CC8H16O-BO2H	G	0	1.61E+02	300	5000	8	17	3	0	0	0
178	BC8H16OH-CO2	G	0	1.61E+02	300	5000	8	17	3	0	0	0
179	BC8H16O-CO2H	G	0	1.61E+02	300	5000	8	17	3	0	0	0
180	DC6H12CHO-D	G	0	1.13E+02	300	5000	7	13	1	0	0	0
181	IC3H7COC3H6-T	G	0	1.13E+02	300	5000	7	13	1	0	0	0
182	TC4H9COC2H5	G	0	1.14E+02	300	5000	7	14	1	0	0	0
183	TC4H9COC2H4S	G	0	1.13E+02	300	5000	7	13	1	0	0	0
184	HC6H12CHO	G	0	1.13E+02	300	5000	7	13	1	0	0	0
185	OC7H13OOH-N	G	0	1.30E+02	300	5000	7	14	2	0	0	0
186	OC7H13O-N	G	0	1.13E+02	300	5000	7	13	1	0	0	0
187	PC7H13OOH-O	G	0	1.30E+02	300	5000	7	14	2	0	0	0
188	OC7H13OOH-Q	G	0	1.30E+02	300	5000	7	14	2	0	0	0
189	OC7H13O-Q	G	0	1.13E+02	300	5000	7	13	1	0	0	0
190	DC6H11-D	G	0	8.32E+01	300	5000	6	11	0	0	0	0
191	IC3H6CHCOCH2	G	0	9.71E+01	300	5000	6	9	1	0	0	0
192	C4H8OH-1	G	0	7.31E+01	300	5000	4	9	1	0	0	0
193	C5H11O2-1	G	0	1.03E+02	300	5000	5	11	2	0	0	0
194	C5H11O2H-1	G	0	1.04E+02	300	5000	5	12	2	0	0	0
195	C5H11O-1	G	0	8.71E+01	300	5000	5	11	1	0	0	0
196	C5H11O-2	G	0	8.71E+01	300	5000	5	11	1	0	0	0
197	C5H10OOH1-2	G	0	1.03E+02	300	5000	5	11	2	0	0	0
198	C5H10OOH1-3	G	0	1.03E+02	300	5000	5	11	2	0	0	0
199	C5H10OOH1-4	G	0	1.03E+02	300	5000	5	11	2	0	0	0
200	C5H10OOH2-3	G	0	1.03E+02	300	5000	5	11	2	0	0	0
201	C5H10OOH1-2O2	G	0	1.35E+02	300	5000	5	11	4	0	0	0
202	C5H10OOH1-3O2	G	0	1.35E+02	300	5000	5	11	4	0	0	0
203	C5H10OOH1-4O2	G	0	1.35E+02	300	5000	5	11	4	0	0	0
204	C5H10OOH2-4O2	G	0	1.35E+02	300	5000	5	11	4	0	0	0
205	C5H10O1-3	G	0	8.61E+01	300	5000	5	10	1	0	0	0

206	C5H10O1-4	G	0	8.61E+01	300	5000	5	10	1	0	0	0
207	NC5KET12	G	0	1.18E+02	300	5000	5	10	3	0	0	0
208	NC5KET13	G	0	1.18E+02	300	5000	5	10	3	0	0	0
209	NC5KET14	G	0	1.18E+02	300	5000	5	10	3	0	0	0
210	NC5KET24	G	0	1.18E+02	300	5000	5	10	3	0	0	0
211	NC3H7COC2H4P	G	0	9.92E+01	300	5000	6	11	1	0	0	0
212	C6H12O1-2	G	0	1.00E+02	300	5000	6	12	1	0	0	0
213	C6H12O1-3	G	0	1.00E+02	300	5000	6	12	1	0	0	0
214	C6H13O2H-1	G	0	1.18E+02	300	5000	6	14	2	0	0	0
215	C6H13O2-1	G	0	1.17E+02	300	5000	6	13	2	0	0	0
216	C6H12OOH1-2	G	0	1.17E+02	300	5000	6	13	2	0	0	0
217	C6H12OOH1-3	G	0	1.17E+02	300	5000	6	13	2	0	0	0
218	C6H12OOH1-4	G	0	1.17E+02	300	5000	6	13	2	0	0	0
219	C6H12OOH1-2O2	G	0	1.49E+02	300	5000	6	13	4	0	0	0
220	C6H12OOH1-3O2	G	0	1.49E+02	300	5000	6	13	4	0	0	0
221	C6H12OOH1-4O2	G	0	1.49E+02	300	5000	6	13	4	0	0	0
222	NC6KET12	G	0	1.32E+02	300	5000	6	12	3	0	0	0
223	NC6KET13	G	0	1.32E+02	300	5000	6	12	3	0	0	0
224	NC6KET14	G	0	1.32E+02	300	5000	6	12	3	0	0	0
225	C6H13O-1	G	0	1.01E+02	300	5000	6	13	1	0	0	0
226	C7H14-2	G	0	9.82E+01	300	5000	7	14	0	0	0	0
227	C7H14-3	G	0	9.82E+01	300	5000	7	14	0	0	0	0
228	C7H15O2-4	G	0	1.31E+02	300	5000	7	15	2	0	0	0
229	C7H15O2H-1	G	0	1.32E+02	300	5000	7	16	2	0	0	0
230	C7H15O-1	G	0	1.15E+02	300	5000	7	15	1	0	0	0
231	C7H14OOH4-2	G	0	1.31E+02	300	5000	7	15	2	0	0	0
232	C7H14OOH1-2O2	G	0	1.63E+02	300	5000	7	15	4	0	0	0
233	C7H14OOH1-3O2	G	0	1.63E+02	300	5000	7	15	4	0	0	0
234	C7H14OOH1-4O2	G	0	1.63E+02	300	5000	7	15	4	0	0	0
235	C7H14OOH4-2O2	G	0	1.63E+02	300	5000	7	15	4	0	0	0
236	NC7KET12	G	0	1.46E+02	300	5000	7	14	3	0	0	0
237	NC7KET13	G	0	1.46E+02	300	5000	7	14	3	0	0	0
238	NC7KET14	G	0	1.46E+02	300	5000	7	14	3	0	0	0
239	NC7KET42	G	0	1.46E+02	300	5000	7	14	3	0	0	0
240	C5H10CHO-1	G	0	9.92E+01	300	5000	6	11	1	0	0	0
241	C5H10CHO-2	G	0	9.92E+01	300	5000	6	11	1	0	0	0
242	C5H10CHO-3	G	0	9.92E+01	300	5000	6	11	1	0	0	0
243	C5H10CHO-4	G	0	9.92E+01	300	5000	6	11	1	0	0	0
244	C5H10CHO-5	G	0	9.92E+01	300	5000	6	11	1	0	0	0
245	NC4H9COCH3	G	0	1.00E+02	300	5000	6	12	1	0	0	0
246	C9H19-3	G	0	1.27E+02	300	5000	9	19	0	0	0	0
247	C9H19-5	G	0	1.27E+02	300	5000	9	19	0	0	0	0
248	C9H18-2	G	0	1.26E+02	300	5000	9	18	0	0	0	0
249	C9H18-3	G	0	1.26E+02	300	5000	9	18	0	0	0	0
250	C10H21O-1	G	0	1.57E+02	300	5000	10	21	1	0	0	0
251	C10H21O-2	G	0	1.57E+02	300	5000	10	21	1	0	0	0

252	C10H21O-3	G	0	1.57E+02	300	5000	10	21	1	0	0	0
253	C10H21O-4	G	0	1.57E+02	300	5000	10	21	1	0	0	0
254	C10H21O-5	G	0	1.57E+02	300	5000	10	21	1	0	0	0
255	C9H19O-1	G	0	1.43E+02	300	5000	9	19	1	0	0	0
256	C8H17O-1	G	0	1.29E+02	300	5000	8	17	1	0	0	0
257	C9H19O2-4	G	0	1.59E+02	300	5000	9	19	2	0	0	0
258	C9H19O2-5	G	0	1.59E+02	300	5000	9	19	2	0	0	0
259	C10H21O2H-1	G	0	1.74E+02	300	5000	10	22	2	0	0	0
260	C10H21O2H-2	G	0	1.74E+02	300	5000	10	22	2	0	0	0
261	C10H21O2H-3	G	0	1.74E+02	300	5000	10	22	2	0	0	0
262	C10H21O2H-4	G	0	1.74E+02	300	5000	10	22	2	0	0	0
263	C10H21O2H-5	G	0	1.74E+02	300	5000	10	22	2	0	0	0
264	C9H19O2H-1	G	0	1.60E+02	300	5000	9	20	2	0	0	0
265	C8H17O2H-1	G	0	1.46E+02	300	5000	8	18	2	0	0	0
266	C10OOH2-1	G	0	1.73E+02	300	5000	10	21	2	0	0	0
267	C10OOH2-6	G	0	1.73E+02	300	5000	10	21	2	0	0	0
268	C10OOH3-1	G	0	1.73E+02	300	5000	10	21	2	0	0	0
269	C10OOH3-7	G	0	1.73E+02	300	5000	10	21	2	0	0	0
270	C10OOH4-7	G	0	1.73E+02	300	5000	10	21	2	0	0	0
271	C10OOH4-8	G	0	1.73E+02	300	5000	10	21	2	0	0	0
272	C10OOH5-9	G	0	1.73E+02	300	5000	10	21	2	0	0	0
273	C9OOH1-2	G	0	1.59E+02	300	5000	9	19	2	0	0	0
274	C9OOH1-3	G	0	1.59E+02	300	5000	9	19	2	0	0	0
275	C9OOH1-4	G	0	1.59E+02	300	5000	9	19	2	0	0	0
276	C9OOH5-3	G	0	1.59E+02	300	5000	9	19	2	0	0	0
277	C8OOH1-2	G	0	1.45E+02	300	5000	8	17	2	0	0	0
278	C8OOH1-3	G	0	1.45E+02	300	5000	8	17	2	0	0	0
279	C8OOH1-4	G	0	1.45E+02	300	5000	8	17	2	0	0	0
280	C10OOH1-2O2	G	0	2.05E+02	300	5000	10	21	4	0	0	0
281	C10OOH1-3O2	G	0	2.05E+02	300	5000	10	21	4	0	0	0
282	C10OOH1-4O2	G	0	2.05E+02	300	5000	10	21	4	0	0	0
283	C10OOH2-1O2	G	0	2.05E+02	300	5000	10	21	4	0	0	0
284	C10OOH2-3O2	G	0	2.05E+02	300	5000	10	21	4	0	0	0
285	C10OOH2-4O2	G	0	2.05E+02	300	5000	10	21	4	0	0	0
286	C10OOH2-5O2	G	0	2.05E+02	300	5000	10	21	4	0	0	0
287	C10OOH3-1O2	G	0	2.05E+02	300	5000	10	21	4	0	0	0
288	C10OOH3-2O2	G	0	2.05E+02	300	5000	10	21	4	0	0	0
289	C10OOH3-4O2	G	0	2.05E+02	300	5000	10	21	4	0	0	0
290	C10OOH3-5O2	G	0	2.05E+02	300	5000	10	21	4	0	0	0
291	C10OOH3-6O2	G	0	2.05E+02	300	5000	10	21	4	0	0	0
292	C10OOH4-1O2	G	0	2.05E+02	300	5000	10	21	4	0	0	0
293	C10OOH4-2O2	G	0	2.05E+02	300	5000	10	21	4	0	0	0
294	C10OOH4-3O2	G	0	2.05E+02	300	5000	10	21	4	0	0	0
295	C10OOH4-5O2	G	0	2.05E+02	300	5000	10	21	4	0	0	0
296	C10OOH4-6O2	G	0	2.05E+02	300	5000	10	21	4	0	0	0
297	C10OOH4-7O2	G	0	2.05E+02	300	5000	10	21	4	0	0	0

298	C10OOH5-2O2	G	0	2.05E+02	300	5000	10	21	4	0	0	0
299	C10OOH5-3O2	G	0	2.05E+02	300	5000	10	21	4	0	0	0
300	C10OOH5-4O2	G	0	2.05E+02	300	5000	10	21	4	0	0	0
301	C10OOH5-6O2	G	0	2.05E+02	300	5000	10	21	4	0	0	0
302	C10OOH5-7O2	G	0	2.05E+02	300	5000	10	21	4	0	0	0
303	C10OOH5-8O2	G	0	2.05E+02	300	5000	10	21	4	0	0	0
304	C9OOH1-2O2	G	0	1.91E+02	300	5000	9	19	4	0	0	0
305	C9OOH1-3O2	G	0	1.91E+02	300	5000	9	19	4	0	0	0
306	C8OOH1-2O2	G	0	1.77E+02	300	5000	8	17	4	0	0	0
307	C8OOH1-3O2	G	0	1.77E+02	300	5000	8	17	4	0	0	0
308	C8OOH1-4O2	G	0	1.77E+02	300	5000	8	17	4	0	0	0
309	C10O2-6	G	0	1.56E+02	300	5000	10	20	1	0	0	0
310	C10O3-4	G	0	1.56E+02	300	5000	10	20	1	0	0	0
311	C10O3-7	G	0	1.56E+02	300	5000	10	20	1	0	0	0
312	C10O4-7	G	0	1.56E+02	300	5000	10	20	1	0	0	0
313	C9O1-3	G	0	1.42E+02	300	5000	9	18	1	0	0	0
314	C9O1-4	G	0	1.42E+02	300	5000	9	18	1	0	0	0
315	C8O1-2	G	0	1.28E+02	300	5000	8	16	1	0	0	0
316	C10KET1-2	G	0	1.88E+02	300	5000	10	20	3	0	0	0
317	C10KET1-3	G	0	1.88E+02	300	5000	10	20	3	0	0	0
318	C10KET1-4	G	0	1.88E+02	300	5000	10	20	3	0	0	0
319	C10KET2-1	G	0	1.88E+02	300	5000	10	20	3	0	0	0
320	C10KET2-3	G	0	1.88E+02	300	5000	10	20	3	0	0	0
321	C10KET2-4	G	0	1.88E+02	300	5000	10	20	3	0	0	0
322	C10KET2-5	G	0	1.88E+02	300	5000	10	20	3	0	0	0
323	C10KET3-1	G	0	1.88E+02	300	5000	10	20	3	0	0	0
324	C10KET3-2	G	0	1.88E+02	300	5000	10	20	3	0	0	0
325	C10KET3-4	G	0	1.88E+02	300	5000	10	20	3	0	0	0
326	C10KET3-5	G	0	1.88E+02	300	5000	10	20	3	0	0	0
327	C10KET3-6	G	0	1.88E+02	300	5000	10	20	3	0	0	0
328	C10KET4-1	G	0	1.88E+02	300	5000	10	20	3	0	0	0
329	C10KET4-2	G	0	1.88E+02	300	5000	10	20	3	0	0	0
330	C10KET4-3	G	0	1.88E+02	300	5000	10	20	3	0	0	0
331	C10KET4-5	G	0	1.88E+02	300	5000	10	20	3	0	0	0
332	C10KET4-6	G	0	1.88E+02	300	5000	10	20	3	0	0	0
333	C10KET4-7	G	0	1.88E+02	300	5000	10	20	3	0	0	0
334	C10KET5-2	G	0	1.88E+02	300	5000	10	20	3	0	0	0
335	C10KET5-3	G	0	1.88E+02	300	5000	10	20	3	0	0	0
336	C10KET5-4	G	0	1.88E+02	300	5000	10	20	3	0	0	0
337	C10KET5-6	G	0	1.88E+02	300	5000	10	20	3	0	0	0
338	C10KET5-7	G	0	1.88E+02	300	5000	10	20	3	0	0	0
339	C10KET5-8	G	0	1.88E+02	300	5000	10	20	3	0	0	0
340	C9KET1-2	G	0	1.74E+02	300	5000	9	18	3	0	0	0
341	C9KET1-3	G	0	1.74E+02	300	5000	9	18	3	0	0	0
342	C8KET1-2	G	0	1.60E+02	300	5000	8	16	3	0	0	0
343	C8KET1-3	G	0	1.60E+02	300	5000	8	16	3	0	0	0

344	C8KET1-4	G	0	1.60E+02	300	5000	8	16	3	0	0	0
345	NC8H17CHO	G	0	1.42E+02	300	5000	9	18	1	0	0	0
346	NC8H17CO	G	0	1.41E+02	300	5000	9	17	1	0	0	0
347	C7H15COCH2	G	0	1.41E+02	300	5000	9	17	1	0	0	0
348	C6COC2H4P	G	0	1.41E+02	300	5000	9	17	1	0	0	0
349	C5COC2H4P	G	0	1.27E+02	300	5000	8	15	1	0	0	0
350	C4COC2H4P	G	0	1.13E+02	300	5000	7	13	1	0	0	0
351	C2H2OH	G	0	4.30E+01	300	5000	2	3	1	0	0	0
352	C2H3CHOCH2	G	0	7.01E+01	300	3000	4	6	1	0	0	0
353	C4H6O23	G	0	7.01E+01	200	5000	4	6	1	0	0	0
354	CH3CHCHCHO	G	0	7.01E+01	298	3000	4	6	1	0	0	0
355	CC3H4	G	0	4.01E+01	300	5000	3	4	0	0	0	0
356	CH3CHCO	G	0	5.61E+01	300	5000	3	4	1	0	0	0
357	CH3CHCHO	G	0	5.71E+01	300	5000	3	5	1	0	0	0
358	C2H5CHCO	G	0	7.01E+01	300	5000	4	6	1	0	0	0
359	NC3H7CO	G	0	7.11E+01	300	5000	4	7	1	0	0	0
360	H	G	0	1.01E+00	300	5000	0	1	0	0	0	0
361	H2	G	0	2.02E+00	300	5000	0	2	0	0	0	0
362	O	G	0	1.60E+01	300	5000	0	0	1	0	0	0
363	OH	G	0	1.70E+01	300	5000	0	1	1	0	0	0
364	HO2	G	0	3.30E+01	300	5000	0	1	2	0	0	0
365	H2O2	G	0	3.40E+01	300	5000	0	2	2	0	0	0
366	CH2O	G	0	3.00E+01	300	5000	1	2	1	0	0	0
367	HCO	G	0	2.90E+01	300	5000	1	1	1	0	0	0
368	HOCH2O	G	0	4.70E+01	300	5000	1	3	2	0	0	0
369	CH3OH	G	0	3.20E+01	300	5000	1	4	1	0	0	0
370	CH2OH	G	0	3.10E+01	250	4000	1	3	1	0	0	0
371	CH3O	G	0	3.10E+01	300	3000	1	3	1	0	0	0
372	CH3O2	G	0	4.70E+01	300	5000	1	3	2	0	0	0
373	CH4	G	0	1.60E+01	300	5000	1	4	0	0	0	0
374	CH3	G	0	1.50E+01	300	5000	1	3	0	0	0	0
375	CH2	G	0	1.40E+01	250	4000	1	2	0	0	0	0
376	CH2(S)	G	0	1.40E+01	300	4000	1	2	0	0	0	0
377	C2H6	G	0	3.01E+01	300	4000	2	6	0	0	0	0
378	C2H5	G	0	2.91E+01	300	5000	2	5	0	0	0	0
379	C2H4	G	0	2.81E+01	300	5000	2	4	0	0	0	0
380	C2H3	G	0	2.70E+01	300	5000	2	3	0	0	0	0
381	C2H2	G	0	2.60E+01	300	5000	2	2	0	0	0	0
382	C2H	G	0	2.50E+01	300	4000	2	1	0	0	0	0
383	CH3CHO	G	0	4.41E+01	300	5000	2	4	1	0	0	0
384	CH3CO	G	0	4.30E+01	300	5000	2	3	1	0	0	0
385	CH2CHO	G	0	4.30E+01	300	5000	2	3	1	0	0	0
386	CH2CO	G	0	4.20E+01	300	5000	2	2	1	0	0	0
387	HCCO	G	0	4.10E+01	300	4000	2	1	1	0	0	0
388	C2H5OH	G	0	4.61E+01	300	5000	2	6	1	0	0	0
389	C2H5O	G	0	4.51E+01	300	5000	2	5	1	0	0	0

390	PC2H4OH	G	0	4.51E+01	300	5000	2	5	1	0	0	0
391	SC2H4OH	G	0	4.51E+01	300	5000	2	5	1	0	0	0
392	C2H5O2	G	0	6.11E+01	300	5000	2	5	2	0	0	0
393	C2H3O1-2	G	0	4.30E+01	300	5000	2	3	1	0	0	0
394	CH3COCH3	G	0	5.81E+01	300	5000	3	6	1	0	0	0
395	CH3COCH2	G	0	5.71E+01	300	5000	3	5	1	0	0	0
396	C2H3CHO	G	0	5.61E+01	300	5000	3	4	1	0	0	0
397	C2H3CO	G	0	5.51E+01	300	5000	3	3	1	0	0	0
398	C2H5CHO	G	0	5.81E+01	300	5000	3	6	1	0	0	0
399	C2H5CO	G	0	5.71E+01	300	5000	3	5	1	0	0	0
400	C3H8	G	0	4.41E+01	300	5000	3	8	0	0	0	0
401	IC3H7	G	0	4.31E+01	300	5000	3	7	0	0	0	0
402	NC3H7	G	0	4.31E+01	300	5000	3	7	0	0	0	0
403	C3H6	G	0	4.21E+01	300	5000	3	6	0	0	0	0
404	C3H5-A	G	0	4.11E+01	300	5000	3	5	0	0	0	0
405	C3H5-S	G	0	4.11E+01	300	5000	3	5	0	0	0	0
406	C3H5-T	G	0	4.11E+01	300	5000	3	5	0	0	0	0
407	C3H4-P	G	0	4.01E+01	300	4000	3	4	0	0	0	0
408	C3H4-A	G	0	4.01E+01	300	4000	3	4	0	0	0	0
409	C3H3	G	0	3.91E+01	300	4000	3	3	0	0	0	0
410	C3H2	G	0	3.80E+01	150	4000	3	2	0	0	0	0
411	C3H5O	G	0	5.71E+01	300	5000	3	5	1	0	0	0
412	C3H6OOH1-2	G	0	7.51E+01	300	5000	3	7	2	0	0	0
413	C3H6OOH1-3	G	0	7.51E+01	300	5000	3	7	2	0	0	0
414	C3H6OOH2-1	G	0	7.51E+01	300	5000	3	7	2	0	0	0
415	C3H6OOH1-2O2	G	0	1.07E+02	300	5000	3	7	4	0	0	0
416	C3H6OOH1-3O2	G	0	1.07E+02	300	5000	3	7	4	0	0	0
417	C3H6OOH2-1O2	G	0	1.07E+02	300	5000	3	7	4	0	0	0
418	NC3H7O2	G	0	7.51E+01	300	5000	3	7	2	0	0	0
419	IC3H7O2	G	0	7.51E+01	300	5000	3	7	2	0	0	0
420	C3H6O1-3	G	0	5.81E+01	300	5000	3	6	1	0	0	0
421	C3KET12	G	0	9.01E+01	300	5000	3	6	3	0	0	0
422	C3KET13	G	0	9.01E+01	300	5000	3	6	3	0	0	0
423	C3KET21	G	0	9.01E+01	300	5000	3	6	3	0	0	0
424	C3H51-2	3OOH	G	0	1.07E+02	300	5000	3	7	4	0	0
425	C3H52-1	3OOH	G	0	1.07E+02	300	5000	3	7	4	0	0
426	AC3H5OOH	G	0	7.41E+01	300	5000	3	6	2	0	0	0
427	C4H10	G	0	5.81E+01	300	5000	4	10	0	0	0	0
428	C4H8-1	G	0	5.61E+01	300	5000	4	8	0	0	0	0
429	C4H8-2	G	0	5.61E+01	300	5000	4	8	0	0	0	0
430	PC4H9	G	0	5.71E+01	300	5000	4	9	0	0	0	0
431	SC4H9	G	0	5.71E+01	300	5000	4	9	0	0	0	0
432	C4H71-1	G	0	5.51E+01	300	5000	4	7	0	0	0	0
433	C4H71-2	G	0	5.51E+01	300	5000	4	7	0	0	0	0
434	C4H71-3	G	0	5.51E+01	300	5000	4	7	0	0	0	0

435	C4H71-4	G	0	5.51E+01	300	5000	4	7	0	0	0	0
436	C4H6	G	0	5.41E+01	300	5000	4	6	0	0	0	0
437	C4H7O	G	0	7.11E+01	300	5000	4	7	1	0	0	0
438	C2H5COCH2	G	0	7.11E+01	300	5000	4	7	1	0	0	0
439	CH3CHCOCH3	G	0	7.11E+01	300	5000	4	7	1	0	0	0
440	C2H3COCH3	G	0	7.01E+01	300	5000	4	6	1	0	0	0
441	NC3H7CHO	G	0	7.21E+01	300	5000	4	8	1	0	0	0
442	C3H6CHO-1	G	0	7.11E+01	300	5000	4	7	1	0	0	0
443	C3H6CHO-2	G	0	7.11E+01	300	5000	4	7	1	0	0	0
444	C3H6CHO-3	G	0	7.11E+01	300	5000	4	7	1	0	0	0
445	SC3H5CHO	G	0	7.01E+01	300	5000	4	6	1	0	0	0
446	SC3H5CO	G	0	6.91E+01	300	5000	4	5	1	0	0	0
447	IC4H10	G	0	5.81E+01	300	5000	4	10	0	0	0	0
448	IC4H9	G	0	5.71E+01	300	5000	4	9	0	0	0	0
449	TC4H9	G	0	5.71E+01	300	5000	4	9	0	0	0	0
450	IC4H8	G	0	5.61E+01	300	5000	4	8	0	0	0	0
451	IC4H7	G	0	5.51E+01	300	5000	4	7	0	0	0	0
452	TC4H9O2	G	0	8.91E+01	300	5000	4	9	2	0	0	0
453	IC4H9O2	G	0	8.91E+01	300	5000	4	9	2	0	0	0
454	TC4H8O2H-I	G	0	8.91E+01	300	5000	4	9	2	0	0	0
455	IC4H8O2H-I	G	0	8.91E+01	300	5000	4	9	2	0	0	0
456	IC4H8O2H-T	G	0	8.91E+01	300	5000	4	9	2	0	0	0
457	IC4H8O	G	0	7.21E+01	300	5000	4	8	1	0	0	0
458	CC4H8O	G	0	7.21E+01	300	5000	4	8	1	0	0	0
459	IC4H9O	G	0	7.31E+01	300	5000	4	9	1	0	0	0
460	TC4H9O	G	0	7.31E+01	300	5000	4	9	1	0	0	0
461	IC4H7O	G	0	7.11E+01	300	5000	4	7	1	0	0	0
462	IC4H8OH	G	0	7.31E+01	300	5000	4	9	1	0	0	0
463	IC3H7CHO	G	0	7.21E+01	300	5000	4	8	1	0	0	0
464	TC3H6CHO	G	0	7.11E+01	300	5000	4	7	1	0	0	0
465	IC3H7CO	G	0	7.11E+01	300	5000	4	7	1	0	0	0
466	IC3H6CHO	G	0	7.11E+01	300	5000	4	7	1	0	0	0
467	IC4H7OH	G	0	7.21E+01	300	5000	4	8	1	0	0	0
468	IC4H6OH	G	0	7.11E+01	300	5000	4	7	1	0	0	0
469	IC3H5CHO	G	0	7.01E+01	300	5000	4	6	1	0	0	0
470	IC3H5CO	G	0	6.91E+01	300	5000	4	5	1	0	0	0
471	IC3H6CO	G	0	7.01E+01	300	5000	4	6	1	0	0	0
472	IC4H7OOH	G	0	8.81E+01	300	5000	4	8	2	0	0	0
473	TC3H6OH	G	0	5.91E+01	300	5000	3	7	1	0	0	0
474	IC3H5OH	G	0	5.81E+01	300	5000	3	6	1	0	0	0
475	CH2CCH2OH	G	0	5.71E+01	300	5000	3	5	1	0	0	0
476	BC5H11	G	0	7.11E+01	300	5000	5	11	0	0	0	0
477	AC5H10	G	0	7.01E+01	300	5000	5	10	0	0	0	0
478	BC5H10	G	0	7.01E+01	300	5000	5	10	0	0	0	0
479	CC5H10	G	0	7.01E+01	300	5000	5	10	0	0	0	0
480	AC5H9-A2	G	0	6.91E+01	300	5000	5	9	0	0	0	0

481	AC5H9-C	G	0	6.91E+01	300	5000	5	9	0	0	0	0
482	CC5H9-B	G	0	6.91E+01	300	5000	5	9	0	0	0	0
483	AC5H9O-C	G	0	8.51E+01	300	5000	5	9	1	0	0	0
484	CC5H9O-B	G	0	8.51E+01	300	5000	5	9	1	0	0	0
485	AC6H12	G	0	8.42E+01	300	5000	6	12	0	0	0	0
486	BC6H12	G	0	8.42E+01	300	5000	6	12	0	0	0	0
487	CC6H12	G	0	8.42E+01	300	5000	6	12	0	0	0	0
488	DC6H12	G	0	8.42E+01	300	5000	6	12	0	0	0	0
489	AC6H11-A2	G	0	8.32E+01	300	5000	6	11	0	0	0	0
490	AC6H11-C	G	0	8.32E+01	300	5000	6	11	0	0	0	0
491	AC6H11-E	G	0	8.32E+01	300	5000	6	11	0	0	0	0
492	BC6H11-E	G	0	8.32E+01	300	5000	6	11	0	0	0	0
493	CC6H11-A	G	0	8.32E+01	300	5000	6	11	0	0	0	0
494	CC6H11-B	G	0	8.32E+01	300	5000	6	11	0	0	0	0
495	AC6H11O-C	G	0	9.92E+01	300	5000	6	11	1	0	0	0
496	CC6H11O-B	G	0	9.92E+01	300	5000	6	11	1	0	0	0
497	C4H7CO1-4	G	0	8.31E+01	300	5000	5	7	1	0	0	0
498	C5H10-1	G	0	7.01E+01	300	5000	5	10	0	0	0	0
499	C5H10-2	G	0	7.01E+01	300	5000	5	10	0	0	0	0
500	C5H91-3	G	0	6.91E+01	300	5000	5	9	0	0	0	0
501	C5H91-4	G	0	6.91E+01	300	5000	5	9	0	0	0	0
502	C5H91-5	G	0	6.91E+01	300	5000	5	9	0	0	0	0
503	CC5H11	G	0	7.11E+01	300	5000	5	11	0	0	0	0
504	C5H92-4	G	0	6.91E+01	300	5000	5	9	0	0	0	0
505	C5H92-5	G	0	6.91E+01	300	5000	5	9	0	0	0	0
506	C5H9O1-3	G	0	8.51E+01	300	5000	5	9	1	0	0	0
507	C5H9O2-4	G	0	8.51E+01	300	5000	5	9	1	0	0	0
508	C5H11-2	G	0	7.11E+01	300	5000	5	11	0	0	0	0
509	NC4H9CHO	G	0	8.61E+01	300	5000	5	10	1	0	0	0
510	NC4H9CO	G	0	8.51E+01	300	5000	5	9	1	0	0	0
511	C4H8CHO-2	G	0	8.51E+01	300	5000	5	9	1	0	0	0
512	C4H8CHO-3	G	0	8.51E+01	300	5000	5	9	1	0	0	0
513	C4H8CHO-4	G	0	8.51E+01	300	5000	5	9	1	0	0	0
514	IC4H7-I1	G	0	5.51E+01	300	5000	4	7	0	0	0	0
515	C5H81-3	G	0	6.81E+01	300	5000	5	8	0	0	0	0
516	XC7H15	G	0	9.92E+01	300	5000	7	15	0	0	0	0
517	YC7H15	G	0	9.92E+01	300	5000	7	15	0	0	0	0
518	ZC7H15	G	0	9.92E+01	300	5000	7	15	0	0	0	0
519	XC7H14	G	0	9.82E+01	300	5000	7	14	0	0	0	0
520	YC7H14	G	0	9.82E+01	300	5000	7	14	0	0	0	0
521	XC7H13-X1	G	0	9.72E+01	300	5000	7	13	0	0	0	0
522	XC7H13-Z	G	0	9.72E+01	300	5000	7	13	0	0	0	0
523	XC7H13-X2	G	0	9.72E+01	300	5000	7	13	0	0	0	0
524	XC7H13-Y2	G	0	9.72E+01	300	5000	7	13	0	0	0	0
525	YC7H13-Y2	G	0	9.72E+01	300	5000	7	13	0	0	0	0
526	YC7H13-X2	G	0	9.72E+01	300	5000	7	13	0	0	0	0



527	XC7H130-Z	G	0	1.13E+02	300	5000	7	13	1	0	0	0
528	YC7H130-Y2	G	0	1.13E+02	300	5000	7	13	1	0	0	0
529	YC7H1502	G	0	1.31E+02	300	5000	7	15	2	0	0	0
530	YC7H1400H-Y2	G	0	1.31E+02	300	5000	7	15	2	0	0	0
531	Y-YC7H140	G	0	1.14E+02	300	5000	7	14	1	0	0	0
532	NEOC5H12	G	0	7.22E+01	300	5000	5	12	0	0	0	0
533	NEOC5H11	G	0	7.11E+01	300	5000	5	11	0	0	0	0
534	NEOC5H11O2	G	0	1.03E+02	300	5000	5	11	2	0	0	0
535	NEOC5H100OH	G	0	1.03E+02	300	5000	5	11	2	0	0	0
536	NEOC6H12	G	0	8.42E+01	300	5000	6	12	0	0	0	0
537	NEOC6H11	G	0	8.32E+01	300	5000	6	11	0	0	0	0
538	NC7H15	G	0	9.92E+01	300	5000	7	15	0	0	0	0
539	OC7H15	G	0	9.92E+01	300	5000	7	15	0	0	0	0
540	PC7H15	G	0	9.92E+01	300	5000	7	15	0	0	0	0
541	QC7H15	G	0	9.92E+01	300	5000	7	15	0	0	0	0
542	OC7H14	G	0	9.82E+01	300	5000	7	14	0	0	0	0
543	PC7H14	G	0	9.82E+01	300	5000	7	14	0	0	0	0
544	OC7H13-N	G	0	9.72E+01	300	5000	7	13	0	0	0	0
545	PC7H13-N	G	0	9.72E+01	300	5000	7	13	0	0	0	0
546	PC7H13-O	G	0	9.72E+01	300	5000	7	13	0	0	0	0
547	AC8H17	G	0	1.13E+02	300	5000	8	17	0	0	0	0
548	BC8H17	G	0	1.13E+02	300	5000	8	17	0	0	0	0
549	CC8H17	G	0	1.13E+02	300	5000	8	17	0	0	0	0
550	DC8H17	G	0	1.13E+02	300	5000	8	17	0	0	0	0
551	IC8H16	G	0	1.12E+02	300	5000	8	16	0	0	0	0
552	JC8H16	G	0	1.12E+02	300	5000	8	16	0	0	0	0
553	IC8H15	G	0	1.11E+02	300	5000	8	15	0	0	0	0
554	AC8H17O2	G	0	1.45E+02	300	5000	8	17	2	0	0	0
555	BC8H17O2	G	0	1.45E+02	300	5000	8	17	2	0	0	0
556	DC8H17O2	G	0	1.45E+02	300	5000	8	17	2	0	0	0
557	AC8H160OH-A	G	0	1.45E+02	300	5000	8	17	2	0	0	0
558	AC8H160OH-B	G	0	1.45E+02	300	5000	8	17	2	0	0	0
559	AC8H160OH-C	G	0	1.45E+02	300	5000	8	17	2	0	0	0
560	BC8H160OH-C	G	0	1.45E+02	300	5000	8	17	2	0	0	0
561	BC8H160OH-A	G	0	1.45E+02	300	5000	8	17	2	0	0	0
562	BC8H160OH-D	G	0	1.45E+02	300	5000	8	17	2	0	0	0
563	DC8H160OH-C	G	0	1.45E+02	300	5000	8	17	2	0	0	0
564	DC8H160OH-B	G	0	1.45E+02	300	5000	8	17	2	0	0	0
565	IC8ETERAA	G	0	1.28E+02	300	5000	8	16	1	0	0	0
566	IC8ETERAB	G	0	1.28E+02	300	5000	8	16	1	0	0	0
567	IC8ETERAC	G	0	1.28E+02	300	5000	8	16	1	0	0	0
568	IC8ETERBC	G	0	1.28E+02	300	5000	8	16	1	0	0	0
569	IC8ETERBD	G	0	1.28E+02	300	5000	8	16	1	0	0	0
570	CC8H16OH-D	G	0	1.29E+02	300	5000	8	17	1	0	0	0
571	YC7H130OH-X1	G	0	1.30E+02	300	5000	7	14	2	0	0	0
572	YC7H130-X1	G	0	1.13E+02	300	5000	7	13	1	0	0	0

573	XC7H13OOH-Z	G	0	1.30E+02	300	5000	7	14	2	0	0	0
574	YC7H13OOH-X2	G	0	1.30E+02	300	5000	7	14	2	0	0	0
575	YC7H13O-X2	G	0	1.13E+02	300	5000	7	13	1	0	0	0
576	CC6H11-D	G	0	8.32E+01	300	5000	6	11	0	0	0	0
577	C4H7	G	0	5.51E+01	300	5000	4	7	0	0	0	0
578	C5H9	G	0	6.91E+01	300	5000	5	9	0	0	0	0
579	IC5H9	G	0	6.91E+01	300	5000	5	9	0	0	0	0
580	C5H11-1	G	0	7.11E+01	300	5000	5	11	0	0	0	0
581	C5H11O2-2	G	0	1.03E+02	300	5000	5	11	2	0	0	0
582	C5H10OOH2-4	G	0	1.03E+02	300	5000	5	11	2	0	0	0
583	C5H10O2-4	G	0	8.61E+01	300	5000	5	10	1	0	0	0
584	C6H13-1	G	0	8.52E+01	300	5000	6	13	0	0	0	0
585	C6H13-2	G	0	8.52E+01	300	5000	6	13	0	0	0	0
586	C6H13-3	G	0	8.52E+01	300	5000	6	13	0	0	0	0
587	C6H12-1	G	0	8.42E+01	300	5000	6	12	0	0	0	0
588	C6H12-2	G	0	8.42E+01	300	5000	6	12	0	0	0	0
589	C6H12-3	G	0	8.42E+01	300	5000	6	12	0	0	0	0
590	C6H11	G	0	8.32E+01	300	5000	6	11	0	0	0	0
591	C6H12O1-4	G	0	1.00E+02	300	5000	6	12	1	0	0	0
592	C7H15-1	G	0	9.92E+01	300	5000	7	15	0	0	0	0
593	C7H15-2	G	0	9.92E+01	300	5000	7	15	0	0	0	0
594	C7H15-3	G	0	9.92E+01	300	5000	7	15	0	0	0	0
595	C7H15-4	G	0	9.92E+01	300	5000	7	15	0	0	0	0
596	C7H14-1	G	0	9.82E+01	300	5000	7	14	0	0	0	0
597	C7H13	G	0	9.72E+01	300	5000	7	13	0	0	0	0
598	C7H15O2-1	G	0	1.31E+02	300	5000	7	15	2	0	0	0
599	C7H14OOH1-2	G	0	1.31E+02	300	5000	7	15	2	0	0	0
600	C7H14OOH1-3	G	0	1.31E+02	300	5000	7	15	2	0	0	0
601	C7H14OOH1-4	G	0	1.31E+02	300	5000	7	15	2	0	0	0
602	C7H14O1-3	G	0	1.14E+02	300	5000	7	14	1	0	0	0
603	C7H14O1-4	G	0	1.14E+02	300	5000	7	14	1	0	0	0
604	NC5H11CHO	G	0	1.00E+02	300	5000	6	12	1	0	0	0
605	NC5H11CO	G	0	9.92E+01	300	5000	6	11	1	0	0	0
606	NC4H9COCH2	G	0	9.92E+01	300	5000	6	11	1	0	0	0
607	C4H7OOH1-4	G	0	8.81E+01	300	5000	4	8	2	0	0	0
608	C4H7O1-4	G	0	7.11E+01	300	5000	4	7	1	0	0	0
609	C10H21-1	G	0	1.41E+02	300	5000	10	21	0	0	0	0
610	C10H21-2	G	0	1.41E+02	300	5000	10	21	0	0	0	0
611	C10H21-3	G	0	1.41E+02	300	5000	10	21	0	0	0	0
612	C10H21-4	G	0	1.41E+02	300	5000	10	21	0	0	0	0
613	C10H21-5	G	0	1.41E+02	300	5000	10	21	0	0	0	0
614	C9H19-1	G	0	1.27E+02	300	5000	9	19	0	0	0	0
615	C9H19-2	G	0	1.27E+02	300	5000	9	19	0	0	0	0
616	C9H19-4	G	0	1.27E+02	300	5000	9	19	0	0	0	0
617	C8H17-1	G	0	1.13E+02	300	5000	8	17	0	0	0	0
618	C8H17-2	G	0	1.13E+02	300	5000	8	17	0	0	0	0

619	C8H17-3	G	0	1.13E+02	300	5000	8	17	0	0	0	0
620	C8H17-4	G	0	1.13E+02	300	5000	8	17	0	0	0	0
621	C10H20-1	G	0	1.40E+02	300	5000	10	20	0	0	0	0
622	C10H20-2	G	0	1.40E+02	300	5000	10	20	0	0	0	0
623	C10H20-3	G	0	1.40E+02	300	5000	10	20	0	0	0	0
624	C10H20-4	G	0	1.40E+02	300	5000	10	20	0	0	0	0
625	C10H20-5	G	0	1.40E+02	300	5000	10	20	0	0	0	0
626	C9H18-1	G	0	1.26E+02	300	5000	9	18	0	0	0	0
627	C8H16-1	G	0	1.12E+02	300	5000	8	16	0	0	0	0
628	C8H16-2	G	0	1.12E+02	300	5000	8	16	0	0	0	0
629	C8H16-3	G	0	1.12E+02	300	5000	8	16	0	0	0	0
630	C8H16-4	G	0	1.12E+02	300	5000	8	16	0	0	0	0
631	C10H21O2-1	G	0	1.73E+02	300	5000	10	21	2	0	0	0
632	C10H21O2-2	G	0	1.73E+02	300	5000	10	21	2	0	0	0
633	C10H21O2-3	G	0	1.73E+02	300	5000	10	21	2	0	0	0
634	C10H21O2-4	G	0	1.73E+02	300	5000	10	21	2	0	0	0
635	C10H21O2-5	G	0	1.73E+02	300	5000	10	21	2	0	0	0
636	C9H19O2-1	G	0	1.59E+02	300	5000	9	19	2	0	0	0
637	C8H17O2-1	G	0	1.45E+02	300	5000	8	17	2	0	0	0
638	C8H17O2-4	G	0	1.45E+02	300	5000	8	17	2	0	0	0
639	C10OOH1-2	G	0	1.73E+02	300	5000	10	21	2	0	0	0
640	C10OOH1-3	G	0	1.73E+02	300	5000	10	21	2	0	0	0
641	C10OOH1-4	G	0	1.73E+02	300	5000	10	21	2	0	0	0
642	C10OOH2-3	G	0	1.73E+02	300	5000	10	21	2	0	0	0
643	C10OOH2-4	G	0	1.73E+02	300	5000	10	21	2	0	0	0
644	C10OOH2-5	G	0	1.73E+02	300	5000	10	21	2	0	0	0
645	C10OOH3-2	G	0	1.73E+02	300	5000	10	21	2	0	0	0
646	C10OOH3-4	G	0	1.73E+02	300	5000	10	21	2	0	0	0
647	C10OOH3-5	G	0	1.73E+02	300	5000	10	21	2	0	0	0
648	C10OOH3-6	G	0	1.73E+02	300	5000	10	21	2	0	0	0
649	C10OOH4-1	G	0	1.73E+02	300	5000	10	21	2	0	0	0
650	C10OOH4-2	G	0	1.73E+02	300	5000	10	21	2	0	0	0
651	C10OOH4-3	G	0	1.73E+02	300	5000	10	21	2	0	0	0
652	C10OOH4-5	G	0	1.73E+02	300	5000	10	21	2	0	0	0
653	C10OOH4-6	G	0	1.73E+02	300	5000	10	21	2	0	0	0
654	C10OOH5-2	G	0	1.73E+02	300	5000	10	21	2	0	0	0
655	C10OOH5-3	G	0	1.73E+02	300	5000	10	21	2	0	0	0
656	C10OOH5-4	G	0	1.73E+02	300	5000	10	21	2	0	0	0
657	C10OOH5-6	G	0	1.73E+02	300	5000	10	21	2	0	0	0
658	C10OOH5-7	G	0	1.73E+02	300	5000	10	21	2	0	0	0
659	C10OOH5-8	G	0	1.73E+02	300	5000	10	21	2	0	0	0
660	C8OOH4-2	G	0	1.45E+02	300	5000	8	17	2	0	0	0
661	C8OOH4-6	G	0	1.45E+02	300	5000	8	17	2	0	0	0
662	C10O1-2	G	0	1.56E+02	300	5000	10	20	1	0	0	0
663	C10O1-3	G	0	1.56E+02	300	5000	10	20	1	0	0	0
664	C10O1-4	G	0	1.56E+02	300	5000	10	20	1	0	0	0

665	C10O2-3	G	0	1.56E+02	300	5000	10	20	1	0	0	0
666	C10O2-4	G	0	1.56E+02	300	5000	10	20	1	0	0	0
667	C10O2-5	G	0	1.56E+02	300	5000	10	20	1	0	0	0
668	C10O3-5	G	0	1.56E+02	300	5000	10	20	1	0	0	0
669	C10O3-6	G	0	1.56E+02	300	5000	10	20	1	0	0	0
670	C10O4-6	G	0	1.56E+02	300	5000	10	20	1	0	0	0
671	C8O1-3	G	0	1.28E+02	300	5000	8	16	1	0	0	0
672	C8O1-4	G	0	1.28E+02	300	5000	8	16	1	0	0	0
673	NC7H15CHO	G	0	1.28E+02	300	5000	8	16	1	0	0	0
674	NC6H13CHO	G	0	1.14E+02	300	5000	7	14	1	0	0	0
675	NC7H15CO	G	0	1.27E+02	300	5000	8	15	1	0	0	0
676	NC6H13CO	G	0	1.13E+02	300	5000	7	13	1	0	0	0
677	C6H13COCH2	G	0	1.27E+02	300	5000	8	15	1	0	0	0
678	C5H11COCH2	G	0	1.13E+02	300	5000	7	13	1	0	0	0
679	C10H19	G	0	1.39E+02	300	5000	10	19	0	0	0	0
680	C9H17	G	0	1.25E+02	300	5000	9	17	0	0	0	0
681	C8H15	G	0	1.11E+02	300	5000	8	15	0	0	0	0
682	C6H6	G	0	7.81E+01	300	5000	6	6	0	0	0	0
683	C6H5	G	0	7.71E+01	300	4000	6	5	0	0	0	0
684	C6H5OO	G	0	1.09E+02	300	5000	6	5	2	0	0	0
685	C6H5O	G	0	9.31E+01	300	4000	6	5	1	0	0	0
686	C6H5OH	G	0	9.41E+01	300	4000	6	6	1	0	0	0
687	C5H6	G	0	6.61E+01	300	5000	5	6	0	0	0	0
688	C5H5	G	0	6.51E+01	300	4000	5	5	0	0	0	0
689	C5H4O	G	0	8.01E+01	200	6000	5	4	1	0	0	0
690	C5H5O	G	0	8.11E+01	300	5000	5	5	1	0	0	0
691	C4H5-I	G	0	5.31E+01	300	3000	4	5	0	0	0	0
692	C4H5-N	G	0	5.31E+01	300	3000	4	5	0	0	0	0
693	C4H4	G	0	5.21E+01	300	5000	4	4	0	0	0	0
694	C4H3-I	G	0	5.11E+01	300	3000	4	3	0	0	0	0
695	C4H3-N	G	0	5.11E+01	300	3000	4	3	0	0	0	0
696	C4H2	G	0	5.01E+01	300	5000	4	2	0	0	0	0
697	H2C4O	G	0	6.61E+01	300	4000	4	2	1	0	0	0
698	C5H7	G	0	6.71E+01	300	5000	5	7	0	0	0	0
699	C*CCJC*C	G	0	6.71E+01	300	5000	5	7	0	0	0	0
700	C*CC*CCJ	G	0	6.71E+01	300	5000	5	7	0	0	0	0
701	C*CC*CC	G	0	6.81E+01	300	5000	5	8	0	0	0	0
702	CJ*CC*CC*O	G	0	8.11E+01	300	5000	5	5	1	0	0	0
703	C*CC*CCJ*O	G	0	8.11E+01	300	5000	5	5	1	0	0	0
704	CJ*CC*O	G	0	5.51E+01	300	5000	3	3	1	0	0	0
705	C4H612	G	0	5.41E+01	300	3000	4	6	0	0	0	0
706	C4H6-2	G	0	5.41E+01	300	3000	4	6	0	0	0	0
707	CH2CHCHCHO	G	0	6.91E+01	200	6000	4	5	1	0	0	0
708	CH3CHCHCO	G	0	6.91E+01	200	6000	4	5	1	0	0	0
709	H2CC	G	0	2.60E+01	200	6000	2	2	0	0	0	0
710	C4H5-2	G	0	5.31E+01	300	3000	4	5	0	0	0	0

711	HCOOH	G	0	4.60E+01	300	4000	1	2	2	0	0	0
712	H2CCCH	G	0	3.91E+01	300	4000	3	3	0	0	0	0
713	C2O	G	0	4.00E+01	300	5000	2	0	1	0	0	0
714	TOLUEN	G	0	9.21E+01	200	6000	7	8	0	0	0	0
715	PHC2H5	G	0	1.06E+02	300	3000	8	10	0	0	0	0
716	STYREN	G	0	1.04E+02	300	5000	8	8	0	0	0	0
717	PHHCO	G	0	1.06E+02	300	5000	7	6	1	0	0	0
718	C5H4OH	G	0	8.11E+01	200	6000	5	5	1	0	0	0
719	NAPHT	G	0	1.28E+02	300	5000	10	8	0	0	0	0
720	INDENE	G	0	1.16E+02	300	5000	9	8	0	0	0	0
721	PHC3H5-1	G	0	1.18E+02	300	5000	9	10	0	0	0	0
722	C14H14	G	0	1.82E+02	300	3000	14	14	0	0	0	0
723	HEX1245	G	0	7.81E+01	300	5000	6	6	0	0	0	0
724	C6H615	G	0	7.81E+01	300	5000	6	6	0	0	0	0
725	MC6H6	G	0	7.81E+01	300	5000	6	6	0	0	0	0
726	FULVENE	G	0	7.81E+01	300	5000	6	6	0	0	0	0
727	C6H4O2	G	0	1.08E+02	300	5000	6	4	2	0	0	0
728	C6H5O2	G	0	1.09E+02	200	6000	6	5	2	0	0	0
729	C6H5O2H	G	0	1.10E+02	200	6000	6	6	2	0	0	0
730	C6H3O2	G	0	1.07E+02	300	5000	6	3	2	0	0	0
731	C6H3O3	G	0	1.23E+02	300	5000	6	3	3	0	0	0
732	C5H4	G	0	6.41E+01	300	5000	5	4	0	0	0	0
733	C5H3	G	0	6.31E+01	300	5000	5	3	0	0	0	0
734	PHCH2	G	0	9.11E+01	200	6000	7	7	0	0	0	0
735	PHCH2OH	G	0	1.08E+02	300	5000	7	8	1	0	0	0
736	PHCH2O	G	0	1.07E+02	300	3000	7	7	1	0	0	0
737	PHCO	G	0	1.05E+02	300	5000	7	5	1	0	0	0
738	PHCH2O2	G	0	1.23E+02	300	5000	7	7	2	0	0	0
739	APHC2H4	G	0	1.05E+02	300	3000	8	9	0	0	0	0
740	BPHC2H4	G	0	1.05E+02	300	3000	8	9	0	0	0	0
741	PHC2H	G	0	1.02E+02	300	3000	8	6	0	0	0	0
742	C6H4C2H3	G	0	1.03E+02	300	5000	8	7	0	0	0	0
743	PHCH2HCO	G	0	1.20E+02	300	5000	8	8	1	0	0	0
744	PHCH2CO	G	0	1.19E+02	300	5000	8	7	1	0	0	0
745	PHCOCH2	G	0	1.19E+02	300	5000	8	7	1	0	0	0
746	C6H5CCO	G	0	1.17E+02	300	5000	8	5	1	0	0	0
747	PHCHCO	G	0	1.18E+02	300	5000	8	6	1	0	0	0
748	PBZJA	G	0	1.19E+02	300	3000	9	11	0	0	0	0
749	PBZJB	G	0	1.19E+02	300	3000	9	11	0	0	0	0
750	PBZJC	G	0	1.19E+02	300	3000	9	11	0	0	0	0
751	BPHPROPY	G	0	1.19E+02	300	3000	9	11	0	0	0	0
752	PHC3H5-2	G	0	1.18E+02	300	5000	9	10	0	0	0	0
753	PHC3H4	G	0	1.17E+02	300	5000	9	9	0	0	0	0
754	PHC2H4HCO	G	0	1.34E+02	300	5000	9	10	1	0	0	0
755	PHC2H4CO	G	0	1.33E+02	300	5000	9	9	1	0	0	0
756	PHCH2COCH2	G	0	1.33E+02	300	5000	9	9	1	0	0	0

757	PHCOC2H4	G	0	1.33E+02	300	5000	9	9	1	0	0	0
758	PHCOC2H3	G	0	1.32E+02	300	5000	9	8	1	0	0	0
759	BPHC3H5OHA	G	0	1.35E+02	300	5000	9	11	1	0	0	0
760	APHC3H5OHB	G	0	1.35E+02	300	5000	9	11	1	0	0	0
761	CPHC3H5OHB	G	0	1.35E+02	300	5000	9	11	1	0	0	0
762	BPHC3H5OHC	G	0	1.35E+02	300	5000	9	11	1	0	0	0
763	PBZOHAQJB	G	0	1.67E+02	300	5000	9	11	3	0	0	0
764	PBZOHBQJA	G	0	1.67E+02	300	5000	9	11	3	0	0	0
765	PBZOHBQJC	G	0	1.67E+02	300	5000	9	11	3	0	0	0
766	PBZOHCQJB	G	0	1.67E+02	300	5000	9	11	3	0	0	0
767	N-C8H7	G	0	1.03E+02	200	6000	8	7	0	0	0	0
768	BSTYRYL	G	0	1.03E+02	300	5000	8	7	0	0	0	0
769	COPHC3H4-1	G	0	1.33E+02	300	5000	9	9	1	0	0	0
770	AOPHC3H4-2	G	0	1.33E+02	300	5000	9	9	1	0	0	0
771	PHCH2CHCO	G	0	1.32E+02	300	5000	9	8	1	0	0	0
772	PHCOCH2CH2O2	G	0	1.65E+02	300	5000	9	9	3	0	0	0
773	PHCOCH2CH2O2H	G	0	1.66E+02	300	5000	9	10	3	0	0	0
774	PHCOCH2CH2O	G	0	1.49E+02	300	5000	9	9	2	0	0	0
775	PHCH2COCH2O2	G	0	1.65E+02	300	5000	9	9	3	0	0	0
776	PHCH2COCH2O2H	G	0	1.66E+02	300	5000	9	10	3	0	0	0
777	PHCH2COCH2O	G	0	1.49E+02	300	5000	9	9	2	0	0	0
778	CH3C6H4C2H3	G	0	1.18E+02	300	5000	9	10	0	0	0	0
779	C10H9	G	0	1.29E+02	200	6000	10	9	0	0	0	0
780	C10H10	G	0	1.30E+02	200	6000	10	10	0	0	0	0
781	C6H4C2H	G	0	1.01E+02	300	3000	8	5	0	0	0	0
782	C7H5	G	0	8.91E+01	300	5000	7	5	0	0	0	0
783	C7H6	G	0	9.01E+01	300	3000	7	6	0	0	0	0
784	c-C4H5	G	0	5.31E+01	300	3000	4	5	0	0	0	0
785	c-C5H4	G	0	6.41E+01	200	6000	5	4	0	0	0	0
786	A1C2HAC	G	0	1.27E+02	300	5000	10	7	0	0	0	0
787	A2O	G	0	1.43E+02	300	5000	10	7	1	0	0	0
788	A2OH	G	0	1.44E+02	300	5000	10	8	1	0	0	0
789	A1C2H3AC	G	0	1.29E+02	200	6000	10	9	0	0	0	0
790	INDENYL	G	0	1.15E+02	300	3000	9	7	0	0	0	0
791	INDENOXY	G	0	1.31E+02	298	5000	9	7	1	0	0	0
792	PHNTHRN	G	0	1.78E+02	300	5000	14	10	0	0	0	0
793	PHCCH2	G	0	1.03E+02	300	3000	8	7	0	0	0	0
794	PHCHCH	G	0	1.03E+02	300	5000	8	7	0	0	0	0
795	C6H4CH3	G	0	9.11E+01	300	3000	7	7	0	0	0	0
796	A2CH3-1	G	0	1.42E+02	300	5000	11	10	0	0	0	0
797	C6H4OH	G	0	9.31E+01	300	5000	6	5	1	0	0	0
798	PHCC	G	0	1.01E+02	300	3000	8	5	0	0	0	0
799	C9H10	G	0	1.18E+02	298	5000	9	10	0	0	0	0
800	C9H9-1	G	0	1.17E+02	300	5000	9	9	0	0	0	0
801	A2T2	G	0	1.26E+02	300	5000	10	6	0	0	0	0
802	A2T1	G	0	1.26E+02	300	5000	10	6	0	0	0	0

803	A2-1	G	0	1.27E+02	300	3000	10	7	0	0	0	0
804	A2-2	G	0	1.27E+02	300	3000	10	7	0	0	0	0
805	BIPHENYL	G	0	1.54E+02	300	5000	12	10	0	0	0	0
806	FLUORENE	G	0	1.66E+02	300	5000	13	10	0	0	0	0
807	A2C2H2	G	0	1.53E+02	300	3000	12	9	0	0	0	0
808	A2C2H	G	0	1.52E+02	300	3000	12	8	0	0	0	0
809	A2R5-	G	0	1.51E+02	300	3000	12	7	0	0	0	0
810	A2R5	G	0	1.52E+02	300	3000	12	8	0	0	0	0
811	P2-	G	0	1.53E+02	300	3000	12	9	0	0	0	0
812	C13H9	G	0	1.65E+02	300	5000	13	9	0	0	0	0
813	A3-1	G	0	1.77E+02	300	3000	14	9	0	0	0	0
814	A3-4	G	0	1.77E+02	300	5000	14	9	0	0	0	0
815	A2(C2H)2	G	0	1.76E+02	300	3000	14	8	0	0	0	0
816	ANTHRCN	G	0	1.78E+02	300	5000	14	10	0	0	0	0
817	C13H9CH2	G	0	1.79E+02	300	5000	14	11	0	0	0	0
818	C13H8CH2	G	0	1.78E+02	300	5000	14	10	0	0	0	0
819	C14H13	G	0	1.81E+02	300	5000	14	13	0	0	0	0
820	C14H11	G	0	1.79E+02	300	5000	14	11	0	0	0	0
821	PHC2H-	G	0	1.01E+02	300	3000	8	5	0	0	0	0
822	C14H13OO	G	0	2.13E+02	300	5000	14	13	2	0	0	0
823	C14H13OOH	G	0	2.14E+02	300	5000	14	14	2	0	0	0
824	C14H13O	G	0	1.97E+02	300	5000	14	13	1	0	0	0
825	C14H12OOH	G	0	2.13E+02	300	5000	14	13	2	0	0	0
826	C14H12O2H-1O2	G	0	2.45E+02	300	5000	14	13	4	0	0	0
827	C14H11O-1O2H	G	0	2.28E+02	300	5000	14	12	3	0	0	0
828	o-C6H4	G	0	7.61E+01	300	5000	6	4	0	0	0	0
829	BICYCLO	G	0	1.54E+02	200	6000	12	10	0	0	0	0
830	DIBZFUR	G	0	1.68E+02	300	5000	12	8	1	0	0	0
831	DIBZFUENYL	G	0	1.67E+02	100	5000	12	7	1	0	0	0
832	DIBZFURNOXY	G	0	1.83E+02	300	5000	12	7	2	0	0	0
833	A3CH3	G	0	1.92E+02	300	5000	15	12	0	0	0	0
834	A3CH2	G	0	1.91E+02	300	5000	15	11	0	0	0	0
835	FLTHN	G	0	2.02E+02	300	5000	16	10	0	0	0	0
836	A3C2H2	G	0	2.03E+02	300	3000	16	11	0	0	0	0
837	A3C2H	G	0	2.02E+02	300	3000	16	10	0	0	0	0
838	PYRENE	G	0	2.02E+02	300	3000	16	10	0	0	0	0
839	A4-1	G	0	2.01E+02	300	5000	16	9	0	0	0	0
840	A4-2	G	0	2.01E+02	300	5000	16	9	0	0	0	0
841	A4-4	G	0	2.01E+02	300	5000	16	9	0	0	0	0
842	C14H12	G	0	1.80E+02	300	3000	14	12	0	0	0	0
843	CHRYSEN	G	0	2.28E+02	300	5000	18	12	0	0	0	0
844	CHRYSEN-1	G	0	2.27E+02	300	5000	18	11	0	0	0	0
845	CHRYSEN-4	G	0	2.27E+02	300	5000	18	11	0	0	0	0
846	CHRYSEN-5	G	0	2.27E+02	300	5000	18	11	0	0	0	0
847	A3C2H-2	G	0	2.01E+02	300	5000	16	9	0	0	0	0
848	A3C2H-1	G	0	2.01E+02	300	5000	16	9	0	0	0	0

849	A2R5R5	G	0	1.76E+02	300	5000	14	8	0	0	0	0
850	C6H2	G	0	7.41E+01	200	6000	6	2	0	0	0	0
851	C6H	G	0	7.31E+01	200	6000	6	1	0	0	0	0
852	C8H2	G	0	9.81E+01	298	5000	8	2	0	0	0	0
853	C8H	G	0	9.71E+01	298	5000	8	1	0	0	0	0
854	C4H	G	0	4.91E+01	200	6000	4	1	0	0	0	0
855	BGHIF	G	0	2.26E+02	300	5000	18	10	0	0	0	0
856	BAPYR	G	0	2.52E+02	300	5000	20	12	0	0	0	0
857	BAPYR*S	G	0	2.51E+02	300	5000	20	11	0	0	0	0
858	A4C2H*	G	0	2.25E+02	300	5000	18	9	0	0	0	0
859	A3C2H*	G	0	2.01E+02	300	3000	16	9	0	0	0	0
860	A2C2H*	G	0	1.51E+02	300	3000	12	7	0	0	0	0
861	A1C2H-	G	0	1.01E+02	300	3000	8	5	0	0	0	0
862	C2H5OO	G	0	6.11E+01	300	3500	2	5	2	0	0	0
863	CH3OOH	G	0	4.80E+01	300	3500	1	4	2	0	0	0
864	CH3OO	G	0	4.70E+01	300	3500	1	3	2	0	0	0
865	C2H5OOH	G	0	6.21E+01	300	3500	2	6	2	0	0	0
866	HCO3	G	0	6.10E+01	300	3500	1	1	3	0	0	0
867	HCO3H	G	0	6.20E+01	300	3500	1	2	3	0	0	0
868	C2-QOOH	G	0	6.11E+01	300	3500	2	5	2	0	0	0
869	CH2CHCH2	G	0	4.11E+01	300	3500	3	5	0	0	0	0
870	CH3CHOOCHO	G	0	8.91E+01	300	3500	3	5	3	0	0	0
871	CH2CHOOHCHO	G	0	8.91E+01	300	3500	3	5	3	0	0	0
872	ETC3H4O2	G	0	7.21E+01	300	3500	3	4	2	0	0	0
873	CH2OOCHOHCH O	G	0	1.21E+02	300	3500	3	5	5	0	0	0
874	C5EN-OO	G	0	1.01E+02	300	3500	5	9	2	0	0	0
875	C5EN-QOOH	G	0	1.01E+02	300	3500	5	9	2	0	0	0
876	C5EN-OOQOOH-35	G	0	1.33E+02	300	3500	5	9	4	0	0	0
877	C5EN-OQOOH-35	G	0	1.16E+02	300	3500	5	8	3	0	0	0
878	C5H8O	G	0	8.41E+01	300	3500	5	8	1	0	0	0
879	C5H8	G	0	6.81E+01	300	3500	5	8	0	0	0	0
880	CYC5H8	G	0	6.81E+01	200	5000	5	8	0	0	0	0
881	NEOC5-QOOH	G	0	1.03E+02	300	3500	5	11	2	0	0	0
882	NEOC5-OOQOOH	G	0	1.35E+02	300	3500	5	11	4	0	0	0
883	NEOC5-OQOOH	G	0	1.18E+02	300	3500	5	10	3	0	0	0
884	NC5H12OO	G	0	1.03E+02	300	3500	5	11	2	0	0	0
885	NC5-QOOH	G	0	1.03E+02	300	3500	5	11	2	0	0	0
886	NC5-OOQOOH	G	0	1.35E+02	300	3500	5	11	4	0	0	0
887	N1C4H9OH	G	0	7.41E+01	300	3500	4	10	1	0	0	0
888	MEK	G	0	7.21E+01	300	3500	4	8	1	0	0	0
889	C3H6O2	G	0	7.41E+01	300	3500	3	6	2	0	0	0
890	C3H7CHO	G	0	7.21E+01	300	3500	4	8	1	0	0	0
891	NC7-QOOH	G	0	1.31E+02	300	3500	7	15	2	0	0	0
892	NC7H14O	G	0	1.14E+02	300	3500	7	14	1	0	0	0
893	NC7-OOQOOH	G	0	1.63E+02	300	3500	7	15	4	0	0	0



894	NC7-OQOOH	G	0	1.46E+02	300	3500	7	14	3	0	0	0
895	C3H4O2	G	0	7.21E+01	300	3500	3	4	2	0	0	0
896	NC7H13OOH	G	0	1.30E+02	300	3500	7	14	2	0	0	0
897	C7KETONE	G	0	1.14E+02	300	3500	7	14	1	0	0	0
898	IC8-QOOH	G	0	1.45E+02	300	3500	8	17	2	0	0	0
899	IC8T-QOOH	G	0	1.45E+02	300	3500	8	17	2	0	0	0
900	IC8H17	G	0	1.13E+02	300	3500	8	17	0	0	0	0
901	IC8H17-OO	G	0	1.45E+02	300	3500	8	17	2	0	0	0
902	IC8H16O	G	0	1.28E+02	300	3500	8	16	1	0	0	0
903	IC8-OOQOOH	G	0	1.77E+02	300	3500	8	17	4	0	0	0
904	IC8-OQOOH	G	0	1.60E+02	300	3500	8	16	3	0	0	0
905	NC10MOOH	G	0	1.72E+02	300	3500	10	20	2	0	0	0
906	NC10-QOOH	G	0	1.73E+02	300	3500	10	21	2	0	0	0
907	NC10-OQOOH	G	0	1.88E+02	300	3500	10	20	3	0	0	0
908	NC10-OOQOOH	G	0	2.05E+02	300	3500	10	21	4	0	0	0
909	NC3H7OO	G	0	7.51E+01	300	3500	3	7	2	0	0	0
910	CH3COOH	G	0	6.01E+01	300	3500	2	4	2	0	0	0
911	TERPHENYL	G	0	2.30E+02	300	5000	18	14	0	0	0	0
912	P3-	G	0	2.29E+02	300	5000	18	13	0	0	0	0
913	QUATERPHENYL	G	0	3.06E+02	250	5000	24	18	0	0	0	0
914	P4-	G	0	3.05E+02	250	5000	24	17	0	0	0	0
915	TRIPHENYLEN	G	0	2.28E+02	300	5000	18	12	0	0	0	0
916	A4T-	G	0	2.27E+02	300	5000	18	11	0	0	0	0
917	QINQUEPHENYL	G	0	3.83E+02	250	5000	30	22	0	0	0	0
918	P5-	G	0	3.82E+02	250	5000	30	21	0	0	0	0
919	BENZYL B	G	0	1.68E+02	300	5000	13	12	0	0	0	0
920	BENZYL B J	G	0	1.67E+02	300	5000	13	11	0	0	0	0
921	A1A1CH2-1	G	0	1.67E+02	300	5000	13	11	0	0	0	0
922	PHCH2CH2	G	0	1.05E+02	300	5000	8	9	0	0	0	0
923	A1CCA1	G	0	1.78E+02	300	5000	14	10	0	0	0	0
924	A2C2H-2J3	G	0	1.51E+02	300	5000	12	7	0	0	0	0
925	A3LJX	G	0	1.77E+02	300	5000	14	9	0	0	0	0
926	A3LJ2	G	0	1.77E+02	300	5000	14	9	0	0	0	0
927	A3LJ9	G	0	1.77E+02	300	5000	14	9	0	0	0	0
928	A2R5YNE1	G	0	1.76E+02	300	5000	14	8	0	0	0	0
929	A2R5YNE3	G	0	1.76E+02	300	5000	14	8	0	0	0	0
930	A2R5YNE4	G	0	1.76E+02	300	5000	14	8	0	0	0	0
931	A2R5YNE5	G	0	1.76E+02	300	5000	14	8	0	0	0	0
932	A3CH2R	G	0	1.90E+02	300	5000	15	10	0	0	0	0
933	A3R5	G	0	2.02E+02	300	5000	16	10	0	0	0	0
934	A2R5YN4J5	G	0	1.75E+02	300	5000	14	7	0	0	0	0
935	A3R5J7	G	0	2.01E+02	300	5000	16	9	0	0	0	0
936	A2R5YN5J4	G	0	1.75E+02	300	5000	14	7	0	0	0	0
937	A3R5J10	G	0	2.01E+02	300	5000	16	9	0	0	0	0
938	A2R5YN3J4	G	0	1.75E+02	300	5000	14	7	0	0	0	0
939	A2R5YN4J3	G	0	1.75E+02	300	5000	14	7	0	0	0	0

940	A3LR5JS	G	0	2.01E+02	300	5000	16	9	0	0	0	0
941	A3LR5	G	0	2.02E+02	300	5000	16	10	0	0	0	0
942	HB	G	0	3.70E+02	300	5000	30	10	0	0	0	0
943	A2A1-1	G	0	2.04E+02	300	5000	16	12	0	0	0	0
944	A2A1-2	G	0	2.04E+02	300	5000	16	12	0	0	0	0
945	A21C6H4	G	0	2.02E+02	300	5000	16	10	0	0	0	0
946	A22C6H4	G	0	2.02E+02	300	5000	16	10	0	0	0	0
947	A2R5YN1J2	G	0	1.75E+02	300	5000	14	7	0	0	0	0
948	FLTHNJ7	G	0	2.01E+02	300	5000	16	9	0	0	0	0
949	FLTHNJ1	G	0	2.01E+02	300	5000	16	9	0	0	0	0
950	FLTHNJ3	G	0	2.01E+02	300	5000	16	9	0	0	0	0
951	BENZNAP	G	0	2.18E+02	300	5000	17	14	0	0	0	0
952	BENZNAPJP	G	0	2.17E+02	300	5000	17	13	0	0	0	0
953	BENZFLRN	G	0	2.16E+02	300	5000	17	12	0	0	0	0
954	A3LC2H-1	G	0	2.02E+02	300	5000	16	10	0	0	0	0
955	A3LC2H-1P	G	0	2.01E+02	300	5000	16	9	0	0	0	0
956	A3LC2H-2	G	0	2.02E+02	300	5000	16	10	0	0	0	0
957	A3LC2H-2P	G	0	2.01E+02	300	5000	16	9	0	0	0	0
958	A3LC2H-2S	G	0	2.01E+02	300	5000	16	9	0	0	0	0
959	A4LJS	G	0	2.27E+02	300	5000	18	11	0	0	0	0
960	A4L	G	0	2.28E+02	300	5000	18	12	0	0	0	0
961	A3A1-1	G	0	2.54E+02	300	5000	20	14	0	0	0	0
962	A3-9	G	0	1.77E+02	300	5000	14	9	0	0	0	0
963	A3A1-9	G	0	2.54E+02	300	5000	20	14	0	0	0	0
964	BBFLUOR	G	0	2.52E+02	300	5000	20	12	0	0	0	0
965	A2A2-12	G	0	2.54E+02	300	5000	20	14	0	0	0	0
966	BKFLUOR	G	0	2.52E+02	300	5000	20	12	0	0	0	0
967	FLRNA1-4	G	0	2.42E+02	300	5000	19	14	0	0	0	0
968	CPTRPHEN	G	0	2.40E+02	300	5000	19	12	0	0	0	0
969	A4C2H*S	G	0	2.25E+02	300	5000	18	9	0	0	0	0
970	BEPYREN	G	0	2.52E+02	300	5000	20	12	0	0	0	0
971	BEPYRENJS	G	0	2.51E+02	300	5000	20	11	0	0	0	0
972	A3A1-4	G	0	2.54E+02	300	5000	20	14	0	0	0	0
973	A2A2-11	G	0	2.54E+02	300	5000	20	14	0	0	0	0
974	PERYLEN	G	0	2.52E+02	300	5000	20	12	0	0	0	0
975	PERYLENJS	G	0	2.51E+02	300	5000	20	11	0	0	0	0
976	PYRNA1-1	G	0	2.78E+02	300	5000	22	14	0	0	0	0
977	PYRNA1-4	G	0	2.78E+02	300	5000	22	14	0	0	0	0
978	INPYR	G	0	2.76E+02	300	5000	22	12	0	0	0	0
979	BBFLUORJS	G	0	2.51E+02	300	5000	20	11	0	0	0	0
980	BGHIFJ	G	0	2.25E+02	300	5000	18	9	0	0	0	0
981	CPCDFLTH	G	0	2.26E+02	300	5000	18	10	0	0	0	0
982	CPCDFLTJS	G	0	2.25E+02	300	5000	18	9	0	0	0	0
983	BGHIFR	G	0	2.50E+02	300	5000	20	10	0	0	0	0
984	BGHIFRJS	G	0	2.49E+02	300	5000	20	9	0	0	0	0
985	COR1	G	0	2.74E+02	300	5000	22	10	0	0	0	0

986	CPCDPYR	G	0	2.26E+02	300	5000	18	10	0	0	0	0
987	DCPCDFG	G	0	2.50E+02	300	5000	20	10	0	0	0	0
988	COR	G	0	2.50E+02	300	5000	20	10	0	0	0	0
989	CPCDPYRJS	G	0	2.25E+02	300	5000	18	9	0	0	0	0
990	CORJ	G	0	2.49E+02	300	5000	20	9	0	0	0	0
991	COR1J	G	0	2.73E+02	300	5000	22	9	0	0	0	0
992	COR2	G	0	2.98E+02	300	5000	24	10	0	0	0	0
993	COR2J	G	0	2.97E+02	300	5000	24	9	0	0	0	0
994	COR3	G	0	3.22E+02	300	5000	26	10	0	0	0	0
995	COR3J	G	0	3.21E+02	300	5000	26	9	0	0	0	0
996	COR4	G	0	3.46E+02	300	5000	28	10	0	0	0	0
997	COR4J	G	0	3.45E+02	300	5000	28	9	0	0	0	0
998	ANTHAN	G	0	2.76E+02	300	5000	22	12	0	0	0	0
999	ANTHANJP	G	0	2.75E+02	300	5000	22	11	0	0	0	0
1000	ANTHANJS	G	0	2.75E+02	300	5000	22	11	0	0	0	0
1001	BGHIPER	G	0	2.76E+02	300	5000	22	12	0	0	0	0
1002	BGHIPEJP1	G	0	2.75E+02	300	5000	22	11	0	0	0	0
1003	CPBPER	G	0	3.00E+02	300	5000	24	12	0	0	0	0
1004	BGHIPEJS1	G	0	2.75E+02	300	5000	22	11	0	0	0	0
1005	CORONEN	G	0	3.00E+02	300	5000	24	12	0	0	0	0
1006	A3L-O	G	0	1.93E+02	100	5000	14	9	1	0	0	0
1007	A3O-4	G	0	1.93E+02	100	5000	14	9	1	0	0	0
1008	A4	G	0	2.28E+02	300	5000	18	12	0	0	0	0
1009	A3LA1-X	G	0	2.27E+02	300	5000	18	11	0	0	0	0
1010	A4-O	G	0	2.43E+02	100	5000	18	11	1	0	0	0
1011	C13H9A1-	G	0	2.15E+02	100	5000	17	11	0	0	0	0
1012	C13H9A1	G	0	2.16E+02	100	5000	17	12	0	0	0	0
1013	CORONEN-O	G	0	3.15E+02	100	5000	24	11	1	0	0	0
1014	CORONENYL	G	0	2.99E+02	100	5000	24	11	0	0	0	0

Table 23 : List of species included in the kinetic model.

## I. Detailed chemical kinetic mechanism

k=A.T <sup>n</sup> .exp(-E/RT))						
Reactions n°	Reactions considered	A (mole-cm-sec-K)	n	E (cal/mole)		
1	H+O2=O+OH	1.18E+16	-0.6	16198		
2	O+H2=H+OH	5.08E+04	2.7	6290		
3	H2+OH=H2O+H	2.16E+08	1.5	3430		
4	O+H2O=2OH	2.97E+06	2	13400		
5	H2+M=2H+M	4.58E+19	-1.4	104380		
	H2	Enhanced	by	2.50E+00		
	H2O	Enhanced	by	1.20E+01		

	CO	Enhanced	by	1.90E+00		
	CO2	Enhanced	by	3.80E+00		
6	2O+M=O2+M	6.16E+15	-0.5	0		
	H2	Enhanced	by	2.50E+00		
	H2O	Enhanced	by	1.20E+01		
	CO	Enhanced	by	1.90E+00		
	CO2	Enhanced	by	3.80E+00		
7	O+H+M=OH+M	4.71E+18	-1	0		
	H2	Enhanced	by	2.50E+00		
	H2O	Enhanced	by	1.20E+01		
	CO	Enhanced	by	1.90E+00		
	CO2	Enhanced	by	3.80E+00		
8	H+OH+M=H2O+M	3.80E+22	-2	0		
	H2	Enhanced	by	2.50E+00		
	H2O	Enhanced	by	1.20E+01		
	CO	Enhanced	by	1.90E+00		
	CO2	Enhanced	by	3.80E+00		
9	H+O2(+M)=HO2(+M)	1.48E+12	0.6	0		
	H2	Enhanced	by	2.00E+00		
	H2O	Enhanced	by	1.10E+01		
	O2	Enhanced	by	7.80E-01		
	CO	Enhanced	by	1.90E+00		
	CO2	Enhanced	by	3.80E+00		
	Low	pressure	limit:	6.37E+20	-1.72E+00	5.25E+02
	TROE	centering:	8.00E-01	1.00E-30	1.00E+30	
10	HO2+H=H2+O2	1.66E+13	0	823		
11	HO2+H=2OH	7.08E+13	0	295		
12	HO2+O=O2+OH	3.25E+13	0	0		
13	HO2+OH=H2O+O2	2.89E+13	0	-497		
14	2HO2=H2O2+O2	4.20E+14	0	11982		
	Declared	duplicate	reaction...			
15	2HO2=H2O2+O2	1.30E+11	0	-1629.3		
	Declared	duplicate	reaction...			
16	H2O2(+M)=2OH(+M)	2.95E+14	0	48430		
	H2	Enhanced	by	2.50E+00		
	H2O	Enhanced	by	1.20E+01		
	CO	Enhanced	by	1.90E+00		
	CO2	Enhanced	by	3.80E+00		
	Low	pressure	limit:	1.20E+17	0.00E+00	4.55E+04
	TROE	centering:	5.00E-01	1.00E-30	1.00E+30	
17	H2O2+H=H2O+OH	2.41E+13	0	3970		
18	H2O2+H=HO2+H2	4.82E+13	0	7950		
19	H2O2+O=OH+HO2	9.55E+06	2	3970		
20	H2O2+OH=HO2+H2O	1.00E+12	0	0		
	Declared	duplicate	reaction...			
21	H2O2+OH=HO2+H2O	5.80E+14	0	9557		

	Declared	duplicate	reaction...			
22	CO+O(+M)=CO2(+M)	1.80E+10	0	2384		
	H2	Enhanced	by	2.50E+00		
	H2O	Enhanced	by	1.20E+01		
	CO	Enhanced	by	1.90E+00		
	CO2	Enhanced	by	3.80E+00		
	Low	pressure	limit:	1.55E+24	-2.79E+00	4.19E+03
23	CO+O2=CO2+O	2.53E+12	0	47700		
24	CO+HO2=CO2+OH	3.01E+13	0	23000		
25	CO+OH=CO2+H	2.23E+05	1.9	-1158.7		
26	HCO+M=H+CO+M	4.75E+11	0.7	14874		
	H2	Enhanced	by	2.50E+00		
	H2O	Enhanced	by	6.00E+00		
	CO	Enhanced	by	1.90E+00		
	CO2	Enhanced	by	3.80E+00		
27	HCO+O2=CO+HO2	7.58E+12	0	410		
28	HCO+H=CO+H2	7.23E+13	0	0		
29	HCO+O=CO+OH	3.02E+13	0	0		
30	HCO+OH=CO+H2O	3.02E+13	0	0		
31	HCO+O=CO2+H	3.00E+13	0	0		
32	HCO+HO2=CO2+OH+H	3.00E+13	0	0		
33	HCO+CH3=CO+CH4	2.65E+13	0	0		
34	2HCO=H2+2CO	3.00E+12	0	0		
35	2HCO=CH2O+CO	3.00E+13	0	0		
36	HCO+O2=O2CHO	1.20E+11	0	-1100		
37	CH2O+O2CHO=HCO+HO2CHO	1.99E+12	0	11660		
38	HO2CHO=OCHO+OH	5.01E+14	0	40150		
39	H+CO2+M=OCHO+M	7.50E+13	0	29000		
40	CH2O+M=HCO+H+M	3.30E+39	-6.3	99900		
	H2	Enhanced	by	2.50E+00		
	H2O	Enhanced	by	1.20E+01		
	CO	Enhanced	by	1.90E+00		
	CO2	Enhanced	by	3.80E+00		
41	CH2O+M=CO+H2+M	3.10E+45	-8	97510		
	H2	Enhanced	by	2.50E+00		
	H2O	Enhanced	by	1.20E+01		
	CO	Enhanced	by	1.90E+00		
	CO2	Enhanced	by	3.80E+00		
42	CH2O+H=HCO+H2	5.74E+07	1.9	2748.6		
43	CH2O+O=HCO+OH	1.81E+13	0	3080		
44	CH2O+OH=HCO+H2O	3.43E+09	1.2	-447		
45	CH2O+O2=HCO+HO2	1.23E+06	3	52000		
46	CH2O+HO2=HCO+H2O2	4.11E+04	2.5	10210		
47	CH2O+CH3=HCO+CH4	3.64E-06	5.4	998		
48	CH3+O=CH2O+H	8.43E+13	0	0		
49	CH3+O2=CH3O+O	1.99E+18	-1.6	29230		

50	$\text{CH}_3+\text{O}_2=\text{CH}_2\text{O}+\text{OH}$	3.51E-01	3.5	7380		
51	$\text{CH}_3+\text{HO}_2=\text{CH}_3\text{O}+\text{OH}$	2.41E+10	0.8	-2325		
52	$2\text{CH}_3(+\text{M})=\text{C}_2\text{H}_6(+\text{M})$	2.28E+15	-0.7	174.9		
	H <sub>2</sub> O	Enhanced	by	5.00E+00		
	CO	Enhanced	by	2.00E+00		
	CO <sub>2</sub>	Enhanced	by	3.00E+00		
	Low	pressure	limit:	8.05E+31	-3.75E+00	9.82E+02
	TROE	centering:	0.00E+00	5.70E+02	0.00E+00	1.00E+30
53	$\text{CH}_3+\text{H}(+\text{M})=\text{CH}_4(+\text{M})$	1.27E+16	-0.6	383		
	Low	pressure	limit:	2.48E+33	-4.76E+00	2.44E+03
	TROE	centering:	7.83E-01	7.40E+01	2.94E+03	6.96E+03
	H <sub>2</sub>	Enhanced	by	2.00E+00		
	H <sub>2</sub> O	Enhanced	by	6.00E+00		
	CH <sub>4</sub>	Enhanced	by	2.00E+00		
	CO	Enhanced	by	1.50E+00		
	CO <sub>2</sub>	Enhanced	by	2.00E+00		
	C <sub>2</sub> H <sub>6</sub>	Enhanced	by	3.00E+00		
	AR	Enhanced	by	7.00E-01		
54	$\text{CH}_4+\text{H}=\text{CH}_3+\text{H}_2$	5.47E+07	2	11210		
55	$\text{CH}_4+\text{O}=\text{CH}_3+\text{OH}$	3.15E+12	0.5	10290		
56	$\text{CH}_4+\text{OH}=\text{CH}_3+\text{H}_2\text{O}$	5.72E+06	2	2639		
57	$\text{CH}_3+\text{HO}_2=\text{CH}_4+\text{O}_2$	3.16E+12	0	0		
58	$\text{CH}_4+\text{HO}_2=\text{CH}_3+\text{H}_2\text{O}_2$	1.81E+11	0	18580		
59	$\text{CH}_3+\text{CH}_3\text{OH}=\text{CH}_4+\text{CH}_3\text{O}$	1.44E+01	3.1	6935		
60	$\text{CH}_3\text{O}+\text{CH}_3=\text{CH}_2\text{O}+\text{CH}_4$	1.20E+13	0	0		
61	$\text{CH}_3\text{O}+\text{H}=\text{CH}_2\text{O}+\text{H}_2$	2.00E+13	0	0		
62	$\text{CH}_3+\text{O}_2(+\text{M})=\text{CH}_3\text{O}_2(+\text{M})$	1.01E+08	1.6	0		
	Low	pressure	limit:	3.82E+31	-4.89E+00	3.43E+03
	TROE	centering:	4.50E-02	8.80E+02	2.50E+09	1.79E+09
63	$\text{CH}_3\text{O}_2+\text{CH}_2\text{O}=\text{CH}_3\text{O}_2\text{H}+\text{HCO}$	1.99E+12	0	11660		
64	$\text{CH}_4+\text{CH}_3\text{O}_2=\text{CH}_3+\text{CH}_3\text{O}_2\text{H}$	1.81E+11	0	18480		
65	$\text{CH}_3\text{OH}+\text{CH}_3\text{O}_2=\text{CH}_2\text{OH}+\text{CH}_3\text{O}_2\text{H}$	1.81E+12	0	13710		
66	$\text{CH}_3\text{O}_2+\text{CH}_3=2\text{CH}_3\text{O}$	5.08E+12	0	-1411		
67	$\text{CH}_3\text{O}_2+\text{HO}_2=\text{CH}_3\text{O}_2\text{H}+\text{O}_2$	2.47E+11	0	-1570		
68	$2\text{CH}_3\text{O}_2=\text{CH}_2\text{O}+\text{CH}_3\text{OH}+\text{O}_2$	3.11E+14	-1.6	-1051		
69	$2\text{CH}_3\text{O}_2=\text{O}_2+2\text{CH}_3\text{O}$	1.40E+16	-1.6	1860		
70	$\text{CH}_3\text{O}_2+\text{H}=\text{CH}_3\text{O}+\text{OH}$	9.60E+13	0	0		
71	$\text{CH}_3\text{O}_2+\text{O}=\text{CH}_3\text{O}+\text{O}_2$	3.60E+13	0	0		
72	$\text{CH}_3\text{O}_2+\text{OH}=\text{CH}_3\text{OH}+\text{O}_2$	6.00E+13	0	0		
73	$\text{CH}_3\text{O}_2\text{H}=\text{CH}_3\text{O}+\text{OH}$	6.31E+14	0	42300		
74	$\text{CH}_2\text{OH}+\text{M}=\text{CH}_2\text{O}+\text{H}+\text{M}$	1.00E+14	0	25100		
75	$\text{CH}_2\text{OH}+\text{H}=\text{CH}_2\text{O}+\text{H}_2$	6.00E+12	0	0		
76	$\text{CH}_2\text{OH}+\text{H}=\text{CH}_3+\text{OH}$	9.64E+13	0	0		
77	$\text{CH}_2\text{OH}+\text{O}=\text{CH}_2\text{O}+\text{OH}$	4.20E+13	0	0		
78	$\text{CH}_2\text{OH}+\text{OH}=\text{CH}_2\text{O}+\text{H}_2\text{O}$	2.40E+13	0	0		
79	$\text{CH}_2\text{OH}+\text{O}_2=\text{CH}_2\text{O}+\text{HO}_2$	2.41E+14	0	5017		

	Declared	duplicate	reaction...			
80	CH2OH+O2=CH2O+HO2	1.51E+15	-1	0		
	Declared	duplicate	reaction...			
81	CH2OH+HO2=CH2O+H2O2	1.20E+13	0	0		
82	CH2OH+HCO=CH3OH+CO	1.00E+13	0	0		
83	CH2OH+HCO=2CH2O	1.50E+13	0	0		
84	2CH2OH=CH3OH+CH2O	3.00E+12	0	0		
85	CH2OH+CH3O=CH3OH+CH2O	2.40E+13	0	0		
86	CH2OH+HO2=HOCH2O+OH	1.00E+13	0	0		
87	CH3O+M=CH2O+H+M	8.30E+17	-1.2	15500		
88	CH3O+H=CH3+OH	3.20E+13	0	0		
89	CH3O+O=CH2O+OH	6.00E+12	0	0		
90	CH3O+OH=CH2O+H2O	1.80E+13	0	0		
91	CH3O+O2=CH2O+HO2	9.03E+13	0	11980		
	Declared	duplicate	reaction...			
92	CH3O+O2=CH2O+HO2	2.20E+10	0	1748		
	Declared	duplicate	reaction...			
93	CH3O+HO2=CH2O+H2O2	3.00E+11	0	0		
94	CH3O+CO=CH3+CO2	1.60E+13	0	11800		
95	CH3O+HCO=CH3OH+CO	9.00E+13	0	0		
96	2CH3O=CH3OH+CH2O	6.00E+13	0	0		
97	OH+CH3(+M)=CH3OH(+M)	2.79E+18	-1.4	1330		
	H2	Enhanced	by	2.00E+00		
	H2O	Enhanced	by	6.00E+00		
	CH4	Enhanced	by	2.00E+00		
	CO	Enhanced	by	1.50E+00		
	CO2	Enhanced	by	2.00E+00		
	C2H6	Enhanced	by	3.00E+00		
	Low	pressure	limit:	4.00E+36	-5.92E+00	3.14E+03
	TROE	centering:	4.12E-01	1.95E+02	5.90E+03	6.39E+03
98	H+CH2OH(+M)=CH3OH(+M)	1.06E+12	0.5	86		
	H2	Enhanced	by	2.00E+00		
	H2O	Enhanced	by	6.00E+00		
	CH4	Enhanced	by	2.00E+00		
	CO	Enhanced	by	1.50E+00		
	CO2	Enhanced	by	2.00E+00		
	C2H6	Enhanced	by	3.00E+00		
	Low	pressure	limit:	4.36E+31	-4.65E+00	5.08E+03
	TROE	centering:	6.00E-01	1.00E+02	9.00E+04	1.00E+04
99	H+CH3O(+M)=CH3OH(+M)	2.43E+12	0.5	50		
	H2	Enhanced	by	2.00E+00		
	H2O	Enhanced	by	6.00E+00		
	CH4	Enhanced	by	2.00E+00		
	CO	Enhanced	by	1.50E+00		
	CO2	Enhanced	by	2.00E+00		
	C2H6	Enhanced	by	3.00E+00		

	Low	pressure	limit:	4.66E+41	-7.44E+00	1.41E+04
	TROE	centering:	7.00E-01	1.00E+02	9.00E+04	1.00E+04
100	CH3OH+H=CH2OH+H2	3.20E+13	0	6095		
101	CH3OH+H=CH3O+H2	8.00E+12	0	6095		
102	CH3OH+O=CH2OH+OH	3.88E+05	2.5	3080		
103	CH3OH+OH=CH3O+H2O	1.00E+06	2.1	496.7		
104	CH3OH+OH=CH2OH+H2O	7.10E+06	1.8	-596		
105	CH3OH+O2=CH2OH+HO2	2.05E+13	0	44900		
106	CH3OH+HCO=CH2OH+CH2O	9.64E+03	2.9	13110		
107	CH3OH+HO2=CH2OH+H2O2	3.98E+13	0	19400		
108	CH3OH+CH3=CH2OH+CH4	3.19E+01	3.2	7172		
109	CH3O+CH3OH=CH3OH+CH2OH	3.00E+11	0	4060		
110	2CH3=H+C2H5	4.99E+12	0.1	10600		
111	CH4+CH2=2CH3	2.46E+06	2	8270		
112	CH4+CH2(S)=2CH3	1.60E+13	0	-570		
113	CH3+OH=CH2+H2O	5.60E+07	1.6	5420		
114	CH3+OH=CH2(S)+H2O	2.50E+13	0	0		
115	CH3+CH2=C2H4+H	4.00E+13	0	0		
116	CH3+CH2(S)=C2H4+H	1.20E+13	0	-570		
117	CH3O+H=CH2(S)+H2O	1.60E+13	0	0		
118	CH2(S)+H2O(+M)=CH3OH(+M)	4.82E+17	-1.2	1145		
	H2	Enhanced	by	2.00E+00		
	H2O	Enhanced	by	6.00E+00		
	CH4	Enhanced	by	2.00E+00		
	CO	Enhanced	by	1.50E+00		
	CO2	Enhanced	by	2.00E+00		
	C2H6	Enhanced	by	3.00E+00		
	Low	pressure	limit:	1.88E+38	-6.36E+00	5.04E+03
	TROE	centering:	6.03E-01	2.08E+02	3.92E+03	1.02E+04
119	CH2+H(+M)=CH3(+M)	2.50E+16	-0.8	0		
	H2	Enhanced	by	2.00E+00		
	H2O	Enhanced	by	6.00E+00		
	CH4	Enhanced	by	2.00E+00		
	CO	Enhanced	by	1.50E+00		
	CO2	Enhanced	by	2.00E+00		
	C2H6	Enhanced	by	3.00E+00		
	Low	pressure	limit:	3.20E+27	-3.14E+00	1.23E+03
	TROE	centering:	6.80E-01	7.80E+01	2.00E+03	5.59E+03
120	CH2+O=HCO+H	8.00E+13	0	0		
121	CH2+OH=CH2O+H	2.00E+13	0	0		
122	CH2+H2=H+CH3	5.00E+05	2	7230		
123	CH2+O2=HCO+OH	1.32E+13	0	1500		
124	CH2+HO2=CH2O+OH	2.00E+13	0	0		
125	CH2+CO(+M)=CH2CO(+M)	8.10E+11	0.5	4510		
	H2	Enhanced	by	2.00E+00		
	H2O	Enhanced	by	6.00E+00		



	CH4	Enhanced	by	2.00E+00		
	CO	Enhanced	by	1.50E+00		
	CO2	Enhanced	by	2.00E+00		
	C2H6	Enhanced	by	3.00E+00		
	Low	pressure	limit:	2.69E+33	-5.11E+00	7.10E+03
	TROE	centering:	5.91E-01	2.75E+02	1.23E+03	5.19E+03
126	2CH2=C2H2+H2	3.20E+13	0	0		
127	CH2(S)+M=CH2+M	9.00E+12	0	600		
	H2O	Enhanced	by	0.00E+00		
	CO	Enhanced	by	0.00E+00		
	CO2	Enhanced	by	0.00E+00		
128	CH2(S)+H2O=CH2+H2O	3.00E+13	0	0		
129	CH2(S)+CO=CH2+CO	9.00E+12	0	0		
130	CH2(S)+CO2=CH2+CO2	7.00E+12	0	0		
131	CH2(S)+O=CO+H2	1.50E+13	0	0		
132	CH2(S)+O=HCO+H	1.50E+13	0	0		
133	CH2(S)+OH=CH2O+H	3.00E+13	0	0		
134	CH2(S)+H2=CH3+H	7.00E+13	0	0		
135	CH2(S)+O2=H+OH+CO	2.80E+13	0	0		
136	CH2(S)+O2=CO+H2O	1.20E+13	0	0		
137	CH2(S)+CO2=CH2O+CO	1.40E+13	0	0		
138	CH2(S)+H=CH+H2	3.00E+13	0	0		
139	CH2+H=CH+H2	1.00E+18	-1.6	0		
	Declared	duplicate	reaction...			
140	CH2+OH=CH+H2O	1.13E+07	2	3000		
141	CH+O2=HCO+O	3.30E+13	0	0		
142	CH+O=CO+H	5.70E+13	0	0		
143	CH+OH=HCO+H	3.00E+13	0	0		
144	CH2+H=CH+H2	2.70E+11	0.7	25700		
	Declared	duplicate	reaction...			
145	CH+H2O=H+CH2O	1.71E+13	0	-755		
146	CH+CO2=HCO+CO	1.70E+12	0	685		
147	HOCH2O=HCOOH+H	1.00E+14	0	14900		
148	CH2O+OH=HOCH2O	4.50E+15	-1.1	0		
149	HCOOH+M=CO+H2O+M	2.30E+13	0	50000		
150	HCOOH+M=CO2+H2+M	1.50E+16	0	57000		
151	HCOOH=HCO+OH	4.59E+18	-0.5	108300		
152	HCOOH+OH=H2O+CO2+H	2.62E+06	2.1	916		
153	HCOOH+OH=H2O+CO+OH	1.85E+07	1.5	-962		
154	HCOOH+H=H2+CO2+H	4.24E+06	2.1	4868		
155	HCOOH+H=H2+CO+OH	6.03E+13	-0.3	2988		
156	HCOOH+CH3=CH4+CO+OH	3.90E-07	5.8	2200		
157	HCOOH+HO2=H2O2+CO+OH	1.00E+12	0	11920		
158	HCOOH+O=CO+2OH	1.77E+18	-1.9	2975		
159	C2H5+H(+M)=C2H6(+M)	5.21E+17	-1	1580		
	H2	Enhanced	by	2.00E+00		

	H2O	Enhanced	by	6.00E+00		
	CO	Enhanced	by	1.50E+00		
	CO2	Enhanced	by	2.00E+00		
	CH4	Enhanced	by	2.00E+00		
	C2H6	Enhanced	by	3.00E+00		
	Low	pressure	limit:	1.99E+41	-7.08E+00	6.69E+03
	TROE	centering:	8.42E-01	1.25E+02	2.22E+03	6.88E+03
160	C2H6+H=C2H5+H2	5.54E+02	3.5	5167		
161	C2H6+O=C2H5+OH	3.55E+06	2.4	5830		
162	C2H6+OH=C2H5+H2O	3.54E+06	2.1	870		
163	C2H6+O2=C2H5+HO2	6.03E+13	0	51870		
164	C2H6+CH3=C2H5+CH4	1.51E-07	6	6047		
165	C2H6+HO2=C2H5+H2O2	3.46E+01	3.6	16920		
166	C2H6+CH3O2=C2H5+CH3O2H	1.94E+01	3.6	17100		
167	C2H6+CH3O=C2H5+CH3OH	2.41E+11	0	7090		
168	C2H6+CH=C2H5+CH2	1.10E+14	0	-260		
169	CH2(S)+C2H6=CH3+C2H5	1.20E+14	0	0		
170	H+C2H4(+M)=C2H5(+M)	5.40E+11	0.5	1820		
	Low	pressure	limit:	6.00E+41	-7.62E+00	6.97E+03
	TROE	centering:	9.75E-01	2.10E+02	9.84E+02	4.37E+03
	H2	Enhanced	by	2.00E+00		
	H2O	Enhanced	by	6.00E+00		
	CH4	Enhanced	by	2.00E+00		
	CO	Enhanced	by	1.50E+00		
	CO2	Enhanced	by	2.00E+00		
	C2H6	Enhanced	by	3.00E+00		
	AR	Enhanced	by	7.00E-01		
171	H2+CH3O2=H+CH3O2H	1.50E+14	0	26030		
172	H2+C2H5O2=H+C2H5O2H	1.50E+14	0	26030		
173	2C2H4=C2H5+C2H3	4.82E+14	0	71530		
174	CH3+C2H5=CH4+C2H4	1.18E+04	2.5	-2921		
175	C2H5+H=C2H4+H2	2.00E+12	0	0		
176	C2H5+O=CH3CHO+H	1.10E+14	0	0		
177	C2H5+HO2=C2H5O+OH	1.10E+13	0	0		
178	CH3O2+C2H5=CH3O+C2H5O	8.00E+12	0	-1000		
179	C2H5O+O2=CH3CHO+HO2	4.28E+10	0	1097		
180	CH3+CH2O=C2H5O	3.00E+11	0	6336		
181	CH3CHO+H=C2H5O	8.00E+12	0	6400		
182	C2H5+O2=C2H5O2	2.88E+56	-13.8	14620		
183	C2H5O2+CH2O=C2H5O2H+HCO	1.99E+12	0	11660		
184	CH4+C2H5O2=CH3+C2H5O2H	1.81E+11	0	18480		
185	CH3OH+C2H5O2=CH2OH+C2H5O2H	1.81E+12	0	13710		
186	C2H5O2+HO2=C2H5O2H+O2	1.75E+10	0	-3275		
187	C2H6+C2H5O2=C2H5+C2H5O2H	8.60E+00	3.8	17200		
188	C2H5O2H=C2H5O+OH	6.31E+14	0	42300		
189	C2H5+O2=C2H4O2H	1.81E+45	-11.5	14600		

190	$C_2H_5+O_2=C_2H_4+HO_2$	7.56E+14	-1	4749		
	Declared	duplicate	reaction...			
191	$C_2H_5+O_2=C_2H_4+HO_2$	4.00E-01	3.9	13620		
	Declared	duplicate	reaction...			
192	$C_2H_5+O_2=C_2H_4O_1-2+OH$	1.63E+11	-0.3	6150		
193	$C_2H_5+O_2=CH_3CHO+OH$	8.26E+02	2.4	5285		
194	$C_2H_4O_2H=C_2H_5O_2$	1.20E+36	-8.1	27020		
195	$C_2H_5O_2=CH_3CHO+OH$	2.52E+41	-10.2	43710		
196	$C_2H_5O_2=C_2H_4+HO_2$	1.82E+38	-8.4	37890		
197	$C_2H_5O_2=C_2H_4O_1-2+OH$	4.00E+43	-10.5	45580		
198	$C_2H_4O_2H=C_2H_4O_1-2+OH$	8.85E+30	-6.1	20660		
199	$C_2H_4O_2H=C_2H_4+HO_2$	3.98E+34	-7.2	23250		
200	$C_2H_4O_2H=CH_3CHO+OH$	1.19E+34	-9	29210		
201	$C_2H_4O_1-2=CH_3+HCO$	3.63E+13	0	57200		
202	$C_2H_4O_1-2=CH_3CHO$	7.41E+12	0	53800		
203	$C_2H_4O_1-2+OH=C_2H_3O_1-2+H_2O$	1.78E+13	0	3610		
204	$C_2H_4O_1-2+H=C_2H_3O_1-2+H_2$	8.00E+13	0	9680		
205	$C_2H_4O_1-2+HO_2=C_2H_3O_1-2+H_2O_2$	1.13E+13	0	30430		
206	$C_2H_4O_1-2+CH_3O_2=C_2H_3O_1-2+CH_3O_2H$	1.13E+13	0	30430		
207	$C_2H_4O_1-2+C_2H_5O_2=C_2H_3O_1-2+C_2H_5O_2H$	1.13E+13	0	30430		
208	$C_2H_4O_1-2+CH_3=C_2H_3O_1-2+CH_4$	1.07E+12	0	11830		
209	$C_2H_4O_1-2+CH_3O=C_2H_3O_1-2+CH_3OH$	1.20E+11	0	6750		
210	$C_2H_3O_1-2=CH_3CO$	8.50E+14	0	14000		
211	$C_2H_3O_1-2=CH_2CHO$	1.00E+14	0	14000		
212	$CH_3+HCO=CH_3CHO$	1.75E+13	0	0		
213	$CH_3CHO+H=CH_3CO+H_2$	1.11E+13	0	3110		
214	$CH_3CHO+O=CH_3CO+OH$	5.94E+12	0	1868		
215	$CH_3CHO+OH=CH_3CO+H_2O$	2.00E+06	1.8	1300		
216	$CH_3CHO+O_2=CH_3CO+HO_2$	3.01E+13	0	39150		
217	$CH_3CHO+CH_3=CH_3CO+CH_4$	1.76E+03	2.8	4950		
218	$CH_3CHO+HO_2=CH_3CO+H_2O_2$	3.01E+12	0	11920		
219	$CH_3O_2+CH_3CHO=CH_3O_2H+CH_3CO$	3.01E+12	0	11920		
220	$CH_3CHO+CH_3CO_3=CH_3CO+CH_3CO_3H$	3.01E+12	0	11920		
221	$CH_3CHO+OH=CH_3+HCOOH$	3.00E+15	-1.1	0		
222	$CH_3CHO+OH=CH_2CHO+H_2O$	1.72E+05	2.4	815		
223	$CH_3CO(+M)=CH_3+CO(+M)$	3.00E+12	0	16720		
	Low	pressure	limit:	1.20E+15	0.00E+00	1.25E+04
224	$CH_3CO+H=CH_2CO+H_2$	2.00E+13	0	0		
225	$CH_3CO+O=CH_2CO+OH$	2.00E+13	0	0		
226	$CH_3CO+CH_3=CH_2CO+CH_4$	5.00E+13	0	0		
227	$CH_3CO+O_2=CH_3CO_3$	1.20E+11	0	-1100		
	Declared	duplicate	reaction...			
228	$CH_3CO_3+HO_2=CH_3CO_3H+O_2$	1.75E+10	0	-3275		
229	$H_2O_2+CH_3CO_3=HO_2+CH_3CO_3H$	2.41E+12	0	9936		
230	$CH_4+CH_3CO_3=CH_3+CH_3CO_3H$	1.81E+11	0	18480		
231	$CH_2O+CH_3CO_3=HCO+CH_3CO_3H$	1.99E+12	0	11660		

232	$C_2H_6+CH_3CO_3=C_2H_5+CH_3CO_3H$	1.70E+13	0	20460		
233	$CH_3CO_3H=CH_3CO_2+OH$	5.01E+14	0	40150		
234	$CH_3CO_2+M=CH_3+CO_2+M$	4.40E+15	0	10500		
235	$CH_2CO+H=CH_2CHO$	5.00E+13	0	12300		
236	$CH_2CHO+O_2=CH_2O+CO+OH$	2.00E+13	0	4200		
237	$CH_2CO+H=CH_3+CO$	1.10E+13	0	3400		
238	$CH_2CO+H=HCCO+H_2$	2.00E+14	0	8000		
239	$CH_2CO+O=CH_2+CO_2$	1.75E+12	0	1350		
240	$CH_2CO+O=HCCO+OH$	1.00E+13	0	8000		
241	$CH_2CO+OH=HCCO+H_2O$	1.00E+13	0	2000		
242	$CH_2CO+OH=CH_2OH+CO$	2.00E+12	0	-1010		
243	$CH_2(S)+CH_2CO=C_2H_4+CO$	1.60E+14	0	0		
244	$HCCO+OH=H_2+2CO$	1.00E+14	0	0		
245	$H+HCCO=CH_2(S)+CO$	1.10E+13	0	0		
246	$HCCO+O=H+2CO$	8.00E+13	0	0		
247	$HCCO+O_2=OH+2CO$	4.20E+10	0	850		
248	$HCCO+M=CH+CO+M$	6.50E+15	0	58820		
249	$CH+CH_2O=H+CH_2CO$	9.46E+13	0	-515		
250	$CH+HCCO=CO+C_2H_2$	5.00E+13	0	0		
251	$C_2H_3+H(+M)=C_2H_4(+M)$	1.36E+14	0.2	660		
	H <sub>2</sub>	Enhanced	by	2.00E+00		
	H <sub>2</sub> O	Enhanced	by	6.00E+00		
	CO	Enhanced	by	1.50E+00		
	CO <sub>2</sub>	Enhanced	by	2.00E+00		
	CH <sub>4</sub>	Enhanced	by	2.00E+00		
	C <sub>2</sub> H <sub>6</sub>	Enhanced	by	3.00E+00		
	Low pressure	limit:		1.40E+30	-3.86E+00	3.32E+03
	TROE centering:		7.82E-01	2.08E+02	2.66E+03	6.10E+03
252	$C_2H_4(+M)=C_2H_2+H_2(+M)$	8.00E+12	0.4	88770		
	H <sub>2</sub>	Enhanced	by	2.00E+00		
	H <sub>2</sub> O	Enhanced	by	6.00E+00		
	CO	Enhanced	by	1.50E+00		
	CO <sub>2</sub>	Enhanced	by	2.00E+00		
	CH <sub>4</sub>	Enhanced	by	2.00E+00		
	C <sub>2</sub> H <sub>6</sub>	Enhanced	by	3.00E+00		
	AR	Enhanced	by	7.00E-01		
	Low pressure	limit:		1.58E+51	-9.30E+00	9.78E+04
	TROE centering:		7.35E-01	1.80E+02	1.04E+03	5.42E+03
253	$C_2H_4+H=C_2H_3+H_2$	1.33E+06	2.5	12241		
254	$C_2H_4+O=CH_3+HCO$	8.56E+06	1.9	183		
255	$C_2H_4+O=CH_2CHO+H$	4.99E+06	1.9	183		
256	$C_2H_4+OH=C_2H_3+H_2O$	1.80E+06	2	2500		
257	$C_2H_4+CH_3=C_2H_3+CH_4$	6.62E+00	3.7	9500		
258	$C_2H_4+O_2=C_2H_3+HO_2$	4.00E+13	0	58200		
259	$C_2H_4+CH_3O=C_2H_3+CH_3OH$	1.20E+11	0	6750		
260	$C_2H_4+CH_3O_2=C_2H_3+CH_3O_2H$	2.23E+12	0	17190		

261	$C_2H_4+C_2H_5O_2=C_2H_3+C_2H_5O_2H$	2.23E+12	0	17190		
262	$C_2H_4+CH_3CO_3=C_2H_3+CH_3CO_3H$	1.13E+13	0	30430		
263	$C_2H_4+CH_3O_2=C_2H_4O_1-2+CH_3O$	2.82E+12	0	17110		
264	$C_2H_4+C_2H_5O_2=C_2H_4O_1-2+C_2H_5O$	2.82E+12	0	17110		
265	$C_2H_4+HO_2=C_2H_4O_1-2+OH$	2.23E+12	0	17190		
266	$CH+CH_4=C_2H_4+H$	6.00E+13	0	0		
267	$C_2H_3(+M)=C_2H_2+H(+M)$	3.86E+08	1.6	37048.2		
	Low	pressure	limit:	2.57E+27	-3.40E+00	3.58E+04
	TROE	centering:	1.98E+00	5.38E+03	4.29E+00	-7.95E-02
	H2	Enhanced	by	2.00E+00		
	H2O	Enhanced	by	6.00E+00		
	CH4	Enhanced	by	2.00E+00		
	CO	Enhanced	by	1.50E+00		
	CO2	Enhanced	by	2.00E+00		
	C2H6	Enhanced	by	3.00E+00		
	AR	Enhanced	by	7.00E-01		
	C2H2	Enhanced	by	3.00E+00		
	C2H4	Enhanced	by	3.00E+00		
268	$C_2H_3+O_2=HCO+CH_2O$	4.58E+16	-1.4	1015		
269	$C_2H_3+O_2=HO_2+C_2H_2$	1.34E+06	1.6	-384		
270	$C_2H_3+O_2=O+CH_2CHO$	3.00E+11	0.3	11		
271	$CH_3+C_2H_3=CH_4+C_2H_2$	3.92E+11	0	0		
272	$C_2H_3+H=C_2H_2+H_2$	9.63E+13	0	0		
273	$C_2H_3+OH=C_2H_2+H_2O$	5.00E+12	0	0		
274	$C_2H+H(+M)=C_2H_2(+M)$	1.00E+17	0	0		
	H2	Enhanced	by	2.00E+00		
	H2O	Enhanced	by	6.00E+00		
	CO	Enhanced	by	1.50E+00		
	CO2	Enhanced	by	2.00E+00		
	CH4	Enhanced	by	2.00E+00		
	C2H6	Enhanced	by	3.00E+00		
	Low	pressure	limit:	3.75E+33	-4.80E+00	1.90E+03
	TROE	centering:	6.46E-01	1.32E+02	1.32E+03	5.57E+03
275	$C_2H_2+O_2=HCCO+OH$	2.00E+08	1.5	30100		
276	$O+C_2H_2=C_2H+OH$	4.60E+19	-1.4	28950		
277	$C_2H_2+O=CH_2+CO$	4.08E+06	2	1900		
278	$C_2H_2+O=HCCO+H$	1.35E+07	2	1900		
279	$C_2H_2+OH=C_2H+H_2O$	3.37E+07	2	14000		
280	$C_2H_2+OH=CH_2CO+H$	3.24E+13	0	12000		
281	$C_2H_2+OH=CH_3+CO$	4.83E-04	4	-2000		
282	$OH+C_2H_2=H+HCCOH$	5.04E+05	2.3	13500		
283	$H+HCCOH=H+CH_2CO$	1.00E+13	0	0		
284	$C_2H_5OH(+M)=CH_2OH+CH_3(+M)$	5.71E+23	-1.7	94400		
	H2	Enhanced	by	2.00E+00		
	H2O	Enhanced	by	5.00E+00		
	CO	Enhanced	by	2.00E+00		

	CO2	Enhanced	by	3.00E+00		
	Low	pressure	limit:	3.11E+85	-1.88E+01	1.13E+05
	TROE	centering:	5.00E-01	5.50E+02	8.25E+02	6.10E+03
285	C2H5OH(+M)=C2H5+OH(+M)	2.40E+23	-1.6	99540		
	H2	Enhanced	by	2.00E+00		
	H2O	Enhanced	by	5.00E+00		
	CO	Enhanced	by	2.00E+00		
	CO2	Enhanced	by	3.00E+00		
	Low	pressure	limit:	5.11E+85	-1.88E+01	1.19E+05
	TROE	centering:	5.00E-01	6.50E+02	8.00E+02	1.00E+15
286	C2H5OH(+M)=C2H4+H2O(+M)	2.79E+13	0.1	66140		
	H2O	Enhanced	by	5.00E+00		
	Low	pressure	limit:	2.57E+83	-1.89E+01	8.65E+04
	TROE	centering:	7.00E-01	3.50E+02	8.00E+02	3.80E+03
287	C2H5OH(+M)=CH3CHO+H2(+M)	7.24E+11	0.1	91010		
	H2O	Enhanced	by	5.00E+00		
	Low	pressure	limit:	4.46E+87	-1.94E+01	1.16E+05
	TROE	centering:	9.00E-01	9.00E+02	1.10E+03	3.50E+03
288	C2H5OH+O2=PC2H4OH+HO2	2.00E+13	0	52800		
289	C2H5OH+O2=SC2H4OH+HO2	1.50E+13	0	50150		
290	C2H5OH+OH=PC2H4OH+H2O	1.74E+11	0.3	600		
291	C2H5OH+OH=SC2H4OH+H2O	4.64E+11	0.1	0		
292	C2H5OH+OH=C2H5O+H2O	7.46E+11	0.3	1634		
293	C2H5OH+H=PC2H4OH+H2	1.23E+07	1.8	5098		
294	C2H5OH+H=SC2H4OH+H2	2.58E+07	1.6	2827		
295	C2H5OH+H=C2H5O+H2	1.50E+07	1.6	3038		
296	C2H5OH+HO2=PC2H4OH+H2O2	1.23E+04	2.5	15750		
297	C2H5OH+HO2=SC2H4OH+H2O2	8.20E+03	2.5	10750		
298	C2H5OH+HO2=C2H5O+H2O2	2.50E+12	0	24000		
299	C2H5OH+CH3O2=PC2H4OH+CH3O2H	1.23E+04	2.5	15750		
300	C2H5OH+CH3O2=SC2H4OH+CH3O2H	8.20E+03	2.5	10750		
301	C2H5OH+CH3O2=C2H5O+CH3O2H	2.50E+12	0	24000		
302	C2H5OH+O=PC2H4OH+OH	9.41E+07	1.7	5459		
303	C2H5OH+O=SC2H4OH+OH	1.88E+07	1.9	1824		
304	C2H5OH+O=C2H5O+OH	1.58E+07	2	4448		
305	C2H5OH+CH3=PC2H4OH+CH4	1.33E+02	3.2	9362		
306	C2H5OH+CH3=SC2H4OH+CH4	4.44E+02	2.9	7690		
307	C2H5OH+CH3=C2H5O+CH4	1.34E+02	2.9	7452		
308	C2H5OH+C2H5=PC2H4OH+C2H6	5.00E+10	0	13400		
309	C2H5OH+C2H5=SC2H4OH+C2H6	5.00E+10	0	10400		
310	C2H4+OH=PC2H4OH	4.17E+20	-2.8	1240		
311	SC2H4OH+M=CH3CHO+H+M	1.00E+14	0	25000		
312	O2C2H4OH=PC2H4OH+O2	3.90E+16	-1	30000		
313	O2C2H4OH=OH+2CH2O	3.12E+09	0	18900		
314	SC2H4OH+O2=CH3CHO+HO2	3.81E+06	2	1641		
315	CH3COCH3(+M)=CH3CO+CH3(+M)	7.11E+21	-1.6	84680		

	Low	pressure	limit:	7.01E+89	-2.04E+01	1.07E+05
	TROE	centering:	8.63E-01	1.00E+10	4.16E+02	3.29E+09
316	CH3COCH3+OH=CH3COCH2+H2O	1.25E+05	2.5	445		
317	CH3COCH3+H=CH3COCH2+H2	9.80E+05	2.4	5160		
318	CH3COCH3+O=CH3COCH2+OH	5.13E+11	0.2	4890		
319	CH3COCH3+CH3=CH3COCH2+CH4	3.96E+11	0	9784		
320	CH3COCH3+CH3O=CH3COCH2+CH3OH	4.34E+11	0	6460		
321	CH3COCH3+O2=CH3COCH2+HO2	6.03E+13	0	48500		
322	CH3COCH3+HO2=CH3COCH2+H2O2	1.70E+13	0	20460		
323	CH3COCH3+CH3O2=CH3COCH2+CH3O2H	1.70E+13	0	20460		
324	CH3COCH2=CH2CO+CH3	1.00E+14	0	31000		
325	CH3COCH2+O2=CH3COCH2O2	1.20E+11	0	-1100		
326	CH3COCH3+CH3COCH2O2=CH3COCH2+CH3COCH2O2H	1.00E+11	0	5000		
327	CH2O+CH3COCH2O2=HCO+CH3COCH2O2H	1.29E+11	0	9000		
328	HO2+CH3COCH2O2=CH3COCH2O2H+O2	1.00E+12	0	0		
329	CH3COCH2O2H=CH3COCH2O+OH	1.00E+16	0	43000		
330	CH3CO+CH2O=CH3COCH2O	1.00E+11	0	11900		
331	C2H3+HCO=C2H3CHO	1.81E+13	0	0		
332	C2H3CHO+H=C2H3CO+H2	1.34E+13	0	3300		
333	C2H3CHO+O=C2H3CO+OH	5.94E+12	0	1868		
334	C2H3CHO+H=C2H4+HCO	2.00E+13	0	3500		
335	C2H3CHO+O=CH2CO+HCO+H	5.00E+07	1.8	76		
336	C2H3CHO+OH=C2H3CO+H2O	9.24E+06	1.5	-962		
337	C2H3CHO+O2=C2H3CO+HO2	1.00E+13	0	40700		
338	C2H3CHO+HO2=C2H3CO+H2O2	3.01E+12	0	11920		
339	C2H3CHO+CH3=C2H3CO+CH4	2.61E+06	1.8	5911		
340	C2H3CHO+C2H3=C2H3CO+C2H4	1.74E+12	0	8440		
341	C2H3CHO+CH3O=C2H3CO+CH3OH	1.00E+12	0	3300		
342	C2H3CHO+CH3O2=C2H3CO+CH3O2H	3.01E+12	0	11920		
343	C2H3+CO=C2H3CO	1.51E+11	0	4810		
344	C2H3CO+O2=CH2CHO+CO2	5.40E+20	-2.7	7000		
345	C2H3CO+O=C2H3+CO2	1.00E+14	0	0		
346	C2H5+HCO=C2H5CHO	1.81E+13	0	0		
347	C2H5CHO+H=C2H5CO+H2	4.00E+13	0	4200		
348	C2H5CHO+O=C2H5CO+OH	5.00E+12	0	1790		
349	C2H5CHO+OH=C2H5CO+H2O	2.69E+10	0.8	-340		
350	C2H5CHO+CH3=C2H5CO+CH4	2.61E+06	1.8	5911		
351	C2H5CHO+HO2=C2H5CO+H2O2	2.80E+12	0	13600		
352	C2H5CHO+CH3O=C2H5CO+CH3OH	1.00E+12	0	3300		
353	C2H5CHO+CH3O2=C2H5CO+CH3O2H	3.01E+12	0	11920		
354	C2H5CHO+C2H5=C2H5CO+C2H6	1.00E+12	0	8000		
355	C2H5CHO+C2H5O=C2H5CO+C2H5OH	6.03E+11	0	3300		
356	C2H5CHO+C2H5O2=C2H5CO+C2H5O2H	3.01E+12	0	11920		
357	C2H5CHO+O2=C2H5CO+HO2	1.00E+13	0	40700		
358	C2H5CHO+CH3CO3=C2H5CO+CH3CO3H	3.01E+12	0	11920		

359	$C_2H_5CHO + C_2H_3 = C_2H_5CO + C_2H_4$	1.70E+12	0	8440		
360	$C_2H_5 + CO = C_2H_5CO$	1.51E+11	0	4810		
361	$CH_3OCH_3(+M) = CH_3 + CH_3O(+M)$	4.85E+21	-1.6	83130		
	Low pressure		limit:	1.12E+71	-1.45E+01	1.00E+05
	TROE centering:		8.43E-01	9.49E+09	5.56E+02	6.71E+09
362	$CH_3OCO + H = CH_3OCHO$	1.00E+14	0	0		
363	$CH_3OCHO(+M) = CH_3OH + CO(+M)$	1.00E+14	0	62500		
	Low pressure		limit:	6.14E+60	-1.21E+01	7.54E+04
	TROE centering:		7.80E-01	8.28E+09	4.39E+02	6.70E+08
364	$CH_3O + HCO = CH_3OCHO$	3.00E+13	0	0		
365	$CH_3 + OCHO = CH_3OCHO$	1.00E+13	0	0		
366	$CH_3OCHO + O_2 = CH_3OCO + HO_2$	1.00E+13	0	49700		
367	$CH_3OCHO + OH = CH_3OCO + H_2O$	1.58E+07	1.8	934		
368	$CH_3OCHO + HO_2 = CH_3OCO + H_2O_2$	4.82E+03	2.6	13910		
369	$CH_3OCHO + O = CH_3OCO + OH$	2.76E+05	2.5	2830		
370	$CH_3OCHO + H = CH_3OCO + H_2$	6.50E+05	2.4	4471		
371	$CH_3OCHO + CH_3 = CH_3OCO + CH_4$	7.55E-01	3.5	5481		
372	$CH_3OCHO + CH_3O = CH_3OCO + CH_3OH$	5.48E+11	0	5000		
373	$CH_3OCHO + CH_3O_2 = CH_3OCO + CH_3O_2H$	4.82E+03	2.6	13910		
374	$CH_3OCHO + HCO = CH_3OCO + CH_2O$	5.40E+06	1.9	17010		
375	$CH_3 + CO_2 = CH_3OCO$	4.76E+07	1.5	34700		
376	$CH_3O + CO = CH_3OCO$	1.55E+06	2	5730		
377	$C_3H_8(+M) = CH_3 + C_2H_5(+M)$	1.29E+37	-5.8	97380		
	H <sub>2</sub>	Enhanced	by	2.00E+00		
	H <sub>2</sub> O	Enhanced	by	6.00E+00		
	CO	Enhanced	by	1.50E+00		
	CO <sub>2</sub>	Enhanced	by	2.00E+00		
	CH <sub>4</sub>	Enhanced	by	2.00E+00		
	C <sub>2</sub> H <sub>6</sub>	Enhanced	by	3.00E+00		
	Low pressure		limit:	5.64E+74	-1.57E+01	9.87E+04
	TROE centering:		3.10E-01	5.00E+01	3.00E+03	9.00E+03
378	$NC_3H_7 + H = C_3H_8$	1.00E+14	0	0		
379	$IC_3H_7 + H = C_3H_8$	1.00E+14	0	0		
380	$C_3H_8 + O_2 = IC_3H_7 + HO_2$	2.00E+13	0	49640		
381	$C_3H_8 + O_2 = NC_3H_7 + HO_2$	6.00E+13	0	52290		
382	$H + C_3H_8 = H_2 + IC_3H_7$	1.30E+06	2.4	4471		
383	$H + C_3H_8 = H_2 + NC_3H_7$	1.33E+06	2.5	6756		
384	$C_3H_8 + O = IC_3H_7 + OH$	5.49E+05	2.5	3140		
385	$C_3H_8 + O = NC_3H_7 + OH$	3.71E+06	2.4	5505		
386	$C_3H_8 + OH = NC_3H_7 + H_2O$	1.05E+10	1	1586		
387	$C_3H_8 + OH = IC_3H_7 + H_2O$	4.67E+07	1.6	-35		
388	$C_3H_8 + HO_2 = IC_3H_7 + H_2O_2$	5.88E+04	2.5	14860		
389	$C_3H_8 + HO_2 = NC_3H_7 + H_2O_2$	8.10E+04	2.5	16690		
390	$CH_3 + C_3H_8 = CH_4 + IC_3H_7$	6.40E+04	2.2	7520		
391	$CH_3 + C_3H_8 = CH_4 + NC_3H_7$	9.04E-01	3.6	7154		
392	$IC_3H_7 + C_3H_8 = NC_3H_7 + C_3H_8$	3.00E+10	0	12900		



393	$C_2H_3+C_3H_8=C_2H_4+IC_3H_7$	1.00E+11	0	10400		
394	$C_2H_3+C_3H_8=C_2H_4+NC_3H_7$	1.00E+11	0	10400		
395	$C_2H_5+C_3H_8=C_2H_6+IC_3H_7$	1.00E+11	0	10400		
396	$C_2H_5+C_3H_8=C_2H_6+NC_3H_7$	1.00E+11	0	10400		
397	$C_3H_8+C_3H_5-A=NC_3H_7+C_3H_6$	7.94E+11	0	20500		
398	$C_3H_8+C_3H_5-A=IC_3H_7+C_3H_6$	7.94E+11	0	16200		
399	$C_3H_8+CH_3O=NC_3H_7+CH_3OH$	3.00E+11	0	7000		
400	$C_3H_8+CH_3O=IC_3H_7+CH_3OH$	3.00E+11	0	7000		
401	$CH_3O_2+C_3H_8=CH_3O_2H+NC_3H_7$	8.10E+04	2.5	16690		
402	$CH_3O_2+C_3H_8=CH_3O_2H+IC_3H_7$	5.88E+04	2.5	14860		
403	$C_2H_5O_2+C_3H_8=C_2H_5O_2H+NC_3H_7$	8.10E+04	2.5	16690		
404	$C_2H_5O_2+C_3H_8=C_2H_5O_2H+IC_3H_7$	5.88E+04	2.5	14860		
405	$NC_3H_7O_2+C_3H_8=NC_3H_7O_2H+NC_3H_7$	1.70E+13	0	20460		
406	$NC_3H_7O_2+C_3H_8=NC_3H_7O_2H+IC_3H_7$	2.00E+12	0	17000		
407	$IC_3H_7O_2+C_3H_8=IC_3H_7O_2H+NC_3H_7$	1.70E+13	0	20460		
408	$IC_3H_7O_2+C_3H_8=IC_3H_7O_2H+IC_3H_7$	2.00E+12	0	17000		
409	$C_3H_8+CH_3CO_3=IC_3H_7+CH_3CO_3H$	2.00E+12	0	17000		
410	$C_3H_8+CH_3CO_3=NC_3H_7+CH_3CO_3H$	1.70E+13	0	20460		
411	$C_3H_8+O_2CHO=NC_3H_7+HO_2CHO$	5.52E+04	2.5	16480		
412	$C_3H_8+O_2CHO=IC_3H_7+HO_2CHO$	1.48E+04	2.6	13910		
413	$H+C_3H_6=IC_3H_7$	2.64E+13	0	2160		
414	$IC_3H_7+H=C_2H_5+CH_3$	2.00E+13	0	0		
415	$IC_3H_7+O_2=C_3H_6+HO_2$	4.50E-19	0	5020		
416	$IC_3H_7+OH=C_3H_6+H_2O$	2.41E+13	0	0		
417	$IC_3H_7+O=CH_3COCH_3+H$	4.82E+13	0	0		
418	$IC_3H_7+O=CH_3CHO+CH_3$	4.82E+13	0	0		
419	$NC_3H_7=CH_3+C_2H_4$	9.97E+40	-8.6	41430		
420	$NC_3H_7=H+C_3H_6$	8.78E+39	-8.1	46580		
421	$NC_3H_7+O_2=C_3H_6+HO_2$	3.00E-19	0	3000		
422	$C_2H_5CHO+NC_3H_7=C_2H_5CO+C_3H_8$	1.70E+12	0	8440		
423	$C_2H_5CHO+IC_3H_7=C_2H_5CO+C_3H_8$	1.70E+12	0	8440		
424	$C_2H_5CHO+C_3H_5-A=C_2H_5CO+C_3H_6$	1.70E+12	0	8440		
425	$C_3H_5-A+H(+M)=C_3H_6(+M)$	2.00E+14	0	0		
	H <sub>2</sub>	Enhanced	by	2.00E+00		
	H <sub>2</sub> O	Enhanced	by	6.00E+00		
	CH <sub>4</sub>	Enhanced	by	2.00E+00		
	CO	Enhanced	by	1.50E+00		
	CO <sub>2</sub>	Enhanced	by	2.00E+00		
	C <sub>2</sub> H <sub>6</sub>	Enhanced	by	3.00E+00		
	Low pressure	limit:		1.33E+60	-1.20E+01	5.97E+03
	TROE centering:		2.00E-02	1.10E+03	1.10E+03	6.86E+03
426	$C_2H_3+CH_3(+M)=C_3H_6(+M)$	2.50E+13	0	0		
	H <sub>2</sub>	Enhanced	by	2.00E+00		
	H <sub>2</sub> O	Enhanced	by	6.00E+00		
	CH <sub>4</sub>	Enhanced	by	2.00E+00		
	CO	Enhanced	by	1.50E+00		

	CO2	Enhanced	by	2.00E+00		
	C2H6	Enhanced	by	3.00E+00		
	C2H4	Enhanced	by	3.00E+00		
	Low	pressure	limit:	4.27E+58	-1.19E+01	9.77E+03
	TROE	centering:	1.75E-01	1.34E+03	6.00E+04	1.01E+04
427	C3H6=C3H5-S+H	7.71E+69	-16.1	140000		
428	C3H6=C3H5-T+H	5.62E+71	-16.6	139300		
429	C3H6+O=C2H5+HCO	1.58E+07	1.8	-1216		
430	C3H6+O=CH2CO+CH3+H	2.50E+07	1.8	76		
431	C3H6+O=CH3CHCO+2H	2.50E+07	1.8	76		
432	C3H6+O=C3H5-A+OH	5.24E+11	0.7	5884		
433	C3H6+O=C3H5-S+OH	1.20E+11	0.7	8959		
434	C3H6+O=C3H5-T+OH	6.03E+10	0.7	7632		
435	C3H6+OH=C3H5-A+H2O	3.12E+06	2	-298		
436	C3H6+OH=C3H5-S+H2O	2.11E+06	2	2778		
437	C3H6+OH=C3H5-T+H2O	1.11E+06	2	1451		
438	C3H6+HO2=C3H5-A+H2O2	2.70E+04	2.5	12340		
439	C3H6+HO2=C3H5-S+H2O2	1.80E+04	2.5	27620		
440	C3H6+HO2=C3H5-T+H2O2	9.00E+03	2.5	23590		
441	C3H6+H=C2H4+CH3	2.60E+08	1.5	2007		
442	C3H6+H=C3H5-A+H2	1.73E+05	2.5	2490		
443	C3H6+H=C3H5-T+H2	4.00E+05	2.5	9790		
444	C3H6+H=C3H5-S+H2	8.04E+05	2.5	12283		
445	C3H6+O2=C3H5-A+HO2	4.00E+12	0	39900		
446	C3H6+O2=C3H5-S+HO2	2.00E+12	0	62900		
447	C3H6+O2=C3H5-T+HO2	1.40E+12	0	60700		
448	C3H6+CH3=C3H5-A+CH4	1.00E+12	0	7989		
449	C3H6+CH3=C3H5-S+CH4	1.35E+00	3.5	12850		
450	C3H6+CH3=C3H5-T+CH4	8.40E-01	3.5	11660		
451	C3H6+C2H5=C3H5-A+C2H6	1.00E+11	0	9800		
452	C3H6+CH3CO3=C3H5-A+CH3CO3H	3.24E+11	0	14900		
453	C3H6+CH3O2=C3H5-A+CH3O2H	3.24E+11	0	14900		
454	C3H6+HO2=C3H6O1-2+OH	1.29E+12	0	14900		
455	C3H6+C2H5O2=C3H5-A+C2H5O2H	3.24E+11	0	14900		
456	C3H6+NC3H7O2=C3H5-A+NC3H7O2H	3.24E+11	0	14900		
457	C3H6+IC3H7O2=C3H5-A+IC3H7O2H	3.24E+11	0	14900		
458	C3H6+OH=C3H6OH	9.93E+11	0	-960		
459	C3H6OH+O2=HOC3H6O2	1.20E+11	0	-1100		
460	HOC3H6O2=CH3CHO+CH2O+OH	1.25E+10	0	18900		
461	C3H5-A+H=C3H4-A+H2	1.80E+13	0	0		
462	C3H5-A+O=C2H3CHO+H	6.00E+13	0	0		
463	C3H5-A+OH=C2H3CHO+2H	1.60E+20	-1.6	26330		
464	C3H5-A+OH=C3H4-A+H2O	6.00E+12	0	0		
465	C3H5-A+O2=C3H4-A+HO2	2.18E+21	-2.9	30755		
466	C3H5-A+O2=CH3CO+CH2O	7.14E+15	-1.2	21046		
467	C3H5-A+O2=C2H3CHO+OH	2.47E+13	-0.5	23017		

468	$C_3H_5-A+HCO=C_3H_6+CO$	6.00E+13	0	0		
469	$C_3H_5-A+CH_3(+M)=C_4H_8-1(+M)$	1.00E+14	-0.3	-262.3		
	H2	Enhanced	by	2.00E+00		
	H2O	Enhanced	by	6.00E+00		
	CH4	Enhanced	by	2.00E+00		
	CO	Enhanced	by	1.50E+00		
	CO2	Enhanced	by	2.00E+00		
	C2H6	Enhanced	by	3.00E+00		
	Low	pressure	limit:	3.91E+60	-1.28E+01	6.25E+03
	TROE	centering:	1.04E-01	1.61E+03	6.00E+04	6.12E+03
470	$C_3H_5-A+CH_3=C_3H_4-A+CH_4$	3.00E+12	-0.3	-131		
471	$C_3H_5-A=C_3H_5-T$	4.86E+53	-12.8	75883		
472	$C_3H_5-A=C_3H_5-S$	9.70E+48	-11.7	73700		
473	$C_2H_2+CH_3=C_3H_5-A$	1.04E+51	-11.9	36476		
474	$C_3H_5-A+CH_3O_2=C_3H_5O+CH_3O$	7.00E+12	0	-1000		
475	$C_3H_5-A+C_2H_5=C_2H_6+C_3H_4-A$	4.00E+11	0	0		
476	$C_3H_5-A+C_2H_5=C_2H_4+C_3H_6$	4.00E+11	0	0		
477	$C_3H_5-A+C_2H_3=C_2H_4+C_3H_4-A$	1.00E+12	0	0		
478	$2C_3H_5-A=C_3H_4-A+C_3H_6$	8.43E+10	0	-262		
479	$C_3H_5-A+C_2H_2=C*CCJC*C$	1.00E+12	0	6883.4		
480	$C_3H_5-A+C_2H_3=C_5H_6+2H$	1.60E+35	-14	61137.7		
481	$C_3H_5-A+C_3H_3=C_6H_6+2H$	5.60E+20	-2.5	1696.9		
482	$C_3H_5-A+HO_2=C_3H_5O+OH$	7.00E+12	0	-1000		
483	$C_2H_2+CH_3=C_3H_5-S$	2.40E+38	-8.2	17100		
484	$C_3H_5-S+H=C_3H_4-P+H_2$	3.34E+12	0	0		
485	$C_3H_5-S+O=C_2H_4+HCO$	6.00E+13	0	0		
486	$C_3H_5-S+OH=C_2H_4+HCO+H$	5.00E+12	0	0		
487	$C_3H_5-S+O_2=CH_3CHO+HCO$	1.00E+11	0	0		
488	$C_3H_5-S+HO_2=C_2H_4+HCO+OH$	2.00E+13	0	0		
489	$C_3H_5-S+HCO=C_3H_6+CO$	9.00E+13	0	0		
490	$C_3H_5-S+CH_3=C_3H_4-P+CH_4$	1.00E+11	0	0		
491	$C_2H_2+CH_3=C_3H_5-T$	7.31E+25	-5.1	21150		
492	$C_3H_5-T=C_3H_5-S$	5.10E+52	-13.4	57200		
493	$C_3H_5-T+H=C_3H_4-P+H_2$	3.34E+12	0	0		
494	$C_3H_5-T+O=CH_3+CH_2CO$	6.00E+13	0	0		
495	$C_3H_5-T+OH=CH_3+CH_2CO+H$	5.00E+12	0	0		
496	$C_3H_5-T+O_2=CH_3CO+CH_2O$	1.00E+11	0	0		
497	$C_3H_5-T+HO_2=CH_3+CH_2CO+OH$	2.00E+13	0	0		
498	$C_3H_5-T+HCO=C_3H_6+CO$	9.00E+13	0	0		
499	$C_3H_5-T+CH_3=C_3H_4-P+CH_4$	1.00E+11	0	0		
500	$C_2H_2+CH_3=C_3H_4-A+H$	9.20E+10	0.5	23950		
501	$C_3H_4-A+H=C_3H_3+H_2$	1.30E+06	2	5500		
502	$C_3H_4-A+H=C_3H_5-S$	2.60E+31	-6.2	18700		
503	$C_3H_4-A+H=C_3H_5-T$	6.98E+44	-9.7	14032		
504	$C_3H_4-A+H=C_3H_5-A$	7.34E+54	-12.1	26187		
505	$C_3H_4-A+O=C_2H_4+CO$	2.00E+07	1.8	1000		

506	C3H4-A+OH=C3H3+H2O	5.30E+06	2	2000			
507	C3H4-A+CH3=C3H3+CH4	1.30E+12	0	7700			
508	C3H4-A+C2H=C2H2+C3H3	1.00E+13	0	0			
509	2C3H4-A=C3H5-A+C3H3	5.00E+14	0	64746.7			
510	C3H4-A+C3H5-A=C3H3+C3H6	2.00E+11	0	7700			
511	C3H4-A+C3H3=C6H6+H	1.40E+12	0	9990.4			
512	C3H4-P=CC3H4	3.92E+40	-8.7	68706			
513	C3H4-P=C3H4-A	3.12E+58	-13.1	92680			
514	C3H4-P+H=C3H4-A+H	1.93E+18	-1	11523			
515	C3H4-P+H=C3H5-T	9.62E+47	-10.6	15910			
516	C3H4-P+H=C3H5-S	1.00E+34	-6.9	8900			
517	C3H4-P+H=C3H5-A	9.02E+59	-13.9	33953			
518	C3H4-P+H=C3H3+H2	1.30E+06	2	5500			
519	C3H4-P+C3H3=C3H4-A+C3H3	6.14E+06	1.7	10450			
520	C3H4-P+O=HCCO+CH3	7.30E+12	0	2250			
521	C3H4-P+O=C2H4+CO	1.00E+13	0	2250			
522	C3H4-P+OH=C3H3+H2O	1.00E+06	2	100			
523	C3H4-P+C2H=C2H2+C3H3	1.00E+13	0	0			
524	C3H4-P+CH3=C3H3+CH4	1.80E+12	0	7700			
525	C2H2+CH3=C3H4-P+H	2.51E+11	0.6	15453			
526	C3H4-P+C2H3=C3H3+C2H4	1.00E+12	0	7700			
527	C3H4-P+C3H5-A=C3H3+C3H6	1.00E+12	0	7700			
528	CC3H4=C3H4-A	4.33E+41	-8.9	50475			
529	C3H3+H=C3H4-P	6.45E+13	0.1	-31.1			
530	C3H3+H=C3H4-A	2.00E+13	0.2	-172.1			
531	C3H3+H=C3H2+H2	1.00E+13	0	1000			
532	C3H3+O=CH2O+C2H	2.00E+13	0	0			
533	C3H3+OH=C3H2+H2O	2.00E+13	0	0			
534	C3H3+O2=CH2CO+HCO	3.00E+10	0	2868			
535	C3H3+HO2=OH+CO+C2H3	8.00E+11	0	0			
536	C3H3+HO2=C3H4-A+O2	3.00E+11	0	0			
537	C3H3+HO2=C3H4-P+O2	2.50E+12	0	0			
538	C3H3+HCO=C3H4-A+CO	2.50E+13	0	0			
539	C3H3+HCO=C3H4-P+CO	2.50E+13	0	0			
540	C3H3+HCCO=C4H4+CO	2.50E+13	0	0			
541	C3H3+CH=C4H3-I+H	5.00E+13	0	0			
542	C3H3+CH2=C4H4+H	5.00E+13	0	0			
543	C3H3+CH3(+M)=C4H612(+M)	1.50E+12	0	0			
	H2	Enhanced	by	2.00E+00			
	H2O	Enhanced	by	6.00E+00			
	CH4	Enhanced	by	2.00E+00			
	CO	Enhanced	by	1.50E+00			
	CO2	Enhanced	by	2.00E+00			
	C2H6	Enhanced	by	3.00E+00			
	Low	pressure	limit:	2.60E+57	-1.19E+01	9.77E+03	
	TROE	centering:		1.75E-01	1.34E+03	6.00E+04	9.77E+03

544	2C3H3=C6H5+H	2.02E+33	-6	15940		
545	2C3H3=C6H6	2.00E+12	0	0		
546	C2H5+C2H=C3H3+CH3	1.81E+13	0	0		
547	C3H2+H(+M)=C3H3(+M)	1.02E+13	0.3	279.6		
	Low	pressure	limit:	2.80E+30	-3.86E+00	3.32E+03
	TROE	centering:	7.82E-01	2.08E+02	2.66E+03	6.10E+03
	H2	Enhanced	by	2.00E+00		
	H2O	Enhanced	by	1.20E+01		
	CO2	Enhanced	by	3.60E+00		
	CO	Enhanced	by	1.75E+00		
	AR	Enhanced	by	7.00E-01		
	CH4	Enhanced	by	2.00E+00		
	C2H6	Enhanced	by	3.00E+00		
548	C3H2+O=C2H2+CO	6.80E+13	0	0		
549	C3H2+OH=HCO+C2H2	6.80E+13	0	0		
550	C3H2+O2=HCCO+H+CO	2.00E+12	0	1000		
551	C3H2+CH=C4H2+H	5.00E+13	0	0		
552	C3H2+CH2=C4H3-N+H	5.00E+13	0	0		
553	C3H2+CH3=C4H4+H	5.00E+12	0	0		
554	C3H2+HCCO=C4H3-N+CO	1.00E+13	0	0		
555	C3H2+C3H3=C6H5	7.00E+12	0	0		
556	C3H2+O2=HCO+HCCO	5.00E+13	0	0		
557	CH3CHCO+OH=C2H5+CO2	1.73E+12	0	-1010		
558	CH3CHCO+OH=SC2H4OH+CO	2.00E+12	0	-1010		
559	CH3CHCO+H=C2H5+CO	4.40E+12	0	1459		
560	CH3CHCO+O=CH3CHO+CO	3.20E+12	0	-437		
561	NC3H7+HO2=NC3H7O+OH	7.00E+12	0	-1000		
562	IC3H7+HO2=IC3H7O+OH	7.00E+12	0	-1000		
563	CH3O2+NC3H7=CH3O+NC3H7O	7.00E+12	0	-1000		
564	CH3O2+IC3H7=CH3O+IC3H7O	7.00E+12	0	-1000		
565	NC3H7+O2=NC3H7O2	4.52E+12	0	0		
566	IC3H7+O2=IC3H7O2	7.54E+12	0	0		
567	NC3H7O2+CH2O=NC3H7O2H+HCO	5.60E+12	0	13600		
568	NC3H7O2+CH3CHO=NC3H7O2H+CH3CO	2.80E+12	0	13600		
569	IC3H7O2+CH2O=IC3H7O2H+HCO	5.60E+12	0	13600		
570	IC3H7O2+CH3CHO=IC3H7O2H+CH3CO	2.80E+12	0	13600		
571	NC3H7O2+HO2=NC3H7O2H+O2	1.75E+10	0	-3275		
572	IC3H7O2+HO2=IC3H7O2H+O2	1.75E+10	0	-3275		
573	C2H4+NC3H7O2=C2H3+NC3H7O2H	1.13E+13	0	30430		
574	C2H4+IC3H7O2=C2H3+IC3H7O2H	1.13E+13	0	30430		
575	CH3OH+NC3H7O2=CH2OH+NC3H7O2H	6.30E+12	0	19360		
576	CH3OH+IC3H7O2=CH2OH+IC3H7O2H	6.30E+12	0	19360		
577	C2H3CHO+NC3H7O2=C2H3CO+NC3H7O2H	2.80E+12	0	13600		
578	C2H3CHO+IC3H7O2=C2H3CO+IC3H7O2H	2.80E+12	0	13600		
579	CH4+NC3H7O2=CH3+NC3H7O2H	1.12E+13	0	24640		
580	CH4+IC3H7O2=CH3+IC3H7O2H	1.12E+13	0	24640		

581	NC3H7O2+CH3O2=NC3H7O+CH3O+O2	1.40E+16	-1.6	1860		
582	IC3H7O2+CH3O2=IC3H7O+CH3O+O2	1.40E+16	-1.6	1860		
583	H2+NC3H7O2=H+NC3H7O2H	3.01E+13	0	26030		
584	H2+IC3H7O2=H+IC3H7O2H	3.01E+13	0	26030		
585	IC3H7O2+C2H6=IC3H7O2H+C2H5	1.70E+13	0	20460		
586	NC3H7O2+C2H6=NC3H7O2H+C2H5	1.70E+13	0	20460		
587	IC3H7O2+C2H5CHO=IC3H7O2H+C2H5CO	2.00E+11	0	9500		
588	NC3H7O2+C2H5CHO=NC3H7O2H+C2H5CO	2.00E+11	0	9500		
589	IC3H7O2+CH3CO3=IC3H7O+CH3CO2+O2	1.40E+16	-1.6	1860		
590	NC3H7O2+CH3CO3=NC3H7O+CH3CO2+O2	1.40E+16	-1.6	1860		
591	IC3H7O2+C2H5O2=IC3H7O+C2H5O+O2	1.40E+16	-1.6	1860		
592	NC3H7O2+C2H5O2=NC3H7O+C2H5O+O2	1.40E+16	-1.6	1860		
593	2IC3H7O2=O2+2IC3H7O	1.40E+16	-1.6	1860		
594	2NC3H7O2=O2+2NC3H7O	1.40E+16	-1.6	1860		
595	IC3H7O2+NC3H7O2=IC3H7O+NC3H7O+O2	1.40E+16	-1.6	1860		
596	IC3H7O2+CH3=IC3H7O+CH3O	7.00E+12	0	-1000		
597	IC3H7O2+C2H5=IC3H7O+C2H5O	7.00E+12	0	-1000		
598	IC3H7O2+IC3H7=2IC3H7O	7.00E+12	0	-1000		
599	IC3H7O2+NC3H7=IC3H7O+NC3H7O	7.00E+12	0	-1000		
600	IC3H7O2+C3H5-A=IC3H7O+C3H5O	7.00E+12	0	-1000		
601	NC3H7O2+CH3=NC3H7O+CH3O	7.00E+12	0	-1000		
602	NC3H7O2+C2H5=NC3H7O+C2H5O	7.00E+12	0	-1000		
603	NC3H7O2+IC3H7=NC3H7O+IC3H7O	7.00E+12	0	-1000		
604	NC3H7O2+NC3H7=2NC3H7O	7.00E+12	0	-1000		
605	NC3H7O2+C3H5-A=NC3H7O+C3H5O	7.00E+12	0	-1000		
606	NC3H7O2H=NC3H7O+OH	1.50E+16	0	42500		
607	IC3H7O2H=IC3H7O+OH	9.45E+15	0	42600		
608	C2H5+CH2O=NC3H7O	1.00E+11	0	3496		
609	C2H5CHO+H=NC3H7O	4.00E+12	0	6260		
610	CH3+CH3CHO=IC3H7O	1.00E+11	0	9256		
611	CH3COCH3+H=IC3H7O	2.00E+12	0	7270		
612	IC3H7O+O2=CH3COCH3+HO2	9.09E+09	0	390		
613	NC3H7O2=C3H6OOH1-2	6.00E+11	0	26850		
614	NC3H7O2=C3H6OOH1-3	1.12E+11	0	24400		
615	IC3H7O2=C3H6OOH2-1	1.80E+12	0	29400		
	Reverse	Arrhenius	coefficients:	1.12E+10	0.1	11810
616	C3H6OOH1-2=C3H6O1-2+OH	6.00E+11	0	22000		
617	C3H6OOH1-3=C3H6O1-3+OH	7.50E+10	0	15250		
618	C3H6OOH2-1=C3H6O1-2+OH	6.00E+11	0	22000		
619	C3H6+HO2=C3H6OOH1-2	1.00E+11	0	11000		
620	C3H6+HO2=C3H6OOH2-1	1.00E+11	0	11750		
621	C3H6OOH1-3=OH+CH2O+C2H4	3.04E+15	-0.8	27400		
622	C3H6OOH1-2=C2H4+CH2O+OH	1.31E+33	-7	48120		
623	C3H6OOH1-2+O2=C3H6OOH1-2O2	5.00E+12	0	0		
624	C3H6OOH1-3+O2=C3H6OOH1-3O2	4.52E+12	0	0		
625	C3H6OOH2-1+O2=C3H6OOH2-1O2	4.52E+12	0	0		

626	C3H6OOH1-2O2=C3KET12+OH	6.00E+11	0	26400		
627	C3H6OOH1-3O2=C3KET13+OH	7.50E+10	0	21400		
628	C3H6OOH2-1O2=C3KET21+OH	3.00E+11	0	23850		
	Reverse	Arrhenius	coefficients:	1.40E+03	1.8	49750
629	C3H6OOH2-1O2=C3H51-2	3OOH	1.12E+11	0	24400	
630	C3H6OOH1-2O2=C3H51-2	3OOH	9.00E+11	0	29400	
631	C3H51-2	3OOH=AC3H5OO H+HO2	2.56E+13	-0.5	17770	
632	C3H6OOH1-3O2=C3H52-1	3OOH	6.00E+11	0	26850	
633	C3H52-1	3OOH=AC3H5OO H+HO2	1.15E+14	-0.6	17250	
634	C3KET12=CH3CHO+HCO+OH	9.45E+15	0	43000		
635	C3KET13=CH2O+CH2CHO+OH	1.00E+16	0	43000		
636	C3KET21=CH2O+CH3CO+OH	1.00E+16	0	43000		
637	C3H5O+OH=AC3H5OOH	2.00E+13	0	0		
638	C3H5O=C2H3CHO+H	1.00E+14	0	29100		
639	C3H5O+O2=C2H3CHO+HO2	1.00E+12	0	6000		
640	C3H6O1-2=C2H4+CH2O	6.00E+14	0	60000		
641	C3H6O1-2+OH=CH2O+C2H3+H2O	5.00E+12	0	0		
642	C3H6O1-2+H=CH2O+C2H3+H2	2.63E+07	2	5000		
643	C3H6O1-2+O=CH2O+C2H3+OH	8.43E+13	0	5200		
644	C3H6O1-2+HO2=CH2O+C2H3+H2O2	1.00E+13	0	15000		
645	C3H6O1-2+CH3O2=CH2O+C2H3+CH3O2H	1.00E+13	0	19000		
646	C3H6O1-2+CH3=CH2O+C2H3+CH4	2.00E+11	0	10000		
647	C3H6O1-3=C2H4+CH2O	6.00E+14	0	60000		
648	C3H6O1-3+OH=CH2O+C2H3+H2O	5.00E+12	0	0		
649	C3H6O1-3+O=CH2O+C2H3+OH	8.43E+13	0	5200		
650	C3H6O1-3+H=CH2O+C2H3+H2	2.63E+07	2	5000		
651	C3H6O1-3+CH3O2=CH2O+C2H3+CH3O2H	1.00E+13	0	19000		
652	C3H6O1-3+HO2=CH2O+C2H3+H2O2	1.00E+13	0	15000		
653	C3H6O1-3+CH3=CH2O+C2H3+CH4	2.00E+11	0	10000		
654	IC3H7O2=C3H6+HO2	1.01E+43	-9.4	41490		
655	NC3H7O2=C3H6+HO2	5.04E+38	-8.1	40490		
656	C4H10(+M)=2C2H5(+M)	2.72E+15	0	75610		
	Low	pressure	limit:	4.72E+18	0.00E+00	4.96E+04
	TROE	centering:	7.20E-01	1.50E+03	1.00E-10	1.00E+10
657	C4H10(+M)=NC3H7+CH3(+M)	4.28E+14	0	69900		
	Low	pressure	limit:	5.34E+17	0.00E+00	4.30E+04
	TROE	centering:	7.20E-01	1.50E+03	1.00E-10	1.00E+10
658	PC4H9+H=C4H10	3.61E+13	0	0		
659	SC4H9+H=C4H10	3.61E+13	0	0		
660	C4H10+O2=PC4H9+HO2	6.00E+13	0	52340		
661	C4H10+O2=SC4H9+HO2	4.00E+13	0	49800		
662	C4H10+C3H5-A=PC4H9+C3H6	7.94E+11	0	20500		
663	C4H10+C3H5-A=SC4H9+C3H6	3.16E+11	0	16400		
664	C4H10+C2H5=PC4H9+C2H6	1.58E+11	0	12300		
665	C4H10+C2H5=SC4H9+C2H6	1.00E+11	0	10400		

666	C4H10+C2H3=PC4H9+C2H4	1.00E+12	0	18000		
667	C4H10+C2H3=SC4H9+C2H4	8.00E+11	0	16800		
668	C4H10+CH3=PC4H9+CH4	9.04E-01	3.6	7154		
669	C4H10+CH3=SC4H9+CH4	3.02E+00	3.5	5481		
670	C4H10+H=PC4H9+H2	1.88E+05	2.8	6280		
671	C4H10+H=SC4H9+H2	2.60E+06	2.4	4471		
672	C4H10+OH=PC4H9+H2O	1.05E+10	1	1586		
673	C4H10+OH=SC4H9+H2O	9.34E+07	1.6	-35		
674	C4H10+O=PC4H9+OH	1.13E+14	0	7850		
675	C4H10+O=SC4H9+OH	5.62E+13	0	5200		
676	C4H10+HO2=PC4H9+H2O2	8.10E+04	2.5	16690		
677	C4H10+HO2=SC4H9+H2O2	1.18E+05	2.5	14860		
678	C4H10+CH3O=PC4H9+CH3OH	3.00E+11	0	7000		
679	C4H10+CH3O=SC4H9+CH3OH	6.00E+11	0	7000		
680	C4H10+C2H5O=PC4H9+C2H5OH	3.00E+11	0	7000		
681	C4H10+C2H5O=SC4H9+C2H5OH	6.00E+11	0	7000		
682	C4H10+PC4H9=SC4H9+C4H10	1.00E+11	0	10400		
683	C4H10+CH3CO3=PC4H9+CH3CO3H	1.70E+13	0	20460		
684	C4H10+CH3CO3=SC4H9+CH3CO3H	1.12E+13	0	17700		
685	C4H10+O2CHO=PC4H9+HO2CHO	1.68E+13	0	20440		
686	C4H10+O2CHO=SC4H9+HO2CHO	1.12E+13	0	17690		
687	CH3O2+C4H10=CH3O2H+PC4H9	8.10E+04	2.5	16690		
688	CH3O2+C4H10=CH3O2H+SC4H9	1.18E+05	2.5	14860		
689	C2H5O2+C4H10=C2H5O2H+PC4H9	1.70E+13	0	20460		
690	C2H5O2+C4H10=C2H5O2H+SC4H9	1.12E+13	0	17700		
691	NC3H7O2+C4H10=NC3H7O2H+PC4H9	1.70E+13	0	20460		
692	NC3H7O2+C4H10=NC3H7O2H+SC4H9	1.12E+13	0	17700		
693	IC3H7O2+C4H10=IC3H7O2H+PC4H9	1.70E+13	0	20460		
694	IC3H7O2+C4H10=IC3H7O2H+SC4H9	1.12E+13	0	17700		
695	PC4H9O2+C3H8=PC4H9O2H+NC3H7	1.70E+13	0	20460		
696	PC4H9O2+C3H8=PC4H9O2H+IC3H7	2.00E+12	0	17000		
697	PC4H9O2+C4H10=PC4H9O2H+PC4H9	1.70E+13	0	20460		
698	PC4H9O2+C4H10=PC4H9O2H+SC4H9	1.12E+13	0	17700		
699	C2H5+C2H4=PC4H9	1.32E+04	2.5	6130		
700	C3H6+CH3=SC4H9	1.76E+04	2.5	6130		
701	C4H8-1+H=PC4H9	2.50E+11	0.5	2620		
702	C4H8-2+H=SC4H9	2.50E+11	0.5	2620		
703	C4H8-1+H=SC4H9	4.24E+11	0.5	1230		
704	PC4H9+O2=C4H8-1+HO2	2.00E-18	0	5000		
705	SC4H9+O2=C4H8-1+HO2	2.00E-18	0	5000		
706	SC4H9+O2=C4H8-2+HO2	2.00E-18	0	5000		
707	C2H3+C2H5=C4H8-1	9.00E+12	0	0		
708	H+C4H71-3=C4H8-1	5.00E+13	0	0		
709	C4H8-1+O2=C4H71-3+HO2	2.00E+13	0	37190		
710	C4H8-1+H=C4H71-1+H2	7.81E+05	2.5	12290		
711	C4H8-1+H=C4H71-2+H2	3.90E+05	2.5	5821		



712	C4H8-1+H=C4H71-3+H2	3.38E+05	2.4	207		
713	C4H8-1+H=C4H71-4+H2	6.65E+05	2.5	6756		
714	C4H8-1+OH=C4H71-1+H2O	2.14E+06	2	2778		
715	C4H8-1+OH=C4H71-2+H2O	2.22E+06	2	1451		
716	C4H8-1+OH=C4H71-3+H2O	2.76E+04	2.6	-1919		
717	C4H8-1+OH=C4H71-4+H2O	5.27E+09	1	1586		
718	C4H8-1+CH3=C4H71-3+CH4	3.69E+00	3.3	4002		
719	C4H8-1+CH3=C4H71-4+CH4	4.52E-01	3.6	7154		
720	C4H8-1+HO2=C4H71-3+H2O2	4.82E+03	2.5	10530		
721	C4H8-1+HO2=C4H71-4+H2O2	2.38E+03	2.5	16490		
722	C4H8-1+CH3O2=C4H71-3+CH3O2H	4.82E+03	2.5	10530		
723	C4H8-1+CH3O2=C4H71-4+CH3O2H	2.38E+03	2.5	16490		
724	C4H8-1+CH3O=C4H71-3+CH3OH	4.00E+01	2.9	8609		
725	C4H8-1+CH3O=C4H71-4+CH3OH	2.17E+11	0	6458		
726	C4H8-1+CH3CO3=C4H71-3+CH3CO3H	1.00E+11	0	8000		
727	C4H8-1+C3H5-A=C4H71-3+C3H6	7.90E+10	0	12400		
728	2C4H71-3=C4H8-1+C4H6	1.60E+12	0	0		
729	C4H8-1+C2H5O2=C4H71-3+C2H5O2H	1.40E+12	0	14900		
730	C4H8-1+NC3H7O2=C4H71-3+NC3H7O2H	1.40E+12	0	14900		
731	C4H8-1+IC3H7O2=C4H71-3+IC3H7O2H	1.40E+12	0	14900		
732	C4H8-1+PC4H9O2=C4H71-3+PC4H9O2H	1.40E+12	0	14900		
733	H+C4H71-3=C4H8-2	5.00E+13	0	0		
734	C4H8-2+O2=C4H71-3+HO2	4.00E+13	0	39390		
735	C4H8-2+H=C4H71-3+H2	3.46E+05	2.5	2492		
736	C4H8-2+OH=C4H71-3+H2O	6.24E+06	2	-298		
737	C4H8-2+CH3=C4H71-3+CH4	4.42E+00	3.5	5675		
738	C4H8-2+HO2=C4H71-3+H2O2	1.93E+04	2.6	13910		
739	C4H8-2+CH3O2=C4H71-3+CH3O2H	1.93E+04	2.6	13910		
740	C4H8-2+CH3O=C4H71-3+CH3OH	1.80E+01	3	11990		
741	C4H8-2+C2H5O2=C4H71-3+C2H5O2H	3.20E+12	0	14900		
742	C4H8-2+NC3H7O2=C4H71-3+NC3H7O2H	3.20E+12	0	14900		
743	C4H8-2+IC3H7O2=C4H71-3+IC3H7O2H	3.20E+12	0	14900		
744	C4H8-2+PC4H9O2=C4H71-3+PC4H9O2H	3.20E+12	0	14900		
745	C4H8-1+OH=C4H8OH-1	4.75E+12	0	-782		
746	C4H8OH-1+O2=C4H8OH-1O2	2.00E+12	0	0		
747	C4H8OH-1O2=C2H5CHO+CH2O+OH	1.00E+16	0	25000		
748	C2H2+C2H5=C4H71-1	2.00E+11	0	7800		
749	C3H4-A+CH3=C4H71-2	2.00E+11	0	7800		
750	C2H4+C2H3=C4H71-4	2.00E+11	0	7800		
751	C4H6+H=C4H71-3	4.00E+13	0	1300		
752	C4H71-3+C2H5=C4H8-1+C2H4	2.59E+12	0	-131		
753	C4H71-3+CH3O=C4H8-1+CH2O	2.41E+13	0	0		
754	C4H71-3+O=C2H3CHO+CH3	6.03E+13	0	0		
755	C4H71-3+HO2=C4H7O+OH	9.64E+12	0	0		
756	C4H71-3+CH3O2=C4H7O+CH3O	9.64E+12	0	0		
757	C3H5-A+C4H71-3=C3H6+C4H6	6.31E+12	0	0		

758	$C_4H_7I-3+O_2=C_4H_6+HO_2$	1.00E+09	0	0		
759	$H+C_4H_7I-3=C_4H_6+H_2$	3.16E+13	0	0		
760	$C_2H_5+C_4H_7I-3=C_4H_6+C_2H_6$	3.98E+12	0	0		
761	$C_2H_3+C_4H_7I-3=C_2H_4+C_4H_6$	3.98E+12	0	0		
762	$C_4H_7I-3+C_2H_5O_2=C_4H_7O+C_2H_5O$	3.80E+12	0	-1200		
763	$IC_3H_7O_2+C_4H_7I-3=IC_3H_7O+C_4H_7O$	3.80E+12	0	-1200		
764	$NC_3H_7O_2+C_4H_7I-3=NC_3H_7O+C_4H_7O$	3.80E+12	0	-1200		
765	$C_4H_7O=CH_3CHO+C_2H_3$	7.94E+14	0	19000		
766	$C_4H_7O=C_2H_3CHO+CH_3$	7.94E+14	0	19000		
767	$C_4H_6=C_4H_5-I+H$	5.70E+36	-6.3	112353		
768	$C_4H_6=C_4H_5-N+H$	5.30E+44	-8.6	123608		
769	$C_4H_6=C_4H_4+H_2$	2.50E+15	0	94700		
770	$C_4H_6+H=C_4H_5-N+H_2$	1.33E+06	2.5	12240		
771	$C_4H_6+H=C_4H_5-I+H_2$	6.65E+05	2.5	9240		
772	$C_4H_6+H=C_2H_4+C_2H_3$	5.45E+30	-4.5	21877		
773	$C_4H_6+H=C_3H_4-P+CH_3$	7.00E+12	0	2000		
774	$C_4H_6+H=C_3H_4-A+CH_3$	7.00E+12	0	2000		
775	$C_4H_6+O=C_4H_5-N+OH$	7.50E+06	1.9	3740		
776	$C_4H_6+O=C_4H_5-I+OH$	7.50E+06	1.9	3740		
777	$C_4H_6+O=CH_3CHCHCO+H$	1.50E+08	1.4	-860		
778	$C_4H_6+O=CH_2CHCHCHO+H$	4.50E+08	1.4	-860		
779	$C_4H_6+OH=C_4H_5-N+H_2O$	6.20E+06	2	3430		
780	$C_4H_6+OH=C_4H_5-I+H_2O$	3.10E+06	2	430		
781	$C_4H_6+HO_2=C_2H_3CHOCH_2+OH$	4.80E+12	0	14000		
782	$C_4H_6+CH_3=C_4H_5-N+CH_4$	2.00E+14	0	22800		
783	$C_4H_6+CH_3=C_4H_5-I+CH_4$	1.00E+14	0	19800		
784	$C_4H_6+C_2H_3=C_4H_5-N+C_2H_4$	5.00E+13	0	22800		
785	$C_4H_6+C_2H_3=C_4H_5-I+C_2H_4$	2.50E+13	0	19800		
786	$C_4H_6+C_3H_3=C_4H_5-N+C_3H_4-A$	1.00E+13	0	22500		
787	$C_4H_6+C_3H_3=C_4H_5-I+C_3H_4-A$	5.00E+12	0	19500		
788	$C_4H_6+C_3H_5-A=C_4H_5-N+C_3H_6$	1.00E+13	0	22500		
789	$C_4H_6+C_3H_5-A=C_4H_5-I+C_3H_6$	5.00E+12	0	19500		
790	$C_4H_6+C_2H_3=C_6H_6+H_2+H$	5.62E+11	0	3240		
791	$C_4H_7I-4=C_4H_6+H$	1.85E+48	-10.5	51770		
792	$C_4H_5-N=C_4H_5-I$	1.50E+67	-16.9	59100		
793	$C_4H_5-N+H=C_4H_5-I+H$	3.10E+26	-3.4	17423		
794	$C_4H_5-N+H=C_4H_4+H_2$	1.50E+13	0	0		
795	$C_4H_5-N+OH=C_4H_4+H_2O$	2.00E+12	0	0		
796	$C_4H_5-N+HCO=C_4H_6+CO$	5.00E+12	0	0		
797	$C_4H_5-N+HO_2=C_2H_3+CH_2CO+OH$	6.60E+12	0	0		
798	$C_4H_5-N+H_2O_2=C_4H_6+HO_2$	1.21E+10	0	-596		
799	$C_4H_5-N+HO_2=C_4H_6+O_2$	6.00E+11	0	0		
800	$C_4H_5-N+O_2=CH_2CHCHCHO+O$	3.00E+11	0.3	11		
801	$C_4H_5-N+O_2=HCO+C_2H_3CHO$	9.20E+16	-1.4	1010		
802	$C_4H_5-N+C_2H_2=C_6H_6+H$	1.60E+16	-1.3	5400		
803	$C_4H_5-N+C_2H_3=C_6H_6+H_2$	1.84E-13	7.1	-3611		

804	C4H5-I+H=C4H4+H2	3.00E+13	0	0		
805	C4H5-I+H=C3H3+CH3	2.00E+13	0	2000		
806	C4H5-I+OH=C4H4+H2O	4.00E+12	0	0		
807	C4H5-I+HCO=C4H6+CO	5.00E+12	0	0		
808	C4H5-I+HO2=C4H6+O2	6.00E+11	0	0		
809	C4H5-I+HO2=C2H3+CH2CO+OH	6.60E+12	0	0		
810	C4H5-I+H2O2=C4H6+HO2	1.21E+10	0	-596		
811	C4H5-I+O2=CH2CO+CH2CHO	2.16E+10	0	2500		
812	C4H5-2=C4H5-I	1.50E+67	-16.9	59100		
813	C4H5-2+H=C4H5-I+H	3.10E+26	-3.4	17423		
814	C4H5-2+HO2=OH+C2H2+CH3CO	8.00E+11	0	0		
815	C4H5-2+O2=CH3CO+CH2CO	2.16E+10	0	2500		
816	C4H5-2+C2H2=C6H6+H	5.00E+14	0	25000		
817	C4H5-2+C2H4=C5H6+CH3	5.00E+14	0	25000		
818	C4H6I2=C4H5-I+H	4.20E+15	0	92600		
819	C4H6I2+H=C4H6+H	2.00E+13	0	4000		
820	C4H6I2+H=C4H5-I+H2	1.70E+05	2.5	2490		
821	C4H6I2+H=C3H4-A+CH3	2.00E+13	0	2000		
822	C4H6I2+H=C3H4-P+CH3	2.00E+13	0	2000		
823	C4H6I2+CH3=C4H5-I+CH4	7.00E+13	0	18500		
824	C4H6I2+O=CH2CO+C2H4	1.20E+08	1.6	327		
825	C4H6I2+O=C4H5-I+OH	1.80E+11	0.7	5880		
826	C4H6I2+OH=C4H5-I+H2O	3.10E+06	2	-298		
827	C4H6I2=C4H6	3.00E+13	0	65000		
828	C4H6-2=C4H6	3.00E+13	0	65000		
829	C4H6-2=C4H6I2	3.00E+13	0	67000		
830	C4H6-2+H=C4H6I2+H	2.00E+13	0	4000		
831	C4H6-2+H=C4H5-2+H2	3.40E+05	2.5	2490		
832	C4H6-2+H=CH3+C3H4-P	2.60E+05	2.5	1000		
833	C4H6-2=H+C4H5-2	5.00E+15	0	87300		
834	C4H6-2+CH3=C4H5-2+CH4	1.40E+14	0	18500		
835	C2H3CHOCH2=C4H6O23	2.00E+14	0	50600		
836	C4H6O23=CH3CHCHCHO	1.95E+13	0	49400		
837	C4H6O23=C2H4+CH2CO	5.75E+15	0	69300		
838	C4H6O23=C2H2+C2H4O1-2	1.00E+16	0	75800		
839	CH3CHCHCHO=C3H6+CO	3.90E+14	0	69000		
840	CH3CHCHCHO+H=CH2CHCHCHO+H2	1.70E+05	2.5	2490		
841	CH3CHCHCHO+H=CH3CHCHCO+H2	1.00E+05	2.5	2490		
842	CH3CHCHCHO+H=CH3+C2H3CHO	4.00E+21	-2.4	11180		
843	CH3CHCHCHO+H=C3H6+HCO	4.00E+21	-2.4	11180		
844	CH3CHCHCHO+CH3=CH2CHCHCHO+CH4	2.10E+00	3.5	5675		
845	CH3CHCHCHO+CH3=CH3CHCHCO+CH4	1.10E+00	3.5	5675		
846	CH3CHCHCHO+C2H3=CH2CHCHCHO+C2H4	2.21E+00	3.5	4682		
847	CH3CHCHCHO+C2H3=CH3CHCHCO+C2H4	1.11E+00	3.5	4682		
848	CH3CHCHCO=C3H5-S+CO	1.00E+14	0	30000		
849	CH3CHCHCO+H=CH3CHCHCHO	1.00E+14	0	0		

850	CH <sub>2</sub> CHCHCHO=C <sub>3</sub> H <sub>5</sub> -A+CO	1.00E+14	0	25000		
851	CH <sub>2</sub> CHCHCHO+H=CH <sub>3</sub> CHCHCHO	1.00E+14	0	0		
852	C <sub>4</sub> H <sub>4</sub> +H=C <sub>4</sub> H <sub>5</sub> -N	1.30E+51	-11.9	16500		
853	C <sub>4</sub> H <sub>4</sub> +H=C <sub>4</sub> H <sub>5</sub> -I	4.90E+51	-11.9	17700		
854	C <sub>4</sub> H <sub>4</sub> +H=C <sub>4</sub> H <sub>3</sub> -N+H <sub>2</sub>	6.65E+05	2.5	12240		
855	C <sub>4</sub> H <sub>4</sub> +H=C <sub>4</sub> H <sub>3</sub> -I+H <sub>2</sub>	3.33E+05	2.5	9240		
856	C <sub>4</sub> H <sub>4</sub> +OH=C <sub>4</sub> H <sub>3</sub> -N+H <sub>2</sub> O	3.10E+07	2	3430		
857	C <sub>4</sub> H <sub>4</sub> +OH=C <sub>4</sub> H <sub>3</sub> -I+H <sub>2</sub> O	1.55E+07	2	430		
858	C <sub>4</sub> H <sub>4</sub> +O=C <sub>3</sub> H <sub>3</sub> +HCO	6.00E+08	1.4	-860		
859	C <sub>4</sub> H <sub>3</sub> -N=C <sub>4</sub> H <sub>3</sub> -I	4.10E+43	-9.5	53000		
860	C <sub>4</sub> H <sub>3</sub> -N+H=C <sub>4</sub> H <sub>3</sub> -I+H	2.50E+20	-1.7	10800		
861	C <sub>4</sub> H <sub>3</sub> -N+H=C <sub>2</sub> H <sub>2</sub> +H <sub>2</sub> CC	6.30E+25	-3.3	10014		
862	C <sub>4</sub> H <sub>3</sub> -N+H=C <sub>4</sub> H <sub>4</sub>	2.00E+47	-10.3	13070		
863	C <sub>4</sub> H <sub>3</sub> -N+H=C <sub>4</sub> H <sub>2</sub> +H <sub>2</sub>	3.00E+13	0	0		
864	C <sub>4</sub> H <sub>3</sub> -N+OH=C <sub>4</sub> H <sub>2</sub> +H <sub>2</sub> O	2.00E+12	0	0		
865	C <sub>4</sub> H <sub>3</sub> -N+C <sub>2</sub> H <sub>2</sub> =C <sub>6</sub> H <sub>5</sub>	9.60E+70	-17.8	31300		
866	C <sub>4</sub> H <sub>3</sub> -I+H=C <sub>2</sub> H <sub>2</sub> +H <sub>2</sub> CC	2.80E+23	-2.5	10780		
867	C <sub>4</sub> H <sub>3</sub> -I+H=C <sub>4</sub> H <sub>4</sub>	3.40E+43	-9	12120		
868	C <sub>4</sub> H <sub>3</sub> -I+H=C <sub>4</sub> H <sub>2</sub> +H <sub>2</sub>	6.00E+13	0	0		
869	C <sub>4</sub> H <sub>3</sub> -I+OH=C <sub>4</sub> H <sub>2</sub> +H <sub>2</sub> O	4.00E+12	0	0		
870	C <sub>4</sub> H <sub>3</sub> -I+O <sub>2</sub> =HCCO+CH <sub>2</sub> CO	7.86E+16	-1.8	0		
871	C <sub>4</sub> H <sub>3</sub> -I+CH <sub>2</sub> =C <sub>3</sub> H <sub>4</sub> -A+C <sub>2</sub> H	2.00E+13	0	0		
872	C <sub>4</sub> H <sub>3</sub> -I+CH <sub>3</sub> =C <sub>5</sub> H <sub>6</sub>	1.00E+12	0	0		
873	C <sub>4</sub> H <sub>2</sub> +H=C <sub>4</sub> H <sub>3</sub> -N	1.70E+49	-11.7	12804		
874	C <sub>4</sub> H <sub>2</sub> +H(+M)=C <sub>4</sub> H <sub>3</sub> -I(+M)	4.31E+10	1.2	1751.9		
	Low	pressure	limit:	2.30E+45	-8.10E+00	2.51E+03
	TROE	centering:	7.48E-02	1.00E+00	-4.22E+03	
	H <sub>2</sub>	Enhanced	by	2.00E+00		
	H <sub>2</sub> O	Enhanced	by	1.20E+01		
	CO <sub>2</sub>	Enhanced	by	3.60E+00		
	CO	Enhanced	by	1.75E+00		
	AR	Enhanced	by	7.00E-01		
	C <sub>2</sub> H <sub>6</sub>	Enhanced	by	3.00E+00		
875	C <sub>4</sub> H <sub>2</sub> +O=C <sub>3</sub> H <sub>2</sub> +CO	2.70E+13	0	1720		
876	C <sub>4</sub> H <sub>2</sub> +OH=H <sub>2</sub> C <sub>4</sub> O+H	6.60E+12	0	-410		
877	H <sub>2</sub> C <sub>4</sub> O+H=C <sub>2</sub> H <sub>2</sub> +HCCO	5.00E+13	0	3000		
878	H <sub>2</sub> C <sub>4</sub> O+OH=CH <sub>2</sub> CO+HCCO	1.00E+07	2	2000		
879	H <sub>2</sub> CC+H=C <sub>2</sub> H <sub>2</sub> +H	1.00E+14	0	0		
880	H <sub>2</sub> CC+OH=CH <sub>2</sub> CO+H	2.00E+13	0	0		
881	H <sub>2</sub> CC+O <sub>2</sub> =2HCO	1.00E+13	0	0		
882	H <sub>2</sub> CC+C <sub>2</sub> H <sub>2</sub> (+M)=C <sub>4</sub> H <sub>4</sub> (+M)	3.50E+05	2.1	-2400		
	H <sub>2</sub>	Enhanced	by	2.00E+00		
	H <sub>2</sub> O	Enhanced	by	6.00E+00		
	CH <sub>4</sub>	Enhanced	by	2.00E+00		
	CO	Enhanced	by	1.50E+00		
	CO <sub>2</sub>	Enhanced	by	2.00E+00		

	C2H6	Enhanced	by	3.00E+00		
	C2H2	Enhanced	by	3.00E+00		
	C2H4	Enhanced	by	3.00E+00		
	Low	pressure	limit:	1.40E+60	-1.26E+01	7.42E+03
	TROE	centering:	9.80E-01	5.60E+01	5.80E+02	4.16E+03
883	H2CC+C2H4=C4H6	1.00E+12	0	0		
884	C4H8O1-3+OH=CH2O+C3H5-A+H2O	5.00E+12	0	0		
885	C4H8O1-3+H=CH2O+C3H5-A+H2	5.00E+12	0	0		
886	C4H8O1-3+O=CH2O+C3H5-A+OH	5.00E+12	0	0		
887	C4H8O1-3+HO2=CH2O+C3H5-A+H2O2	1.00E+13	0	15000		
888	C4H8O1-3+CH3O2=CH2O+C3H5-A+CH3O2H	1.00E+13	0	19000		
889	C4H8O1-3+CH3=CH2O+C3H5-A+CH4	2.00E+11	0	10000		
890	C4H8O1-4+OH=CH2O+C3H5-A+H2O	5.00E+12	0	0		
891	C4H8O1-4+H=CH2O+C3H5-A+H2	5.00E+12	0	0		
892	C4H8O1-4+O=CH2O+C3H5-A+OH	5.00E+12	0	0		
893	C4H8O1-4+HO2=CH2O+C3H5-A+H2O2	1.00E+13	0	15000		
894	C4H8O1-4+CH3O2=CH2O+C3H5-A+CH3O2H	1.00E+13	0	19000		
895	C4H8O1-4+CH3=CH2O+C3H5-A+CH4	2.00E+11	0	10000		
896	PC4H9+O2=PC4H9O2	4.52E+12	0	0		
897	SC4H9+O2=SC4H9O2	7.54E+12	0	0		
898	IC3H7O2+PC4H9=IC3H7O+PC4H9O	7.00E+12	0	-1000		
899	IC3H7O2+SC4H9=IC3H7O+SC4H9O	7.00E+12	0	-1000		
900	NC3H7O2+PC4H9=NC3H7O+PC4H9O	7.00E+12	0	-1000		
901	NC3H7O2+SC4H9=NC3H7O+SC4H9O	7.00E+12	0	-1000		
902	2SC4H9O2=O2+2SC4H9O	1.40E+16	-1.6	1860		
903	SC4H9O2+NC3H7O2=SC4H9O+NC3H7O+O2	1.40E+16	-1.6	1860		
904	SC4H9O2+IC3H7O2=SC4H9O+IC3H7O+O2	1.40E+16	-1.6	1860		
905	SC4H9O2+C2H5O2=SC4H9O+C2H5O+O2	1.40E+16	-1.6	1860		
906	SC4H9O2+CH3O2=SC4H9O+CH3O+O2	1.40E+16	-1.6	1860		
907	SC4H9O2+CH3CO3=SC4H9O+CH3CO2+O2	1.40E+16	-1.6	1860		
908	PC4H9O2+HO2=PC4H9O+OH+O2	1.40E-14	-1.6	1860		
909	SC4H9O2+HO2=SC4H9O+OH+O2	1.40E-14	-1.6	1860		
910	H2+PC4H9O2=H+PC4H9O2H	3.01E+13	0	26030		
911	C2H6+PC4H9O2=C2H5+PC4H9O2H	1.70E+13	0	20460		
912	PC4H9O2+C2H5CHO=PC4H9O2H+C2H5CO	2.00E+11	0	9500		
913	SC4H9O2+CH3=SC4H9O+CH3O	7.00E+12	0	-1000		
914	SC4H9O2+C2H5=SC4H9O+C2H5O	7.00E+12	0	-1000		
915	SC4H9O2+IC3H7=SC4H9O+IC3H7O	7.00E+12	0	-1000		
916	SC4H9O2+NC3H7=SC4H9O+NC3H7O	7.00E+12	0	-1000		
917	SC4H9O2+PC4H9=SC4H9O+PC4H9O	7.00E+12	0	-1000		
918	SC4H9O2+SC4H9=2SC4H9O	7.00E+12	0	-1000		
919	SC4H9O2+C3H5-A=SC4H9O+C3H5O	7.00E+12	0	-1000		
920	PC4H9O2+CH2O=PC4H9O2H+HCO	5.60E+12	0	13600		
921	PC4H9O2+CH3CHO=PC4H9O2H+CH3CO	2.80E+12	0	13600		
922	PC4H9O2+HO2=PC4H9O2H+O2	1.75E+10	0	-3275		
923	C3H6+PC4H9O2=C3H5-A+PC4H9O2H	3.24E+11	0	14900		

924	$C_2H_4+PC_4H_9O_2=C_2H_3+PC_4H_9O_2H$	1.13E+13	0	30430		
925	$CH_3OH+PC_4H_9O_2=CH_2OH+PC_4H_9O_2H$	6.30E+12	0	19360		
926	$C_2H_3CHO+PC_4H_9O_2=C_2H_3CO+PC_4H_9O_2H$	2.80E+12	0	13600		
927	$CH_4+PC_4H_9O_2=CH_3+PC_4H_9O_2H$	1.12E+13	0	24640		
928	$C_4H_7-3+PC_4H_9O_2=C_4H_7O+PC_4H_9O$	7.00E+12	0	-1000		
929	$C_4H_7-3+SC_4H_9O_2=C_4H_7O+SC_4H_9O$	7.00E+12	0	-1000		
930	$H_2O_2+PC_4H_9O_2=HO_2+PC_4H_9O_2H$	2.40E+12	0	10000		
931	$2PC_4H_9O_2=O_2+2PC_4H_9O$	1.40E+16	-1.6	1860		
932	$PC_4H_9O_2+SC_4H_9O_2=PC_4H_9O+SC_4H_9O+O_2$	1.40E+16	-1.6	1860		
933	$PC_4H_9O_2+NC_3H_7O_2=PC_4H_9O+NC_3H_7O+O_2$	1.40E+16	-1.6	1860		
934	$PC_4H_9O_2+IC_3H_7O_2=PC_4H_9O+IC_3H_7O+O_2$	1.40E+16	-1.6	1860		
935	$PC_4H_9O_2+C_2H_5O_2=PC_4H_9O+C_2H_5O+O_2$	1.40E+16	-1.6	1860		
936	$PC_4H_9O_2+CH_3O_2=PC_4H_9O+CH_3O+O_2$	1.40E+16	-1.6	1860		
937	$PC_4H_9O_2+CH_3CO_3=PC_4H_9O+CH_3CO_2+O_2$	1.40E+16	-1.6	1860		
938	$PC_4H_9O_2+CH_3=PC_4H_9O+CH_3O$	7.00E+12	0	-1000		
939	$PC_4H_9O_2+C_2H_5=PC_4H_9O+C_2H_5O$	7.00E+12	0	-1000		
940	$PC_4H_9O_2+IC_3H_7=PC_4H_9O+IC_3H_7O$	7.00E+12	0	-1000		
941	$PC_4H_9O_2+NC_3H_7=PC_4H_9O+NC_3H_7O$	7.00E+12	0	-1000		
942	$PC_4H_9O_2+PC_4H_9=2PC_4H_9O$	7.00E+12	0	-1000		
943	$PC_4H_9O_2+SC_4H_9=PC_4H_9O+SC_4H_9O$	7.00E+12	0	-1000		
944	$PC_4H_9O_2+C_3H_5-A=PC_4H_9O+C_3H_5O$	7.00E+12	0	-1000		
945	$PC_4H_9+HO_2=PC_4H_9O+OH$	7.00E+12	0	-1000		
946	$SC_4H_9+HO_2=SC_4H_9O+OH$	7.00E+12	0	-1000		
947	$CH_3O_2+PC_4H_9=CH_3O+PC_4H_9O$	7.00E+12	0	-1000		
948	$CH_3O_2+SC_4H_9=CH_3O+SC_4H_9O$	7.00E+12	0	-1000		
949	$PC_4H_9O_2H=PC_4H_9O+OH$	1.50E+16	0	42500		
950	$NC_3H_7+CH_2O=PC_4H_9O$	5.00E+10	0	3457		
951	$CH_3+C_2H_5CHO=SC_4H_9O$	5.00E+10	0	9043		
952	$C_2H_5+CH_3CHO=SC_4H_9O$	3.33E+10	0	6397		
953	$PC_4H_9O_2=C_4H_8OOH1-2$	2.00E+11	0	26850		
954	$PC_4H_9O_2=C_4H_8OOH1-3$	2.50E+10	0	20850		
955	$PC_4H_9O_2=C_4H_8OOH1-4$	4.69E+09	0	22350		
956	$PC_4H_9O_2=C_4H_8-1+HO_2$	5.04E+38	-8.1	40490		
957	$SC_4H_9O_2=C_4H_8-1+HO_2$	5.07E+42	-9.4	41490		
958	$SC_4H_9O_2=C_4H_8-2+HO_2$	5.04E+38	-8.1	40490		
959	$C_4H_8-1+HO_2=C_4H_8OOH1-2$	1.00E+11	0	11000		
960	$C_4H_8OOH1-3=C_4H_8O1-3+OH$	7.50E+10	0	15250		
961	$C_4H_8OOH1-4=C_4H_8O1-4+OH$	9.38E+09	0	6000		
962	$C_4H_8OOH1-3=OH+CH_2O+C_3H_6$	6.64E+13	-0.2	29900		
963	$C_4H_8OOH1-2+O_2=C_4H_8OOH1-2O_2$	7.54E+12	0	0		
964	$C_4H_8OOH1-3+O_2=C_4H_8OOH1-3O_2$	7.54E+12	0	0		
965	$C_4H_8OOH1-2O_2=NC_4KET12+OH$	2.00E+11	0	26400		
966	$C_4H_8OOH1-3O_2=NC_4KET13+OH$	2.50E+10	0	21400		
967	$NC_4KET12=C_2H_5CHO+HCO+OH$	1.05E+16	0	41600		
968	$NC_4KET13=CH_3CHO+CH_2CHO+OH$	1.05E+16	0	41600		
969	$C_2H_5COCH_3+OH=CH_2CH_2COCH_3+H_2O$	7.55E+09	1	1586		

970	$C_2H_5COCH_3+OH=CH_3CHCOCH_3+H_2O$	8.45E+11	0	-228		
971	$C_2H_5COCH_3+OH=C_2H_5COCH_2+H_2O$	5.10E+11	0	1192		
972	$C_2H_5COCH_3+HO_2=CH_2CH_2COCH_3+H_2O_2$	2.38E+04	2.5	16490		
973	$C_2H_5COCH_3+HO_2=CH_3CHCOCH_3+H_2O_2$	2.00E+11	0	8698		
974	$C_2H_5COCH_3+HO_2=C_2H_5COCH_2+H_2O_2$	2.38E+04	2.5	14690		
975	$C_2H_5COCH_3+O=CH_2CH_2COCH_3+OH$	2.25E+13	0	7700		
976	$C_2H_5COCH_3+O=CH_3CHCOCH_3+OH$	3.07E+13	0	3400		
977	$C_2H_5COCH_3+O=C_2H_5COCH_2+OH$	5.00E+12	0	5962		
978	$C_2H_5COCH_3+H=CH_2CH_2COCH_3+H_2$	9.16E+06	2	7700		
979	$C_2H_5COCH_3+H=CH_3CHCOCH_3+H_2$	4.46E+06	2	3200		
980	$C_2H_5COCH_3+H=C_2H_5COCH_2+H_2$	9.30E+12	0	6357		
981	$C_2H_5COCH_3+O_2=CH_2CH_2COCH_3+HO_2$	2.05E+13	0	51310		
982	$C_2H_5COCH_3+O_2=CH_3CHCOCH_3+HO_2$	1.55E+13	0	41970		
983	$C_2H_5COCH_3+O_2=C_2H_5COCH_2+HO_2$	2.05E+13	0	49150		
984	$C_2H_5COCH_3+CH_3=CH_2CH_2COCH_3+CH_4$	3.19E+01	3.2	7172		
985	$C_2H_5COCH_3+CH_3=CH_3CHCOCH_3+CH_4$	1.74E+00	3.5	3680		
986	$C_2H_5COCH_3+CH_3=C_2H_5COCH_2+CH_4$	1.62E+11	0	9630		
987	$C_2H_5COCH_3+CH_3O=CH_2CH_2COCH_3+CH_3OH$	2.17E+11	0	6460		
988	$C_2H_5COCH_3+CH_3O=CH_3CHCOCH_3+CH_3OH$	1.45E+11	0	2771		
989	$C_2H_5COCH_3+CH_3O=C_2H_5COCH_2+CH_3OH$	2.17E+11	0	4660		
990	$C_2H_5COCH_3+CH_3O_2=CH_2CH_2COCH_3+CH_3O_2H$	3.01E+12	0	19380		
991	$C_2H_5COCH_3+CH_3O_2=CH_3CHCOCH_3+CH_3O_2H$	2.00E+12	0	15250		
992	$C_2H_5COCH_3+CH_3O_2=C_2H_5COCH_2+CH_3O_2H$	3.01E+12	0	17580		
993	$C_2H_5COCH_3+C_2H_3=CH_2CH_2COCH_3+C_2H_4$	5.00E+11	0	10400		
994	$C_2H_5COCH_3+C_2H_3=CH_3CHCOCH_3+C_2H_4$	3.00E+11	0	3400		
995	$C_2H_5COCH_3+C_2H_3=C_2H_5COCH_2+C_2H_4$	6.15E+10	0	4278		
996	$C_2H_5COCH_3+C_2H_5=CH_2CH_2COCH_3+C_2H_6$	5.00E+10	0	13400		
997	$C_2H_5COCH_3+C_2H_5=CH_3CHCOCH_3+C_2H_6$	3.00E+10	0	8600		
998	$C_2H_5COCH_3+C_2H_5=C_2H_5COCH_2+C_2H_6$	5.00E+10	0	11600		
999	$CH_2CH_2CHO=C_2H_4+HCO$	3.13E+13	-0.5	24590		
1000	$CH_2CH_2COCH_3=C_2H_4+CH_3CO$	1.00E+14	0	18000		
1001	$C_2H_5COCH_2=CH_2CO+C_2H_5$	1.00E+14	0	35000		
1002	$C_2H_3COCH_3+H=CH_3CHCOCH_3$	5.00E+12	0	1200		
1003	$CH_3CHCO+CH_3=CH_3CHCOCH_3$	1.23E+11	0	7800		
1004	$NC_3H_7CHO+O_2=NC_3H_7CO+HO_2$	1.20E+05	2.5	37560		
1005	$NC_3H_7CHO+OH=NC_3H_7CO+H_2O$	2.00E+06	1.8	-1300		
1006	$NC_3H_7CHO+H=NC_3H_7CO+H_2$	4.14E+09	1.1	2320		
1007	$NC_3H_7CHO+O=NC_3H_7CO+OH$	5.94E+12	0	1868		
1008	$NC_3H_7CHO+HO_2=NC_3H_7CO+H_2O_2$	4.09E+04	2.5	10200		
1009	$NC_3H_7CHO+CH_3=NC_3H_7CO+CH_4$	2.89E-03	4.6	3210		
1010	$NC_3H_7CHO+CH_3O=NC_3H_7CO+CH_3OH$	1.00E+12	0	3300		
1011	$NC_3H_7CHO+CH_3O_2=NC_3H_7CO+CH_3O_2H$	4.09E+04	2.5	10200		
1012	$NC_3H_7CHO+OH=C_3H_6CHO-1+H_2O$	5.28E+09	1	1586		
1013	$NC_3H_7CHO+OH=C_3H_6CHO-2+H_2O$	4.68E+07	1.6	-35		
1014	$NC_3H_7CHO+OH=C_3H_6CHO-3+H_2O$	5.52E+02	3.1	-1176		

1015	NC3H7CHO+HO2=C3H6CHO-1+H2O2	2.38E+04	2.5	16490		
1016	NC3H7CHO+HO2=C3H6CHO-2+H2O2	9.64E+03	2.6	13910		
1017	NC3H7CHO+HO2=C3H6CHO-3+H2O2	3.44E+12	0.1	17880		
1018	NC3H7CHO+CH3O2=C3H6CHO-1+CH3O2H	2.38E+04	2.5	16490		
1019	NC3H7CHO+CH3O2=C3H6CHO-2+CH3O2H	9.64E+03	2.6	13910		
1020	NC3H7CHO+CH3O2=C3H6CHO-3+CH3O2H	3.44E+12	0.1	17880		
1021	NC3H7CO=NC3H7+CO	1.00E+11	0	9600		
1022	C3H6CHO-1=C2H4+CH2CHO	7.40E+11	0	21970		
1023	C2H5CHCO+H=C3H6CHO-3	5.00E+12	0	1200		
1024	C2H3CHO+CH3=C3H6CHO-3	1.23E+11	0	7800		
1025	SC3H5CHO+H=C3H6CHO-2	5.00E+12	0	2900		
1026	C3H6+HCO=C3H6CHO-2	1.00E+11	0	6000		
1027	C2H5CHCO+OH=NC3H7+CO2	3.73E+12	0	-1010		
1028	C2H5CHCO+H=NC3H7+CO	4.40E+12	0	1459		
1029	C2H5CHCO+O=C3H6+CO2	3.20E+12	0	-437		
1030	SC3H5CHO+OH=SC3H5CO+H2O	2.69E+10	0.8	-340		
1031	SC3H5CO=C3H5-S+CO	8.60E+15	0	23000		
1032	SC3H5CHO+HO2=SC3H5CO+H2O2	1.00E+12	0	11920		
1033	SC3H5CHO+CH3=SC3H5CO+CH4	3.98E+12	0	8700		
1034	SC3H5CHO+O=SC3H5CO+OH	7.18E+12	0	1389		
1035	SC3H5CHO+O2=SC3H5CO+HO2	4.00E+13	0	37600		
1036	SC3H5CHO+H=SC3H5CO+H2	2.60E+12	0	2600		
1037	C2H3COCH3+OH=CH3CHO+CH3CO	1.00E+11	0	0		
1038	C2H3COCH3+OH=CH2CO+C2H3+H2O	5.10E+11	0	1192		
1039	C2H3COCH3+HO2=CH2CHO+CH3CO+OH	6.03E+09	0	7949		
1040	C2H3COCH3+HO2=CH2CO+C2H3+H2O2	8.50E+12	0	20460		
1041	C2H3COCH3+CH3O2=CH2CHO+CH3CO+CH3O	3.97E+11	0	17050		
1042	C2H3COCH3+CH3O2=CH2CO+C2H3+CH3O2H	3.01E+12	0	17580		
1043	IC4H10(+M)=CH3+IC3H7(+M)	4.83E+16	0	79900		
	Low pressure	limit:	2.41E+19	0.00E+00	5.26E+04	
	TROE centering:	2.50E-01	7.50E+02	1.00E-10	1.00E+10	
1044	IC4H10=TC4H9+H	2.51E+98	-23.8	145300		
1045	IC4H10=IC4H9+H	9.85E+95	-23.1	147600		
1046	IC4H10+H=TC4H9+H2	1.81E+06	2.5	6756		
1047	IC4H10+H=IC4H9+H2	6.02E+05	2.4	2583		
1048	IC4H10+CH3=TC4H9+CH4	1.36E+00	3.6	7154		
1049	IC4H10+CH3=IC4H9+CH4	9.04E-01	3.5	4598		
1050	IC4H10+OH=TC4H9+H2O	5.73E+10	0.5	63		
1051	IC4H10+OH=IC4H9+H2O	2.29E+08	1.5	776		
1052	IC4H10+C2H5=IC4H9+C2H6	1.51E+12	0	10400		
1053	IC4H10+C2H5=TC4H9+C2H6	1.00E+11	0	7900		
1054	IC4H10+HO2=IC4H9+H2O2	1.22E+05	2.5	16690		
1055	IC4H10+HO2=TC4H9+H2O2	1.50E+04	2.5	12260		
1056	IC4H10+O=TC4H9+OH	1.97E+05	2.4	1150		
1057	IC4H10+O=IC4H9+OH	4.05E+07	2	5136		



1058	IC4H10+CH3O=IC4H9+CH3OH	4.80E+11	0	7000		
1059	IC4H10+CH3O=TC4H9+CH3OH	1.90E+10	0	2800		
1060	IC4H10+O2=IC4H9+HO2	1.80E+14	0	46000		
1061	IC4H10+O2=TC4H9+HO2	2.04E+13	0	41350		
1062	IC4H10+CH3O2=IC4H9+CH3O2H	1.22E+05	2.5	16690		
1063	IC4H10+C2H5O2=IC4H9+C2H5O2H	2.55E+13	0	20460		
1064	IC4H10+CH3CO3=IC4H9+CH3CO3H	2.55E+13	0	20460		
1065	IC4H10+NC3H7O2=IC4H9+NC3H7O2H	2.55E+13	0	20460		
1066	IC4H10+IC3H7O2=IC4H9+IC3H7O2H	2.55E+13	0	20460		
1067	IC4H10+IC4H9O2=IC4H9+IC4H9O2H	2.55E+13	0	20460		
1068	IC4H10+TC4H9O2=IC4H9+TC4H9O2H	2.55E+13	0	20460		
1069	IC4H10+O2CHO=IC4H9+HO2CHO	2.52E+13	0	20440		
1070	IC4H10+O2CHO=TC4H9+HO2CHO	2.80E+12	0	16010		
1071	IC4H10+PC4H9O2=IC4H9+PC4H9O2H	2.25E+13	0	20460		
1072	IC4H10+PC4H9O2=TC4H9+PC4H9O2H	2.80E+12	0	16000		
1073	IC4H10+CH3O2=TC4H9+CH3O2H	1.50E+04	2.5	12260		
1074	IC4H10+C2H5O2=TC4H9+C2H5O2H	2.80E+12	0	16000		
1075	IC4H10+CH3CO3=TC4H9+CH3CO3H	2.80E+12	0	16000		
1076	IC4H10+NC3H7O2=TC4H9+NC3H7O2H	2.80E+12	0	16000		
1077	IC4H10+IC3H7O2=TC4H9+IC3H7O2H	2.80E+12	0	16000		
1078	IC4H10+IC4H9O2=TC4H9+IC4H9O2H	2.80E+12	0	16000		
1079	IC4H10+TC4H9O2=TC4H9+TC4H9O2H	2.80E+12	0	16000		
1080	IC4H10+IC4H9=TC4H9+IC4H10	2.50E+10	0	7900		
1081	IC4H9+HO2=IC4H9O+OH	7.00E+12	0	-1000		
1082	TC4H9+HO2=TC4H9O+OH	7.00E+12	0	-1000		
1083	CH3O2+IC4H9=CH3O+IC4H9O	7.00E+12	0	-1000		
1084	CH3O2+TC4H9=CH3O+TC4H9O	7.00E+12	0	-1000		
1085	IC4H9=IC4H8+H	4.98E+32	-6.2	40070		
1086	IC4H9=C3H6+CH3	1.64E+37	-7.4	38670		
1087	TC4H9=H+IC4H8	4.65E+46	-9.8	55080		
1088	TC4H9+O2=IC4H8+HO2	2.00E-18	0	5000		
1089	IC4H9+O2=IC4H8+HO2	2.00E-18	0	5000		
1090	NC3H7O2+IC4H9=NC3H7O+IC4H9O	7.00E+12	0	-1000		
1091	NC3H7O2+TC4H9=NC3H7O+TC4H9O	7.00E+12	0	-1000		
1092	NC3H7O2+IC4H7=NC3H7O+IC4H7O	7.00E+12	0	-1000		
1093	SC4H9O2+IC4H9=SC4H9O+IC4H9O	7.00E+12	0	-1000		
1094	SC4H9O2+TC4H9=SC4H9O+TC4H9O	7.00E+12	0	-1000		
1095	PC4H9O2+IC4H9=PC4H9O+IC4H9O	7.00E+12	0	-1000		
1096	PC4H9O2+TC4H9=PC4H9O+TC4H9O	7.00E+12	0	-1000		
1097	PC4H9O2+IC4H7=PC4H9O+IC4H7O	7.00E+12	0	-1000		
1098	SC4H9O2+IC4H7=SC4H9O+IC4H7O	7.00E+12	0	-1000		
1099	IC4H9+O2=IC4H9O2	2.26E+12	0	0		
1100	TC4H9+O2=TC4H9O2	1.41E+13	0	0		
1101	IC4H9O2+C4H10=IC4H9O2H+SC4H9	1.12E+13	0	17700		
1102	TC4H9O2+C4H10=TC4H9O2H+SC4H9	1.12E+13	0	17700		
1103	IC4H9O2+C4H10=IC4H9O2H+PC4H9	1.70E+13	0	20460		

1104	TC4H9O2+C4H10=TC4H9O2H+PC4H9	1.70E+13	0	20460		
1105	IC3H7O2+IC4H9=IC3H7O+IC4H9O	7.00E+12	0	-1000		
1106	IC3H7O2+TC4H9=IC3H7O+TC4H9O	7.00E+12	0	-1000		
1107	IC3H7O2+IC4H7=IC3H7O+IC4H7O	7.00E+12	0	-1000		
1108	IC4H9O2+C3H6=IC4H9O2H+C3H5-A	3.24E+11	0	14900		
1109	TC4H9O2+C3H6=TC4H9O2H+C3H5-A	3.24E+11	0	14900		
1110	IC4H9O2+IC4H8=IC4H9O2H+IC4H7	1.40E+12	0	14900		
1111	TC4H9O2+IC4H8=TC4H9O2H+IC4H7	1.40E+12	0	14900		
1112	PC4H9O2+IC4H8=PC4H9O2H+IC4H7	1.40E+12	0	14900		
1113	IC3H7O2+IC4H8=IC3H7O2H+IC4H7	1.40E+12	0	14900		
1114	NC3H7O2+IC4H8=NC3H7O2H+IC4H7	1.40E+12	0	14900		
1115	IC4H9O2+C4H8-1=IC4H9O2H+C4H71-3	1.40E+12	0	14900		
1116	TC4H9O2+C4H8-1=TC4H9O2H+C4H71-3	1.40E+12	0	14900		
1117	IC4H9O2+C4H8-2=IC4H9O2H+C4H71-3	1.40E+12	0	14900		
1118	TC4H9O2+C4H8-2=TC4H9O2H+C4H71-3	1.40E+12	0	14900		
1119	CC4H8O+OH=CH2O+C3H5-A+H2O	5.00E+12	0	0		
1120	CC4H8O+H=CH2O+C3H5-A+H2	3.51E+07	2	5000		
1121	CC4H8O+O=CH2O+C3H5-A+OH	1.12E+14	0	5200		
1122	CC4H8O+HO2=CH2O+C3H5-A+H2O2	1.00E+13	0	15000		
1123	CC4H8O+CH3O2=CH2O+C3H5-A+CH3O2H	1.00E+13	0	19000		
1124	CC4H8O+CH3=CH2O+C3H5-A+CH4	2.00E+11	0	10000		
1125	C2H4+TC4H9O2=C2H3+TC4H9O2H	7.00E+11	0	17110		
1126	TC4H9O2+CH4=TC4H9O2H+CH3	1.13E+13	0	20460		
1127	H2+TC4H9O2=H+TC4H9O2H	3.01E+13	0	26030		
1128	TC4H9O2+C2H6=TC4H9O2H+C2H5	1.70E+13	0	20460		
1129	TC4H9O2+C3H8=TC4H9O2H+IC3H7	2.00E+12	0	17000		
1130	TC4H9O2+C3H8=TC4H9O2H+NC3H7	1.70E+13	0	20460		
1131	TC4H9O2+CH3OH=TC4H9O2H+CH2OH	6.30E+12	0	19360		
1132	TC4H9O2+C2H5OH=TC4H9O2H+PC2H4OH	6.30E+12	0	19360		
1133	TC4H9O2+C2H5OH=TC4H9O2H+SC2H4OH	4.20E+12	0	15000		
1134	IC4H9O2+CH3CHO=IC4H9O2H+CH3CO	2.80E+12	0	13600		
1135	TC4H9O2+CH3CHO=TC4H9O2H+CH3CO	2.80E+12	0	13600		
1136	IC4H9O2+C2H3CHO=IC4H9O2H+C2H3CO	2.80E+12	0	13600		
1137	TC4H9O2+C2H3CHO=TC4H9O2H+C2H3CO	2.80E+12	0	13600		
1138	IC4H9O2+C2H5CHO=IC4H9O2H+C2H5CO	2.80E+12	0	13600		
1139	TC4H9O2+C2H5CHO=TC4H9O2H+C2H5CO	2.80E+12	0	13600		
1140	IC4H9O2+HO2=IC4H9O2H+O2	1.75E+10	0	-3275		
1141	TC4H9O2+HO2=TC4H9O2H+O2	1.75E+10	0	-3275		
1142	IC4H9O2+H2O2=IC4H9O2H+HO2	2.40E+12	0	10000		
1143	TC4H9O2+H2O2=TC4H9O2H+HO2	2.40E+12	0	10000		
1144	IC4H9O2+CH2O=IC4H9O2H+HCO	1.30E+11	0	9000		
1145	TC4H9O2+CH2O=TC4H9O2H+HCO	1.30E+11	0	9000		
1146	IC4H9O2+CH3O2=IC4H9O+CH3O+O2	1.40E+16	-1.6	1860		
1147	TC4H9O2+CH3O2=TC4H9O+CH3O+O2	1.40E+16	-1.6	1860		
1148	IC4H9O2+C2H5O2=IC4H9O+C2H5O+O2	1.40E+16	-1.6	1860		
1149	TC4H9O2+C2H5O2=TC4H9O+C2H5O+O2	1.40E+16	-1.6	1860		

1150	IC4H9O2+CH3CO3=IC4H9O+CH3CO2+O2	1.40E+16	-1.6	1860		
1151	TC4H9O2+CH3CO3=TC4H9O+CH3CO2+O2	1.40E+16	-1.6	1860		
1152	2IC4H9O2=O2+2IC4H9O	1.40E+16	-1.6	1860		
1153	IC4H9O2+TC4H9O2=IC4H9O+TC4H9O+O2	1.40E+16	-1.6	1860		
1154	2TC4H9O2=O2+2TC4H9O	1.40E+16	-1.6	1860		
1155	IC4H9O2+PC4H9O2=IC4H9O+PC4H9O+O2	1.40E+16	-1.6	1860		
1156	TC4H9O2+PC4H9O2=TC4H9O+PC4H9O+O2	1.40E+16	-1.6	1860		
1157	IC4H9O2+SC4H9O2=IC4H9O+SC4H9O+O2	1.40E+16	-1.6	1860		
1158	TC4H9O2+SC4H9O2=TC4H9O+SC4H9O+O2	1.40E+16	-1.6	1860		
1159	IC4H9O2+NC3H7O2=IC4H9O+NC3H7O+O2	1.40E+16	-1.6	1860		
1160	TC4H9O2+NC3H7O2=TC4H9O+NC3H7O+O2	1.40E+16	-1.6	1860		
1161	IC4H9O2+IC3H7O2=IC4H9O+IC3H7O+O2	1.40E+16	-1.6	1860		
1162	TC4H9O2+IC3H7O2=TC4H9O+IC3H7O+O2	1.40E+16	-1.6	1860		
1163	IC4H9O2+HO2=IC4H9O+OH+O2	1.40E+16	-1.6	1860		
1164	TC4H9O2+HO2=TC4H9O+OH+O2	1.40E+16	-1.6	1860		
1165	IC4H9O2+CH3=IC4H9O+CH3O	7.00E+12	0	-1000		
1166	IC4H9O2+C2H5=IC4H9O+C2H5O	7.00E+12	0	-1000		
1167	IC4H9O2+IC3H7=IC4H9O+IC3H7O	7.00E+12	0	-1000		
1168	IC4H9O2+NC3H7=IC4H9O+NC3H7O	7.00E+12	0	-1000		
1169	IC4H9O2+PC4H9=IC4H9O+PC4H9O	7.00E+12	0	-1000		
1170	IC4H9O2+SC4H9=IC4H9O+SC4H9O	7.00E+12	0	-1000		
1171	IC4H9O2+IC4H9=2IC4H9O	7.00E+12	0	-1000		
1172	IC4H9O2+TC4H9=IC4H9O+TC4H9O	7.00E+12	0	-1000		
1173	IC4H9O2+C3H5-A=IC4H9O+C3H5O	7.00E+12	0	-1000		
1174	IC4H9O2+C4H71-3=IC4H9O+C4H7O	7.00E+12	0	-1000		
1175	IC4H9O2+IC4H7=IC4H9O+IC4H7O	7.00E+12	0	-1000		
1176	TC4H9O2+CH3=TC4H9O+CH3O	7.00E+12	0	-1000		
1177	TC4H9O2+C2H5=TC4H9O+C2H5O	7.00E+12	0	-1000		
1178	TC4H9O2+IC3H7=TC4H9O+IC3H7O	7.00E+12	0	-1000		
1179	TC4H9O2+NC3H7=TC4H9O+NC3H7O	7.00E+12	0	-1000		
1180	TC4H9O2+PC4H9=TC4H9O+PC4H9O	7.00E+12	0	-1000		
1181	TC4H9O2+SC4H9=TC4H9O+SC4H9O	7.00E+12	0	-1000		
1182	TC4H9O2+IC4H9=TC4H9O+IC4H9O	7.00E+12	0	-1000		
1183	TC4H9O2+TC4H9=2TC4H9O	7.00E+12	0	-1000		
1184	TC4H9O2+C3H5-A=TC4H9O+C3H5O	7.00E+12	0	-1000		
1185	TC4H9O2+C4H71-3=TC4H9O+C4H7O	7.00E+12	0	-1000		
1186	TC4H9O2+IC4H7=TC4H9O+IC4H7O	7.00E+12	0	-1000		
1187	IC4H9O2+C2H4=IC4H9O2H+C2H3	2.00E+11	0	6000		
1188	IC4H9O2+CH4=IC4H9O2H+CH3	1.13E+13	0	20460		
1189	H2+IC4H9O2=H+IC4H9O2H	3.01E+13	0	26030		
1190	IC4H9O2+C2H6=IC4H9O2H+C2H5	1.70E+13	0	20460		
1191	IC4H9O2+C3H8=IC4H9O2H+IC3H7	2.00E+12	0	17000		
1192	IC4H9O2+C3H8=IC4H9O2H+NC3H7	1.70E+13	0	20460		
1193	IC4H9O2+CH3OH=IC4H9O2H+CH2OH	6.30E+12	0	19360		
1194	IC4H9O2+C2H5OH=IC4H9O2H+PC2H4OH	6.30E+12	0	19360		
1195	IC4H9O2+C2H5OH=IC4H9O2H+SC2H4OH	4.20E+12	0	15000		

1196	IC4H9O2H=IC4H9O+OH	1.50E+16	0	42500		
1197	TC4H9O2H=TC4H9O+OH	5.95E+15	0	42540		
1198	IC4H9O+HO2=IC3H7CHO+H2O2	1.00E+12	0	0		
1199	IC4H9O+OH=IC3H7CHO+H2O	1.81E+13	0	0		
1200	IC4H9O+CH3=IC3H7CHO+CH4	2.40E+13	0	0		
1201	IC4H9O+O=IC3H7CHO+OH	6.00E+12	0	0		
1202	IC4H9O+H=IC3H7CHO+H2	1.99E+13	0	0		
1203	IC4H9O=IC3H7CHO+H	4.00E+14	0	21500		
1204	IC4H9O=CH2O+IC3H7	2.00E+14	0	17500		
1205	CH3COCH3+CH3=TC4H9O	1.50E+11	0	11900		
1206	IC4H9O+O2=IC3H7CHO+HO2	1.93E+11	0	1660		
1207	TC4H9O+O2=IC4H8O+HO2	8.10E+11	0	4700		
1208	IC4H8O=IC3H7CHO	4.18E+13	0	52720		
1209	IC4H8O+OH=IC3H6CHO+H2O	1.25E+12	0	0		
1210	IC4H8O+H=IC3H6CHO+H2	1.25E+12	0	0		
1211	IC4H8O+HO2=IC3H6CHO+H2O2	2.50E+12	0	15000		
1212	IC4H8O+CH3O2=IC3H6CHO+CH3O2H	2.50E+12	0	19000		
1213	IC4H8O+CH3=IC3H6CHO+CH4	5.00E+10	0	10000		
1214	IC4H8O+O=IC3H6CHO+OH	1.25E+12	0	0		
1215	TC3H6CHO+H=IC3H7CHO	2.00E+14	0	0		
1216	IC3H7+HCO=IC3H7CHO	1.81E+13	0	0		
1217	IC3H7CHO+HO2=IC3H7CO+H2O2	3.00E+12	0	11920		
1218	IC3H7CHO+HO2=TC3H6CHO+H2O2	8.00E+10	0	11920		
1219	IC3H7CHO+CH3=IC3H7CO+CH4	3.98E+12	0	8700		
1220	IC3H7CHO+O=IC3H7CO+OH	7.18E+12	0	1389		
1221	IC3H7CHO+O2=IC3H7CO+HO2	4.00E+13	0	37600		
1222	IC3H7CHO+OH=IC3H7CO+H2O	2.69E+10	0.8	-340		
1223	IC3H7CHO+OH=TC3H6CHO+H2O	1.68E+12	0	-781		
1224	IC3H7CHO+H=IC3H7CO+H2	2.60E+12	0	2600		
1225	IC3H7CHO+OH=IC3H6CHO+H2O	3.12E+06	2	-298		
1226	IC3H7CHO+HO2=IC3H6CHO+H2O2	2.74E+04	2.5	15500		
1227	IC3H7CHO+CH3O2=IC3H6CHO+CH3O2H	4.76E+04	2.5	16490		
1228	IC3H7+CO=IC3H7CO	1.50E+11	0	4810		
1229	C3H6+HCO=IC3H6CHO	1.00E+11	0	7800		
1230	C2H3CHO+CH3=IC3H6CHO	1.00E+11	0	7800		
1231	IC4H8+OH=IC4H8OH	9.93E+11	0	-960		
1232	IC4H8OH+O2=IO2C4H8OH	1.20E+11	0	-1100		
1233	IO2C4H8OH=CH3COCH3+CH2O+OH	1.25E+10	0	18900		
1234	IC4H9O2=IC4H8O2H-I	7.50E+10	0	24400		
1235	TC4H9O2=TC4H8O2H-I	9.00E+11	0	29400		
1236	IC4H9O2=IC4H8O2H-T	1.00E+11	0	24100		
1237	IC4H9O2=IC4H8+HO2	4.53E+35	-7.2	39490		
1238	TC4H9O2=IC4H8+HO2	1.52E+43	-9.4	41490		
1239	IC4H8O2H-I+O2=IC4H8OOH-IO2	2.26E+12	0	0		
1240	TC4H8O2H-I+O2=TC4H8OOH-IO2	2.26E+12	0	0		
1241	IC4H8O2H-T+O2=IC4H8OOH-TO2	1.41E+13	0	0		

1242	IC4H8OOH-IO2=IC4KETII+OH	2.50E+10	0	21400		
1243	IC4H8OOH-TO2=IC4KETIT+OH	2.00E+11	0	26400		
1244	IC4KETII=CH2O+C2H5CO+OH	1.50E+16	0	42000		
1245	IC4KETIT=CH3COCH3+HCO+OH	9.50E+15	0	42540		
1246	IC4H8+HO2=TC4H8O2H-I	3.97E+11	0	12620		
1247	IC4H8+HO2=IC4H8O2H-T	3.97E+11	0	12620		
1248	IC4H8O2H-I=CC4H8O+OH	7.50E+10	0	15250		
1249	IC4H8O2H-T=IC4H8O+OH	6.00E+11	0	22000		
1250	TC4H8O2H-I=IC4H8O+OH	6.00E+11	0	22000		
1251	IC4H8O2H-I=OH+CH2O+C3H6	8.45E+15	-0.7	29170		
1252	IC4H8=C3H5-T+CH3	1.92E+66	-14.2	128100		
1253	IC4H8=IC4H7+H	3.07E+55	-11.5	114300		
1254	IC4H8+H=C3H6+CH3	5.68E+33	-5.7	20000		
1255	IC4H8+H=IC4H7+H2	3.40E+05	2.5	2492		
1256	IC4H8+O=CH2CO+2CH3	3.33E+07	1.8	76		
1257	IC4H8+O=IC3H6CO+2H	1.66E+07	1.8	76		
1258	IC4H8+O=IC4H7+OH	1.21E+11	0.7	7633		
1259	IC4H8+CH3=IC4H7+CH4	4.42E+00	3.5	5675		
1260	IC4H8+HO2=IC4H7+H2O2	1.93E+04	2.6	13910		
1261	IC4H8+O2CHO=IC4H7+HO2CHO	1.93E+04	2.6	13910		
1262	IC4H8+O2=IC4H7+HO2	6.00E+12	0	39900		
1263	IC4H8+C3H5-A=IC4H7+C3H6	7.94E+11	0	20500		
1264	IC4H8+C3H5-S=IC4H7+C3H6	7.94E+11	0	20500		
1265	IC4H8+C3H5-T=IC4H7+C3H6	7.94E+11	0	20500		
1266	IC4H8+OH=IC4H7+H2O	5.20E+06	2	-298		
1267	IC4H8+O=IC3H7+HCO	1.58E+07	1.8	-1216		
1268	IC4H8+CH3O2=IC4H7+CH3O2H	1.93E+04	2.6	13910		
1269	IC4H8+HO2=IC4H8O+OH	1.29E+12	0	13340		
1270	IC4H7+O2=IC3H5CHO+OH	2.47E+13	-0.5	23020		
1271	IC4H7+O2=CH3COCH2+CH2O	7.14E+15	-1.2	21050		
1272	IC4H7+O2=C3H4-A+CH2O+OH	7.29E+29	-5.7	21450		
1273	IC4H7+O=IC3H5CHO+H	6.03E+13	0	0		
1274	IC4H7=C3H4-A+CH3	7.09E+10	1.4	56360		
1275	CH3O2+IC4H7=CH3O+IC4H7O	7.00E+12	0	-1000		
1276	IC4H7+HO2=IC4H7O+OH	7.00E+12	0	-1000		
1277	C3H5-T+CH2O=IC4H7O	1.00E+11	0	12600		
1278	IC4H7O=IC4H6OH	1.39E+11	0	15600		
1279	IC4H7O=IC3H5CHO+H	5.00E+13	0	29100		
1280	IC4H6OH+H2=IC4H7OH+H	2.16E+04	2.4	18990		
1281	IC4H7OH+O2=IC4H6OH+HO2	6.00E+13	0	39900		
1282	IC4H6OH+CH2O=IC4H7OH+HCO	6.30E+08	1.9	18190		
1283	IC4H6OH+IC4H8=IC4H7OH+IC4H7	4.70E+02	3.3	19840		
1284	IC4H6OH+H=IC4H7OH	1.00E+14	0	0		
1285	IC4H6OH+H2O2=IC4H7OH+HO2	7.83E+05	2	13580		
1286	C3H4-A+CH2OH=IC4H6OH	1.00E+11	0	9200		
1287	IC4H7O+O2=IC3H5CHO+HO2	3.00E+10	0	1649		

1288	IC4H7O+HO2=IC3H5CHO+H2O2	3.00E+11	0	0		
1289	IC4H7O+CH3=IC3H5CHO+CH4	2.40E+13	0	0		
1290	IC4H7O+O=IC3H5CHO+OH	6.00E+12	0	0		
1291	IC4H7O+OH=IC3H5CHO+H2O	1.81E+13	0	0		
1292	IC4H7O+H=IC3H5CHO+H2	1.99E+13	0	0		
1293	IC3H5CHO+OH=IC3H5CO+H2O	2.69E+10	0.8	-340		
1294	IC3H5CHO+HO2=IC3H5CO+H2O2	1.00E+12	0	11920		
1295	IC3H5CHO+CH3=IC3H5CO+CH4	3.98E+12	0	8700		
1296	IC3H5CHO+O=IC3H5CO+OH	7.18E+12	0	1389		
1297	IC3H5CHO+O2=IC3H5CO+HO2	2.00E+13	0	40700		
1298	IC3H5CHO+H=IC3H5CO+H2	2.60E+12	0	2600		
1299	C3H5-T+CO=IC3H5CO	1.51E+11	0	4809		
1300	TC3H6CHO+HO2=TC3H6OCHO+OH	9.64E+12	0	0		
1301	TC3H6OCHO=CH3COCH3+HCO	3.98E+13	0	9700		
1302	IC3H5CHO+H=TC3H6CHO	1.30E+13	0	1200		
1303	IC3H6CO+H=TC3H6CHO	1.30E+13	0	4800		
1304	TC3H6CHO+H2=IC3H7CHO+H	2.16E+05	2.4	18990		
1305	IC4H7OOH<=>IC4H7O+OH	6.40E+15	0	45550		
1306	IC4H7O+H=IC4H7OH	4.00E+13	0	0		
1307	IC4H7OH+H=IC4H8OH	1.00E+13	0	1200		
1308	IC4H7O+H2=IC4H7OH+H	9.05E+06	2	17830		
1309	IC4H7+OH=IC4H7OH	3.00E+13	0	0		
1310	IC4H7OH+HCO=IC4H7O+CH2O	3.02E+11	0	18160		
1311	TC3H6CHO+CH2O=IC3H7CHO+HCO	2.52E+08	1.9	18190		
1312	TC3H6CHO+IC4H8=IC3H7CHO+IC4H7	4.70E+02	3.3	19840		
1313	IC3H6CO+OH=IC3H7+CO2	1.73E+12	0	-1010		
1314	CH3COCH3+H=TC3H6OH	1.00E+12	0	0		
1315	IC3H5OH+H=TC3H6OH	1.30E+13	0	1560		
1316	C3H5-T+OH=IC3H5OH	5.00E+13	0	0		
1317	TC3H6CHO+O2=TC3H6O2CHO	1.99E+17	-2.1	0		
1318	TC3H6O2CHO=IC3H5O2HCHO	6.00E+11	0	29880		
1319	TC3H6O2CHO=TC3H6O2HCO	1.00E+11	0	25750		
1320	IC3H5CHO+HO2=IC3H5O2HCHO	2.23E+11	0	10600		
1321	TC3H6O2HCO=CH3COCH3+CO+OH	4.24E+18	-1.4	4800		
1322	TC3H6OH+O2=CH3COCH3+HO2	2.23E+13	0	0		
1323	IC3H6CO+OH=TC3H6OH+CO	2.00E+12	0	-1010		
1324	TC3H6CHO+O2=IC3H5CHO+HO2	2.72E-19	0	7240		
1325	TC3H6CHO+O2=CH3COCH3+CO+OH	3.62E-20	0	0		
1326	TC3H6CHO+HO2=IC3H7CHO+O2	3.68E+12	0	1310		
1327	TC3H6CHO+CH3=IC3H5CHO+CH4	3.01E+12	-0.3	-131		
1328	TC4H8CHO=IC3H5CHO+CH3	1.00E+13	0	26290		
1329	TC4H8CHO=IC4H8+HCO	8.52E+12	0	20090		
1330	TC4H8CHO+O2=O2C4H8CHO	2.00E+12	0	0		
1331	O2C4H8CHO=O2HC4H8CO	2.16E+11	0	15360		
1332	IC4H8O2H-T+CO=O2HC4H8CO	1.50E+11	0	4809		
1333	IC4H7O+IC4H8=IC4H7OH+IC4H7	2.70E+11	0	4000		

1334	IC4H6OH+HO2=CH2CCH2OH+CH2O+OH	1.45E+13	0	0		
1335	CH2CCH2OH+CH3=IC4H7OH	3.00E+13	0	0		
1336	CH2CCH2OH+O2=CH2OH+CO+CH2O	4.34E+12	0	0		
1337	CH2CCH2OH=C2H2+CH2OH	2.16E+40	-8.3	45110		
1338	C3H4-A+OH=CH2CCH2OH	8.50E+12	0	2000		
1339	AC5H11=C3H6+C2H5	2.91E+13	0.4	29710		
	Reverse	Arrhenius	coefficients:	1.42E+03	2.7	6850
1340	AC5H11=C4H8-1+CH3	4.84E+11	0.8	30800		
	Reverse	Arrhenius	coefficients:	1.89E+03	2.7	6850
1341	AC5H11=AC5H10+H	1.89E+13	0.2	34220		
	Reverse	Arrhenius	coefficients:	6.25E+11	0.5	2620
1342	AC5H11=DC5H11	3.00E+11	0	21100		
	Reverse	Arrhenius	coefficients:	3.00E+11	0	21100
1343	BC5H11=IC4H8+CH3	5.27E+10	1.2	30220		
	Reverse	Arrhenius	coefficients:	4.40E+04	2.5	6130
1344	BC5H11=AC5H10+H	3.66E+11	0.7	37150		
	Reverse	Arrhenius	coefficients:	1.06E+12	0.5	1230
1345	BC5H11=BC5H10+H	6.17E+11	0.5	35580		
	Reverse	Arrhenius	coefficients:	6.25E+11	0.5	2620
1346	CC5H11=C4H8-2+CH3	5.28E+10	0.9	30620		
	Reverse	Arrhenius	coefficients:	1.89E+03	2.7	6850
1347	CC5H11=BC5H10+H	1.48E+12	0.3	33780		
	Reverse	Arrhenius	coefficients:	2.50E+11	0.5	2620
1348	CC5H11=CC5H10+H	6.26E+11	0.6	38150		
	Reverse	Arrhenius	coefficients:	6.25E+11	0.5	2620
1349	DC5H11=C2H4+IC3H7	1.24E+14	0.1	28960		
	Reverse	Arrhenius	coefficients:	8.80E+03	2.5	6130
1350	DC5H11=CC5H10+H	3.66E+12	0.2	35630		
	Reverse	Arrhenius	coefficients:	2.50E+11	0.5	2620
1351	AC5H11+O2=AC5H10+HO2	2.00E-18	0	5000		
	Reverse	Arrhenius	coefficients:	2.00E-19	0	17500
1352	BC5H11+O2=AC5H10+HO2	2.00E-18	0	5000		
	Reverse	Arrhenius	coefficients:	2.00E-19	0	17500
1353	BC5H11+O2=BC5H10+HO2	2.00E-18	0	5000		
	Reverse	Arrhenius	coefficients:	2.00E-19	0	17500
1354	CC5H11+O2=BC5H10+HO2	2.00E-18	0	5000		
	Reverse	Arrhenius	coefficients:	2.00E-19	0	17500
1355	CC5H11+O2=CC5H10+HO2	2.00E-18	0	5000		
	Reverse	Arrhenius	coefficients:	2.00E-19	0	17500
1356	DC5H11+O2=CC5H10+HO2	2.00E-18	0	5000		
	Reverse	Arrhenius	coefficients:	2.00E-19	0	17500
1357	AC5H10=IC4H7+CH3	1.90E+20	-1.6	75930		
	Reverse	Arrhenius	coefficients:	2.55E+13	-0.3	-131
1358	AC5H10=C3H5-T+C2H5	8.92E+24	-2.4	100500		
	Reverse	Arrhenius	coefficients:	1.00E+13	0	0
1359	BC5H10=IC4H7+CH3	2.61E+19	-1	79020		

	Reverse	Arrhenius	coefficients:	1.00E+13	0	0
1360	CC5H10=C4H71-3+CH3	1.30E+21	-1.6	76140		
	Reverse	Arrhenius	coefficients:	1.00E+13	0	0
1361	AC5H10+OH=SC4H9+CH2O	2.00E+10	0	4000		
	Reverse	Arrhenius	coefficients:	2.00E+13	0	20000
1362	BC5H10+OH=IC3H7+CH3CHO	2.00E+10	0	4000		
	Reverse	Arrhenius	coefficients:	2.00E+13	0	20000
1363	CC5H10+OH=IC4H9+CH2O	2.00E+10	0	4000		
	Reverse	Arrhenius	coefficients:	2.00E+13	0	20000
1364	AC5H10+O=SC4H9+HCO	7.23E+05	2.3	-1050		
	Reverse	Arrhenius	coefficients:	2.00E+05	2.3	80300
1365	AC5H10+O=IC3H7+CH3CO	7.23E+05	2.3	-1050		
	Reverse	Arrhenius	coefficients:	2.00E+05	2.3	80300
1366	AC5H10+O=IC4H9+HCO	7.23E+05	2.3	-1050		
	Reverse	Arrhenius	coefficients:	2.00E+05	2.3	80300
1367	AC5H10+H=AC5H9-A2+H2	1.73E+05	2.5	2492		
	Reverse	Arrhenius	coefficients:	6.95E+06	1.9	20100
1368	AC5H10+H=AC5H9-C+H2	3.38E+05	2.4	207		
	Reverse	Arrhenius	coefficients:	4.35E+06	2.1	20330
1369	AC5H10+OH=AC5H9-A2+H2O	3.12E+06	2	-298		
	Reverse	Arrhenius	coefficients:	5.43E+08	1.4	32470
1370	AC5H10+OH=AC5H9-C+H2O	2.76E+04	2.6	-1919		
	Reverse	Arrhenius	coefficients:	1.54E+06	2.4	33360
1371	AC5H10+CH3=AC5H9-A2+CH4	2.21E+00	3.5	5675		
	Reverse	Arrhenius	coefficients:	2.32E+03	2.9	23770
1372	AC5H10+CH3=AC5H9-C+CH4	3.69E+00	3.3	4002		
	Reverse	Arrhenius	coefficients:	1.24E+03	3	24600
1373	AC5H10+HO2=AC5H9-A2+H2O2	9.64E+03	2.6	13910		
	Reverse	Arrhenius	coefficients:	9.96E+06	1.7	15210
1374	AC5H10+HO2=AC5H9-C+H2O2	4.82E+03	2.5	10530		
	Reverse	Arrhenius	coefficients:	1.60E+06	2	14340
1375	AC5H10+CH3O2=AC5H9-A2+CH3O2H	9.64E+03	2.6	13910		
	Reverse	Arrhenius	coefficients:	2.07E+07	1.5	12190
1376	AC5H10+CH3O2=AC5H9-C+CH3O2H	4.82E+03	2.5	10530		
	Reverse	Arrhenius	coefficients:	3.33E+06	1.8	11320
1377	AC5H10+CH3O=AC5H9-A2+CH3OH	9.00E+01	3	11990		
	Reverse	Arrhenius	coefficients:	1.74E+03	2.4	27870
1378	AC5H10+CH3O=AC5H9-C+CH3OH	4.00E+01	2.9	8609		
	Reverse	Arrhenius	coefficients:	2.49E+02	2.7	27000
1379	BC5H10+H=AC5H9-C+H2	3.46E+05	2.5	2492		
	Reverse	Arrhenius	coefficients:	1.27E+07	2	19650
1380	BC5H10+H=CC5H9-B+H2	1.73E+05	2.5	2492		
	Reverse	Arrhenius	coefficients:	7.02E+06	2.2	20400
1381	BC5H10+OH=AC5H9-C+H2O	6.24E+06	2	-298		
	Reverse	Arrhenius	coefficients:	9.94E+08	1.5	32020
1382	BC5H10+OH=CC5H9-B+H2O	3.12E+06	2	-298		



	Reverse	Arrhenius	coefficients:	5.48E+08	1.7	32770
1383	BC5H10+CH3=AC5H9-C+CH4	4.42E+00	3.5	5675		
	Reverse	Arrhenius	coefficients:	4.25E+03	3	23320
1384	BC5H10+CH3=CC5H9-B+CH4	2.21E+00	3.5	5675		
	Reverse	Arrhenius	coefficients:	2.34E+03	3.2	24060
1385	BC5H10+HO2=AC5H9-C+H2O2	1.93E+04	2.6	13910		
	Reverse	Arrhenius	coefficients:	1.82E+07	1.8	14760
1386	BC5H10+HO2=CC5H9-B+H2O2	9.64E+03	2.6	13910		
	Reverse	Arrhenius	coefficients:	1.00E+07	1.9	15510
1387	BC5H10+CH3O2=AC5H9-C+CH3O2H	1.93E+04	2.6	13910		
	Reverse	Arrhenius	coefficients:	3.80E+07	1.6	11740
1388	BC5H10+CH3O2=CC5H9-B+CH3O2H	9.64E+03	2.6	13910		
	Reverse	Arrhenius	coefficients:	2.09E+07	1.8	12490
1389	BC5H10+CH3O=AC5H9-C+CH3OH	1.80E+02	3	11990		
	Reverse	Arrhenius	coefficients:	3.19E+03	2.5	27420
1390	BC5H10+CH3O=CC5H9-B+CH3OH	9.00E+01	3	11990		
	Reverse	Arrhenius	coefficients:	1.76E+03	2.6	28170
1391	CC5H10+H=CC5H9-B+H2	2.65E+06	2.2	0		
	Reverse	Arrhenius	coefficients:	1.82E+07	2.1	22280
1392	CC5H10+OH=CC5H9-B+H2O	6.14E+02	3.2	-3500		
	Reverse	Arrhenius	coefficients:	1.83E+04	3.1	33940
1393	CC5H10+CH3=CC5H9-B+CH4	4.61E+00	3.1	2330		
	Reverse	Arrhenius	coefficients:	8.28E+02	3	25090
1394	CC5H10+HO2=CC5H9-B+H2O2	1.81E+03	2.5	7154		
	Reverse	Arrhenius	coefficients:	3.20E+05	2.1	13130
1395	CC5H10+CH3O2=CC5H9-B+CH3O2H	1.81E+03	2.5	7154		
	Reverse	Arrhenius	coefficients:	6.66E+05	1.9	10110
1396	CC5H10+CH3O=CC5H9-B+CH3OH	1.00E+01	2.9	5231		
	Reverse	Arrhenius	coefficients:	3.31E+01	2.8	25790
1397	AC5H9-C+HO2=AC5H9O-C+OH	9.64E+12	0	0		
	Reverse	Arrhenius	coefficients:	2.73E+15	-1	15620
1398	AC5H9-C+CH3O2=AC5H9O-C+CH3O	9.64E+12	0	0		
	Reverse	Arrhenius	coefficients:	2.67E+17	-1.5	20380
1399	AC5H9-C+C2H5O2=AC5H9O-C+C2H5O	9.64E+12	0	0		
	Reverse	Arrhenius	coefficients:	1.75E+14	-0.6	18220
1400	CC5H9-B+HO2=CC5H9O-B+OH	9.64E+12	0	0		
	Reverse	Arrhenius	coefficients:	2.94E+15	-1	16870
1401	CC5H9-B+CH3O2=CC5H9O-B+CH3O	9.64E+12	0	0		
	Reverse	Arrhenius	coefficients:	2.87E+17	-1.6	21640
1402	CC5H9-B+C2H5O2=CC5H9O-B+C2H5O	9.64E+12	0	0		
	Reverse	Arrhenius	coefficients:	1.88E+14	-0.7	19480
1403	AC5H9O-C=CH3CHO+C3H5-T	3.23E+22	-2.6	30310		
	Reverse	Arrhenius	coefficients:	1.00E+11	0	11900
1404	CC5H9O-B=CH3COCH3+C2H3	7.81E+13	-0.2	22330		
	Reverse	Arrhenius	coefficients:	1.00E+11	0	11900
1405	CH3CHCHO=C2H3CHO+H	3.52E+15	-0.5	41060		

	Reverse	Arrhenius	coefficients:	6.50E+12	0	2900
1406	CH3CHCHO=CH3CHCO+H	1.14E+16	-0.7	40310		
	Reverse	Arrhenius	coefficients:	5.00E+12	0	1200
1407	CH3CHCHO+H2=C2H5CHO+H	2.16E+05	2.4	18990		
	Reverse	Arrhenius	coefficients:	4.31E+04	2.6	5265
1408	AC6H13=NC3H7+C3H6	1.82E+21	-2.2	32260		
	Reverse	Arrhenius	coefficients:	1.50E+11	0	9200
1409	AC6H13=C5H10-1+CH3	2.12E+18	-1.4	33320		
	Reverse	Arrhenius	coefficients:	1.50E+11	0	9200
1410	AC6H13=AC6H12+H	2.12E+14	-0.3	35160		
	Reverse	Arrhenius	coefficients:	1.00E+13	0	3200
1411	BC6H13=IC4H8+C2H5	1.05E+19	-1.6	30790		
	Reverse	Arrhenius	coefficients:	1.50E+11	0	7200
1412	BC6H13=AC6H12+H	3.92E+12	0.3	37660		
	Reverse	Arrhenius	coefficients:	1.00E+13	0	1200
1413	BC6H13=BC6H12+H	8.02E+12	0.1	36490		
	Reverse	Arrhenius	coefficients:	1.00E+13	0	2900
1414	DC6H13=IC3H7+C3H6	7.77E+20	-2.2	30830		
	Reverse	Arrhenius	coefficients:	1.50E+11	0	7800
1415	DC6H13=CC6H12+H	1.37E+13	-0.1	35920		
	Reverse	Arrhenius	coefficients:	1.00E+13	0	2900
1416	DC6H13=DC6H12+H	6.43E+12	0.1	36820		
	Reverse	Arrhenius	coefficients:	1.00E+13	0	1200
1417	EC6H13=IC4H9+C2H4	2.15E+19	-1.9	30740		
	Reverse	Arrhenius	coefficients:	1.70E+11	0	7200
1418	EC6H13=DC6H12+H	9.53E+13	-0.3	36010		
	Reverse	Arrhenius	coefficients:	1.00E+13	0	2900
1419	AC6H13+O2=AC6H12+HO2	1.50E-19	0	2000		
	Reverse	Arrhenius	coefficients:	2.00E-19	0	17500
1420	BC6H13+O2=AC6H12+HO2	9.00E-19	0	5020		
	Reverse	Arrhenius	coefficients:	2.00E-19	0	17500
1421	BC6H13+O2=BC6H12+HO2	3.00E-19	0	3000		
	Reverse	Arrhenius	coefficients:	2.00E-19	0	17500
1422	DC6H13+O2=CC6H12+HO2	3.00E-19	0	3000		
	Reverse	Arrhenius	coefficients:	2.00E-19	0	17500
1423	DC6H13+O2=DC6H12+HO2	4.50E-19	0	5020		
	Reverse	Arrhenius	coefficients:	2.00E-19	0	17500
1424	EC6H13+O2=DC6H12+HO2	3.00E-19	0	3000		
	Reverse	Arrhenius	coefficients:	2.00E-19	0	17500
1425	AC6H13=DC6H13	2.00E+11	0	18100		
	Reverse	Arrhenius	coefficients:	6.00E+11	0	21100
1426	AC6H13=EC6H13	3.00E+11	0	14100		
	Reverse	Arrhenius	coefficients:	6.00E+11	0	14100
1427	BC6H13=EC6H13	3.00E+11	0	21100		
	Reverse	Arrhenius	coefficients:	1.00E+11	0	16100
1428	AC6H12+OH=>C5H11-2+CH2O	1.00E+11	0	-4000		

1429	BC6H12+OH=>CH3COCH3+NC3H7	1.00E+11	0	-4000		
1430	BC6H12+OH=>C2H5CHO+IC3H7	1.00E+11	0	-4000		
1431	CC6H12+OH=>IC4H9+CH3CHO	1.00E+11	0	-4000		
1432	DC6H12+OH=>DC5H11+CH2O	1.00E+11	0	-4000		
1433	AC6H12+O=>C5H11-2+HCO	1.00E+11	0	-1050		
1434	CC6H12+O=>IC4H9+CH3CO	1.00E+11	0	-1050		
1435	DC6H12+O=>DC5H11+HCO	1.00E+11	0	-1050		
1436	AC6H12=IC4H7+C2H5	1.00E+16	0	71000		
	Reverse	Arrhenius	coefficients:	1.00E+13	0	0
1437	BC6H12=CH3+CC5H9-B	1.00E+16	0	71000		
	Reverse	Arrhenius	coefficients:	1.00E+13	0	0
1438	CC6H12=CH3+C5H92-4	1.00E+16	0	71000		
	Reverse	Arrhenius	coefficients:	1.00E+13	0	0
1439	DC6H12=IC3H7+C3H5-A	1.00E+16	0	71000		
	Reverse	Arrhenius	coefficients:	1.00E+13	0	0
1440	AC6H12+H=AC6H11-A2+H2	1.73E+05	2.5	2492		
	Reverse	Arrhenius	coefficients:	7.05E+06	1.9	20100
1441	AC6H12+H=AC6H11-C+H2	3.38E+05	2.4	207		
	Reverse	Arrhenius	coefficients:	4.37E+06	2.1	20330
1442	AC6H12+H=AC6H11-E+H2	6.65E+05	2.5	6756		
	Reverse	Arrhenius	coefficients:	3.08E+04	2.5	11040
1443	AC6H12+OH=AC6H11-A2+H2O	3.12E+06	2	-298		
	Reverse	Arrhenius	coefficients:	5.50E+08	1.4	32470
1444	AC6H12+OH=AC6H11-C+H2O	2.76E+04	2.6	-1919		
	Reverse	Arrhenius	coefficients:	1.55E+06	2.4	33360
1445	AC6H12+OH=AC6H11-E+H2O	5.27E+09	1	1586		
	Reverse	Arrhenius	coefficients:	1.06E+09	1	21020
1446	AC6H12+CH3=AC6H11-A2+CH4	2.21E+00	3.5	5675		
	Reverse	Arrhenius	coefficients:	2.35E+03	2.9	23760
1447	AC6H12+CH3=AC6H11-C+CH4	3.69E+00	3.3	4002		
	Reverse	Arrhenius	coefficients:	1.25E+03	3	24600
1448	AC6H12+CH3=AC6H11-E+CH4	4.52E-01	3.6	7154		
	Reverse	Arrhenius	coefficients:	5.46E-01	3.6	11910
1449	AC6H12+HO2=AC6H11-A2+H2O2	9.64E+03	2.6	13910		
	Reverse	Arrhenius	coefficients:	1.01E+07	1.7	15210
1450	AC6H12+HO2=AC6H11-C+H2O2	4.82E+03	2.5	10530		
	Reverse	Arrhenius	coefficients:	1.60E+06	2	14340
1451	AC6H12+HO2=AC6H11-E+H2O2	2.38E+04	2.5	16490		
	Reverse	Arrhenius	coefficients:	2.83E+04	2.2	4466
1452	AC6H12+CH3O2=AC6H11-A2+CH3O2H	9.64E+03	2.6	13910		
	Reverse	Arrhenius	coefficients:	2.10E+07	1.5	12190
1453	AC6H12+CH3O2=AC6H11-C+CH3O2H	4.82E+03	2.5	10530		
	Reverse	Arrhenius	coefficients:	3.34E+06	1.8	11320
1454	AC6H12+CH3O2=AC6H11-E+CH3O2H	2.38E+04	2.5	16490		
	Reverse	Arrhenius	coefficients:	5.89E+04	2	1446
1455	AC6H12+CH3O=AC6H11-A2+CH3OH	9.00E+01	3	11990		

	Reverse	Arrhenius	coefficients:	1.77E+03	2.4	27870
1456	AC6H12+CH3O=AC6H11-C+CH3OH	4.00E+01	2.9	8609		
	Reverse	Arrhenius	coefficients:	2.50E+02	2.7	27000
1457	AC6H12+CH3O=AC6H11-E+CH3OH	2.17E+11	0	6458		
	Reverse	Arrhenius	coefficients:	4.84E+09	0	9008
1458	BC6H12+H=AC6H11-C+H2	3.46E+05	2.5	2492		
	Reverse	Arrhenius	coefficients:	9.18E+06	2.1	19740
1459	BC6H12+H=CC6H11-B+H2	3.38E+05	2.4	207		
	Reverse	Arrhenius	coefficients:	2.50E+06	2.3	21040
1460	BC6H12+H=BC6H11-E+H2	6.65E+05	2.5	6756		
	Reverse	Arrhenius	coefficients:	3.09E+04	2.5	11040
1461	BC6H12+OH=AC6H11-C+H2O	6.24E+06	2	-298		
	Reverse	Arrhenius	coefficients:	7.17E+08	1.6	32110
1462	BC6H12+OH=CC6H11-B+H2O	2.76E+04	2.6	-1919		
	Reverse	Arrhenius	coefficients:	8.85E+05	2.5	34070
1463	BC6H12+OH=BC6H11-E+H2O	5.27E+09	1	1586		
	Reverse	Arrhenius	coefficients:	1.06E+09	1	21020
1464	BC6H12+CH3=AC6H11-C+CH4	4.42E+00	3.5	5675		
	Reverse	Arrhenius	coefficients:	3.06E+03	3.1	23410
1465	BC6H12+CH3=CC6H11-B+CH4	3.69E+00	3.3	4002		
	Reverse	Arrhenius	coefficients:	7.13E+02	3.2	25310
1466	BC6H12+CH3=BC6H11-E+CH4	4.52E-01	3.6	7154		
	Reverse	Arrhenius	coefficients:	5.49E-01	3.6	11910
1467	BC6H12+HO2=AC6H11-C+H2O2	1.93E+04	2.6	13910		
	Reverse	Arrhenius	coefficients:	1.32E+07	1.8	14850
1468	BC6H12+HO2=CC6H11-B+H2O2	4.82E+03	2.5	10530		
	Reverse	Arrhenius	coefficients:	9.16E+05	2.1	15050
1469	BC6H12+HO2=BC6H11-E+H2O2	2.38E+04	2.5	16490		
	Reverse	Arrhenius	coefficients:	2.84E+04	2.2	4466
1470	BC6H12+CH3O2=AC6H11-C+CH3O2H	1.93E+04	2.6	13910		
	Reverse	Arrhenius	coefficients:	2.74E+07	1.7	11830
1471	BC6H12+CH3O2=CC6H11-B+CH3O2H	4.82E+03	2.5	10530		
	Reverse	Arrhenius	coefficients:	1.91E+06	1.9	12030
1472	BC6H12+CH3O2=BC6H11-E+CH3O2H	2.38E+04	2.5	16490		
	Reverse	Arrhenius	coefficients:	5.92E+04	2	1446
1473	BC6H12+CH3O=AC6H11-C+CH3OH	1.80E+02	3	11990		
	Reverse	Arrhenius	coefficients:	2.30E+03	2.5	27510
1474	BC6H12+CH3O=CC6H11-B+CH3OH	4.00E+01	2.9	8609		
	Reverse	Arrhenius	coefficients:	1.43E+02	2.8	27710
1475	BC6H12+CH3O=BC6H11-E+CH3OH	2.17E+11	0	6458		
	Reverse	Arrhenius	coefficients:	4.86E+09	0	9008
1476	CC6H12+H=CC6H11-A+H2	1.33E+06	2.5	6756		
	Reverse	Arrhenius	coefficients:	6.09E+04	2.5	11050
1477	CC6H12+H=CC6H11-B+H2	2.65E+06	2.2	0		
	Reverse	Arrhenius	coefficients:	9.15E+06	2.1	22250
1478	CC6H12+OH=CC6H11-A+H2O	1.05E+10	1	1586		

	Reverse	Arrhenius	coefficients:	2.09E+09	1	21030
1479	CC6H12+OH=CC6H11-B+H2O	6.14E+02	3.2	-3500		
	Reverse	Arrhenius	coefficients:	9.18E+03	3.1	33910
1480	CC6H12+CH3=CC6H11-A+CH4	9.04E-01	3.6	7154		
	Reverse	Arrhenius	coefficients:	1.08E+00	3.6	11920
1481	CC6H12+CH3=CC6H11-B+CH4	4.61E+00	3.1	2330		
	Reverse	Arrhenius	coefficients:	4.16E+02	3	25060
1482	CC6H12+HO2=CC6H11-A+H2O2	4.76E+04	2.5	16490		
	Reverse	Arrhenius	coefficients:	5.60E+04	2.2	4476
1483	CC6H12+HO2=CC6H11-B+H2O2	1.81E+03	2.5	7154		
	Reverse	Arrhenius	coefficients:	1.61E+05	2.1	13100
1484	CC6H12+CH3O2=CC6H11-A+CH3O2H	4.76E+04	2.5	16490		
	Reverse	Arrhenius	coefficients:	1.17E+05	2	1456
1485	CC6H12+CH3O2=CC6H11-B+CH3O2H	1.81E+03	2.5	7154		
	Reverse	Arrhenius	coefficients:	3.35E+05	1.9	10080
1486	CC6H12+CH3O=CC6H11-A+CH3OH	4.34E+11	0	6458		
	Reverse	Arrhenius	coefficients:	9.58E+09	0	9018
1487	CC6H12+CH3O=CC6H11-B+CH3OH	1.00E+01	2.9	5231		
	Reverse	Arrhenius	coefficients:	1.66E+01	2.8	25750
1488	AC6H11-C+HO2=AC6H11O-C+OH	9.64E+12	0	0		
	Reverse	Arrhenius	coefficients:	1.77E+15	-0.9	15560
1489	AC6H11-C+CH3O2=AC6H11O-C+CH3O	9.64E+12	0	0		
	Reverse	Arrhenius	coefficients:	1.73E+17	-1.5	20330
1490	AC6H11-C+C2H5O2=AC6H11O-C+C2H5O	9.64E+12	0	0		
	Reverse	Arrhenius	coefficients:	1.13E+14	-0.6	18170
1491	AC6H11-E=AC6H11-A2	4.17E+11	0	26400		
	Reverse	Arrhenius	coefficients:	3.67E+14	-0.6	39730
1492	CC6H11-B+HO2=CC6H11O-B+OH	9.64E+12	0	0		
	Reverse	Arrhenius	coefficients:	5.16E+15	-1	17070
1493	CC6H11-B+CH3O2=CC6H11O-B+CH3O	9.64E+12	0	0		
	Reverse	Arrhenius	coefficients:	5.04E+17	-1.6	21830
1494	CC6H11-B+C2H5O2=CC6H11O-B+C2H5O	9.64E+12	0	0		
	Reverse	Arrhenius	coefficients:	3.30E+14	-0.7	19670
1495	AC6H11O-C=C2H5CHO+C3H5-T	3.24E+22	-2.6	30010		
	Reverse	Arrhenius	coefficients:	1.00E+11	0	11900
1496	CC6H11O-B=CH3COCH3+C3H5-S	7.18E+17	-1.2	28370		
	Reverse	Arrhenius	coefficients:	1.00E+11	0	11900
1497	AC6H11-A2=C3H4-A+NC3H7	1.28E+28	-4.4	72370		
	Reverse	Arrhenius	coefficients:	1.00E+11	0	9200
1498	AC6H11-E=C2H4+IC4H7	4.96E+23	-3.5	43590		
	Reverse	Arrhenius	coefficients:	1.00E+11	0	7800
1499	BC6H11-E=C2H4+IC4H7-I1	2.01E+17	-1.3	43260		
	Reverse	Arrhenius	coefficients:	2.00E+11	0	7800
1500	CC6H11-A=C5H81-3+CH3	2.46E+12	0	24210		
	Reverse	Arrhenius	coefficients:	1.00E+11	0	9200
1501	C4H7CO1-4=C4H71-4+CO	2.79E+09	0.5	-160		

	Reverse	Arrhenius	coefficients:	1.50E+11	0	4810
1502	IC4H9COCH3+OH=IC4H9COCH2+H2O	5.10E+11	0	1192		
	Reverse	Arrhenius	coefficients:	6.76E+13	-0.7	27670
1503	IC4H9COCH3+OH=IC3H6CH2COCH3+H2O	1.51E+10	1	1586		
	Reverse	Arrhenius	coefficients:	2.78E+09	1	21000
1504	IC4H9COCH3+OH=TC3H6CH2COCH3+H2O	5.73E+10	0.5	63		
	Reverse	Arrhenius	coefficients:	1.78E+08	1.1	23970
1505	IC4H9COCH3+HO2=IC4H9COCH2+H2O2	2.38E+04	2.5	14690		
	Reverse	Arrhenius	coefficients:	1.87E+07	1.5	9702
1506	IC4H9COCH3+HO2=IC3H6CH2COCH3+H2O2	4.76E+04	2.5	16490		
	Reverse	Arrhenius	coefficients:	5.20E+04	2.2	4442
1507	IC4H9COCH3+HO2=TC3H6CH2COCH3+H2O2	2.80E+12	0	16000		
	Reverse	Arrhenius	coefficients:	5.16E+10	0.3	8442
1508	IC4H9COCH3+CH3O2=IC4H9COCH2+CH3O2 H	3.01E+12	0	17580		
	Reverse	Arrhenius	coefficients:	9.74E+15	-1.2	11870
1509	IC4H9COCH3+CH3O2=IC3H6CH2COCH3+CH 3O2H	6.02E+12	0	19380		
	Reverse	Arrhenius	coefficients:	2.70E+13	-0.5	6612
1510	IC4H9COCH3+CH3O2=TC3H6CH2COCH3+CH 3O2H	3.61E+03	2.5	10530		
	Reverse	Arrhenius	coefficients:	2.73E+02	2.6	2254
1511	IC4H9COCH2=IC4H9+CH2CO	8.29E+18	-1.5	44360		
	Reverse	Arrhenius	coefficients:	1.00E+11	0	12600
1512	IC3H6CH2COCH3=C3H6+CH3COCH2	3.61E+17	-1.2	30350		
	Reverse	Arrhenius	coefficients:	1.00E+11	0	12600
1513	TC3H6CH2COCH3=IC4H8+CH3CO	6.15E+17	-1.4	31780		
	Reverse	Arrhenius	coefficients:	1.00E+11	0	12600
1514	NC3H7COCH3+OH=C3H6COCH3-2+H2O	3.62E+07	1.6	-247		
	Reverse	Arrhenius	coefficients:	3.67E+05	2	21660
1515	NC3H7COCH3+OH=NC3H7COCH2+H2O	5.10E+11	0	1192		
	Reverse	Arrhenius	coefficients:	9.29E+13	-0.7	27730
1516	NC3H7COCH3+HO2=C3H6COCH3-2+H2O2	5.60E+12	0	17700		
	Reverse	Arrhenius	coefficients:	3.37E+11	0.1	8142
1517	NC3H7COCH3+HO2=NC3H7COCH2+H2O2	2.38E+04	2.5	14690		
	Reverse	Arrhenius	coefficients:	2.57E+07	1.5	9762
1518	NC3H7COCH3+CH3O2=C3H6COCH3- 2+CH3O2H	1.99E+12	0	17050		
	Reverse	Arrhenius	coefficients:	4.93E+11	-0.1	6774
1519	NC3H7COCH3+CH3O2=NC3H7COCH2+CH3O 2H	3.01E+12	0	17580		
	Reverse	Arrhenius	coefficients:	1.34E+16	-1.2	11930
1520	C3H6COCH3-2=C3H6+CH3CO	2.72E+16	-1.1	25590		
	Reverse	Arrhenius	coefficients:	1.00E+11	0	7800
1521	NC3H7COCH2=NC3H7+CH2CO	1.23E+18	-1.4	43450		
	Reverse	Arrhenius	coefficients:	1.00E+11	0	11600
1522	AC3H5CHO=C3H5-A+HCO	1.81E+19	-1.1	68480		
	Reverse	Arrhenius	coefficients:	1.00E+13	0	0
1523	C5H10-1+OH=PC4H9+CH2O	2.00E+10	0	-4000		

	Reverse	Arrhenius	coefficients:	3.00E+11	0	20400
1524	C5H10-2+OH=C2H5+C2H5CHO	1.00E+10	0	-4000		
	Reverse	Arrhenius	coefficients:	2.00E+13	0	20000
1525	C5H10-2+OH=NC3H7+CH3CHO	2.00E+10	0	-4000		
	Reverse	Arrhenius	coefficients:	2.00E+13	0	20000
1526	C5H10-2+O=C3H6+CH3CHO	1.00E+10	0	0		
	Reverse	Arrhenius	coefficients:	1.00E+12	0	81000
1527	C5H10-1+O=>PC4H9+HCO	1.00E+11	0	0		
1528	C5H10-1+O=>NC3H7+CH3CO	1.00E+11	0	0		
1529	C5H10-1+OH=>NC3H7+CH3CHO	1.00E+11	0	0		
1530	C5H10-1+H=C5H9-3+H2	3.38E+05	2.4	207		
	Reverse	Arrhenius	coefficients:	3.10E+05	2.5	20320
1531	C5H10-1+H=C5H9-4+H2	1.30E+06	2.4	4471		
	Reverse	Arrhenius	coefficients:	2.78E+02	3.2	11240
1532	C5H10-1+H=C5H9-5+H2	6.65E+05	2.5	6756		
	Reverse	Arrhenius	coefficients:	2.19E+03	3	11020
1533	C5H10-1+O=C5H9-3+OH	6.60E+05	2.4	1210		
	Reverse	Arrhenius	coefficients:	2.66E+05	2.6	19230
1534	C5H10-1+O=C5H9-4+OH	5.51E+05	2.5	2830		
	Reverse	Arrhenius	coefficients:	5.17E+01	3.2	7505
1535	C5H10-1+O=C5H9-5+OH	9.80E+05	2.4	4750		
	Reverse	Arrhenius	coefficients:	1.42E+03	2.9	6915
1536	C5H10-1+OH=C5H9-3+H2O	2.76E+04	2.6	-1919		
	Reverse	Arrhenius	coefficients:	1.10E+05	2.8	33350
1537	C5H10-1+OH=C5H9-4+H2O	4.67E+07	1.6	-35		
	Reverse	Arrhenius	coefficients:	4.32E+04	2.4	21890
1538	C5H10-1+OH=C5H9-5+H2O	5.27E+09	1	1586		
	Reverse	Arrhenius	coefficients:	7.52E+07	1.4	21000
1539	C5H10-1+CH3=C5H9-3+CH4	3.69E+00	3.3	4002		
	Reverse	Arrhenius	coefficients:	8.84E+01	3.5	24590
1540	C5H10-1+CH3=C5H9-4+CH4	1.51E+00	3.5	5481		
	Reverse	Arrhenius	coefficients:	8.43E-03	4.2	12730
1541	C5H10-1+CH3=C5H9-5+CH4	4.52E-01	3.6	7154		
	Reverse	Arrhenius	coefficients:	3.89E-02	4.1	11890
1542	C5H10-1+O2=C5H9-3+HO2	2.20E+12	0	37220		
	Reverse	Arrhenius	coefficients:	3.66E+10	0.5	-152
1543	C5H10-1+O2=C5H9-4+HO2	2.00E+13	0	49640		
	Reverse	Arrhenius	coefficients:	7.76E+07	1.1	-1072
1544	C5H10-1+O2=C5H9-5+HO2	3.00E+13	0	52290		
	Reverse	Arrhenius	coefficients:	1.80E+09	0.8	-932
1545	C5H10-1+HO2=C5H9-3+H2O2	4.82E+03	2.5	10530		
	Reverse	Arrhenius	coefficients:	1.14E+05	2.4	14330
1546	C5H10-1+HO2=C5H9-4+H2O2	9.64E+03	2.6	13910		
	Reverse	Arrhenius	coefficients:	5.29E+01	3	4372
1547	C5H10-1+HO2=C5H9-5+H2O2	2.38E+04	2.5	16490		
	Reverse	Arrhenius	coefficients:	2.02E+03	2.6	4446

1548	C5H10-1+CH3O2=C5H91-3+CH3O2H	4.82E+03	2.5	10530		
	Reverse	Arrhenius	coefficients:	2.37E+05	2.2	11310
1549	C5H10-1+CH3O2=C5H91-4+CH3O2H	9.64E+03	2.6	13910		
	Reverse	Arrhenius	coefficients:	1.10E+02	2.9	1352
1550	C5H10-1+CH3O2=C5H91-5+CH3O2H	2.38E+04	2.5	16490		
	Reverse	Arrhenius	coefficients:	4.20E+03	2.5	1426
1551	C5H10-1+CH3O=C5H91-3+CH3OH	4.00E+01	2.9	8609		
	Reverse	Arrhenius	coefficients:	1.77E+01	3.1	26990
1552	C5H10-1+CH3O=C5H91-4+CH3OH	1.45E+11	0	4571		
	Reverse	Arrhenius	coefficients:	1.49E+07	0.8	9611
1553	C5H10-1+CH3O=C5H91-5+CH3OH	2.17E+11	0	6458		
	Reverse	Arrhenius	coefficients:	3.45E+08	0.5	8988
1554	C5H10-2+H=C5H91-3+H2	1.73E+05	2.5	2492		
	Reverse	Arrhenius	coefficients:	4.56E+06	2.1	19750
1555	C5H10-2+H=C5H92-4+H2	3.38E+05	2.4	207		
	Reverse	Arrhenius	coefficients:	4.36E+06	2.1	20330
1556	C5H10-2+H=C5H92-5+H2	6.65E+05	2.5	6756		
	Reverse	Arrhenius	coefficients:	3.08E+04	2.5	11030
1557	C5H10-2+O=C5H91-3+OH	4.41E+05	2.4	3150		
	Reverse	Arrhenius	coefficients:	5.11E+06	2	18310
1558	C5H10-2+O=C5H92-4+OH	9.90E+05	2.4	1210		
	Reverse	Arrhenius	coefficients:	5.62E+06	2.2	19240
1559	C5H10-2+O=C5H92-5+OH	9.80E+05	2.4	4750		
	Reverse	Arrhenius	coefficients:	2.00E+04	2.4	6931
1560	C5H10-2+OH=C5H91-3+H2O	3.12E+06	2	-298		
	Reverse	Arrhenius	coefficients:	3.56E+08	1.6	32110
1561	C5H10-2+OH=C5H92-4+H2O	2.76E+04	2.6	-1919		
	Reverse	Arrhenius	coefficients:	1.55E+06	2.4	33360
1562	C5H10-2+OH=C5H92-5+H2O	5.27E+09	1	1586		
	Reverse	Arrhenius	coefficients:	1.06E+09	1	21020
1563	C5H10-2+CH3=C5H91-3+CH4	2.21E+00	3.5	5675		
	Reverse	Arrhenius	coefficients:	1.52E+03	3.1	23410
1564	C5H10-2+CH3=C5H92-4+CH4	3.69E+00	3.3	4002		
	Reverse	Arrhenius	coefficients:	1.24E+03	3	24610
1565	C5H10-2+CH3=C5H92-5+CH4	4.52E-01	3.6	7154		
	Reverse	Arrhenius	coefficients:	5.48E-01	3.6	11910
1566	C5H10-2+O2=C5H91-3+HO2	3.30E+12	0	39900		
	Reverse	Arrhenius	coefficients:	1.58E+12	-0.1	-326
1567	C5H10-2+O2=C5H92-4+HO2	2.20E+12	0	37220		
	Reverse	Arrhenius	coefficients:	5.16E+11	0.1	-136
1568	C5H10-2+O2=C5H92-5+HO2	3.00E+13	0	52290		
	Reverse	Arrhenius	coefficients:	2.53E+10	0.3	-916
1569	C5H10-2+HO2=C5H91-3+H2O2	9.64E+03	2.6	13910		
	Reverse	Arrhenius	coefficients:	6.53E+06	1.8	14860
1570	C5H10-2+HO2=C5H92-4+H2O2	4.82E+03	2.5	10530		
	Reverse	Arrhenius	coefficients:	1.60E+06	2	14350



1571	$C_5H_{10-2}+HO_2=C_5H_9-5+H_2O_2$	2.38E+04	2.5	16490		
	Reverse	Arrhenius	coefficients:	2.84E+04	2.2	4462
1572	$C_5H_{10-2}+CH_3O_2=C_5H_9-3+CH_3O_2H$	9.64E+03	2.6	13910		
	Reverse	Arrhenius	coefficients:	1.36E+07	1.7	11840
1573	$C_5H_{10-2}+CH_3O_2=C_5H_9-4+CH_3O_2H$	4.82E+03	2.5	10530		
	Reverse	Arrhenius	coefficients:	3.33E+06	1.8	11330
1574	$C_5H_{10-2}+CH_3O_2=C_5H_9-5+CH_3O_2H$	2.38E+04	2.5	16490		
	Reverse	Arrhenius	coefficients:	5.91E+04	2	1442
1575	$C_5H_{10-2}+CH_3O=C_5H_9-3+CH_3OH$	9.00E+01	3	11990		
	Reverse	Arrhenius	coefficients:	1.14E+03	2.5	27510
1576	$C_5H_{10-2}+CH_3O=C_5H_9-4+CH_3OH$	4.00E+01	2.9	8609		
	Reverse	Arrhenius	coefficients:	2.49E+02	2.7	27010
1577	$C_5H_{10-2}+CH_3O=C_5H_9-5+CH_3OH$	2.17E+11	0	6458		
	Reverse	Arrhenius	coefficients:	4.85E+09	0	9004
1578	$C_5H_9-3+HO_2=C_5H_9O-3+OH$	9.64E+12	0	0		
	Reverse	Arrhenius	coefficients:	6.09E+15	-1.1	15720
1579	$C_5H_9-3+CH_3O_2=C_5H_9O-3+CH_3O$	9.64E+12	0	0		
	Reverse	Arrhenius	coefficients:	5.95E+17	-1.6	20480
1580	$C_5H_9-3+C_2H_5O_2=C_5H_9O-3+C_2H_5O$	9.64E+12	0	0		
	Reverse	Arrhenius	coefficients:	3.89E+14	-0.7	18330
1581	$C_5H_9-4+HO_2=C_5H_9O-4+OH$	9.64E+12	0	0		
	Reverse	Arrhenius	coefficients:	7.03E+15	-1.2	15890
1582	$C_5H_9-4+CH_3O_2=C_5H_9O-4+CH_3O$	9.64E+12	0	0		
	Reverse	Arrhenius	coefficients:	6.86E+17	-1.8	20650
1583	$C_5H_9-4+C_2H_5O_2=C_5H_9O-4+C_2H_5O$	9.64E+12	0	0		
	Reverse	Arrhenius	coefficients:	4.49E+14	-0.9	18490
1584	$C_5H_{11-2}=C_3H_6+C_2H_5$	2.00E+13	0	29100		
	Reverse	Arrhenius	coefficients:	4.00E+10	0	7500
1585	$C_5H_{11-2}=C_5H_{10-1}+H$	5.00E+12	0	40400		
	Reverse	Arrhenius	coefficients:	7.90E+12	0	2900
1586	$C_5H_{11-2}=C_5H_{10-2}+H$	5.00E+12	0	37900		
	Reverse	Arrhenius	coefficients:	2.50E+12	0	1200
1587	$NC_4H_9CHO+O_2=NC_4H_9CO+HO_2$	2.00E+13	0.5	42200		
	Reverse	Arrhenius	coefficients:	1.00E+07	0	40000
1588	$NC_4H_9CHO+OH=NC_4H_9CO+H_2O$	2.69E+10	0.8	-340		
	Reverse	Arrhenius	coefficients:	2.14E+10	0.7	31240
1589	$NC_4H_9CHO+H=NC_4H_9CO+H_2$	4.00E+13	0	4200		
	Reverse	Arrhenius	coefficients:	1.80E+13	0	24000
1590	$NC_4H_9CHO+O=NC_4H_9CO+OH$	5.00E+12	0	1790		
	Reverse	Arrhenius	coefficients:	1.00E+12	0	19000
1591	$NC_4H_9CHO+HO_2=NC_4H_9CO+H_2O_2$	2.80E+12	0	13600		
	Reverse	Arrhenius	coefficients:	1.00E+12	0	10000
1592	$NC_4H_9CHO+CH_3=NC_4H_9CO+CH_4$	1.70E+12	0	8440		
	Reverse	Arrhenius	coefficients:	1.50E+13	0	28000
1593	$NC_4H_9CHO+CH_3O=NC_4H_9CO+CH_3OH$	1.15E+11	0	1280		
	Reverse	Arrhenius	coefficients:	3.00E+11	0	18000

1594	NC4H9CHO+CH3O2=NC4H9CO+CH3O2H	1.00E+12	0	9500		
	Reverse	Arrhenius	coefficients:	2.50E+10	0	10000
1595	NC4H9CHO+OH=C4H8CHO-1+H2O	5.27E+09	1	1586		
	Reverse	Arrhenius	coefficients:	1.23E+09	0.9	21040
1596	NC4H9CHO+OH=C4H8CHO-2+H2O	4.67E+07	1.6	-35		
	Reverse	Arrhenius	coefficients:	6.84E+05	1.9	21920
1597	NC4H9CHO+OH=C4H8CHO-3+H2O	4.67E+07	1.6	-35		
	Reverse	Arrhenius	coefficients:	6.84E+05	1.9	21920
1598	NC4H9CHO+OH=C4H8CHO-4+H2O	4.67E+07	1.6	-35		
	Reverse	Arrhenius	coefficients:	1.20E+09	1.3	28870
1599	NC4H9CO=PC4H9+CO	1.00E+11	0	9600		
	Reverse	Arrhenius	coefficients:	1.00E+11	0	0
1600	NC4H9CHO+HO2=C4H8CHO-1+H2O2	2.76E+04	2.5	16480		
	Reverse	Arrhenius	coefficients:	3.83E+04	2.2	4471
1601	NC4H9CHO+HO2=C4H8CHO-2+H2O2	1.48E+04	2.6	13910		
	Reverse	Arrhenius	coefficients:	1.28E+03	2.6	4399
1602	NC4H9CHO+HO2=C4H8CHO-3+H2O2	1.48E+04	2.6	13910		
	Reverse	Arrhenius	coefficients:	1.28E+03	2.6	4399
1603	NC4H9CHO+HO2=C4H8CHO-4+H2O2	2.95E+04	2.6	13910		
	Reverse	Arrhenius	coefficients:	4.51E+06	2	11350
1604	NC4H9CHO+CH3O2=C4H8CHO-1+CH3O2H	6.03E+12	0	19380		
	Reverse	Arrhenius	coefficients:	3.44E+13	-0.5	6646
1605	NC4H9CHO+CH3O2=C4H8CHO-2+CH3O2H	1.99E+12	0	17050		
	Reverse	Arrhenius	coefficients:	7.11E+11	-0.2	6821
1606	NC4H9CHO+CH3O2=C4H8CHO-3+CH3O2H	1.99E+12	0	17050		
	Reverse	Arrhenius	coefficients:	7.11E+11	-0.2	6821
1607	NC4H9CHO+CH3O2=C4H8CHO-4+CH3O2H	3.98E+12	0	17050		
	Reverse	Arrhenius	coefficients:	2.50E+15	-0.8	13770
1608	C4H8CHO-1=C2H4+CH2CH2CHO	5.98E+18	-1.6	30430		
	Reverse	Arrhenius	coefficients:	2.50E+11	0	7800
1609	C4H8CHO-2=C3H6+CH2CHO	2.98E+14	-0.8	23320		
	Reverse	Arrhenius	coefficients:	1.00E+11	0	7800
1610	C4H8CHO-3=C4H8-1+HCO	4.80E+14	-0.7	24350		
	Reverse	Arrhenius	coefficients:	1.00E+11	0	7800
1611	C4H8CHO-3=AC3H5CHO+CH3	3.64E+13	-0.4	30330		
	Reverse	Arrhenius	coefficients:	1.00E+11	0	7800
1612	C4H8CHO-4=C2H3CHO+C2H5	1.86E+18	-1.3	30830		
	Reverse	Arrhenius	coefficients:	1.00E+11	0	7800
1613	C2H5COC2H5+OH=C2H5COC2H4P+H2O	6.34E+10	1	1586		
	Reverse	Arrhenius	coefficients:	7.18E+09	0.9	21030
1614	C2H5COC2H5+HO2=C2H5COC2H4P+H2O2	2.86E+05	2.5	16490		
	Reverse	Arrhenius	coefficients:	1.92E+05	2.2	4472
1615	C2H5COC2H5+O2=C2H5COC2H4P+HO2	3.60E+14	0	52290		
	Reverse	Arrhenius	coefficients:	1.71E+11	0.3	-902
1616	C2H5COC2H5+H=C2H5COC2H4P+H2	7.99E+06	2.5	6756		
	Reverse	Arrhenius	coefficients:	2.09E+05	2.5	11050

1617	$C_2H_5COC_2H_5 + C_2H_3 = C_2H_5COC_2H_4P + C_2H_4$	1.00E+12	0	10400		
	Reverse	Arrhenius	coefficients:	3.85E+08	0.8	14040
1618	$C_2H_5COC_2H_5 + C_2H_5 = C_2H_5COC_2H_4P + C_2H_6$	1.00E+11	0	13400		
	Reverse	Arrhenius	coefficients:	1.07E+13	-0.6	14000
1619	$C_2H_5COC_2H_5 + CH_3O = C_2H_5COC_2H_4P + CH_3O$ H	4.34E+11	0	6458		
	Reverse	Arrhenius	coefficients:	7.18E+08	0.4	9013
1620	$C_2H_5COC_2H_5 + CH_3O_2 = C_2H_5COC_2H_4P + CH_3O$ 2H	2.86E+05	2.5	16490		
	Reverse	Arrhenius	coefficients:	3.87E+05	2	1244
1621	$C_2H_5COC_2H_4P = C_2H_5CO + C_2H_4$	1.77E+17	-1.5	29540		
	Reverse	Arrhenius	coefficients:	8.00E+10	0	11300
1622	$C_2H_5COC_2H_3 + OH = C_2H_5COCH_2 + CH_2O$	1.00E+10	0	0		
	Reverse	Arrhenius	coefficients:	1.67E+11	-0.4	18220
1623	$C_2H_5COC_2H_3 + OH = PC_2H_4COC_2H_3 + H_2O$	7.55E+09	1	1586		
	Reverse	Arrhenius	coefficients:	1.28E+08	2.5	20210
1624	$C_2H_5COC_2H_3 + HO_2 = C_2H_5CO + CH_2CHO + OH$	6.03E+09	0	7949		
	Reverse	Arrhenius	coefficients:	1.00E+00	0	0
1625	$C_2H_5COC_2H_3 + HO_2 = PC_2H_4COC_2H_3 + H_2O_2$	2.38E+04	2.5	16490		
	Reverse	Arrhenius	coefficients:	2.40E+03	3.8	3652
1626	$C_2H_5COC_2H_3 + CH_3O_2 = C_2H_5CO + CH_2CHO + C$ H <sub>3</sub> O	3.97E+11	0	17050		
	Reverse	Arrhenius	coefficients:	1.00E+00	0	0
1627	$C_2H_5COC_2H_3 + CH_3O_2 = PC_2H_4COC_2H_3 + CH_3O$ 2H	3.01E+12	0	19380		
	Reverse	Arrhenius	coefficients:	1.25E+12	1.1	5822
1628	$PC_2H_4COC_2H_3 = C_2H_3CO + C_2H_4$	5.26E+14	0.4	21460		
	Reverse	Arrhenius	coefficients:	8.00E+10	0	11300
1629	$C_5H_9O_2-4 = SC_3H_5CHO + CH_3$	5.98E+15	-1.1	9941		
	Reverse	Arrhenius	coefficients:	1.00E+11	0	9600
1630	$C_5H_9O_2-4 = CH_3CHO + C_3H_5-S$	1.07E+22	-2.7	29650		
	Reverse	Arrhenius	coefficients:	1.00E+11	0	9600
1631	$IC_4H_7-I1 = C_3H_4-P + CH_3$	2.10E+12	0.1	29950		
	Reverse	Arrhenius	coefficients:	1.00E+11	0	9200
1632	$C_5H_81-3 + OH = CH_2O + C_4H_71-3$	1.00E+12	0	0		
	Reverse	Arrhenius	coefficients:	1.00E+11	0	15000
1633	$C_5H_81-3 + OH = C_2H_3CHO + C_2H_5$	1.00E+12	0	0		
	Reverse	Arrhenius	coefficients:	1.00E+11	0	15000
1634	$C_5H_81-3 + OH = CH_3CHO + C_3H_5-S$	1.00E+12	0	0		
	Reverse	Arrhenius	coefficients:	1.00E+11	0	15000
1635	$C_7H16-24 = XC_7H15 + H$	6.73E+16	-0.4	101200		
	Reverse	Arrhenius	coefficients:	3.61E+13	0	0
1636	$C_7H16-24 = YC_7H15 + H$	2.63E+18	-0.9	96690		
	Reverse	Arrhenius	coefficients:	3.61E+13	0	0
1637	$C_7H16-24 = ZC_7H15 + H$	9.93E+17	-0.7	98710		
	Reverse	Arrhenius	coefficients:	3.61E+13	0	0
1638	$C_7H16-24 = DC_6H13 + CH_3$	2.33E+24	-2.2	89140		
	Reverse	Arrhenius	coefficients:	4.00E+12	0	-596

1639	C7H16-24=IC3H7+IC4H9	2.40E+25	-2.6	88320		
	Reverse	Arrhenius	coefficients:	4.00E+12	0	-596
1640	C7H16-24+H=XC7H15+H2	3.76E+05	2.8	6280		
	Reverse	Arrhenius	coefficients:	8.05E+01	3.4	8612
1641	C7H16-24+H=YC7H15+H2	1.20E+06	2.4	2583		
	Reverse	Arrhenius	coefficients:	6.60E+00	3.6	9453
1642	C7H16-24+H=ZC7H15+H2	1.30E+06	2.4	4471		
	Reverse	Arrhenius	coefficients:	1.89E+01	3.4	9324
1643	C7H16-24+CH3=XC7H15+CH4	1.81E+00	3.6	7154		
	Reverse	Arrhenius	coefficients:	3.54E-01	3.8	11030
1644	C7H16-24+CH3=YC7H15+CH4	1.20E-09	6.4	893		
	Reverse	Arrhenius	coefficients:	6.01E-12	7.1	9303
1645	C7H16-24+CH3=ZC7H15+CH4	8.40E+04	2.1	7574		
	Reverse	Arrhenius	coefficients:	1.11E+03	2.7	13970
1646	C7H16-24+C2H5=XC7H15+C2H6	2.00E+11	0	13400		
	Reverse	Arrhenius	coefficients:	3.20E+11	0	12300
1647	C7H16-24+C2H5=YC7H15+C2H6	2.00E+11	0	7900		
	Reverse	Arrhenius	coefficients:	3.00E+11	0	21000
1648	C7H16-24+C2H5=ZC7H15+C2H6	5.00E+10	0	10400		
	Reverse	Arrhenius	coefficients:	1.00E+11	0	12900
1649	C7H16-24+O=XC7H15+OH	5.39E+07	2	5136		
	Reverse	Arrhenius	coefficients:	6.06E+03	2.6	6056
1650	C7H16-24+O=YC7H15+OH	7.94E+05	2.4	1150		
	Reverse	Arrhenius	coefficients:	2.28E+00	3.5	6608
1651	C7H16-24+O=ZC7H15+OH	5.95E+05	2.4	2846		
	Reverse	Arrhenius	coefficients:	4.53E+00	3.4	6287
1652	C7H16-24+OH=XC7H15+H2O	2.11E+10	1	1586		
	Reverse	Arrhenius	coefficients:	4.80E+07	1.5	18810
1653	C7H16-24+OH=YC7H15+H2O	1.15E+10	0.5	63		
	Reverse	Arrhenius	coefficients:	1.17E+11	0.5	21600
1654	C7H16-24+OH=ZC7H15+H2O	4.68E+07	1.6	-35		
	Reverse	Arrhenius	coefficients:	6.40E+05	1.9	21910
1655	C7H16-24+HO2=XC7H15+H2O2	1.62E+05	2.5	16690		
	Reverse	Arrhenius	coefficients:	2.01E+04	2.4	3022
1656	C7H16-24+HO2=YC7H15+H2O2	1.50E+04	2.5	12260		
	Reverse	Arrhenius	coefficients:	4.76E+01	3	3129
1657	C7H16-24+HO2=ZC7H15+H2O2	5.88E+04	2.5	14860		
	Reverse	Arrhenius	coefficients:	4.94E+02	2.8	3715
1658	C7H16-24+CH3O=XC7H15+CH3OH	6.40E+11	0	7000		
	Reverse	Arrhenius	coefficients:	1.20E+10	0	9200
1659	C7H16-24+CH3O=YC7H15+CH3OH	3.80E+10	0	2800		
	Reverse	Arrhenius	coefficients:	1.00E+10	0	5200
1660	C7H16-24+CH3O=ZC7H15+CH3OH	1.10E+11	0	5000		
	Reverse	Arrhenius	coefficients:	8.90E+09	0	7200
1661	C7H16-24+O2=XC7H15+HO2	8.40E+13	0	52800		
	Reverse	Arrhenius	coefficients:	9.43E+10	0.3	448

1662	C7H16-24+O2=YC7H15+HO2	1.40E+13	0	48000		
	Reverse	Arrhenius	coefficients:	4.02E+08	0.8	186
1663	C7H16-24+O2=ZC7H15+HO2	1.40E+13	0	50160		
	Reverse	Arrhenius	coefficients:	1.07E+09	0.6	319
1664	C7H16-24+C2H3=XC7H15+C2H4	2.00E+12	0	18000		
	Reverse	Arrhenius	coefficients:	2.60E+12	0	25400
1665	C7H16-24+C2H3=YC7H15+C2H4	4.00E+11	0	14300		
	Reverse	Arrhenius	coefficients:	2.40E+12	0	23000
1666	C7H16-24+C2H3=ZC7H15+C2H4	4.00E+11	0	16800		
	Reverse	Arrhenius	coefficients:	2.00E+12	0	24200
1667	C7H16-24+CH3O2=XC7H15+CH3O2H	1.62E+05	2.5	16690		
	Reverse	Arrhenius	coefficients:	3.90E+05	2	1427
1668	C7H16-24+CH3O2=YC7H15+CH3O2H	1.50E+04	2.5	12260		
	Reverse	Arrhenius	coefficients:	9.26E+02	2.5	1534
1669	C7H16-24+CH3O2=ZC7H15+CH3O2H	5.88E+04	2.5	14860		
	Reverse	Arrhenius	coefficients:	9.62E+03	2.3	2120
1670	C7H16-24+XC7H15=YC7H15+C7H16-24	3.36E+13	0	7900		
	Reverse	Arrhenius	coefficients:	5.00E+12	0	12300
1671	C7H16-24+XC7H15=ZC7H15+C7H16-24	5.60E+12	0	10400		
	Reverse	Arrhenius	coefficients:	1.60E+11	0	12300
1672	C7H16-24+YC7H15=ZC7H15+C7H16-24	5.60E+12	0	10400		
	Reverse	Arrhenius	coefficients:	3.30E+11	0	7900
1673	C7H16-24+O2CHO=XC7H15+HO2CHO	3.36E+13	0	20440		
	Reverse	Arrhenius	coefficients:	2.29E+03	2.3	3057
1674	C7H16-24+O2CHO=YC7H15+HO2CHO	5.60E+12	0	16010		
	Reverse	Arrhenius	coefficients:	9.78E+00	2.8	3173
1675	C7H16-24+O2CHO=ZC7H15+HO2CHO	5.60E+12	0	17690		
	Reverse	Arrhenius	coefficients:	2.59E+01	2.6	2829
1676	XC7H15=C3H6+IC4H9	8.43E+20	-2.2	32420		
	Reverse	Arrhenius	coefficients:	1.00E+11	0	9200
1677	XC7H15=DC6H12+CH3	2.01E+19	-1.8	33330		
	Reverse	Arrhenius	coefficients:	1.00E+11	0	9200
1678	YC7H15=>IC3H7+IC4H8	3.64E+21	-2.3	33260		
1679	XC7H14+H=>C3H6+IC4H7+H2	1.98E+06	2.5	6760		
1680	XC7H14+CH3=>C3H6+IC4H7+CH4	9.00E+02	3.6	7150		
1681	XC7H14=>IC3H7+IC4H7	2.50E+16	0	71000		
1682	XC7H14+H=>XC7H15	1.00E+13	0	2900		
1683	XC7H14+H=>YC7H15	1.00E+13	0	1200		
1684	AC8H17=>XC7H14+CH3	3.38E+21	-2.4	29640		
1685	YC7H14+H=>YC7H15	1.00E+13	0	2900		
1686	YC7H14+H=>C3H6+IC4H7+H2	1.98E+06	2.5	6760		
1687	YC7H14+CH3=>C3H6+IC4H7+CH4	9.00E+02	3.6	7150		
1688	BC8H17=>YC7H14+CH3	1.38E+21	-2.2	29550		
1689	YC7H14=>CH3+CC6H11-B	2.50E+16	0	71000		
1690	ZC7H15=CC6H12+CH3	2.91E+18	-1.6	33250		
	Reverse	Arrhenius	coefficients:	1.00E+11	0	9200

1691	ZC7H15=YC7H14+H	8.20E+13	-0.1	34370		
	Reverse	Arrhenius	coefficients:	2.60E+13	0	2500
1692	XC7H15+O2=XC7H14+HO2	1.50E-29	0	2000		
	Reverse	Arrhenius	coefficients:	2.00E-29	0	17500
1693	YC7H15+O2=XC7H14+HO2	6.00E-29	0	5020		
	Reverse	Arrhenius	coefficients:	2.00E-29	0	17500
1694	YC7H15+O2=YC7H14+HO2	3.00E-29	0	3000		
	Reverse	Arrhenius	coefficients:	2.00E-29	0	17500
1695	ZC7H15+O2=YC7H14+HO2	3.00E-29	0	2000		
	Reverse	Arrhenius	coefficients:	2.00E-29	0	17500
1696	XC7H15=YC7H15	3.71E+11	0	23720		
	Reverse	Arrhenius	coefficients:	9.49E+09	0.5	28260
1697	YC7H15+HO2=YC7H15O+OH	7.00E+12	0	-1000		
	Reverse	Arrhenius	coefficients:	2.41E+18	-1.3	28400
1698	ZC7H15+HO2=ZC7H15O+OH	7.00E+12	0	-1000		
	Reverse	Arrhenius	coefficients:	7.78E+17	-1.2	28100
1699	YC7H15+CH3O2=YC7H15O+CH3O	7.00E+12	0	-1000		
	Reverse	Arrhenius	coefficients:	1.51E+17	-1	32640
1700	ZC7H15+CH3O2=ZC7H15O+CH3O	7.00E+12	0	-1000		
	Reverse	Arrhenius	coefficients:	4.86E+16	-0.9	32340
1701	XC7H14+OH=>CH2O+DC6H13	2.00E+10	0	-4000		
1702	XC7H14+OH=>CH3COCH3+IC4H9	2.00E+10	0	-4000		
1703	YC7H14+OH=>CH3COCH3+IC4H9	2.00E+10	0	-4000		
1704	XC7H14+O=>CH2O+CC6H12	2.00E+10	0	-1050		
1705	YC7H14+O=>CH3COCH3+IC4H8	2.00E+10	0	-1050		
1706	XC7H14+OH=XC7H13-X1+H2O	3.12E+06	2	-298		
	Reverse	Arrhenius	coefficients:	5.50E+08	1.4	32500
1707	XC7H14+OH=XC7H13-Z+H2O	2.76E+04	2.6	-1919		
	Reverse	Arrhenius	coefficients:	1.57E+06	2.4	33400
1708	XC7H14+OH=XC7H13-Y2+H2O	5.73E+10	0.5	63		
	Reverse	Arrhenius	coefficients:	1.95E+08	1.1	23820
1709	XC7H14+OH=XC7H13-X2+H2O	1.05E+10	1	1586		
	Reverse	Arrhenius	coefficients:	2.36E+09	0.9	21060
1710	XC7H14+HO2=XC7H13-X1+H2O2	9.64E+03	2.6	13910		
	Reverse	Arrhenius	coefficients:	1.01E+07	1.7	15240
1711	XC7H14+HO2=XC7H13-Z+H2O2	4.82E+03	2.5	10530		
	Reverse	Arrhenius	coefficients:	1.62E+06	2	14380
1712	XC7H14+HO2=XC7H13-Y2+H2O2	3.61E+03	2.5	10530		
	Reverse	Arrhenius	coefficients:	7.30E+01	2.8	2824
1713	XC7H14+HO2=XC7H13-X2+H2O2	4.76E+04	2.5	16490		
	Reverse	Arrhenius	coefficients:	6.33E+04	2.2	4506
1714	XC7H14+CH3O2=XC7H13-X1+CH3O2H	9.64E+03	2.6	13910		
	Reverse	Arrhenius	coefficients:	2.10E+07	1.5	12220
1715	XC7H14+CH3O2=XC7H13-Z+CH3O2H	4.82E+03	2.5	10530		
	Reverse	Arrhenius	coefficients:	3.38E+06	1.8	11360
1716	XC7H14+CH3O2=XC7H13-Y2+CH3O2H	3.61E+03	2.5	10530		

	Reverse	Arrhenius	coefficients:	1.52E+02	2.6	-196
1717	$\text{XC7H14+CH3O2=XC7H13-X2+CH3O2H}$	4.76E+04	2.5	16490		
	Reverse	Arrhenius	coefficients:	1.32E+05	2	1486
1718	$\text{XC7H14+CH3O=XC7H13-X1+CH3OH}$	9.00E+01	3	11990		
	Reverse	Arrhenius	coefficients:	1.77E+03	2.4	27900
1719	$\text{XC7H14+CH3O=XC7H13-Z+CH3OH}$	4.00E+01	2.9	8609		
	Reverse	Arrhenius	coefficients:	2.52E+02	2.7	27040
1720	$\text{XC7H14+CH3O=XC7H13-Y2+CH3OH}$	2.29E+10	0	2873		
	Reverse	Arrhenius	coefficients:	8.69E+06	0.6	9743
1721	$\text{XC7H14+CH3O=XC7H13-X2+CH3OH}$	4.34E+11	0	6458		
	Reverse	Arrhenius	coefficients:	1.08E+10	0	9048
1722	$\text{YC7H14+OH=XC7H13-Z+H2O}$	6.24E+06	2	-298		
	Reverse	Arrhenius	coefficients:	7.61E+08	1.6	32420
1723	$\text{YC7H14+OH=YC7H13-Y2+H2O}$	6.14E+02	3.2	-3500		
	Reverse	Arrhenius	coefficients:	1.84E+04	3.1	33940
1724	$\text{YC7H14+OH=YC7H13-X2+H2O}$	1.05E+10	1	1586		
	Reverse	Arrhenius	coefficients:	2.12E+09	1	21060
1725	$\text{XC7H13-Z+HO2=XC7H13O-Z+OH}$	9.64E+12	0	0		
	Reverse	Arrhenius	coefficients:	5.41E+14	-0.7	15380
1726	$\text{XC7H13-Z+CH3O2=XC7H13O-Z+CH3O}$	9.64E+12	0	0		
	Reverse	Arrhenius	coefficients:	5.28E+16	-1.3	20140
1727	$\text{XC7H13-Z+C2H5O2=XC7H13O-Z+C2H5O}$	9.64E+12	0	0		
	Reverse	Arrhenius	coefficients:	3.46E+13	-0.4	17980
1728	$\text{YC7H13-Y2+HO2=YC7H13O-Y2+OH}$	9.64E+12	0	0		
	Reverse	Arrhenius	coefficients:	2.11E+15	-1	17000
1729	$\text{YC7H13-Y2+CH3O2=YC7H13O-Y2+CH3O}$	9.64E+12	0	0		
	Reverse	Arrhenius	coefficients:	2.06E+17	-1.6	21760
1730	$\text{YC7H13-Y2+C2H5O2=YC7H13O-Y2+C2H5O}$	9.64E+12	0	0		
	Reverse	Arrhenius	coefficients:	1.35E+14	-0.6	19610
1731	$\text{YC7H13-X2=C3H6+IC4H7-I1}$	1.23E+18	-1.4	43840		
	Reverse	Arrhenius	coefficients:	7.50E+10	0	9200
1732	$\text{XC7H13O-Z=IC3H7CHO+C3H5-T}$	7.52E+21	-2.4	30190		
	Reverse	Arrhenius	coefficients:	1.00E+11	0	11900
1733	$\text{YC7H13O-Y2=CH3COCH3+IC4H7-I1}$	1.31E+18	-1.3	29420		
	Reverse	Arrhenius	coefficients:	1.00E+11	0	11900
1734	$\text{YC7H15O2=YC7H15+O2}$	3.41E+23	-2.4	37210		
	Reverse	Arrhenius	coefficients:	3.00E+12	0	0
1735	$\text{ZC7H15O2=ZC7H15+O2}$	2.97E+22	-2.2	37940		
	Reverse	Arrhenius	coefficients:	2.25E+12	0	0
1736	$\text{YC7H15+YC7H15O2=2YC7H15O}$	7.00E+12	0	-1000		
	Reverse	Arrhenius	coefficients:	5.36E+16	-1	32910
1737	$\text{YC7H15+ZC7H15O2=YC7H15O+ZC7H15O}$	7.00E+12	0	-1000		
	Reverse	Arrhenius	coefficients:	1.49E+17	-1.1	31890
1738	$\text{ZC7H15+YC7H15O2=ZC7H15O+YC7H15O}$	7.00E+12	0	-1000		
	Reverse	Arrhenius	coefficients:	1.73E+16	-0.8	32620
1739	$\text{ZC7H15+ZC7H15O2=2ZC7H15O}$	7.00E+12	0	-1000		

	Reverse	Arrhenius	coefficients:	4.79E+16	-0.9	31600
1740	YC7H15O2+CH3O2=>YC7H15O+CH3O+O2	1.40E+16	-1.6	1860		
1741	ZC7H15O2+CH3O2=>ZC7H15O+CH3O+O2	1.40E+16	-1.6	1860		
1742	2YC7H15O2=>O2+2YC7H15O	1.40E+16	-1.6	1860		
1743	YC7H15O2+ZC7H15O2=>YC7H15O+ZC7H15O+O2	1.40E+16	-1.6	1860		
1744	2ZC7H15O2=>O2+2ZC7H15O	1.40E+16	-1.6	1860		
1745	YC7H15O=IC4H9+CH3COCH3	8.19E+23	-2.9	18020		
	Reverse	Arrhenius	coefficients:	1.00E+11	0	11900
1746	ZC7H15O=IC3H7+IC3H7CHO	2.63E+24	-3	21010		
	Reverse	Arrhenius	coefficients:	1.00E+11	0	11900
1747	YC7H15O2=YC7H14OOH-X1	6.00E+11	0	29400		
	Reverse	Arrhenius	coefficients:	1.46E+12	-0.5	13940
1748	YC7H15O2=YC7H14OOH-Z	2.00E+11	0	26850		
	Reverse	Arrhenius	coefficients:	2.11E+10	-0.1	13840
1749	YC7H15O2=YC7H14OOH-Y2	1.25E+10	0	19100		
	Reverse	Arrhenius	coefficients:	2.79E+08	0.1	7940
1750	YC7H15O2=YC7H14OOH-X2	9.38E+09	0	22350		
	Reverse	Arrhenius	coefficients:	2.28E+10	-0.5	6890
1751	ZC7H15O2=ZC7H14OOH-Y	2.00E+11	0	24100		
	Reverse	Arrhenius	coefficients:	8.11E+09	0	12990
1752	YC7H15O2=XC7H14+HO2	1.01E+43	-9.4	41490		
	Reverse	Arrhenius	coefficients:	3.39E+32	-7.3	16660
1753	YC7H15O2=YC7H14+HO2	5.04E+38	-8.1	40490		
	Reverse	Arrhenius	coefficients:	7.82E+27	-5.8	18260
1754	ZC7H15O2=YC7H14+HO2	9.06E+35	-7.2	39490		
	Reverse	Arrhenius	coefficients:	4.56E+25	-4.9	18550
1755	YC7H14OOH-Y2=>Y-YC7H14O+OH	7.50E+10	0	15250		
1756	YC7H14OOH-X2=>X-Y2C7H14O+OH	9.38E+09	0	7000		
1757	YC7H14OOH-X1=XC7H14+HO2	4.19E+22	-2.7	21270		
	Reverse	Arrhenius	coefficients:	5.75E+11	0	11900
1758	YC7H14OOH-Z=YC7H14+HO2	9.83E+20	-2.4	18730		
	Reverse	Arrhenius	coefficients:	1.44E+11	0	9512
1759	ZC7H14OOH-Y=YC7H14+HO2	1.16E+20	-2.3	19340		
	Reverse	Arrhenius	coefficients:	1.44E+11	0	9512
1760	YC7H14OOH-Y2=>OH+CH3COCH3+IC4H8	5.00E+13	0	25500		
1761	YC7H14OOH-X1O2=YC7H14OOH-X1+O2	1.61E+20	-1.6	35710		
	Reverse	Arrhenius	coefficients:	4.52E+12	0	0
1762	YC7H14OOH-ZO2=YC7H14OOH-Z+O2	2.56E+22	-2.3	38020		
	Reverse	Arrhenius	coefficients:	2.25E+12	0	0
1763	YC7H14OOH-Y2O2=YC7H14OOH-Y2+O2	1.20E+24	-2.5	37480		
	Reverse	Arrhenius	coefficients:	3.00E+12	0	0
1764	YC7H14OOH-X2O2=YC7H14OOH-X2+O2	1.61E+20	-1.6	35710		
	Reverse	Arrhenius	coefficients:	4.52E+12	0	0
1765	X-Y2C7H14O+OH=>IC4H8+CH3CHCHO+H2O	2.50E+12	0	0		
1766	Y-YC7H14O+OH=>CH3COCH3+IC4H7+H2O	2.50E+12	0	0		



1767	X-Y2C7H14O+OH=>CH3COCH3+IC4H7+H2O	2.50E+12	0	0		
1768	Y-YC7H14O+OH=>CH3COCH3+IC4H7-I1+H2O	2.50E+12	0	0		
1769	X- Y2C7H14O+HO2=>IC4H8+CH3CHCHO+H2O2	5.00E+12	0	17700		
1770	Y- YC7H14O+HO2=>CH3COCH3+IC4H7+H2O2	5.00E+12	0	17700		
1771	X- Y2C7H14O+HO2=>CH3COCH3+IC4H7+H2O2	5.00E+12	0	17700		
1772	Y-YC7H14O+HO2=>CH3COCH3+IC4H7-I1+H2O2	5.00E+12	0	17700		
1773	XC7H14OH=XC7H14+OH	6.82E+13	-0.3	28150		
	Reverse	Arrhenius	coefficients:	1.00E+12	0	-1042
1774	XO2C7H14OH=XC7H14OH+O2	2.26E+22	-2.2	37130		
	Reverse	Arrhenius	coefficients:	2.00E+12	0	0
1775	XO2C7H14OH=>IC4H9COCH3+CH2O+OH	2.50E+10	0	18860		
1776	YC7H14OH=YC7H14+OH	1.91E+16	-0.9	30050		
	Reverse	Arrhenius	coefficients:	1.00E+12	0	-1042
1777	YO2C7H14OH=YC7H14OH+O2	4.84E+21	-2.1	37100		
	Reverse	Arrhenius	coefficients:	2.00E+12	0	0
1778	YO2C7H14OH=>IC3H7CHO+CH3COCH3+OH	2.50E+10	0	18860		
1779	NEOC5H12+H=NEOC5H11+H2	9.79E+05	2.8	8147		
	Reverse	Arrhenius	coefficients:	4.42E-01	4	9641
1780	NEOC5H12+O=NEOC5H11+OH	1.14E+04	3	3123		
	Reverse	Arrhenius	coefficients:	2.67E-03	4.2	3205
1781	NEOC5H12+OH=NEOC5H11+H2O	3.16E+07	1.8	298.1		
	Reverse	Arrhenius	coefficients:	1.51E+02	2.9	16680
1782	NEOC5H12+CH3=NEOC5H11+CH4	5.68E-14	8.1	4150		
	Reverse	Arrhenius	coefficients:	2.34E-17	8.8	7184
1783	NEOC5H12+HO2=NEOC5H11+H2O2	8.16E+01	3.6	17160		
	Reverse	Arrhenius	coefficients:	2.13E-02	4.1	2654
1784	NEOC5H12+CH3O=NEOC5H11+CH3OH	6.40E+11	0	7000		
	Reverse	Arrhenius	coefficients:	1.20E+10	0	9200
1785	NEOC5H12+O2=NEOC5H11+HO2	4.95E+13	0	49000		
	Reverse	Arrhenius	coefficients:	1.17E+08	0.9	-4195
1786	NEOC5H12+C2H5=NEOC5H11+C2H6	2.00E+11	0	13400		
	Reverse	Arrhenius	coefficients:	3.20E+11	0	12300
1787	NEOC5H12+C2H3=NEOC5H11+C2H4	2.00E+12	0	18000		
	Reverse	Arrhenius	coefficients:	2.60E+12	0	25400
1788	NEOC5H12+O2CHO=NEOC5H11+HO2CHO	7.20E+04	2.5	16680		
	Reverse	Arrhenius	coefficients:	1.08E+03	2.5	3125
1789	NEOC5H12+CH3O2=NEOC5H11+CH3O2H	8.16E+01	3.6	17160		
	Reverse	Arrhenius	coefficients:	4.15E-01	3.7	1059
1790	IC4H6OH+NEOC5H12=IC4H7OH+NEOC5H11	9.40E+02	3.3	19840		
	Reverse	Arrhenius	coefficients:	5.08E-01	3.7	7668
1791	IC4H7O+NEOC5H12=IC4H7OH+NEOC5H11	5.40E+11	0	4000		
	Reverse	Arrhenius	coefficients:	1.00E+10	0	9000
1792	TC3H6CHO+NEOC5H12=IC3H7CHO+NEOC5H11	9.40E+02	3.3	19840		

	Reverse	Arrhenius	coefficients:	7.16E+01	3.2	9819
1793	NEOC5H11=IC4H8+CH3	8.47E+17	-1.1	32930		
	Reverse	Arrhenius	coefficients:	1.30E+03	2.5	8520
1794	NEOC5H11+HO2=NEOC5H11O+OH	7.00E+12	0	-1000		
	Reverse	Arrhenius	coefficients:	1.45E+11	0.8	24900
1795	NEOC5H11+CH3O2=NEOC5H11O+CH3O	7.00E+12	0	-1000		
	Reverse	Arrhenius	coefficients:	9.05E+09	1.1	29140
1796	NEOC5H11O2=NEOC5H11+O2	9.75E+20	-2.4	34530		
	Reverse	Arrhenius	coefficients:	1.99E+17	-2.1	0
	Declared	duplicate	reaction...			
1797	NEOC5H11O2+NEOC5H12=NEOC5H11O2H+N EOC5H11	2.42E+13	0	20430		
	Reverse	Arrhenius	coefficients:	1.44E+10	0	15000
1798	NEOC5H11+NEOC5H11O2=2NEOC5H11O	7.00E+12	0	-1000		
	Reverse	Arrhenius	coefficients:	4.47E+09	1.1	28610
1799	NEOC5H11O2+HO2=NEOC5H11O2H+O2	1.75E+10	0	-3275		
	Reverse	Arrhenius	coefficients:	3.84E+13	-0.8	33620
1800	NEOC5H11O2+H2O2=NEOC5H11O2H+HO2	2.40E+12	0	10000		
	Reverse	Arrhenius	coefficients:	2.40E+12	0	10000
1801	NEOC5H11O2+CH3O2=>NEOC5H11O+CH3O+ O2	1.40E+16	-1.6	1860		
1802	2NEOC5H11O2=>O2+2NEOC5H11O	1.40E+16	-1.6	1860		
1803	NEOC5H11O2H=NEOC5H11O+OH	1.50E+16	0	42500		
	Reverse	Arrhenius	coefficients:	2.88E+07	1.9	-3022
1804	NEOC5H11O=CH2O+TC4H9	2.65E+25	-3.2	23930		
	Reverse	Arrhenius	coefficients:	2.00E+11	0	11900
1805	NEOC5H11O2=NEOC5H10OOH	1.12E+11	0	24400		
	Reverse	Arrhenius	coefficients:	9.14E+10	-0.5	8950
1806	NEOC5H10OOH=>NEO-C5H10O+OH	2.50E+10	0	15250		
1807	NEOC5H10OOH=>OH+CH2O+IC4H8	3.01E+17	-1.2	29950		
1808	NEOC5H10OOH=IC4H7OOH+CH3	9.03E+21	-2.3	32830		
	Reverse	Arrhenius	coefficients:	1.25E+11	0	10100
1809	NEOC5H10OOH-O2=NEOC5H10OOH+O2	1.37E+25	-3.7	35700		
	Reverse	Arrhenius	coefficients:	1.99E+17	-2.1	0
1810	NEOC5H10OOH-O2=NEOC5H9Q2	7.50E+10	0	24400		
	Reverse	Arrhenius	coefficients:	1.76E+11	-0.5	8940
1811	NEOC5H10OOH-O2=NEOC5H9Q2-N	2.50E+10	0	21400		
	Reverse	Arrhenius	coefficients:	4.44E+10	-0.5	10960
1812	NEOC5H9Q2-N=NEOC5KET+OH	9.00E+14	0	1500		
	Reverse	Arrhenius	coefficients:	1.67E+09	1.6	31880
1813	NEOC5KET=NEOC5KETOX+OH	1.50E+16	0	42000		
	Reverse	Arrhenius	coefficients:	2.01E+09	1.5	-4125
1814	NEOC5KETOX=TC3H6CHO+CH2O	2.48E+21	-2.5	15830		
	Reverse	Arrhenius	coefficients:	1.00E+11	0	11900
1815	NEO-C5H10O+OH=>TC4H8CHO+H2O	2.50E+12	0	0		
1816	NEO-C5H10O+OH=>IC4H7+CH2O+H2O	2.50E+12	0	0		
1817	NEO-C5H10O+HO2=>TC4H8CHO+H2O2	5.00E+12	0	17700		

1818	NEO-C5H10O+HO2=>IC4H7+CH2O+H2O2	5.00E+12	0	17700		
1819	NEO-C5H10O+H=>TC4H8CHO+H2	3.54E+07	2	5000		
1820	NEO-C5H10O+H=>IC4H7+CH2O+H2	1.33E+06	2.5	6756		
1821	NEO-C5H10O=IC4H8+CH2O	3.80E+15	0	60700		
	Reverse	Arrhenius	coefficients:	3.15E+04	2	59730
1822	HC6H13=C2H4+TC4H9	5.46E+23	-3	30610		
	Reverse	Arrhenius	coefficients:	1.70E+11	0	8300
1823	HC6H13=NEOC6H12+H	1.04E+14	-0.3	37030		
	Reverse	Arrhenius	coefficients:	1.00E+13	0	2900
1824	HC6H13+O2=NEOC6H12+HO2	3.00E-29	0	3000		
	Reverse	Arrhenius	coefficients:	2.00E-29	0	17500
1825	NEOC6H12=CH3+CC5H9-B	1.53E+23	-2.2	74190		
	Reverse	Arrhenius	coefficients:	1.00E+13	0	0
1826	NEOC6H12+OH=NEOC6H11+H2O	3.00E+13	0	1230		
	Reverse	Arrhenius	coefficients:	9.80E+10	0.6	10480
1827	NEOC6H12+H=NEOC6H11+H2	3.70E+13	0	3900		
	Reverse	Arrhenius	coefficients:	1.14E+10	0.7	-1740
1828	NEOC6H12+CH3=NEOC6H11+CH4	1.00E+12	0	7300		
	Reverse	Arrhenius	coefficients:	2.80E+11	0.2	3200
1829	NEOC6H12+O=NEOC6H11+OH	4.34E+15	-0.7	36950		
	Reverse	Arrhenius	coefficients:	7.00E+11	0	29900
1830	NEOC6H12+OH=>NEOC5H11+CH2O	1.00E+11	0	-4000		
1831	NEOC6H12+O=>NEOC5H11+HCO	1.00E+11	0	-1050		
1832	NEOC6H11=IC4H8+C2H3	4.79E+17	-1.2	29640		
	Reverse	Arrhenius	coefficients:	7.50E+10	0	10600
1833	TC4H9CHO+HO2=TC4H9CO+H2O2	1.00E+12	0	11920		
	Reverse	Arrhenius	coefficients:	3.85E+12	-0.3	12000
1834	TC4H9CHO+CH3=TC4H9CO+CH4	3.98E+12	0	8700		
	Reverse	Arrhenius	coefficients:	1.56E+13	0	25570
1835	TC4H9CHO+O=TC4H9CO+OH	7.18E+12	0	1389		
	Reverse	Arrhenius	coefficients:	4.73E+11	0	15680
1836	TC4H9CHO+O2=TC4H9CO+HO2	4.00E+13	0	37600		
	Reverse	Arrhenius	coefficients:	1.09E+11	0.3	-3492
1837	TC4H9CHO+OH=TC4H9CO+H2O	2.69E+10	0.8	-340		
	Reverse	Arrhenius	coefficients:	1.75E+10	0.8	31200
1838	TC4H9CO=TC4H9+CO	2.52E+23	-2.9	13490		
	Reverse	Arrhenius	coefficients:	1.50E+11	0	4810
1839	TC4H9CHO+OH=TC4H8CHO+H2O	2.29E+08	1.5	775		
	Reverse	Arrhenius	coefficients:	7.78E+06	1.5	20210
1840	TC4H9CHO+H=TC4H8CHO+H2	1.81E+06	2.5	6756		
	Reverse	Arrhenius	coefficients:	1.42E+04	2.5	11040
1841	TC4H9CHO+HO2=TC4H8CHO+H2O2	3.01E+04	2.5	15500		
	Reverse	Arrhenius	coefficients:	6.07E+03	2.2	3472
1842	TC4H9CHO+CH3=TC4H8CHO+CH4	1.36E+00	3.6	7154		
	Reverse	Arrhenius	coefficients:	2.79E-01	3.6	11910
1843	TC4H9CHO+CH3O=TC4H8CHO+CH3OH	4.82E+11	0	7313		

	Reverse	Arrhenius	coefficients:	1.82E+09	0	9863
1844	TC4H9CHO+CH3O2=TC4H8CHO+CH3O2H	3.01E+04	2.5	15500		
	Reverse	Arrhenius	coefficients:	2.49E+04	2	2752
1845	IC3H6CHCHO+OH=IC3H6CHCO+H2O	3.37E+12	0	-616		
	Reverse	Arrhenius	coefficients:	5.78E+12	0	36810
1846	IC3H6CHCHO+OH=TC3H6CHO+CH2O	1.00E+11	0	0		
	Reverse	Arrhenius	coefficients:	1.39E+11	0.1	16080
1847	NC7H15=IC4H8+NC3H7	7.64E+22	-2.6	32570		
	Reverse	Arrhenius	coefficients:	1.50E+11	0	10600
1848	NC7H15=AC6H12+CH3	1.25E+21	-2.2	34280		
	Reverse	Arrhenius	coefficients:	1.50E+11	0	10600
1849	OC7H15=BC6H12+CH3	4.96E+20	-2	33920		
	Reverse	Arrhenius	coefficients:	1.50E+11	0	10600
1850	OC7H15=NEOC6H12+CH3	2.37E+17	-1.4	32500		
	Reverse	Arrhenius	coefficients:	1.50E+11	0	7200
1851	OC7H15=OC7H14+H	3.33E+13	-0.1	36260		
	Reverse	Arrhenius	coefficients:	2.60E+13	0	2500
1852	PC7H15=TC4H9+C3H6	2.31E+23	-2.8	29340		
	Reverse	Arrhenius	coefficients:	1.50E+11	0	7200
1853	PC7H15=PC7H14+H	1.53E+13	0.1	36810		
	Reverse	Arrhenius	coefficients:	2.60E+13	0	1200
1854	PC7H15=OC7H14+H	1.28E+13	-0.1	36260		
	Reverse	Arrhenius	coefficients:	1.00E+13	0	2500
1855	QC7H15=C2H4+NEOC5H11	4.06E+15	-0.6	29100		
	Reverse	Arrhenius	coefficients:	3.30E+11	0	7200
1856	QC7H15=PC7H14+H	2.36E+14	-0.2	35600		
	Reverse	Arrhenius	coefficients:	2.60E+13	0	2500
1857	OC7H15+O2=OC7H14+HO2	3.00E-29	0	3000		
	Reverse	Arrhenius	coefficients:	2.00E-29	0	17500
1858	PC7H15+O2=OC7H14+HO2	3.00E-29	0	3000		
	Reverse	Arrhenius	coefficients:	2.00E-29	0	17500
1859	PC7H15+O2=PC7H14+HO2	4.50E-29	0	5020		
	Reverse	Arrhenius	coefficients:	2.00E-29	0	17500
1860	QC7H15+O2=PC7H14+HO2	3.00E-29	0	3000		
	Reverse	Arrhenius	coefficients:	2.00E-29	0	17500
1861	NC7H15=PC7H15	2.00E+11	0	18100		
	Reverse	Arrhenius	coefficients:	9.00E+11	0	21100
1862	NC7H15=QC7H15	3.00E+11	0	14100		
	Reverse	Arrhenius	coefficients:	9.00E+11	0	14100
1863	PC7H14=TC4H9+C3H5-A	1.86E+27	-3.4	74280		
	Reverse	Arrhenius	coefficients:	7.22E+14	-0.8	-131
1864	OC7H14=CC6H11-B+CH3	3.09E+24	-2.5	74100		
	Reverse	Arrhenius	coefficients:	1.02E+14	-0.3	-131
1865	OC7H14+OH=>C2H5CHO+TC4H9	2.00E+10	0	-4000		
1866	OC7H14+OH=>NEOC5H11+CH3CHO	2.00E+10	0	-4000		
1867	PC7H14+OH=>NEOC5H11+CH3CHO	2.00E+10	0	-4000		

1868	PC7H14+OH=>CH2O+HC6H13	2.00E+10	0	-4000		
1869	OC7H14+O=>TC4H9+HCO+C2H4	2.00E+10	0	-1050		
1870	PC7H14+O=>CH2O+NEOC6H12	2.00E+10	0	-1050		
1871	OC7H14+H=OC7H13-N+H2	2.00E+06	2.5	6756		
	Reverse	Arrhenius	coefficients:	3.10E+04	2.5	11120
1872	OC7H14+H=PC7H13-O+H2	1.73E+04	2.5	2492		
	Reverse	Arrhenius	coefficients:	4.86E+05	2.1	20850
1873	OC7H14+OH=OC7H13-N+H2O	1.58E+10	1	1586		
	Reverse	Arrhenius	coefficients:	1.06E+09	1	21100
1874	OC7H14+OH=PC7H13-O+H2O	3.12E+06	2	-298		
	Reverse	Arrhenius	coefficients:	3.80E+08	1.6	33220
1875	PC7H14+H=PC7H13-N+H2	2.00E+06	2.5	6756		
	Reverse	Arrhenius	coefficients:	3.09E+04	2.5	11120
1876	PC7H14+H=PC7H13-O+H2	3.38E+05	2.4	207		
	Reverse	Arrhenius	coefficients:	4.35E+06	2.1	20420
1877	PC7H14+OH=PC7H13-N+H2O	1.58E+10	1	1586		
	Reverse	Arrhenius	coefficients:	1.06E+09	1	21100
1878	PC7H14+OH=PC7H13-O+H2O	2.76E+04	2.6	-1919		
	Reverse	Arrhenius	coefficients:	1.54E+06	2.4	33450
1879	OC7H13-N=IC4H8+C3H5-S	3.48E+21	-2.4	44670		
	Reverse	Arrhenius	coefficients:	1.00E+11	0	10600
1880	PC7H13-N=IC4H8+C3H5-A	4.89E+19	-2.1	19390		
	Reverse	Arrhenius	coefficients:	1.00E+11	0	10600
1881	PC7H13-O=PC7H13-N	4.17E+11	0	26400		
	Reverse	Arrhenius	coefficients:	5.01E+08	0.2	10550
1882	PC7H13-O+HO2=PC7H13O-O+OH	9.64E+12	0	0		
	Reverse	Arrhenius	coefficients:	8.72E+15	-1.1	15690
1883	PC7H13-O+CH3O2=PC7H13O-O+CH3O	9.64E+12	0	0		
	Reverse	Arrhenius	coefficients:	8.52E+17	-1.7	20450
1884	PC7H13-O+C2H5O2=PC7H13O-O+C2H5O	9.64E+12	0	0		
	Reverse	Arrhenius	coefficients:	5.58E+14	-0.8	18290
1885	PC7H13O-O=C2H3CHO+TC4H9	4.56E+21	-2.3	7565		
	Reverse	Arrhenius	coefficients:	1.00E+11	0	9600
1886	PC7H13O-O=TC4H9CHO+C2H3	8.53E+17	-1.5	24330		
	Reverse	Arrhenius	coefficients:	1.00E+11	0	9600
1887	NC7H15O2=NC7H15+O2	1.48E+20	-1.7	35790		
	Reverse	Arrhenius	coefficients:	1.24E+12	0	0
	Declared	duplicate	reaction...			
1888	PC7H15O2=PC7H15+O2	2.76E+22	-2.4	38110		
	Reverse	Arrhenius	coefficients:	1.25E+12	0	0
1889	QC7H15O2=QC7H15+O2	5.41E+20	-1.7	35790		
	Reverse	Arrhenius	coefficients:	4.52E+12	0	0
1890	NC7H15O2=NC7H14OOH-N2	7.50E+10	0	24400		
	Reverse	Arrhenius	coefficients:	1.83E+11	-0.5	8940
1891	NC7H15O2=NC7H14OOH-O	2.50E+10	0	20850		
	Reverse	Arrhenius	coefficients:	2.34E+09	-0.1	7830

1892	PC7H15O2=PC7H14OOH-N	1.41E+10	0	22350		
	Reverse	Arrhenius	coefficients:	1.31E+10	-0.5	6910
1893	PC7H15O2=PC7H14OOH-O	2.00E+11	0	26850		
	Reverse	Arrhenius	coefficients:	1.46E+10	-0.1	13800
1894	QC7H15O2=QC7H14OOH-O	2.50E+10	0	20850		
	Reverse	Arrhenius	coefficients:	2.33E+09	-0.1	7830
1895	PC7H15O2=OC7H14+HO2	5.04E+38	-8.1	40490		
	Reverse	Arrhenius	coefficients:	3.74E+28	-5.7	17490
1896	PC7H15O2=PC7H14+HO2	5.07E+42	-9.4	41490		
	Reverse	Arrhenius	coefficients:	8.20E+32	-7.2	16640
1897	QC7H15O2=PC7H14+HO2	5.04E+38	-8.1	40490		
	Reverse	Arrhenius	coefficients:	9.71E+29	-6.2	20470
1898	PC7H14OOH-N=>N-PC7H14O+OH	9.38E+09	0	6000		
1899	PC7H14OOH-O=OC7H14+HO2	1.23E+20	-2.5	23350		
	Reverse	Arrhenius	coefficients:	1.25E+11	0	13400
1900	NC7H14OOH-N2=>OH+CH2O+AC6H12	5.00E+13	0	25500		
1901	NC7H14OOH-O=>OH+CH2O+BC6H12	5.00E+13	0	25500		
1902	QC7H14OOH-O=>OH+CH2O+NEOC6H12	5.00E+13	0	25500		
1903	NC7H14OOH-OO2=NC7H14OOH-O+O2	2.80E+22	-2.3	38060		
	Reverse	Arrhenius	coefficients:	1.75E+12	0	0
1904	PC7H14OOH-NO2=PC7H14OOH-N+O2	5.58E+19	-1.6	35650		
	Reverse	Arrhenius	coefficients:	1.24E+12	0	0
1905	PC7H14OOH-OO2=PC7H14OOH-O+O2	2.10E+22	-2.3	38020		
	Reverse	Arrhenius	coefficients:	1.75E+12	0	0
1906	QC7H14OOH-OO2=QC7H14OOH-O+O2	2.80E+22	-2.3	38060		
	Reverse	Arrhenius	coefficients:	1.75E+12	0	0
1907	PC7H14OOH-NO2=NEOC7KETPN+OH	1.56E+09	0	16050		
	Reverse	Arrhenius	coefficients:	8.38E+00	1.9	42230
1908	PC7H14OOH-OO2=NEOC7KETPO+OH	1.00E+11	0	23850		
	Reverse	Arrhenius	coefficients:	1.80E+03	1.7	49170
1909	QC7H14OOH-OO2=NEOC7KETQO+OH	2.50E+10	0	21400		
	Reverse	Arrhenius	coefficients:	9.34E+02	1.5	44680
1910	NEOC7KETPN=>CH2O+TC3H6CH2COCH3+O H	1.00E+16	0	39000		
1911	NEOC7KETPO=>TC4H9CHO+CH3CO+OH	1.00E+16	0	39000		
1912	NEOC7KETQO=>TC4H9CHO+CH2CHO+OH	1.00E+16	0	39000		
1913	N-PC7H14O+OH=>C3H6+TC3H6CHO+H2O	2.50E+12	0	0		
1914	N-PC7H14O+OH=>IC4H8+CH3COCH2+H2O	2.50E+12	0	0		
1915	N-PC7H14O+HO2=>C3H6+TC3H6CHO+H2O2	5.00E+12	0	17700		
1916	N-PC7H14O+HO2=>IC4H8+CH3COCH2+H2O2	5.00E+12	0	17700		
1917	IC8H18=AC8H17+H	5.75E+17	-0.4	101200		
	Reverse	Arrhenius	coefficients:	1.00E+14	0	0
1918	IC8H18=BC8H17+H	3.30E+18	-0.7	98730		
	Reverse	Arrhenius	coefficients:	1.00E+14	0	0
1919	IC8H18=CC8H17+H	1.15E+19	-0.9	95430		
	Reverse	Arrhenius	coefficients:	1.00E+14	0	0

1920	IC8H18=DC8H17+H	1.92E+17	-0.4	100400		
	Reverse	Arrhenius	coefficients:	1.00E+14	0	0
1921	IC8H18=YC7H15+CH3	1.64E+27	-2.8	83930		
	Reverse	Arrhenius	coefficients:	1.63E+13	0	-596
1922	IC8H18=PC7H15+CH3	1.38E+26	-2.6	85860		
	Reverse	Arrhenius	coefficients:	1.93E+14	-0.3	0
1923	IC8H18=TC4H9+IC4H9	7.83E+29	-3.9	84150		
	Reverse	Arrhenius	coefficients:	3.59E+14	-0.8	0
1924	IC8H18=NEOC5H11+IC3H7	2.45E+23	-2	83400		
	Reverse	Arrhenius	coefficients:	3.59E+14	-0.8	0
1925	IC8H18+H=AC8H17+H2	7.34E+05	2.8	8147		
	Reverse	Arrhenius	coefficients:	5.10E+01	3.4	10480
1926	IC8H18+H=BC8H17+H2	5.74E+05	2.5	4124		
	Reverse	Arrhenius	coefficients:	6.94E+00	3.5	8954
1927	IC8H18+H=CC8H17+H2	6.02E+05	2.4	2583		
	Reverse	Arrhenius	coefficients:	2.10E+00	3.6	10710
1928	IC8H18+H=DC8H17+H2	1.88E+05	2.8	6280		
	Reverse	Arrhenius	coefficients:	3.91E+01	3.4	9417
1929	IC8H18+O=AC8H17+OH	8.55E+03	3	3123		
	Reverse	Arrhenius	coefficients:	3.12E-01	3.7	4048
1930	IC8H18+O=BC8H17+OH	4.77E+04	2.7	2106		
	Reverse	Arrhenius	coefficients:	3.03E-01	3.7	5524
1931	IC8H18+O=CC8H17+OH	3.83E+05	2.4	1140		
	Reverse	Arrhenius	coefficients:	7.00E-01	3.6	7858
1932	IC8H18+O=DC8H17+OH	2.85E+05	2.5	3645		
	Reverse	Arrhenius	coefficients:	3.12E+01	3.1	5370
1933	IC8H18+OH=AC8H17+H2O	2.63E+07	1.8	1431		
1934	IC8H18+OH=BC8H17+H2O	9.00E+05	2	-1133		
	Reverse	Arrhenius	coefficients:	1.16E+02	2.9	18590
1935	IC8H18+OH=CC8H17+H2O	1.70E+06	1.9	-1450		
	Reverse	Arrhenius	coefficients:	6.30E+01	3	21570
1936	IC8H18+OH=DC8H17+H2O	1.78E+07	1.8	1431		
	Reverse	Arrhenius	coefficients:	3.94E+04	2.3	19460
1937	IC8H18+CH3=AC8H17+CH4	4.26E-14	8.1	4154		
	Reverse	Arrhenius	coefficients:	2.70E-15	8.2	8031
1938	IC8H18+CH3=BC8H17+CH4	2.70E+04	2.3	7287		
	Reverse	Arrhenius	coefficients:	2.99E+02	2.8	13660
1939	IC8H18+CH3=CC8H17+CH4	6.01E-10	6.4	893		
	Reverse	Arrhenius	coefficients:	1.91E-12	7.1	10560
1940	IC8H18+CH3=DC8H17+CH4	1.47E-01	3.9	6808		
	Reverse	Arrhenius	coefficients:	2.79E-02	4.1	11480
1941	IC8H18+HO2=AC8H17+H2O2	7.29E+04	2.5	16680		
1942	IC8H18+HO2=BC8H17+H2O2	3.53E+04	2.5	14680		
1943	IC8H18+HO2=CC8H17+H2O2	9.00E+03	2.5	12260		
1944	IC8H18+HO2=DC8H17+H2O2	4.86E+04	2.5	16690		
1945	IC8H18+CH3O=AC8H17+CH3OH	4.74E+11	0	7000		

	Reverse	Arrhenius	coefficients:	1.20E+10	0	9200
1946	IC8H18+CH3O=BC8H17+CH3OH	1.10E+11	0	5000		
	Reverse	Arrhenius	coefficients:	8.90E+09	0	7200
1947	IC8H18+CH3O=CC8H17+CH3OH	1.90E+10	0	2800		
	Reverse	Arrhenius	coefficients:	1.00E+10	0	5200
1948	IC8H18+CH3O=DC8H17+CH3OH	3.20E+11	0	7000		
	Reverse	Arrhenius	coefficients:	1.20E+10	0	9200
1949	IC8H18+O2=AC8H17+HO2	6.30E+13	0	50760		
	Reverse	Arrhenius	coefficients:	2.30E+10	0.3	-1592
1950	IC8H18+O2=BC8H17+HO2	1.40E+13	0	48210		
	Reverse	Arrhenius	coefficients:	8.89E+08	0.6	-1649
1951	IC8H18+O2=CC8H17+HO2	7.00E+12	0	46060		
	Reverse	Arrhenius	coefficients:	1.28E+08	0.9	-499
1952	IC8H18+O2=DC8H17+HO2	4.20E+13	0	50760		
	Reverse	Arrhenius	coefficients:	4.58E+10	0.3	-792
1953	IC8H18+C2H5=AC8H17+C2H6	1.50E+11	0	13400		
	Reverse	Arrhenius	coefficients:	3.20E+11	0	12300
1954	IC8H18+C2H5=BC8H17+C2H6	5.00E+10	0	10400		
	Reverse	Arrhenius	coefficients:	1.00E+11	0	12900
1955	IC8H18+C2H5=CC8H17+C2H6	1.00E+11	0	7900		
	Reverse	Arrhenius	coefficients:	3.00E+11	0	21000
1956	IC8H18+C2H5=DC8H17+C2H6	1.00E+11	0	13400		
	Reverse	Arrhenius	coefficients:	3.20E+11	0	12300
1957	IC8H18+C2H3=AC8H17+C2H4	1.50E+12	0	18000		
	Reverse	Arrhenius	coefficients:	2.57E+12	0	25400
1958	IC8H18+C2H3=BC8H17+C2H4	4.00E+11	0	16800		
	Reverse	Arrhenius	coefficients:	2.00E+12	0	24200
1959	IC8H18+C2H3=CC8H17+C2H4	2.00E+11	0	14300		
	Reverse	Arrhenius	coefficients:	2.50E+12	0	23000
1960	IC8H18+C2H3=DC8H17+C2H4	1.00E+12	0	18000		
	Reverse	Arrhenius	coefficients:	2.57E+12	0	25400
1961	IC4H8+IC4H9=AC8H17	4.00E+02	2.5	8520		
1962	OC7H14+CH3=BC8H17	1.30E+03	2.5	8520		
1963	IC4H8+TC4H9=CC8H17	4.00E+02	2.5	6130		
1964	PC7H14+CH3=DC8H17	1.30E+03	2.5	8520		
1965	C3H6+NEOC5H11=DC8H17	4.00E+02	2.5	8520		
1966	BC8H17=IC8H16+H	1.84E+12	0.4	35240		
	Reverse	Arrhenius	coefficients:	6.25E+11	0.5	2620
1967	CC8H17=IC8H16+H	9.00E+11	0.6	37150		
	Reverse	Arrhenius	coefficients:	1.06E+12	0.5	1230
1968	CC8H17=JC8H16+H	4.21E+11	0.8	36690		
	Reverse	Arrhenius	coefficients:	1.06E+12	0.5	1230
1969	CC8H17+O2=IC8H16+HO2	3.00E-19	0	5000		
	Reverse	Arrhenius	coefficients:	2.00E-19	0	17500
1970	CC8H17+O2=JC8H16+HO2	1.50E-19	0	4000		
	Reverse	Arrhenius	coefficients:	2.00E-19	0	17500



1971	DC8H17=JC8H16+H	1.48E+13	0.2	33090		
	Reverse	Arrhenius	coefficients:	6.25E+11	0.5	2620
1972	AC8H17=DC8H17	1.39E+11	0	15400		
	Reverse	Arrhenius	coefficients:	4.16E+11	0	16200
1973	AC8H17=CC8H17	3.71E+11	0	20400		
	Reverse	Arrhenius	coefficients:	1.86E+10	0.6	26190
1974	DC8H17+O2=JC8H16+HO2	2.00E-18	0	5000		
	Reverse	Arrhenius	coefficients:	2.00E-19	0	17500
1975	IC8H16+H=IC8H15+H2	3.70E+13	0	3900		
	Reverse	Arrhenius	coefficients:	3.42E+12	0	19570
1976	JC8H16+H=IC8H15+H2	3.70E+13	0	3900		
	Reverse	Arrhenius	coefficients:	1.60E+12	0.2	19110
1977	IC8H16+O=IC8H15+OH	3.70E+13	0	3900		
	Reverse	Arrhenius	coefficients:	1.80E+12	0	18160
1978	JC8H16+O=IC8H15+OH	3.70E+13	0	3900		
	Reverse	Arrhenius	coefficients:	8.42E+11	0.2	17700
1979	IC8H16+OH=IC8H15+H2O	3.70E+13	0	3900		
	Reverse	Arrhenius	coefficients:	3.64E+13	-0.1	34460
1980	JC8H16+OH=IC8H15+H2O	3.70E+13	0	3900		
	Reverse	Arrhenius	coefficients:	1.71E+13	0.1	34000
1981	IC8H15=IC4H8+IC4H7-I1	8.99E+24	-3	53600		
	Reverse	Arrhenius	coefficients:	1.00E+11	0	10600
1982	IC8H16+CH3=IC8H15+CH4	2.00E+12	0	7300		
	Reverse	Arrhenius	coefficients:	1.69E+14	-0.4	24510
1983	JC8H16+CH3=IC8H15+CH4	2.00E+12	0	7300		
	Reverse	Arrhenius	coefficients:	7.91E+13	-0.2	24050
1984	IC8H16+OH=>CH3COCH3+NEOC5H11	1.00E+11	0	-4000		
1985	JC8H16+OH=>CH2O+PC7H15	1.00E+11	0	-4000		
1986	JC8H16+O=>CH2O+PC7H14	1.00E+11	0	-1050		
1987	IC8H18+CH3O2=AC8H17+CH3O2H	8.51E+04	2.5	16690		
1988	IC8H18+CH3O2=BC8H17+CH3O2H	4.12E+04	2.5	14680		
1989	IC8H18+CH3O2=CC8H17+CH3O2H	1.05E+04	2.5	12260		
1990	IC8H18+CH3O2=DC8H17+CH3O2H	5.67E+04	2.5	16690		
1991	IC8H18+AC8H17O2=AC8H17+AC8H17O2H	1.81E+13	0	20430		
	Reverse	Arrhenius	coefficients:	1.44E+10	0	15000
1992	IC8H18+BC8H17O2=AC8H17+BC8H17O2H	1.81E+13	0	20430		
	Reverse	Arrhenius	coefficients:	1.44E+10	0	15000
1993	IC8H18+CC8H17O2=AC8H17+CC8H17O2H	1.81E+13	0	20430		
	Reverse	Arrhenius	coefficients:	1.44E+10	0	15000
1994	IC8H18+DC8H17O2=AC8H17+DC8H17O2H	1.81E+13	0	20430		
	Reverse	Arrhenius	coefficients:	1.44E+10	0	15000
1995	IC8H18+AC8H17O2=BC8H17+AC8H17O2H	4.03E+12	0	17700		
	Reverse	Arrhenius	coefficients:	1.44E+10	0	15000
1996	IC8H18+BC8H17O2=BC8H17+BC8H17O2H	4.03E+12	0	17700		
	Reverse	Arrhenius	coefficients:	1.44E+10	0	15000
1997	IC8H18+CC8H17O2=BC8H17+CC8H17O2H	4.03E+12	0	17700		

	Reverse	Arrhenius	coefficients:	1.44E+10	0	15000
1998	IC8H18+DC8H17O2=BC8H17+DC8H17O2H	4.03E+12	0	17700		
	Reverse	Arrhenius	coefficients:	1.44E+10	0	15000
1999	IC8H18+AC8H17O2=CC8H17+AC8H17O2H	2.00E+12	0	16000		
	Reverse	Arrhenius	coefficients:	1.44E+10	0	15000
2000	IC8H18+BC8H17O2=CC8H17+BC8H17O2H	2.00E+12	0	16000		
	Reverse	Arrhenius	coefficients:	1.44E+10	0	15000
2001	IC8H18+CC8H17O2=CC8H17+CC8H17O2H	2.00E+12	0	16000		
	Reverse	Arrhenius	coefficients:	1.44E+10	0	15000
2002	IC8H18+DC8H17O2=CC8H17+DC8H17O2H	2.00E+12	0	16000		
	Reverse	Arrhenius	coefficients:	1.44E+10	0	15000
2003	IC8H18+AC8H17O2=DC8H17+AC8H17O2H	1.21E+13	0	20430		
	Reverse	Arrhenius	coefficients:	1.44E+10	0	15000
2004	IC8H18+BC8H17O2=DC8H17+BC8H17O2H	1.21E+13	0	20430		
	Reverse	Arrhenius	coefficients:	1.44E+10	0	15000
2005	IC8H18+CC8H17O2=DC8H17+CC8H17O2H	1.21E+13	0	20430		
	Reverse	Arrhenius	coefficients:	1.44E+10	0	15000
2006	IC8H18+DC8H17O2=DC8H17+DC8H17O2H	1.21E+13	0	20430		
	Reverse	Arrhenius	coefficients:	1.44E+10	0	15000
2007	IC8H18+O2CHO=AC8H17+HO2CHO	2.52E+13	0	20440		
	Reverse	Arrhenius	coefficients:	5.58E+02	2.3	3062
2008	IC8H18+O2CHO=BC8H17+HO2CHO	5.60E+12	0	17690		
	Reverse	Arrhenius	coefficients:	2.16E+01	2.7	2806
2009	IC8H18+O2CHO=CC8H17+HO2CHO	2.80E+12	0	16010		
	Reverse	Arrhenius	coefficients:	3.11E+00	2.9	4633
2010	IC8H18+O2CHO=DC8H17+HO2CHO	1.68E+13	0	20440		
	Reverse	Arrhenius	coefficients:	1.11E+03	2.3	3862
2011	IC8H18+IC4H6OH=AC8H17+IC4H7OH	7.05E+02	3.3	19840		
	Reverse	Arrhenius	coefficients:	2.77E-01	3.9	6526
2012	IC8H18+IC4H6OH=BC8H17+IC4H7OH	1.57E+02	3.3	18170		
	Reverse	Arrhenius	coefficients:	1.07E-02	4.3	7350
2013	IC8H18+IC4H6OH=CC8H17+IC4H7OH	8.44E+01	3.3	17170		
	Reverse	Arrhenius	coefficients:	1.66E-03	4.5	9648
2014	IC8H18+IC4H6OH=DC8H17+IC4H7OH	4.70E+02	3.3	19840		
	Reverse	Arrhenius	coefficients:	5.53E-01	3.9	7326
2015	AC8H17O2=AC8H17+O2	3.46E+20	-1.7	35720		
	Reverse	Arrhenius	coefficients:	4.52E+12	0	0
2016	BC8H17O2=BC8H17+O2	1.05E+23	-2.3	38840		
	Reverse	Arrhenius	coefficients:	7.54E+12	0	0
2017	CC8H17O2=CC8H17+O2	3.62E+24	-2.6	36010		
	Reverse	Arrhenius	coefficients:	1.41E+13	0	0
2018	DC8H17O2=DC8H17+O2	3.46E+20	-1.7	34920		
	Reverse	Arrhenius	coefficients:	4.52E+12	0	0
2019	AC8H17+AC8H17O2=2AC8H17O	7.00E+12	0	-1000		
	Reverse	Arrhenius	coefficients:	6.48E+13	-0.2	29360
2020	AC8H17+BC8H17O2=AC8H17O+BC8H17O	7.00E+12	0	-1000		

	Reverse	Arrhenius	coefficients:	4.99E+13	-0.1	28230
2021	AC8H17+CC8H17O2=AC8H17O+CC8H17O	7.00E+12	0	-1000		
	Reverse	Arrhenius	coefficients:	4.35E+13	-0.2	30170
2022	AC8H17+DC8H17O2=AC8H17O+DC8H17O	7.00E+12	0	-1000		
	Reverse	Arrhenius	coefficients:	3.25E+13	-0.2	29360
2023	BC8H17+AC8H17O2=BC8H17O+AC8H17O	7.00E+12	0	-1000		
	Reverse	Arrhenius	coefficients:	9.04E+15	-0.8	31350
2024	BC8H17+BC8H17O2=2BC8H17O	7.00E+12	0	-1000		
	Reverse	Arrhenius	coefficients:	6.96E+15	-0.8	30220
2025	BC8H17+CC8H17O2=BC8H17O+CC8H17O	7.00E+12	0	-1000		
	Reverse	Arrhenius	coefficients:	6.07E+15	-0.8	32160
2026	BC8H17+DC8H17O2=BC8H17O+DC8H17O	7.00E+12	0	-1000		
	Reverse	Arrhenius	coefficients:	4.54E+15	-0.8	31350
2027	CC8H17+AC8H17O2=CC8H17O+AC8H17O	7.00E+12	0	-1000		
	Reverse	Arrhenius	coefficients:	1.46E+17	-1.1	30460
2028	CC8H17+BC8H17O2=CC8H17O+BC8H17O	7.00E+12	0	-1000		
	Reverse	Arrhenius	coefficients:	1.12E+17	-1	29330
2029	CC8H17+CC8H17O2=2CC8H17O	7.00E+12	0	-1000		
	Reverse	Arrhenius	coefficients:	9.80E+16	-1.1	31270
2030	CC8H17+DC8H17O2=CC8H17O+DC8H17O	7.00E+12	0	-1000		
	Reverse	Arrhenius	coefficients:	7.32E+16	-1.1	30460
2031	DC8H17+AC8H17O2=DC8H17O+AC8H17O	7.00E+12	0	-1000		
	Reverse	Arrhenius	coefficients:	3.25E+13	-0.2	28560
2032	DC8H17+BC8H17O2=DC8H17O+BC8H17O	7.00E+12	0	-1000		
	Reverse	Arrhenius	coefficients:	2.50E+13	-0.1	27430
2033	DC8H17+CC8H17O2=DC8H17O+CC8H17O	7.00E+12	0	-1000		
	Reverse	Arrhenius	coefficients:	2.18E+13	-0.2	29370
2034	DC8H17+DC8H17O2=2DC8H17O	7.00E+12	0	-1000		
	Reverse	Arrhenius	coefficients:	1.63E+13	-0.2	28560
2035	AC8H17+HO2=AC8H17O+OH	7.00E+12	0	-1000		
	Reverse	Arrhenius	coefficients:	2.18E+15	-0.5	25880
2036	BC8H17+HO2=BC8H17O+OH	7.00E+12	0	-1000		
	Reverse	Arrhenius	coefficients:	3.04E+17	-1.1	27870
2037	CC8H17+HO2=CC8H17O+OH	7.00E+12	0	-1000		
	Reverse	Arrhenius	coefficients:	4.91E+18	-1.4	26980
2038	DC8H17+HO2=DC8H17O+OH	7.00E+12	0	-1000		
	Reverse	Arrhenius	coefficients:	1.09E+15	-0.5	25080
2039	AC8H17+CH3O2=AC8H17O+CH3O	7.00E+12	0	-1000		
	Reverse	Arrhenius	coefficients:	1.36E+14	-0.2	30120
2040	BC8H17+CH3O2=BC8H17O+CH3O	7.00E+12	0	-1000		
	Reverse	Arrhenius	coefficients:	1.90E+16	-0.8	32110
2041	CC8H17+CH3O2=CC8H17O+CH3O	7.00E+12	0	-1000		
	Reverse	Arrhenius	coefficients:	3.07E+17	-1.1	31220
2042	DC8H17+CH3O2=DC8H17O+CH3O	7.00E+12	0	-1000		
	Reverse	Arrhenius	coefficients:	6.84E+13	-0.2	29320
2043	AC8H17O2+HO2=AC8H17O2H+O2	1.75E+10	0	-3275		

	Reverse	Arrhenius	coefficients:	4.07E+13	-0.8	33620
2044	BC8H17O2+HO2=BC8H17O2H+O2	1.75E+10	0	-3275		
	Reverse	Arrhenius	coefficients:	3.75E+13	-0.8	33610
2045	CC8H17O2+HO2=CC8H17O2H+O2	1.75E+10	0	-3275		
	Reverse	Arrhenius	coefficients:	3.75E+13	-0.8	33610
2046	DC8H17O2+HO2=DC8H17O2H+O2	1.75E+10	0	-3275		
	Reverse	Arrhenius	coefficients:	4.07E+13	-0.8	33620
2047	H2O2+AC8H17O2=HO2+AC8H17O2H	2.40E+12	0	10000		
	Reverse	Arrhenius	coefficients:	2.40E+12	0	10000
2048	H2O2+BC8H17O2=HO2+BC8H17O2H	2.40E+12	0	10000		
	Reverse	Arrhenius	coefficients:	2.40E+12	0	10000
2049	H2O2+CC8H17O2=HO2+CC8H17O2H	2.40E+12	0	10000		
	Reverse	Arrhenius	coefficients:	2.40E+12	0	10000
2050	H2O2+DC8H17O2=HO2+DC8H17O2H	2.40E+12	0	10000		
	Reverse	Arrhenius	coefficients:	2.40E+12	0	10000
2051	AC8H17O2+CH3O2=>AC8H17O+CH3O+O2	1.40E+16	-1.6	1860		
2052	BC8H17O2+CH3O2=>BC8H17O+CH3O+O2	1.40E+16	-1.6	1860		
2053	CC8H17O2+CH3O2=>CC8H17O+CH3O+O2	1.40E+16	-1.6	1860		
2054	DC8H17O2+CH3O2=>DC8H17O+CH3O+O2	1.40E+16	-1.6	1860		
2055	2AC8H17O2=>O2+2AC8H17O	1.40E+16	-1.6	1860		
2056	AC8H17O2+BC8H17O2=>AC8H17O+BC8H17O+O2	1.40E+16	-1.6	1860		
2057	AC8H17O2+CC8H17O2=>AC8H17O+CC8H17O+O2	1.40E+16	-1.6	1860		
2058	AC8H17O2+DC8H17O2=>AC8H17O+DC8H17O+O2	1.40E+16	-1.6	1860		
2059	2BC8H17O2=>O2+2BC8H17O	1.40E+16	-1.6	1860		
2060	BC8H17O2+CC8H17O2=>BC8H17O+CC8H17O+O2	1.40E+16	-1.6	1860		
2061	BC8H17O2+DC8H17O2=>BC8H17O+DC8H17O+O2	1.40E+16	-1.6	1860		
2062	2CC8H17O2=>O2+2CC8H17O	1.40E+16	-1.6	1860		
2063	CC8H17O2+DC8H17O2=>CC8H17O+DC8H17O+O2	1.40E+16	-1.6	1860		
2064	2DC8H17O2=>O2+2DC8H17O	1.40E+16	-1.6	1860		
2065	AC8H17O2H=AC8H17O+OH	1.00E+16	0	39000		
	Reverse	Arrhenius	coefficients:	1.75E+07	1.9	-6742
2066	BC8H17O2H=BC8H17O+OH	1.00E+16	0	39000		
	Reverse	Arrhenius	coefficients:	1.46E+07	2	-7862
2067	CC8H17O2H=CC8H17O+OH	1.00E+16	0	39000		
	Reverse	Arrhenius	coefficients:	1.27E+07	1.9	-5922
2068	DC8H17O2H=DC8H17O+OH	1.00E+16	0	39000		
	Reverse	Arrhenius	coefficients:	8.77E+06	1.9	-6742
2069	AC8H17O=YC7H15+CH2O	5.69E+24	-3.2	19140		
	Reverse	Arrhenius	coefficients:	1.00E+11	0	11900
2070	BC8H17O=TC4H9+IC3H7CHO	3.11E+26	-3.6	15980		
	Reverse	Arrhenius	coefficients:	1.00E+11	0	11900
2071	BC8H17O=IC3H7+TC4H9CHO	3.33E+23	-2.9	18470		
	Reverse	Arrhenius	coefficients:	6.25E+10	0	12900

2072	CC8H17O=NEOC5H11+CH3COCH3	1.21E+20	-1.7	12340		
	Reverse	Arrhenius	coefficients:	1.00E+11	0	11900
2073	DC8H17O=PC7H15+CH2O	6.08E+22	-2.7	20470		
	Reverse	Arrhenius	coefficients:	1.00E+11	0	11900
2074	AC8H17O2=AC8H16OOH-A	7.50E+10	0	24000		
2075	AC8H17O2=AC8H16OOH-B	2.50E+10	0	20450		
2076	AC8H17O2=AC8H16OOH-C	1.56E+09	0	16650		
2077	AC8H17O2=AC8H16OOH-D	1.17E+09	0	25150		
2078	BC8H17O2=BC8H16OOH-A	1.12E+11	0	24000		
2079	BC8H17O2=BC8H16OOH-C	1.00E+11	0	23700		
2080	BC8H17O2=BC8H16OOH-D	7.50E+10	0	24000		
2081	CC8H17O2=CC8H16OOH-A	1.41E+10	0	21950		
2082	CC8H17O2=CC8H16OOH-B	2.00E+11	0	26450		
2083	CC8H17O2=CC8H16OOH-D	6.00E+11	0	29000		
2084	DC8H17O2=DC8H16OOH-A	1.76E+09	0	25150		
2085	DC8H17O2=DC8H16OOH-B	2.50E+10	0	20450		
2086	DC8H17O2=DC8H16OOH-C	1.00E+11	0	23700		
2087	DC8H17O2=DC8H16OOH-D	3.75E+10	0	24000		
2088	BC8H17O2=IC8H16+HO2	1.25E+36	-7.2	41490		
2089	CC8H17O2=IC8H16+HO2	1.50E+39	-8.1	42490		
2090	CC8H17O2=JC8H16+HO2	3.02E+43	-9.4	43490		
2091	DC8H17O2=JC8H16+HO2	1.25E+36	-7.2	41490		
2092	AC8H16OOH-A=>IC8ETERAA+OH	3.00E+11	0	14250		
2093	AC8H16OOH-B=>IC8ETERAB+OH	3.00E+11	0	14250		
2094	AC8H16OOH-C=>IC8ETERAC+OH	2.74E+10	0	7000		
2095	AC8H16OOH-D=>IC8ETERAD+OH	2.17E+09	0	1800		
2096	BC8H16OOH-C=>IC8ETERBC+OH	1.80E+12	0	22000		
2097	BC8H16OOH-A=>IC8ETERAB+OH	3.00E+11	0	14250		
2098	BC8H16OOH-D=>IC8ETERBD+OH	3.00E+11	0	14250		
2099	CC8H16OOH-B=>IC8ETERBC+OH	1.80E+12	0	22000		
2100	CC8H16OOH-A=>IC8ETERAC+OH	2.74E+10	0	7000		
2101	DC8H16OOH-D=>IC8ETERDD+OH	3.00E+11	0	14250		
2102	DC8H16OOH-B=>IC8ETERBD+OH	3.00E+11	0	14250		
2103	DC8H16OOH-A=>IC8ETERAD+OH	3.17E+09	0	1800		
2104	BC8H16OOH-C=IC8H16+HO2	1.53E+20	-2.4	24400		
	Reverse	Arrhenius	coefficients:	1.00E+11	0	12900
2105	CC8H16OOH-D=JC8H16+HO2	1.17E+22	-2.7	16740		
	Reverse	Arrhenius	coefficients:	1.00E+11	0	9600
2106	CC8H16OOH-B=IC8H16+HO2	1.13E+21	-2.5	22960		
	Reverse	Arrhenius	coefficients:	1.00E+11	0	12900
2107	DC8H16OOH-C=JC8H16+HO2	1.88E+18	-1.8	14960		
	Reverse	Arrhenius	coefficients:	1.00E+11	0	9600
2108	AC8H16OOH-A=>OH+CH2O+XC7H14	9.09E+17	-1.3	28580		
2109	AC8H16OOH-B=>OH+CH2O+YC7H14	1.25E+17	-1.1	28210		
2110	BC8H16OOH-A=>OH+IC3H7CHO+IC4H8	3.12E+21	-2.4	26330		
2111	BC8H16OOH-D=>OH+TC4H9CHO+C3H6	1.29E+21	-2.2	32970		

2112	DC8H16OOH-B=>OH+CH2O+OC7H14	1.12E+15	-0.5	30930		
2113	DC8H16OOH-D=>OH+CH2O+PC7H14	8.01E+15	-0.7	30890		
2114	AC8H16OOH-A=IC4H7OOH+TC4H9	1.51E+24	-3.1	26840		
	Reverse	Arrhenius	coefficients:	1.25E+11	0	12300
2115	AC8H16OOH-B=YC7H13OOH-X1+CH3	1.03E+16	-0.8	27450		
	Reverse	Arrhenius	coefficients:	1.25E+11	0	10900
2116	AC8H16OOH-B=OC7H13OOH-N+CH3	3.76E+14	-0.6	27330		
	Reverse	Arrhenius	coefficients:	1.25E+11	0	10200
2117	BC8H16OOH-A=XC7H13OOH-Z+CH3	2.14E+16	-0.8	29150		
	Reverse	Arrhenius	coefficients:	1.25E+11	0	10600
2118	BC8H16OOH-D=PC7H13OOH-O+CH3	1.40E+15	-0.7	31780		
	Reverse	Arrhenius	coefficients:	1.25E+11	0	9200
2119	DC8H16OOH-B=OC7H13OOH-Q+CH3	2.49E+14	-0.5	26930		
	Reverse	Arrhenius	coefficients:	1.25E+11	0	9200
2120	DC8H16OOH-B=YC7H13OOH-X2+CH3	4.77E+17	-1	29600		
	Reverse	Arrhenius	coefficients:	1.25E+11	0	13600
2121	DC8H16OOH-D=NEOC5H11+AC3H5OOH	2.01E+22	-2.4	30980		
	Reverse	Arrhenius	coefficients:	1.25E+11	0	9200
2122	AC8H16OOH-C=IC4H8+IC4H8O2H-T	5.57E+21	-2.4	27120		
	Reverse	Arrhenius	coefficients:	1.25E+11	0	7800
2123	CC8H16OOH-A=IC4H8+TC4H8O2H-I	1.73E+23	-2.8	29800		
	Reverse	Arrhenius	coefficients:	1.25E+11	0	10600
2124	AC8H16OOH-D=C3H6+NEOC5H10OOH	2.02E+19	-1.9	28830		
	Reverse	Arrhenius	coefficients:	1.42E+11	-0.3	9864
2125	AC8H16OOH-AO2=AC8H16OOH-A+O2	3.25E+20	-1.6	34920		
	Reverse	Arrhenius	coefficients:	4.52E+12	0	0
2126	AC8H16OOH-BO2=AC8H16OOH-B+O2	1.36E+23	-2.4	37280		
	Reverse	Arrhenius	coefficients:	7.54E+12	0	0
2127	AC8H16OOH-CO2=AC8H16OOH-C+O2	3.26E+24	-2.5	36700		
	Reverse	Arrhenius	coefficients:	1.41E+13	0	0
2128	BC8H16OOH-CO2=BC8H16OOH-C+O2	1.53E+24	-2.4	36620		
	Reverse	Arrhenius	coefficients:	1.41E+13	0	0
2129	BC8H16OOH-AO2=BC8H16OOH-A+O2	2.98E+20	-1.6	34900		
	Reverse	Arrhenius	coefficients:	4.52E+12	0	0
2130	BC8H16OOH-DO2=BC8H16OOH-D+O2	2.98E+20	-1.6	34900		
	Reverse	Arrhenius	coefficients:	4.52E+12	0	0
2131	CC8H16OOH-BO2=CC8H16OOH-B+O2	1.11E+23	-2.3	38060		
	Reverse	Arrhenius	coefficients:	7.54E+12	0	0
2132	CC8H16OOH-AO2=CC8H16OOH-A+O2	3.36E+20	-1.6	35720		
	Reverse	Arrhenius	coefficients:	4.52E+12	0	0
2133	DC8H16OOH-CO2=DC8H16OOH-C+O2	3.27E+24	-2.5	37500		
	Reverse	Arrhenius	coefficients:	1.41E+13	0	0
2134	DC8H16OOH-DO2=DC8H16OOH-D+O2	1.63E+20	-1.6	35720		
	Reverse	Arrhenius	coefficients:	4.52E+12	0	0
2135	DC8H16OOH-BO2=DC8H16OOH-B+O2	1.36E+23	-2.4	38080		
	Reverse	Arrhenius	coefficients:	7.54E+12	0	0

2136	AC8H16OOH-AO2=IC8KETAA+OH	2.50E+10	0	21000		
2137	AC8H16OOH-BO2=IC8KETAB+OH	2.50E+10	0	21000		
2138	AC8H16OOH-CO2=IC8KETAC+OH	3.12E+09	0	18950		
2139	BC8H16OOH-CO2=IC8KETBC+OH	1.00E+11	0	23450		
2140	BC8H16OOH-AO2=IC8KETBA+OH	1.25E+10	0	17450		
2141	BC8H16OOH-DO2=IC8KETBD+OH	1.25E+10	0	17450		
2142	DC8H16OOH-CO2=IC8KETDC+OH	2.00E+11	0	26000		
2143	DC8H16OOH-DO2=IC8KETDD+OH	2.50E+10	0	21000		
2144	DC8H16OOH-BO2=IC8KETDB+OH	2.50E+10	0	21000		
2145	IC8ETERAA+OH=>XC7H14+HCO+H2O	1.25E+12	0	0		
2146	IC8ETERAB+OH=>YC7H14+HCO+H2O	1.25E+12	0	0		
2147	IC8ETERAC+OH=>IC4H8+TC3H6CHO+H2O	1.25E+12	0	0		
2148	IC8ETERAD+OH=>C3H6+TC4H8CHO+H2O	1.25E+12	0	0		
2149	IC8ETERBC+OH=>IC3H5CHO+TC4H9+H2O	1.25E+12	0	0		
2150	IC8ETERBD+OH=>OC7H14+HCO+H2O	1.25E+12	0	0		
2151	IC8ETERDD+OH=>C2H3CHO+NEOC5H11+H2O	1.25E+12	0	0		
2152	IC8ETERAA+OH=>IC3H5CHO+IC4H9+H2O	1.25E+12	0	0		
2153	IC8ETERAB+OH=>IC4H8+IC3H7CO+H2O	1.25E+12	0	0		
2154	IC8ETERAC+OH=>CH2O+YC7H13-Y2+H2O	1.25E+12	0	0		
2155	IC8ETERAD+OH=>IC4H8+IC3H6CHO+H2O	1.25E+12	0	0		
2156	IC8ETERBC+OH=>IC3H6CO+TC4H9+H2O	1.25E+12	0	0		
2157	IC8ETERBD+OH=>C3H6+TC4H9CO+H2O	1.25E+12	0	0		
2158	IC8ETERDD+OH=>CH2O+PC7H13-O+H2O	1.25E+12	0	0		
2159	IC8ETERAA+HO2=>XC7H14+HCO+H2O2	2.50E+12	0	17700		
2160	IC8ETERAB+HO2=>YC7H14+HCO+H2O2	2.50E+12	0	17700		
2161	IC8ETERAC+HO2=>IC4H8+TC3H6CHO+H2O2	2.50E+12	0	17700		
2162	IC8ETERAD+HO2=>C3H6+TC4H8CHO+H2O2	2.50E+12	0	17700		
2163	IC8ETERBC+HO2=>IC3H5CHO+TC4H9+H2O2	2.50E+12	0	17700		
2164	IC8ETERBD+HO2=>OC7H14+HCO+H2O2	2.50E+12	0	17700		
2165	IC8ETERDD+HO2=>C2H3CHO+NEOC5H11+H2O2	2.50E+12	0	17700		
2166	IC8ETERAA+HO2=>IC3H5CHO+IC4H9+H2O2	2.50E+12	0	17700		
2167	IC8ETERAB+HO2=>IC4H8+IC3H7CO+H2O2	2.50E+12	0	17700		
2168	IC8ETERAC+HO2=>CH2O+YC7H13-Y2+H2O2	2.50E+12	0	17700		
2169	IC8ETERAD+HO2=>IC4H8+IC3H6CHO+H2O2	2.50E+12	0	17700		
2170	IC8ETERBC+HO2=>IC3H6CO+TC4H9+H2O2	2.50E+12	0	17700		
2171	IC8ETERBD+HO2=>C3H6+TC4H9CO+H2O2	2.50E+12	0	17700		
2172	IC8ETERDD+HO2=>CH2O+PC7H13-O+H2O2	2.50E+12	0	17700		
2173	IC8KETAA=>CH2O+DC6H12CHO-D+OH	1.00E+16	0	39000		
2174	IC8KETAB=>IC3H7CHO+TC3H6CHO+OH	1.00E+16	0	39000		
2175	IC8KETAC=>CH3COCH3+TC4H8CHO+OH	1.00E+16	0	39000		
2176	IC8KETBC=>CH3COCH3+TC4H9CO+OH	1.00E+16	0	39000		
2177	IC8KETBA=>CH2O+IC3H7COC3H6-T+OH	1.00E+16	0	39000		
2178	IC8KETBD=>CH2O+TC4H9COC2H4S+OH	1.00E+16	0	39000		
2179	IC8KETDD=>CH2O+HC6H12CHO+OH	1.00E+16	0	39000		
2180	IC8KETDB=>TC4H9CHO+CH3CHCHO+OH	1.00E+16	0	39000		

2181	CC8H16OH-B=IC8H16+OH	5.84E+16	-1	35400		
	Reverse	Arrhenius	coefficients:	1.00E+12	0	-1042
2182	BC8H16OH-C=IC8H16+OH	6.33E+15	-0.8	34880		
	Reverse	Arrhenius	coefficients:	1.00E+12	0	-1042
2183	CC8H16OH-D=JC8H16+OH	8.35E+17	-1.3	32550		
	Reverse	Arrhenius	coefficients:	1.00E+12	0	-1042
2184	CC8H16OH-D=NEOC5H11+IC3H5OH	1.62E+22	-2.5	31020		
	Reverse	Arrhenius	coefficients:	1.00E+11	0	9200
2185	BC8H16OH-C=TC4H9+IC4H7OH	3.44E+22	-2.6	32690		
	Reverse	Arrhenius	coefficients:	1.00E+11	0	9200
2186	CC8H16OH-BO2=CC8H16OH-B+O2	7.68E+20	-2	35510		
	Reverse	Arrhenius	coefficients:	1.50E+12	0	0
2187	BC8H16OH-CO2=BC8H16OH-C+O2	1.03E+22	-2.2	34770		
	Reverse	Arrhenius	coefficients:	2.00E+12	0	0
2188	CC8H16OH-BO2=CC8H16O-BO2H	1.20E+12	0	18900		
	Reverse	Arrhenius	coefficients:	1.42E+15	-0.9	3590
2189	BC8H16OH-CO2=BC8H16O-CO2H	1.20E+12	0	18900		
	Reverse	Arrhenius	coefficients:	1.38E+15	-0.9	3580
2190	CC8H16O- BO2H=>TC4H9CHO+CH3COCH3+OH	3.86E+23	-3.1	13000		
2191	BC8H16O- CO2H=>TC4H9CHO+CH3COCH3+OH	1.61E+23	-2.9	15090		
2192	DC6H12CHO-D=IC3H5CHO+IC3H7	7.83E+15	-0.6	31510		
	Reverse	Arrhenius	coefficients:	1.00E+11	0	8300
2193	IC3H7COC3H6-T=IC3H6CO+IC3H7	1.22E+17	-0.6	42050		
	Reverse	Arrhenius	coefficients:	1.00E+11	0	11900
2194	TC4H9COC2H5+OH=TC4H9COC2H4S+H2O	8.95E+11	0	-228		
	Reverse	Arrhenius	coefficients:	1.59E+13	-0.2	28620
2195	TC4H9COC2H5+HO2=TC4H9COC2H4S+H2O2	2.00E+11	0	8698		
	Reverse	Arrhenius	coefficients:	2.11E+13	-0.6	6080
2196	TC4H9COC2H5+CH3O2=TC4H9COC2H4S+CH 3O2H	2.00E+12	0	15250		
	Reverse	Arrhenius	coefficients:	8.65E+14	-0.7	11910
2197	TC4H9COC2H4S=CH3CHCO+TC4H9	4.60E+20	-1.9	38250		
	Reverse	Arrhenius	coefficients:	1.00E+11	0	10600
2198	HC6H12CHO=C2H3CHO+TC4H9	6.88E+19	-1.8	27690		
	Reverse	Arrhenius	coefficients:	1.00E+11	0	7800
2199	YC7H13OOH-X1=YC7H13O-X1+OH	4.18E+20	-1.7	47810		
	Reverse	Arrhenius	coefficients:	2.00E+13	0	0
2200	XC7H13OOH-Z=XC7H13O-Z+OH	3.76E+21	-1.9	46430		
	Reverse	Arrhenius	coefficients:	2.00E+13	0	0
2201	YC7H13OOH-X2=YC7H13O-X2+OH	1.88E+20	-1.5	47030		
	Reverse	Arrhenius	coefficients:	2.00E+13	0	0
2202	OC7H13OOH-N=OC7H13O-N+OH	1.83E+20	-1.5	47020		
	Reverse	Arrhenius	coefficients:	2.00E+13	0	0
2203	OC7H13OOH-Q=OC7H13O-Q+OH	4.19E+20	-1.7	47840		
	Reverse	Arrhenius	coefficients:	2.00E+13	0	0
2204	PC7H13OOH-O=PC7H13O-O+OH	8.22E+19	-1.2	42490		



	Reverse	Arrhenius	coefficients:	2.00E+13	0	0
2205	YC7H13O-X1=CH2O+CC6H11-D	2.66E+21	-2.4	34870		
	Reverse	Arrhenius	coefficients:	1.00E+11	0	11900
2206	YC7H13O-X2=CH2O+CC6H11-D	7.56E+18	-2.2	10260		
	Reverse	Arrhenius	coefficients:	1.00E+11	0	11900
2207	OC7H13O-N=CH2O+CC6H11-B	1.14E+18	-1.8	2305		
	Reverse	Arrhenius	coefficients:	1.00E+11	0	9600
2208	OC7H13O-Q=CH2O+NEOC6H11	2.72E+16	-1	29510		
	Reverse	Arrhenius	coefficients:	1.00E+11	0	9600
2209	CC6H11-D=C3H4-P+IC3H7	4.79E+12	0.3	28960		
	Reverse	Arrhenius	coefficients:	1.00E+11	0	7800
2210	DC6H11-D=C3H4-A+IC3H7	2.69E+16	-0.9	30540		
	Reverse	Arrhenius	coefficients:	1.00E+11	0	7800
2211	IC4H6OH+H2O=IC4H7OH+OH	5.88E+06	1.9	30240		
	Reverse	Arrhenius	coefficients:	3.12E+06	2	-298
2212	IC4H6OH+CH4=IC4H7OH+CH3	3.57E+02	3.1	22870		
	Reverse	Arrhenius	coefficients:	2.21E+00	3.5	5675
2213	IC4H6OH+C3H6=IC4H7OH+C3H5-A	2.51E+02	3.2	18640		
	Reverse	Arrhenius	coefficients:	5.75E+02	3.1	18660
2214	IC4H6OH+CH3CHO=IC4H7OH+CH3CO	1.36E+09	1.4	17940		
	Reverse	Arrhenius	coefficients:	5.30E+06	2	16240
2215	C3H5-A+CH2O=C3H6+HCO	6.30E+08	1.9	18190		
	Reverse	Arrhenius	coefficients:	9.16E+06	2.2	17700
2216	IC3H6CHCOCH2=IC4H7+CH2CO	1.40E+14	-1.6	50750		
	Reverse	Arrhenius	coefficients:	8.00E+10	0	11900
2217	CH3COCH3=CH3CO+CH3	1.22E+23	-2	83950		
	Reverse	Arrhenius	coefficients:	1.00E+13	0	0
2218	AC5H10+OH=IC5H9+H2O	1.00E+12	0	1230		
	Reverse	Arrhenius	coefficients:	5.00E+12	0	26500
2219	BC5H10+OH=IC5H9+H2O	1.00E+12	0	1230		
	Reverse	Arrhenius	coefficients:	5.00E+12	0	26500
2220	CC5H10+OH=IC5H9+H2O	1.00E+12	0	1230		
	Reverse	Arrhenius	coefficients:	5.00E+12	0	26500
2221	AC5H10+H=IC5H9+H2	1.00E+12	0	3800		
	Reverse	Arrhenius	coefficients:	1.00E+12	0	25000
2222	BC5H10+H=IC5H9+H2	1.00E+12	0	3800		
	Reverse	Arrhenius	coefficients:	1.00E+12	0	25000
2223	CC5H10+H=IC5H9+H2	1.00E+12	0	3800		
	Reverse	Arrhenius	coefficients:	1.00E+12	0	25000
2224	AC5H10+CH3=IC5H9+CH4	5.00E+11	0	7300		
	Reverse	Arrhenius	coefficients:	6.00E+11	0	25000
2225	BC5H10+CH3=IC5H9+CH4	5.00E+11	0	7300		
	Reverse	Arrhenius	coefficients:	6.00E+11	0	25000
2226	CC5H10+CH3=IC5H9+CH4	5.00E+11	0	7300		
	Reverse	Arrhenius	coefficients:	6.00E+11	0	25000
2227	AC5H10+O=IC5H9+OH	3.70E+05	2.6	-1130		

	Reverse	Arrhenius	coefficients:	1.00E+12	0	25000
2228	BC5H10+O=IC5H9+OH	3.70E+05	2.6	-1130		
	Reverse	Arrhenius	coefficients:	1.00E+12	0	25000
2229	CC5H10+O=IC5H9+OH	3.70E+05	2.6	-1130		
	Reverse	Arrhenius	coefficients:	1.00E+12	0	25000
2230	IC5H9=C3H4-A+C2H5	1.98E+20	-1.6	59240		
	Reverse	Arrhenius	coefficients:	2.00E+11	0	8300
2231	C5H11-1=C2H4+NC3H7	7.97E+17	-1.4	29790		
	Reverse	Arrhenius	coefficients:	3.30E+11	0	7200
2232	C5H11-1=H+C5H10-1	3.48E+15	-0.7	37880		
	Reverse	Arrhenius	coefficients:	1.00E+13	0	2900
2233	C5H11-1+O2=C5H10-1+HO2	3.00E-19	0	3000		
	Reverse	Arrhenius	coefficients:	2.00E-19	0	17500
2234	C5H11-1=C5H11-2	3.88E+09	0.3	19760		
	Reverse	Arrhenius	coefficients:	1.83E+13	-0.6	24360
2235	C5H11-2+O2=C5H10-1+HO2	4.50E-19	0	5020		
	Reverse	Arrhenius	coefficients:	2.00E-19	0	17500
2236	C5H11-2+O2=C5H10-2+HO2	3.00E-19	0	3000		
	Reverse	Arrhenius	coefficients:	2.00E-19	0	17500
2237	C5H10-2=CH3+C4H7	1.00E+16	0	71000		
	Reverse	Arrhenius	coefficients:	1.00E+13	0	0
2238	C5H10-2+H=C5H9+H2	2.90E+13	0	4000		
	Reverse	Arrhenius	coefficients:	1.00E+12	0	14000
2239	C5H10-2+O=C5H9+OH	2.43E+05	2.6	-1130		
	Reverse	Arrhenius	coefficients:	7.00E+11	0	29900
2240	C5H10-2+OH=C5H9+H2O	4.30E+13	0	3060		
	Reverse	Arrhenius	coefficients:	5.00E+12	0	26500
2241	C5H10-2+CH3=C5H9+CH4	1.00E+11	0	8200		
	Reverse	Arrhenius	coefficients:	6.00E+11	0	18800
2242	NEOC5H12=TC4H9+CH3	1.74E+22	-1.6	84020		
	Reverse	Arrhenius	coefficients:	4.00E+12	0	-596
2243	NEOC5H12=NEOC5H11+H	1.51E+19	-0.8	102000		
	Reverse	Arrhenius	coefficients:	1.00E+14	0	0
2244	C2H5O+M=CH3+CH2O+M	1.35E+38	-7	23800		
	Reverse	Arrhenius	coefficients:	6.44E+36	-7	16850
2245	C2H5O+M=CH3CHO+H+M	1.16E+35	-5.9	25270		
	Reverse	Arrhenius	coefficients:	3.06E+30	-4.8	6100
2246	IC3H7O2+C4H7=IC3H7O+C4H7O	7.00E+12	0	-1000		
	Reverse	Arrhenius	coefficients:	7.63E+08	0.8	19530
2247	NC3H7O2+C4H7=NC3H7O+C4H7O	7.00E+12	0	-1000		
	Reverse	Arrhenius	coefficients:	6.13E+08	0.8	19790
2248	C4H7+HO2=C4H7O+OH	7.00E+12	0	-1000		
	Reverse	Arrhenius	coefficients:	1.01E+11	0.3	16890
2249	C4H7+CH3O2=C4H7O+CH3O	7.00E+12	0	-1000		
	Reverse	Arrhenius	coefficients:	9.84E+12	-0.3	21650
2250	C4H7+C2H5O2=C4H7O+C2H5O	7.00E+12	0	-1000		

	Reverse	Arrhenius	coefficients:	6.95E+08	0.8	19810
2251	C4H7+PC4H9O2=C4H7O+PC4H9O	7.00E+12	0	-1000		
	Reverse	Arrhenius	coefficients:	5.78E+08	0.8	19780
2252	C4H7+SC4H9O2=C4H7O+SC4H9O	7.00E+12	0	-1000		
	Reverse	Arrhenius	coefficients:	6.76E+08	0.8	19510
2253	C4H8-2+CH3CO3=C4H7+CH3CO3H	1.00E+11	0	8000		
	Reverse	Arrhenius	coefficients:	2.00E+10	0	10000
2254	C4H8-2+CH3O2=C4H7+CH3O2H	3.20E+12	0	14900		
	Reverse	Arrhenius	coefficients:	1.58E+11	0	14700
2255	C4H8-2+C2H5O2=C4H7+C2H5O2H	3.20E+12	0	14900		
	Reverse	Arrhenius	coefficients:	1.58E+11	0	14700
2256	C4H8-2+NC3H7O2=C4H7+NC3H7O2H	3.20E+12	0	14900		
	Reverse	Arrhenius	coefficients:	1.58E+11	0	14700
2257	C4H8-2+IC3H7O2=C4H7+IC3H7O2H	3.20E+12	0	14900		
	Reverse	Arrhenius	coefficients:	1.58E+11	0	14700
2258	C4H8-2+PC4H9O2=C4H7+PC4H9O2H	3.20E+12	0	14900		
	Reverse	Arrhenius	coefficients:	1.58E+11	0	14700
2259	IC4H9O2+C4H8-2=IC4H9O2H+C4H7	1.40E+12	0	14900		
	Reverse	Arrhenius	coefficients:	3.16E+11	0	13000
2260	TC4H9O2+C4H8-2=TC4H9O2H+C4H7	1.40E+12	0	14900		
	Reverse	Arrhenius	coefficients:	3.16E+11	0	13000
2261	C4H8-1+OH=NC3H7+CH2O	1.00E+12	0	0		
	Reverse	Arrhenius	coefficients:	1.62E+12	0	13230
2262	C4H8-1+O=C3H6+CH2O	7.23E+05	2.3	-1050		
	Reverse	Arrhenius	coefficients:	2.00E+05	2.3	80280
2263	C4H8-1+O=CH3CHO+C2H4	1.30E+13	0	850		
	Reverse	Arrhenius	coefficients:	2.07E+12	0	85100
2264	C4H8-1+O=CH3CO+C2H5	1.30E+13	0	850		
	Reverse	Arrhenius	coefficients:	2.35E+12	0	38150
2265	C4H8-1+OH=CH3CHO+C2H5	1.00E+12	0	0		
	Reverse	Arrhenius	coefficients:	9.33E+12	0	19930
2266	C4H8-1+OH=CH3CO+C2H6	5.00E+11	0	0		
	Reverse	Arrhenius	coefficients:	9.83E+12	0	32430
2267	C4H8-1+O=C2H5CHO+CH2	1.30E+13	0	850		
	Reverse	Arrhenius	coefficients:	5.71E+09	0	11000
2268	C4H8-1+O=C2H5CO+CH3	1.30E+13	0	850		
	Reverse	Arrhenius	coefficients:	4.80E+11	0	32550
2269	C4H8-1+OH=C2H5CHO+CH3	1.00E+12	0	0		
	Reverse	Arrhenius	coefficients:	4.95E+10	0	16940
2270	C4H8-1+OH=C2H5CO+CH4	5.00E+11	0	0		
	Reverse	Arrhenius	coefficients:	2.20E+13	0	34270
2271	C4H8-1+CH3CO3=C4H7+CH3CO3H	1.00E+11	0	8000		
	Reverse	Arrhenius	coefficients:	2.00E+10	0	10000
2272	C4H8-1+CH3O2=C4H7+CH3O2H	1.40E+12	0	14900		
	Reverse	Arrhenius	coefficients:	3.16E+11	0	13000
2273	C4H8-1+C2H5O2=C4H7+C2H5O2H	1.40E+12	0	14900		

	Reverse	Arrhenius	coefficients:	3.16E+11	0	13000
2274	C4H8-1+NC3H7O2=C4H7+NC3H7O2H	1.40E+12	0	14900		
	Reverse	Arrhenius	coefficients:	3.16E+11	0	13000
2275	C4H8-1+IC3H7O2=C4H7+IC3H7O2H	1.40E+12	0	14900		
	Reverse	Arrhenius	coefficients:	3.16E+11	0	13000
2276	C4H8-1+PC4H9O2=C4H7+PC4H9O2H	1.40E+12	0	14900		
	Reverse	Arrhenius	coefficients:	3.16E+11	0	13000
2277	IC4H9O2+C4H8-1=IC4H9O2H+C4H7	1.40E+12	0	14900		
	Reverse	Arrhenius	coefficients:	3.16E+11	0	13000
2278	TC4H9O2+C4H8-1=TC4H9O2H+C4H7	1.40E+12	0	14900		
	Reverse	Arrhenius	coefficients:	3.16E+11	0	13000
2279	IC4H9O2+C4H7=IC4H9O+C4H7O	7.00E+12	0	-1000		
	Reverse	Arrhenius	coefficients:	5.85E+08	0.8	19580
2280	TC4H9O2+C4H7=TC4H9O+C4H7O	7.00E+12	0	-1000		
	Reverse	Arrhenius	coefficients:	2.62E+08	0.8	20600
2281	C2H5CHO+PC4H9=C2H5CO+C4H10	1.70E+12	0	8440		
	Reverse	Arrhenius	coefficients:	9.70E+13	0	18820
2282	C2H5CHO+SC4H9=C2H5CO+C4H10	1.70E+12	0	8440		
	Reverse	Arrhenius	coefficients:	9.70E+13	0	18820
2283	C2H5CHO+C4H7=C2H5CO+C4H8-1	1.70E+12	0	8440		
	Reverse	Arrhenius	coefficients:	1.00E+13	0	28000
2284	C2H5CHO+C4H7=C2H5CO+C4H8-2	1.70E+12	0	8440		
	Reverse	Arrhenius	coefficients:	1.00E+13	0	28000
2285	C5H11O2-1=C5H11-1+O2	1.96E+20	-1.5	35810		
	Reverse	Arrhenius	coefficients:	4.52E+12	0	0
2286	C5H11-1+C5H11O2-1=2C5H11O-1	7.00E+12	0	-1000		
	Reverse	Arrhenius	coefficients:	3.87E+13	0	29890
2287	C5H11-1+C5H11O2-2=C5H11O-1+C5H11O-2	7.00E+12	0	-1000		
	Reverse	Arrhenius	coefficients:	3.44E+13	0	29580
2288	C5H11O2-2=C5H11-2+O2	5.19E+17	-0.8	35970		
	Reverse	Arrhenius	coefficients:	7.54E+12	0	0
2289	C5H11-2+C5H11O2-1=C5H11O-2+C5H11O-1	7.00E+12	0	-1000		
	Reverse	Arrhenius	coefficients:	5.47E+10	0.7	29740
2290	C5H11-2+C5H11O2-2=2C5H11O-2	7.00E+12	0	-1000		
	Reverse	Arrhenius	coefficients:	4.87E+10	0.7	29430
2291	C5H11O2-1=C5H10OOH1-2	2.00E+11	0	26850		
	Reverse	Arrhenius	coefficients:	2.08E+10	-0.1	13850
2292	C5H11O2-1=C5H10OOH1-3	2.50E+10	0	20850		
	Reverse	Arrhenius	coefficients:	2.60E+09	-0.1	7850
2293	C5H11O2-1=C5H10OOH1-4	3.12E+09	0	19050		
	Reverse	Arrhenius	coefficients:	3.26E+08	-0.1	6050
2294	C5H11O2-1+C5H11O2-2=>O2+C5H11O-1+C5H11O-2	1.40E+16	-1.6	1860		
2295	C5H11O2-1+CH3O2=>O2+C5H11O-1+CH3O	1.40E+16	-1.6	1860		
2296	2C5H11O2-1=>O2+2C5H11O-1	1.40E+16	-1.6	1860		
2297	H2O2+C5H11O2-1=HO2+C5H11O2H-1	2.40E+12	0	10000		

	Reverse	Arrhenius	coefficients:	2.40E+12	0	10000
2298	C5H11O2-1+HO2=C5H11O2H-1+O2	1.75E+10	0	-3275		
	Reverse	Arrhenius	coefficients:	4.98E+13	-0.8	34480
2299	C5H11O2-2=C5H10OOH2-3	2.00E+11	0	26850		
	Reverse	Arrhenius	coefficients:	2.70E+10	-0.1	13900
2300	C5H11O2-2=C5H10OOH2-4	2.50E+10	0	20850		
	Reverse	Arrhenius	coefficients:	3.37E+09	-0.1	7900
2301	C5H11O2-2+CH3O2=>O2+C5H11O-2+CH3O	1.40E+16	-1.6	1860		
2302	2C5H11O2-2=>O2+2C5H11O-2	1.40E+16	-1.6	1860		
2303	C5H11O2H-1=C5H11O-1+OH	1.50E+16	0	42500		
	Reverse	Arrhenius	coefficients:	1.41E+08	1.8	-3055
2304	C5H11O-1=CH2O+PC4H9	4.24E+16	-1	20010		
	Reverse	Arrhenius	coefficients:	6.25E+10	0	11900
2305	C5H11O-2=CH3CHO+NC3H7	1.66E+21	-2.3	20880		
	Reverse	Arrhenius	coefficients:	7.50E+10	0	11900
2306	C5H10OOH1-3=>C5H10O1-3+OH	5.00E+10	0	15250		
2307	C5H10OOH1-4=>C5H10O1-4+OH	6.25E+09	0	6000		
2308	C5H10OOH2-4=>C5H10O2-4+OH	5.00E+10	0	15250		
2309	C5H10OOH1-2=C5H10-1+HO2	5.73E+17	-1.6	15900		
	Reverse	Arrhenius	coefficients:	1.25E+11	0	8070
2310	C5H10OOH2-3=C5H10-2+HO2	1.60E+20	-2.5	17860		
	Reverse	Arrhenius	coefficients:	1.25E+11	0	8070
2311	C5H10OOH1-3=>OH+CH2O+C4H8-1	8.28E+13	-0.2	30090		
2312	C5H10OOH2-4=>OH+CH3CHO+C3H6	8.31E+17	-1.4	27170		
2313	C5H10OOH1-2O2=C5H10OOH1-2+O2	8.04E+22	-2.3	37970		
	Reverse	Arrhenius	coefficients:	7.54E+12	0	0
2314	C5H10OOH1-3O2=C5H10OOH1-3+O2	8.04E+22	-2.3	37970		
	Reverse	Arrhenius	coefficients:	7.54E+12	0	0
2315	C5H10OOH1-4O2=C5H10OOH1-4+O2	8.04E+22	-2.3	37970		
	Reverse	Arrhenius	coefficients:	7.54E+12	0	0
2316	C5H10OOH2-4O2=C5H10OOH2-4+O2	7.25E+22	-2.3	37910		
	Reverse	Arrhenius	coefficients:	7.54E+12	0	0
2317	C5H10OOH1-2O2=NC5KET12+OH	2.00E+11	0	26400		
	Reverse	Arrhenius	coefficients:	1.34E+05	1.2	48910
2318	C5H10OOH1-3O2=NC5KET13+OH	2.50E+10	0	21400		
	Reverse	Arrhenius	coefficients:	5.33E+03	1.4	44700
2319	C5H10OOH1-4O2=NC5KET14+OH	3.12E+09	0	19350		
	Reverse	Arrhenius	coefficients:	6.66E+02	1.4	42650
2320	C5H10OOH2-4O2=NC5KET24+OH	1.25E+10	0	17850		
	Reverse	Arrhenius	coefficients:	2.70E+02	1.8	43880
2321	C5H10O1-3+OH=>C2H4+C2H5CO+H2O	2.50E+12	0	0		
2322	C5H10O1-4+OH=>CH3COCH2+C2H4+H2O	2.50E+12	0	0		
2323	C5H10O2-4+OH=>CH3CO+C3H6+H2O	2.50E+12	0	0		
2324	C5H10O1-3+OH=>HCO+C4H8-1+H2O	2.50E+12	0	0		
2325	C5H10O1-4+OH=>CH2CHO+C3H6+H2O	2.50E+12	0	0		
2326	C5H10O2-4+OH=>CH3CHO+C3H5-S+H2O	2.50E+12	0	0		

2327	$C_5H_{10}O_1-3+HO_2 \Rightarrow C_2H_4+C_2H_5CO+H_2O_2$	5.00E+12	0	17700		
2328	$C_5H_{10}O_1-4+HO_2 \Rightarrow CH_3COCH_2+C_2H_4+H_2O_2$	5.00E+12	0	17700		
2329	$C_5H_{10}O_2-4+HO_2 \Rightarrow CH_3CO+C_3H_6+H_2O_2$	5.00E+12	0	17700		
2330	$C_5H_{10}O_1-3+HO_2 \Rightarrow HCO+C_4H_8-1+H_2O_2$	5.00E+12	0	17700		
2331	$C_5H_{10}O_1-4+HO_2 \Rightarrow CH_2CHO+C_3H_6+H_2O_2$	5.00E+12	0	17700		
2332	$C_5H_{10}O_2-4+HO_2 \Rightarrow CH_3CHO+C_3H_5-S+H_2O_2$	5.00E+12	0	17700		
2333	$C_3H_5-A+HO_2=C_2H_3+CH_2O+OH$	1.00E-18	0	0		
	Reverse	Arrhenius	coefficients:	1.00E-30	0	0
2334	$C_3H_5-T+O_2=CH_3COCH_2+O$	3.81E+17	-1.4	5580		
	Reverse	Arrhenius	coefficients:	2.00E+11	0	17500
2335	$NC_5KET12 \Rightarrow NC_3H_7CHO+HCO+OH$	1.05E+16	0	41600		
2336	$NC_5KET13 \Rightarrow C_2H_5CHO+CH_2CHO+OH$	1.05E+16	0	41600		
2337	$NC_5KET14 \Rightarrow CH_3CHO+CH_2CH_2CHO+OH$	1.05E+16	0	41600		
2338	$NC_5KET24 \Rightarrow CH_3CHO+CH_3COCH_2+OH$	1.50E+16	0	42000		
2339	$HCCO+O_2=CO_2+HCO$	2.40E+11	0	-854		
	Reverse	Arrhenius	coefficients:	1.47E+14	0	133600
2340	$C_2H_4+H_2=2CH_3$	3.77E+12	0.8	84710		
	Reverse	Arrhenius	coefficients:	1.00E+14	0	32000
2341	$IC_3H_6CO+H \Rightarrow IC_3H_7+CO$	4.40E+12	0	1459		
2342	$IC_3H_6CO+O \Rightarrow CH_3COCH_3+CO$	3.20E+12	0	-437		
2343	$CH_3CHCHO+HO_2=C_2H_5CHO+O_2$	7.35E+12	0	1310		
	Reverse	Arrhenius	coefficients:	8.07E+13	-0.1	45070
2344	$CH_3CHCHO+HO_2=CH_3CHOCHO+OH$	9.64E+12	0	0		
	Reverse	Arrhenius	coefficients:	1.55E+16	-1	21740
2345	$CH_3CHOCHO=CH_3CHO+HCO$	3.98E+13	0	9700		
	Reverse	Arrhenius	coefficients:	4.34E+05	1.7	8282
2346	$C_2H_5CHO+HO_2=CH_3CHCHO+H_2O_2$	8.00E+10	0	11920		
	Reverse	Arrhenius	coefficients:	1.03E+13	-0.6	9337
2347	$CH_3CHCHO+O_2=CH_3CHCO+HO_2$	1.81E+11	0	1840		
	Reverse	Arrhenius	coefficients:	2.73E+10	0	12690
2348	$CH_3CHCHO+O_2=C_2H_3CHO+HO_2$	2.72E+11	0	7240		
	Reverse	Arrhenius	coefficients:	1.73E+11	-0.2	19040
2349	$CH_3CHCHO+O_2 \Rightarrow CH_3CHO+CO+OH$	3.62E+10	0	0		
2350	$NC_3H_7COC_2H_4P=NC_3H_7CO+C_2H_4$	5.40E+17	-1.4	26040		
	Reverse	Arrhenius	coefficients:	2.50E+11	0	7800
2351	$NEOC_5H_9Q_2 \Rightarrow IC_4H_7OOH+CH_2O+OH$	3.42E+14	0.4	30920		
2352	$C_5H_{11}-1+HO_2=C_5H_{11}O-1+OH$	7.00E+12	0	-1000		
	Reverse	Arrhenius	coefficients:	8.08E+15	-0.6	27010
2353	$C_5H_{11}-2+HO_2=C_5H_{11}O-2+OH$	7.00E+12	0	-1000		
	Reverse	Arrhenius	coefficients:	1.14E+13	0.1	26860
2354	$C_5H_{11}-1+CH_3O_2=C_5H_{11}O-1+CH_3O$	7.00E+12	0	-1000		
	Reverse	Arrhenius	coefficients:	7.89E+17	-1.2	31770
2355	$C_5H_{11}-2+CH_3O_2=C_5H_{11}O-2+CH_3O$	7.00E+12	0	-1000		
	Reverse	Arrhenius	coefficients:	1.12E+15	-0.4	31620
2356	$C_6H_{13}-1+O_2=C_6H_{12}-1+HO_2$	3.00E-19	0	3000		
	Reverse	Arrhenius	coefficients:	2.00E-19	0	17500

2357	$C_6H_{13-2}+O_2=C_6H_{12-1}+HO_2$	4.50E-19	0	5020		
	Reverse	Arrhenius	coefficients:	2.00E-19	0	17500
2358	$C_6H_{13-2}+O_2=C_6H_{12-2}+HO_2$	3.00E-19	0	3000		
	Reverse	Arrhenius	coefficients:	2.00E-19	0	17500
2359	$C_6H_{13-3}+O_2=C_6H_{12-2}+HO_2$	3.00E-19	0	3000		
	Reverse	Arrhenius	coefficients:	2.00E-19	0	17500
2360	$C_6H_{13-3}+O_2=C_6H_{12-3}+HO_2$	3.00E-19	0	3000		
	Reverse	Arrhenius	coefficients:	2.00E-19	0	17500
2361	$C_6H_{13-1}=C_2H_4+PC_4H_9$	5.45E+17	-1.3	29580		
	Reverse	Arrhenius	coefficients:	3.30E+11	0	7200
2362	$C_6H_{13-1}=C_6H_{12-1}+H$	2.09E+16	-0.9	37940		
	Reverse	Arrhenius	coefficients:	1.00E+13	0	2900
2363	$C_6H_{13-2}=C_3H_6+NC_3H_7$	2.08E+16	-0.9	29400		
	Reverse	Arrhenius	coefficients:	1.50E+11	0	7200
2364	$C_6H_{13-2}=C_6H_{12-1}+H$	1.36E+15	-0.6	38760		
	Reverse	Arrhenius	coefficients:	1.00E+13	0	1200
2365	$C_6H_{13-2}=C_6H_{12-2}+H$	2.76E+15	-0.7	37590		
	Reverse	Arrhenius	coefficients:	1.00E+13	0	2900
2366	$C_6H_{13-3}=C_4H_8-1+C_2H_5$	5.61E+17	-1.3	29600		
	Reverse	Arrhenius	coefficients:	1.50E+11	0	7200
2367	$C_6H_{13-3}=C_5H_{10-1}+CH_3$	6.27E+12	0	28680		
	Reverse	Arrhenius	coefficients:	1.50E+11	0	7200
2368	$C_6H_{13-3}=C_6H_{12-2}+H$	2.76E+15	-0.7	37590		
	Reverse	Arrhenius	coefficients:	1.00E+13	0	2900
2369	$C_6H_{13-3}=C_6H_{12-3}+H$	1.01E+15	-0.7	37680		
	Reverse	Arrhenius	coefficients:	1.00E+13	0	2900
2370	$C_6H_{13-1}=C_6H_{13-2}$	5.48E+08	1.6	38760		
	Reverse	Arrhenius	coefficients:	3.56E+07	2	41270
2371	$C_6H_{13-1}=C_6H_{13-3}$	1.50E+09	1	33760		
	Reverse	Arrhenius	coefficients:	9.71E+07	1.3	36270
2372	$C_6H_{12-1}+OH=C_6H_{11}+H_2O$	3.00E+13	0	1230		
	Reverse	Arrhenius	coefficients:	9.76E+14	-0.1	39260
2373	$C_6H_{12-2}+OH=C_6H_{11}+H_2O$	3.00E+13	0	1230		
	Reverse	Arrhenius	coefficients:	1.99E+15	-0.3	36380
2374	$C_6H_{12-3}+OH=C_6H_{11}+H_2O$	3.00E+13	0	1230		
	Reverse	Arrhenius	coefficients:	7.28E+14	-0.2	36480
2375	$C_6H_{12-1}+H=C_6H_{11}+H_2$	3.70E+13	0	3900		
	Reverse	Arrhenius	coefficients:	2.78E+14	-0.1	26770
2376	$C_6H_{12-2}+H=C_6H_{11}+H_2$	3.70E+13	0	3900		
	Reverse	Arrhenius	coefficients:	5.66E+14	-0.3	23900
2377	$C_6H_{12-3}+H=C_6H_{11}+H_2$	3.70E+13	0	3900		
	Reverse	Arrhenius	coefficients:	2.07E+14	-0.2	23990
2378	$C_6H_{12-1}+CH_3=C_6H_{11}+CH_4$	1.00E+12	0	7300		
	Reverse	Arrhenius	coefficients:	1.96E+14	-0.1	30650
2379	$C_6H_{12-2}+CH_3=C_6H_{11}+CH_4$	1.00E+12	0	7300		
	Reverse	Arrhenius	coefficients:	3.99E+14	-0.3	27780

2380	C6H12-3+CH3=C6H11+CH4	1.00E+12	0	7300		
	Reverse	Arrhenius	coefficients:	1.46E+14	-0.2	27870
2381	C6H12-1+O=C6H11+OH	2.12E+11	0.1	9125		
	Reverse	Arrhenius	coefficients:	7.00E+11	0	29900
2382	C6H12-2+O=C6H11+OH	1.04E+11	0.3	12000		
	Reverse	Arrhenius	coefficients:	7.00E+11	0	29900
2383	C6H12-3+O=C6H11+OH	2.84E+11	0.2	11900		
	Reverse	Arrhenius	coefficients:	7.00E+11	0	29900
2384	C6H12-1+OH=>C5H11-1+CH2O	1.00E+11	0	-4000		
2385	C6H12-2+OH=>PC4H9+CH3CHO	1.00E+11	0	-4000		
2386	C6H12-3+OH=>PC4H9+CH3CHO	1.00E+11	0	-4000		
2387	C6H12-1+O=>C5H11-1+HCO	1.00E+11	0	-1050		
2388	C6H12-2+O=>PC4H9+CH3CO	1.00E+11	0	-1050		
2389	C6H11=C3H6+C3H5-A	2.50E+13	0	45000		
	Reverse	Arrhenius	coefficients:	1.00E+10	0	17000
2390	C6H11=C4H8-1+C2H3	2.50E-17	0	45000		
	Reverse	Arrhenius	coefficients:	1.50E-20	0	7400
2391	C6H11=C4H7+C2H4	2.50E-17	0	45000		
	Reverse	Arrhenius	coefficients:	1.50E-20	0	7400
2392	C6H12-1=NC3H7+C3H5-A	1.00E+16	0	71000		
	Reverse	Arrhenius	coefficients:	1.00E+13	0	0
2393	C6H12-2=C2H5+C4H7	1.00E+16	0	71000		
	Reverse	Arrhenius	coefficients:	1.00E+13	0	0
2394	C6H12-3=CH3+C5H9	1.00E+16	0	71000		
	Reverse	Arrhenius	coefficients:	1.00E+13	0	0
2395	C6H13O2-1=C6H13-1+O2	5.15E+20	-1.7	35780		
	Reverse	Arrhenius	coefficients:	4.52E+12	0	0
2396	C6H13-1+C6H13O2-1=2C6H13O-1	7.00E+12	0	-1000		
	Reverse	Arrhenius	coefficients:	9.78E+13	-0.2	29840
2397	C6H13O2-1=C6H12OOH1-2	2.00E+11	0	26850		
	Reverse	Arrhenius	coefficients:	2.40E+10	-0.1	13860
2398	C6H13O2-1=C6H12OOH1-3	2.50E+10	0	20850		
	Reverse	Arrhenius	coefficients:	3.00E+09	-0.1	7860
2399	C6H13O2-1=C6H12OOH1-4	3.12E+09	0	19050		
	Reverse	Arrhenius	coefficients:	3.75E+08	-0.1	6060
2400	C6H13O2-1+HO2=C6H13O2H-1+O2	1.75E+10	0	-3275		
	Reverse	Arrhenius	coefficients:	4.70E+13	-0.8	34460
2401	C6H13O2-1+H2O2=C6H13O2H-1+HO2	2.40E+12	0	10000		
	Reverse	Arrhenius	coefficients:	2.40E+12	0	10000
2402	C6H13O2-1+CH3O2=>C6H13O-1+CH3O+O2	1.40E+16	-1.6	1860		
2403	2C6H13O2-1=>O2+2C6H13O-1	1.40E+16	-1.6	1860		
2404	C6H13O2H-1=C6H13O-1+OH	1.50E+16	0	42500		
	Reverse	Arrhenius	coefficients:	1.46E+08	1.7	-3045
2405	C6H13O-1=C5H11-1+CH2O	1.81E+17	-1.1	20300		
	Reverse	Arrhenius	coefficients:	1.00E+11	0	11900
2406	C6H12OOH1-2=>C6H12O1-2+OH	6.00E+11	0	22000		



2407	C6H12OOH1-3=>C6H12O1-3+OH	7.50E+10	0	15250		
2408	C6H12OOH1-4=>C6H12O1-4+OH	9.38E+09	0	7000		
2409	C6H12OOH1-2=C6H12-1+HO2	1.35E+19	-2	20570		
	Reverse	Arrhenius	coefficients:	1.62E+11	0	12690
2410	C6H12OOH1-3=>OH+CH2O+C5H10-1	7.70E+13	-0.2	30090		
2411	C6H12OOH1-2O2=C6H12OOH1-2+O2	8.87E+22	-2.3	37980		
	Reverse	Arrhenius	coefficients:	7.54E+12	0	0
2412	C6H12OOH1-3O2=C6H12OOH1-3+O2	8.87E+22	-2.3	37980		
	Reverse	Arrhenius	coefficients:	7.54E+12	0	0
2413	C6H12OOH1-4O2=C6H12OOH1-4+O2	8.87E+22	-2.3	37980		
	Reverse	Arrhenius	coefficients:	7.54E+12	0	0
2414	C6H12OOH1-2O2=NC6KET12+OH	2.00E+11	0	26400		
	Reverse	Arrhenius	coefficients:	1.25E-11	6	39660
2415	C6H12OOH1-3O2=NC6KET13+OH	2.50E+10	0	21400		
	Reverse	Arrhenius	coefficients:	4.24E+03	1.4	44670
2416	C6H12OOH1-4O2=NC6KET14+OH	3.12E+09	0	19350		
	Reverse	Arrhenius	coefficients:	5.30E+02	1.4	42620
2417	NC6KET12=>NC4H9CHO+HCO+OH	1.05E+16	0	41600		
2418	NC6KET13=>NC3H7CHO+CH2CHO+OH	1.05E+16	0	41600		
2419	NC6KET14=>C2H5CHO+CH2CH2CHO+OH	1.05E+16	0	41600		
2420	C6H12O1-2+OH=>C2H3CHO+NC3H7+H2O	2.50E+12	0	0		
2421	C6H12O1-3+OH=>C5H10-1+HCO+H2O	2.50E+12	0	0		
2422	C6H12O1-4+OH=>C4H8-1+CH2CHO+H2O	2.50E+12	0	0		
2423	C6H12O1-2+OH=>CH2CO+PC4H9+H2O	2.50E+12	0	0		
2424	C6H12O1-3+OH=>C2H4+NC3H7CO+H2O	2.50E+12	0	0		
2425	C6H12O1-4+OH=>C2H4+C2H5COCH2+H2O	2.50E+12	0	0		
2426	C6H12O1-2+HO2=>C2H3CHO+NC3H7+H2O2	5.00E+12	0	17700		
2427	C6H12O1-3+HO2=>C5H10-1+HCO+H2O2	5.00E+12	0	17700		
2428	C6H12O1-4+HO2=>C4H8-1+CH2CHO+H2O2	5.00E+12	0	17700		
2429	C6H12O1-2+HO2=>CH2CO+PC4H9+H2O2	5.00E+12	0	17700		
2430	C6H12O1-3+HO2=>C2H4+NC3H7CO+H2O2	5.00E+12	0	17700		
2431	C6H12O1-4+HO2=>C2H4+C2H5COCH2+H2O2	5.00E+12	0	17700		
2432	C6H13-1+HO2=C6H13O-1+OH	7.00E+12	0	-1000		
	Reverse	Arrhenius	coefficients:	2.08E+16	-0.8	26970
2433	C6H13-1+CH3O2=C6H13O-1+CH3O	7.00E+12	0	-1000		
	Reverse	Arrhenius	coefficients:	2.04E+18	-1.4	31740
2434	C7H15-1=C5H11-1+C2H4	8.16E+17	-1.4	30840		
	Reverse	Arrhenius	coefficients:	1.00E+11	0	8200
2435	C7H15-1=C7H14-1+H	4.20E+16	-0.9	37940		
	Reverse	Arrhenius	coefficients:	1.00E+13	0	2900
2436	C7H15-2=PC4H9+C3H6	2.22E+16	-0.9	30130		
	Reverse	Arrhenius	coefficients:	1.00E+11	0	8200
2437	C7H15-2=C7H14-1+H	1.34E+15	-0.6	38760		
	Reverse	Arrhenius	coefficients:	1.00E+13	0	1200
2438	C7H15-2=C7H14-2+H	2.71E+15	-0.7	37590		
	Reverse	Arrhenius	coefficients:	1.00E+13	0	2900

2439	C7H15-3=C4H8-1+NC3H7	9.63E+17	-1.4	30580		
	Reverse	Arrhenius	coefficients:	1.00E+11	0	7700
2440	C7H15-3=C6H12-1+CH3	1.03E+14	-0.4	28690		
	Reverse	Arrhenius	coefficients:	1.75E+11	0	7200
2441	C7H15-3=C7H14-2+H	2.71E+15	-0.7	37590		
	Reverse	Arrhenius	coefficients:	1.00E+13	0	2900
2442	C7H15-3=C7H14-3+H	2.02E+15	-0.7	37680		
	Reverse	Arrhenius	coefficients:	1.00E+13	0	2900
2443	C7H15-4=C2H5+C5H10-1	5.43E+16	-0.9	30590		
	Reverse	Arrhenius	coefficients:	1.00E+11	0	8200
2444	C7H15-4=C7H14-3+H	4.02E+15	-0.7	37680		
	Reverse	Arrhenius	coefficients:	1.00E+13	0	2900
2445	C7H15-1+O2=C7H14-1+HO2	3.00E-09	0	3000		
	Reverse	Arrhenius	coefficients:	2.44E-10	0.3	17920
2446	C7H15-2+O2=C7H14-1+HO2	4.50E-09	0	5020		
	Reverse	Arrhenius	coefficients:	1.15E-08	-0.1	17420
2447	C7H15-2+O2=C7H14-2+HO2	3.00E-09	0	3000		
	Reverse	Arrhenius	coefficients:	3.79E-09	0.1	18270
2448	C7H15-3+O2=C7H14-2+HO2	3.00E-09	0	3000		
	Reverse	Arrhenius	coefficients:	3.79E-09	0.1	18270
2449	C7H15-3+O2=C7H14-3+HO2	3.00E-09	0	3000		
	Reverse	Arrhenius	coefficients:	5.09E-09	0	18180
2450	C7H15-4+O2=C7H14-3+HO2	6.00E-09	0	3000		
	Reverse	Arrhenius	coefficients:	5.11E-09	0	18180
2451	C7H15-1=C7H15-3	1.39E+09	1	33760		
	Reverse	Arrhenius	coefficients:	4.41E+07	1.4	36280
2452	C7H15-1=C7H15-4	2.54E+09	0.3	19760		
	Reverse	Arrhenius	coefficients:	1.61E+08	0.7	22280
2453	C7H15-2=C7H15-3	9.59E+08	1.4	39700		
	Reverse	Arrhenius	coefficients:	9.59E+08	1.4	39700
2454	C7H15-1=C7H15-2	5.48E+08	1.6	38760		
	Reverse	Arrhenius	coefficients:	1.74E+07	2	41280
2455	C7H14-1+OH=C7H13+H2O	3.00E+13	0	1230		
	Reverse	Arrhenius	coefficients:	7.92E+14	-0.5	36480
2456	C7H14-2+OH=C7H13+H2O	3.00E+13	0	1230		
	Reverse	Arrhenius	coefficients:	1.60E+15	-0.6	33600
2457	C7H14-3+OH=C7H13+H2O	3.00E+13	0	1230		
	Reverse	Arrhenius	coefficients:	1.19E+15	-0.6	33700
2458	C7H14-1+H=C7H13+H2	3.70E+13	0	3900		
	Reverse	Arrhenius	coefficients:	2.26E+14	-0.5	23990
2459	C7H14-2+H=C7H13+H2	3.70E+13	0	3900		
	Reverse	Arrhenius	coefficients:	4.57E+14	-0.6	21120
2460	C7H14-3+H=C7H13+H2	3.70E+13	0	3900		
	Reverse	Arrhenius	coefficients:	3.40E+14	-0.6	21210
2461	C7H14-1+CH3=C7H13+CH4	1.00E+12	0	7300		
	Reverse	Arrhenius	coefficients:	1.59E+14	-0.5	27870

2462	$C_7H_{14-2}+CH_3=C_7H_{13}+CH_4$	1.00E+12	0	7300		
	Reverse	Arrhenius	coefficients:	3.23E+14	-0.6	25000
2463	$C_7H_{14-3}+CH_3=C_7H_{13}+CH_4$	1.00E+12	0	7300		
	Reverse	Arrhenius	coefficients:	2.40E+14	-0.6	25090
2464	$C_7H_{14-1}+O=C_7H_{13}+OH$	2.62E+11	0.5	11900		
	Reverse	Arrhenius	coefficients:	7.00E+11	0	29900
2465	$C_7H_{14-2}+O=C_7H_{13}+OH$	1.29E+11	0.6	14780		
	Reverse	Arrhenius	coefficients:	7.00E+11	0	29900
2466	$C_7H_{14-3}+O=C_7H_{13}+OH$	1.73E+11	0.6	14680		
	Reverse	Arrhenius	coefficients:	7.00E+11	0	29900
2467	$C_7H_{14-1}+OH=>CH_2O+C_6H_{13-1}$	1.00E+11	0	-4000		
2468	$C_7H_{14-1}+OH=>CH_3CHO+C_5H_{11-1}$	1.00E+11	0	-4000		
2469	$C_7H_{14-2}+OH=>CH_3CHO+C_5H_{11-1}$	1.00E+11	0	-4000		
2470	$C_7H_{14-2}+OH=>C_2H_5CHO+PC_4H_9$	1.00E+11	0	-4000		
2471	$C_7H_{14-3}+OH=>C_2H_5CHO+PC_4H_9$	1.00E+11	0	-4000		
2472	$C_7H_{14-1}+O=>CH_2CHO+C_5H_{11-1}$	1.00E+11	0	-1050		
2473	$C_7H_{14-2}+O=>CH_3CHO+C_5H_{10-1}$	1.00E+11	0	-1050		
2474	$C_7H_{14-3}+O=>CH_3CHO+C_5H_{10-1}$	1.00E+11	0	-1050		
2475	$C_7H_{13}=C_3H_5-A+C_4H_8-1$	2.50E+13	0	45000		
	Reverse	Arrhenius	coefficients:	1.00E+13	0	9600
2476	$C_7H_{13}=C_4H_7+C_3H_6$	2.50E+13	0	45000		
	Reverse	Arrhenius	coefficients:	1.00E+13	0	9600
2477	$C_7H_{14-1}=PC_4H_9+C_3H_5-A$	1.00E+16	0	71000		
	Reverse	Arrhenius	coefficients:	1.00E+13	0	0
2478	$C_7H_{14-2}=C_4H_7+NC_3H_7$	1.00E+16	0	71000		
	Reverse	Arrhenius	coefficients:	1.00E+13	0	0
2479	$C_7H_{14-3}=C_4H_7+NC_3H_7$	1.00E+16	0	71000		
	Reverse	Arrhenius	coefficients:	1.00E+13	0	0
2480	$C_7H_{15O_2-1}=C_7H_{15-1}+O_2$	2.66E+20	-1.7	35400		
	Reverse	Arrhenius	coefficients:	4.52E+12	0	0
2481	$C_7H_{15O_2-4}=C_7H_{15-4}+O_2$	1.36E+23	-2.4	37670		
	Reverse	Arrhenius	coefficients:	7.54E+12	0	0
2482	$C_7H_{15-1}+C_7H_{15O_2-1}=2C_7H_{15O-1}$	7.00E+12	0	-1000		
	Reverse	Arrhenius	coefficients:	5.56E+13	-0.2	30260
2483	$C_7H_{15O_2-1}=C_7H_{14OOH1-2}$	2.00E+11	0	26850		
	Reverse	Arrhenius	coefficients:	2.12E+10	-0.1	14240
2484	$C_7H_{15O_2-1}=C_7H_{14OOH1-3}$	2.50E+10	0	20850		
	Reverse	Arrhenius	coefficients:	2.65E+09	-0.1	8240
2485	$C_7H_{15O_2-1}=C_7H_{14OOH1-4}$	3.12E+09	0	19050		
	Reverse	Arrhenius	coefficients:	3.32E+08	-0.1	6440
2486	$C_7H_{15O_2-4}=C_7H_{14OOH4-2}$	5.00E+10	0	20850		
	Reverse	Arrhenius	coefficients:	5.66E+09	-0.1	8270
2487	$C_7H_{15O_2-1}+HO_2=C_7H_{15O_2H-1}+O_2$	1.75E+10	0	-3275		
	Reverse	Arrhenius	coefficients:	5.02E+13	-0.8	34870
2488	$H_2O_2+C_7H_{15O_2-1}=HO_2+C_7H_{15O_2H-1}$	2.40E+12	0	10000		
	Reverse	Arrhenius	coefficients:	2.40E+12	0	10000

2489	$C7H15O2-1+CH3O2 \Rightarrow C7H15O-1+CH3O+O2$	1.40E+16	-1.6	1860		
2490	$2C7H15O2-1 \Rightarrow O2+2C7H15O-1$	1.40E+16	-1.6	1860		
2491	$C7H15O2H-1=C7H15O-1+OH$	1.50E+16	0	42500		
	Reverse	Arrhenius	coefficients:	1.43E+08	1.7	-3055
2492	$C7H15O-1=CH2O+C6H13-1$	4.68E+17	-1.3	20260		
	Reverse	Arrhenius	coefficients:	1.00E+11	0	11900
2493	$C7H14OOH1-2=C7H14-1+HO2$	7.66E+18	-2	18400		
	Reverse	Arrhenius	coefficients:	1.00E+11	0	10530
2494	$C7H14OOH1-3 \Rightarrow C7H14O1-3+OH$	7.50E+10	0	15250		
2495	$C7H14OOH1-4 \Rightarrow C7H14O1-4+OH$	9.38E+09	0	7000		
2496	$C7H14OOH1-3 \Rightarrow OH+CH2O+C6H12-1$	8.12E+13	-0.1	31090		
2497	$C7H14OOH4-2 \Rightarrow OH+NC3H7CHO+C3H6$	1.30E+18	-1.5	26800		
2498	$C7H14OOH1-2O2=C7H14OOH1-2+O2$	1.37E+23	-2.4	37640		
	Reverse	Arrhenius	coefficients:	7.54E+12	0	0
2499	$C7H14OOH1-3O2=C7H14OOH1-3+O2$	1.37E+23	-2.4	37640		
	Reverse	Arrhenius	coefficients:	7.54E+12	0	0
2500	$C7H14OOH1-4O2=C7H14OOH1-4+O2$	1.37E+23	-2.4	37640		
	Reverse	Arrhenius	coefficients:	7.54E+12	0	0
2501	$C7H14OOH4-2O2=C7H14OOH4-2+O2$	6.97E+22	-2.4	37600		
	Reverse	Arrhenius	coefficients:	7.54E+12	0	0
2502	$C7H14OOH1-2O2=NC7KET12+OH$	2.00E+11	0	26400		
	Reverse	Arrhenius	coefficients:	1.38E+05	1.2	46790
2503	$C7H14OOH1-3O2=NC7KET13+OH$	2.50E+10	0	21400		
	Reverse	Arrhenius	coefficients:	3.30E+03	1.4	45040
2504	$C7H14OOH1-4O2=NC7KET14+OH$	3.12E+09	0	19350		
	Reverse	Arrhenius	coefficients:	4.13E+02	1.4	42990
2505	$C7H14OOH4-2O2=NC7KET42+OH$	1.25E+10	0	17850		
	Reverse	Arrhenius	coefficients:	1.62E+02	1.8	44200
2506	$NC7KET12 \Rightarrow NC5H11CHO+HCO+OH$	1.05E+16	0	41600		
2507	$NC7KET13 \Rightarrow NC4H9CHO+CH2CHO+OH$	1.05E+16	0	41600		
2508	$NC7KET14 \Rightarrow NC3H7CHO+CH2CH2CHO+OH$	1.05E+16	0	41600		
2509	$NC7KET42 \Rightarrow CH3CHO+NC3H7COCH2+OH$	1.05E+16	0	41600		
2510	$C7H14O1-3+OH \Rightarrow C6H12-1+HCO+H2O$	2.50E+12	0	0		
2511	$C7H14O1-4+OH \Rightarrow C5H10-1+CH2CHO+H2O$	2.50E+12	0	0		
2512	$C7H14O1-3+OH \Rightarrow C2H4+NC4H9CO+H2O$	2.50E+12	0	0		
2513	$C7H14O1-4+OH \Rightarrow C2H4+NC3H7COCH2+H2O$	2.50E+12	0	0		
2514	$C7H14O1-3+HO2 \Rightarrow C6H12-1+HCO+H2O2$	5.00E+12	0	17700		
2515	$C7H14O1-4+HO2 \Rightarrow C5H10-1+CH2CHO+H2O2$	5.00E+12	0	17700		
2516	$C7H14O1-3+HO2 \Rightarrow C2H4+NC4H9CO+H2O2$	5.00E+12	0	17700		
2517	$C7H14O1-4+HO2 \Rightarrow C2H4+NC3H7COCH2+H2O2$	5.00E+12	0	17700		
2518	$NC5H11CHO+O2=NC5H11CO+HO2$	2.00E+13	0.5	42200		
	Reverse	Arrhenius	coefficients:	1.00E+07	0	40000
2519	$NC5H11CHO+OH=NC5H11CO+H2O$	2.69E+10	0.8	-340		
	Reverse	Arrhenius	coefficients:	1.74E+10	0.8	31200
2520	$NC5H11CHO+H=NC5H11CO+H2$	4.00E+13	0	4200		

	Reverse	Arrhenius	coefficients:	1.80E+13	0	24000
2521	NC5H11CHO+O=NC5H11CO+OH	5.00E+12	0	1790		
	Reverse	Arrhenius	coefficients:	1.00E+12	0	19000
2522	NC5H11CHO+HO2=NC5H11CO+H2O2	2.80E+12	0	13600		
	Reverse	Arrhenius	coefficients:	1.00E+12	0	10000
2523	NC5H11CHO+CH3=NC5H11CO+CH4	1.70E+12	0	8440		
	Reverse	Arrhenius	coefficients:	1.50E+13	0	28000
2524	NC5H11CHO+CH3O=NC5H11CO+CH3OH	1.15E+11	0	1280		
	Reverse	Arrhenius	coefficients:	3.00E+11	0	18000
2525	NC5H11CHO+CH3O2=NC5H11CO+CH3O2H	1.00E+12	0	9500		
	Reverse	Arrhenius	coefficients:	2.50E+10	0	10000
2526	NC5H11CHO+OH=C5H10CHO-1+H2O	5.27E+09	1	1586		
	Reverse	Arrhenius	coefficients:	1.07E+09	1	21010
2527	NC5H11CHO+OH=C5H10CHO-2+H2O	4.67E+07	1.6	-35		
	Reverse	Arrhenius	coefficients:	1.75E+06	1.9	23880
2528	NC5H11CHO+OH=C5H10CHO-3+H2O	4.67E+07	1.6	-35		
	Reverse	Arrhenius	coefficients:	1.75E+06	1.9	23880
2529	NC5H11CHO+OH=C5H10CHO-4+H2O	4.67E+07	1.6	-35		
	Reverse	Arrhenius	coefficients:	1.75E+06	1.9	23880
2530	NC5H11CHO+OH=C5H10CHO-5+H2O	4.67E+07	1.6	-35		
	Reverse	Arrhenius	coefficients:	3.32E+09	1.2	30840
2531	NC5H11CO=C5H11-1+CO	1.00E+11	0	9600		
	Reverse	Arrhenius	coefficients:	1.00E+11	0	0
2532	NC5H11CHO+HO2=C5H10CHO-1+H2O2	2.76E+04	2.5	16480		
	Reverse	Arrhenius	coefficients:	3.33E+04	2.2	4442
2533	NC5H11CHO+HO2=C5H10CHO-2+H2O2	1.48E+04	2.6	13910		
	Reverse	Arrhenius	coefficients:	3.28E+03	2.5	6362
2534	NC5H11CHO+HO2=C5H10CHO-3+H2O2	1.48E+04	2.6	13910		
	Reverse	Arrhenius	coefficients:	3.28E+03	2.5	6362
2535	NC5H11CHO+HO2=C5H10CHO-4+H2O2	1.48E+04	2.6	13910		
	Reverse	Arrhenius	coefficients:	3.28E+03	2.5	6362
2536	NC5H11CHO+HO2=C5H10CHO-5+H2O2	2.95E+04	2.6	13910		
	Reverse	Arrhenius	coefficients:	1.24E+07	1.9	13320
2537	NC5H11CHO+CH3O2=C5H10CHO-1+CH3O2H	6.03E+12	0	19380		
	Reverse	Arrhenius	coefficients:	2.99E+13	-0.5	6617
2538	NC5H11CHO+CH3O2=C5H10CHO-2+CH3O2H	1.99E+12	0	17050		
	Reverse	Arrhenius	coefficients:	1.82E+12	-0.3	8784
2539	NC5H11CHO+CH3O2=C5H10CHO-3+CH3O2H	1.99E+12	0	17050		
	Reverse	Arrhenius	coefficients:	1.82E+12	-0.3	8784
2540	NC5H11CHO+CH3O2=C5H10CHO-4+CH3O2H	1.99E+12	0	17050		
	Reverse	Arrhenius	coefficients:	1.82E+12	-0.3	8784
2541	NC5H11CHO+CH3O2=C5H10CHO-5+CH3O2H	3.98E+12	0	17050		
	Reverse	Arrhenius	coefficients:	6.90E+15	-0.9	15740
2542	C5H10CHO-1=C2H4+C3H6CHO-1	2.68E+18	-1.6	30410		
	Reverse	Arrhenius	coefficients:	2.50E+11	0	7800
2543	C5H10CHO-2=C3H6+CH2CH2CHO	9.38E+17	-1.3	31970		

	Reverse	Arrhenius	coefficients:	1.00E+11	0	7800
2544	C5H10CHO-3=C4H8-1+CH2CHO	6.27E+16	-1.4	25990		
	Reverse	Arrhenius	coefficients:	1.00E+11	0	7800
2545	C5H10CHO-4=AC3H5CHO+C2H5	7.19E+17	-1.4	33230		
	Reverse	Arrhenius	coefficients:	1.00E+11	0	7800
2546	C5H10CHO-4=C5H10-1+HCO	1.06E+14	-0.4	26330		
	Reverse	Arrhenius	coefficients:	1.00E+11	0	7800
2547	C5H10CHO-5=C2H3CHO+NC3H7	1.56E+19	-1.5	33310		
	Reverse	Arrhenius	coefficients:	1.00E+11	0	7800
2548	C4H7CO1-4=C4H7+CO	2.79E+09	0.5	-160		
	Reverse	Arrhenius	coefficients:	1.50E+11	0	4810
2549	NC4H9COCH3+OH=NC4H9COCH2+H2O	5.10E+11	0	1192		
	Reverse	Arrhenius	coefficients:	6.79E+13	-0.7	27680
2550	NC4H9COCH3+HO2=NC4H9COCH2+H2O2	2.38E+04	2.5	14690		
	Reverse	Arrhenius	coefficients:	1.88E+07	1.5	9712
2551	NC4H9COCH3+CH3O2=NC4H9COCH2+CH3O2H	3.01E+12	0	17580		
	Reverse	Arrhenius	coefficients:	9.77E+15	-1.2	11880
2552	NC4H9COCH2=PC4H9+CH2CO	1.55E+18	-1.4	43140		
	Reverse	Arrhenius	coefficients:	1.00E+11	0	11600
2553	C7H14OOH1-3=C4H7OOH1-4+NC3H7	3.82E+14	-0.7	27470		
	Reverse	Arrhenius	coefficients:	8.50E+10	0	7800
2554	C7H14OOH1-4=>C5H10-1+C2H4+HO2	2.44E+16	-1.1	29450		
2555	C7H15-1+HO2=C7H15O-1+OH	7.00E+12	0	-1000		
	Reverse	Arrhenius	coefficients:	1.13E+16	-0.8	26980
2556	C7H15-1+CH3O2=C7H15O-1+CH3O	7.00E+12	0	-1000		
	Reverse	Arrhenius	coefficients:	1.10E+18	-1.3	31750
2557	C4H7OOH1-4=C4H7O1-4+OH	2.02E+20	-1.5	47040		
	Reverse	Arrhenius	coefficients:	2.00E+13	0	0
2558	C4H7O1-4=CH2O+C3H5-A	2.41E+16	-1.1	7550		
	Reverse	Arrhenius	coefficients:	1.00E+11	0	11900
2559	C10H21-1+H=NC10H22	1.00E+14	0	0		
2560	C10H21-2+H=NC10H22	1.00E+14	0	0		
2561	C10H21-3+H=NC10H22	1.00E+14	0	0		
2562	C10H21-4+H=NC10H22	1.00E+14	0	0		
2563	C10H21-5+H=NC10H22	1.00E+14	0	0		
2564	C9H19-1+CH3=NC10H22	1.00E+13	0	0		
2565	C8H17-1+C2H5=NC10H22	8.00E+12	0	0		
2566	C7H15-1+NC3H7=NC10H22	8.00E+12	0	0		
2567	C6H13-1+PC4H9=NC10H22	8.00E+12	0	0		
2568	2C5H11-1=NC10H22	8.00E+12	0	0		
2569	NC10H22+H=C10H21-1+H2	1.88E+05	2.8	6280		
	Reverse	Arrhenius	coefficients:	8.93E+03	2.7	10550
2570	NC10H22+H=C10H21-2+H2	2.60E+06	2.4	4471		
	Reverse	Arrhenius	coefficients:	3.93E+03	2.7	11260
2571	NC10H22+H=C10H21-3+H2	2.60E+06	2.4	4471		

	Reverse	Arrhenius	coefficients:	3.93E+03	2.7	11260
2572	NC10H22+H=C10H21-4+H2	2.60E+06	2.4	4471		
	Reverse	Arrhenius	coefficients:	3.93E+03	2.7	11260
2573	NC10H22+H=C10H21-5+H2	2.60E+06	2.4	4471		
	Reverse	Arrhenius	coefficients:	3.93E+03	2.7	11260
2574	NC10H22+OH=C10H21-1+H2O	1.05E+10	1	1590		
	Reverse	Arrhenius	coefficients:	1.50E+10	1.1	23330
2575	NC10H22+OH=C10H21-2+H2O	9.40E+07	1.6	-35		
	Reverse	Arrhenius	coefficients:	6.15E+05	1.9	21910
2576	NC10H22+OH=C10H21-3+H2O	9.40E+07	1.6	-35		
	Reverse	Arrhenius	coefficients:	6.15E+05	1.9	21910
2577	NC10H22+OH=C10H21-4+H2O	9.40E+07	1.6	-35		
	Reverse	Arrhenius	coefficients:	6.15E+05	1.9	21910
2578	NC10H22+OH=C10H21-5+H2O	9.40E+07	1.6	-35		
	Reverse	Arrhenius	coefficients:	6.15E+05	1.9	21910
2579	NC10H22+O=C10H21-1+OH	1.93E+05	2.7	3716		
	Reverse	Arrhenius	coefficients:	4.02E+03	2.6	5893
2580	NC10H22+O=C10H21-2+OH	9.54E+04	2.7	2106		
	Reverse	Arrhenius	coefficients:	6.33E+01	3	6798
2581	NC10H22+O=C10H21-3+OH	9.54E+04	2.7	2106		
	Reverse	Arrhenius	coefficients:	6.33E+01	3	6798
2582	NC10H22+O=C10H21-4+OH	9.54E+04	2.7	2106		
	Reverse	Arrhenius	coefficients:	6.33E+01	3	6798
2583	NC10H22+O=C10H21-5+OH	9.54E+04	2.7	2106		
	Reverse	Arrhenius	coefficients:	6.33E+01	3	6798
2584	NC10H22+HO2=C10H21-1+H2O2	1.68E+13	0	20440		
	Reverse	Arrhenius	coefficients:	2.05E+13	-0.4	8399
2585	NC10H22+HO2=C10H21-2+H2O2	1.12E+13	0	17690		
	Reverse	Arrhenius	coefficients:	4.35E+11	0	8165
2586	NC10H22+HO2=C10H21-3+H2O2	1.12E+13	0	17690		
	Reverse	Arrhenius	coefficients:	4.35E+11	0	8165
2587	NC10H22+HO2=C10H21-4+H2O2	1.12E+13	0	17690		
	Reverse	Arrhenius	coefficients:	4.35E+11	0	8165
2588	NC10H22+HO2=C10H21-5+H2O2	1.12E+13	0	17690		
	Reverse	Arrhenius	coefficients:	4.35E+11	0	8165
2589	NC10H22+CH3=C10H21-1+CH4	9.04E-01	3.6	7154		
	Reverse	Arrhenius	coefficients:	1.12E+00	3.6	11910
2590	NC10H22+CH3=C10H21-2+CH4	5.41E+04	2.3	7287		
	Reverse	Arrhenius	coefficients:	2.14E+03	2.6	14550
2591	NC10H22+CH3=C10H21-3+CH4	5.41E+04	2.3	7287		
	Reverse	Arrhenius	coefficients:	2.14E+03	2.6	14550
2592	NC10H22+CH3=C10H21-4+CH4	5.41E+04	2.3	7287		
	Reverse	Arrhenius	coefficients:	2.14E+03	2.6	14550
2593	NC10H22+CH3=C10H21-5+CH4	5.41E+04	2.3	7287		
	Reverse	Arrhenius	coefficients:	2.14E+03	2.6	14550
2594	NC10H22+O2=C10H21-1+HO2	6.00E+13	0	52800		

	Reverse	Arrhenius	coefficients:	5.18E+10	0.3	-406
2595	NC10H22+O2=C10H21-2+HO2	4.00E+13	0	50150		
	Reverse	Arrhenius	coefficients:	1.10E+09	0.7	-541
2596	NC10H22+O2=C10H21-3+HO2	4.00E+13	0	50150		
	Reverse	Arrhenius	coefficients:	1.10E+09	0.7	-541
2597	NC10H22+O2=C10H21-4+HO2	4.00E+13	0	50150		
	Reverse	Arrhenius	coefficients:	1.10E+09	0.7	-541
2598	NC10H22+O2=C10H21-5+HO2	4.00E+13	0	50150		
	Reverse	Arrhenius	coefficients:	1.10E+09	0.7	-541
2599	NC10H22+C2H3=C10H21-1+C2H4	1.00E+12	0	18000		
	Reverse	Arrhenius	coefficients:	2.57E+12	0	25400
2600	NC10H22+C2H3=C10H21-2+C2H4	8.00E+11	0	16800		
	Reverse	Arrhenius	coefficients:	2.00E+12	0	24200
2601	NC10H22+C2H3=C10H21-3+C2H4	8.00E+11	0	16800		
	Reverse	Arrhenius	coefficients:	2.00E+12	0	24200
2602	NC10H22+C2H3=C10H21-4+C2H4	8.00E+11	0	16800		
	Reverse	Arrhenius	coefficients:	2.00E+12	0	24200
2603	NC10H22+C2H3=C10H21-5+C2H4	8.00E+11	0	16800		
	Reverse	Arrhenius	coefficients:	2.00E+12	0	24200
2604	NC10H22+C2H5=C10H21-1+C2H6	1.00E+11	0	13400		
	Reverse	Arrhenius	coefficients:	3.20E+11	0	12300
2605	NC10H22+C2H5=C10H21-2+C2H6	1.00E+11	0	10400		
	Reverse	Arrhenius	coefficients:	1.00E+11	0	12900
2606	NC10H22+C2H5=C10H21-3+C2H6	1.00E+11	0	10400		
	Reverse	Arrhenius	coefficients:	1.00E+11	0	12900
2607	NC10H22+C2H5=C10H21-4+C2H6	1.00E+11	0	10400		
	Reverse	Arrhenius	coefficients:	1.00E+11	0	12900
2608	NC10H22+C2H5=C10H21-5+C2H6	1.00E+11	0	10400		
	Reverse	Arrhenius	coefficients:	1.00E+11	0	12900
2609	NC10H22+C10H21O2-1=C10H21-1+C10H21O2H-1	1.00E+11	0	13400		
	Reverse	Arrhenius	coefficients:	3.20E+11	0	12300
2610	NC10H22+C10H21O2-1=C10H21-2+C10H21O2H-1	1.00E+11	0	10400		
	Reverse	Arrhenius	coefficients:	1.00E+11	0	12900
2611	NC10H22+C10H21O2-1=C10H21-3+C10H21O2H-1	1.00E+11	0	10400		
	Reverse	Arrhenius	coefficients:	1.00E+11	0	12900
2612	NC10H22+C10H21O2-1=C10H21-4+C10H21O2H-1	1.00E+11	0	10400		
	Reverse	Arrhenius	coefficients:	1.00E+11	0	12900
2613	NC10H22+C10H21O2-1=C10H21-5+C10H21O2H-1	1.00E+11	0	10400		
	Reverse	Arrhenius	coefficients:	1.00E+11	0	12900
2614	NC10H22+C10H21O2-2=C10H21-1+C10H21O2H-2	1.00E+11	0	13400		
	Reverse	Arrhenius	coefficients:	3.20E+11	0	12300
2615	NC10H22+C10H21O2-2=C10H21-2+C10H21O2H-2	1.00E+11	0	10400		
	Reverse	Arrhenius	coefficients:	1.00E+11	0	12900



2616	NC10H22+C10H21O2-2=C10H21-3+C10H21O2H-2	1.00E+11	0	10400		
	Reverse	Arrhenius	coefficients:	1.00E+11	0	12900
2617	NC10H22+C10H21O2-2=C10H21-4+C10H21O2H-2	1.00E+11	0	10400		
	Reverse	Arrhenius	coefficients:	1.00E+11	0	12900
2618	NC10H22+C10H21O2-2=C10H21-5+C10H21O2H-2	1.00E+11	0	10400		
	Reverse	Arrhenius	coefficients:	1.00E+11	0	12900
2619	NC10H22+C10H21O2-3=C10H21-1+C10H21O2H-3	1.00E+11	0	13400		
	Reverse	Arrhenius	coefficients:	3.20E+11	0	12300
2620	NC10H22+C10H21O2-3=C10H21-2+C10H21O2H-3	1.00E+11	0	10400		
	Reverse	Arrhenius	coefficients:	1.00E+11	0	12900
2621	NC10H22+C10H21O2-3=C10H21-3+C10H21O2H-3	1.00E+11	0	10400		
	Reverse	Arrhenius	coefficients:	1.00E+11	0	12900
2622	NC10H22+C10H21O2-3=C10H21-4+C10H21O2H-3	1.00E+11	0	10400		
	Reverse	Arrhenius	coefficients:	1.00E+11	0	12900
2623	NC10H22+C10H21O2-3=C10H21-5+C10H21O2H-3	1.00E+11	0	10400		
	Reverse	Arrhenius	coefficients:	1.00E+11	0	12900
2624	NC10H22+C10H21O2-4=C10H21-1+C10H21O2H-4	1.00E+11	0	13400		
	Reverse	Arrhenius	coefficients:	3.20E+11	0	12300
2625	NC10H22+C10H21O2-4=C10H21-2+C10H21O2H-4	1.00E+11	0	10400		
	Reverse	Arrhenius	coefficients:	1.00E+11	0	12900
2626	NC10H22+C10H21O2-4=C10H21-3+C10H21O2H-4	1.00E+11	0	10400		
	Reverse	Arrhenius	coefficients:	1.00E+11	0	12900
2627	NC10H22+C10H21O2-4=C10H21-4+C10H21O2H-4	1.00E+11	0	10400		
	Reverse	Arrhenius	coefficients:	1.00E+11	0	12900
2628	NC10H22+C10H21O2-4=C10H21-5+C10H21O2H-4	1.00E+11	0	10400		
	Reverse	Arrhenius	coefficients:	1.00E+11	0	12900
2629	NC10H22+C10H21O2-5=C10H21-1+C10H21O2H-5	1.00E+11	0	13400		
	Reverse	Arrhenius	coefficients:	3.20E+11	0	12300
2630	NC10H22+C10H21O2-5=C10H21-2+C10H21O2H-5	1.00E+11	0	10400		
	Reverse	Arrhenius	coefficients:	1.00E+11	0	12900
2631	NC10H22+C10H21O2-5=C10H21-3+C10H21O2H-5	1.00E+11	0	10400		
	Reverse	Arrhenius	coefficients:	1.00E+11	0	12900
2632	NC10H22+C10H21O2-5=C10H21-4+C10H21O2H-5	1.00E+11	0	10400		
	Reverse	Arrhenius	coefficients:	1.00E+11	0	12900
2633	NC10H22+C10H21O2-5=C10H21-5+C10H21O2H-5	1.00E+11	0	10400		
	Reverse	Arrhenius	coefficients:	1.00E+11	0	12900
2634	C2H4+C8H17-1=C10H21-1	1.00E+11	0	8200		
2635	H+C10H20-1=C10H21-1	1.00E+13	0	2900		
2636	C3H6+C7H15-1=C10H21-2	1.00E+11	0	8200		

2637	H+C10H20-1=C10H21-2	1.00E+13	0	1200		
2638	H+C10H20-2=C10H21-2	1.00E+13	0	2900		
2639	C4H8-1+C6H13-1=C10H21-3	1.00E+11	0	8200		
2640	CH3+C9H18-1=C10H21-3	1.00E+11	0	8200		
2641	H+C10H20-2=C10H21-3	1.00E+13	0	2900		
2642	H+C10H20-3=C10H21-3	1.00E+13	0	2900		
2643	C5H10-1+C5H11-1=C10H21-4	1.00E+11	0	8200		
2644	C2H5+C8H16-1=C10H21-4	1.00E+11	0	8200		
2645	H+C10H20-3=C10H21-4	1.00E+13	0	2900		
2646	H+C10H20-4=C10H21-4	1.00E+13	0	2900		
2647	C6H12-1+PC4H9=C10H21-5	1.00E+11	0	8200		
2648	NC3H7+C7H14-1=C10H21-5	1.00E+11	0	8200		
2649	H+C10H20-4=C10H21-5	1.00E+13	0	2900		
2650	H+C10H20-5=C10H21-5	1.00E+13	0	2900		
2651	C2H4+C7H15-1=C9H19-1	1.00E+11	0	8200		
2652	H+C9H18-1=C9H19-1	1.00E+13	0	2900		
2653	C3H6+C6H13-1=C9H19-2	1.00E+11	0	8200		
2654	H+C9H18-1=C9H19-2	1.00E+13	0	1200		
2655	H+C9H18-2=C9H19-2	1.00E+13	0	2900		
2656	C4H8-1+C5H11-1=C9H19-3	1.00E+11	0	8200		
2657	CH3+C8H16-1=C9H19-3	1.00E+11	0	8200		
2658	H+C9H18-2=C9H19-3	1.00E+13	0	2900		
2659	H+C9H18-3=C9H19-3	1.00E+13	0	2900		
2660	C5H10-1+PC4H9=C9H19-4	1.00E+11	0	8200		
2661	C2H5+C7H14-1=C9H19-4	1.00E+11	0	8200		
2662	H+C9H18-3=C9H19-4	1.00E+13	0	2900		
2663	C6H12-1+NC3H7=C9H19-5	1.00E+11	0	8200		
2664	C2H4+C6H13-1=C8H17-1	1.00E+11	0	8200		
2665	H+C8H16-1=C8H17-1	1.00E+13	0	2900		
2666	C3H6+C5H11-1=C8H17-2	1.00E+11	0	8200		
2667	H+C8H16-1=C8H17-2	1.00E+13	0	1200		
2668	H+C8H16-2=C8H17-2	1.00E+13	0	2900		
2669	C4H8-1+PC4H9=C8H17-3	1.00E+11	0	8200		
2670	CH3+C7H14-1=C8H17-3	1.00E+11	0	8200		
2671	H+C8H16-2=C8H17-3	1.00E+13	0	2900		
2672	H+C8H16-3=C8H17-3	1.00E+13	0	2900		
2673	C5H10-1+NC3H7=C8H17-4	1.00E+11	0	8200		
2674	C2H5+C6H12-1=C8H17-4	1.00E+11	0	8200		
2675	H+C8H16-3=C8H17-4	1.00E+13	0	2900		
2676	H+C8H16-4=C8H17-4	1.00E+13	0	2900		
2677	C10H21-1+O2=C10H20-1+HO2	3.00E-09	0	3000		
2678	C10H21-2+O2=C10H20-1+HO2	3.00E-09	0	3000		
2679	C10H21-2+O2=C10H20-2+HO2	3.00E-09	0	3000		
2680	C10H21-3+O2=C10H20-2+HO2	3.00E-09	0	3000		
2681	C10H21-3+O2=C10H20-3+HO2	3.00E-09	0	3000		
2682	C10H21-4+O2=C10H20-3+HO2	3.00E-09	0	3000		

2683	C10H21-4+O2=C10H20-4+HO2	3.00E-09	0	3000		
2684	C10H21-5+O2=C10H20-4+HO2	3.00E-09	0	3000		
2685	C10H21-5+O2=C10H20-5+HO2	3.00E-09	0	3000		
2686	C9H19-1+O2=C9H18-1+HO2	3.00E-09	0	3000		
2687	C9H19-2+O2=C9H18-1+HO2	3.00E-09	0	3000		
2688	C9H19-2+O2=C9H18-2+HO2	3.00E-09	0	3000		
2689	C9H19-3+O2=C9H18-2+HO2	3.00E-09	0	3000		
2690	C9H19-3+O2=C9H18-3+HO2	3.00E-09	0	3000		
2691	C9H19-4+O2=C9H18-3+HO2	3.00E-09	0	3000		
2692	C8H17-1+O2=C8H16-1+HO2	3.00E-09	0	3000		
2693	C8H17-2+O2=C8H16-1+HO2	3.00E-09	0	3000		
2694	C8H17-2+O2=C8H16-2+HO2	3.00E-09	0	3000		
2695	C8H17-3+O2=C8H16-2+HO2	3.00E-09	0	3000		
2696	C8H17-3+O2=C8H16-3+HO2	3.00E-09	0	3000		
2697	C8H17-4+O2=C8H16-3+HO2	3.00E-09	0	3000		
2698	C8H17-4+O2=C8H16-4+HO2	3.00E-09	0	3000		
2699	C10H21-1=C10H21-2	5.48E+08	1.6	38760		
	Reverse	Arrhenius	coefficients:	1.74E+07	2	41280
2700	C10H21-1=C10H21-3	1.39E+09	1	33760		
	Reverse	Arrhenius	coefficients:	4.41E+07	1.4	36280
2701	C10H21-1=C10H21-4	2.54E+09	0.3	19760		
	Reverse	Arrhenius	coefficients:	8.05E+07	0.7	22280
2702	C10H21-1=C10H21-5	4.28E+11	-1.1	11760		
	Reverse	Arrhenius	coefficients:	1.36E+10	-0.7	14280
2703	C10H21-2=C10H21-3	9.59E+08	1.4	39700		
	Reverse	Arrhenius	coefficients:	9.59E+08	1.4	39700
2704	C10H21-2=C10H21-4	1.76E+09	0.8	34700		
	Reverse	Arrhenius	coefficients:	1.76E+09	0.8	34700
2705	C10H21-2=C10H21-5	3.22E+09	0.1	20700		
	Reverse	Arrhenius	coefficients:	3.22E+09	0.1	20700
	Declared	duplicate	reaction...			
2706	C10H21-2=C10H21-5	5.00E+11	-1.2	12760		
	Reverse	Arrhenius	coefficients:	1.60E+10	-0.9	15280
	Declared	duplicate	reaction...			
2707	C10H21-3=C10H21-4	9.59E+08	1.4	39700		
	Reverse	Arrhenius	coefficients:	9.59E+08	1.4	39700
	Declared	duplicate	reaction...			
2708	C10H21-3=C10H21-5	1.76E+09	0.8	34700		
	Reverse	Arrhenius	coefficients:	3.50E+09	0.8	34700
	Declared	duplicate	reaction...			
2709	C10H21-3=C10H21-5	3.22E+09	0.1	20700		
	Reverse	Arrhenius	coefficients:	3.22E+09	0.1	20700
	Declared	duplicate	reaction...			
2710	C10H21-3=C10H21-4	5.00E+11	-1.2	12760		
	Reverse	Arrhenius	coefficients:	1.60E+10	-0.9	15280
	Declared	duplicate	reaction...			

2711	C10H21-4=C10H21-5	9.59E+08	1.4	39700		
	Reverse	Arrhenius	coefficients:	9.59E+08	1.4	39700
	Declared	duplicate	reaction...			
2712	C10H21-4=C10H21-5	1.76E+09	0.8	34700		
	Reverse	Arrhenius	coefficients:	3.50E+09	0.8	34700
	Declared	duplicate	reaction...			
2713	C9H19-1=C9H19-2	5.48E+08	1.6	38760		
	Reverse	Arrhenius	coefficients:	1.74E+07	2	41280
2714	C9H19-1=C9H19-3	1.39E+09	1	33760		
	Reverse	Arrhenius	coefficients:	4.41E+07	1.4	36280
2715	C9H19-1=C9H19-4	2.54E+09	0.3	19760		
	Reverse	Arrhenius	coefficients:	8.05E+07	0.7	22280
2716	C9H19-1=C9H19-5	4.28E+11	-1.1	11760		
	Reverse	Arrhenius	coefficients:	1.36E+10	-0.7	14280
2717	C9H19-2=C9H19-3	9.59E+08	1.4	39700		
	Reverse	Arrhenius	coefficients:	9.59E+08	1.4	39700
2718	C9H19-2=C9H19-4	1.76E+09	0.8	34700		
	Reverse	Arrhenius	coefficients:	1.76E+09	0.8	34700
	Declared	duplicate	reaction...			
2719	C9H19-2=C9H19-5	3.22E+09	0.1	20700		
	Reverse	Arrhenius	coefficients:	3.22E+09	0.1	20700
2720	C9H19-2=C9H19-4	5.00E+11	-1.2	12760		
	Reverse	Arrhenius	coefficients:	1.60E+10	-0.9	15280
	Declared	duplicate	reaction...			
2721	C9H19-3=C9H19-4	9.59E+08	1.4	39700		
	Reverse	Arrhenius	coefficients:	9.59E+08	1.4	39700
	Declared	duplicate	reaction...			
2722	C9H19-3=C9H19-5	1.76E+09	0.8	34700		
	Reverse	Arrhenius	coefficients:	3.50E+09	0.8	34700
2723	C9H19-3=C9H19-4	3.22E+09	0.1	20700		
	Reverse	Arrhenius	coefficients:	3.22E+09	0.1	20700
	Declared	duplicate	reaction...			
2724	C9H19-4=C9H19-5	9.59E+08	1.4	39700		
	Reverse	Arrhenius	coefficients:	9.59E+08	1.4	39700
2725	C8H17-1=C8H17-2	5.48E+08	1.6	38760		
	Reverse	Arrhenius	coefficients:	1.74E+07	2	41280
2726	C8H17-1=C8H17-3	1.39E+09	1	33760		
	Reverse	Arrhenius	coefficients:	4.41E+07	1.4	36280
2727	C8H17-1=C8H17-4	2.54E+09	0.3	19760		
	Reverse	Arrhenius	coefficients:	8.05E+07	0.7	22280
	Declared	duplicate	reaction...			
2728	C8H17-1=C8H17-4	4.28E+11	-1.1	11760		
	Reverse	Arrhenius	coefficients:	1.36E+10	-0.7	14280
	Declared	duplicate	reaction...			
2729	C8H17-2=C8H17-3	9.59E+08	1.4	39700		
	Reverse	Arrhenius	coefficients:	9.59E+08	1.4	39700

	Declared	duplicate	reaction...			
2730	C8H17-2=C8H17-4	1.76E+09	0.8	34700		
	Reverse	Arrhenius	coefficients:	1.76E+09	0.8	34700
	Declared	duplicate	reaction...			
2731	C8H17-2=C8H17-4	3.22E+09	0.1	20700		
	Reverse	Arrhenius	coefficients:	3.22E+09	0.1	20700
	Declared	duplicate	reaction...			
2732	C8H17-2=C8H17-3	5.00E+11	-1.2	12760		
	Reverse	Arrhenius	coefficients:	1.60E+10	-0.9	15280
	Declared	duplicate	reaction...			
2733	C8H17-3=C8H17-4	9.59E+08	1.4	39700		
	Reverse	Arrhenius	coefficients:	9.59E+08	1.4	39700
	Declared	duplicate	reaction...			
2734	C8H17-3=C8H17-4	1.76E+09	0.8	34700		
	Reverse	Arrhenius	coefficients:	3.50E+09	0.8	34700
	Declared	duplicate	reaction...			
2735	C10H20-1+OH=C10H19+H2O	3.00E+13	0	1230		
	Reverse	Arrhenius	coefficients:	7.92E+14	-0.5	36480
2736	C10H20-2+OH=C10H19+H2O	3.00E+13	0	1230		
	Reverse	Arrhenius	coefficients:	7.92E+14	-0.5	36480
2737	C10H20-3+OH=C10H19+H2O	3.00E+13	0	1230		
	Reverse	Arrhenius	coefficients:	7.92E+14	-0.5	36480
2738	C10H20-4+OH=C10H19+H2O	3.00E+13	0	1230		
	Reverse	Arrhenius	coefficients:	7.92E+14	-0.5	36480
2739	C10H20-5+OH=C10H19+H2O	3.00E+13	0	1230		
	Reverse	Arrhenius	coefficients:	7.92E+14	-0.5	36480
2740	C10H20-1+H=C10H19+H2	3.70E+13	0	3900		
	Reverse	Arrhenius	coefficients:	2.26E+14	-0.5	23990
2741	C10H20-2+H=C10H19+H2	3.70E+13	0	3900		
	Reverse	Arrhenius	coefficients:	2.26E+14	-0.5	23990
2742	C10H20-3+H=C10H19+H2	3.70E+13	0	3900		
	Reverse	Arrhenius	coefficients:	2.26E+14	-0.5	23990
2743	C10H20-4+H=C10H19+H2	3.70E+13	0	3900		
	Reverse	Arrhenius	coefficients:	2.26E+14	-0.5	23990
2744	C10H20-5+H=C10H19+H2	3.70E+13	0	3900		
	Reverse	Arrhenius	coefficients:	2.26E+14	-0.5	23990
2745	C10H20-1+CH3=C10H19+CH4	1.00E+12	0	7300		
	Reverse	Arrhenius	coefficients:	3.23E+14	-0.6	25000
2746	C10H20-2+CH3=C10H19+CH4	1.00E+12	0	7300		
	Reverse	Arrhenius	coefficients:	3.23E+14	-0.6	25000
2747	C10H20-3+CH3=C10H19+CH4	1.00E+12	0	7300		
	Reverse	Arrhenius	coefficients:	3.23E+14	-0.6	25000
2748	C10H20-4+CH3=C10H19+CH4	1.00E+12	0	7300		
	Reverse	Arrhenius	coefficients:	3.23E+14	-0.6	25000
2749	C10H20-5+CH3=C10H19+CH4	1.00E+12	0	7300		
	Reverse	Arrhenius	coefficients:	3.23E+14	-0.6	25000

2750	C10H20-1+O=C10H19+OH	1.00E+12	0	4000		
	Reverse	Arrhenius	coefficients:	7.00E+11	0	29900
2751	C10H20-2+O=C10H19+OH	1.00E+12	0	4000		
	Reverse	Arrhenius	coefficients:	7.00E+11	0	29900
2752	C10H20-3+O=C10H19+OH	1.00E+12	0	4000		
	Reverse	Arrhenius	coefficients:	7.00E+11	0	29900
2753	C10H20-4+O=C10H19+OH	1.00E+12	0	4000		
	Reverse	Arrhenius	coefficients:	7.00E+11	0	29900
2754	C10H20-5+O=C10H19+OH	1.00E+12	0	4000		
	Reverse	Arrhenius	coefficients:	7.00E+11	0	29900
2755	C9H18-1+OH=C9H17+H2O	3.00E+13	0	1230		
	Reverse	Arrhenius	coefficients:	7.92E+14	-0.5	36480
2756	C9H18-2+OH=C9H17+H2O	3.00E+13	0	1230		
	Reverse	Arrhenius	coefficients:	7.92E+14	-0.5	36480
2757	C9H18-3+OH=C9H17+H2O	3.00E+13	0	1230		
	Reverse	Arrhenius	coefficients:	7.92E+14	-0.5	36480
2758	C9H18-1+H=C9H17+H2	3.70E+13	0	3900		
	Reverse	Arrhenius	coefficients:	2.26E+14	-0.5	23990
2759	C9H18-2+H=C9H17+H2	3.70E+13	0	3900		
	Reverse	Arrhenius	coefficients:	2.26E+14	-0.5	23990
2760	C9H18-3+H=C9H17+H2	3.70E+13	0	3900		
	Reverse	Arrhenius	coefficients:	2.26E+14	-0.5	23990
2761	C9H18-1+CH3=C9H17+CH4	1.00E+12	0	7300		
	Reverse	Arrhenius	coefficients:	3.23E+14	-0.6	25000
2762	C9H18-2+CH3=C9H17+CH4	1.00E+12	0	7300		
	Reverse	Arrhenius	coefficients:	3.23E+14	-0.6	25000
2763	C9H18-3+CH3=C9H17+CH4	1.00E+12	0	7300		
	Reverse	Arrhenius	coefficients:	3.23E+14	-0.6	25000
2764	C9H18-1+O=C9H17+OH	1.00E+12	0	4000		
	Reverse	Arrhenius	coefficients:	7.00E+11	0	29900
2765	C9H18-2+O=C9H17+OH	1.00E+12	0	4000		
	Reverse	Arrhenius	coefficients:	7.00E+11	0	29900
2766	C9H18-3+O=C9H17+OH	1.00E+12	0	4000		
	Reverse	Arrhenius	coefficients:	7.00E+11	0	29900
2767	C8H16-1+OH=C8H15+H2O	3.00E+13	0	1230		
	Reverse	Arrhenius	coefficients:	7.92E+14	-0.5	36480
2768	C8H16-2+OH=C8H15+H2O	3.00E+13	0	1230		
	Reverse	Arrhenius	coefficients:	7.92E+14	-0.5	36480
2769	C8H16-3+OH=C8H15+H2O	3.00E+13	0	1230		
	Reverse	Arrhenius	coefficients:	7.92E+14	-0.5	36480
2770	C8H16-4+OH=C8H15+H2O	3.00E+13	0	1230		
	Reverse	Arrhenius	coefficients:	7.92E+14	-0.5	36480
2771	C8H16-1+H=C8H15+H2	3.70E+13	0	3900		
	Reverse	Arrhenius	coefficients:	2.26E+14	-0.5	23990
2772	C8H16-2+H=C8H15+H2	3.70E+13	0	3900		
	Reverse	Arrhenius	coefficients:	2.26E+14	-0.5	23990

2773	C8H16-3+H=C8H15+H2	3.70E+13	0	3900		
	Reverse	Arrhenius	coefficients:	2.26E+14	-0.5	23990
2774	C8H16-4+H=C8H15+H2	3.70E+13	0	3900		
	Reverse	Arrhenius	coefficients:	2.26E+14	-0.5	23990
2775	C8H16-1+CH3=C8H15+CH4	1.00E+12	0	7300		
	Reverse	Arrhenius	coefficients:	3.23E+14	-0.6	25000
2776	C8H16-2+CH3=C8H15+CH4	1.00E+12	0	7300		
	Reverse	Arrhenius	coefficients:	3.23E+14	-0.6	25000
2777	C8H16-3+CH3=C8H15+CH4	1.00E+12	0	7300		
	Reverse	Arrhenius	coefficients:	3.23E+14	-0.6	25000
2778	C8H16-4+CH3=C8H15+CH4	1.00E+12	0	7300		
	Reverse	Arrhenius	coefficients:	3.23E+14	-0.6	25000
2779	C8H16-1+O=C8H15+OH	1.00E+12	0	4000		
	Reverse	Arrhenius	coefficients:	7.00E+11	0	29900
2780	C8H16-2+O=C8H15+OH	1.00E+12	0	4000		
	Reverse	Arrhenius	coefficients:	7.00E+11	0	29900
2781	C8H16-3+O=C8H15+OH	1.00E+12	0	4000		
	Reverse	Arrhenius	coefficients:	7.00E+11	0	29900
2782	C8H16-4+O=C8H15+OH	1.00E+12	0	4000		
	Reverse	Arrhenius	coefficients:	7.00E+11	0	29900
2783	C10H20-1+OH=>CH2O+C9H19-1	1.00E+11	0	-4000		
2784	C10H20-1+OH=>CH3CHO+C8H17-1	1.00E+11	0	-4000		
2785	C10H20-1+O=>CH2CHO+C8H17-1	1.00E+11	0	-1050		
2786	C10H20-2+OH=>CH3CHO+C8H17-1	1.00E+11	0	-4000		
2787	C10H20-2+OH=>C2H5CHO+C7H15-1	1.00E+11	0	-4000		
2788	C10H20-2+O=>CH3CHO+C8H16-1	1.00E+11	0	-1050		
2789	C10H20-3+OH=>C2H5CHO+C7H15-1	1.00E+11	0	-4000		
2790	C10H20-3+OH=>NC3H7CHO+C6H13-1	1.00E+11	0	-4000		
2791	C10H20-3+O=>C2H5CHO+C7H14-1	1.00E+11	0	-1050		
2792	C10H20-4+OH=>NC3H7CHO+C6H13-1	1.00E+11	0	-4000		
2793	C10H20-4+OH=>NC4H9CHO+C5H11-1	1.00E+11	0	-4000		
2794	C10H20-4+O=>NC3H7CHO+C6H12-1	1.00E+11	0	-1050		
2795	C10H20-5+OH=>NC4H9CHO+C5H11-1	1.00E+11	0	-4000		
2796	C10H20-5+O=>NC4H9CHO+C5H10-1	1.00E+11	0	-1050		
2797	C9H18-1+OH=>CH2O+C8H17-1	1.00E+11	0	-4000		
2798	C9H18-1+OH=>CH3CHO+C7H15-1	1.00E+11	0	-4000		
2799	C9H18-1+O=>CH2CHO+C7H15-1	1.00E+11	0	-1050		
2800	C9H18-2+OH=>CH3CHO+C7H15-1	1.00E+11	0	-4000		
2801	C9H18-2+OH=>C2H5CHO+C6H13-1	1.00E+11	0	-4000		
2802	C9H18-2+O=>CH3CHO+C7H14-1	1.00E+11	0	-1050		
2803	C9H18-3+OH=>C2H5CHO+C6H13-1	1.00E+11	0	-4000		
2804	C9H18-3+OH=>NC3H7CHO+C5H11-1	1.00E+11	0	-4000		
2805	C9H18-3+O=>C2H5CHO+C6H12-1	1.00E+11	0	-1050		
2806	C8H16-1+OH=>CH2O+C7H15-1	1.00E+11	0	-4000		
2807	C8H16-1+OH=>CH3CHO+C6H13-1	1.00E+11	0	-4000		
2808	C8H16-1+O=>CH2CHO+C6H13-1	1.00E+11	0	-1050		

2809	C8H16-2+OH=>CH3CHO+C6H13-1	1.00E+11	0	-4000		
2810	C8H16-2+OH=>C2H5CHO+C5H11-1	1.00E+11	0	-4000		
2811	C8H16-2+O=>CH3CHO+C6H12-1	1.00E+11	0	-1050		
2812	C8H16-3+OH=>C2H5CHO+C5H11-1	1.00E+11	0	-4000		
2813	C8H16-3+OH=>NC3H7CHO+PC4H9	1.00E+11	0	-4000		
2814	C8H16-3+O=>C2H5CHO+C5H10-1	1.00E+11	0	-1050		
2815	C8H16-4+OH=>NC3H7CHO+PC4H9	1.00E+11	0	-4000		
2816	C8H16-4+O=>NC3H7CHO+C4H8-1	1.00E+11	0	-1050		
2817	C10H19=C2H3+C8H16-1	1.00E+13	0	45000		
	Reverse	Arrhenius	coefficients:	1.00E+11	0	9600
2818	C10H19=C3H5-A+C7H14-1	1.00E+13	0	45000		
	Reverse	Arrhenius	coefficients:	1.00E+11	0	9600
2819	C10H19=C4H7+C6H12-1	1.00E+13	0	45000		
	Reverse	Arrhenius	coefficients:	1.00E+11	0	9600
2820	C10H19=C5H9+C5H10-1	1.00E+13	0	45000		
	Reverse	Arrhenius	coefficients:	1.00E+11	0	9600
2821	C10H19=C6H11+C4H8-1	1.00E+13	0	45000		
	Reverse	Arrhenius	coefficients:	1.00E+11	0	9600
2822	C10H19=C7H13+C3H6	1.00E+13	0	45000		
	Reverse	Arrhenius	coefficients:	1.00E+11	0	9600
2823	C10H19=C8H15+C2H4	1.00E+13	0	45000		
	Reverse	Arrhenius	coefficients:	1.00E+11	0	9600
2824	C9H17=C2H3+C7H14-1	1.00E+13	0	45000		
	Reverse	Arrhenius	coefficients:	1.00E+11	0	9600
2825	C9H17=C3H5-A+C6H12-1	1.00E+13	0	45000		
	Reverse	Arrhenius	coefficients:	1.00E+11	0	9600
2826	C9H17=C4H7+C5H10-1	1.00E+13	0	45000		
	Reverse	Arrhenius	coefficients:	1.00E+11	0	9600
2827	C9H17=C5H9+C4H8-1	1.00E+13	0	45000		
	Reverse	Arrhenius	coefficients:	1.00E+11	0	9600
2828	C9H17=C6H11+C3H6	1.00E+13	0	45000		
	Reverse	Arrhenius	coefficients:	1.00E+11	0	9600
2829	C9H17=C7H13+C2H4	1.00E+13	0	45000		
	Reverse	Arrhenius	coefficients:	1.00E+11	0	9600
2830	C8H15=C2H3+C6H12-1	1.00E+13	0	45000		
	Reverse	Arrhenius	coefficients:	1.00E+11	0	9600
2831	C8H15=C3H5-A+C5H10-1	1.00E+13	0	45000		
	Reverse	Arrhenius	coefficients:	1.00E+11	0	9600
2832	C8H15=C4H7+C4H8-1	1.00E+13	0	45000		
	Reverse	Arrhenius	coefficients:	1.00E+11	0	9600
2833	C8H15=C5H9+C3H6	1.00E+13	0	45000		
	Reverse	Arrhenius	coefficients:	1.00E+11	0	9600
2834	C8H15=C6H11+C2H4	1.00E+13	0	45000		
	Reverse	Arrhenius	coefficients:	1.00E+11	0	9600
2835	C10H20-1=C7H15-1+C3H5-A	1.00E+16	0	71000		
	Reverse	Arrhenius	coefficients:	1.00E+13	0	0



2836	C10H20-2=C4H7+C6H13-1	1.00E+16	0	71000		
	Reverse	Arrhenius	coefficients:	1.00E+13	0	0
2837	C10H20-3=C5H9+C5H11-1	1.00E+16	0	71000		
	Reverse	Arrhenius	coefficients:	1.00E+13	0	0
2838	C10H20-4=C6H11+PC4H9	1.00E+16	0	71000		
	Reverse	Arrhenius	coefficients:	1.00E+13	0	0
2839	C10H20-5=C7H13+NC3H7	1.00E+16	0	71000		
	Reverse	Arrhenius	coefficients:	1.00E+13	0	0
2840	C9H18-1=C6H13-1+C3H5-A	1.00E+16	0	71000		
	Reverse	Arrhenius	coefficients:	1.00E+13	0	0
2841	C9H18-2=C4H7+C5H11-1	1.00E+16	0	71000		
	Reverse	Arrhenius	coefficients:	1.00E+13	0	0
2842	C9H18-3=C5H9+PC4H9	1.00E+16	0	71000		
	Reverse	Arrhenius	coefficients:	1.00E+13	0	0
2843	C8H16-1=C5H11-1+C3H5-A	1.00E+16	0	71000		
	Reverse	Arrhenius	coefficients:	1.00E+13	0	0
2844	C8H16-2=C4H7+PC4H9	1.00E+16	0	71000		
	Reverse	Arrhenius	coefficients:	1.00E+13	0	0
2845	C8H16-3=C5H9+NC3H7	1.00E+16	0	71000		
	Reverse	Arrhenius	coefficients:	1.00E+13	0	0
2846	C8H16-4=C6H11+C2H5	1.00E+16	0	71000		
	Reverse	Arrhenius	coefficients:	1.00E+13	0	0
2847	C10H21O2-1=C10H21-1+O2	2.66E+20	-1.7	35400		
	Reverse	Arrhenius	coefficients:	4.52E+12	0	0
	Declared	duplicate	reaction...			
2848	C10H21O2-2=C10H21-2+O2	1.36E+23	-2.4	37670		
	Reverse	Arrhenius	coefficients:	7.54E+12	0	0
2849	C10H21O2-3=C10H21-3+O2	1.36E+23	-2.4	37670		
	Reverse	Arrhenius	coefficients:	7.54E+12	0	0
2850	C10H21O2-4=C10H21-4+O2	1.36E+23	-2.4	37670		
	Reverse	Arrhenius	coefficients:	7.54E+12	0	0
2851	C10H21O2-5=C10H21-5+O2	1.36E+23	-2.4	37670		
	Reverse	Arrhenius	coefficients:	7.54E+12	0	0
2852	C9H19O2-1=C9H19-1+O2	2.66E+20	-1.7	35400		
	Reverse	Arrhenius	coefficients:	4.52E+12	0	0
2853	C9H19O2-4=C9H19-4+O2	1.36E+23	-2.4	37670		
	Reverse	Arrhenius	coefficients:	7.54E+12	0	0
2854	C9H19O2-5=C9H19-5+O2	1.36E+23	-2.4	37670		
	Reverse	Arrhenius	coefficients:	7.54E+12	0	0
2855	C8H17O2-1=C8H17-1+O2	2.66E+20	-1.7	35400		
	Reverse	Arrhenius	coefficients:	4.52E+12	0	0
2856	C8H17O2-4=C8H17-4+O2	1.36E+23	-2.4	37670		
	Reverse	Arrhenius	coefficients:	7.54E+12	0	0
2857	C10H21-1+C10H21O2-1=2C10H21O-1	7.00E+12	0	-1000		
	Reverse	Arrhenius	coefficients:	7.57E+16	-1.1	31600
2858	C10H21-1+C10H21O2-2=C10H21O-	7.00E+12	0	-1000		

	1+C10H21O-2					
	Reverse	Arrhenius	coefficients:	7.57E+16	-1.1	31600
2859	C10H21-1+C10H21O2-3=C10H21O-1+C10H21O-3	7.00E+12	0	-1000		
	Reverse	Arrhenius	coefficients:	7.57E+16	-1.1	31600
2860	C10H21-1+C10H21O2-4=C10H21O-1+C10H21O-4	7.00E+12	0	-1000		
	Reverse	Arrhenius	coefficients:	7.57E+16	-1.1	31600
2861	C10H21-1+C10H21O2-5=C10H21O-1+C10H21O-5	7.00E+12	0	-1000		
	Reverse	Arrhenius	coefficients:	7.57E+16	-1.1	31600
2862	C10H21-2+C10H21O2-1=C10H21O-2+C10H21O-1	7.00E+12	0	-1000		
	Reverse	Arrhenius	coefficients:	7.57E+16	-1.1	31600
2863	C10H21-2+C10H21O2-2=2C10H21O-2	7.00E+12	0	-1000		
	Reverse	Arrhenius	coefficients:	7.57E+16	-1.1	31600
2864	C10H21-2+C10H21O2-3=C10H21O-2+C10H21O-3	7.00E+12	0	-1000		
	Reverse	Arrhenius	coefficients:	7.57E+16	-1.1	31600
2865	C10H21-2+C10H21O2-4=C10H21O-2+C10H21O-4	7.00E+12	0	-1000		
	Reverse	Arrhenius	coefficients:	7.57E+16	-1.1	31600
2866	C10H21-2+C10H21O2-5=C10H21O-2+C10H21O-5	7.00E+12	0	-1000		
	Reverse	Arrhenius	coefficients:	7.57E+16	-1.1	31600
2867	C10H21-3+C10H21O2-1=C10H21O-3+C10H21O-1	7.00E+12	0	-1000		
	Reverse	Arrhenius	coefficients:	7.57E+16	-1.1	31600
2868	C10H21-3+C10H21O2-2=C10H21O-3+C10H21O-2	7.00E+12	0	-1000		
	Reverse	Arrhenius	coefficients:	7.57E+16	-1.1	31600
2869	C10H21-3+C10H21O2-3=2C10H21O-3	7.00E+12	0	-1000		
	Reverse	Arrhenius	coefficients:	7.57E+16	-1.1	31600
2870	C10H21-3+C10H21O2-4=C10H21O-3+C10H21O-4	7.00E+12	0	-1000		
	Reverse	Arrhenius	coefficients:	7.57E+16	-1.1	31600
2871	C10H21-3+C10H21O2-5=C10H21O-3+C10H21O-5	7.00E+12	0	-1000		
	Reverse	Arrhenius	coefficients:	7.57E+16	-1.1	31600
2872	C10H21-4+C10H21O2-1=C10H21O-4+C10H21O-1	7.00E+12	0	-1000		
	Reverse	Arrhenius	coefficients:	7.57E+16	-1.1	31600
2873	C10H21-4+C10H21O2-2=C10H21O-4+C10H21O-2	7.00E+12	0	-1000		
	Reverse	Arrhenius	coefficients:	7.57E+16	-1.1	31600
2874	C10H21-4+C10H21O2-3=C10H21O-4+C10H21O-3	7.00E+12	0	-1000		
	Reverse	Arrhenius	coefficients:	7.57E+16	-1.1	31600
2875	C10H21-4+C10H21O2-4=2C10H21O-4	7.00E+12	0	-1000		
	Reverse	Arrhenius	coefficients:	7.57E+16	-1.1	31600
2876	C10H21-4+C10H21O2-5=C10H21O-4+C10H21O-5	7.00E+12	0	-1000		
	Reverse	Arrhenius	coefficients:	7.57E+16	-1.1	31600
2877	C10H21-5+C10H21O2-1=C10H21O-5+C10H21O-1	7.00E+12	0	-1000		
	Reverse	Arrhenius	coefficients:	7.57E+16	-1.1	31600

2878	$C_{10}H_{21-5}+C_{10}H_{21}O_{2-2}=C_{10}H_{21}O-5+C_{10}H_{21}O-2$	7.00E+12	0	-1000		
	Reverse	Arrhenius	coefficients:	7.57E+16	-1.1	31600
2879	$C_{10}H_{21-5}+C_{10}H_{21}O_{2-3}=C_{10}H_{21}O-5+C_{10}H_{21}O-3$	7.00E+12	0	-1000		
	Reverse	Arrhenius	coefficients:	7.57E+16	-1.1	31600
2880	$C_{10}H_{21-5}+C_{10}H_{21}O_{2-4}=C_{10}H_{21}O-5+C_{10}H_{21}O-4$	7.00E+12	0	-1000		
	Reverse	Arrhenius	coefficients:	7.57E+16	-1.1	31600
2881	$C_{10}H_{21-5}+C_{10}H_{21}O_{2-5}=2C_{10}H_{21}O-5$	7.00E+12	0	-1000		
	Reverse	Arrhenius	coefficients:	7.57E+16	-1.1	31600
2882	$C_9H_{19-1}+C_9H_{19}O_{2-1}=2C_9H_{19}O-1$	7.00E+12	0	-1000		
	Reverse	Arrhenius	coefficients:	7.57E+16	-1.1	31600
2883	$C_8H_{17-1}+C_8H_{17}O_{2-1}=2C_8H_{17}O-1$	7.00E+12	0	-1000		
	Reverse	Arrhenius	coefficients:	7.57E+16	-1.1	31600
2884	$C_{10}H_{21-1}+HO_2=C_{10}H_{21}O-1+OH$	7.00E+12	0	-1000		
	Reverse	Arrhenius	coefficients:	1.13E+16	-0.8	26980
2885	$C_{10}H_{21-2}+HO_2=C_{10}H_{21}O-2+OH$	7.00E+12	0	-1000		
	Reverse	Arrhenius	coefficients:	1.97E+18	-1.4	28890
2886	$C_{10}H_{21-3}+HO_2=C_{10}H_{21}O-3+OH$	7.00E+12	0	-1000		
	Reverse	Arrhenius	coefficients:	1.97E+18	-1.4	28890
2887	$C_{10}H_{21-4}+HO_2=C_{10}H_{21}O-4+OH$	7.00E+12	0	-1000		
	Reverse	Arrhenius	coefficients:	1.97E+18	-1.4	28890
2888	$C_{10}H_{21-5}+HO_2=C_{10}H_{21}O-5+OH$	7.00E+12	0	-1000		
	Reverse	Arrhenius	coefficients:	1.97E+18	-1.4	28890
2889	$C_9H_{19-1}+HO_2=C_9H_{19}O-1+OH$	7.00E+12	0	-1000		
	Reverse	Arrhenius	coefficients:	1.13E+16	-0.8	26980
2890	$C_8H_{17-1}+HO_2=C_8H_{17}O-1+OH$	7.00E+12	0	-1000		
	Reverse	Arrhenius	coefficients:	1.13E+16	-0.8	26980
2891	$C_{10}H_{21}O_{2-1}=C_{10}OOH_{1-2}$	2.00E+11	0	26850		
	Reverse	Arrhenius	coefficients:	2.12E+10	-0.1	14240
2892	$C_{10}H_{21}O_{2-1}=C_{10}OOH_{1-3}$	2.50E+10	0	20850		
	Reverse	Arrhenius	coefficients:	2.65E+09	-0.1	8240
2893	$C_{10}H_{21}O_{2-1}=C_{10}OOH_{1-4}$	3.12E+09	0	19050		
	Reverse	Arrhenius	coefficients:	3.32E+08	-0.1	6440
2894	$C_{10}H_{21}O_{2-2}=C_{10}OOH_{2-1}$	3.00E+11	0	29400		
	Reverse	Arrhenius	coefficients:	8.06E+11	-0.5	14360
2895	$C_{10}H_{21}O_{2-2}=C_{10}OOH_{2-3}$	2.00E+11	0	26850		
	Reverse	Arrhenius	coefficients:	2.26E+10	-0.1	14270
2896	$C_{10}H_{21}O_{2-2}=C_{10}OOH_{2-4}$	2.50E+10	0	20850		
	Reverse	Arrhenius	coefficients:	2.65E+09	-0.1	8240
2897	$C_{10}H_{21}O_{2-2}=C_{10}OOH_{2-5}$	3.12E+09	0	19050		
	Reverse	Arrhenius	coefficients:	3.32E+08	-0.1	6440
2898	$C_{10}H_{21}O_{2-2}=C_{10}OOH_{2-6}$	3.91E+08	0	22050		
	Reverse	Arrhenius	coefficients:	4.15E+07	-0.1	9440
2899	$C_{10}H_{21}O_{2-3}=C_{10}OOH_{3-1}$	3.75E+10	0	24400		
	Reverse	Arrhenius	coefficients:	1.38E+12	-0.9	9170
2900	$C_{10}H_{21}O_{2-3}=C_{10}OOH_{3-2}$	2.00E+11	0	26850		

	Reverse	Arrhenius	coefficients:	2.26E+10	-0.1	14270
2901	C10H21O2-3=C10OOH3-4	2.00E+11	0	26850		
	Reverse	Arrhenius	coefficients:	2.26E+10	-0.1	14270
2902	C10H21O2-3=C10OOH3-5	2.50E+10	0	20850		
	Reverse	Arrhenius	coefficients:	2.65E+09	-0.1	8240
2903	C10H21O2-3=C10OOH3-6	3.12E+09	0	19050		
	Reverse	Arrhenius	coefficients:	3.32E+08	-0.1	6440
2904	C10H21O2-3=C10OOH3-7	3.91E+08	0	22050		
	Reverse	Arrhenius	coefficients:	4.15E+07	-0.1	9440
2905	C10H21O2-4=C10OOH4-1	9.38E+09	0	22350		
	Reverse	Arrhenius	coefficients:	2.52E+10	-0.5	7310
2906	C10H21O2-4=C10OOH4-2	2.50E+10	0	20850		
	Reverse	Arrhenius	coefficients:	2.65E+09	-0.1	8240
2907	C10H21O2-4=C10OOH4-3	2.00E+11	0	26850		
	Reverse	Arrhenius	coefficients:	2.26E+10	-0.1	14270
2908	C10H21O2-4=C10OOH4-5	2.00E+11	0	26850		
	Reverse	Arrhenius	coefficients:	2.26E+10	-0.1	14270
2909	C10H21O2-4=C10OOH4-6	2.50E+10	0	20850		
	Reverse	Arrhenius	coefficients:	2.65E+09	-0.1	8240
2910	C10H21O2-4=C10OOH4-7	3.12E+09	0	19050		
	Reverse	Arrhenius	coefficients:	3.32E+08	-0.1	6440
2911	C10H21O2-4=C10OOH4-8	3.91E+08	0	22050		
	Reverse	Arrhenius	coefficients:	4.15E+07	-0.1	9440
2912	C10H21O2-5=C10OOH5-2	3.12E+09	0	19050		
	Reverse	Arrhenius	coefficients:	3.32E+08	-0.1	6440
2913	C10H21O2-5=C10OOH5-3	2.50E+10	0	20850		
	Reverse	Arrhenius	coefficients:	2.65E+09	-0.1	8240
2914	C10H21O2-5=C10OOH5-4	2.00E+11	0	26850		
	Reverse	Arrhenius	coefficients:	2.26E+10	-0.1	14270
2915	C10H21O2-5=C10OOH5-6	2.00E+11	0	26850		
	Reverse	Arrhenius	coefficients:	2.26E+10	-0.1	14270
2916	C10H21O2-5=C10OOH5-7	2.50E+10	0	20850		
	Reverse	Arrhenius	coefficients:	2.65E+09	-0.1	8240
2917	C10H21O2-5=C10OOH5-8	3.12E+09	0	19050		
	Reverse	Arrhenius	coefficients:	3.32E+08	-0.1	6440
2918	C10H21O2-5=C10OOH5-9	3.91E+08	0	22050		
	Reverse	Arrhenius	coefficients:	4.15E+07	-0.1	9440
2919	C9H19O2-1=C9OOH1-2	2.00E+11	0	26850		
	Reverse	Arrhenius	coefficients:	2.12E+10	-0.1	14240
2920	C9H19O2-1=C9OOH1-3	2.50E+10	0	20850		
	Reverse	Arrhenius	coefficients:	2.65E+09	-0.1	8240
2921	C9H19O2-1=C9OOH1-4	3.12E+09	0	19050		
	Reverse	Arrhenius	coefficients:	3.32E+08	-0.1	6440
2922	C9H19O2-5=C9OOH5-3	2.50E+10	0	20850		
	Reverse	Arrhenius	coefficients:	2.65E+09	-0.1	8240
2923	C8H17O2-1=C8OOH1-2	2.00E+11	0	26850		

	Reverse	Arrhenius	coefficients:	2.12E+10	-0.1	14240
2924	C8H17O2-1=C8OOH1-3	2.50E+10	0	20850		
	Reverse	Arrhenius	coefficients:	2.65E+09	-0.1	8240
2925	C8H17O2-1=C8OOH1-4	3.12E+09	0	19050		
	Reverse	Arrhenius	coefficients:	3.32E+08	-0.1	6440
2926	C8H17O2-4=C8OOH4-2	2.50E+10	0	20850		
	Reverse	Arrhenius	coefficients:	2.65E+09	-0.1	8240
2927	C8H17O2-4=C8OOH4-6	2.50E+10	0	20850		
	Reverse	Arrhenius	coefficients:	2.65E+09	-0.1	8240
2928	C10H21O2-1+HO2=C10H21O2H-1+O2	1.75E+10	0	-3275		
	Reverse	Arrhenius	coefficients:	5.97E+13	-0.8	34900
2929	C10H21O2-2+HO2=C10H21O2H-2+O2	1.75E+10	0	-3275		
	Reverse	Arrhenius	coefficients:	5.97E+13	-0.8	34900
2930	C10H21O2-3+HO2=C10H21O2H-3+O2	1.75E+10	0	-3275		
	Reverse	Arrhenius	coefficients:	5.97E+13	-0.8	34900
2931	C10H21O2-4+HO2=C10H21O2H-4+O2	1.75E+10	0	-3275		
	Reverse	Arrhenius	coefficients:	5.97E+13	-0.8	34900
2932	C10H21O2-5+HO2=C10H21O2H-5+O2	1.75E+10	0	-3275		
	Reverse	Arrhenius	coefficients:	5.97E+13	-0.8	34900
2933	C9H19O2-1+HO2=C9H19O2H-1+O2	1.75E+10	0	-3275		
	Reverse	Arrhenius	coefficients:	5.97E+13	-0.8	34900
2934	C8H17O2-1+HO2=C8H17O2H-1+O2	1.75E+10	0	-3275		
	Reverse	Arrhenius	coefficients:	5.97E+13	-0.8	34900
2935	C10H21O2-1+H2O2=C10H21O2H-1+HO2	2.40E+12	0	10000		
	Reverse	Arrhenius	coefficients:	2.40E+12	0	10000
2936	C10H21O2-2+H2O2=C10H21O2H-2+HO2	2.40E+12	0	10000		
	Reverse	Arrhenius	coefficients:	2.40E+12	0	10000
2937	C10H21O2-3+H2O2=C10H21O2H-3+HO2	2.40E+12	0	10000		
	Reverse	Arrhenius	coefficients:	2.40E+12	0	10000
2938	C10H21O2-4+H2O2=C10H21O2H-4+HO2	2.40E+12	0	10000		
	Reverse	Arrhenius	coefficients:	2.40E+12	0	10000
2939	C10H21O2-5+H2O2=C10H21O2H-5+HO2	2.40E+12	0	10000		
	Reverse	Arrhenius	coefficients:	2.40E+12	0	10000
2940	C9H19O2-1+H2O2=C9H19O2H-1+HO2	2.40E+12	0	10000		
	Reverse	Arrhenius	coefficients:	2.40E+12	0	10000
2941	C8H17O2-1+H2O2=C8H17O2H-1+HO2	2.40E+12	0	10000		
	Reverse	Arrhenius	coefficients:	2.40E+12	0	10000
2942	C10H21O2-1+CH3O2=>C10H21O-1+CH3O+O2	1.40E+16	-1.6	1860		
2943	C10H21O2-2+CH3O2=>C10H21O-2+CH3O+O2	1.40E+16	-1.6	1860		
2944	C10H21O2-3+CH3O2=>C10H21O-3+CH3O+O2	1.40E+16	-1.6	1860		
2945	C10H21O2-4+CH3O2=>C10H21O-4+CH3O+O2	1.40E+16	-1.6	1860		
2946	C10H21O2-5+CH3O2=>C10H21O-5+CH3O+O2	1.40E+16	-1.6	1860		
2947	C9H19O2-1+CH3O2=>C9H19O-1+CH3O+O2	1.40E+16	-1.6	1860		
2948	C8H17O2-1+CH3O2=>C8H17O-1+CH3O+O2	1.40E+16	-1.6	1860		
2949	2C10H21O2-1=>2C10H21O-1+O2	1.40E+16	-1.6	1860		
2950	C10H21O2-1+C10H21O2-2	1.40E+16	-1.6	1860		

	=>C10H21O-1+C10H21O-2+O2				
2951	C10H21O2-1+C10H21O2-3	1.40E+16	-1.6	1860	
	=>C10H21O-1+C10H21O-3+O2				
2952	C10H21O2-1+C10H21O2-4	1.40E+16	-1.6	1860	
	=>C10H21O-1+C10H21O-4+O2				
2953	C10H21O2-1+C10H21O2-5	1.40E+16	-1.6	1860	
	=>C10H21O-1+C10H21O-5+O2				
2954	2C10H21O2-2=>2C10H21O-2+O2	1.40E+16	-1.6	1860	
2955	C10H21O2-2+C10H21O2-3	1.40E+16	-1.6	1860	
	=>C10H21O-2+C10H21O-3+O2				
2956	C10H21O2-2+C10H21O2-4	1.40E+16	-1.6	1860	
	=>C10H21O-2+C10H21O-4+O2				
2957	C10H21O2-2+C10H21O2-5	1.40E+16	-1.6	1860	
	=>C10H21O-2+C10H21O-5+O2				
2958	2C10H21O2-3=>2C10H21O-3+O2	1.40E+16	-1.6	1860	
2959	C10H21O2-3+C10H21O2-4	1.40E+16	-1.6	1860	
	=>C10H21O-3+C10H21O-4+O2				
2960	C10H21O2-3+C10H21O2-5	1.40E+16	-1.6	1860	
	=>C10H21O-3+C10H21O-5+O2				
2961	2C10H21O2-4=>2C10H21O-4+O2	1.40E+16	-1.6	1860	
2962	C10H21O2-4+C10H21O2-5	1.40E+16	-1.6	1860	
	=>C10H21O-4+C10H21O-5+O2				
2963	2C10H21O2-5=>2C10H21O-5+O2	1.40E+16	-1.6	1860	
2964	2C9H19O2-1=>2C9H19O-1+O2	1.40E+16	-1.6	1860	
2965	2C8H17O2-1=>2C8H17O-1+O2	1.40E+16	-1.6	1860	
2966	C10H21O2H-1=C10H21O-1+OH	1.50E+16	0	42500	
2967	C10H21O2H-2=C10H21O-2+OH	1.25E+16	0	41600	
2968	C10H21O2H-3=C10H21O-3+OH	1.25E+16	0	41600	
2969	C10H21O2H-4=C10H21O-4+OH	1.25E+16	0	41600	
2970	C10H21O2H-5=C10H21O-5+OH	1.25E+16	0	41600	
2971	C9H19O2H-1=C9H19O-1+OH	1.50E+16	0	42500	
2972	C8H17O2H-1=C8H17O-1+OH	1.50E+16	0	42500	
2973	CH2O+C9H19-1=C10H21O-1	1.00E+11	0	11900	
2974	CH3CHO+C8H17-1=C10H21O-2	1.00E+11	0	12900	
2975	C2H5CHO+C7H15-1=C10H21O-3	1.00E+11	0	12900	
2976	NC3H7CHO+C6H13-1=C10H21O-4	1.00E+11	0	12900	
2977	NC4H9CHO+C5H11-1=C10H21O-5	1.00E+11	0	12900	
2978	CH2O+C8H17-1=C9H19O-1	1.00E+11	0	11900	
2979	CH2O+C7H15-1=C8H17O-1	1.00E+11	0	11900	
2980	C10OOH1-2=>C10O1-2+OH	6.00E+11	0	22000	
2981	C10OOH2-1=>C10O1-2+OH	6.00E+11	0	22000	
2982	C10OOH2-3=>C10O2-3+OH	6.00E+11	0	22000	
2983	C10OOH3-2=>C10O2-3+OH	6.00E+11	0	22000	
2984	C10OOH3-4=>C10O3-4+OH	6.00E+11	0	22000	
2985	C10OOH4-3=>C10O3-4+OH	6.00E+11	0	22000	
2986	C8OOH1-2=>C8O1-2+OH	6.00E+11	0	22000	

2987	C10OOH1-3=>C10O1-3+OH	7.50E+10	0	15250		
2988	C10OOH3-1=>C10O1-3+OH	7.50E+10	0	15250		
2989	C10OOH2-4=>C10O2-4+OH	7.50E+10	0	15250		
2990	C10OOH4-2=>C10O2-4+OH	7.50E+10	0	15250		
2991	C10OOH3-5=>C10O3-5+OH	7.50E+10	0	15250		
2992	C10OOH5-3=>C10O3-5+OH	7.50E+10	0	15250		
2993	C10OOH4-6=>C10O4-6+OH	7.50E+10	0	15250		
2994	C9OOH1-3=>C9O1-3+OH	7.50E+10	0	15250		
2995	C8OOH1-3=>C8O1-3+OH	7.50E+10	0	15250		
2996	C10OOH1-4=>C10O1-4+OH	9.38E+09	0	7000		
2997	C10OOH4-1=>C10O1-4+OH	9.38E+09	0	7000		
2998	C10OOH2-5=>C10O2-5+OH	9.38E+09	0	7000		
2999	C10OOH5-2=>C10O2-5+OH	9.38E+09	0	7000		
3000	C10OOH3-6=>C10O3-6+OH	9.38E+09	0	7000		
3001	C10OOH5-8=>C10O3-6+OH	9.38E+09	0	7000		
3002	C10OOH4-7=>C10O4-7+OH	9.38E+09	0	7000		
3003	C9OOH1-4=>C9O1-4+OH	9.38E+09	0	7000		
3004	C8OOH1-4=>C8O1-4+OH	9.38E+09	0	7000		
3005	C10OOH2-6=>C10O2-6+OH	1.17E+09	0	1800		
3006	C10OOH5-9=>C10O2-6+OH	1.17E+09	0	1800		
3007	C10OOH3-7=>C10O3-7+OH	1.17E+09	0	1800		
3008	C10OOH4-8=>C10O3-7+OH	1.17E+09	0	1800		
3009	C10OOH1-2=C10H20-1+HO2	1.61E+20	-2.5	21350		
	Reverse	Arrhenius	coefficients:	1.00E+11	0	11530
3010	C10OOH2-1=C10H20-1+HO2	1.61E+20	-2.5	21350		
	Reverse	Arrhenius	coefficients:	1.00E+11	0	11530
3011	C10OOH2-3=C10H20-2+HO2	1.61E+20	-2.5	21350		
	Reverse	Arrhenius	coefficients:	1.00E+11	0	11530
3012	C10OOH3-2=C10H20-2+HO2	1.61E+20	-2.5	21350		
	Reverse	Arrhenius	coefficients:	1.00E+11	0	11530
3013	C10OOH3-4=C10H20-3+HO2	1.61E+20	-2.5	21350		
	Reverse	Arrhenius	coefficients:	1.00E+11	0	11530
3014	C10OOH4-3=C10H20-3+HO2	1.61E+20	-2.5	21350		
	Reverse	Arrhenius	coefficients:	1.00E+11	0	11530
3015	C10OOH4-5=C10H20-4+HO2	1.61E+20	-2.5	21350		
	Reverse	Arrhenius	coefficients:	1.00E+11	0	11530
3016	C10OOH5-4=C10H20-4+HO2	1.61E+20	-2.5	21350		
	Reverse	Arrhenius	coefficients:	1.00E+11	0	11530
3017	C10OOH5-6=C10H20-5+HO2	1.61E+20	-2.5	21350		
	Reverse	Arrhenius	coefficients:	1.00E+11	0	11530
3018	C9OOH1-2=C9H18-1+HO2	1.61E+20	-2.5	21350		
	Reverse	Arrhenius	coefficients:	1.00E+11	0	11530
3019	C8OOH1-2=C8H16-1+HO2	1.61E+20	-2.5	21350		
	Reverse	Arrhenius	coefficients:	1.00E+11	0	11530
3020	C10OOH1-3=>OH+CH2O+C9H18-1	8.12E+13	-0.1	31090		
3021	C10OOH2-4=>OH+CH3CHO+C8H16-1	5.36E+17	-1.4	26750		

3022	C10OOH3-1=>OH+C2H4+NC7H15CHO	2.21E+19	-1.7	26980		
3023	C10OOH3-5=>OH+C2H5CHO+C7H14-1	2.47E+18	-1.6	27020		
3024	C10OOH4-2=>OH+C3H6+NC6H13CHO	1.30E+18	-1.5	26800		
3025	C10OOH4-6=>OH+NC3H7CHO+C6H12-1	2.47E+18	-1.6	27020		
3026	C10OOH5-3=>OH+C4H8-1+NC5H11CHO	2.47E+18	-1.6	27020		
3027	C10OOH5-7=>OH+NC4H9CHO+C5H10-1	2.47E+18	-1.6	27020		
3028	C9OOH1-3=>OH+CH2O+C8H16-1	8.12E+13	-0.1	31090		
3029	C9OOH5-3=>OH+C4H8-1+NC4H9CHO	2.47E+18	-1.6	27020		
3030	C8OOH1-3=>OH+CH2O+C7H14-1	8.12E+13	-0.1	31090		
3031	C8OOH4-2=>OH+C3H6+NC4H9CHO	1.30E+18	-1.5	26800		
3032	C8OOH4-6=>OH+NC3H7CHO+C4H8-1	2.47E+18	-1.6	27020		
3033	C10OOH1-2O2=C10OOH1-2+O2	1.37E+23	-2.4	37640		
	Reverse	Arrhenius	coefficients:	7.54E+12	0	0
3034	C10OOH1-3O2=C10OOH1-3+O2	1.37E+23	-2.4	37640		
	Reverse	Arrhenius	coefficients:	7.54E+12	0	0
3035	C10OOH1-4O2=C10OOH1-4+O2	1.37E+23	-2.4	37640		
	Reverse	Arrhenius	coefficients:	7.54E+12	0	0
3036	C10OOH2-1O2=C10OOH2-1+O2	1.67E+20	-1.6	35280		
	Reverse	Arrhenius	coefficients:	4.52E+12	0	0
3037	C10OOH2-3O2=C10OOH2-3+O2	1.37E+23	-2.4	37640		
	Reverse	Arrhenius	coefficients:	7.54E+12	0	0
3038	C10OOH2-4O2=C10OOH2-4+O2	1.37E+23	-2.4	37640		
	Reverse	Arrhenius	coefficients:	7.54E+12	0	0
3039	C10OOH2-5O2=C10OOH2-5+O2	1.37E+23	-2.4	37640		
	Reverse	Arrhenius	coefficients:	7.54E+12	0	0
3040	C10OOH3-1O2=C10OOH3-1+O2	1.67E+20	-1.6	35280		
	Reverse	Arrhenius	coefficients:	4.52E+12	0	0
3041	C10OOH3-2O2=C10OOH3-2+O2	1.37E+23	-2.4	37640		
	Reverse	Arrhenius	coefficients:	7.54E+12	0	0
3042	C10OOH3-4O2=C10OOH3-4+O2	1.37E+23	-2.4	37640		
	Reverse	Arrhenius	coefficients:	7.54E+12	0	0
3043	C10OOH3-5O2=C10OOH3-5+O2	1.37E+23	-2.4	37640		
	Reverse	Arrhenius	coefficients:	7.54E+12	0	0
3044	C10OOH3-6O2=C10OOH3-6+O2	1.37E+23	-2.4	37640		
	Reverse	Arrhenius	coefficients:	7.54E+12	0	0
3045	C10OOH4-1O2=C10OOH4-1+O2	1.67E+20	-1.6	35280		
	Reverse	Arrhenius	coefficients:	4.52E+12	0	0
3046	C10OOH4-2O2=C10OOH4-2+O2	1.37E+23	-2.4	37640		
	Reverse	Arrhenius	coefficients:	7.54E+12	0	0
3047	C10OOH4-3O2=C10OOH4-3+O2	1.37E+23	-2.4	37640		
	Reverse	Arrhenius	coefficients:	7.54E+12	0	0
3048	C10OOH4-5O2=C10OOH4-5+O2	1.37E+23	-2.4	37640		
	Reverse	Arrhenius	coefficients:	7.54E+12	0	0
3049	C10OOH4-6O2=C10OOH4-6+O2	1.37E+23	-2.4	37640		
	Reverse	Arrhenius	coefficients:	7.54E+12	0	0
3050	C10OOH4-7O2=C10OOH4-7+O2	1.37E+23	-2.4	37640		



	Reverse	Arrhenius	coefficients:	7.54E+12	0	0
3051	C10OOH5-2O2=C10OOH5-2+O2	1.37E+23	-2.4	37640		
	Reverse	Arrhenius	coefficients:	7.54E+12	0	0
3052	C10OOH5-3O2=C10OOH5-3+O2	1.37E+23	-2.4	37640		
	Reverse	Arrhenius	coefficients:	7.54E+12	0	0
3053	C10OOH5-4O2=C10OOH5-4+O2	1.37E+23	-2.4	37640		
	Reverse	Arrhenius	coefficients:	7.54E+12	0	0
3054	C10OOH5-6O2=C10OOH5-6+O2	1.37E+23	-2.4	37640		
	Reverse	Arrhenius	coefficients:	7.54E+12	0	0
3055	C10OOH5-7O2=C10OOH5-7+O2	1.37E+23	-2.4	37640		
	Reverse	Arrhenius	coefficients:	7.54E+12	0	0
3056	C10OOH5-8O2=C10OOH5-8+O2	1.37E+23	-2.4	37640		
	Reverse	Arrhenius	coefficients:	7.54E+12	0	0
3057	C9OOH1-2O2=C9OOH1-2+O2	1.37E+23	-2.4	37640		
	Reverse	Arrhenius	coefficients:	7.54E+12	0	0
3058	C9OOH1-3O2=C9OOH1-3+O2	1.37E+23	-2.4	37640		
	Reverse	Arrhenius	coefficients:	7.54E+12	0	0
3059	C8OOH1-2O2=C8OOH1-2+O2	1.37E+23	-2.4	37640		
	Reverse	Arrhenius	coefficients:	7.54E+12	0	0
3060	C8OOH1-3O2=C8OOH1-3+O2	1.37E+23	-2.4	37640		
	Reverse	Arrhenius	coefficients:	7.54E+12	0	0
3061	C8OOH1-4O2=C8OOH1-4+O2	1.37E+23	-2.4	37640		
	Reverse	Arrhenius	coefficients:	7.54E+12	0	0
3062	C10OOH1-2O2=C10KET1-2+OH	2.00E+11	0	26400		
	Reverse	Arrhenius	coefficients:	1.38E+05	1.2	46790
3063	C10OOH1-3O2=C10KET1-3+OH	2.50E+10	0	21400		
	Reverse	Arrhenius	coefficients:	3.30E+03	1.4	45040
3064	C10OOH1-4O2=C10KET1-4+OH	3.12E+09	0	19350		
	Reverse	Arrhenius	coefficients:	4.13E+02	1.4	42990
3065	C10OOH2-1O2=C10KET2-1+OH	1.00E+11	0	23850		
	Reverse	Arrhenius	coefficients:	1.18E+04	1.4	47350
3066	C10OOH2-3O2=C10KET2-3+OH	1.00E+11	0	23850		
	Reverse	Arrhenius	coefficients:	1.18E+04	1.4	47350
3067	C10OOH2-4O2=C10KET2-4+OH	1.25E+10	0	17850		
	Reverse	Arrhenius	coefficients:	1.62E+02	1.8	44200
3068	C10OOH2-5O2=C10KET2-5+OH	1.56E+09	0	16050		
	Reverse	Arrhenius	coefficients:	2.02E+01	1.8	42400
3069	C10OOH3-1O2=C10KET3-1+OH	1.25E+10	0	17850		
	Reverse	Arrhenius	coefficients:	1.62E+02	1.8	44200
3070	C10OOH3-2O2=C10KET3-2+OH	1.00E+11	0	23850		
	Reverse	Arrhenius	coefficients:	1.18E+04	1.4	47350
3071	C10OOH3-4O2=C10KET3-4+OH	1.00E+11	0	23850		
	Reverse	Arrhenius	coefficients:	1.18E+04	1.4	47350
3072	C10OOH3-5O2=C10KET3-5+OH	1.25E+10	0	17850		
	Reverse	Arrhenius	coefficients:	1.62E+02	1.8	44200
3073	C10OOH3-6O2=C10KET3-6+OH	1.56E+09	0	16050		

	Reverse	Arrhenius	coefficients:	2.02E+01	1.8	42400
3074	C10OOH4-1O2=C10KET4-1+OH	1.56E+09	0	16050		
	Reverse	Arrhenius	coefficients:	2.02E+01	1.8	42400
3075	C10OOH4-2O2=C10KET4-2+OH	1.25E+10	0	17850		
	Reverse	Arrhenius	coefficients:	1.62E+02	1.8	44200
3076	C10OOH4-3O2=C10KET4-3+OH	1.00E+11	0	23850		
	Reverse	Arrhenius	coefficients:	1.18E+04	1.4	47350
3077	C10OOH4-5O2=C10KET4-5+OH	1.00E+11	0	23850		
	Reverse	Arrhenius	coefficients:	1.18E+04	1.4	47350
3078	C10OOH4-6O2=C10KET4-6+OH	1.25E+10	0	17850		
	Reverse	Arrhenius	coefficients:	1.62E+02	1.8	44200
3079	C10OOH4-7O2=C10KET4-7+OH	1.56E+09	0	16050		
	Reverse	Arrhenius	coefficients:	2.02E+01	1.8	42400
3080	C10OOH5-2O2=C10KET5-2+OH	1.56E+09	0	16050		
	Reverse	Arrhenius	coefficients:	2.02E+01	1.8	42400
3081	C10OOH5-3O2=C10KET5-3+OH	1.25E+10	0	17850		
	Reverse	Arrhenius	coefficients:	1.62E+02	1.8	44200
3082	C10OOH5-4O2=C10KET5-4+OH	1.00E+11	0	23850		
	Reverse	Arrhenius	coefficients:	1.18E+04	1.4	47350
3083	C10OOH5-6O2=C10KET5-6+OH	1.00E+11	0	23850		
	Reverse	Arrhenius	coefficients:	1.18E+04	1.4	47350
3084	C10OOH5-7O2=C10KET5-7+OH	1.25E+10	0	17850		
	Reverse	Arrhenius	coefficients:	1.62E+02	1.8	44200
3085	C10OOH5-8O2=C10KET5-8+OH	1.56E+09	0	16050		
	Reverse	Arrhenius	coefficients:	2.02E+01	1.8	42400
3086	C9OOH1-2O2=C9KET1-2+OH	2.00E+11	0	26400		
	Reverse	Arrhenius	coefficients:	1.38E+05	1.2	46790
3087	C9OOH1-3O2=C9KET1-3+OH	2.50E+10	0	21400		
	Reverse	Arrhenius	coefficients:	3.30E+03	1.4	45040
3088	C8OOH1-2O2=C8KET1-2+OH	2.00E+11	0	26400		
	Reverse	Arrhenius	coefficients:	1.38E+05	1.2	46790
3089	C8OOH1-3O2=C8KET1-3+OH	2.50E+10	0	21400		
	Reverse	Arrhenius	coefficients:	3.30E+03	1.4	45040
3090	C8OOH1-4O2=C8KET1-4+OH	3.12E+09	0	19350		
	Reverse	Arrhenius	coefficients:	4.13E+02	1.4	42990
3091	C10KET1-2=>OH+HCO+NC8H17CHO	1.05E+16	0	41600		
3092	C10KET1-3=>OH+CH2CHO+NC7H15CHO	1.05E+16	0	41600		
3093	C10KET1-4=>OH+CH2CH2CHO+NC6H13CHO	1.05E+16	0	41600		
3094	C10KET2-1=>OH+CH2O+NC8H17CO	1.50E+16	0	42000		
3095	C10KET2-3=>OH+CH3CO+NC7H15CHO	1.05E+16	0	41600		
3096	C10KET2-4=>OH+CH3COCH2+NC6H13CHO	1.05E+16	0	41600		
3097	C10KET2-5=>OH+CH2CH2COCH3+NC5H11CHO	1.05E+16	0	41600		
3098	C10KET3-1=>OH+CH2O+C7H15COCH2	1.50E+16	0	42000		
3099	C10KET3-2=>OH+CH3CHO+NC7H15CO	1.05E+16	0	41600		
3100	C10KET3-4=>OH+C2H5CO+NC6H13CHO	1.05E+16	0	41600		

3101	C10KET3-5=>OH+C2H5COCH2+NC5H11CHO	1.05E+16	0	41600		
3102	C10KET3-6=>OH+C2H5COC2H4P+NC4H9CHO	1.05E+16	0	41600		
3103	C10KET4-1=>OH+CH2O+C6COC2H4P	1.50E+16	0	42000		
3104	C10KET4-2=>OH+CH3CHO+C6H13COCH2	1.05E+16	0	41600		
3105	C10KET4-3=>OH+C2H5CHO+NC6H13CO	1.05E+16	0	41600		
3106	C10KET4-5=>OH+NC3H7CO+NC5H11CHO	1.05E+16	0	41600		
3107	C10KET4-6=>OH+NC3H7COCH2+NC4H9CHO	1.05E+16	0	41600		
3108	C10KET4-7=>OH+NC3H7COC2H4P+NC3H7CHO	1.05E+16	0	41600		
3109	C10KET5-2=>OH+CH3CHO+C5COC2H4P	1.05E+16	0	41600		
3110	C10KET5-3=>OH+C2H5CHO+C5H11COCH2	1.05E+16	0	41600		
3111	C10KET5-4=>OH+NC3H7CHO+NC5H11CO	1.05E+16	0	41600		
3112	C10KET5-6=>OH+NC4H9CO+NC4H9CHO	1.05E+16	0	41600		
3113	C10KET5-7=>OH+NC4H9COCH2+NC3H7CHO	1.05E+16	0	41600		
3114	C10KET5-8=>OH+C4COC2H4P+C2H5CHO	1.05E+16	0	41600		
3115	C9KET1-2=>OH+HCO+NC7H15CHO	1.05E+16	0	41600		
3116	C9KET1-3=>OH+CH2CHO+NC6H13CHO	1.05E+16	0	41600		
3117	C8KET1-2=>OH+HCO+NC6H13CHO	1.05E+16	0	41600		
3118	C8KET1-3=>OH+CH2CHO+NC5H11CHO	1.05E+16	0	41600		
3119	C8KET1-4=>OH+CH2CH2CHO+NC4H9CHO	1.05E+16	0	41600		
3120	C10O1-2+OH=>C2H3CHO+C7H15-1+H2O	2.50E+12	0	0		
3121	C10O1-2+OH=>CH2CO+C8H17-1+H2O	2.50E+12	0	0		
3122	C10O1-3+OH=>C9H18-1+HCO+H2O	2.50E+12	0	0		
3123	C10O1-3+OH=>C2H4+NC7H15CO+H2O	2.50E+12	0	0		
3124	C10O1-4+OH=>CH2CHO+C8H16-1+H2O	2.50E+12	0	0		
3125	C10O1-4+OH=>C2H4+C6H13COCH2+H2O	2.50E+12	0	0		
3126	C10O2-3+OH=>C2H3COCH3+C6H13-1+H2O	2.50E+12	0	0		
3127	C10O2-3+OH=>CH3CHCO+C7H15-1+H2O	2.50E+12	0	0		
3128	C10O2-4+OH=>CH3CO+C8H16-1+H2O	2.50E+12	0	0		
3129	C10O2-4+OH=>C3H6+NC6H13CO+H2O	2.50E+12	0	0		
3130	C10O2-5+OH=>CH3COCH2+C7H14-1+H2O	2.50E+12	0	0		
3131	C10O2-5+OH=>C3H6+C5H11COCH2+H2O	2.50E+12	0	0		
3132	C10O2-6+OH=>CH2CH2COCH3+C6H12-1+H2O	2.50E+12	0	0		
3133	C10O2-6+OH=>C3H6+C4COC2H4P+H2O	2.50E+12	0	0		
3134	C10O3-4+OH=>C2H5COC2H3+C5H11-1+H2O	2.50E+12	0	0		
3135	C10O3-4+OH=>C2H5CHCO+C6H13-1+H2O	2.50E+12	0	0		
3136	C10O3-5+OH=>C2H5CO+C7H14-1+H2O	2.50E+12	0	0		
3137	C10O3-5+OH=>C4H8-1+NC5H11CO+H2O	2.50E+12	0	0		
3138	C10O3-6+OH=>C2H5COCH2+C6H12-1+H2O	2.50E+12	0	0		
3139	C10O3-6+OH=>C4H8-1+NC4H9COCH2+H2O	2.50E+12	0	0		
3140	C10O3-7+OH=>C2H5COC2H4P+C5H10-1+H2O	2.50E+12	0	0		
3141	C10O3-7+OH=>C4H8-1+NC3H7COC2H4P+H2O	2.50E+12	0	0		
3142	C10O4-6+OH=>NC3H7CO+C6H12-1+H2O	2.50E+12	0	0		
3143	C10O4-6+OH=>C5H10-1+NC4H9CO+H2O	2.50E+12	0	0		
3144	C10O4-7+OH=>NC3H7COCH2+C5H10-1+H2O	2.50E+12	0	0		

3145	C1001-2+HO2=>C2H3CHO+C7H15-1+H2O2	5.00E+12	0	17700		
3146	C1001-2+HO2=>CH2CO+C8H17-1+H2O2	5.00E+12	0	17700		
3147	C1001-3+HO2=>C9H18-1+HCO+H2O2	5.00E+12	0	17700		
3148	C1001-3+HO2=>C2H4+NC7H15CO+H2O2	5.00E+12	0	17700		
3149	C1001-4+HO2=>CH2CHO+C8H16-1+H2O2	5.00E+12	0	17700		
3150	C1001-4+HO2=>C2H4+C6H13COCH2+H2O2	5.00E+12	0	17700		
3151	C1002-3+HO2=>C2H3COCH3+C6H13-1+H2O2	5.00E+12	0	17700		
3152	C1002-3+HO2=>CH3CHCO+C7H15-1+H2O2	5.00E+12	0	17700		
3153	C1002-4+HO2=>CH3CO+C8H16-1+H2O2	5.00E+12	0	17700		
3154	C1002-4+HO2=>C3H6+NC6H13CO+H2O2	5.00E+12	0	17700		
3155	C1002-5+HO2=>CH3COCH2+C7H14-1+H2O2	5.00E+12	0	17700		
3156	C1002-5+HO2=>C3H6+C5H11COCH2+H2O2	5.00E+12	0	17700		
3157	C1002-6+HO2=>CH2CH2COCH3+C6H12-1+H2O2	5.00E+12	0	17700		
3158	C1002-6+HO2=>C3H6+C4COC2H4P+H2O2	5.00E+12	0	17700		
3159	C1003-4+HO2=>C2H5COC2H3+C5H11-1+H2O2	5.00E+12	0	17700		
3160	C1003-4+HO2=>C2H5CHCO+C6H13-1+H2O2	5.00E+12	0	17700		
3161	C1003-5+HO2=>C2H5CO+C7H14-1+H2O2	5.00E+12	0	17700		
3162	C1003-5+HO2=>C4H8-1+NC5H11CO+H2O2	5.00E+12	0	17700		
3163	C1003-6+HO2=>C2H5COCH2+C6H12-1+H2O2	5.00E+12	0	17700		
3164	C1003-6+HO2=>C4H8-1+NC4H9COCH2+H2O2	5.00E+12	0	17700		
3165	C1003-7+HO2=>C2H5COC2H4P+C5H10-1+H2O2	5.00E+12	0	17700		
3166	C1003-7+HO2=>C4H8-1+NC3H7COC2H4P+H2O2	5.00E+12	0	17700		
3167	C1004-6+HO2=>NC3H7CO+C6H12-1+H2O2	5.00E+12	0	17700		
3168	C1004-6+HO2=>C5H10-1+NC4H9CO+H2O2	5.00E+12	0	17700		
3169	C1004-7+HO2=>NC3H7COCH2+C5H10-1+H2O2	5.00E+12	0	17700		
3170	C901-3+OH=>C8H16-1+HCO+H2O	2.50E+12	0	0		
3171	C901-3+OH=>C2H4+NC6H13CO+H2O	2.50E+12	0	0		
3172	C901-4+OH=>CH2CHO+C7H14-1+H2O	2.50E+12	0	0		
3173	C901-4+OH=>C2H4+C5H11COCH2+H2O	2.50E+12	0	0		
3174	C901-3+HO2=>C8H16-1+HCO+H2O2	5.00E+12	0	17700		
3175	C901-3+HO2=>C2H4+NC6H13CO+H2O2	5.00E+12	0	17700		
3176	C901-4+HO2=>CH2CHO+C7H14-1+H2O2	5.00E+12	0	17700		
3177	C901-4+HO2=>C2H4+C5H11COCH2+H2O2	5.00E+12	0	17700		
3178	C801-2+OH=>C2H3CHO+C5H11-1+H2O	2.50E+12	0	0		
3179	C801-2+OH=>CH2CO+C6H13-1+H2O	2.50E+12	0	0		
3180	C801-3+OH=>C7H14-1+HCO+H2O	2.50E+12	0	0		
3181	C801-3+OH=>C2H4+NC5H11CO+H2O	2.50E+12	0	0		
3182	C801-4+OH=>CH2CHO+C6H12-1+H2O	2.50E+12	0	0		
3183	C801-4+OH=>C2H4+NC4H9COCH2+H2O	2.50E+12	0	0		
3184	C801-2+HO2=>C2H3CHO+C5H11-1+H2O2	5.00E+12	0	17700		
3185	C801-2+HO2=>CH2CO+C6H13-1+H2O2	5.00E+12	0	17700		
3186	C801-3+HO2=>C7H14-1+HCO+H2O2	5.00E+12	0	17700		
3187	C801-3+HO2=>C2H4+NC5H11CO+H2O2	5.00E+12	0	17700		

3188	$C8O1-4+HO2=>CH2CHO+C6H12-1+H2O2$	5.00E+12	0	17700		
3189	$C8O1-4+HO2=>C2H4+NC4H9COCH2+H2O2$	5.00E+12	0	17700		
3190	$NC8H17CHO+O2=NC8H17CO+HO2$	2.00E+13	0.5	42200		
	Reverse	Arrhenius	coefficients:	1.00E+07	0	40000
3191	$NC8H17CHO+OH=NC8H17CO+H2O$	2.69E+10	0.8	-340		
	Reverse	Arrhenius	coefficients:	1.74E+10	0.8	31200
3192	$NC8H17CHO+H=NC8H17CO+H2$	4.00E+13	0	4200		
	Reverse	Arrhenius	coefficients:	1.80E+13	0	24000
3193	$NC8H17CHO+O=NC8H17CO+OH$	5.00E+12	0	1790		
	Reverse	Arrhenius	coefficients:	1.00E+12	0	19000
3194	$NC8H17CHO+HO2=NC8H17CO+H2O2$	2.80E+12	0	13600		
	Reverse	Arrhenius	coefficients:	1.00E+12	0	10000
3195	$NC8H17CHO+CH3=NC8H17CO+CH4$	1.70E+12	0	8440		
	Reverse	Arrhenius	coefficients:	1.50E+13	0	28000
3196	$NC8H17CHO+CH3O=NC8H17CO+CH3OH$	1.15E+11	0	1280		
	Reverse	Arrhenius	coefficients:	3.00E+11	0	18000
3197	$NC8H17CHO+CH3O2=NC8H17CO+CH3O2H$	1.00E+12	0	9500		
	Reverse	Arrhenius	coefficients:	2.50E+10	0	10000
3198	$NC8H17CO=C8H17-1+CO$	1.00E+11	0	9600		
	Reverse	Arrhenius	coefficients:	1.00E+11	0	0
3199	$NC7H15CHO+O2=NC7H15CO+HO2$	2.00E+13	0.5	42200		
	Reverse	Arrhenius	coefficients:	1.00E+07	0	40000
3200	$NC7H15CHO+OH=NC7H15CO+H2O$	2.69E+10	0.8	-340		
	Reverse	Arrhenius	coefficients:	1.74E+10	0.8	31200
3201	$NC7H15CHO+H=NC7H15CO+H2$	4.00E+13	0	4200		
	Reverse	Arrhenius	coefficients:	1.80E+13	0	24000
3202	$NC7H15CHO+O=NC7H15CO+OH$	5.00E+12	0	1790		
	Reverse	Arrhenius	coefficients:	1.00E+12	0	19000
3203	$NC7H15CHO+HO2=NC7H15CO+H2O2$	2.80E+12	0	13600		
	Reverse	Arrhenius	coefficients:	1.00E+12	0	10000
3204	$NC7H15CHO+CH3=NC7H15CO+CH4$	1.70E+12	0	8440		
	Reverse	Arrhenius	coefficients:	1.50E+13	0	28000
3205	$NC7H15CHO+CH3O=NC7H15CO+CH3OH$	1.15E+11	0	1280		
	Reverse	Arrhenius	coefficients:	3.00E+11	0	18000
3206	$NC7H15CHO+CH3O2=NC7H15CO+CH3O2H$	1.00E+12	0	9500		
	Reverse	Arrhenius	coefficients:	2.50E+10	0	10000
3207	$NC7H15CO=C7H15-1+CO$	1.00E+11	0	9600		
	Reverse	Arrhenius	coefficients:	1.00E+11	0	0
3208	$NC6H13CHO+O2=NC6H13CO+HO2$	2.00E+13	0.5	42200		
	Reverse	Arrhenius	coefficients:	1.00E+07	0	40000
3209	$NC6H13CHO+OH=NC6H13CO+H2O$	2.69E+10	0.8	-340		
	Reverse	Arrhenius	coefficients:	1.74E+10	0.8	31200
3210	$NC6H13CHO+H=NC6H13CO+H2$	4.00E+13	0	4200		
	Reverse	Arrhenius	coefficients:	1.80E+13	0	24000
3211	$NC6H13CHO+O=NC6H13CO+OH$	5.00E+12	0	1790		
	Reverse	Arrhenius	coefficients:	1.00E+12	0	19000

3212	NC6H13CHO+HO2=NC6H13CO+H2O2	2.80E+12	0	13600		
	Reverse	Arrhenius	coefficients:	1.00E+12	0	10000
3213	NC6H13CHO+CH3=NC6H13CO+CH4	1.70E+12	0	8440		
	Reverse	Arrhenius	coefficients:	1.50E+13	0	28000
3214	NC6H13CHO+CH3O=NC6H13CO+CH3OH	1.15E+11	0	1280		
	Reverse	Arrhenius	coefficients:	3.00E+11	0	18000
3215	NC6H13CHO+CH3O2=NC6H13CO+CH3O2H	1.00E+12	0	9500		
	Reverse	Arrhenius	coefficients:	2.50E+10	0	10000
3216	NC6H13CO=C6H13-1+CO	1.00E+11	0	9600		
	Reverse	Arrhenius	coefficients:	1.00E+11	0	0
3217	C7H15COCH2=C7H15-1+CH2CO	2.00E+13	0	31000		
	Reverse	Arrhenius	coefficients:	2.00E+11	0	7350
3218	C6H13COCH2=C6H13-1+CH2CO	2.00E+13	0	31000		
	Reverse	Arrhenius	coefficients:	2.00E+11	0	7350
3219	C5H11COCH2=C5H11-1+CH2CO	2.00E+13	0	31000		
	Reverse	Arrhenius	coefficients:	2.00E+11	0	7350
3220	C6COC2H4P=NC6H13CO+C2H4	5.00E+17	-1.5	26000		
	Reverse	Arrhenius	coefficients:	2.50E+11	0	7800
3221	C5COC2H4P=NC5H11CO+C2H4	5.00E+17	-1.5	26000		
	Reverse	Arrhenius	coefficients:	2.50E+11	0	7800
3222	C4COC2H4P=NC4H9CO+C2H4	5.00E+17	-1.5	26000		
	Reverse	Arrhenius	coefficients:	2.50E+11	0	7800
3223	C6H5+H(+M)=C6H6(+M)	1.00E+14	0	0		
	H2	Enhanced	by	2.00E+00		
	H2O	Enhanced	by	6.00E+00		
	CH4	Enhanced	by	2.00E+00		
	CO	Enhanced	by	1.50E+00		
	CO2	Enhanced	by	2.00E+00		
	Low	pressure	limit:	6.60E+75	-1.63E+01	7.00E+03
	TROE	centering:	1.00E+00	1.00E-01	5.85E+02	6.11E+03
3224	C6H6+O2=C6H5+HO2	6.30E+13	0	60000		
3225	C6H6+O=C6H5O+H	2.20E+13	0	4530		
3226	C6H6+O=C6H5+OH	2.00E+13	0	14700		
3227	C6H5+H2=C6H6+H	5.71E+04	2.4	6277.6		
3228	C6H6+CH3=C6H5+CH4	7.32E+12	0	18920		
3229	C6H6+HO2=C6H5+H2O2	5.50E+12	0	28900		
3230	C6H6+OH=C6H5+H2O	1.20E+00	4.1	-301		
3231	C6H6+OH=C6H5OH+H	1.32E+02	3.2	5590		
3232	C6H5=>H+C4H2+C2H2	4.30E+12	0.6	77294		
3233	C6H5+CH2O=C6H6+HCO	8.55E+04	2.2	38		
3234	C6H5+HCO=C6H6+CO	8.55E+04	2.2	38		
3235	C6H5+HO2=C6H5O+OH	5.00E+12	0	0		
3236	C6H5+O2=C6H5O+O	2.60E+13	0	6120		
3237	C6H5+O2=C6H5OO	1.86E+13	-0.2	-711		
3238	C6H5OO=C6H5O+O	1.27E+15	-0.2	38536		
3239	C6H5OH+O2=C6H5O+HO2	1.00E+13	0	38800		

3240	C6H5OH+H=C6H5O+H2	1.20E+14	0	12400		
3241	C6H5OH+O=C6H5O+OH	1.30E+13	0	2900		
3242	C6H5OH+OH=C6H5O+H2O	1.40E+08	1.4	-960		
3243	C6H5OH+HO2=C6H5O+H2O2	1.00E+12	0	10000		
3244	C6H5OH+CH3=C6H5O+CH4	1.80E+11	0	7700		
3245	C6H5OH+C6H5=C6H5O+C6H6	4.90E+12	0	4400		
3246	C6H5OH+C3H5-A=C6H5O+C3H6	4.90E+11	0	9400		
3247	C6H5OH+C4H5-I=C6H5O+C4H6	4.90E+11	0	9400		
3248	C6H5O+H(+M)=C6H5OH(+M)	2.50E+14	0	0		
	Declared	duplicate	reaction...			
	Low	pressure	limit:	1.00E+94	-2.18E+01	1.39E+04
	TROE	centering:	4.30E-02	3.04E+02	6.00E+04	5.90E+03
3249	C6H5OH=C5H6+CO	5.00E+11	0	60808		
	Declared	duplicate	reaction...			
3250	C6H5O=CO+C5H5	2.00E+11	0	43900		
3251	C6H5O+H=CO+C5H6	1.00E+13	0	0		
3252	C6H5O+O=C5H5+CO2	1.00E+13	0	0		
3253	C5H5+H(+M)=C5H6(+M)	2.60E+14	0	0		
	CO	Enhanced	by	1.50E+00		
	CO2	Enhanced	by	2.00E+00		
	H2O	Enhanced	by	6.00E+00		
	H2	Enhanced	by	2.00E+00		
	CH4	Enhanced	by	2.00E+00		
	Low	pressure	limit:	4.40E+80	-1.83E+01	1.30E+04
	TROE	centering:	6.80E-02	4.01E+02	4.14E+03	5.50E+03
3254	C5H6(+M)=C3H4-A+C2H2(+M)	3.80E+17	0	104000		
	CO	Enhanced	by	1.50E+00		
	CO2	Enhanced	by	2.00E+00		
	H2O	Enhanced	by	6.00E+00		
	H2	Enhanced	by	2.00E+00		
	CH4	Enhanced	by	2.00E+00		
	Low	pressure	limit:	1.00E+98	-2.23E+01	1.26E+05
	TROE	centering:	1.44E-01	5.36E+00	3.28E+03	6.71E+09
3255	C5H6+O2=C5H5+HO2	4.00E+13	0	37150		
3256	C5H6+HO2=C5H5+H2O2	1.10E+04	2.6	12900		
3257	C5H6+OH=C5H5+H2O	3.08E+06	2	0		
3258	C5H6+H=C5H5+H2	3.03E+08	1.7	5590		
3259	C5H6+H=C2H2+C3H5-A	7.74E+36	-6.2	32890		
3260	C5H6+O=C5H5+OH	4.80E+04	2.7	1100		
3261	C5H6+C2H3=C5H5+C2H4	1.20E-01	4	0		
3262	C5H6+C6H5O=C5H5+C6H5OH	3.16E+11	0	8000		
3263	C5H6+CH3=C5H5+CH4	1.80E-01	4	0		
3264	C5H6+C6H5=C5H5+C6H6	1.00E-01	4	0		
3265	C5H6+C5H5=C6H6+C4H5-N	5.00E+09	0	0		
3266	C5H5(+M)=C2H2+C3H3(+M)	6.31E+13	-0.1	62300		
	Low	pressure	limit:	1.00E+45	-8.40E+00	4.75E+04

3267	$C_5H_5+O=C_4H_5-N+CO$	3.20E+13	-0.2	440		
3268	$C_5H_5+O=C_5H_4O+H$	5.80E+13	0	20		
3269	$C_5H_5+OH=C_4H_6+CO$	4.00E+14	0	4500		
3270	$C_5H_5+HO_2=C_5H_5O+OH$	6.30E+29	-4.7	11650		
3271	$C_5H_5O=C_5H_4O+H$	2.90E+32	-6.5	21220		
3272	$C_5H_5O=C_4H_5-N+CO$	1.10E+79	-19.6	66250		
3273	$C_5H_5O=CJ*CC*CC*O$	2.00E+13	0	14338		
3274	$CJ*CC*CC*O=C*CC*CCJ*O$	4.30E+11	-1.1	4118		
3275	$C_4H_5-N+CO=C*CC*CCJ*O$	1.51E+11	0	4810		
3276	$CJ*CC*CC*O=C_2H_2+CJ*CC*O$	3.00E+13	0	43710		
3277	$CJ*CC*O=C_2H_3CO$	1.40E+09	1	32100		
3278	$C_2H_2+HCO=CJ*CC*O$	7.77E+06	1.4	7755		
3279	$C_5H_4O=CO+2C_2H_2$	5.70E+32	-6.8	68500		
	Declared	duplicate	reaction...			
3280	$C_5H_4O=CO+2C_2H_2$	6.20E+41	-7.9	98700		
	Declared	duplicate	reaction...			
3281	$C_5H_4O+H=C_4H_5-N+CO$	2.10E+61	-13.3	40810		
3282	$C_5H_4O+O=C_4H_4+CO_2$	1.00E+13	0	2000		
3283	$C_5H_7=C*CCJC*C$	3.20E+15	0	39500		
3284	$C_5H_7+H=C_5H_6+H_2$	3.60E+12	0	0		
3285	$C_5H_7+O=C_5H_6+OH$	1.00E+13	0	0		
3286	$C_5H_7+OH=C_5H_6+H_2O$	2.40E+13	0	0		
3287	$C_5H_6+H=C_5H_7$	2.40E+73	-17.9	31500		
3288	$C_5H_6+H=C*CCJC*C$	1.10E+14	-0.2	3100		
3289	$C_5H_6+O=C_5H_5O+H$	8.90E+12	-0.1	590		
	Declared	duplicate	reaction...			
3290	$C_5H_6+O=C_5H_5O+H$	5.60E+12	-0.1	200		
	Declared	duplicate	reaction...			
3291	$C_5H_6+HO_2=C_5H_7+O_2$	1.30E+15	-1.1	9530		
3292	$C_5H_6+HCO=C_5H_5+CH_2O$	1.08E+08	1.9	16000		
3293	$C_5H_6+C_2H_3=C_6H_6+CH_3$	2.10E+67	-16.1	42460		
3294	$C_5H_6+C_4H_5-I=C_5H_5+C_4H_6$	6.00E+12	0	0		
3295	$C*CCJC*C=C*CC*CCJ$	5.40E+11	-0.7	60		
3296	$C*CC*CCJ+H=C*CC*CC$	2.30E+20	-1.6	3020		
3297	$C*CC*CC+H=C_4H_6+CH_3$	5.20E+71	-16.4	51000		
3298	$C*CC*CC+H=C*CC*CCJ+H_2$	7.00E+06	2	5000		
3299	$C*CC*CC+OH=C*CC*CCJ+H_2O$	7.00E+06	2	0		
3300	$C*CCJC*C+O_2=C_2H_3CHO+CH_2CHO$	1.20E+36	-7.2	33600		
3301	$C*CC*CCJ+H=C_4H_5-N+CH_3$	2.90E+26	-2.2	36770		
3302	$C*CCJC*C+O=C_2H_3CHO+C_2H_3$	2.00E+14	0	0		
3303	$C_2H_2+OH=C_2H_2OH$	9.93E+11	0	-960		
3304	$C_2H+O=CH+CO$	5.00E+13	0	0		
3305	$C_2H+OH=HCCO+H$	2.00E+13	0	0		
3306	$C_2H+O_2=2CO+H$	9.04E+12	0	-457		
3307	$HCCO+C_2H_2=H_2CCCH+CO$	1.00E+11	0	3000		
3308	$HCCO+O=CH+CO_2$	2.95E+13	0	1113		



3309	HCCO+O2=HCO+CO+O	9.78E+11	0	850		
3310	2HCCO=C2H2+2CO	1.00E+13	0	0		
3311	HCCO+OH=C2O+H2O	3.00E+13	0	0		
3312	C2O+H=CH+CO	1.00E+13	0	0		
3313	C2O+O=2CO	5.00E+13	0	0		
3314	C2O+OH=2CO+H	2.00E+13	0	0		
3315	C2O+O2=2CO+O	2.00E+13	0	0		
3316	CH2+HCCO=C2H3+CO	3.00E+13	0	0		
3317	C2H+H2=C2H2+H	4.09E+05	2.4	864.3		
3318	C2H+C2H2=C4H2+H	9.64E+13	0	0		
3319	C2H+C2H4=C4H4+H	1.20E+13	0	0		
3320	CH2+C2H2=H2CCCH+H	1.20E+13	0	6600		
3321	CH+C2H2=C3H2+H	1.00E+14	0	0		
3322	CH+CH2=C2H2+H	4.00E+13	0	0		
3323	CH+CH3=C2H3+H	3.00E+13	0	0		
3324	CH2(S)+C2H2=H2CCCH+H	1.50E+14	0	0		
3325	CH2(S)+C2H4=C3H5-A+H	1.30E+14	0	0		
3326	2C3H3=C6H615	4.00E+12	0	0		
3327	C6H615=HEX1245	1.80E+11	0	35804		
3328	HEX1245=MC6H6	5.00E+11	0	22081		
3329	MC6H6=FULVENE	4.26E+13	0	49282		
3330	MC6H6=C6H6	3.79E+13	0	22000		
3331	C5H6+H=C3H3+C2H4	2.00E+14	0	10000		
3332	C5H6+C2H5=C5H5+C2H6	3.11E+11	0	5500		
3333	C5H6+C4H5-N=C5H5+C4H6	3.11E+11	0	5500		
3334	C5H5+OH=C5H4OH+H	9.00E+13	0	0		
3335	C5H4OH=C5H4O+H	2.10E+13	0	48000		
3336	C5H4O=>CO+C4H4	1.00E+12	0	53000		
3337	C5H4+H=C5H3+H2	1.00E+06	2.5	5000		
3338	C5H4+O=C5H3+OH	1.00E+06	2.5	3000		
3339	C5H4+OH=C5H3+H2O	1.00E+07	2	0		
3340	C5H3+O2=C2H2+HCCO+CO	1.00E+12	0	0		
3341	C6H6+C2H5=C6H5+C2H6	6.31E+11	0	14864		
3342	C6H6+C2H3=C6H5+C2H4	4.08E-01	4	88023		
	Reverse	Arrhenius	coefficients:	9.44E-03	4.5	4470
3343	C6H6+C4H5-N=C6H5+C4H6	4.10E-01	4	8803		
3344	C6H6+C4H5-I=C6H5+C4H6	4.10E-01	4	8803		
3345	C6H5+O=C5H5+CO	9.00E+13	0	0		
3346	C6H5+OH=C6H5O+H	5.00E+13	0	0		
3347	C6H5+C2H=PHC2H	3.00E+08	0	1391		
3348	C6H5+C2H2=PHC2H+H	1.00E+13	0	7647		
	Declared	duplicate	reaction...			
3349	C6H5+C4H2=PHC2H+C2H	2.00E+13	0	0		
3350	C6H5+C4H4=PHC2H+C2H3	1.00E+13	0	7647		
3351	C6H5+O2=C6H5O2	1.86E+13	-0.2	-711		
3352	C6H5O+O=C6H5O2	2.81E+13	-0.2	-1935		

3353	C6H5+C3H6=C3H5-A+C6H6	1.36E+00	3.8	1437		
3354	C6H5OH+C4H5-N=C4H6+C6H5O	3.00E+02	3	7650		
	Declared	duplicate	reaction...			
3355	C6H5OH+C2H5=C6H5O+C2H6	3.00E+02	3	7650		
3356	C6H5OH+C2H3=C6H5O+C2H4	3.00E+02	3	7650		
3357	C6H5O+O=C6H4O2+H	3.00E+13	0	0		
3358	C6H5O2=C6H4O2+H	4.00E+08	0	0		
3359	C6H5O2=C5H5+CO2	1.20E+08	0	0		
3360	C6H5O2+H=C6H5O2H	2.50E+14	0	0		
3361	C6H5O+OH=C6H5O2H	1.00E+12	0	0		
3362	C6H5O2+HO2=C6H5O2H+O2	1.87E+12	0	1540		
3363	C6H5O2+C6H5OH=C6H5O2H+C6H5O	1.00E+12	0	6961		
3364	C6H5O+HO2=C6H5O2+OH	1.50E+14	0	23650		
3365	C6H4O2=C5H4+CO2	3.50E+12	0	67000		
3366	C6H4O2+H=>C5H5O+CO	2.50E+13	0	4700		
3367	C6H4O2+H=>C6H3O2+H2	2.00E+12	0	8100		
3368	C6H4O2+OH=>C6H3O2+H2O	1.00E+06	2	4000		
3369	C6H4O2+O=>C6H3O3+H	1.50E+13	0	4530		
3370	C6H4O2+O=>C6H3O2+OH	1.40E+13	0	14700		
3371	C6H3O2+H=>2C2H2+2CO	1.00E+14	0	0		
3372	C6H3O2+O=>C2H2+HCCO+2CO	1.00E+14	0	0		
3373	C6H3O3=>C2H2+HCCO+2CO	1.00E+12	0	50000		
3374	C4H5-N+C3H4-A=TOLUEN+H	2.00E+11	0	3700		
3375	C4H5-N+C3H4-P=TOLUEN+H	6.32E+11	0	3700		
3376	TOLUEN+O2=PHCH2+HO2	3.00E+14	0	43062		
3377	TOLUEN+H=C6H6+CH3	2.40E+13	0	5123		
3378	TOLUEN+C2H5=PHCH2+C2H6	1.01E+11	0	9514		
3379	TOLUEN+C6H5=PHCH2+C6H6	2.10E+12	0	4400		
3380	TOLUEN+C4H5-N=PHCH2+C4H6	4.00E+12	0	7500		
3381	TOLUEN+C2H3=PHCH2+C2H4	4.00E+12	0	7500		
3382	TOLUEN(+M)=C6H5+CH3(+M)	1.95E+27	-3.2	107447		
	Low	pressure	limit:	1.00E+98	-2.30E+01	1.22E+05
	TROE	centering:	7.05E-01	1.00E+10	4.60E+02	8.21E+09
3383	PHCH2+H(+M)=TOLUEN(+M)	7.22E+13	0.1	-44		
	Low	pressure	limit:	0.30200+137	-3.34E+01	5.56E+04
	TROE	centering:	5.00E-01	6.00E+02	9.00E+02	5.50E+03
	H2	Enhanced	by	2.00E+00		
	H2O	Enhanced	by	6.00E+00		
	CH4	Enhanced	by	2.00E+00		
	CO	Enhanced	by	1.50E+00		
	CO2	Enhanced	by	2.00E+00		
	C2H6	Enhanced	by	3.00E+00		
3384	TOLUEN+HO2=PHCH2+H2O2	1.02E+04	2.5	12340.5		
3385	TOLUEN+OH=PHCH2+H2O	1.77E+05	2.4	-602		
3386	TOLUEN+OH=C6H5OH+CH3	7.83E+02	2.9	3221		
3387	TOLUEN+O=PHCH2+OH	6.30E+11	0	0		

3388	TOLUEN+H=PHCH2+H2	6.47E+00	4	3384		
3389	TOLUEN+CH3=PHCH2+CH4	3.16E+11	0	9500		
3390	PHCH2=C4H4+C3H3	2.00E+14	0	83600		
3391	PHCH2=C5H5+C2H2	6.00E+13	0	70000		
3392	PHCH2+HO2=PHCH2O+OH	1.19E+09	1	-2250		
3393	PHCH2+O=C6H5+CH2O	1.00E+13	0	0		
3394	PHCH2+C3H3=TOLUEN+C3H2	1.00E+12	0	0		
3395	PHCH2+C6H5OH=TOLUEN+C6H5O	1.05E+11	0	9500		
3396	PHCH2+O2=PHCH2O+O	6.31E+12	0	42924		
3397	PHCH2+O2=PHCH2O2	8.28E+51	-12.6	14813		
3398	PHCH2O2=PHHCO+OH	3.88E+68	-17.7	58456		
3399	PHCH2OH+O2=>PHHCO+HO2+H	2.00E+14	0	41400		
3400	PHCH2OH+OH=>PHHCO+H2O+H	8.43E+12	0	2583		
3401	PHCH2OH+H=C6H6+CH2OH	1.20E+13	0	5148		
3402	PHCH2OH+PHCH2=>PHHCO+TOLUEN+H	2.11E+11	0	9500		
3403	PHCH2OH+C6H5=>PHHCO+C6H6+H	1.40E+12	0	4400		
3404	PHCH2O=PHHCO+H	1.27E+14	0	1103		
3405	PHHCO=PHCO+H	3.98E+15	0	83701		
3406	PHHCO+O2=PHCO+HO2	1.02E+13	0	39000		
3407	PHHCO+HO2=PHCO+H2O2	2.00E+12	0	11665		
3408	PHHCO+OH=PHCO+H2O	1.71E+09	1.2	-447		
3409	PHHCO+OH=C6H5OH+HCO	1.20E+13	0	5123		
3410	PHHCO+O=PHCO+OH	9.04E+12	0	3080		
3411	PHHCO+H=PHCO+H2	5.00E+13	0	4928		
3412	PHHCO+H=C6H6+HCO	1.20E+13	0	5148		
3413	PHHCO+CH3=PHCO+CH4	2.77E+03	2.8	5773		
3414	PHHCO+C6H5=PHCO+C6H6	7.01E+11	0	4400		
3415	PHCO=C6H5+CO	3.98E+14	0	29401		
3416	PHCO+O2=C6H5O+CO2	3.00E+10	0	2870		
3417	PHCO+HO2=>C6H5+CO2+OH	2.00E+13	0	0		
3418	PHC2H5=C6H6+C2H4	1.15E+09	0	51699		
3419	PHC2H5=STYREN+H2	5.01E+12	0	63988		
3420	PHC2H5=PHCH2+CH3	8.91E+15	0	74720		
3421	PHC2H5=C6H5+C2H5	1.00E+16	0	100000		
3422	PHC2H5=BPHC2H4+H	2.51E+15	0	81262		
3423	PHC2H5+O2=>BPHC2H4+HO2	4.00E+13	0	38220		
3424	PHC2H5+H=C2H5+C6H6	2.40E+13	0	5123		
3425	PHC2H5+H=BPHC2H4+H2	2.65E+02	3.4	1003.5		
3426	PHC2H5+H=APHC2H4+H2	2.35E+02	1.9	6637.2		
3427	PHC2H5+OH=APHC2H4+H2O	1.99E+07	1.8	1133		
3428	PHC2H5+OH=BPHC2H4+H2O	4.80E+12	0	0		
3429	PHC2H5+O=APHC2H4+OH	5.00E+08	1.5	5802		
3430	PHC2H5+O=BPHC2H4+OH	2.23E+13	0	3795.5		
3431	PHC2H5+HO2=>APHC2H4+H2O2	1.80E+04	2.5	16792		
3432	PHC2H5+HO2=>BPHC2H4+H2O2	6.80E+03	2.5	10115		
3433	PHC2H5+CH3=APHC2H4+CH4	2.75E-01	4	8287		

3434	PHC2H5+CH3=BPHC2H4+CH4	7.50E-01	3.5	4485		
3435	APHC2H4=STYREN+H	3.79E+06	2	32106		
	Reverse	Arrhenius	coefficients:	1.63E+06	2.2	1994
3436	C6H5+C2H4=APHC2H4	4.04E+03	2.6	1459		
	Reverse	Arrhenius	coefficients:	1.72E+11	0.8	38704
3437	BPHC2H4=STYREN+H	3.74E+08	1.6	44609		
	Reverse	Arrhenius	coefficients:	1.19E+07	1.9	-108
3438	BPHC2H4+O2=STYREN+HO2	1.58E+12	0	15200		
3439	BPHC2H4+O=C6H5+CH3CHO	1.60E+13	0	0		
3440	BPHC2H4+O=PHHCO+CH3	1.60E+13	0	0		
3441	BPHC2H4+OH=PHHCO+CH4	1.60E+13	0	0		
3442	BPHC2H4+HO2=>PHHCO+CH3+OH	5.00E+12	0	0		
3443	APHC2H4=BPHC2H4	5.95E+05	2.1	29582		
	Reverse	Arrhenius	coefficients:	2.31E+07	1.7	44456
3444	C4H5-N+C4H4=STYREN+H	3.16E+11	0	3700		
3445	2C4H4=STYREN	1.48E+14	0	38003		
3446	C6H5+C2H3=STYREN	1.00E+13	0	0		
3447	C6H5+C2H4=STYREN+H	5.10E+12	0	6190		
3448	STYREN=C6H6+C2H2	1.60E+11	0	58438		
3449	STYREN=N-C8H7+H	5.00E+15	0	109400		
3450	STYREN=BSTYRYL+H	5.00E+15	0	109400		
3451	STYREN+O2=N-C8H7+HO2	4.00E+13	0	59800		
3452	STYREN+O2=BSTYRYL+HO2	4.00E+13	0	59800		
3453	STYREN+OH=N-C8H7+H2O	5.00E+12	0	6936		
3454	STYREN+OH=BSTYRYL+H2O	5.00E+12	0	5936		
3455	STYREN+H=N-C8H7+H2	5.00E+13	0	15009		
3456	STYREN+H=BSTYRYL+H2	5.00E+13	0	14009		
3457	STYREN+HO2=N-C8H7+H2O2	7.50E+10	0	14190		
3458	STYREN+HO2=BSTYRYL+H2O2	7.50E+10	0	13190		
3459	STYREN+O=PHCH2+HCO	1.20E+08	1.4	530		
3460	STYREN+O=C6H5+CH2CHO	6.00E+07	1.4	530		
3461	STYREN+C6H5=N-C8H7+C6H6	2.00E+11	0	20000		
3462	STYREN+C6H5=BSTYRYL+C6H6	2.00E+11	0	19000		
3463	STYREN+C6H5O=N-C8H7+C6H5OH	2.00E+11	0	20000		
3464	STYREN+C6H5O=BSTYRYL+C6H5OH	2.00E+11	0	19000		
3465	STYREN+C5H5=N-C8H7+C5H6	2.00E+11	0	20000		
3466	STYREN+C5H5=BSTYRYL+C5H6	2.00E+11	0	19000		
3467	STYREN+OH=C6H4C2H3+H2O	1.63E+07	1.4	1454		
3468	STYREN+H=>C6H4C2H3+H2	1.90E+07	2	9698		
3469	STYREN+HO2=>PHCH2+HCO+OH	2.50E+12	1	25000		
3470	STYREN+HO2=>PHHCO+CH2+OH	2.50E+12	1	25000		
3471	STYREN+H=C6H6+C2H3	2.40E+13	0	5123		
3472	N-C8H7+H=BSTYRYL+H	1.00E+14	0	0		
3473	N-C8H7=C6H5+C2H2	1.00E+14	0	36850		
3474	N-C8H7=PHC2H+H	3.00E+12	0	37830		
3475	N-C8H7+O2=PHHCO+HCO	2.00E+11	0	14000		

3476	N-C8H7+C6H5=PHC2H+C6H6	1.00E+13	0	0		
3477	BSTYRYL+O2=PHCO+CH2O	2.00E+11	0	14000		
3478	BSTYRYL+O=C6H5+CH2CO	1.60E+13	0	0		
3479	BSTYRYL=PHC2H+H	3.00E+12	0	48030		
3480	BSTYRYL+C6H5=PHC2H+C6H6	1.00E+13	0	0		
3481	BSTYRYL+OH=PHC2H+H2O	2.00E+13	0	0		
3482	BSTYRYL+H=PHC2H+H2	5.00E+13	0	0		
3483	PHCH2HCO+O2=>PHCH2CO+HO2	2.00E+13	0.5	42200		
3484	PHCH2HCO+HO2=>PHCH2CO+H2O2	4.10E+04	2.5	10204		
3485	PHCH2HCO+OH=>PHCH2CO+H2O	2.69E+08	1.4	-1574		
3486	PHCH2HCO+O=>PHCH2CO+OH	5.85E+12	0	1808		
3487	PHCH2HCO+H=>PHCH2CO+H2	4.10E+09	1.2	2404		
3488	PHCH2HCO+CH3=>PHCH2CO+CH4	3.50E-08	6.2	1639		
3489	PHCH2HCO=>PHCH2+HCO	5.00E+16	0	71600		
3490	PHCH2HCO+H=C6H6+CH2CHO	5.78E+13	0	8088		
3491	PHCH2CO=PHCH2+CO	3.98E+14	0	29401		
3492	PHCH2CO+O2=PHCH2O+CO2	3.00E+10	0	2870		
3493	PHCH2CO+HO2=>PHCH2+CO2+OH	2.00E+13	0	0		
3494	C6H5+CH2CO=PHCH2CO	3.20E+04	2.4	489		
3495	C6H5+CH2CO=PHCOCH2	6.20E+19	-2.3	15083		
3496	PHC2H+OH=>C6H6+HCCO	1.00E+13	0	0		
3497	PHC2H+H=C6H4C2H+H2	5.00E+13	-0.5	1500		
3498	PHC2H+OH=C6H4C2H+H2O	1.05E+13	0	4565		
3499	PHC2H+C2H=C6H4C2H+C2H2	2.00E+13	0	0		
3500	PHC2H+O=C6H5CCO+H	4.80E+09	1	0		
3501	PHC2H+CH3=C6H4C2H+CH4	1.67E+12	0	15057		
3502	C6H4C2H+C2H2=A1C2HAC	1.90E+21	-2.9	8100		
3503	C6H4C2H+C2H2=A2-1	5.10E+48	-10.5	28000		
3504	C6H4C2H+H=PHC2H	4.20E+11	0.5	-71.7		
3505	C6H5CCO+O2=PHCO+CO2	1.00E+12	0	0		
3506	PHCHCO+OH=PHCH2+CO2	3.73E+12	0	-1010		
3507	PHCHCO+H=PHCH2+CO	4.40E+12	0	1459		
3508	PHCHCO+O=PHHCO+CO	3.20E+12	0	-437		
3509	PBZ(+M)=PHCH2+C2H5(+M)	2.30E+22	-1.6	77244		
	Low	pressure	limit:	1.00E+75	-1.72E+01	5.91E+04
	TROE	centering:	8.66E-05	2.14E+02	2.14E+02	3.57E+03
3510	PBZ(+M)=APHC2H4+CH3(+M)	7.06E+20	-1.3	89013		
	Low	pressure	limit:	3.63E+47	-9.31E+00	6.87E+04
	TROE	centering:	7.99E-02	4.42E+02	1.55E+10	2.77E+03
3511	PBZ(+M)=C6H5+NC3H7(+M)	1.26E+22	-1.3	102320		
	Low	pressure	limit:	6.71E+41	-7.34E+00	8.48E+04
	TROE	centering:	2.57E-01	5.43E+02	3.93E+12	3.22E+03
3512	PBZ=PBZJA+H	9.00E+15	0	100210		
3513	PBZ=PBZJB+H	6.00E+15	0	99110		
3514	PBZ=PBZJC+H	6.00E+15	0	86210		
3515	PBZ+O2=PBZJA+HO2	4.00E+13	0	50600		

3516	PBZ+O2=PBZJB+HO2	4.00E+13	0	49500		
3517	PBZ+O2=PBZJC+HO2	4.00E+13	0	35800		
3518	PBZ+H=NC3H7+C6H6	5.78E+13	0	8087		
3519	PBZ+H=PBZJA+H2	5.75E+07	1.9	5599.2		
3520	PBZ+H=PBZJB+H2	7.97E+07	1.9	6819.3		
3521	PBZ+H=PBZJC+H2	6.31E+06	2.2	8640.7		
3522	PBZ+O=PBZJA+OH	1.93E+05	2.7	3716		
3523	PBZ+O=PBZJB+OH	4.77E+04	2.7	2106		
3524	PBZ+O=PBZJC+OH	4.77E+04	2.7	1106		
3525	PBZ+OH=PBZJA+H2O	3.16E+07	1.8	934		
3526	PBZ+OH=PBZJB+H2O	7.08E+06	1.9	-159		
3527	PBZ+OH=PBZJC+H2O	2.76E+04	2.6	-1919		
3528	PBZ+HO2=PBZJA+H2O2	4.76E+04	2.5	16494		
3529	PBZ+HO2=PBZJB+H2O2	9.64E+03	2.6	13910		
3530	PBZ+HO2=PBZJC+H2O2	4.82E+03	2.5	10530		
3531	PBZ+CH3=PBZJA+CH4	2.75E-01	3.6	7150		
3532	PBZ+CH3=PBZJB+CH4	6.00E+11	0	10120		
3533	PBZ+CH3=PBZJC+CH4	3.69E+00	3.3	4002		
3534	PBZ+C2H3=PBZJA+C2H4	6.00E+02	3.3	10502		
3535	PBZ+C2H3=PBZJB+C2H4	1.00E+03	3.1	8829		
3536	PBZ+C2H3=PBZJC+C2H4	1.00E+03	3.1	8829		
3537	PBZ+C2H5=PBZJA+C2H6	3.16E+11	0	12300		
3538	PBZ+C2H5=PBZJB+C2H6	5.01E+10	0	10400		
3539	PBZ+C2H5=PBZJC+C2H6	5.01E+10	0	10400		
3540	PBZ+C3H5-A=PBZJA+C3H6	7.94E+11	0	20500		
3541	PBZ+C3H5-A=PBZJB+C3H6	7.94E+11	0	16200		
3542	PBZ+C3H5-A=PBZJC+C3H6	7.94E+11	0	16200		
3543	PBZ+C3H5-T=PBZJA+C3H6	7.94E+11	0	20500		
3544	PBZ+C3H5-T=PBZJB+C3H6	7.94E+11	0	16200		
3545	PBZ+C3H5-T=PBZJC+C3H6	7.94E+11	0	16200		
3546	PBZ+C3H5-S=PBZJA+C3H6	7.94E+11	0	20500		
3547	PBZ+C3H5-S=PBZJB+C3H6	7.94E+11	0	16200		
3548	PBZ+C3H5-S=PBZJC+C3H6	7.94E+11	0	16200		
3549	PBZ+C6H5=PBZJA+C6H6	7.94E+11	0	20500		
3550	PBZ+C6H5=PBZJB+C6H6	7.94E+11	0	16200		
3551	PBZ+C6H5=PBZJC+C6H6	7.94E+11	0	16200		
3552	PBZ+PHCH2=PBZJA+TOLUEN	7.94E+11	0	20500		
3553	PBZ+PHCH2=PBZJB+TOLUEN	7.94E+11	0	16200		
3554	PBZ+PHCH2=PBZJC+TOLUEN	7.94E+11	0	16200		
3555	PBZ+BPHC2H4=PBZJA+PHC2H5	7.94E+11	0	20500		
3556	PBZ+BPHC2H4=PBZJB+PHC2H5	7.94E+11	0	16200		
3557	PBZ+BPHC2H4=PBZJC+PHC2H5	7.94E+11	0	16200		
3558	PBZ+CH3O=PBZJA+CH3OH	3.18E+11	0	7050		
3559	PBZ+CH3O=PBZJB+CH3OH	7.20E+10	0	4470		
3560	PBZ+CH3O=PBZJC+CH3OH	4.00E+01	2.9	8609		
3561	PBZJA=PHCH2+C2H4	2.00E+13	0	12836		

3562	PBZJB=C6H5+C3H6	2.00E+13	0	35390		
3563	PBZJC=STYREN+CH3	1.00E+14	0	34860		
3564	BPHPROPY=STYREN+CH3	1.00E+14	0	24000		
3565	PBZJB+O=PHCH2+CH3CHO	1.60E+13	0	0		
3566	PBZJB+OH=TOLUEN+CH3CHO	1.60E+13	0	0		
3567	PBZJB+HO2=>PHCH2+CH3CHO+OH	5.00E+12	0	0		
3568	PBZJC+O=PHHCO+C2H5	1.60E+13	0	0		
3569	PBZJC+OH=PHHCO+C2H6	1.60E+13	0	0		
3570	PBZJC+HO2=>PHHCO+C2H5+OH	5.00E+12	0	0		
3571	PHC3H5-1=PHCH2+C2H3	8.00E+15	0	88500		
3572	PHC3H5-1=PHC3H4+H	1.40E+15	0	86250		
3573	PHC3H5-1+H=PHC3H4+H2	2.63E+14	0	8820		
3574	PHC3H5-1+O=PHC3H4+OH	4.00E+11	0.7	-2100		
3575	PHC3H5-1+OH=PHC3H4+H2O	3.12E+06	2	-1300		
3576	PHC3H5-1+HO2=PHC3H4+H2O2	2.66E+11	0	11270		
3577	PHC3H5-1+O2=PHC3H4+HO2	1.95E+12	0	38000		
3578	PHC3H5-1+CH3=PHC3H4+CH4	1.90E+12	0	9010		
3579	PHC3H5-1+C6H5=PHC3H4+C6H6	2.80E+12	0	11220		
3580	PHC3H5-1+PHCH2=PHC3H4+TOLUEN	2.80E+12	0	11220		
3581	PHC3H5-1+APHC2H4=PHC3H4+PHC2H5	2.80E+12	0	11220		
3582	PHC3H5-1+H=C6H6+C3H5-A	5.80E+13	0	5123		
3583	PHC3H5-1+HO2=>APHC2H4+HCO+OH	2.50E+12	1	25000		
3584	PHC3H5-1+HO2=>PHCH2CO+CH3+OH	2.50E+12	1	25000		
3585	PHC3H5-1+O=STYREN+CH2O	7.02E+07	1.6	-1628		
3586	PHC3H5-1+O=PHHCO+C2H4	4.69E+07	1.6	-1628		
3587	PHC3H5-1+OH=>APHC2H4+CH2O	1.00E+12	0	0		
3588	PHC3H5-1+OH=>PHCH2HCO+CH3	1.00E+12	0	0		
3589	PHC3H5-2=N-C8H7+CH3	3.00E+17	0	99000		
3590	PHC3H5-2=C6H5+C3H5-S	8.00E+15	0	163800		
3591	PHC3H5-2=PHC3H4+H	2.10E+15	0	88230		
3592	PHC3H5-2+H=PHC3H4+H2	5.00E+13	0	3900		
3593	PHC3H5-2+O=PHC3H4+OH	1.75E+11	0.7	5884		
3594	PHC3H5-2+OH=PHC3H4+H2O	2.25E+13	0	2217		
3595	PHC3H5-2+HO2=PHC3H4+H2O2	3.20E+12	0	14900		
3596	PHC3H5-2+O2=PHC3H4+HO2	1.95E+12	0	39000		
3597	PHC3H5-2+CH3=PHC3H4+CH4	1.00E+11	0	7300		
3598	PHC3H5-2+C6H5=PHC3H4+C6H6	2.80E+12	0	11220		
3599	PHC3H5-2+PHCH2=PHC3H4+TOLUEN	2.80E+12	0	11220		
3600	PHC3H5-2+APHC2H4=PHC3H4+PHC2H5	2.80E+12	0	11220		
3601	PHC3H5-2+O=PHHCO+C2H4	7.00E+07	1.6	-628		
3602	PHC3H5-2+O=STYREN+CH2O	4.70E+07	1.6	-628		
3603	PHC3H5-2+OH=>PHHCO+C2H5	2.60E+13	0	0		
3604	PHC3H5-2+OH=>PHCH2+CH3CHO	2.60E+13	0	0		
3605	PHC3H5-2+OH=CPHC3H5OHB	4.75E+12	0	-782		
3606	PHC3H5-2+OH=BPHC3H5OHC	4.75E+12	0	-782		
3607	PHC3H4+HO2=COPHC3H4-1+OH	1.90E+12	0	-1200		

3608	PHC3H4+HO2=AOPHC3H4-2+OH	1.90E+12	0	-1200		
3609	PHC3H4+CH3O2=COPHC3H4-1+CH3O	1.90E+12	0	-1200		
3610	PHC3H4+CH3O2=AOPHC3H4-2+CH3O	1.90E+12	0	-1200		
3611	PHC3H4+C2H5O2=COPHC3H4-1+C2H5O	1.90E+12	0	-1200		
3612	PHC3H4+C2H5O2=AOPHC3H4-2+C2H5O	1.90E+12	0	-1200		
3613	PHC3H4+NC3H7O2=COPHC3H4-1+NC3H7O	1.90E+12	0	-1200		
3614	PHC3H4+NC3H7O2=AOPHC3H4-2+NC3H7O	1.90E+12	0	-1200		
3615	PHC3H4+IC3H7O2=COPHC3H4-1+IC3H7O	1.90E+12	0	-1200		
3616	PHC3H4+IC3H7O2=AOPHC3H4-2+IC3H7O	1.90E+12	0	-1200		
3617	PHC3H4+O2=PHHCO+CH2CHO	1.06E+10	0.3	12838		
3618	COPHC3H4-1=PHHCO+C2H3	7.94E+14	0	19000		
3619	AOPHC3H4-2=CH2O+N-C8H7	7.94E+14	0	19000		
3620	CPHC3H5OHB+O2=PBZOHBQJC	4.58E+11	0	-378		
3621	BPHC3H5OHC+O2=PBZOHCQJB	2.00E+12	0	0		
3622	BPHC3H5OHA+O2=PBZOHAQJB	2.00E+12	0	0		
3623	APHC3H5OHB+O2=PBZOHBQJA	2.00E+12	0	0		
3624	PBZOHBQJC=PHHCO+CH3CHO+OH	1.00E+16	0	25000		
3625	PBZOHCQJB=PHHCO+CH3CHO+OH	1.00E+16	0	25000		
3626	PBZOHAQJB=PHCH2HCO+CH2O+OH	1.00E+16	0	25000		
3627	PBZOHBQJA=PHCH2HCO+CH2O+OH	1.00E+16	0	25000		
3628	PHC2H4HCO+O2=>PHC2H4CO+HO2	2.00E+13	0.5	42200		
3629	PHC2H4HCO+HO2=>PHC2H4CO+H2O2	1.70E+12	0	10700		
3630	PHC2H4HCO+OH=>PHC2H4CO+H2O	2.35E+10	0.7	-1113		
3631	PHC2H4HCO+O=>PHC2H4CO+OH	5.85E+12	0	1808		
3632	PHC2H4HCO+H=>PHC2H4CO+H2	5.54E+02	3.5	5167		
3633	PHC2H4HCO+CH3=>PHC2H4CO+CH4	2.25E+00	4	8285		
3634	PHC2H4HCO=>APHC2H4+HCO	5.00E+16	0	72250		
3635	PHC2H4CO=APHC2H4+CO	8.00E+13	0	30000		
3636	PHC2H4CO+HO2=>APHC2H4+CO2+OH	2.00E+13	0	0		
3637	PHCH2COCH2=PHCH2+CH2CO	4.00E+13	0	13500		
3638	PHCH2COCH2+O2=PHCH2COCH2O2	9.00E+18	-2.5	0		
3639	PHCH2COCH2O2+HO2=PHCH2COCH2O2H+O 2	2.29E+11	0	-1790		
3640	PHCH2COCH2O2H=PHCH2COCH2O+OH	1.50E+16	0	42500		
3641	PHCH2CO+CH2O=PHCH2COCH2O	1.50E+11	0	11900		
3642	PHCOC2H4=PHCO+C2H4	4.00E+13	0	27870		
3643	PHCOC2H4+O2=PHCOC2H3+HO2	5.00E+12	0	5000		
3644	PHCOC2H4+O2=PHCOCH2CH2O2	9.00E+18	-2.5	0		
3645	PHCOCH2CH2O2+HO2=PHCOCH2CH2O2H+O 2	2.29E+11	0	-1790		
3646	PHCOCH2CH2O2H=PHCOCH2CH2O+OH	1.50E+16	0	42500		
3647	PHCOCH2+CH2O=PHCOCH2CH2O	1.50E+11	0	11900		
3648	PHCOC2H3=>PHCO+C2H3	1.22E+23	-2	83950		
3649	PHCOC2H3=>C6H5+C2H3CO	1.22E+23	-2	83950		
3650	PHCH2CHCO+OH=APHC2H4+CO2	3.73E+12	0	-1010		
3651	PHCH2CHCO+H=APHC2H4+CO	4.40E+12	0	1459		
3652	PHCH2CHCO+O=PHCH2HCO+CO	3.20E+12	0	-437		



3653	2PHCH2=C14H14	2.51E+11	0.4	0		
3654	2C5H5=NAPHT+H2	1.00E+13	0	7000		
3655	2C5H5=NAPHT+2H	5.00E+12	0	8000		
3656	A1C2H3AC=NAPHT+H	1.00E+10	0	4780.1		
3657	PHCH2+C3H3=C10H10	1.00E+10	0	0		
3658	NAPHT+H=C10H9	5.00E+14	0	5000		
3659	NAPHT=A2-1+H	4.50E+15	0	107433.1		
3660	NAPHT+H=A2-1+H2	2.50E+14	0	15999		
3661	NAPHT+OH=A2-1+H2O	1.63E+08	1.4	1450.8		
3662	NAPHT+CH3=A2-1+CH4	2.00E+12	0	15060		
3663	NAPHT+O=A2O+H	2.23E+13	0	4530.7		
3664	NAPHT+O=A2-1+OH	2.00E+13	0	14704		
3665	NAPHT+O2=A2-1+HO2	6.30E+13	0	60000		
3666	A2-1+HO2=A2O+OH	5.00E+13	0	999		
3667	A2-1+O2=A2O+O	2.09E+12	0	7468.9		
3668	A2-1+OH=A2O+H	5.00E+13	0	0		
3669	A2O+H=A2OH	5.06E+14	0	0		
3670	A2O=>INDENYL+CO	7.40E+11	0	43853		
3671	A2OH+OH=A2O+H2O	3.00E+13	0	0		
3672	A2OH+H=A2O+H2	1.15E+14	0	12399.6		
3673	A2OH+H=NAPHT+OH	2.23E+13	0	7927.8		
3674	A2OH+O=A2O+OH	1.26E+13	0	2899.1		
3675	C10H10+OH=C10H9+H2O	5.00E+06	2	0		
3676	C10H10+O=C10H9+OH	7.00E+11	0.7	6000		
3677	C10H10+H=C10H9+H2	2.00E+05	2.5	2500		
3678	C10H9+H=C10H10	1.00E+14	0	0		
3679	C6H4C2H3+C2H2=A1C2H3AC	5.00E+12	0	0		
3680	PHCH2+C2H2=INDENE+H	3.20E+11	0	7000		
3681	C6H4C2H3+CH3=INDENE+2H	5.00E+13	0	0		
3682	CH3C6H4C2H3+OH=INDENE+H+H2O	1.26E+13	0	2583		
3683	CH3C6H4C2H3+H=INDENE+H+H2	3.98E+02	3.4	3120		
3684	INDENE+H=INDENYL+H2	4.38E+08	1.8	2999.5		
3685	INDENE+O=INDENYL+OH	1.81E+13	0	3080.8		
3686	INDENE+OH=INDENYL+H2O	6.86E+09	1.2	-446.9		
3687	INDENE+HO2=INDENYL+H2O2	1.99E+12	0	11658.7		
3688	INDENE+O2=INDENYL+HO2	2.00E+13	0	25000		
3689	INDENE+O2=INDENOXY+OH	1.00E+13	0	20712.2		
3690	INDENYL+O=N-C8H7+CO	1.00E+14	0	0		
3691	INDENYL+HO2=N-C8H7+CO+OH	1.00E+13	0	0		
3692	INDENYL+C5H5=PHNTHRN+2H	1.00E+13	0	4000		
3693	INDENYL+CO=>A2O	9.50E+03	1.4	26555.9		
3694	INDENYL+H(+M)=INDENE(+M)	1.00E+14	0	0		
	Low	pressure	limit:	4.40E+81	-1.83E+01	1.30E+04
	TROE	centering:	6.80E-02	4.01E+02	4.14E+03	5.50E+03
	H2	Enhanced	by	2.00E+00		
	H2O	Enhanced	by	6.00E+00		

	CH4	Enhanced	by	2.00E+00		
	CO	Enhanced	by	1.50E+00		
	CO2	Enhanced	by	2.00E+00		
3695	INDENYL+O=BSTYRYL+CO	1.00E+14	0	0		
3696	INDENYL+O=INDENOXY	1.00E+13	0	0		
3697	INDENYL+HO2=INDENOXY+OH	1.50E+13	0	0		
3698	INDENOXY=BSTYRYL+CO	2.51E+11	0	43900.6		
3699	CH2+CH2=C2H2+H+H	4.00E+13	0	0		
3700	C2H3+C2H=C2H2+C2H2	3.00E+13	0	0		
3701	C2H3+HCO=C2H4+CO	9.00E+13	0	0		
3702	C2H3+C2H3=H2CCCH+CH3	1.80E+13	0	0		
3703	C2H3+C2H3=C2H4+C2H2	6.30E+13	0	0		
3704	C2H3+CH=CH2+C2H2	5.00E+13	0	0		
3705	C2H+CH4=CH3+C2H2	7.23E+12	0	976		
3706	C2H3+C2H2(+M)<=>C4H4+H(+M)	5.00E+13	-1.2	11800		
	Low	pressure	limit:	5.00E+14	-7.50E-01	5.00E+03
	TROE	centering:	1.00E+00	1.00E-30	1.71E+02	1.07E+03
3707	C2H3+C2H2(+M)<=>C4H5-N(+M)	1.00E+30	-5.7	8700		
	Low	pressure	limit:	1.00E+30	-4.80E+00	-5.90E+01
	TROE	centering:	1.00E-02	1.00E-30	3.00E+02	1.00E+03
3708	C2H3+C2H2(+M)<=>C4H5-I(+M)	1.00E+28	-5.1	12000		
	Low	pressure	limit:	1.00E+30	-5.10E+00	-9.50E+02
	TROE	centering:	1.00E-01	1.00E-30	3.50E+03	1.50E+03
3709	C2H3+C2H3(+M)<=>C4H5-I+H(+M)	1.20E+14	-1.5	11900		
	Low	pressure	limit:	4.00E+20	-2.26E+00	5.06E+03
	TROE	centering:	1.00E+00	1.00E-30	1.00E+02	3.00E+03
3710	C2H3+C2H3(+M)<=>C4H5-N+H(+M)	2.00E+12	-0.7	14200		
	Low	pressure	limit:	1.00E+19	-1.95E+00	6.00E+03
	TROE	centering:	1.00E+00	1.00E-30	4.00E-01	1.00E+03
3711	c-C4H5=C4H4+H	3.00E+12	0	52000		
3712	C4H4+C2H2=C6H6	4.47E+11	0	30010		
3713	C2H2+CH2=C3H3+H	1.20E+13	0	6620		
3714	C2H2+CH2(S)=C3H3+H	2.00E+13	0	0		
3715	C7H6+H=>C5H5+C2H2	7.00E+12	0	0		
3716	C7H6=C7H5+H	1.02+116	-28.5	157860		
3717	C7H6=c-C5H4+C2H2	1.26+130	-32.2	173970		
3718	C7H6+CH3=C7H5+CH4	1.87E+04	2.7	6008		
3719	C7H5(+M)=C4H2+C3H3(+M)	3.00E+12	-0.1	62300		
	Low	pressure	limit:	1.00E+45	8.40E+00	4.75E+04
3720	C7H6+H=C7H5+H2	1.90E+08	1.8	4965		
3721	C7H5(+M)=C2H2+C5H3(+M)	2.00E+11	-0.1	62300		
	Low	pressure	limit:	1.00E+45	8.40E+00	4.75E+04
3722	C6H5O+H=C5H5+HCO	1.00E+13	0	12000		
3723	C5H6=C5H5+H	2.50E+15	0	82000		
3724	CH3+HCCO=C2H4+CO	5.00E+13	0	0		
3725	STYREN+H=PHCCH2+H2	3.33E+05	2.5	9240		

3726	C6H5+C2H3=PHCCH2+H	1.80E+31	-4.6	31652		
3727	C6H5+C2H3=PHCHCH+H	1.50E+32	-4.9	35504		
3728	PHCHCH+H=PHCCH2+H	2.30E+37	-6	35164		
3729	C6H5+C2H2=PHCHCH	7.70E+40	-9.2	13400		
3730	PHC2H+H=PHCHCH	5.00E+54	-12.8	17185		
3731	PHC2H+H=PHCCH2	5.00E+54	-12.8	17185		
3732	PHCHCH+H=PHC2H+H2	1.50E+13	0	0		
3733	PHCCH2+H=PHC2H+H2	3.00E+13	0	0		
3734	PHCHCH+O2=PHHCO+HCO	4.60E+16	-1.4	1010		
3735	PHCCH2+O2=PHCO+CH2O	4.60E+16	-1.4	1010		
3736	PHCCH2+OH=PHHCO+CH2	4.00E+07	1.8	220		
3737	PHCHCH+OH=PHC2H+H2O	2.50E+12	0	0		
3738	PHCCH2+OH=PHC2H+H2O	5.00E+12	0	0		
3739	PHCCH2+O=CH2CO+C6H5	4.80E+13	0	0		
3740	STYREN=PHCCH2+H	6.00E+46	-9.1	118323		
3741	STYREN+OH=PHCCH2+H2O	1.55E+06	2	430		
3742	STYREN+O2=PHCCH2+HO2	2.00E+13	0	57900		
3743	STYREN+H=PHCHCH+H2	6.65E+05	2.5	12240		
3744	C6H5+C3H3=INDENE	1.50E+75	-17.8	39600		
	Declared	duplicate	reaction...			
3745	H2CCCH+H2CCCH=FULVENE	7.25E+65	-16	25035		
	Declared	duplicate	reaction...			
3746	H2CCCH+H2CCCH=FULVENE	4.19E+39	-9	6098		
	Declared	duplicate	reaction...			
3747	H2CCCH+OH=C2H3+HCO	5.00E+13	0	0		
3748	H2CCCH+OH=C2H4+CO	3.00E+13	0	0		
3749	C3H4-A+H=H2CCCH+H2	6.60E+03	3.1	5522		
3750	C3H4-A+OH=H2CCCH+H2O	2.00E+07	2	5000		
3751	C3H4-A+OH=CH2O+C2H3	1.00E+12	0	-198.7		
3752	C3H4-A+OH=CH2CO+CH3	3.04E+12	0	-198.7		
3753	C3H4-P+H=H2CCCH+H2	3.57E+04	2.8	4821		
3754	H2CCCH+H2CCCH=C6H6	1.64E+66	-15.9	27529		
	Declared	duplicate	reaction...			
3755	H2CCCH+H2CCCH=C6H6	1.20E+35	-7.4	5058		
	Declared	duplicate	reaction...			
3756	C3H3+C3H5-A=FULVENE+H+H	3.26E+29	-5.4	3390		
3757	FULVENE+H(+M)=C6H6+H(+M)	4.50E+08	1.2	12500		
	Low	pressure	limit:	4.26E+17	-9.71E-01	6.00E+03
	TROE	centering:	-3.74E-01	6.90E+02	1.00E+01	1.51E+03
3758	C2H2+C4H5-I(+M)=H+FULVENE(+M)	1.00E+40	-7.9	39600		
	Low	pressure	limit:	2.00E+24	-3.45E+00	1.40E+04
	TROE	centering:	5.00E-01	2.00E+00	1.00E+00	1.63E+03
3759	C4H3-I+H2=C2H2+C2H3	5.01E+10	0	20000		
3760	C2H+C4H4=C2H2+C4H3-I	4.00E+13	0	0		
3761	C4H4+C6H5=C6H6+C4H3-N	1.00E+12	0	0		
3762	C4H4+C6H5=C6H6+C4H3-I	1.00E+12	0	0		

3763	$C_6H_5+C_2H_2=C_6H_6+C_2H$	1.13E+12	0	14100		
3764	$C_2H_3+C_4H_2=C_4H_4+C_2H$	3.01E+13	0	23000		
3765	$C_2H_3+C_4H_4=C_2H_4+C_4H_3-N$	5.00E+11	0	16300		
3766	$C_2H_3+C_4H_4=C_2H_4+C_4H_3-I$	5.00E+11	0	16300		
3767	$C_4H_4=C_2H+C_2H_3$	1.00E+16	0	105000		
3768	$H+C_2H_2=C_2H_3$	5.50E+12	0	2500		
3769	$C_6H_4CH_3+H(+M)=TOLUEN(+M)$	1.00E+14	0	0		
	Low	pressure	limit:	6.60E+75	-1.63E+01	7.00E+03
	TROE	centering:	1.00E+00	1.00E-01	5.85E+02	6.11E+03
	H2	Enhanced	by	2.00E+00		
	H2O	Enhanced	by	6.00E+00		
	CH4	Enhanced	by	2.00E+00		
	CO	Enhanced	by	1.50E+00		
	CO2	Enhanced	by	2.00E+00		
	C2H6	Enhanced	by	3.00E+00		
3770	$TOLUEN+H=C_6H_4CH_3+H_2$	3.91E+08	1.8	16352.8		
3771	$TOLUEN+CH_3=C_6H_4CH_3+CH_4$	1.79E-02	4.5	13637.7		
3772	$TOLUEN+OH=C_6H_4CH_3+H_2O$	1.36E+04	2.7	620		
3773	$TOLUEN+O=C_6H_4CH_3+OH$	2.00E+14	0	14700		
3774	$TOLUEN+HO_2=C_6H_4CH_3+H_2O_2$	3.61E+12	0	30982		
3775	$TOLUEN+O_2=>C_6H_4CH_3+HO_2$	1.70E+07	2	51633.9		
3776	$C_4H_3-N+C_3H_4-P=>C_6H_4CH_3$	2.40E+10	0	0		
3777	$C_6H_4CH_3=>C_4H_3-N+C_3H_4-P$	4.50E+13	0	72500		
3778	$C_3H_3+C_6H_4CH_3=>NAPHT+H+H$	5.00E+12	0	3000		
3779	$C_4H_5-N+C_6H_4CH_3=>A_2CH_3-1+H+H$	5.00E+13	0	1000		
3780	$C_6H_4CH_3+H=PHCH_2+H$	1.00E+13	0	0		
3781	$C_6H_4CH_3+C_2H_2=INDENE+H$	1.00E+12	0	5000		
3782	$O+C_6H_5O=>HCO+C_2H_2+C_2H_2+CO$	6.00E+12	0	0		
3783	$C_6H_5O+H(+M)=C_6H_5OH(+M)$	5.00E+13	0	0		
	Declared	duplicate	reaction...			
	Low	pressure	limit:	1.00E+94	-2.18E+01	1.39E+04
	TROE	centering:	4.30E-02	3.40E+02	6.00E+04	5.90E+03
	H2	Enhanced	by	2.00E+00		
	H2O	Enhanced	by	6.00E+00		
	CH4	Enhanced	by	2.00E+00		
	CO	Enhanced	by	1.50E+00		
	CO2	Enhanced	by	2.00E+00		
3784	$C_6H_5OH=C_5H_6+CO$	5.02E+15	-0.6	74115		
	Declared	duplicate	reaction...			
3785	$C_6H_5OH+C_4H_5-N=C_6H_5O+C_4H_6$	6.00E+12	0	0		
	Declared	duplicate	reaction...			
3786	$C_6H_4OH+H=C_6H_5OH$	1.00E+14	0	0		
3787	$C_6H_5OH+H=C_6H_4OH+H_2$	1.70E+14	0	16000		
3788	$C_6H_5OH+O=C_6H_4OH+OH$	2.00E+13	0	14700		
3789	$C_6H_5OH+OH=C_6H_4OH+H_2O$	1.40E+13	0	4600		
3790	$C_6H_5OH+HO_2=C_6H_4OH+H_2O_2$	4.00E+11	0	28900		

3791	C6H5OH+CH3=C6H4OH+CH4	2.00E+12	0	15000		
3792	H+C14H14=TOLUEN+C6H4CH3	2.50E+12	0	15000		
3793	H+C14H14=>C6H6+H+STYREN	2.50E+12	0	5000		
3794	A3-1+H(+M)=PHNTHRN(+M)	1.00E+14	0	0		
	Low	pressure	limit:	0.40000+149	-3.75E+01	2.06E+04
	TROE	centering:	1.00E+00	5.36E+02	1.45E+02	5.63E+03
	H2	Enhanced	by	2.00E+00		
	H2O	Enhanced	by	6.00E+00		
	CH4	Enhanced	by	2.00E+00		
	CO	Enhanced	by	1.50E+00		
	CO2	Enhanced	by	2.00E+00		
	C2H6	Enhanced	by	3.00E+00		
3795	A3-4+H(+M)=PHNTHRN(+M)	1.00E+14	0	0		
	Low	pressure	limit:	0.21000+140	-3.48E+01	1.84E+04
	TROE	centering:	1.00E-03	1.71E+02	1.71E+02	4.99E+03
	H2	Enhanced	by	2.00E+00		
	H2O	Enhanced	by	6.00E+00		
	CH4	Enhanced	by	2.00E+00		
	CO	Enhanced	by	1.50E+00		
	CO2	Enhanced	by	2.00E+00		
	C2H6	Enhanced	by	3.00E+00		
3796	A2C2H*+C2H2=A2(C2H)2+H	5.50E+32	-5.5	27600		
3797	A2C2H+C2H=A2(C2H)2+H	5.00E+13	0	0		
3798	PHNTHRN+H=A3-1+H2	2.50E+14	0	16000		
3799	PHNTHRN+H=A3-4+H2	2.50E+14	0	16000		
3800	A3-1+H=A3-4+H	1.70E+72	-15.2	77175		
3801	NAPHT+C4H3-N=>PHNTHRN+H	4.00E+13	0	15976		
3802	A2-1+C4H3-N=>PHNTHRN	1.50E+75	-17.8	39600		
3803	A2-2+C4H3-N=>PHNTHRN	1.50E+75	-17.8	39600		
3804	A2-1+C4H4=PHNTHRN+H	3.30E+33	-5.7	25500		
3805	A2-2+C4H4=PHNTHRN+H	3.30E+33	-5.7	25500		
3806	A2R5+C2H2=A3-4	2.00E+13	0	55000		
3807	PHCC+C6H6=PHNTHRN+H	5.60E+12	-0.1	7550		
3808	C6H5+PHC2H=PHNTHRN+H	1.00E+13	0	2430		
3809	A2-2+C4H4=ANTHRCN+H	1.26E+04	2.6	1434		
3810	NAPHT+C4H3-N=ANTHRCN+H	1.00E+13	0	0		
3811	ANTHRCN=PHNTHRN	7.94E+12	0	65000		
3812	PHCH2+C7H5=C13H9CH2+H	1.56E+13	-1	-3266.5		
3813	C13H8CH2+H=PHNTHRN+H	5.35E+11	0.6	2422.4		
3814	A2(C2H)2+H=A3-1	1.50E+51	-10.8	25500		
3815	A2C2H*+C2H2(+M)=A3-4(+M)	1.00E+33	-5.9	20000		
	Low	pressure	limit:	2.00E+33	-5.40E+00	-5.00E+03
	TROE	centering:	1.00E-05	1.00E-28	1.00E+02	1.00E+03
3816	A2(C2H)2+H(+M)=A3-4(+M)	1.30E+42	-7.8	23000		
	Low	pressure	limit:	3.70E+49	-9.40E+00	0.00E+00
	TROE	centering:	6.84E-01	5.00E+03	1.00E+01	2.00E+04

3817	$C_{13}H_9CH_2(+M)=C_{13}H_8CH_2+H(+M)$	1.00E+45	-5	70000		
	Low	pressure	limit:	2.10E+34	-4.90E+00	5.40E+04
	TROE	centering:	5.00E-01	1.00E+03	1.50E+04	2.00E+04
3818	$C_{13}H_9CH_2(+M)=PHNTHRN+H(+M)$	1.00E+45	-5	70000		
	Low	pressure	limit:	2.00E+36	-5.40E+00	5.00E+04
	TROE	centering:	1.00E-03	1.00E-30	7.00E+03	2.00E+04
3819	$C_{13}H_9+CH_3(+M)\Rightarrow C_{13}H_9CH_2+H(+M)$	1.00E+52	-11	52000		
	Low	pressure	limit:	1.30E+28	-4.00E+00	2.20E+04
	TROE	centering:	1.00E+00	1.00E+01	1.00E+01	3.15E+02
3820	$C_2H_5OO\Rightarrow O_2+C_2H_5$	1.00E+14	0	30000		
3821	$CH_3OOH=OH+CH_3O$	2.00E+15	0	42500		
3822	$CH_3OO+H=CH_3OOH$	5.00E+13	0	0		
3823	$CH_3OO=CH_2O+OH$	1.50E+13	0	47000		
3824	$HO_2+C_2H_5=C_2H_5OOH$	3.00E+12	0	0		
3825	$C_2H_5OOH\Rightarrow CH_2O+CH_3+OH$	1.00E+15	0	40000		
3826	$C_2-QOOH\Rightarrow CH_2OH+CH_2O$	2.00E+13	0	27500		
3827	$C_2-QOOH\Rightarrow C_2H_4+HO_2$	1.50E+13	0	24000		
3828	$C_2-QOOH\Rightarrow C_2H_5OO$	1.00E+11	0	18100		
3829	$HO_2+C_2H_4\Rightarrow C_2-QOOH$	5.00E+11	0	14000		
3830	$CH_3OO+OH\Rightarrow CH_3O+HO_2$	3.00E+12	0	0		
3831	$CH_3OO+CH_3\Rightarrow CH_3O+CH_3O$	3.00E+13	0	-1200		
3832	$CH_3OO+HO_2=CH_3OOH+O_2$	4.00E+10	0	-2600		
3833	$CH_3OO+HO_2\Rightarrow O_2+CH_2O+H_2O$	5.00E+10	0	0		
3834	$CH_3OO+CH_3O\Rightarrow CH_3OOH+CH_2O$	6.00E+11	0	0		
3835	$CH_3OO+CH_3OO\Rightarrow O_2+CH_3O+CH_3O$	2.00E+11	0	0		
3836	$CH_3OO+CH_3OO\Rightarrow O_2+CH_3OH+CH_2O$	1.00E+10	0	0		
3837	$CH_3OO+CH_2CHCH_2\Rightarrow O_2+C_4H_8-1$	1.50E+11	0	0		
3838	$CH_3OO+CH_2CHCH_2\Rightarrow CH_3O+C_2H_3+CH_2O$	7.50E+10	0	0		
3839	$C_2H_5OO+HO_2=C_2H_5OOH+O_2$	1.00E+11	0	-2600		
3840	$C_2H_5OO+CH_3\Rightarrow CH_3+CH_2O+CH_3O$	2.00E+12	0	-1200		
3841	$C_2H_5OO+CH_3OO\Rightarrow O_2+CH_3O+CH_3+CH_2O$	2.00E+11	0	0		
3842	$C_2H_5OO+C_2H_5OO\Rightarrow O_2+CH_3+CH_2O+CH_3+C$ H <sub>2</sub> O	2.00E+11	0	0		
3843	$CH_3O+CH_3OOH\Rightarrow CH_3OH+OH+CH_2O$	1.50E+11	0	6500		
3844	$CH_3OO+CH_2O\Rightarrow CO+H_2+CH_2O+OH$	2.00E+11	0	11000		
3845	$CH_3OO+CO\Rightarrow CO_2+CH_3O$	1.00E+14	0	24000		
3846	$C_2H_5OO+CO\Rightarrow CO_2+CH_3+CH_2O$	1.00E+14	0	24000		
3847	$O_2+HCO\Rightarrow HCO_3$	2.00E+11	0	0		
3848	$HCO_3\Rightarrow O_2+HCO$	7.00E+12	0	34000		
3849	$HCO_3+HO_2\Rightarrow O_2+HCO_3H$	2.00E+11	0	0		
3850	$HCO_3+CH_3OO\Rightarrow O_2+CO+CH_3O+OH$	2.00E+11	0	0		
3851	$HCO_3H\Rightarrow OH+OH+CO$	2.00E+14	0	38000		
3852	$CH_3CO_3H\Rightarrow CH_3+CO_2+OH$	1.00E+15	0	37400		
3853	$CH_3CO_3\Rightarrow CH_3CO+O_2$	2.50E+12	0	32000		
	Declared	duplicate	reaction...			
3854	$CH_3CO_3+HO_2\Rightarrow CH_3+CO_2+O_2+OH$	1.00E+12	0	0		

3855	CH3CO3+CH3OO=>O2+CH3+CO2+CH3O	9.00E+11	0	0		
3856	CH3CO3+CH3CO3=>2CO2+2CH3+O2	2.50E+12	0	0		
3857	CH2CHCH2+HO2=>AC3H5OOH	7.00E+12	-0.8	0		
3858	AC3H5OOH=>OH+CH2O+C2H3	1.00E+15	0	45000		
3859	CH3CHOOCHO=>CO+CH3CHO+OH	6.00E+11	0	24500		
3860	CH2CHOOHCHO=C2H3CHO+HO2	1.00E+14	0	23000		
3861	CH2CHOOHCHO=OH+ETC3H4O2	1.00E+12	0	18000		
3862	O2+CH2CHOOHCHO=>CH2OOCCHOOHCHO	2.00E+12	0	0		
3863	CH2OOCCHOOHCHO=>O2+CH2CHOOHCHO	3.00E+13	0	31000		
3864	O2+C5H11-1=>NC5H12OO	2.00E+12	0	0		
3865	NC5H12OO=>C5H11-1+O2	3.00E+13	0	30000		
3866	NC5H12OO=>NC5-QOOH	3.00E+12	0	24100		
3867	NC5-QOOH=>NC5H12OO	9.00E+10	0	16100		
3868	NC5-QOOH=>HO2+C5H10-1	2.00E+13	0	23500		
3869	NC5-QOOH=>OH+CH3CHO+C3H6	3.00E+13	0	24000		
3870	NC5-QOOH =>OH+.625CH2O+.625C4H8- 1+.375C2H5CHO+.375C2H4	2.00E+13	0	24000		
3871	O2+NC5-QOOH=>NC5-OOQOOH	2.00E+12	0	0		
3872	NC5-OOQOOH=>NC5-QOOH+O2	1.00E+14	0	29000		
3873	NC5H12OO+HO2=>C5H11O2H-1+O2	1.00E+11	0	-1200		
3874	C5H11O2H-1 =>OH+.5C2H5+.5PC4H9+.5C2H5CHO+.5CH2O	2.00E+14	0	44000		
3875	C5H11O2H-1=>OH+NC3H7+CH3CHO	2.00E+14	0	44000		
3876	NC5H12OO+CH3OO=>O2+CH3CHO+N1C4H9 OH	5.00E+10	0	-1200		
3877	NC5H12OO+CH3OO=>O2+C2H5OH+MEK	5.00E+10	0	-1200		
3878	NC5H12OO+NC5H12OO =>O2+1.6CH3CHO+1.6NC3H7+.4CH2O+.4PC4 H9	1.00E+11	0	-1200		
3879	NC5H12OO+NC5H12OO =>O2+NC4H9CHO+N1C4H9OH+.5C2H4	5.00E+10	0	-1200		
3880	NC5-OOQOOH+HO2 =>O2+H2O2+.5CH2O+.5CH3CHO+.5C2H5CHO +.5C3H7CHO	1.00E+11	0	-1200		
3881	NC5-OOQOOH+CH3OO =>O2+CH3OOH+.5CH2O+.5CH3CHO+.5C2H5 CHO+.5C3H7CHO	1.00E+11	0	-1200		
3882	HO2+C5H10-1=>NC5-QOOH	1.00E+12	0	13000		
3883	C5H91-3+O2=>C5EN-OO	1.00E+12	0	0		
3884	C5EN-OO=>C5H91-3+O2	5.00E+13	0	30000		
3885	C5EN-OO=>C5EN-QOOH	2.50E+10	0	20000		
3886	C5EN-QOOH=>C5EN-OO	2.00E+10	0	12000		
3887	C5EN-QOOH+O2=>C5EN-OOQOOH-35	1.00E+12	0	0		
3888	C5EN-OOQOOH-35=>C5EN-QOOH+O2	5.00E+13	0	30000		
3889	C5EN-OOQOOH-35=>C5EN-OQOOH-35+OH	2.50E+10	0	16000		
3890	C5EN-OQOOH-35=>OH+C2H3+CH2CO+CH2O	5.00E+14	0	42000		
3891	C5EN-OQOOH-35=>OH+C2H3CHO+CH2CHO	5.00E+14	0	42000		
3892	C5EN-QOOH=>OH+C2H3CHO+C2H4	5.00E+11	0	16000		

3893	C5EN-QOOH=>.5C5H8+.5CYC5H8+HO2	2.00E+12	0	18000		
3894	C5EN-QOOH=>C5H8O+OH	2.50E+11	0	17000		
3895	O2+NEOC5H11=>NEOC5H11O2	1.50E+12	0	0		
	Declared	duplicate	reaction...			
3896	NEOC5H11O2=>NEOC5-QOOH	2.00E+12	0	22800		
3897	NEOC5-QOOH=>NEOC5H11O2	3.00E+10	0	12500		
3898	NEOC5-QOOH=>NEO-C5H10O+OH	1.60E+11	0	15000		
3899	NEOC5-QOOH=>CH2O+IC4H8+OH	3.00E+13	0	24000		
3900	NEOC5-QOOH+O2=>NEOC5-OOQOOH	1.50E+12	0	0		
3901	NEOC5-OOQOOH=>NEOC5-QOOH+O2	3.00E+13	0	31000		
3902	NEOC5- OOQOOH=>CH2O+CH2O+CH3COCH3+OH	5.00E+11	0	23500		
3903	NEOC5-OOQOOH=>NEOC5-OQOOH+OH	6.50E+10	0	20500		
3904	NEOC5-OQOOH=>OH+CH2O+IC3H5CHO+H	4.00E+14	0	43300		
3905	NEOC5- OQOOH=>OH+CH3COCH3+.25IC4H8+H+CO	2.00E+14	0	42300		
3906	NEOC5-OQOOH=>2OH+IC4H8+CO	8.00E+13	0	41000		
3907	MEK=CH3COCH2+CH3	2.00E+16	0	84000		
3908	MEK=CH3CO+C2H5	2.00E+16	0	80000		
3909	HO2+C7H14-1=>NC7-QOOH	8.00E+11	0	15000		
3910	O2+NC7H15=>NC7H15O2	2.00E+12	0	0		
	Declared	duplicate	reaction...			
3911	NC7H15O2=>NC7-QOOH	3.00E+12	0	25100		
3912	NC7-QOOH=>NC7H15O2	2.00E+10	0	16100		
3913	NC7-QOOH=>NC7H14O+OH	1.00E+10	0	14100		
3914	NC7-QOOH=>HO2+C7H14-1	2.00E+12	0	24000		
3915	NC7-QOOH=>OH+CH2O+C4H8-1+C2H4	3.00E+11	0	22500		
3916	NC7-QOOH =>OH+CH3CHO+.75C5H10- 1+.1C2H4+.15C7H14-1	5.00E+11	0	22500		
3917	NC7-QOOH=>OH+NC3H7CHO+C3H6	2.50E+11	0	22500		
3918	NC7-QOOH=>OH+NC4H9CHO+C2H4	5.00E+10	0	22500		
3919	NC7-QOOH =>OH+.5CH3CHO+.5C2H5CHO+C3H6+.25C4H 8-1+.25C2H4	3.00E+11	0	22500		
3920	NC7- QOOH=>OH+C2H5CHO+.9C3H6+.25C2H4+.2C 4H8-1	6.00E+11	0	22500		
3921	NC7-QOOH+O2=>NC7-OOQOOH	2.00E+12	0	0		
3922	NC7-OOQOOH=>NC7-QOOH+O2	2.00E+14	0	28500		
3923	NC7-OOQOOH=>NC7-OQOOH+OH	1.00E+12	0	25000		
3924	NC7-OQOOH=>OH+NC3H7CHO+CH3COCH2	7.50E+14	0	42000		
3925	NC7- OQOOH=>OH+CH3CHO+1.5C2H4+CH3CO	1.80E+15	0	42000		
3926	NC7-OQOOH=>OH+C3H4O2+PC4H9	4.00E+14	0	42000		
3927	NC7-OQOOH=>OH+NC4H9CHO+CH2CHO	3.00E+14	0	42000		
3928	NC7-OQOOH=>OH+C2H5CHO+CH2CO+C2H5	6.00E+14	0	42000		
3929	NC7-OQOOH=>OH+CH2O+CH2CO+PC4H9	4.00E+14	0	42000		
3930	C7H15O2H-1=>OH+C2H5+C2H5CHO+.2C4H8- 1+.4C3H6	1.40E+14	0	42000		



3931	C7H15O2H- 1=>OH+NC3H7+CH3CHO+.7C2H4+.2C3H6	1.20E+14	0	42000		
3932	C7H15O2H-1=>OH+PC4H9+CH2O+.4C5H10-1	1.40E+14	0	42000		
3933	NC7-OOQOOH+HO2=>NC7-OQOOH+H2O+O2	1.00E+11	0	-1200		
3934	NC7H15O2+HO2=>C7H15O2H-1+O2	1.00E+11	0	-1200		
3935	NC7H15O2+NC7H15O2=>C7H15O2H- 1+O2+C7H14-1	1.00E+11	0	-1200		
3936	NC7H15O2+NC7- OOQOOH=>NC7H13OOH+C7H15O2H-1+O2	1.00E+11	0	-1200		
3937	NC7-OOQOOH+NC7-OOQOOH =>NC7H13OOH+C7H15O2H-1+2O2	1.00E+11	0	-1200		
3938	C7H13=>C4H6+NC3H7	1.25E+13	0	31000		
3939	C7H13=>C5H8+C2H5	2.50E+12	0	31000		
3940	NC7H13OOH=>C2H3CHO+OH+PC4H9	2.00E+14	0	46000		
3941	NC7H15O2+HO2=>H2O+C7KETONE+O2	5.00E+10	0	-1200		
3942	NC7H15O2+CH3OO=>CH3OH+C7KETONE+O 2	2.50E+10	0	-1200		
3943	NC7H15O2+NC7H15O2=>N1C4H9OH+C3H6+ C7KETONE+O2	2.50E+10	0	-1200		
3944	NC7-OQOOH=>HCOOH+MEK+C2H4	1.70E+05	1.1	26100		
3945	NC7-OQOOH=>CH3COOH+NC4H9CHO	5.10E+05	1.1	26100		
3946	NC7-OQOOH=>C3H6O2+MEK	3.40E+05	1.1	26100		
3947	NC7-OQOOH=>CH3COOH+CH3COCH3+C2H4	1.70E+05	1.1	26100		
3948	HO2+IC8H16=>.4IC8-QOOH+.6IC8T-QOOH	5.00E+11	0	12000		
3949	O2+IC8H17=>IC8H17-OO	1.60E+12	0	0		
3950	IC8H17-OO=>IC8H17+O2	3.00E+13	0	30500		
3951	IC8H17-OO=>IC8T-QOOH	1.10E+12	0	26000		
3952	IC8H17-OO=>IC8-QOOH	9.00E+11	0	26000		
3953	IC8-QOOH=>IC8H17-OO	3.00E+11	0	18650		
3954	IC8T-QOOH=>IC8H17-OO	3.00E+11	0	18650		
3955	IC8-QOOH=>IC8H16O+OH	4.00E+10	0	14000		
3956	IC8-QOOH=>HO2+IC8H16	2.00E+12	0	21500		
3957	IC8-QOOH=>OH+CH2O+C3H6+IC4H8	1.75E+13	0	25600		
3958	IC8- QOOH=>OH+IC3H7CHO+.4IC8H16+.4C2H4	1.75E+13	0	25600		
3959	IC8T-QOOH=>IC8H16O+OH	6.00E+10	0	14000		
3960	IC8T-QOOH=>HO2+IC8H16	1.20E+12	0	21500		
3961	IC8-QOOH+O2=>IC8-OOQOOH	1.60E+12	0	0		
3962	IC8-OOQOOH=>IC8-QOOH+O2	3.00E+13	0	30500		
3963	IC8-OQOOH =>OH+CH2CHO+.5CH3CHO+.5C2H5CHO+.5I C4H8+.5C3H6	1.50E+16	0	43000		
3964	IC8-OQOOH =>OH+CH3COCH2+.5CH2O+.5IC3H7CHO+.62 5IC4H8	1.50E+16	0	43000		
3965	IC8-OOQOOH=>IC8-OQOOH+OH	9.00E+09	0	18000		
3966	IC8-OOQOOH =>OH+CH2O+CH3COCH3+.79IC3H7CHO+.21 C2H5CHO+.0525IC4H8	1.50E+11	0	22600		
3967	IC8- OOQOOH=>HO2+IC3H7CHO+.25IC4H8+CH3C OCH3	2.50E+08	0	16500		

3968	IC8H17-OO+HO2 =>OH+O2+.5CH3COCH3+.5NEOC5H11+.5IC3H7CHO+.5IC4H9	1.00E+11	0	-2600		
3969	C10H19+HO2=>NC10MOOH	1.00E+13	0	0		
3970	NC10MOOH=>C2H3CHO+OH+NC7H15	1.00E+16	0	52000		
3971	O2+C10H21-1=>C10H21O2-1	2.00E+12	0	0		
	Declared	duplicate	reaction...			
3972	O2+NC10-QOOH=>NC10-OOQOOH	2.00E+12	0	0		
3973	NC10-OOQOOH=>OH+NC10-OQOOH	1.50E+12	0	24500		
3974	NC10-OQOOH =>OH+CH3CO+CH2O+.45C10H20-1+.5C5H10-1	1.50E+15	0	42000		
3975	NC10-OQOOH =>OH+CH3CO+C2H5CHO+.31C10H20-1+.1C5H10-1+.2C7H14-1	1.50E+15	0	42000		
3976	NC10-OQOOH =>OH+CO+C2H5+CH3CHO+.65C7H14-1+.09C5H10-1	2.00E+15	0	42000		
3977	NC10-OQOOH =>OH+CO+C2H5+CH2O+.65C7H14-1+.29C5H10-1	2.00E+15	0	42000		
3978	NC10-OQOOH =>OH+CH3COCH2+.5C3H7CHO+.5CH2O+.70666667C3H6+.34C7H14-1	1.00E+15	0	42000		
3979	O2+NC3H7=>NC3H7OO	1.50E+12	0	0		
3980	H+C14H14=BENZYL+CH3	6.00E+12	0	5000		
3981	C14H13+H(+M)=C14H14(+M)	5.21E+17	-1	1580		
	Low	pressure	limit:	1.99E+41	-7.08E+00	6.69E+03
	TROE	centering:	8.42E-01	1.25E+02	2.22E+03	6.88E+03
	H2	Enhanced	by	2.00E+00		
	H2O	Enhanced	by	6.00E+00		
	CH4	Enhanced	by	2.00E+00		
	CO	Enhanced	by	1.50E+00		
	CO2	Enhanced	by	2.00E+00		
	C2H6	Enhanced	by	3.00E+00		
	AR	Enhanced	by	7.00E-01		
3982	C14H14+H=C14H13+H2	3.16E+12	0	0		
3983	C14H14+O2=C14H13+HO2	2.80E+12	0	35000		
3984	C14H14+O=C14H13+OH	8.40E+11	0	-2000		
3985	C14H14+OH=C14H13+H2O	7.00E+09	1	-1100		
3986	C14H14+HO2=C14H13+H2O2	5.40E+11	0	12000		
3987	C14H14+CH3=C14H13+CH4	2.20E+12	0	9100		
3988	C14H14+C3H5-A=C14H13+C3H6	2.20E+12	0	9100		
3989	C14H14+C6H5=C14H13+C6H6	1.06E+14	0	9949		
3990	C14H14+C6H5O=C14H13+C6H5OH	5.43E+12	0	20923		
3991	C14H13+O2=PHHCO+PHCH2O	3.94E+50	-11.5	42250		
3992	C14H13+HO2=PHCH2+PHHCO+OH	1.92E+13	0	0		
3993	C14H12+O2=HO2+C14H11	4.00E+13	0	58200		
3994	C14H12+H=C14H11+H2	8.42E-03	4.6	2583		

3995	C14H12+OH=C14H11+H2O	2.02E+13	0	5955		
3996	C14H12+O=PHCO+PHCH2	7.95E+03	1.7	657.4		
3997	C14H11=>C6H5+C2H+C6H5	1.07E+25	-2.2	88474.6		
3998	C14H11+O2=PHCO+PHHCO	1.70E+29	-5.3	6500		
3999	C14H12+O=C14H11+OH	4.20E+11	0	-1940		
4000	C14H12+HO2=C14H11+H2O2	2.70E+11	0	11640		
4001	C14H12+CH3=C14H11+CH4	1.10E+12	0	8827		
4002	C14H12+C3H5-A=C14H11+C3H6	1.10E+12	0	8827		
4003	C14H12+C6H5O=C14H11+C6H5OH	5.43E+12	0	20923		
4004	C14H12+PHCH2=C14H11+TOLUEN	1.10E+11	0	8827		
4005	PHCH2+PHCH2=C14H13+H	3.36E+38	-6.9	47618.9		
4006	STYREN+C6H5=C14H12+H	1.86E+13	-0.4	4163.4		
4007	C14H13(+M)=C14H12+H(+M)	1.00E+45	-9	60000		
	Low	pressure	limit:	1.00E+35	-5.30E+00	1.90E+03
	TROE	centering:	1.00E-02	1.00E-30	2.30E+02	4.00E+04
4008	C14H12(+M)=C14H11+H(+M)	1.00E+35	-5.9	100000		
	Low	pressure	limit:	1.00E+34	-5.00E+00	2.00E+03
	TROE	centering:	1.00E-04	1.00E-30	7.00E+03	7.00E+04
4009	C14H11(+M)=PHNTHRN+H(+M)	5.00E+15	0	41000		
	Low	pressure	limit:	9.00E+19	-1.80E+00	1.20E+04
	TROE	centering:	5.00E-01	1.93E+01	1.80E+01	3.11E+03
4010	C14H11(+M)=PHC2H+C6H5(+M)	1.70E+41	-7.8	59000		
	Low	pressure	limit:	4.00E+98	-2.30E+01	8.50E+04
	TROE	centering:	5.00E-01	1.00E+02	2.00E+03	1.00E+03
4011	C7H5+C7H5=PHNTHRN	6.39E+29	-4	35205.5		
4012	PHCC+C6H5=PHNTHRN	5.00E+12	0	6000		
4013	PHC2H+C6H5=PHNTHRN	5.00E+12	0	6000		
4014	PHC2H+C6H6=PHNTHRN+H	1.00E+13	0	6000		
4015	P2-+C2H2=PHNTHRN+H	4.60E+06	2	7300		
4016	BIPHENYL+C2H=PHNTHRN+H	1.00E+13	0	0		
4017	PHNTHRN+OH=A3-1+H2O	2.34E+04	2.7	733.2		
4018	PHNTHRN+OH=A3-4+H2O	2.34E+04	2.7	733.2		
4019	PHNTHRN+O=A2C2H+CH2CO	2.20E+13	0	4530		
4020	PHNTHRN+OH=>A2C2H+CH3+CO	1.10E+02	3.2	5590.3		
4021	A3-1+O2=>A2C2H2+2CO	8.57E+20	-2.3	7189.3		
4022	A3-4+O2=>A2C2H2+2CO	8.57E+20	-2.3	7189.3		
4023	C14H13+O2=C14H13OO	8.00E+12	0	0		
4024	C14H13+HO2=C14H13OOH	7.00E+12	0	-1000		
4025	PHCH2+PHHCO=C14H13O	1.00E+11	0	12900		
4026	C14H13OOH+PHCH2=C14H13OO+TOLUEN	1.44E+10	0	17700		
4027	C14H13OO+HO2=C14H13OOH+O2	1.75E+10	0	-3275		
4028	C14H13OO+H2O2=C14H13OOH+HO2	2.40E+12	0	10000		
4029	C14H13O+OH=C14H13OOH	2.00E+13	0	0		
4030	C14H13OO=C14H12OOH	2.59E+12	0	21374		
4031	C14H12+HO2=C14H12OOH	1.00E+11	0	10530		
4032	C14H12OOH+O2=C14H12O2H-1O2	8.00E+12	0	0		

4033	C14H12O2H-1O2=C14H11O-1O2H+OH	1.30E+12	0	18374		
4034	C14H11O-1O2H=PHHCO+PHCO+OH	1.00E+16	0	43000		
4035	o-C6H4+C6H6=>BICYCLO	1.16E+04	2.5	5915.9		
4036	BICYCLO=>o-C6H4+C6H6	4.91E+16	0	66811		
4037	BICYCLO=NAPHT+C2H2	7.46E+14	0.1	54780.1		
4038	C6H5O+C6H5O=>DIBZFUR+H2O	4.00E+13	0	11000		
4039	DIBZFUR+OH=>CO+NAPHT+HCO	2.00E+13	0	0		
4040	DIBZFUR+H=DIBZFURNYL+H2	2.50E+14	0	15999		
4041	DIBZFURNYL+O2=DIBZFURNOXY+O	1.46E+19	-0.9	18104		
4042	BIPHENYL+C3H3=A3CH3+H	3.00E+13	0	16000		
4043	A3CH3(+M)=A3-1+CH3(+M)	1.00E+40	-5	10000		
	Low	pressure	limit:	1.00E+43	-6.00E+00	1.20E+05
	TROE	centering:	1.00E-01	1.00E-28	1.00E+03	5.00E+03
4044	A3CH3(+M)=A3-4+CH3(+M)	1.00E+40	-5	10000		
	Low	pressure	limit:	1.00E+43	-6.00E+00	1.20E+05
	TROE	centering:	1.00E-01	1.00E-28	1.00E+03	5.00E+03
4045	A3CH3+H=A3CH2+H2	3.98E+02	3.4	3120		
4046	A3CH3+H=PHNTHRN+CH3	5.78E+13	0	8090		
4047	A2T2+C6H5=FLTHN+H	5.00E+12	0	0		
4048	A2-1+C6H5=FLTHN+H+H	1.39E+13	0	111		
4049	A2-1+C6H6=FLTHN+H+H2	8.51E+11	0	3986		
4050	A2T2+o-C6H4=FLTHN	6.50E+39	-7.6	27260		
4051	A2T1+o-C6H4=FLTHN	6.50E+39	-7.6	27260		
4052	PHNTHRN+C2H=A3C2H+H	5.00E+13	0	0		
4053	A3-4+C2H2(+M)=A3C2H2(+M)	1.00E+27	-3.1	26000		
	Low	pressure	limit:	1.00E+29	-3.80E+00	6.50E+03
	TROE	centering:	1.00E-04	1.00E+03	8.00E+03	9.00E+03
4054	A3-4+C2H2=A3C2H+H	8.00E+17	-1.2	22600		
4055	A3-4+C2H2=PYRENE+H	1.87E+07	1.8	3262		
4056	C13H9+C3H3=PYRENE+H2	1.50E+75	-17.8	39600		
4057	C13H9+C3H2=PYRENE+H	1.50E+75	-17.8	39600		
4058	FLUORENE+C3H2=PYRENE+H2	1.50E+12	1.8	56500		
4059	PHC2H-+PHC2H=PYRENE+H	1.10E+23	-2.9	15890		
4060	PHCC+PHCC=PYRENE	5.00E+12	0	6000		
4061	PHC2H-+PHC2H-=PYRENE	5.00E+12	0	6000		
4062	PHCC+PHC2H-=PYRENE	5.00E+12	0	6000		
4063	A3C2H+H(+M)=A3C2H2(+M)	1.00E+30	-2.8	26000		
	Low	pressure	limit:	2.00E+40	-7.00E+00	7.10E+03
	TROE	centering:	1.00E-02	1.00E-30	2.00E+00	1.19E+03
4064	A3C2H+H=PYRENE+H	3.18E+09	1.2	4580		
	Declared	duplicate	reaction...			
4065	A3C2H2(+M)=PYRENE+H(+M)	4.00E+28	-5	26000		
	Low	pressure	limit:	1.00E+29	-4.40E+00	8.00E+03
	TROE	centering:	1.00E-02	1.00E-30	2.00E+04	5.00E+01
4066	PYRENE+H=A4-1+H2	2.50E+14	0	16000		
4067	PYRENE+H=A4-2+H2	2.50E+14	0	16000		

4068	PYRENE+H=A4-4+H2	2.50E+14	0	16000		
4069	A4-1+CH4=>PYRENE+CH3	4.48E-02	4.2	4277		
4070	PYRENE+CH3=>A4-2+CH4	7.98E-01	3.9	11771		
4071	A4-2+CH4=>PYRENE+CH3	4.48E-02	4.2	4277		
4072	PYRENE+CH3=>A4-4+CH4	7.98E-01	3.9	11771		
4073	A4-4+CH4=>PYRENE+CH3	4.48E-02	4.2	4277		
4074	A4-1+H(+M)=PYRENE(+M)	1.00E+14	0	0		
	Low	pressure	limit:	6.60E+75	-1.63E+01	7.00E+03
	TROE	centering:	1.00E+00	1.00E-01	5.85E+02	6.11E+03
4075	A4-2+H(+M)=PYRENE(+M)	1.00E+14	0	0		
	Low	pressure	limit:	6.60E+75	-1.63E+01	7.00E+03
	TROE	centering:	1.00E+00	1.00E-01	5.85E+02	6.11E+03
4076	A4-4+H(+M)=PYRENE(+M)	1.00E+14	0	0		
	Low	pressure	limit:	6.60E+75	-1.63E+01	7.00E+03
	TROE	centering:	1.00E+00	1.00E-01	5.85E+02	6.11E+03
4077	PHNTHRN+C2H=PYRENE+H	1.00E+13	0	0		
4078	A2R5-C2H2=A2R5R5+H	8.20E+30	-5.4	16900		
4079	A2R5+C2H=A2R5R5+H	8.20E+30	-5.4	16900		
4080	PYRENE+OH=A4-1+H2O	2.34E+04	2.7	733.2		
4081	PYRENE+OH=A4-2+H2O	2.34E+04	2.7	733.2		
4082	PYRENE+OH=A4-4+H2O	2.34E+04	2.7	733.2		
4083	PYRENE+OH=>A3-4+CH2CO	1.30E+13	0	10600		
4084	PYRENE+OH=>PHNTHRN+HCCO	5.50E+02	3.2	5590.3		
4085	PYRENE+O=>A3-4+HCCO	2.20E+13	0	4530		
4086	A4-1+O2=>A3-4+CO+CO	2.10E+12	0	7470		
4087	A4-2+O2=>A3-4+CO+CO	2.10E+12	0	7470		
4088	A4-4+O2=>A3-4+CO+CO	2.10E+12	0	7470		
4089	A3C2H-2+C2H2=CHRYSEN-1	5.60E+05	2.3	3261		
4090	A3C2H-1+C2H2=CHRYSEN-4	1.87E+07	1.8	3262		
4091	A2-2+PHC2H=CHRYSEN+H	8.51E+11	0	3986		
4092	NAPHT+PHC2H=CHRYSEN+H	8.51E+11	0	3986		
4093	CHRYSEN+H=CHRYSEN-4+H2	6.67E+11	-0.7	20011.2		
4094	CHRYSEN+H=CHRYSEN-5+H2	6.67E+11	-0.7	20011.2		
4095	CHRYSEN-1+H(+M)=CHRYSEN(+M)	1.00E+14	0	0		
	Low	pressure	limit:	6.60E+75	-1.63E+01	7.00E+03
	TROE	centering:	1.00E+00	1.00E-01	5.85E+02	6.11E+03
4096	CHRYSEN-4+H(+M)=CHRYSEN(+M)	1.00E+14	0	0		
	Low	pressure	limit:	6.60E+75	-1.63E+01	7.00E+03
	TROE	centering:	1.00E+00	1.00E-01	5.85E+02	6.11E+03
4097	CHRYSEN-5+H(+M)=CHRYSEN(+M)	1.00E+14	0	0		
	Low	pressure	limit:	6.60E+75	-1.63E+01	7.00E+03
	TROE	centering:	1.00E+00	1.00E-01	5.85E+02	6.11E+03
4098	P2-C6H5=CHRYSEN+H2	1.00E+13	0	0		
4099	INDENYL+INDENYL=CHRYSEN+2H	1.00E+12	0	6000		
	Declared	duplicate	reaction...			
4100	C4H5-I+C4H2=PHC2H+H	3.16E+11	0	900		

4101	C6H5+C2H3=PHC2H+H2	7.90E+12	0	3200		
4102	C6H6+C2H=PHC2H+H	1.00E+12	0	0		
4103	PHC2H+O=PHC2H.+OH	1.10E+13	0	4100		
4104	PHC2H+O=C6H5+HCCO	2.10E+07	2	950		
4105	PHC2H+O=C6H5O+C2H	2.20E+13	0	2260		
4106	PHC2H+H=PHC2H.+H2	2.70E+13	0	4882		
4107	PHC2H+H=C6H5+C2H2	2.00E+14	0	4882		
	Declared	duplicate	reaction...			
4108	PHC2H+OH=C6H5+CH2CO	2.18E-04	4.5	-500		
4109	C5H5+C4H4=INDENE+H	6.00E+11	0	5030		
4110	C5H5+C4H3-N=INDENE	3.00E+36	-7.2	4234		
4111	C6H5+C3H3=INDENE	3.86E+11	0	6850.5		
	Declared	duplicate	reaction...			
4112	C4H6+C6H5=INDENE+CH3	1.42E+13	0	14000		
4113	C4H5-I+C6H6=INDENE+CH3	1.42E+13	0	14000		
4114	C6H5+C3H4-P=INDENE+H	1.00E+16	0	16600		
4115	C6H5+C3H4-A=INDENE+H	1.00E+16	0	16600		
4116	INDENE+H=PHC2H+CH3	4.00E+14	0	23000		
4117	INDENE+H=C6H6+C3H3	2.00E+14	0	24500		
4118	INDENE+OH=C6H4CH3+CH2CO	1.00E+13	0	5000		
4119	INDENE+C3H3=INDENYL+C3H4-P	7.80E+10	0	2770.2		
4120	INDENE+H2CCCH=INDENYL+C3H4-P	7.80E+10	0	2770.2		
4121	INDENE+H2CCCH=INDENYL+C3H4-A	7.80E+10	0	2770.2		
4122	INDENE+C3H3=INDENYL+C3H4-A	7.80E+10	0	2770.2		
4123	INDENE+C6H5=INDENYL+C6H6	5.00E+11	0	3000		
4124	C5H5+C4H2=INDENYL	1.20E+12	0	5030		
4125	INDENYL=>C2H2+C4H2+H2CCCH	1.00E+14	0	37500		
4126	INDENYL+HO2=>PHC2H+CO+H2O	1.00E+13	0	0		
4127	C4H5-I+C6H6=>NAPHT+H2+H	1.00E+12	0	1503.5		
4128	C4H6+C6H5=>NAPHT+H2+H	5.00E+11	0	1503.5		
4129	C6H5+C4H3-N=NAPHT	3.18E+23	-3.2	2130		
4130	C6H5+C4H4=NAPHT+H	3.30E+33	-5.7	12750		
4131	C6H4CH3+H2CCCH=>NAPHT+2H	4.00E+11	0	7000		
4132	PHC2H.+C2H2=A2-1	4.00E+13	0	5100		
4133	N-C8H7+C2H2=NAPHT+H	1.60E+16	-1.3	3300		
4134	INDENE+CH2=>NAPHT+2H	2.00E+13	0	4370		
4135	INDENE+CH2(S)=NAPHT+2H	4.00E+13	0	4370		
4136	NAPHT+O=CH2CO+PHC2H	2.20E+13	0	2265		
4137	NAPHT+O=>INDENYL+CO+H	3.60E+14	0	22093		
4138	NAPHT+O=N-C8H7+HCCO	2.00E+13	0	21000		
4139	NAPHT+OH=>PHC2H+CH2CO+H	1.30E+13	0	5300		
4140	NAPHT+C2H=A2-1+C2H2	5.00E+13	0	8000		
4141	NAPHT+C2H=A2C2H+H	5.00E+13	0	0		
4142	A2-1+O2=>PHC2H+HCO+CO	2.00E+13	0	3700		
4143	A2-1+O=>INDENYL+CO	1.00E+14	0	0		
4144	A2-1+HO2=>INDENYL+CO+OH	1.00E+13	0	0		

4145	A2-1+C2H2=A2C2H+H	1.30E+24	-3.1	11300		
4146	A2C2H+H=A2C2H*+H2	2.50E+14	0	8000		
4147	A2C2H+OH=A2-1+CH2CO	2.18E-04	4.5	-500		
4148	A2C2H+OH=A2C2H*+H2O	2.10E+13	0	2300		
4149	INDENYL+H2CCCH=>A2C2H+2H	6.00E+11	0	0		
4150	C4H+C2H2=C6H2+H	2.30E+13	0.3	-37		
4151	2C3H2=>C6H2+H2	2.00E+13	0	42500		
4152	C6H+C2H2=C8H2+H	2.30E+13	0.3	-37		
4153	C2H+C6H2=C8H2+H	2.30E+13	0.3	-37		
4154	C4H2+C2H=C4H+C2H2	2.00E+13	0	0		
4155	C4H2+C2H=H+C6H2	2.30E+13	0.3	-37		
4156	2C4H2=>C8H2+2H	1.51E+14	0	28000		
4157	2C4H2=C8H2+H2	1.51E+13	0	21000		
4158	C6H2+M=C6H+H+M	1.14E+17	0	68000		
	AR	Enhanced	by	3.50E-01		
	O2	Enhanced	by	4.00E-01		
	CO	Enhanced	by	7.50E-01		
	CO2	Enhanced	by	1.50E+00		
	H2O	Enhanced	by	6.50E+00		
	CH4	Enhanced	by	3.00E+00		
	C2H6	Enhanced	by	3.00E+00		
4159	C6H2+H=C6H+H2	7.70E+14	0	20000		
4160	C6H2+OH=C6H+H2O	6.00E+13	0	7499.9		
4161	C6H2+C2H=C4H+C4H2	1.00E+13	0	0		
4162	C8H2+M=C8H+H+M	1.14E+17	0	68000		
	AR	Enhanced	by	3.50E-01		
	O2	Enhanced	by	4.00E-01		
	CO	Enhanced	by	7.50E-01		
	CO2	Enhanced	by	1.50E+00		
	H2O	Enhanced	by	6.50E+00		
	CH4	Enhanced	by	3.00E+00		
	C2H6	Enhanced	by	3.00E+00		
4163	C8H2+H=C8H+H2	7.70E+14	0	13000		
4164	C8H2+OH=C8H+H2O	6.00E+13	0	6499.9		
4165	C6H5+C6H6=BIPHENYL+H	1.10E+23	-2.9	7450		
4166	INDENYL+H2CCCH=>BIPHENYL	4.00E+11	0	7000		
4167	INDENE+H2CCCH=>BIPHENYL+H	1.55E+14	0	25912.2		
4168	2C6H5=BIPHENYL	2.00E+19	-2	1450		
4169	2C6H5=P2-+H	2.30E-01	4.6	14500		
4170	BIPHENYL=P2-+H	1.10E+19	-2.7	57300		
4171	P2-+O2=NAPHT+HCO+CO	2.00E+12	0	3700		
4172	BIPHENYL+H=P2-+H2	2.50E+14	0	8000		
4173	BIPHENYL+OH=P2-+H2O	1.60E+08	1.4	770		
4174	PHC2H-+C4H4=A2R5+H	1.60E+16	-1.3	3300		
4175	N-C8H7+C4H2=A2R5+H	1.60E+16	-1.3	2700		
4176	INDENYL+H2CCCH=>A2R5+2H	8.30E+13	0	4888.3		

4177	INDENE+H2CCCH=>A2R5+H+H2	1.55E+14	0	25912.2		
4178	INDENYL+H2CCCH=A2R5+H2	9.50E+12	0	0		
4179	A2-1+C2H2=A2R5+H	1.90E+31	-5.3	10500		
4180	A2C2H*+H=A2R5	5.00E+13	0	0		
4181	A2C2H+H=A2R5+H	4.60E+37	-7	11550		
4182	A2R5-+H(+M)=A2R5(+M)	1.00E+14	0	0		
	O2	Enhanced	by	4.00E-01		
	CO	Enhanced	by	7.50E-01		
	CO2	Enhanced	by	1.50E+00		
	H2O	Enhanced	by	6.50E+00		
	CH4	Enhanced	by	3.00E+00		
	C2H6	Enhanced	by	3.00E+00		
	AR	Enhanced	by	2.00E-01		
	Low	pressure	limit:	6.60E+75	-1.63E+01	3.50E+00
	TROE	centering:	1.00E+00	1.00E-01	5.85E+02	6.11E+03
4183	A2R5+O=A2R5-+OH	2.00E+13	0	7400		
4184	A2R5+O=>A2-1+HCCO	2.00E+13	0	7400		
4185	A2R5+H=A2R5-+H2	2.50E+14	0	8000		
4186	A2R5+OH=A2R5-+H2O	1.60E+08	1.4	725		
4187	A2R5+OH=A2-1+CH2CO	1.00E+13	0	5000		
4188	INDENYL+C5H5=>PHNTHRN+H2	4.30E+36	-6.3	22530		
4189	A2-1+C4H2=A3-1	3.30E+33	-5.7	25337		
4190	A2C2H*+C2H2=A3-1	1.10E+62	-14.6	16550		
4191	A2R5-+C2H2=A3-1	7.00E+37	-8	8200		
4192	NAPHT+C4H2=>PHNTHRN	2.77E+04	2.5	14635.8		
4193	PHNTHRN+O=>HCCO+P2-	2.00E+13	0	21000		
4194	PHNTHRN+OH=CH2CO+P2-	4.00E+13	0	16000		
4195	PHNTHRN+CH3=A3-1+CH4	2.00E+12	0	7530		
4196	A3C2H+OH=A3-1+CH2CO	2.18E-04	4.5	-500		
4197	A3-1+O2=>CO+HCO+A2R5	2.00E+12	0	3700		
4198	A3-1+C2H2=A3C2H+H	1.20E+26	-3.4	15100		
4199	PHNTHRN+CH2=A3CH3	2.20E+13	0	3596		
4200	PHNTHRN+CH2(S)=A3CH3	4.20E+13	0	3596		
4201	A3CH2+CH2=PYRENE+H2+H	2.40E+14	0	0		
4202	N-C8H7+PHC2H=>PYRENE+H2+H	1.10E+24	-2.9	8010		
4203	N-C8H7+A1C2H-=PYRENE+H2	4.30E+37	-6.3	22530		
4204	INDENYL+C6H4CH3=>PYRENE+2H2	4.30E+37	-6.3	22530		
4205	2INDENYL=>PYRENE+C2H2+H2	4.30E+36	-6.3	22530		
4206	NAPHT+C6H=A4-1	7.00E+37	-8	8200		
4207	NAPHT+C6H5=PYRENE+H+H2	1.00E+11	0	2500		
4208	A2-1+C6H6=PYRENE+H+H2	1.00E+12	0	2500		
4209	A2-1+C6H5=>PYRENE+H2	4.30E+37	-6.3	22530		
4210	A2-1+C6H2=A4-1	7.00E+37	-8	8200		
4211	A2R5-+C4H2=>A4-1	7.00E+37	-8	8200		
4212	A2R5-+C4H3-N=PYRENE	6.40E+23	-3.2	2130		
4213	A3-1+C2H2=PYRENE+H	6.60E+24	-3.4	8900		



4214	A3C2H+H=PYRENE+H	9.00E+38	-7.4	10400		
	Declared	duplicate	reaction...			
4215	A4C2H*+H=BGHIF	5.00E+13	0	0		
4216	BIPHENYL+C6H=CHRYSEN-1	7.00E+37	-8	8200		
4217	P2-+C6H2=BGHIF+H	1.10E+24	-2.9	8010		
4218	P2-+C6H2=CHRYSEN-1	7.00E+37	-8	8200		
4219	A3-1+C4H4=CHRYSEN+H	3.30E+33	-5.7	12750		
4220	A2R5+C6H2=>BGHIF	2.41E+02	2.2	-569.2		
4221	PHC2H-+NAPHT=>BGHIF+H2+H	2.10E+25	-2.9	8010		
4222	PHC2H+A2-1=>BGHIF+H2+H	2.10E+25	-2.9	8010		
4223	INDENE+INDENYL=>CHRYSEN+H2+H	1.10E+24	-2.9	8010		
4224	INDENYL+INDENYL=>CHRYSEN+2H	4.30E+14	0	4888.3		
	Declared	duplicate	reaction...			
4225	2INDENYL=>BGHIF+2H2	8.30E+38	-6.3	22530		
4226	A2C2H+C6H5=CHRYSEN+H	1.10E+24	-2.9	8010		
4227	A2C2H*+C6H6=CHRYSEN+H	1.10E+24	-2.9	8010		
4228	A2R5-+C6H5=>BGHIF+2H	4.30E+15	0	4888.3		
4229	A2R5-+C6H6=>BGHIF+H2+H	1.10E+25	-2.9	8010		
4230	A3C2H*+C4H4=BAPYR+H	3.30E+33	-5.7	12750		
4231	A4-1+C4H4=BAPYR+H	3.30E+33	-5.7	12750		
4232	A4C2H*+C2H2=BAPYR*S	7.00E+37	-8	8200		
4233	BAPYR*S+H=BAPYR	1.00E+14	0	0		
4234	P2-+PHC2H=>BAPYR+2H	4.30E+15	0	4888.3		
4235	P2-+PHC2H=>BAPYR+H2	8.30E+38	-6.3	22530		
4236	BIPHENYL+PHC2H=>BAPYR+H2+H	1.10E+24	-2.9	8010		
4237	P2-+N-C8H7=>BAPYR+2H2	8.30E+38	-6.3	22530		
4238	A2R5-+PHC2H=BAPYR	8.30E+38	-6.3	22530		
4239	A2R5+PHC2H=BAPYR+H	2.10E+25	-2.9	8010		
4240	A2R5-+PHC2H=BAPYR+H	2.10E+25	-2.9	8010		
4241	CHRYSEN-1+O2=>HCO+CO+PYRENE	2.00E+13	0	3700		
4242	CHRYSEN-1+H=BGHIF+H2	1.00E+14	0	0		
4243	CHRYSEN-1+C2H=>BAPYR	5.24E+14	-0.5	350		
4244	CHRYSEN-1+C2H2=BAPYR+H	2.10E+24	-3.4	8900		
4245	CHRYSEN+O=CHRYSEN-1+OH	2.00E+13	0	7400		
4246	CHRYSEN+H=CHRYSEN-1+H2	3.03E+02	3.3	2870		
4247	CHRYSEN+OH=CHRYSEN-1+H2O	1.70E+08	1.4	732.8		
4248	BGHIF+O=HCCO+A4-1	2.00E+13	0	7400		
4249	BGHIF+OH=CH2CO+A4-1	1.30E+13	0	5300		
4250	BAPYR*S+O2=>HCO+CO+BGHIF	2.00E+13	0	3700		
4251	C4H2+PYRENE=>BAPYR	6.00E+02	2.2	-569.2		
4252	BAPYR+O=HCCO+CHRYSEN-1	2.00E+13	0	21000		
4253	BAPYR+OH=>CH2CO+CHRYSEN-1	1.30E+13	0	5300		
4254	STYREN+O=N-C8H7+OH	7.55E+06	1.9	1880		
4255	C5H5+H2CCCH=N-C8H7+H	1.50E+35	-7.2	4234		
4256	C6H6+C2H=N-C8H7	7.00E+38	-8	8200		
4257	C6H5+C2H3=N-C8H7+H	9.40E+00	4.1	11617		

4258	N-C8H7+M=PHC2H+H+M	2.00E+17	0	20000		
4259	N-C8H7+H=PHC2H+H2	1.00E+13	0	0		
4260	N-C8H7+OH=PHC2H+H2O	1.00E+13	0	0		
4261	N-C8H7+PHC2H=>PYRENE+2H	4.30E+14	0	4888.3		
4262	A2C2H*+N-C8H7=BAPYR+H2	8.30E+38	-6.3	22530		
4263	C4H5-I+C2H2=C6H6+H	1.60E+15	-1.3	5365		
4264	INDENYL+CH3=NAPHT+H+H	3.00E+18	0	36500		
4265	PHCH2+C3H3=NAPHT+H+H	2.00E+13	0.3	5000		
4266	P2-+C6H5=TERPHENYL	5.94E+42	-8.8	13822		
4267	P2-+C6H5=P3-+H	8.60E+13	0.5	34797.5		
4268	BIPHENYL+C6H5=TERPHENYL+H	9.50E+75	-18.9	39445.4		
4269	P2-+C6H6=TERPHENYL+H	9.50E+75	-18.9	39445.4		
4270	TERPHENYL+H=P3-+H2	3.23E+07	2.1	15833.1		
4271	P3-+H=TERPHENYL	1.17E+33	-5.6	8753.7		
4272	TERPHENYL+CH3=P3-+CH4	2.00E+12	0	14975.6		
4273	TERPHENYL+C2H3=P3-+C2H4	6.00E+11	0	12969.3		
4274	P2-+C6H6=>TRIPHENYLEN+H2+H	8.51E+11	0	3983.9		
4275	BIPHENYL+C6H5=>TRIPHENYLEN+H2+H	8.51E+11	0	3983.9		
4276	P2-+C6H5=>TRIPHENYLEN+H+H	1.39E+13	0	109.9		
4277	P3-+H=TRIPHENYLEN+H	9.50E+75	-18.9	39445.4		
4278	TRIPHENYLEN+CH3=A4T-+CH4	2.00E+12	0	14975.6		
4279	TRIPHENYLEN+C2H3=A4T-+C2H4	6.00E+11	0	12969.3		
4280	A4T-+H=TRIPHENYLEN	5.00E+13	0	0		
4281	A4T-+C2H2=>BEPYREN+H	1.87E+07	1.8	3260.2		
4282	TRIPHENYLEN+H=A4T-+H2	3.23E+07	2.1	15833.1		
4283	P3-+C6H5=QUATERPHENYL	5.94E+48	-8.8	13829.2		
4284	P3-+C6H5=P4-+H	8.60E+19	0.5	34799.8		
4285	TERPHENYL+C6H5=QUATERPHENYL+H	1.00E+83	-18.9	39529		
4286	P3-+C6H6=QUATERPHENYL+H	1.00E+83	-18.9	39529		
4287	BIPHENYL+P2-+H=QUATERPHENYL+H	1.80E+83	-18.9	39529		
4288	QUATERPHENYL+H=P4-+H2	3.53E+13	2.1	15835.5		
4289	P4-+H=QUATERPHENYL	1.17E+39	-5.6	8765.6		
4290	P2-+P2-+H=QUATERPHENYL	3.56E+49	-8.8	13829.2		
4291	P2-+P2-+H=P4-+H	5.16E+20	0.5	34799.8		
4292	P4-+C6H5=QINQUEPHENYL	5.94E+48	-8.8	13829.2		
4293	P4-+C6H5=P5-+H	8.60E+19	0.5	34799.8		
4294	QUATERPHENYL+C6H5=QINQUEPHENYL+H	1.00E+83	-18.9	39529		
4295	P4-+C6H6=QINQUEPHENYL+H	1.00E+83	-18.9	39529		
4296	P3-+P2-+H=QINQUEPHENYL	1.78E+49	-8.8	13829.2		
4297	P3-+P2-+H=P5-+H	2.58E+19	0.5	34799.8		
4298	TERPHENYL+P2-+H=QINQUEPHENYL+H	3.00E+83	-18.9	39457.3		
4299	P3-+BIPHENYL=QINQUEPHENYL+H	3.00E+83	-18.9	39457.3		
4300	QINQUEPHENYL+H=P5-+H2	6.46E+13	2.1	15835.5		
4301	P5-+H=QINQUEPHENYL	2.34E+39	-5.6	8765.6		
4302	C9H9-1+H=C9H10	2.00E+13	0	0		

4303	C9H10+H=C9H9-1+H2	3.90E+06	2.4	4471		
4304	C9H10+CH3=C9H9-1+CH4	4.53E+00	3.5	5481		
4305	INDENE+H=C9H9-1	1.30E+13	0	1560		
4306	BSTYRYL+CH3=C9H9-1+H	1.00E+13	0	0		
4307	C5H5+C4H3-I=INDENE	1.00E+13	0	0		
4308	C6H5+C3H4-A=PHCH2+C2H2	5.13E+01	3.2	2787.8		
4309	C6H5+C3H4-A=PHC2H+CH3	2.56E+01	3.2	2787.8		
4310	C6H5+C3H4-P=C6H6+C3H3	1.79E+04	2.5	2759.1		
4311	C6H5+C3H4-P=PHC2H+CH3	7.18E+03	2.5	2759.1		
4312	o-C6H4+C3H3=INDENYL	7.46+100	-25	61541.8		
	Reverse	Arrhenius	coefficients:	1.53+108	-26	180368.9
4313	PHCH2+C2H4=C9H10+H	2.81E-06	4.7	1417.5		
4314	o-C6H4+C3H5-A=INDENE+H	1.52E+09	1	-1035.5		
4315	o-C6H4+C3H4-A=INDENE	1.00E+13	0	10000		
4316	o-C6H4+C3H4-P=INDENE	1.00E+13	0	10000		
4317	BENZYLH+H=C6H6+PHCH2	1.69E+08	1.6	4448.3		
4318	C6H5+PHCH2=BENZYLBJ+H	2.47E+50	-10.1	43638.8		
4319	C6H5+PHCH2=BENZYLBJ	4.42E+49	-11.1	14751.9		
	Reverse	Arrhenius	coefficients:	4.33+127	-31.9	158358.6
4320	BENZYLBJ=BENZYLBJ+H	2.25+123	-30.9	153559.2		
4321	BENZYLBJ+H=BENZYLBJ+H2	4.31E+00	4	3384		
4322	BENZYLBJ+CH3=BENZYLBJ+CH4	2.67E-05	5.6	9000		
4323	BENZYLBJ+C6H5=BENZYLBJ+C6H6	5.29E+13	0	11935		
4324	BENZYLBJ=FLUORENE+H	7.65+107	-26.9	126128.4		
4325	FLUORENE+H=C13H9+H2	2.80E+13	0	2259		
	Declared	duplicate	reaction...			
4326	FLUORENE+CH3=C13H9+CH4	1.80E-01	4	0		
	Declared	duplicate	reaction...			
4327	C13H9+H=FLUORENE	1.08E+63	-14.8	21050		
4328	FLUORENE+H=C13H9+H2	4.34E+16	-0.7	20011.2		
	Declared	duplicate	reaction...			
4329	FLUORENE+CH3=C13H9+CH4	6.65E+11	0	15060		
	Declared	duplicate	reaction...			
4330	C13H9+H(+M)=FLUORENE(+M)	1.00E+14	0	0		
	Low	pressure	limit:	6.60E+75	-1.63E+01	7.00E+03
	TROE	centering:	1.00E+00	1.00E-01	5.85E+02	6.11E+03
4331	o-C6H4+PHCH2=FLUORENE+H	5.12E+12	0	2416.2		
4332	A1A1CH2-1=FLUORENE+H	7.65+107	-26.9	128628.4		
4333	C14H14=C14H13+H	6.25+174	-46.9	171781.4		
4334	C14H14+H=C6H6+PHCH2CH2	1.69E+08	1.6	4448.3		
4335	C14H13=C14H12+H	1.80E+85	-22.4	66243.9		
4336	C14H13=STYREN+C6H5	1.69E+88	-22.8	67565.8		
4337	C14H12+C6H5=C14H11+C6H6	2.56E+02	3.2	2787.8		
4338	C14H11=PHC2H+C6H5	6.47E+89	-23.3	73055.8		
4339	PHC2H+C6H5=A1CCA1+H	1.63E+23	-2.8	12667.1		
4340	A1CCA1+H=PHNTHRN+H	4.34E+30	-4.9	13387.3		

4341	A2C2H-2J3+C2H2=A3LJX	4.67E+06	1.8	3262		
4342	ANTHRCN+H=A3LJX+H2	8.67E+16	-0.7	20011.2		
4343	A3LJX+H(+M)=ANTHRCN(+M)	1.00E+14	0	0		
	Low	pressure	limit:	6.60E+75	-1.63E+01	7.00E+03
	TROE	centering:	1.00E+00	1.00E-01	5.85E+02	6.11E+03
4344	A2R5-+C2H2=A2R5YNE1+H	1.12E+26	-3.4	20870		
4345	A2R5-+C2H2=A2R5YNE3+H	1.12E+26	-3.4	20870		
4346	A2R5-+C2H2=A2R5YNE4+H	1.12E+26	-3.4	20870		
4347	A2R5-+C2H2=A2R5YNE5+H	2.50E-09	6.6	8850		
4348	A3CH2=A3CH2R+H	7.65+107	-26.9	128628.4		
4349	C13H9+C2H2=A3CH2R+H	3.59E+22	-2.5	16160		
4350	A3-1+C2H2=A3R5+H	3.59E+22	-2.5	16160		
4351	A2T1+o-C6H4=A3R5	5.12E+60	-13.1	48980		
4352	A2T2+o-C6H4=A3R5	5.12E+60	-13.1	48980		
4353	A2R5YNE4+H=A2R5YN4J5+H2	2.17E+16	-0.7	20011.2		
4354	A2R5YN4J5+C2H2=A3R5J7	1.87E+07	1.8	3262		
4355	A2R5YNE5+H=A2R5YN5J4+H2	2.17E+16	-0.7	20011.2		
4356	A2R5YN5J4+C2H2=A3R5J10	1.87E+07	1.8	3262		
4357	A3R5J7+H(+M)=A3R5(+M)	1.00E+14	0	0		
	Low	pressure	limit:	6.60E+75	-1.63E+01	7.00E+03
	TROE	centering:	1.00E+00	1.00E-01	5.85E+02	6.11E+03
4358	A3R5J10+H(+M)=A3R5(+M)	1.00E+14	0	0		
	Low	pressure	limit:	6.60E+75	-1.63E+01	7.00E+03
	TROE	centering:	1.00E+00	1.00E-01	5.85E+02	6.11E+03
4359	A3LJX+C2H2=A3LR5+H	3.59E+22	-2.5	16160		
4360	A2T1+o-C6H4=A3LR5	7.85E+55	-12	43790		
4361	A2T2+o-C6H4=A3LR5	7.85E+55	-12	43790		
4362	A2R5YNE3+H=A2R5YN3J4+H2	2.17E+16	-0.7	20011.2		
4363	A2R5YNE4+H=A2R5YN4J3+H2	2.17E+16	-0.7	20011.2		
4364	A2R5YN3J4+C2H2=A3LR5JS	1.87E+07	1.8	3262		
4365	A2R5YN4J3+C2H2=A3LR5JS	1.87E+07	1.8	3262		
4366	A3LR5JS+H(+M)=A3LR5(+M)	1.00E+14	0	0		
	Low	pressure	limit:	6.60E+75	-1.63E+01	7.00E+03
	TROE	centering:	1.00E+00	1.00E-01	5.85E+02	6.11E+03
4367	A2-1+C6H5=A2A1-1	1.66E+64	-14.7	33265.8		
4368	A2-1+C6H6=A2A1-1+H	9.55E+11	0	4308.3		
4369	NAPHT+C6H5=A2A1-1+H	6.37E+11	0	4308.3		
4370	A2-2+C6H5=A2A1-2	1.66E+64	-14.7	33265.8		
4371	A2-2+C6H6=A2A1-2+H	9.55E+11	0	4308.3		
4372	NAPHT+C6H5=A2A1-2+H	6.37E+11	0	4308.3		
4373	A2A1-1+H=FLTHN+H2+H	4.34E+16	-0.7	20011.2		
4374	A2A1-1+CH3=FLTHN+CH4+H	6.67E+11	0	15060		
4375	A2A1-2+H=A21C6H4+H2+H	4.34E+16	-0.7	20011.2		
4376	A2A1-2+CH3=A21C6H4+CH4+H	6.67E+11	0	15060		
4377	A2A1-2+H=A22C6H4+H2+H	4.34E+16	-0.7	20011.2		
4378	A2A1-2+CH3=A22C6H4+CH4+H	6.67E+11	0	15060		

4379	A2R5YNE1+H=A2R5YN1J2+H2	2.17E+16	-0.7	20011.2		
4380	A2R5YN1J2+C2H2=FLTHNJ7	1.87E+07	1.8	3262		
4381	FLTHN+H=FLTHNJ1+H2	4.34E+16	-0.7	20011.2		
4382	FLTHN+H=FLTHNJ3+H2	4.34E+16	-0.7	20011.2		
4383	FLTHN+H=FLTHNJ7+H2	4.34E+16	-0.7	20011.2		
4384	FLTHNJ1+H(+M)=FLTHN(+M)	1.00E+14	0	0		
	Low	pressure	limit:	6.60E+75	-1.63E+01	7.00E+03
	TROE	centering:	1.00E+00	1.00E-01	5.85E+02	6.11E+03
4385	FLTHNJ3+H(+M)=FLTHN(+M)	1.00E+14	0	0		
	Low	pressure	limit:	6.60E+75	-1.63E+01	7.00E+03
	TROE	centering:	1.00E+00	1.00E-01	5.85E+02	6.11E+03
4386	FLTHNJ7+H(+M)=FLTHN(+M)	1.00E+14	0	0		
	Low	pressure	limit:	6.60E+75	-1.63E+01	7.00E+03
4387	A21C6H4=FLTHN	8.51E+12	0	62860		
4388	A22C6H4=A3LR5	8.51E+12	0	62860		
4389	A3R5=FLTHN	8.51E+12	0	62860		
4390	A3LR5=A3R5	8.51E+12	0	62860		
4391	A3LR5=FLTHN	8.51E+12	0	62860		
4392	BENZNAP+H=NAPHT+PHCH2	1.69E+08	1.6	4448.3		
4393	A2-2+PHCH2=BENZNAP	4.42E+49	-11.1	14751.9		
4394	BENZNAP+H=BENZNAPJP+H2	4.31E+00	4	3384		
4395	BENZNAP+CH3=BENZNAPJP+CH4	2.67E-05	5.6	9000		
4396	BENZNAP+C6H5=BENZNAPJP+C6H6	5.29E+13	0	11935		
4397	BENZNAPJP=BENZFLRN+H	7.20E+79	-20.4	62809.9		
4398	A3LJX+C2H2=A3LC2H-1+H	1.01E-10	7.1	9210		
4399	A3LC2H-1+H=A3LC2H-1P+H2	2.17E+16	-0.7	20011.2		
4400	A3LC2H-1P+C2H2=A3LA1-X	1.87E+07	1.8	3262		
4401	A3LC2H-2+H=A3LC2H-2S+H2	2.17E+16	-0.7	20011.2		
4402	A3LC2H-2S+C2H2=A3LA1-X	1.87E+07	1.8	3262		
4403	A2-2+PHC2H=A4+H	8.51E+11	0	3986		
4404	NAPHT+PHC2H=A4+H	8.51E+11	0	3986		
4405	A4+H=A3LA1-X+H2	2.17E+16	-0.7	20011.2		
4406	A3LA1-X+H(+M)=A4(+M)	1.00E+14	0	0		
	Low	pressure	limit:	6.60E+75	-1.63E+01	7.00E+03
	TROE	centering:	1.00E+00	1.00E-01	5.85E+02	6.11E+03
4407	A3LC2H-2+H=A3LC2H-2P+H2	2.17E+16	-0.7	20011.2		
4408	A3LC2H-2P+C2H2=A4LJS	1.87E+07	1.8	3262		
4409	A4LJS+H(+M)=A4L(+M)	1.00E+14	0	0		
	Low	pressure	limit:	6.60E+75	-1.63E+01	7.00E+03
	TROE	centering:	1.00E+00	1.00E-01	5.85E+02	6.11E+03
4410	A3-1+C6H5=A3A1-1	1.66E+64	-14.7	33265.8		
4411	A3-9+C6H5=A3A1-9	1.66E+64	-14.7	33265.8		
4412	PHNTHRN+C6H5=A3A1-1+H	3.18E+11	0	4308.3		
4413	PHNTHRN+C6H5=A3A1-9+H	3.18E+11	0	4308.3		
4414	A3-1+C6H6=A3A1-1+H	9.55E+11	0	4308.3		
4415	A3-1+C6H6=A3A1-9+H	9.55E+11	0	4308.3		

4416	A3A1-1+H=BBFLUOR+H2+H	2.17E+16	-0.7	20011.2		
4417	A3A1-9+H=BBFLUOR+H2+H	2.17E+16	-0.7	20011.2		
4418	A3A1-1+CH3=BBFLUOR+CH4+H	6.67E+11	0	15060		
4419	A3A1-9+CH3=BBFLUOR+CH4+H	6.67E+11	0	15060		
4420	A2-2+A2-1=A2A2-12	1.66E+64	-14.7	33265.8		
4421	NAPHT+A2-2=A2A2-12+H	6.37E+11	0	4308.3		
4422	NAPHT+A2-1=A2A2-12+H	6.37E+11	0	4308.3		
4423	A2A2-12+H=BKFLUOR+H2+H	2.17E+16	-0.7	20011.2		
4424	A2A2-12+CH3=BKFLUOR+CH4+H	6.67E+11	0	15060		
4425	C13H9+C6H5=FLRNA1-4	1.66E+64	-14.7	33265.8		
4426	FLUORENE+C6H5=FLRNA1-4+H	3.18E+11	0	4308.3		
4427	C13H9+C6H6=FLRNA1-4+H	9.55E+11	0	4308.3		
4428	FLRNA1-4+H=CPTRPHEN+H2+H	4.34E+16	-0.7	20011.2		
4429	FLRNA1-4+CH3=CPTRPHEN+CH4+H	6.67E+11	0	15060		
4430	CHRYSEN-4+C2H2=BAPYR+H	1.87E+07	1.8	3262		
4431	CHRYSEN-5+C2H2=BAPYR+H	1.87E+07	1.8	3262		
4432	BAPYR+H=BAPYR*S+H2	4.34E+16	-0.7	20011.2		
4433	BAPYR*S+H(+M)=BAPYR(+M)	1.00E+14	0	0		
	Low	pressure	limit:	6.60E+75	-1.63E+01	7.00E+03
	TROE	centering:	1.00E+00	1.00E-01	5.85E+02	6.11E+03
4434	A4C2H*S+C2H2=BEPYRENJS	1.87E+07	1.8	3262		
4435	BEPYREN+H=BEPYRENJS+H2	8.67E+16	-0.7	20011.2		
4436	BEPYRENJS+H(+M)=BEPYREN(+M)	1.00E+14	0	0		
	Low	pressure	limit:	6.60E+75	-1.63E+01	7.00E+03
	TROE	centering:	1.00E+00	1.00E-01	5.85E+02	6.11E+03
4437	A3-4+C6H5=A3A1-4	1.66E+64	-14.7	33265.8		
4438	PHNTHRN+C6H5=A3A1-4+H	3.18E+11	0	4308.3		
4439	A3-4+C6H6=A3A1-4+H	9.55E+11	0	4308.3		
4440	A3A1-4+H=BEPYREN+H2+H	2.17E+16	-0.7	20011.2		
4441	A3A1-4+CH3=BEPYREN+CH4+H	6.67E+11	0	15060		
4442	A2-1+A2-1=A2A2-11	1.66E+64	-14.7	33265.8		
4443	NAPHT+A2-1=A2A2-11+H	6.37E+11	0	4308.3		
4444	A2A2-11+H=PERYLEN+H2+H	2.17E+16	-0.7	20011.2		
4445	A2A2-11+CH3=PERYLEN+CH4+H	6.67E+11	0	15060		
4446	PERYLEN+H=PERYLENJS+H2	1.74E+17	-0.7	20011.2		
4447	PERYLENJS+H(+M)=PERYLEN(+M)	1.00E+14	0	0		
	Low	pressure	limit:	6.60E+75	-1.63E+01	7.00E+03
	TROE	centering:	1.00E+00	1.00E-01	5.85E+02	6.11E+03
4448	A4-1+C6H5=PYRNA1-1	1.66E+64	-14.7	33265.8		
4449	A4-4+C6H5=PYRNA1-4	1.66E+64	-14.7	33265.8		
4450	PYRENE+C6H5=PYRNA1-1+H	1.27E+12	0	4308.3		
4451	PYRENE+C6H5=PYRNA1-4+H	1.27E+12	0	4308.3		
4452	A4-1+C6H6=PYRNA1-4+H	9.55E+11	0	4308.3		
4453	A4-4+C6H6=PYRNA1-4+H	9.55E+11	0	4308.3		
4454	PYRNA1-1+H=INPYR+H2+H	2.17E+16	-0.7	20011.2		
4455	PYRNA1-4+H=INPYR+H2+H	2.17E+16	-0.7	20011.2		

4456	PYRNA1-1+CH3=INPYR+CH4+H	6.67E+11	0	15060		
4457	PYRNA1-4+CH3=INPYR+CH4+H	6.67E+11	0	15060		
4458	BBFLUOR+H=BBFLUORJS+H2	4.34E+16	-0.7	20011.2		
4459	BBFLUORJS+H(+M)=BBFLUOR(+M)	1.00E+14	0	0		
	Low	pressure	limit:	6.60E+75	-1.63E+01	7.00E+03
	TROE	centering:	1.00E+00	1.00E-01	5.85E+02	6.11E+03
4460	BBFLUORJS+C2H2=INPYR+H	1.87E+07	1.8	3262		
4461	FLTHNJ1+C2H2=BGHIF+H	1.87E+07	1.8	3262		
4462	FLTHNJ7+C2H2=BGHIF+H	1.87E+07	1.8	3262		
4463	BGHIF+H=BGHIFJ+H2	8.67E+16	-0.7	20011.2		
4464	BGHIFJ+H(+M)=BGHIF(+M)	1.00E+14	0	0		
	Low	pressure	limit:	6.60E+75	-1.63E+01	7.00E+03
	TROE	centering:	1.00E+00	1.00E-01	5.85E+02	6.11E+03
4465	FLTHNJ3+C2H2=CPCDFLTH+H	3.80E+22	-2.5	16880		
4466	CPCDFLTH+H=CPCDFLTJS+H2	4.34E+16	-0.7	20011.2		
4467	CPCDFLTJS+H(+M)=CPCDFLTH(+M)	1.00E+14	0	0		
	Low	pressure	limit:	6.60E+75	-1.63E+01	7.00E+03
	TROE	centering:	1.00E+00	1.00E-01	5.85E+02	6.11E+03
4468	CPCDFLTJS+C2H2=BGHIFR+H	1.87E+07	1.8	3262		
4469	BGHIFJ+C2H2=BGHIFR+H	3.80E+22	-2.5	16880		
4470	BGHIFR+H=BGHIFRJS+H2	4.34E+16	-0.7	20011.2		
4471	BGHIFRJS+H(+M)=BGHIFR(+M)	1.00E+14	0	0		
	Low	pressure	limit:	6.60E+75	-1.63E+01	7.00E+03
	TROE	centering:	1.00E+00	1.00E-01	5.85E+02	6.11E+03
4472	BGHIFRJS+C2H2=COR1+H	1.87E+07	1.8	3262		
4473	A4-1+C2H2=CPCDPYR+H	3.80E+22	-2.5	16880		
4474	A4-4+C2H2=CPCDPYR+H	3.80E+22	-2.5	16880		
4475	CPCDPYR+H=CPCDPYRJS+H2	1.30E+17	-0.7	20011.2		
4476	CPCDPYRJS+H(+M)=CPCDPYR(+M)	1.00E+14	0	0		
	Low	pressure	limit:	6.60E+75	-1.63E+01	7.00E+03
	TROE	centering:	1.00E+00	1.00E-01	5.85E+02	6.11E+03
4477	CPCDPYRJS+C2H2=DCPCDFG+H	3.80E+22	-2.5	16880		
4478	BGHIFJ+C2H2=COR+H	1.87E+07	1.8	3262		
4479	CPCDPYRJS+C2H2=COR+H	3.80E+22	-2.5	16880		
4480	COR+H=CORJ+H2	2.17E+17	-0.7	20011.2		
4481	CORJ+H(+M)=COR(+M)	1.00E+14	0	0		
	Low	pressure	limit:	6.60E+75	-1.63E+01	7.00E+03
	TROE	centering:	1.00E+00	1.00E-01	5.85E+02	6.11E+03
4482	CORJ+C2H2=COR1+H	3.80E+22	-2.5	16880		
4483	COR1+H=COR1J+H2	1.74E+17	-0.7	20011.2		
4484	COR1J+H(+M)=COR1(+M)	1.00E+14	0	0		
	Low	pressure	limit:	6.60E+75	-1.63E+01	7.00E+03
	TROE	centering:	1.00E+00	1.00E-01	5.85E+02	6.11E+03
4485	COR1J+C2H2=COR2+H	1.87E+07	1.8	3262		
4486	COR2+H=COR2J+H2	1.30E+17	-0.7	20011.2		
4487	COR2J+H(+M)=COR2(+M)	1.00E+14	0	0		

	Low	pressure	limit:	6.60E+75	-1.63E+01	7.00E+03
	TROE	centering:	1.00E+00	1.00E-01	5.85E+02	6.11E+03
4488	COR2J+C2H2=COR3+H	1.87E+07	1.8	3262		
4489	COR3+H=COR3J+H2	8.67E+16	-0.7	20011.2		
4490	COR3J+H(+M)=COR3(+M)	1.00E+14	0	0		
	Low	pressure	limit:	6.60E+75	-1.63E+01	7.00E+03
	TROE	centering:	1.00E+00	1.00E-01	5.85E+02	6.11E+03
4491	COR3J+C2H2=COR4+H	1.87E+07	1.8	3262		
4492	COR4+H=COR4J+H2	4.34E+16	-0.7	20011.2		
4493	COR4J+H(+M)=COR4(+M)	1.00E+14	0	0		
	Low	pressure	limit:	6.60E+75	-1.63E+01	7.00E+03
	TROE	centering:	1.00E+00	1.00E-01	5.85E+02	6.11E+03
4494	COR4J+C2H2=HB+H	1.87E+07	1.8	3262		
4495	BAPYR*S+C2H2=ANTHAN+H	1.87E+07	1.8	3262		
4496	ANTHAN+H=ANTHANJP+H2	1.74E+17	-0.7	20011.2		
4497	ANTHAN+H=ANTHANJS+H2	8.67E+16	-0.7	20011.2		
4498	ANTHANJP+H(+M)=ANTHAN(+M)	1.00E+14	0	0		
	Low	pressure	limit:	6.60E+75	-1.63E+01	7.00E+03
	TROE	centering:	1.00E+00	1.00E-01	5.85E+02	6.11E+03
4499	ANTHANJS+H(+M)=ANTHAN(+M)	1.00E+14	0	0		
	Low	pressure	limit:	6.60E+75	-1.63E+01	7.00E+03
	TROE	centering:	1.00E+00	1.00E-01	5.85E+02	6.11E+03
4500	BEPYRENJS+C2H2=BGHIPER+H	1.87E+07	1.8	3262		
4501	PERYLENJS+C2H2=BGHIPER+H	1.87E+07	1.8	3262		
4502	BGHIPER+H=BGHIPEJP1+H2	1.74E+17	-0.7	20011.2		
4503	BGHIPEJP1+H(+M)=BGHIPER(+M)	1.00E+14	0	0		
	Low	pressure	limit:	6.60E+75	-1.63E+01	7.00E+03
	TROE	centering:	1.00E+00	1.00E-01	5.85E+02	6.11E+03
4504	BGHIPEJP1+C2H2=CPBPER+H	3.80E+22	-2.5	16880		
4505	BGHIPER+H=BGHIPEJS1+H2	4.34E+16	-0.7	20011.2		
4506	BGHIPEJS1+H(+M)=BGHIPER(+M)	1.00E+14	0	0		
	Low	pressure	limit:	6.60E+75	-1.63E+01	7.00E+03
	TROE	centering:	1.00E+00	1.00E-01	5.85E+02	6.11E+03
4507	BGHIPEJS1+C2H2=CORONEN+H	1.87E+07	1.8	3262		
4508	C5H5+C5H6=>INDENE+CH3	1.30E+28	-3.9	23108.3		
4509	C5H5+C5H6=>STYREN+C2H3	4.00E+15	0	25556.5		
4510	C5H5+TOLUEN=>BIPHENYL+H+H2	4.00E+14	0	19107.7		
4511	C5H5+PHC2H=FLUORENE+H	4.00E+14	0	19107.7		
4512	C5H5+STYREN=FLUORENE+H+H2	1.00E+14	0	19107.7		
4513	C5H5+PHC2H5=>BIPHENYL+H2+CH3	4.00E+14	0	19107.7		
4514	C5H5+PHCH2=>BIPHENYL+H+H	5.00E+14	0	5971.1		
4515	C5H5+C3H3=>STYREN	5.00E+15	0	5971.1		
4516	C5H5+PHC2H=>FLUORENE	2.00E+15	0	3009.5		
4517	C5H5+N-C8H7=>FLUORENE+H+H	2.00E+15	0	3009.5		
4518	A3-4+O2=A3O-4+O	4.00E+03	2.4	41320.3		
4519	A3O-4=C13H9+CO	6.42E+10	1	242627.5		



4520	A3LJX+O2=A3L-O+O	7.30E+03	2.4	37260		
4521	A3L-O=C13H9+CO	6.42E+10	1	242627.5		
4522	A3LA1-X+O2=A4-O+O	7.30E+03	2.4	37260		
4523	A4-O=C13H9A1-+CO	6.42E+10	1	242627.5		
4524	C13H9A1-+H=C13H9A1	1.00E+14	0	0		
4525	ANTHAN+OH=ANTHANJS+H2O	2.10E+13	0	4600		
4526	ANTHAN+OH=ANTHANJP+H2O	2.10E+13	0	4600		
4527	ANTHAN+OH=BAPYR*S+CH2CO	1.30E+13	0	10600		
4528	ANTHAN+O=BAPYR*S+HCCO	2.20E+13	0	4530		
4529	ANTHANJS+O2=BAPYR*S+2CO	2.10E+12	0	7470		
4530	ANTHANJP+O2=BAPYR*S+2CO	2.10E+12	0	7470		
4531	BGHIPEP+OH=BGHIPEJP1+H2O	2.10E+13	0	4600		
4532	BGHIPEJP1+O2=PERYLENJS+2CO	2.10E+12	0	7470		
4533	PERYLEN+OH=PERYLENJS+H2O	2.10E+13	0	4600		
4534	BEPYREN+OH=BEPYRENJS+H2O	2.10E+13	0	4600		
4535	BAPYR*S+O2=A3LA1-X+2CO	2.10E+12	0	7470		
4536	COR+OH=CORJ+H2O	2.10E+13	0	4600		
4537	COR1+OH=COR1J+H2O	2.10E+13	0	4600		
4538	COR2+OH=COR2J+H2O	2.10E+13	0	4600		
4539	COR3+OH=COR3J+H2O	2.10E+13	0	4600		
4540	COR4+OH=COR4J+H2O	2.10E+13	0	4600		
4541	CPCDPYR+OH=CPCDPYRJS+H2O	2.10E+13	0	4600		
4542	BGHIF+OH=BGHIFJ+H2O	2.10E+13	0	4600		
4543	BGHIFR+OH=BGHIFRJS+H2O	2.10E+13	0	4600		
4544	CPCDFLTH+OH=CPCDFLTJS+H2O	2.10E+13	0	4600		
4545	FLTHN+OH=FLTHNJ1+H2O	2.10E+13	0	4600		
4546	FLTHN+OH=FLTHNJ3+H2O	2.10E+13	0	4600		
4547	CORONENYL+O2=BGHIPEJS1+2CO	2.10E+12	0	7470		
4548	CORONEN+H=CORONENYL+H2	2.62E+07	2.1	15842		
4549	CORONEN+OH=CORONENYL+H2O	1.71E+13	0	4571		
4550	CORONENYL+H=CORONEN	7.83E+13	0	0		

Table 24 : List of reactions considered in the present detailed kinetic mechanism.

